DISSERTATION

zur

Erlangung der Doktorwürde

der

Naturwissenschaftlich-Mathematischen Gesamtfakultät

der

Ruprecht-Karls-Universität Heidelberg

Zu Heidelberg

vorgelegt von

M. Sc. Jinsong Han

Tag der mündlichen Prüfung: 14.07.2017

Conjugated Polymer-Based Chemical Tongues

Hypothesis-Free Sensor Arrays for the Discrimination of

Chemical and Biological Analytes

Gutachter: Prof. Dr. Uwe H. F. Bunz

Prof. Dr. A. Stephen K. Hashmi

Acknowledgement

I would like to express my sincere appreciation to my PhD mentor, Prof. Dr. Uwe H. F. Bunz, for his generous support and guidance during the time of my research, his consistent interest in the progress of my work, as well as valuable ideas, suggestions and discussions. Furthermore, I would like to thank Dr. Kai Seehafer for an overall pleasant atmosphere, kind help for my research study, the fruitful discussions, suggestions and his anytime accessibilities. I would also like to thank Prof. Dr. A. Stephen K. Hashmi for kindly accepting to be my second reviewer.

I thank my collaborators, Prof. Dr. Andreas Herrmann (Zernike Institute for Advanced Materials, University of Groningen, Netherlands) and his PhD student Chao Ma, for their kind support on the preparation of supercharged GFPs and fruitful discussions on the project of whisky sensing.

I thank my collaborators, Prof. Dr. Michael Wink (IPMB, University of Heidelberg) and his group members, especially Haoran Cheng, for their kind supports and fruitful discussions on the project of bacterial discrimination, especially for the assistances on the biological experiments (preparation of antimicrobial peptides, bacterial culturing, fluorescence microscopy and experiments of bacterial discrimination).

I thank Prof. Dr. Rasmus Schröder and Dr. Irene Wacker (Bioquant, University of Heidelberg), for their discussions and assistances on the scanning electron microscope and confocal fluorescence microscopy. I also thank Prof. Dr. Vincent M. Rotello, Prof. Dr. Caren M. Rotello and Mahdieh Yazdani from University of Massachusetts Amherst, USA, for their kind help of statistical methods, especially bootstrapping analysis.

I thank Dr. Jürgen Gross and colleagues for the MS spectra and UPLC-MS analysis. I also acknowledge the colleagues from the NMR and elemental analysis department for their kind supports.

I thank Benhua Wang, Markus Bender, Soh Kushida and Emanuel Smarsly for their collaboration, kind help and fruitful discussions during my research study. I also thank all of my intelligent colleagues, in particular Wei Huang, Gaozhan Xie, Kerstin Windisch, Kerstin Brödner, Andrea Uptmoor, Dr. Jan Freudenberg, Allan Bastos, Sebastian Hahn, Yury Kozhemyakin, Andreas Kretzschmar, Olena Tverskoy, Maximilian Bojanowski, Maximilian Ackermann, Zeyu Li, Gerard Bollmann, Manuela Casutt for their parties, suggestions, discussions and general supports. It is really a pleasure to work with you.

Last but not least, I am deeply grateful for the consistent and strong support from my beloved family, for their support on my academic career.

Abstract

This doctoral thesis is divided into four chapters. The main focus of this thesis is on the development of conjugated polymer-based chemical tongues and their sensory applications. In the first chapter, introductions on the synthesis of conjugated polymers and their sensory applications are summarized. In chapters 2-4, several types of polyelectrolyte-based chemical tongues have been constructed and been applied to the discrimination of small molecular analytes, complex mixtures and bioanalytes. In the last chapter, experimental details are provided.

In Chapter 1, an introduction is first given to the synthesis of conjugated polymers, especially the water-soluble poly(*p*-aryleneethynylene)s (PAEs). Then, introductions of the recent progress in the field of chemical tongue/nose and their applications toward small molecules, complex mixtures and bio-analytes are described. Finally, the basic properties of PAEs and the concept of hypothesis-free sensor array are introduced.

In Chapter 2, several PAE-based sensor arrays (PAEs alone or their electrostatic complexes) were constructed. They reliably discriminate different types of small molecular analytes, including 13 structurally related aliphatic organic acids and 21 aromatic carboxylic acids. Next, methods to generate the minimalist tongue were developed. Such simple tongue successfully discerns 11 NSAIDs and 19 different antibiotics, even commercial drugs (over-the-counter) and their "counterfeits".

In Chapter 3, my work was focused on the development of chemical tongues for the quality control of food, beverages and other complex analytes. Several types of hypothesis-free sensor arrays have been constructed based upon PAEs (complexes) or green fluorescent proteins; they successfully discriminated white wines and fruit juices. Especially, 33 different whiskies have been identified according to their country of origin (Ireland, US, Scotland), brand, blend status (blend/single malt), age and taste (rich/light). Our tongues do not need any sample preparation and are superior to state-of-the-art methods.

In Chapter 4, our focus was transferred to the detection of bioanalytes in complex biofluids. We developed a new sensor array comprised of four complexes, formed from one cationic PPE and four anionic antimicrobial peptides (AMPs). This simple tongue successfully identifies fourteen bacteria in water and in human urine, at a disease-related concentration. Interestingly, clusters formed according to staining (Gram-positive and Gram-negative) and genetic similarity (genera, species and strains), indicate a potential application in clinical settings.

Zusammenfassung

Diese Doktorarbeit ist in vier Kapitel unterteilt. Der Schwerpunkt dieser Arbeit liegt auf der Entwicklung konjugierter polymerbasierter chemischer Zungen und deren sensorischen Anwendungen. Im ersten Kapitel werden Einführungen zur Synthese von konjugierten Polymeren und deren sensorischen Anwendungen zusammengefasst. In den Kapiteln 2-4 wurden verschiedene Arten von chemischen Zungen auf Polyelektrolytbasis aufgebaut und auf die Unterscheidung von kleinen molekularen Analyten, komplexen Mischungen und Bioanalyten angewendet. Im letzten Kapitel werden experimentelle Details bereitgestellt.

In Kapitel 1 wird zunächst die Synthese von konjugierten Polymeren, insbesondere der wasserlöslichen Poly(*p*-arylenethinylene) (PAEs), eingeführt. Anschließend werden die Einführungen der jüngsten Fortschritte auf dem Gebiet der chemischen Zunge / Nase und ihren Anwendungen auf kleine Moleküle, komplexe Mischungen und Bioanalyten beschrieben. Schließlich werden die Grundeigenschaften von PAEs und das Konzept der hypothesenfreien Sensoranordnung eingeführt.

In Kapitel 2 wurden mehrerer PAE-basierter Sensor-Arrays (PAEs allein oder ihre elektrostatischen Komplexe) konstruiert. Sie unterscheiden zuverlässig verschiedene Arten von kleinen molekularen Analyten, darunter 13 strukturell verwandte aliphatische organische Säuren und 21 aromatische Carbonsäuren. Als nächstes wurden Methoden zur Erzeugung der minimalistischen Zunge entwickelt. Eine solche einfache Zunge erkennt erfolgreich 11 NSAIDs und 19 verschiedene Antibiotika, auch kommerzielle Arzneistoffe und ihre "Fälschungen".

In Kapitel 3 konzentrierte sich meine Arbeit auf die Entwicklung von chemischen Zungen für die Qualitätskontrolle von Nahrungsmitteln, Getränken und anderen komplexen Analyten. Mehrere Arten von hypothesenfreien Sensorarrays wurden auf der Basis von PAEs (Komplexen) oder GFPs (green fluorescent protein) konstruiert; Sie haben erfolgreich weiße Weine und Fruchtsäfte unterschieden. Vor allem 33 verschiedene Whiskeys wurden nach ihrem Herkunftsland, Marke, Blend Status, Alter und Geschmack identifiziert. Unsere Zungen brauchen keine aufwendige Probenvorbereitung und sind dem Stand der Technik überlegen.

In Kapitel 4 wurde unser Fokus auf den Nachweis von Bioanalyten in komplexen Biofluiden übertragen. Wir entwickelten eine neue Sensoranordnung aus vier Komplexen, die aus einem kationischen PPE und vier anionischen antimikrobiellen Peptiden (AMPs) gebildet wurden. Diese einfache Zunge identifiziert erfolgreich 14 Bakterien in Wasser und im menschlichen Urin, in pathogenen Konzentrationen. Interessanterweise gruppierten sich Bakterien die in ihrem Färbeverhalten (Gram-positiv und Gram-negativ) und ihrer Genetik (Gattungen, Arten und Stämme) ähneln, was eine Anwendung im klinischen Rahmen möglich machen könnte.

Publications

Refereed Publications

Jinsong Han, Chao Ma, Benhua Wang, Markus Bender, Maximilian Bojanowski, Marcel Hergert, Kai Seehafer, Andreas Herrmann and Uwe H. F. Bunz, A hypothesis-free sensor array discriminates whiskies for brand, age and taste. *Chem (Cell Press).***2017**, DOI: 10.1016/j.chempr.2017.04.008.

Jinsong Han[†], Benhua Wang[†], Markus Bender, Jessica Pfisterer, Wei Huang, Kai Seehafer, Mahdieh Yazdani, Vincent M. Rotello, Caren M. Rotello and Uwe H. F. Bunz, Fingerprinting antibiotics with PAE-based fluorescent sensor arrays. *Polymer Chemistry.* **2017**, 8, 2723-2732.

Jinsong Han, Benhua Wang, Markus Bender, Kai Seehafer and Uwe H. F. Bunz, Poly(*p*-phenyleneethynylene)-based tongues discriminate fruit juices. *Analyst.* **2017**, 142, 537-543.

Highlighted by: *ChemistryWorld from RSC*

Jinsong Han[†], Benhua Wang[†], Markus Bender, Soh Kushida, Kai Seehafer and Uwe H. F. Bunz, Poly(aryleneethynylene) tongue that identifies nonsteroidal anti-inflammatory drugs in water: A test case for combating counterfeit drugs. *ACS Applied Materials & Interfaces.* **2017**, 9, 790-797.

Jinsong Han[†], Benhua Wang[†], Markus Bender, Kai Seehafer and Uwe H. F. Bunz, Water-soluble poly(p-aryleneethynylene)s: A sensor array discriminates aromatic carboxylic acids. *ACS Applied Materials & Interfaces.* **2016**, 8, 20415–20421.

Jinsong Han, Markus Bender, Kai Seehafer and Uwe H. F. Bunz, Identification of white wines by using two oppositely charged poly(*p*-phenyleneethynylene)s individually and in complex. *Angewandte Chemie International Edition.* **2016**, *55*, 7689-7692. *Angewandte Chemie*. **2016**, 128, 7820–7823.

Highlighted by: *Angew. Chem. Int. Ed. Press Release, C&EN 2016, 94, 26, p9, Heidelberg University Press, ChemistryViews, analytica-world.com, chemie.de, q-more.chemie.de, PHYSORG news, Spektrum.de, LABORWELT, Pro-Physik.de, Yumda, IDW, EATON, WijnWijs.eu, innovations-report, Analytik-News, X-MOL.*

Jinsong Han[†], Markus Bender[†], Kai Seehafer and Uwe H. F. Bunz, Polyelectrolyte complexes formed from conjugated polymers: Array-based sensing of organic acids. *Chemistry - A European Journal.* **2016**, 22, 3230-3233.

Benhua Wang[†], **Jinsong Han[†],** Markus Bender, Kai Seehafer and Uwe H. F. Bunz, Array-Based Sensing of Explosives by Water-Soluble Poly(para-phenylene-ethynylene)s. *Macromolecules*, **2017,** DOI: 10.1021/acs.macromol.7b00738. ([†] co-first author)

Wei Huang, Emanuel Smarsly, **Jinsong Han**, Markus Bender, Kai Seehafer, Irene Wacker, Rasmus R. Schröder, and Uwe H. F. Bunz, Truxene-Based hyperbranched conjugated polymers: fluorescent micelles detect explosives in water. *ACS Applied Materials & Interfaces.* **2017**, 9, 3068-3074.

Jinsong Han[†], Haoran Cheng[†], Benhua Wang[†], Markus Braun, Xiaobo Fan, Markus Bender, Wei Huang, Cornelius Domhan, Walter Mier, Thomas Lindner, Kai Seehafer, Michael Wink and Uwe H. F. Bunz. Polymer/Peptide Complex-Based Tongues Discriminate Bacteria in Complex Biological Milieu. **2017**, *Manuscript submitted.*

Benhua Wang[†], **Jinsong Han[†],** Chao Ma, Markus Bender, Kai Seehafer, Andreas Herrmann and Uwe H. F. Bunz, A Simple Tongue Discriminates Amino Acids. **2017**, *Manuscript submitted.* ([†] co-first author)

Patents

Uwe Bunz, Kai Seehafer, **Jinsong Han**, Markus Bender, Method for identifying a complex analyte.
EU pending patent, **10. 2016.**

Abbreviations

AIE	aggregation-induced emission
AMR	antibiotic resistance of microbes
CIU	correctly identified unknowns
CP	conjugated polymers
CPE	conjugated polyelectrolytes
CTMA	cetyltrimethylammonium chloride
CMC	critical micelle concentration
DART	direct analysis real time
DIEA	N,N-Diisopropylethylamine
FRET	fluorescence resonance energy transfer
GC-MS	gas chromatography–mass spectrometry
GFP	green fluorescent protein
GPC	gel permeation chromatography
HCA	hierarchical cluster analysis
HR-MS	high resolution mass spectra
IR	infrared spectroscopy
LDA	linear discriminant analysis
MALDI	matrix-assisted laser desorption/ionization
MANOVA	multivariate analysis of variance
MDR	microbes multidrug resistant strains
MDRS	multidrug resistant strains
MeOH	Methanol
MRSA	methicillin-resistant Staphylococcus aureus
NMR	Nuclear magnetic resonance
NP	nanoparticle
NSAIDs	nonsteroidal anti-inflammatory drugs
OTC	over-the-counter
PAE	poly(*para*-aryleneethynylene)
PPP	poly(*para*-phenylene)
PPV	poly(*para*-phenylenevinylene
PPE	poly(*para*-phenyleneethynylene)
PF	poly(fluorene)
PA	polyacetylene
PPy	polypyrrole
PT	polythiophene
PANI	polyaniline

PCA	principal component analysis
PCR	polymerase chain reaction
PDI	polydispersities
RT	room temperature
SDBS	sodium dodecylbenzenesulfonate
SERS	surface-enhanced Raman spectroscopy
SW	swallowtail
THF	tetrahydrofuran
TCA	citric acid cycle
TLC	thin layer chromatography
TMS	Trimethylsilyl
TOF-MS	Time-of-flight mass spectrometry
UV-Vis	ultraviolet-visible spectrophotometry
VOC	volatile organic compound
WSCP	water-soluble conjugated polymer
Φ	Quantum yields
calcd.	calculated
h	hours
min	minutes
m.p.	melting point
ppm	parts per million

Table of Contents

Chapter 1. Introduction

1.1 Synthesis of Poly(aryleneethynylene)s

1.1.1 Introduction of Conjugated Polyelectrolytes

In 2000, the Nobel Prize for Chemistry was awarded to Prof. Alan J. Heeger, Prof. Alan G. MacDiarmid and Prof. Hideki Shirakawa "for the discovery and development of conductive polymers". Conjugated polymers (CPs), have emerged as the promising materials during the last few decades due to their optical and electronic properties. Based on the difference of their backbones, various types of CPs (Figure 1A) have been developed and studied. They include poly(*para*-phenylene (**PPP**), poly(*para*-phenylenevinylene (**PPV**), poly(*para*-phenyleneethynylene) (**PPE**), poly(fluorene) (**PF**), polyacetylene (**PA**), polypyrrole (**PPy**), polythiophene (**PT**) and polyaniline (**PANI**). Large numbers of conjugated polymers with unique, tunable electronic and optical properties were designed and synthesized.

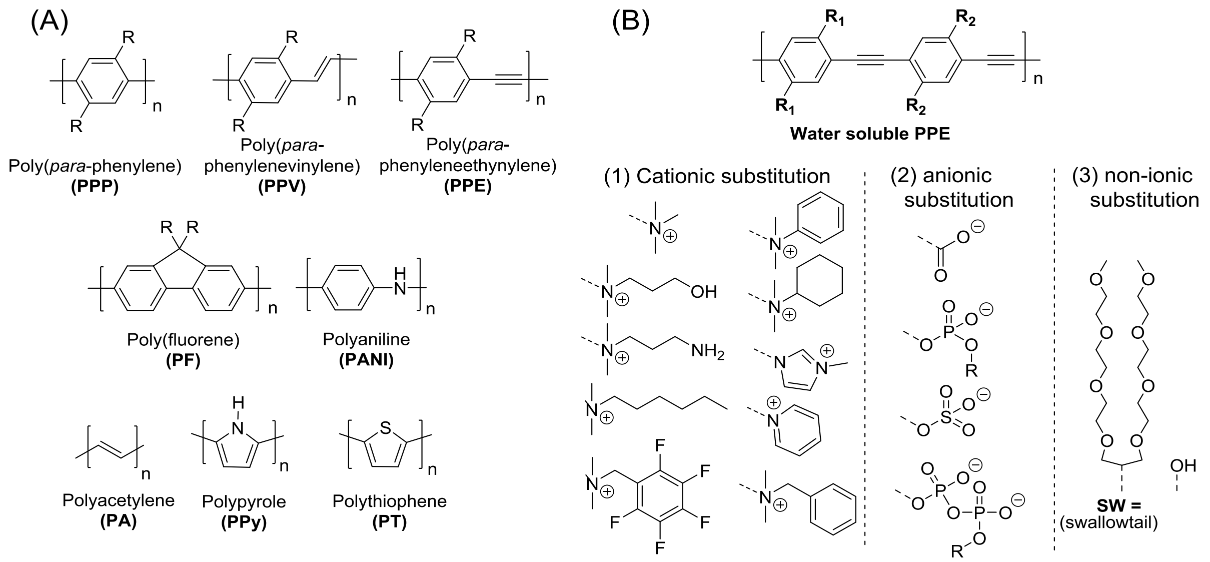

Figure 1. (A) Molecular structures and backbones of extensively studied conjugated polymers. **(B)** Design and construction of water soluble conjugated polymers.

With the rapid development of the conjugated polymers area, specifically designed conjugated polymers were developed. They are used for applications, including light-emitting diodes,[1-2] photovoltaic cells,[3-4] field effect transistors,[5-6] and chemical and biological sensors[7-10]. To improve the chemical and physical properties including solubility of a polymer material, methods have been found by adding side chains. Water-soluble poly(*para*-phenyleneethynylene)s (PPEs), functionalized with oligoethyleneglycol side-chains, carboxylate or ammonium groups, show strong ability for chemical tongue sensing application.

1.1.2 Synthesis of Water Soluble Poly(aryleneethynylene)s

Conjugated polyelectrolytes (CPEs) are conjugated polymers functionalized with water-soluble ionic side chains. Typically, CPEs can be divided into three categories (Figure 1B) depending on the charge properties of their side chains: (**1**) Cationic conjugated polyelectrolytes, typically functionalized with quaternary ammonium (NR_3^+) and pyridinium; (**2**) Anionic conjugated polyelectrolytes, the side chain of anionic groups mainly are carboxylate (CO_2^-), phosphonate (PO_3^{2-}), and sulfonate (SO_3^-). (**3**) Zwitterionic conjugated polyelectrolytes, which combined the anionic and cationic side groups. However, it should be noted that conjugated polymer which not including any ionic group, but containing oligoethyleneglycol side-chains (swallowtail) may also have good water solubility. Thus, the solubility of conjugated polymers in polar solvents (e.g., water and methanol) is dependent on the ionic side groups, the hydrophobic aromatic backbones, and hydrophilic side chain.

During the past few decades, large numbers of CPEs have been synthesized via carbon–carbon bond-forming reactions using organometallic catalysts. For poly(arylene)s, the most widely used polymerization methods include $FeCl_3$-catalyzed, electrochemical oxidization, the Yamamoto and Suzuki coupling reactions. For poly(arylene vinylene)s, the Wittig, Gilch, Wessling, and Heck reactions are the most common methods.

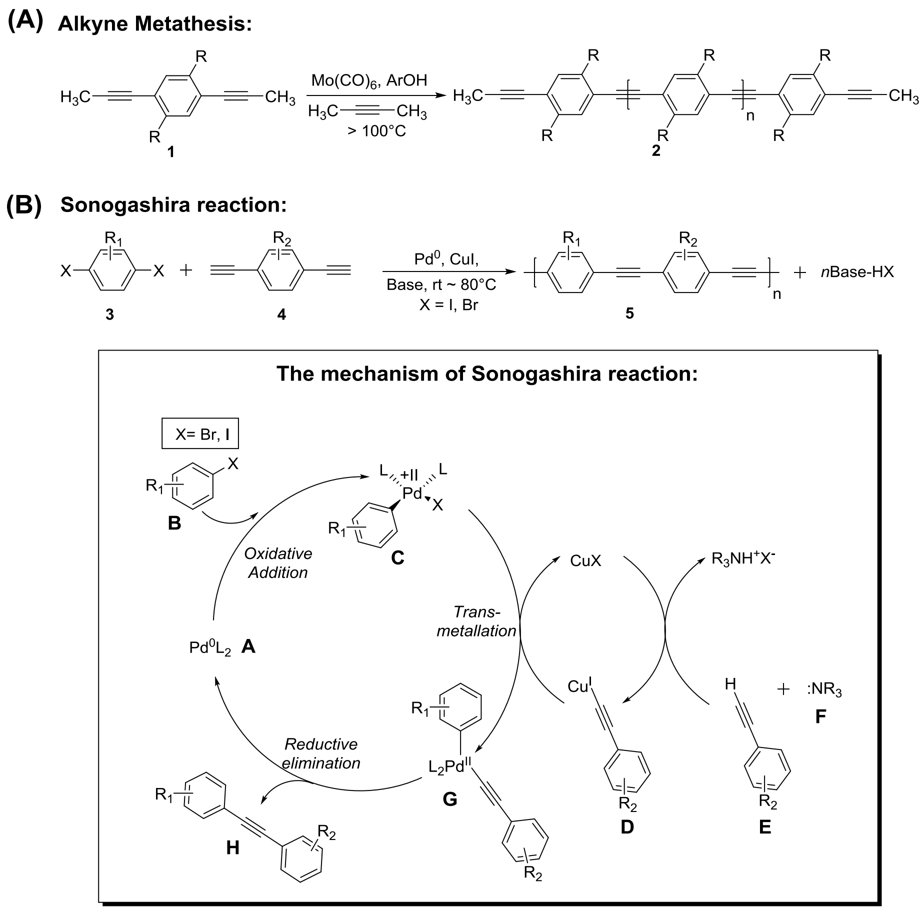

Figure 2. (A) Synthesis of PAEs by alkyne metathesis. **(B)** Synthesis route and mechanism of sonogashira coupling reactions for PAEs.

Among water soluble conjugated polymers, we are interested in PAEs and their sensory application. In comparison to the other conjugated polymers, PAEs show advantages such as fairly quick syntheses of large scales, functional groups (sulfonate, carboxylate, phosphonate, quaternary ammonium and pyridinium) can easily be incorporated into the side chains, high fluorescence quantum yields. Several reviews focus on the syntheses and physical properties of water soluble PAEs.[9, 11-14] The most common methods include palladium-catalyzed Sonogashira coupling reactions and alkyne metathesis found by Bunz etc. (Figure 2A). We employ Sonogashira coupling reactions, because of tolerance to functional groups, mild reaction conditions, and the capability to produce different backbone structures. More specifically, the coupling of aryl diiodides with aromatic diynes using $(Ph_3P)_2PdCl_2$ as the catalyst with low (0.1–0.2 mol%) loadings and piperidine–THF as the solvent–base mixture at reaction temperatures of 20–80 °C are optimal. Higher temperatures can give PAEs of higher molecular weight. For the situation that monomers are sensitive towards piperidine, triethylamine is an alternative choice. For aryl bromides, triethylamine in the presence of THF is preferred. Generally, high reaction temperatures (>80 °C) are necessary, unless the bromides are attached to electron poor arenes, which increase the reactivity towards the Sonogashira reaction.

The mechanism of the reaction, following Figure 2B, begins with a Pd^0 species undergoing oxidative addition to the aryl–X bond of **B** to give **C**. Transmetallation with the putative Cu^I acetylide **D** leads to **G**, which undergoes reductive elimination to yield the product, **H**, and regenerating **A**.

1.2 Application of Chemical Tongue/Nose

1.2.1 Introduction of Chemical Tongue/Nose

"The Nobel Prize in Physiology or Medicine 2004" was awarded jointly to Richard Axel and Linda B. Buck "for their discoveries of odorant receptors and the organization of the olfactory system".[15-17] The mammalian olfactory system recognizes and discriminates odorant molecules by the mucosa composed of sensing cells. The human taste sensing system recognizes over 10,000 different complex tastes according to the combination of salty, sweet, sour, bitter, umami, and hotness.[18] Similar to the human organ, scientists try to make artificial tongues/noses, which mimic the olfactory/taste sensing elements by constructing the sensor arrays with various signals (optical, electronic, mechanical, etc.) from artificial devices. In 1982, the first artificial nose was reported by Persaud and Dodd, which mimic the mammalian olfactory system using semiconductor transducers. This model nose successfully discriminated among odorant mixtures without using highly specific receptors.[19] Based on the difference of signal transduction, various sensors have been developed, mainly including electrical and electrochemical sensors,[20-23] thermometric sensors[24-31] and optical sensors (colorimetry[32] and fluorometry[33]). In our study, we are interested in optical sensor arrays that use absorbance, reflectance or fluorescence array detectors; fluorescence detection is particularly desirable because of its high sensitivity and the associated convenient data acquisition (plate reader).[34-35]

Chemical tongues/noses, composed of a number of sensor or receptor elements, discriminate multiple types of analytes. Instead of a specific response of a single sensor or dosimeter for a single analyte (lock-and-key method), chemical tongues/noses consist of combinations of different highly cross-reactive sensors, which respond to selective, but not specific signals to the offered analytes.[36-37] In our study, chemical tongues exploit the change in fluorescence intensities upon exposure of the sensor field towards the selected analytes. The numerical power of the created data field is high, as one element in such a sensor field can attain 100 - 200 (or more) values. For example, a small field of 4 sensor elements, a power of up to $200^4 = 1.6 \times 10^9$ different responses are possible, suggesting that analyte groups containing 10-100 elements would be easily discerned, if the sensor field is even only somewhat suitable. Based on this hypothesis, we have employed small sensor fields to identify the following analytes: (1) small molecular compounds - aliphatic organic acids, diacids, aromatic acid, metal ion, phosphate, explosives, nonsteroidal anti-inflammatory drugs and antibiotics;[38-45] (2) complex analytes - white wines, fruit juices and whiskies;[46-47] (3) biomacromolecules - glycosaminoglycan, proteins, bacteria, cells etc.[48-58]

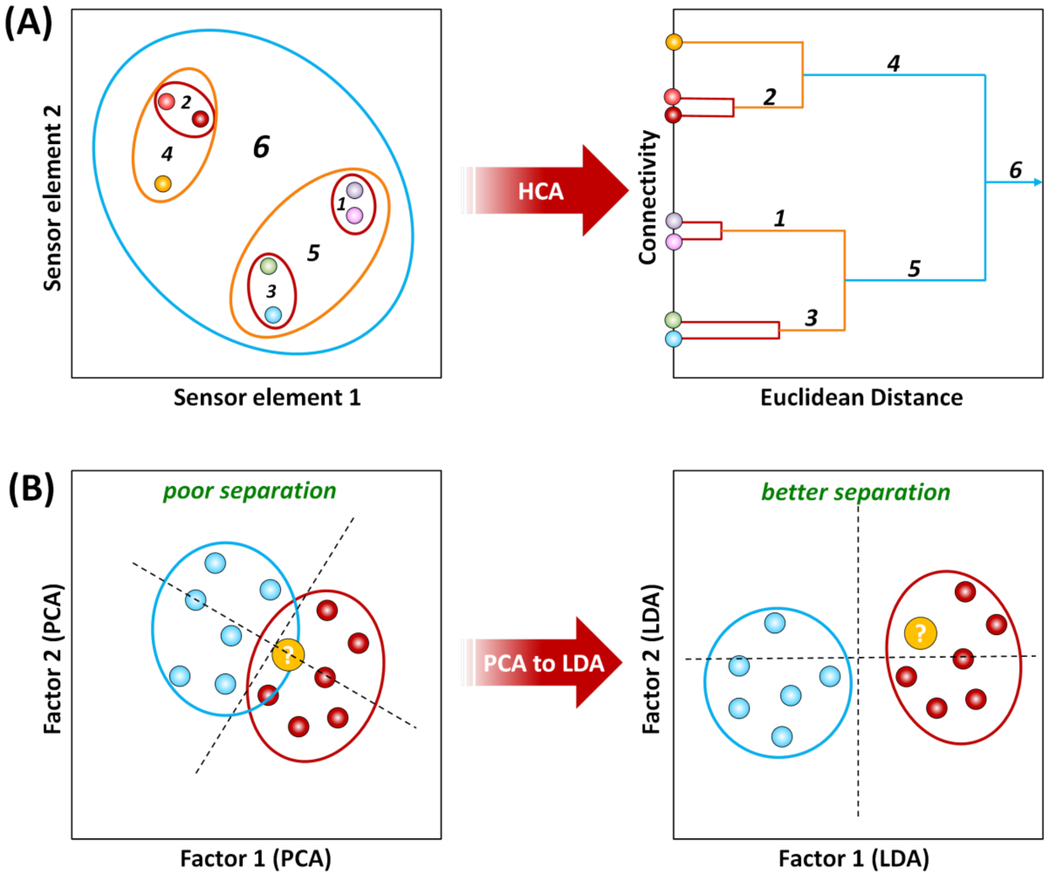

Figure 3. (A) Schematic representation of a hierarchical cluster analysis (HCA) of multidimensional data that forms a dendrogram based on clustering of those experimental measurements (shown on the right). (B) Score plots comparing data analyzed with PCA (left) and LDA (right). Circled areas represent 95% confidence intervals. The most obvious separation by eye in the PCA plot is along dimension A, which is orthogonal to dimension B; this is used as the first dimension in LDA analysis and is a visualization of the between-sample variance. The orange circle is clearly identified as being in the red class using LDA, while identification is ambiguous using PCA.

Chemical tongues with fewer sensor elements have difficulty to identify large libraries of similar, complex analytes. Thus, an increase of sensor elements can improve the accuracy and resolution, this is the reason why the olfactory system consist of hundreds of highly cross-reactive receptors. However, for the pattern recognition of similar analytes, the greater dimensionality of sensor elements, the more sophisticated approach of statistics are needed. There are many statistical methods available to deal with the high dimensional data; they share the common goals that reduce the dimensionality and predict the unknown samples based on a known library.[59] The most commonly used three approaches for chemical tongue are: hierarchical cluster analysis (HCA), principal component analysis (PCA), and linear discriminant analysis (LDA).[36, 60-63]

HCA is a statistical method which provides a straightforward dendrogram based on the cluster similarity determined by Euclidean distance (Figure 3A).[60, 64] However, HCA can not be used for quantitatively analyzing and predicting unknown analytes. Thus it is often used as an auxiliary method for cluster observation of similar analytes. PCA is a dimensional reduction method that condenses the variance among several possibly - correlated dimensions by creating a new orthogonal set of dimensions, using linear combinations of the initial dimensions. As "chemical tongue" sensor arrays are often composed of many components (4-30 sensor elements), it is difficult to show all data in a visualized 2D or 3D plots; by employing PCA, two or three optimized components were obtained from a dimensional reduction method, depending on the contribution of all sensor elements. Thus, PCA is a powerful tool for evaluating "chemical tongue" sensor arrays with several disparate sensor elements and screening the best elements with the most discriminative power. While similar to HCA, PCA is an unbiased method that is best suited for evaluation of data sets rather than prediction, which is realized by LDA.

Like PCA, LDA is also a statistical method of dimensional reduction and has been widely used for pattern-based identification in chemical tongues. LDA converts the training matrix with multiple sensor elements into canonical scores according to their Mahalanobis distance by calculation. While This is an important advantage, LDA can be applied to predict unknown samples by using a training set, called "blind test". Furthermore, when compared with PCA, LDA shows better distinguishing ability because of the arithmetic difference between groups (Figure 3B). For this reason, we use PCA for the screening of the best sensor elements based on the contribution of each element, then distinguish various analytes and predict the unknown samples with LDA.

1.2.2 Chemical Tongue for Sensing of Small Molecular Analytes

Identification and recognization of different kinds of small molecular analytes with chemical tongues have been widely investigated, including explosive, acids, amine, nervous toxic, drug etc. In this area, the groups of Suslick[65-71], Anslyn[37, 72-73] and Anzenbacher[74-83] have made key contributions during the past decade. Small molecular analytes are mainly divided into three types based on ionic condition, including cationic, neutral and anionic. Based on their physical properties, the analytes can be identified by chemical tongues constructed by charged PAEs and GFPs employing nonspecific interaction.

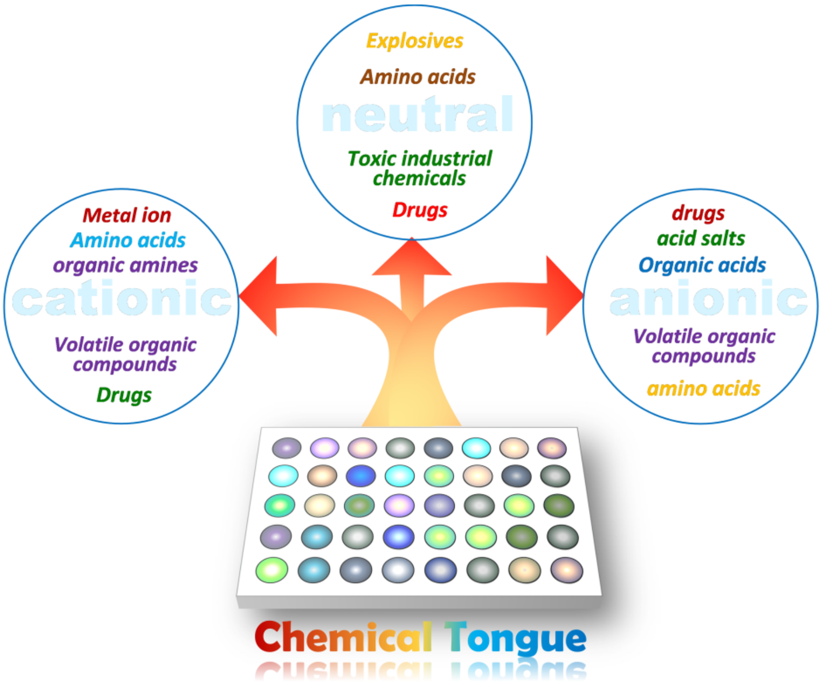

Figure 4. Chemical tongue for small molecular sensing.

As the case for cationic analyte sensing (Figure 4), heavy metal ions are important and widely investigated targets because of their serious harmfulness. Heavy metal ion pollution has posed a severe threat to human health, their accumulation in the soft tissues of the body could cause serious damage to the brain. Numbers of studies and methods have been reported for the detection and removal of metal ions in water. For example, Anzenbacher and co-workers reported a fluorescent sensor array for qualitative and quantitative identification of 10 metal ions (Ca^{2+}, Mg^{2+}, Cd^{2+}, Hg^{2+}, Co^{2+}, Zn^{2+}, Cu^{2+}, Ni^{2+}, Al^{3+}, and Ga^{3+}) with 100% accuracy[84]; to illustrate the utility of the approach to a real-world application, soft drinks based on their different Ca^{2+}, Mg^{2+}, and Zn^{2+} cation content were successfully discriminated[83]. In addition, other cationic analytes, such as cancer-associated nitrosamines[85], amino acids[86-87] etc. have also been widely studied.

The recognition and sensing of anions is also of significant importance due to their biological occurrence, as a variety of biological molecules, such as amino acids, peptides, and nucleotides, can have an anionic motif. However, small anions sensing is challenging, particularly in water, because anions are larger than isoelectric cations, resulting in lower charge-to-radius ratio, a feature which makes the electrostatic binding of anions to receptors less effective.[88] Recently, several chemical tongues focused on small molecular anions have been reported, which successfully identified anions in water with high accuracy. For example, an eight-member sensor array composed of dye elements successfully identified 10 inorganic anions in water, including F^-, Cl^-, Br^-, AcO^-, BzO^-, NO_3^-, HSO_4^-, $H_2PO_4^-$, PPi, and HS^-.[88] Other examples focus on phosphate anions (AMP, ADP, ATP, CMP, GMP, Pi, and PPi)[81, 89] and recognition of carboxylate drugs[79-80] has also been reported.

Small neutral molecules are among the largest group of analytes investigated, which include industrial chemicals, explosives, amino acids, drugs, organic gases, vapors etc. Suslick's group has made significant contributions to this field by developing a large variety of sensor arrays for organic gases and vapors.[65-66, 69-70, 90-94] Volatile organic compounds (VOCs) are numerous, varied, and ubiquitous. They include human-made and naturally occurring chemical compounds. VOCs play a key role in human health, such as cancer diagnostics,[95] but can also cause harm to the environment. Thus, development of a low-cost, sensitive sensor array for the detection and identification of VOCs is important. During the past ten years, a full list of 115 VOCs have been reported in the literature as cancer biomarkers.

Developing new diagnostic and detection technologies for disease-related biomarkers is challenging. Haick's group have made key contributions to this area, and analyzed disease-related VOCs by means of nanomaterial-based sensors, a non-invasive diagnostic tool; various diseases have been detected successfully.[95-96] However, most of the work is based on highly selective receptors/detectors to bind or detect the disease-related VOCs specifically; the one analyte one receptor method limits the application with a complicated design process of the specific receptor. An emerging method that is complementary to the selective sensing approach is the cross-reactive sensor array, chemical tongue, which identifies a variety of disease-related VOCs in minutes.[36, 97-100]

Chemical tongue based colorimetric sensors and electro-acoustic sensors have also been developed and applied successfully to cancer testing. Suslick et al. reported that a colorimetric sensor made from 24 sensor elements that was used in a clinical trial on 229 subjects (92 lung cancer with different histology, 137 healthy controls). Results showed that better accuracies are achieved in the comparison of individual histologies and the control group (e.g., squamous cell carcinoma, adenocarcinoma) than in the case of non-small cell lung cancer compared with the control group, which gave a sensitivity and specificity of 70% and 86%, respectively.[92]

Development of rapid, sensitive, portable and inexpensive techniques for the identification of a wide range of hazardous analytes (toxic gases, vapors, and aqueous solutions) are crucial for human health and safety. Many efforts have been undertaken toward developing methods to identify the hazardous chemicals. Especially, new approaches of chemical tongue sensor arrays or artificial noses have been proved to show strong discriminatory powers for the monitoring of toxic gases at sub-ppm levels.[72, 101] Among hazardous analytes, explosives and chemical warfare agents (nerve agents) detection are extremely important for national security, military defense and criminal investigations. In addition to that, toxic industrial chemicals (heavy metal ion, drug residue, pesticide etc.) are also threat to human health and the environment. Because of the structural similarity of various hazardous analytes, traditional optical sensors with specific or nonspecific interaction are difficult for detection. The use of chemical tongues in combination with pattern recognition algorithms (LDA, PCA) can overcome the problem. Therefore, many studies have been reported for the detection of hazardous chemicals with chemical tongue methods, including colorimetric and fluorescence sensor array.[66, 68, 94, 102-105]

1.2.3 Chemical Tongue for Sensing of Complex Mixtures

Quality control and quality assurance of food, beverages and other complex analytes is a practical, important, yet intellectually ambitious task. Although different analytical methods have been exploited, including mass spectrometry,[106-110] electrochemical tongues and noses,[111-113] also biological methods (antibodies, genetics),[114-115] the analysis of complex mixtures is still challenging, because of the similarity and complexity of their compositions. One specific method are chemo-optical tongues.[36, 116] These indicate the spoiling of fish,[117-118] fingerprint coffees,[119] whiskeys,[120] beers,[121] softdrinks,[122] red wines[123-125] and white wines,[47] to highlight applications of tongues that react by color change or fluorescence intensity modulation. These tongues are composed of sensor arrays with different receptors that are bound to colored or fluorescent indicator-dyes, replaced by the analytes. Their action principle is different from that of classic sensors but also of that of instrumental analytical methods. Suslick described in his superb review[36] some of the features that are (presumably) necessary to achieve successful discrimination for complex analytes and stressed that "*…in general, an optimal sensor array for general sensing purposes will incorporate as much chemical diversity as possible…*".[36] This statement guided the development of arrays in which a wide variety of different colorimetric indicator molecules are employed to identify analytes. Suslick's (printed) sensor libraries typically consist of 16-36 elements for successful identification of different classes of analytes.[65-66, 70-71, 90, 119, 121-122, 126-128]

A second accepted tenet of these chemo-optical tongues was formulated by Anslyn, and is a weakened variation of the lock and key-principle of Fischer as nicely shown in Figure 1 of ref.[129] In this picture molecular keys fit into many locks with a varying degree of fit. Several of such partially fitting receptors identify and discriminate groups of analytes by the unique signal patterns of the sum of the sensor elements. Here the most practical approach is to offer small libraries of receptors that are "filled" with dyes to be replaced by the analytes with differential efficiency.[130]

Both of these approaches stress that cross-reactivity, structural differentiation and structural variation of the sensor elements are important, as expressed by the wish to obtain high dimensionality sensor arrays that differentiate a broad variety of similar but complex analytes, including soft drinks, coffees, beers, whiskeys, etc. Both approaches, i.e. the weakened lock and key principle but also the chemical diversity of the sensors are *sufficient* to guide the production of useful sensor arrays. Are they necessary though? Both concepts have generated in the past an arbitrary and large number of exceptionally well-working tongues and sensors, but neither predicts or defines the minimum structural variation in sensor elements necessary to discriminate complex analytes. As optical tongues are constructed in a glass-bead game of nature, there must be rules that guide the arrays' rational and minimalist construction. What are the rules of this game and are the rules defined, to construct minimalist tongues, the simplest systems discriminating a given set of analytes? The overall chemical tongue is not only defined by the selection of the cross-reactive or promiscuous sensor elements (ProSE) but also by the mathematical workup of the collected raw data.

For optimizing chemical tongue/nose system, Bunz et al. have developed minimalist sensor arrays (2-5 sensor elements) with charged poly(*para*-phenyleneethynylene) (PPE) or green fluorescent protein (GFP), which successfully discern different brands of apple, black currant and red grape juice, as well as different white wine and whiskies of various origin, age, brand, blend status and taste. These chemical tongues, based upon fluorescence quenching or turn-on of conjugated polymers in water, allow the assessment and discrimination of commercially available beverages and their mixtures.[46-47]

1.2.4 Chemical Tongues for Sensing of Bio-analytes

The discrimination and quantification of bio-analytes (proteins, cells, bacteria and other biological analytes) in complex mixtures or biological liquids (serum, urine, plasma or saliva etc.) are one key to the detection and diagnosis of diseases. Traditional approaches for the detection of diseases-related biomacromolecule generally depend on a specific interaction, such as enzymatic or antibody-antigen, thereby limiting the scope of the analytes. Instead of a specific response of a single sensor or dosimeter for a single analyte, "chemical tongues/noses" consist of several sensor elements, which respond to selective, but not specific signals to the offered analytes.

Bacterial infections are still the leading cause of human death (approaching 40%), and at the same time antibiotic resistance of microbes (AMR) increases to projected alarming levels. Around 6000 humans die in Germany and around 0.7 million human in the whole world as a consequence of AMR, as a growing number of microbes is un-responsive towards antibiotics; multidrug resistant strains (MDR) have developed. The reason for this situation is multifaceted and includes antibiotics use in livestock, uncontrolled sales in second world countries and over-prescription in first world countries. This situation makes the rapid and efficient identification and classification of bacteria a vital issue. Conventionally are planting and culturing;[131] while the gold standard of bacteriology it takes time (up to 48 h), and some bacteria are only cultured on specific substrates. Yet the high sensitivity and at the same time the fairly simple screening for MDR, this method is still the method of choice in most settings. Yet, the time lag can be a problem for a patient with any serious infection.

More recently polymerase chain reaction (PCR),[132-133] antibodies, gene microarray,[134-135] mass spectrometry[136] and surface-enhanced Raman spectroscopy (SERS)[137] as well as bio- and chemo-materials functionalized with recognition elements, such as antibodies (IgG),[138-139] aptamers,[140] phage[141-142] and carbohydrates,[143] have been[144] developed as alternatives, which however have other disadvantages such as their non-generality, high cost for purchase and maintenance of expensive highly complex instrumentation, complex procedures etc. We have recently developed a simple array composed of an anionic PPE and three different cationic gold nanoparticles. The three electrostatic complexes formed from the nanoparticles and the PPE are greatly reduced in their fluorescence and form a small array. The addition of different bacteria to this simple array led to fluorescence intensity modulation that, upon linear discriminant analysis (LDA), led to their identification. All of the different microorganisms could be discriminated, even several *E. coli* strains[145]. Other systems were used by Bazan et al.[146] electrostatic complexes containing a cationic conjugated oligoelectrolyte and fluorescein (FAM)-labeled single-stranded DNA (ssDNA), identified 7 bacteria. Jiang et al.[147] designed a fluorescent turn-on sensor array with five small molecular aggregation-induced emission (AIE) probes, eight kinds of bacteria have been identified successfully.

1.3 PAE-based Chemical Tongue for Sensing Application

1.3.1 Properties of PAE-based Sensor

Poly(*para*-aryleneethynylene)s (PAEs) are a versatile class of conjugated polymers and have been widely used for sensor applications because of their fluorescence properties.[10] Generally, PAEs are highly fluorescent materials with bright blue color in organic solvents (dichloromethane, chloroform, or THF etc.) and poor solubilities in water.[9, 14, 148] Meanwhile, the fluorescence quantum yield of PAEs decreases in methanol, ethanol or water, which strongly limited the sensory application, as most of the analytes are water soluble. By substitution with oligoethyleneglycol side-chains, carboxylate, ammonium and other charged groups, PAEs are rendered water-soluble and higher fluorescent and can be applied for sensor applications in water. Unlike the traditional small-molecule color change dyes or fluorophores, the fluorescence change of PAEs with delocalized electronic structure are very sensitive towards analytes. Thus, a fairly low concentration of analytes can be detected.

The mode of fluorescence change of PAEs towards various analytes includes fluorescence quenching, fluorescence turn-on and ratiometric mode. Fluorescence quenching is the most commonly used and most direct method, which may be caused by a mechanism of static quenching, dynamic quenching or a combination of them. In static quenching, a ground state complex formed between the analytes and PAEs before the irradiation, thus excited state is immediately and efficiently deactivated. While in dynamic quenching, the complex formed after the excitation of PAEs, and the fluorescence lifetime decreases after the addition of a quencher. Currently, the most popular and useful tool for the mathematical evaluation of the quenching process is the Stern–Volmer equation. If the quenching data do not fit, a modified Stern–Volmer equation has to be used. Based on our experiences, modified Stern–Volmer equation is more useful when PAEs were employed as sensor elements, because of superquenching and molecular wire effects. Rotello and Bunz have reported a ratiometric array composed of conjugated polymers and green fluorescent protein for the detection of mammalian cells. A fluorescence resonance energy transfer (FRET)-based ratiometric biosensor array was constructed and diverse cell types were correctly identified in minutes. Fluorescence turn-on methods have also been applied in our study; electrostatic complexes are constructed by using charged PAEs with oppositely charged gold nanoparticles or PAEs (used as quencher). These formed electrostatic complexes are non-fluorescent, but complexes can be disrupted by the addition of different analytes and the fluorescence of PAEs can be restored (see Figure 5).[49, 52, 54-57, 59, 149] Polyvalent interactions play a key role, both in the formation as well as in the destruction of the electrostatic complexes by various analytes, such as proteins, bacteria, cells and cell lysates.[150]

Compared with the traditional small molecular dye, PAEs have the advantages including (**1**) amplified quenching, which caused superquenching when response to analytes. (**2**) Changes in fluorescence are more sensitive towards analytes than changes in absorption spectra or color change. (**3**) A low concentration of PAEs can be used for sensing (100nM – 10uM) based on the concentration of the repeat unit, while much higher concentrations were needed for the colorimetric sensors.

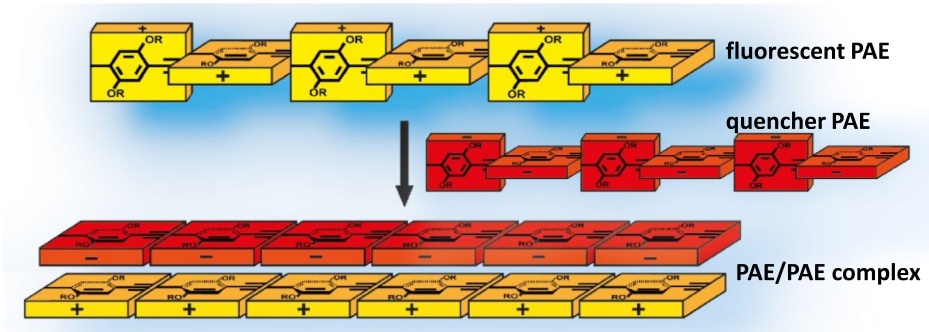

Figure 5. The non-fluorescent electrostatic complexes formed between highly fluorescent PAE (positive) and PAE quencher (negative) for the construction of a fluorescence turn-on sensor array.

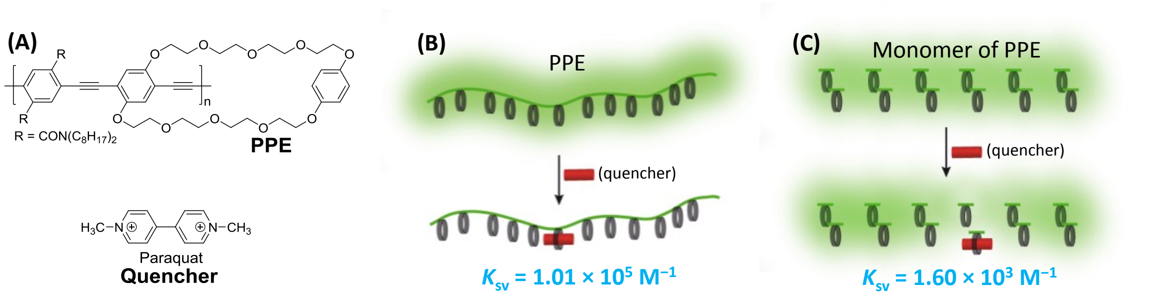

Figure 6. **(A)** Structure of cyclophane-appended PPE and the employed quencher paraquat. **(B)** One paraquat molecule (red cylinder) quenches in this picture a PPE with appended receptors; **(C)** one paraquat molecule quenches one of the monomer of PPE, the others are still fluorescent.

The "molecular wire effect" was first presented in a model study published by Swager group in 1995, which serves as a general introduction to the mechanism of chemical sensing by amplified fluorescence quenching with conjugated polymers. Cyclophane-appended PPE (Pn is approximately 60 repeat units) was designed and reacted with paraquat, a powerful electron acceptor and well-known electron-transfer quenching agent (Figure 6). Cyclophane receptors were chosen because they form complexes with paraquat. The binding constant K_{sv} between PPE and paraquat was measured to be 1.01×10^5 M^{-1} on a per repeat unit base. A controlled study, paraquat quenched the cyclophane-appended monomer with a K_{sv} of 1.6×10^3 M^{-1}. Thus, on a per receptor basis, PPE showed 63 times stronger quenching ability than the monomer, the amplification of PPEs' quenching ability is due to exciton mobility.

1.3.2 PAE-based Hypothesis-free Sensor Arrays

Suslick et al.[36, 69, 71] and by Anslyn et al.,[37, 129, 151] have made significant contributions to the development of "Chemical tongue/nose" sensor arrays field, even though now more and more groups start working in this area.[10, 54, 62, 116, 152-153] A hypothesis-free sensor array would fundamentally allow to sense "everything" with any fluorescent dye. Conjugated polyelectrolytes may represent such hypothesis-free arrays; they discriminate white wines,[47] fruit juices,[46] non-steroidal anti-inflammatories[39] and proteins[58] with small selected sensor arrays, based upon fluorescence modulation, i.e. either quenching or fluorescence enhancement. The excited state of conjugated polymers lives for about 0.5-1 ns and is exquisitely sensitive towards environmental change, be it solvent but also any type of analyte that interacts either via hydrophobic or electrostatic interactions or other forces. The magnitude of the effect, the analyte has on the fluorescence intensity is not predictable. A sensor arrays' fluorescence response towards complex analytes such as whiskies can neither be predicted nor modeled, due to its large interactome. If the complex analyte is colored (such as whisky etc.), differential quenching of all of the sensor elements' fluorescence is observed. Here we exploit arrays to discriminate whiskies according to their region of origin, brand, age and taste.

Chapter 2. PAE-Based Chemical Tongue for Sensing of Small Molecular Analytes

2.1 PAE/PAE Complexes for Sensing of Organic Acids

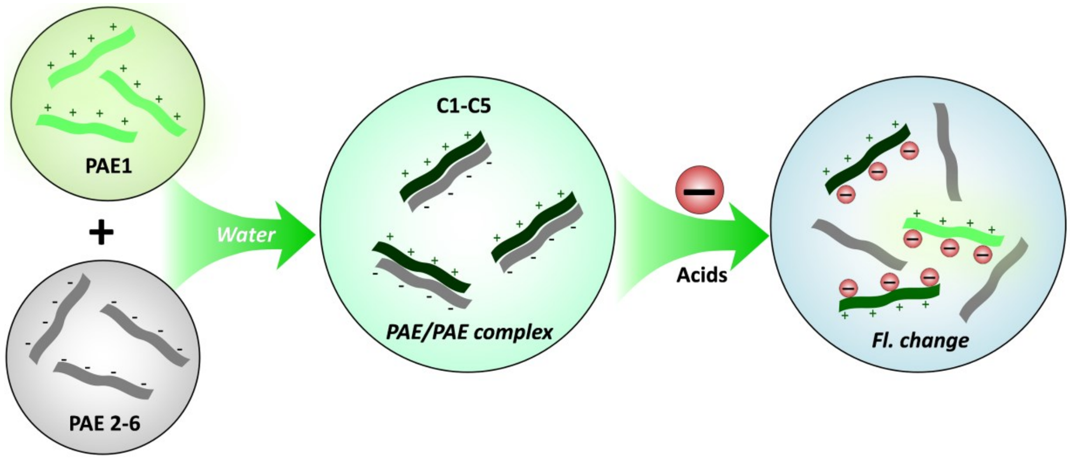

Figure 7. Systematic illustration of the formation of complexes **C1-C5** by mixing **PAE 1** (fluorophore) with PAEs **2-6** (quencher). The complexes were disrupted by adding different carboxylic acids, lead to the fluorescence change.

In this section, we constructed a chemical tongue composed of one fluorescent, positively charged poly(*para*-phenylene-ethynylene) (**PAE 1**) with five negatively charged pyridine- or benzothiadiazole-containing poly(*para*-aryleneethynylene)s (**PAE**s **2-6**). The **PAE**s **2-6** are less fluorescent in water and act as quenchers for **PAE 1** in their electrostatic complexes **C1-C5**; the PAE-complexes (2 µM) are exposed to thirteen different carboxylic acids (50 mM) in buffered aqueous solution. The fluorescence responses of the small library of electrostatic PAE-complexes towards the acids is analyzed; discrimination of all of the thirteen acids is achieved. The investigated acids include acetic, butyric, tartaric, maleic, lactic, sorbic, oxalic, aspartic and citric acids. A random, simple, ad-hoc library of electrostatic polymer complexes, **C1-C5**, discerns 13 carboxylic acids in water.

2.1.1 Screening of PAEs Toward Small Molecular Analytes

Negatively charged PAEs and their sensory application have been investigated for metal ion sensing,[45, 154-155] pH-dependent optical properties,[156] phosphate sensing[43] etc. However, the sensory application of positively charged and neutral PAEs are less often reported. To investigate the interactions between PAEs and various small molecular analytes, we selected PAEs **1**, **7-8**, functionalized with different side chains (positively charged and neutral) and explored the sensory properties towards small molecular analytes. As shown in Figure 8, PAEs **1, 7-8** were treated with various small molecular acids which contain different numbers of carboxylic acids group in different pH buffer solution. Based on this small photograph array, we can easily see that all acids have their unique response fingerprint towards PPEs. Especially, maleic acid strongly quenched all PAEs art pH10 and pH13.

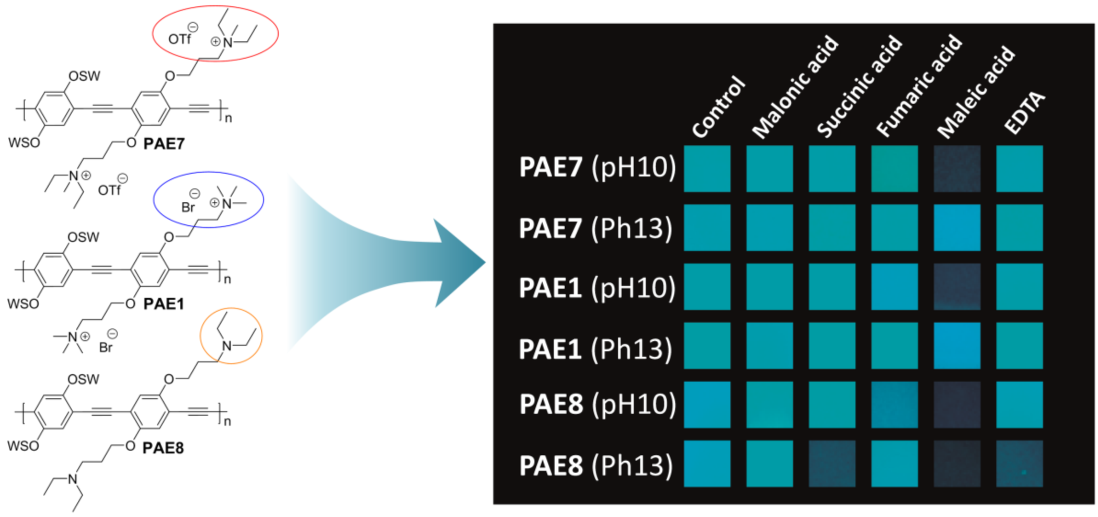

Figure 8. Structure and photographs of PPEs **1**, **7-8** in different pH buffer condition response to five acids under a hand-held black light with illumination at 365 nm.

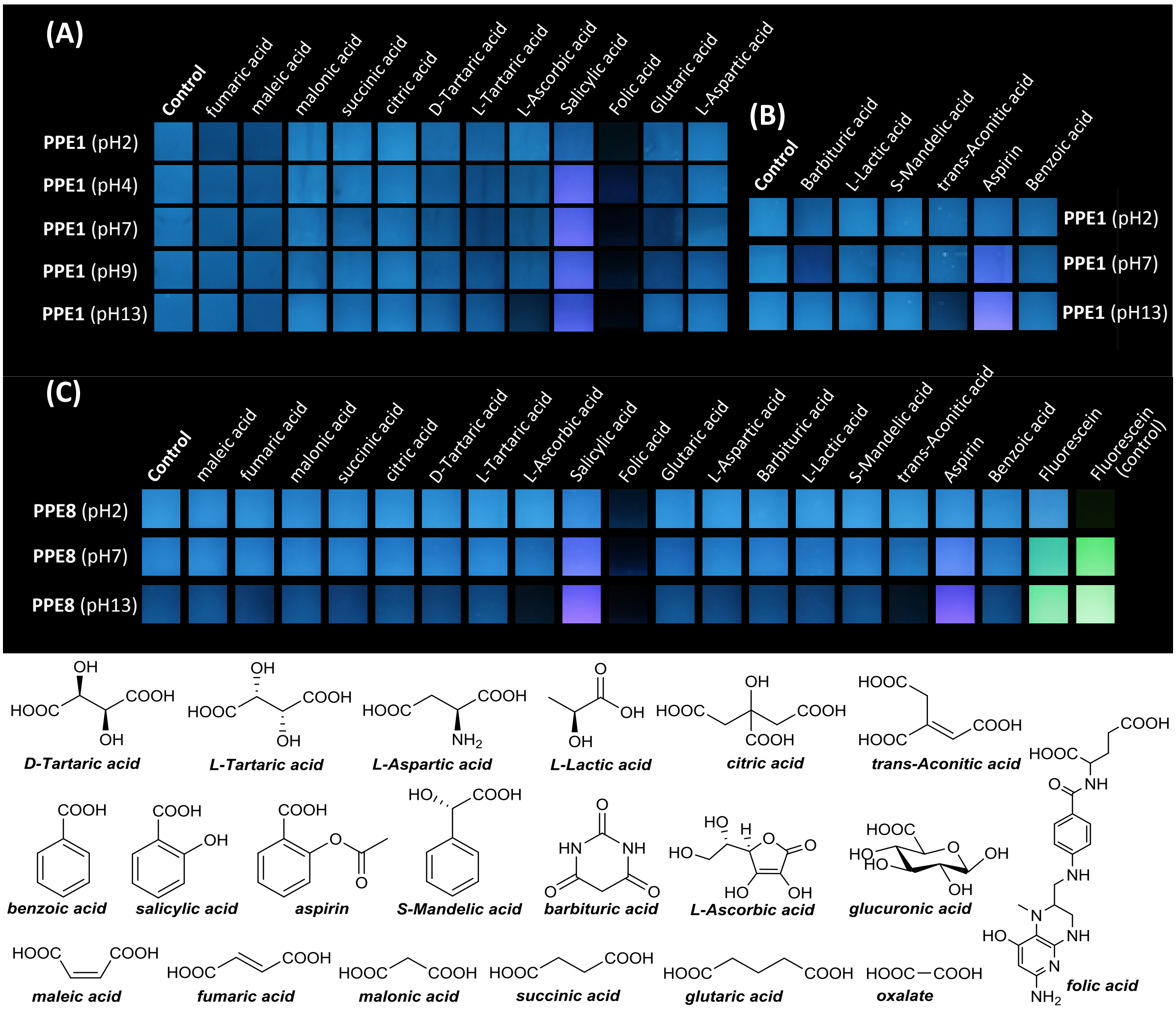

Figure 9. (A-B) Photographs of **PAE 1** (1.1 µM) in different pH buffer condition treated with all small molecular analytes (1mg/mL) under a hand-held black light with illumination at 365 nm. **(C)** Photographs of **PAE 3** (1.1 µM) in different pH buffer condition treated with all small molecular analytes (1mg/ml) under a hand-held black light with illumination at 365 nm.

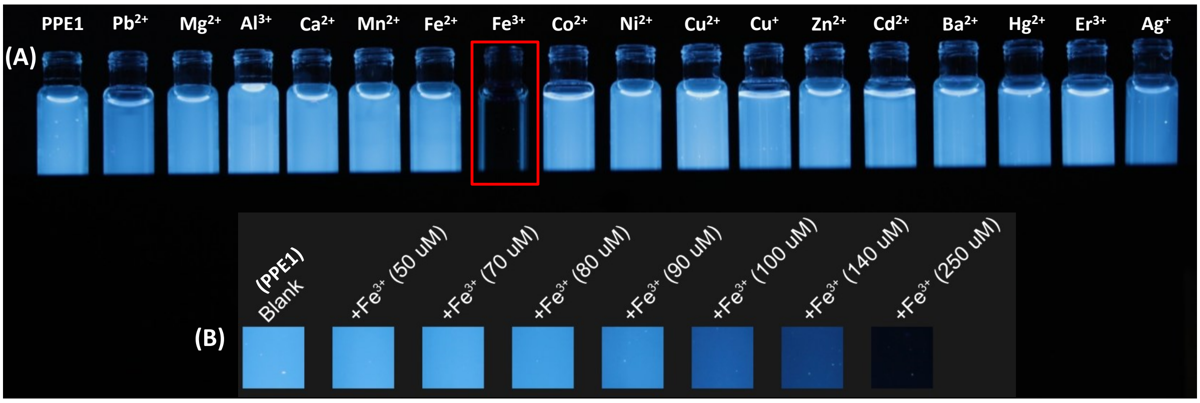

Figure 10. (A) Photographs of **PPE 2** (c = 2 µM, in DI water) with different metal cations, excellent selectivity of Fe^{3+} were observed which shown the only quenching to **PPE 2**. Fe^{3+}, Co^{2+}, Cu^{2+}, Hg^{2+} (c = 1 mM), the other metal cations (c > 1 mM), added all metal were added as perchlorates except CuI, $Er(CF_3SO_3)_3$, $Ag(CF_3SO_3)$ and $Fe(ClO_4)_3$. **(B)** Photographs of **PPE 2** (c = 2 µM, in DI water) with Fe^{3+} in various concentrations (0–250 µM). All of the photographs were shown under a hand-held black light with illumination at 365 nm.

These results inspired us to further try different other groups of small analytes. Figure 9 shows the photographs of **PAE 1** and **PAE 8** (1.1 µM) in various pH buffer condition treated with small molecular analytes (1mg/mL) under a hand-held black light with illumination at 365 nm. Twenty different acids including aliphatic acids, aromatic acids and some special acids with mono-, di-, tri-acid groups were investigated for the fluorescence color change. On the whole, each acid has their unique optical properties response to PAEs in different pH condition. Folic acid show strong quenching of both **PAE 1** and **PAE 8** at all pH condition, L-ascorbic acid only works in base condition.

In addition to that, we especially investigated **PAE 1** with different metal ions (Figure 10), according to the previously results, metal ions showed strong quench ability to the negatively charged PAEs.[154-155] Interestingly, after treating **PAE 1** with 18 different metal salts at the same condition, we found that only Fe^{3+} shows strong quenching ability, which is different from the negatively charged PAEs. Furthermore, we tested the response of **PAE 1** with Fe^{3+} at various concentration, 250 µM of the Fe^{3+} can cause almost the fully quench of the fluorescence of **PAE 1**.

2.1.2 Construction of PAE-based Sensor Array

Carboxylic acid are essential and useful chemicals in our daily life. Such carboxylic acids relate to citric acid cycle (TCA), the structures of them are highly similar. Detection of these acids is challenging and important for various diseases. Inspired by the first result of three PAEs towards various small molecular analytes, we developed a sensor array composed of one fluorescent, positively charged poly(*para*-phenyleneethynylene) (**PAE 1**) that forms electrostatic complexes with five negatively charged pyridine- or benzothiadiazole-containing poly(*para*-aryleneethynylene)s (PAEs **2-6**). The PAEs **2-6** are less fluorescent in water and act as quenchers for PAE **1** in their electrostatic complexes **C1-C5**; the PAE-complexes are exposed to thirteen different carboxylic acids (50 mM) in buffered aqueous solution. The fluorescence responses of the small library of electrostatic PAE-complexes towards the acids is analyzed; discrimination of all of the thirteen acids is achieved. The investigated acids include acetic, butyric, tartaric, maleic, lactic, sorbic, oxalic, aspartic and citric acids. A random, simple, ad-hoc library of electrostatic polymer complexes, C1-C5, therefore discerns the thirteen carboxylic acids in water.

Chemical tongues and noses discriminate multiple types of analytes.[10, 36-37, 51] Instead of a specific response of a single sensor or dosimeter for a single analyte, chemical tongues/noses consist of combinations of different sensors, which respond with selective, but not specific signals to the offered analytes. Such sensor fields work similar to biological noses or tongues, which also do not possess receptors for specific smells or tastes, but create the specific response to a smell or a taste by the combination of different selective responses. Synthetic versions of such a tongue can be fairly primitive and just consist of a collection of dyes, for example. Anslyn et al.,[157-159] Suslick et al.,[36, 91, 127-128] Rotello et al.[42, 51, 56] and other groups[118, 160-162] have developed sensor fields, which identify disparate analytes. A subset of such chemical tongues consists of electrostatic complexes of a fluorophore and a quencher. An example is the gold-nanoparticle-PPE-constructs by Rotello and us.[51] Such electrostatic constructs form in water by simple mixing a polyelectrolyte fluorophore with a polyelectrolyte quencher; Rotello et al. deploy positively charged gold-nanoparticles as quencher and emissive anionic PPEs as fluorophore. Upon addition of charged analytes to these complexes, they are disrupted, the quencher is removed from the fluorophore, and the fluorescence turns on. Gold-nanoparticles are powerful quenchers, but require some degree of finessed synthesis and characterization. Herein we describe, that one can employ simple complexes of positively and negatively charged polyelectrolytes, to discern a number of carboxylic acids in aqueous solution (Figure 13).

Rotello et al. have reported sensor system formed from PPE/gold nanoparticle, GFP/nanoparticle and single PPE arrays, and remarkable achievements were obtained.[42, 48-49, 51-52, 54-58, 163] Herein, we construct a sensor array with PAE/PAE complexes formed from two oppositely charged PAEs (one fluorophore and one quencher). To realize this idea, PAEs **1-6** were designed and synthesized via the Sonogashira protocol by Markus Bender and me. For anionic PAEs, PPE-acetate ester was first synthesized, and for cationic PAEs, a bromo-substituted side chain PAE precursor was first synthesized. Sonogashira reaction with the two building blocks of ester-substituted or bromo-substituted diiodobenzene and 1,4-diethynylbenzene using $Pd(PPh_3)_4$ and CuI as catalysts follow. The subsequent hydrolysis of the ester polymer or substitution of bromine polymer gave the final polymers PAEs **1**-**6** (detailed synthesis protocols see Chapter 5.2.1). Figure 11 shows the structure of PAEs **1-6**. Of these, **PAE 1** is positively charged and highly fluorescent, while PAEs **2-6** are negatively charged and less fluorescent in aqueous solution. PAE **1** is substituted with oligoethyleneglycol side-chains (swallowtail) and ammonium groups, water-soluble with high fluorescence. PAEs **2**-**6** were synthesized with the pyridine-based or benzothiadiazole-based backbone and different number of carboxylic groups in their side chains, used as a quencher to PAE **1**. Table 1 and Figure 12 show the detailed analytical data of PAE **1-6** (optical properties, emissive lifetimes and quantum yield et al.).

These poly(aryleneethynylene)s (PAEs) have a degree of polymerization P_n of 4 to 18 repeat units, with polydispersities ranging from M_n/M_w = 1.2–6.5.

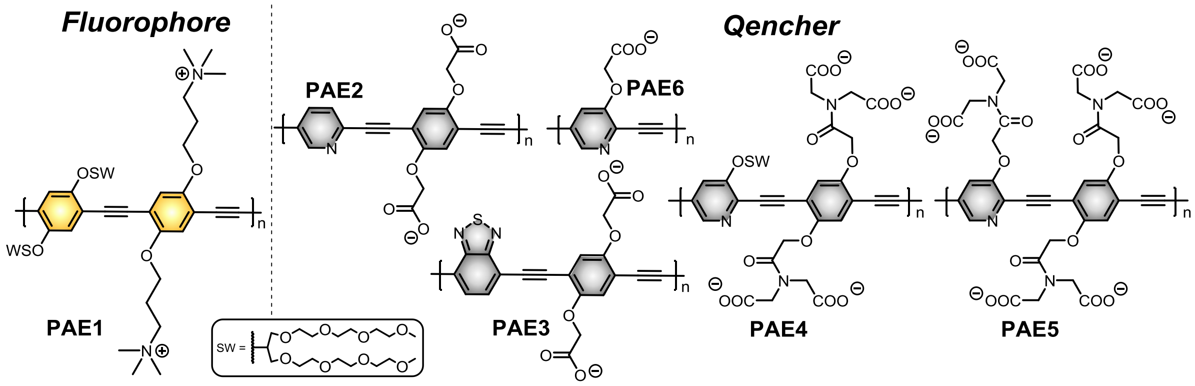

Figure 11. Structure of PAEs **1-6**, PAE **1** is positively charged and highly fluorescent (fluorophore), while PAEs **2-6** are negatively charged and less fluorescent in aqueous solution (quencher).

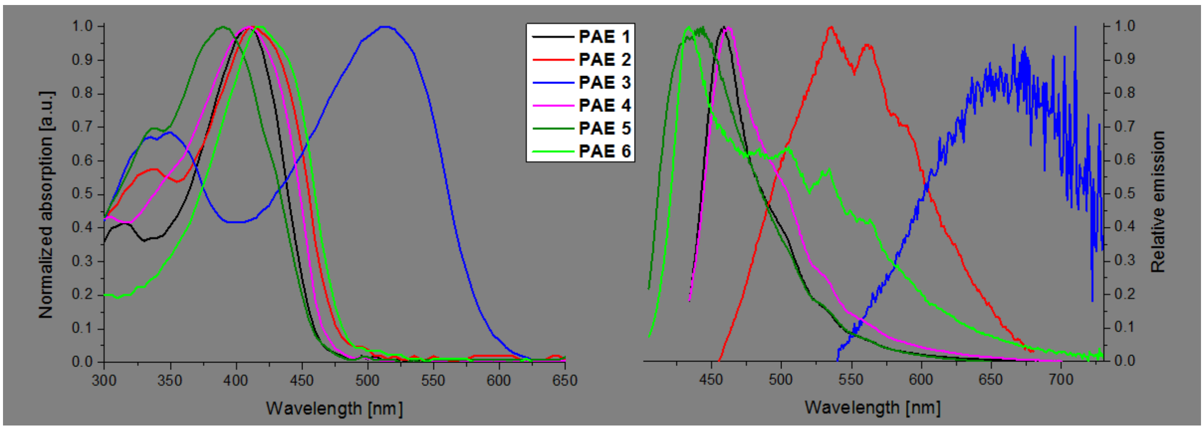

Figure 12. Normalized absorption (left) and emission (right) spectra of PAE **1-6** at pH7 buffer solution.

Table 1. Analytical data of PAE **1-6** for sensing.

No.	M_n [g/mol][a]	M_w [g/mol][a]	PDI[b]	P_n[c]	$\lambda_{abs.}^{max}$ [nm][d]	$\lambda_{em.}^{max}$ [nm][d]	Φ [%][d]	τ [ns][e]
PAE1	1.4 x 10^4	5.5 x 10^4	3.9	11	410	459	37	--
PAE2	6.9 x 10^3	1.3 x 10^3	1.9	17	415	536	1	0.5
PAE3	1.8 x 10^3	5.6 x 10^3	3.1	4	515	665	n.a.[f]	n.a.[f]
PAE4	1.9 x 10^4	1.3 x 10^4	6.5	18	410	462	4	0.3
PAE5	1.1 x 10^4	1.8 x 10^4	1.5	12	390	443	8	0.3
PAE6	3.2 x 10^3	3.7 x 10^3	1.2	16	410	433	6	0.7

[a] determined by gel permeation chromatography of the corresponding organosoluble precursors; [b] Ratio of weight-average molecular weight (Mw) and number-average molar mass (Mn); [c] The ratio of the number-average molar mass (Mn) and the molecular mass of the smallest repeat unit; [d] measured in KH_2PO_4/Na_2HPO_4 buffer solution; [e] Radiated at the emission maximum; [f] too low to measure;

For the construction of polyelectrolyte complexes, K_{sv} constants have been determined by titration methods. Equimolar (based on a per repeat unit) solutions of PAE **1** combined with either one of non-fluorescent PAEs **2-6** form five different complexes **C1-C5**. We titrated PAE **1** (2.0 x 10^{-6} M) with the PAEs **2-6** in aqueous buffered solution and obtained the binding constants for **C1-C5** using a modified Stern-Volmer equation (Table 2). All titrations were performed in KH_2PO4/Na_2HPO_4 buffered solution (pH = 7). The corresponding emission spectra are shown in the inset of the figures (see

Chapter 5.4.1 , Figure 129). The molecular structure of the fluorophore, K_{sv} and log K_{sv} is shown on the right. The fitting of quenching data was performed using the following modified Stern-Volmer equation.

$$I_q = I_0 + \frac{I_{final} - I_0}{2} \times \left\{1 + \frac{[Q]}{[F]} + \frac{1}{K_{SV}[F]} - \left[(1 + \frac{[Q]}{[F]} + \frac{1}{K_{SV}[F]})^2 - 4\frac{[Q]}{[F]}\right]^{1/2}\right\} \quad \textbf{(eq. 1)}$$

Here, I_0 = initial fluorescence intensity of the fluorophore, I_{final} = final fluorescence intensity of the fluorophore, I_q = fluorescence intensity at a given quencher concentration, $[F]$ = concentration of the fluorophore, $[Q]$ = total concentration of the added quencher Q and K_{SV} = Stern-Volmer constant.

The log K_{SV}-values for these complexes are in the range of 5.1-7.2 and rise - as expected - with the number of carboxylic groups in the side chains of the quencher PAEs (Table 2, detailed quenching titrations see Chapter 5.4.1 Figure 129). Thus, the log K_{SV} of the polyelectrolyte complexes are lower than the log K_{SV}-values obtained for the complexation of PPEs with gold-nanoparticles (log K_{SV} ~ 8-11),[49, 150] but should be sufficient to advance **C1-C5** as sensor materials.

Table 2. Binding Constants (log K_{sv}) Obtained from Quenching Data by Mixing **PAE1** ^{F} with PAEs **2-6** ^{Q} to Form **C1-C5** (Detailed Quenching Titrations see Chapter 5.4.1 , **Figure 129**).

Complex (PAE1 ^{F}+PAE ^{Q})	**Complex 1 C1 PAE2 ^{Q}**	**Complex 2 C2 PAE3 ^{Q}**	**Complex 3 C3 PAE4 ^{Q}**	**Complex 4 C4 PAE5 ^{Q}**	**Complex 5 C5 PAE6 ^{Q}**
log *Ksv*	6.33±0.46	6.25±0.05	7.18±0.68	6.95±0.34	5.08±0.20

^{F} Fluorophore; ^{Q} Quencher.

2.1.3 Array-Based Identification of Organic Acids

After we had established (by modified Stern-Volmer quenching) that **C1-5** form in water, we investigated the five complexes, using thirteen non-aromatic mono-, di-, tri- as well as hydroxyl-substituted carboxylic acids (Figure 13C). Figure 13A shows the fluorescence response patterns. The acids were used at a concentration of 50 mM. **C1-C5** were combined with the analytes, when the fluorescence intensity of **PAE 1** was reduced to about 20-30%, after addition of the quencher PAE. We record additional quenching by the analytes but also fluorescence turn-on through disruption of the complexes, independently from the pK_a values of the acids. From Figure 13A we glean that the hydrophobic sorbic acid (**A4**) turns the fluorescence on. This is not the case for butyric acid (**A2**), which also should be somewhat hydrophobic. Other acids that lead to a fluorescence turn-on are oxalic acid (**A5**), malic acid (**A7**) and tartaric acid (**A8**). Acids **A9** and **A12** (maleic and aconitic acids) lead to additional quenching. The other acids show a more mixed response to the different complexes. If one treats these data using LDA (linear discriminant analysis, quintuplet data sets) one can discern all of the acids according to their Mahalanobis distances, employing two dimensionless factors (Figure 13B).[63, 150] LDA converts the training matrix (5 polymer complexes x 13 acid-analytes x 5 replicates) into canonical scores. The first two canonical factors represent 87% of the total variation (see Figure 100). The canonical scores are clustered into thirteen different groups. The jackknifed classification matrix with cross-validation reveals a 94% accuracy (Table 20). These initial results indicate the ability of **C1-C5** to differentiate between the different organic acids.

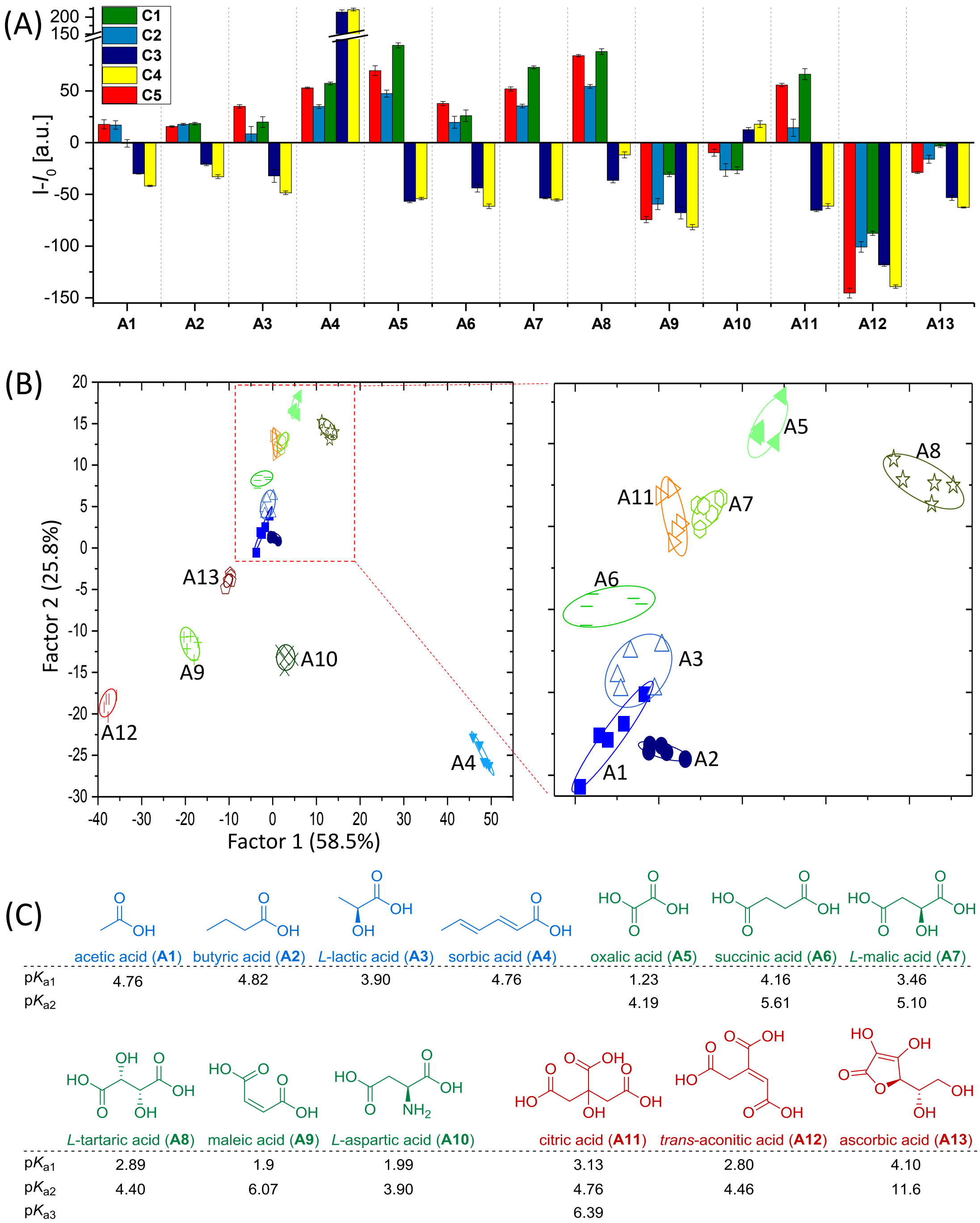

Figure 13. (A) Fluorescence response pattern ($I - I_0$) obtained by **C1-5** after addition of different acids **A1-A13** (c = 50 mM). Each value is the average of five measurements. Measurements were done in KH_2PO_4/Na_2HPO_4 buffered solution (pH = 7). **(B)** Canonical score plot for the first two factors of simplified fluorescence response patterns obtained with the polymer complex arrays with confidence ellipses (90%). Each point represents the response pattern for a single acid to the polymer complex array. All monoacids, diacids and triacids are held in blue, green and red, respectively. Open symbols correspond to hydroxy acids. The bottom picture shows a detailed view of the framed inset within the top picture. **(C)** 13 organic acids and corresponding pK*a* values used in this study.

To validate the efficiency of our sensing system, we performed tests with randomly chosen acids of our training set. The new cases are classified into groups, generated through the training matrix, based on their shortest Mahalanobis distance to the respective group.[57] 1 of 39 unknown samples of acids was misclassified, representing an accuracy of 97% (see Table 21). In this experiment, the factor 1

(59%) can be correlated with a physical quantity, viz. the overall fluorescence intensity. Acids that lead to turn-on are located to the right-hand side of the plot, while the ones, which quench the complexes' fluorescence further, are located on the left-hand side of the plot. The second, the vertical factor is more diffuse and is not attributable to an easily identifiable physical quantity.

2.1.4 Conclusions

In conclusion, a simple, randomly generated small library of polyelectrolyte complexes containing two oppositely charged PAEs, one fluorescent, the other one less fluorescent, discerns thirteen relatively closely related carboxylic acid analytes in water. These results are somewhat discomfiting, as the amount of design put into the library was minimal: the quencher molecules carry one or several carboxylate groups at the repeat unit. No other design principle was followed. Strangely, one either does not need any design (i.e. other than a very basic understanding of the involved electrostatic forces), or design might even be harmful; alternatively, with an improved design we might create libraries of super-sensors, almost insensitive towards groups of analytes but zooming into a specific one, while responding only weakly towards others. A series of such discerning, “super-selective” compounded sensors could achieve the concentration dependent identification of analytes, in this case carboxylic acids. This is a hard challenge, as one would not only have to identify a given analyte but also would have to deal with varying concentrations of the analyte. A second, more easily achieved challenge is the identification and quality control of different commercial samples with bona fide fixed compositions using our polyelectrolyte complexes. Here, the discrimination of white wines or hard liquor would be a useful test bed. The field is wide open and we hope to “sniff out” the potential of these simple complexes.

2.2 Water-Soluble PAE-Based Sensor Array Discriminates Aromatic Carboxylic Acids

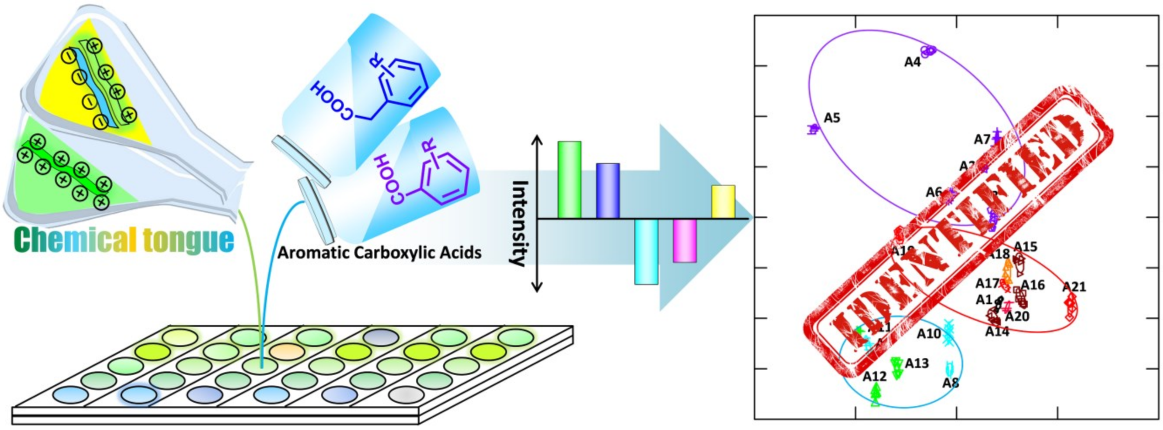

Figure 14. Systematic illustration of the formation of complexes **C1-C5** by mixing **PAE 1** (fluorophore) with PAEs (quencher). The complexes were disrupted by adding different carboxylic acids, lead to the fluorescence change.

The excellent discrimination capacity of the PAE-based tongue towards organic acids inspired us to further extend our work to aromatic carboxylic acids. Chemicals contain free carboxylic acid group (or their salts) are popular in a significant number of prescription drugs, such as Artesunate, Lipitor, Crestor, Cellcept, aspirin, ibuprofen, penicillin and Sector etc. (partial examples listed in Figure 15).

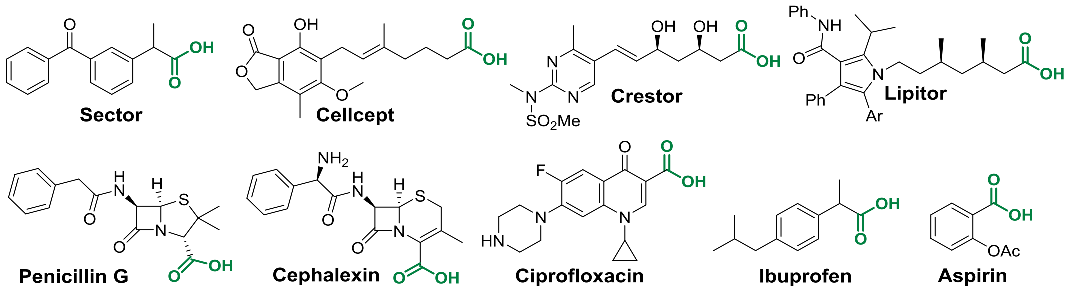

Figure 15. Drugs displaying carboxylate groups.

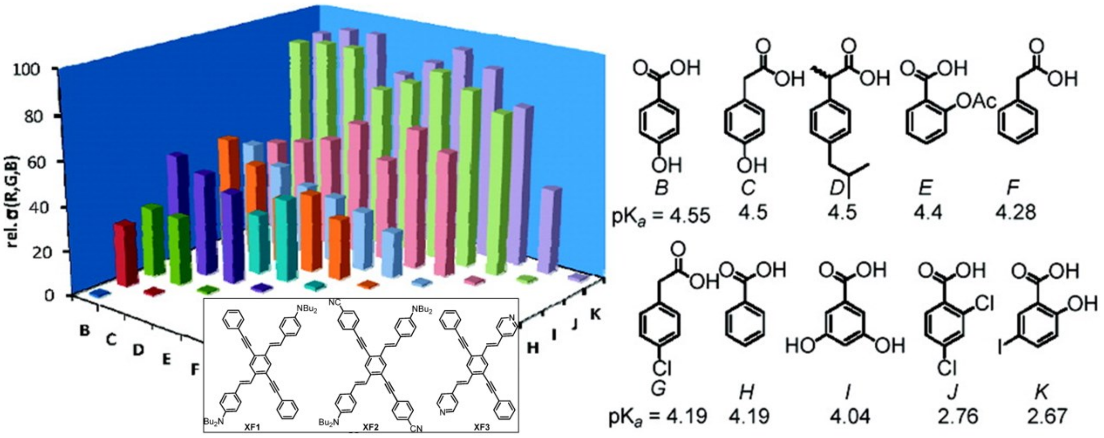

Figure 16. Discrimination of organic acids using a three molecule array based upon cruciform fluorophores. Reproduced with permission from liter [164]. Copyright 2011, American Chemical Society.

The detection of counterfeit drugs is critically important and challenging, as one wants to avoid ingestion of poisonous substances or the use of (for example) malaria medications that contain wrong or adulterated ingredients or have just expired. A simple fluorescence-based test that can discern organic acids might therefore be of great interest, as it would have the potential to perform quality control of drug samples of questionable origin. Such a tool would also be useful for public health applications.[164] Our group previously reported a small array formed from three reactive cruciform fluorophores in six different solvents (Figure 16). Such array can discern ten different aromatic carboxylic acids by protonation-induced fluorescence change, recorded by digital photography. Aromatic carboxylic acids with closely spaced pKa values can be identified.[164]

In this chapter, a chemical tongue consisting of 11 elements (four poly(*p*-aryleneethynylene)s (PAEs) at pH7 and pH13, and seven electrostatic complexes formed from oppositely charged poly(*p*-aryleneethynylene)s at pH7) discriminate 21 benzoic and phenylacetic acid derivatives in aqueous solution. The mechanism of discrimination is the fluorescence modulation of the PAEs, leading to quenching or fluorescence turn-on. The PAEs alone at both pH-values and the tongue, consisting of the complexes only, discriminate the 21 acids with 92% (PAEs at pH7), 95% (PAEs at pH13) and 99% (complexes at pH7) reliability after linear discriminant analysis (LDA). A sensor field with all 14 elements, according to LDA, discriminates all of the 21 acids with 100% accuracy.

2.2.1 Design and Construction of Chemical Tongue

In this contribution, a chemical tongue sensor array consisting of conjugated polyelectrolytes alone or their complexes formed from oppositely charged PAE were constructed; they reliably discern structurally similar aromatic carboxylic acids in water. Electrostatic complexes formed from rigid rod fluorescent polyelectrolytes and quencher and/or FRET entities (cationic gold nanoparticles, other oppositely charged polyelectrolytes, green fluorescent protein) often result in sensory systems of exquisite selectivity. These chemical tongues identify analytes in aqueous solution[43, 48, 51, 53, 56] and do not operate at the principle “one sensor one analyte”, instead, one creates a library of sensor elements to achieve the identification.[58] These “chemical noses” or “chemical tongues” work well if a series of test analytes builds a frame of reference for the identification of unknowns.[10, 128, 165-169] The test analytes render such sensor field competent and lead to successful fingerprinting of the unknowns.

The herein used chemical tongues exploit their change in fluorescence intensities upon exposure of the sensor field towards the selected analytes. The numerical power of the created data field is high, as one element in such a sensor field can attain 100-200 (or more) values. For a small field of 4 sensor elements, a power of up to $200^4 = 1.6 \times 10^9$ different responses are possible, suggesting that analyte groups containing 10-100 elements would be easily discerned, if the sensor field *is even only somewhat suitable*. We have employed small sensor fields in the past to identify proteins, bacteria, cells etc. and more recently also to discriminate aliphatic acids and diacids.[41] This work has directly led to the discrimination of different white wines.[47] Aliphatic carboxylic acids, diacids and hydroxyacids are present in all type of beverages, including white wine and are important for their discrimination. Aromatic acids, on the other hand, are important as structural elements in medicinal compounds and most, if not all analgesics carry carboxylate groups. For any practical application as sensor unit, identification of medicinal compounds or industrial effluvia etc. has work in water. Consequently, we developed an aqueous sensory system. We herein discriminate a series of closely related aromatic carboxylic acids in water, using ionic, fluorescent poly(*p*-aryleneethynylene)s (PAE) and their complexes.[45] We investigate the PAEs by themselves but also as complexes to successfully discriminate a group of 21 different aromatic carboxylic acids.

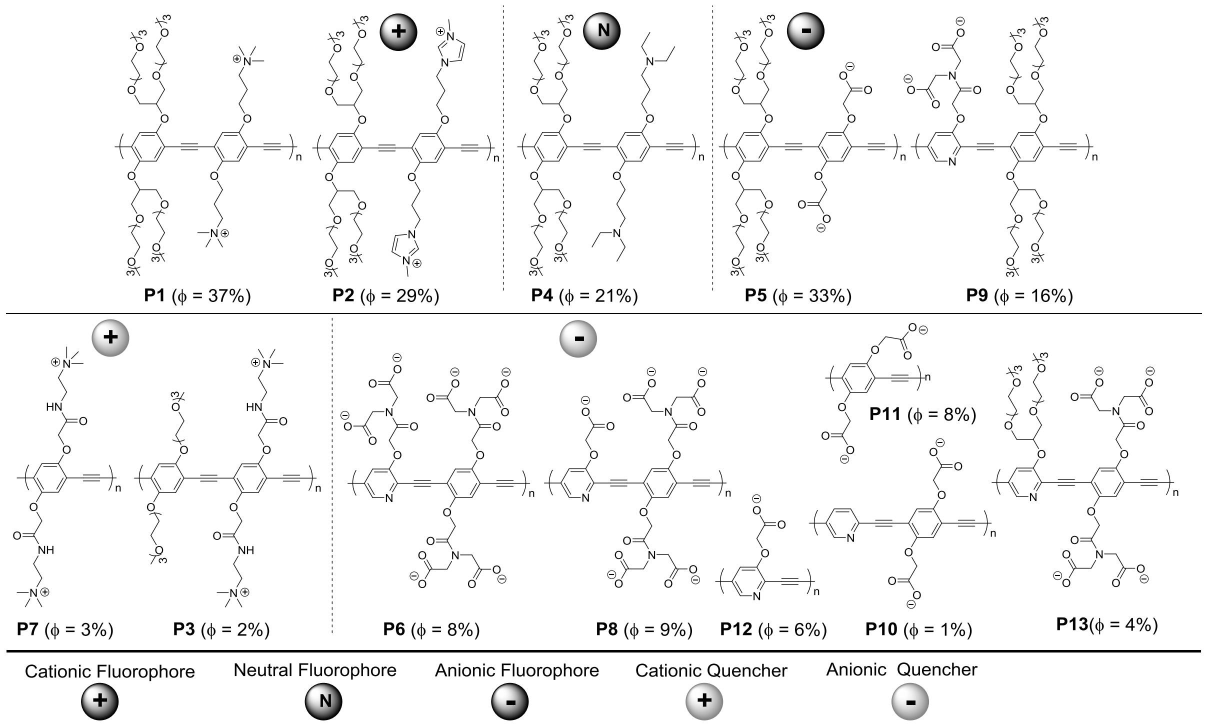

Figure 17. Chemical structures and quantum yields (ϕ) of the used PAEs **P1-P13** grouped in cationic (+), anionic (-) and neutral (N) fluorophores (colored) or quenchers (grey, low quantum yield).

To build up a useful library resulting in a working chemical tongue for the discrimination of aromatic carboxylic acids, we pre-selected (Figure 17) negatively charged, neutral and positively charged PAE-based fluorophores and several PAE-types of lower fluorescent quenchers. Polymer **P1-P13** have been synthesized via the standard Sonogashira protocol, detailed of the synthesis protocols see Chapter 5.2.2 . Often, but not always, the introduction of a pyridine unit into the PAEs results in reduced fluorescence in water.[154-155, 170] Table 3 shows the detailed analytical data of PAEs **1-13**. These poly(aryleneethynylene)s (PAEs) have a degree of polymerization P_n of 7 to 21 repeat units, with polydispersities ranging from M_n/M_w = 1.2–14. All of these water soluble conjugated polymers were employed for the next screening and identification processes of 21 structurally similar aromatic acids **A1-A21** (Detailed structure see Figure 18).

Table 3. Additional analytical data of **P1-P13**.

No.	M_n [g/mol]	M_w [g/mol]	PDI	P_n
P1[a]	1.4 x 10^4	5.5 x 10^4	3.9	11
P2[a]	1.4 x 10^4	5.5 x 10^4	3.9	11
P3	1.1 x 10^4	1.6 x 10^4	1.5	16
P4[a]	7.9 x 10^3	2.0 x 10^4	2.5	7
P5	1.7 x 10^4	5.6 x 10^4	3.3	15
P6	1.1 x 10^4	1.8 x 10^4	1.5	12
P7	4.0 x 10^3	1.1 x 10^4	2.7	13
P8	8.4 x 10^3	1.0 x 10^4	1.2	11
P9	2.4 x 10^4	3.4 x 10^5	14	21
P10	6.9 x 10^3	1.3 x 10^4	1.9	17
P11	4.0 x 10^3	1.1 x 10^4	2.7	13
P12	3.2 x 10^3	3.7 x 10^3	1.2	16
P13	1.9 x 10^4	1.3 x 10^5	6.5	18

a determined by gel permeation chromtography of the corresponding organosoluble precursors;

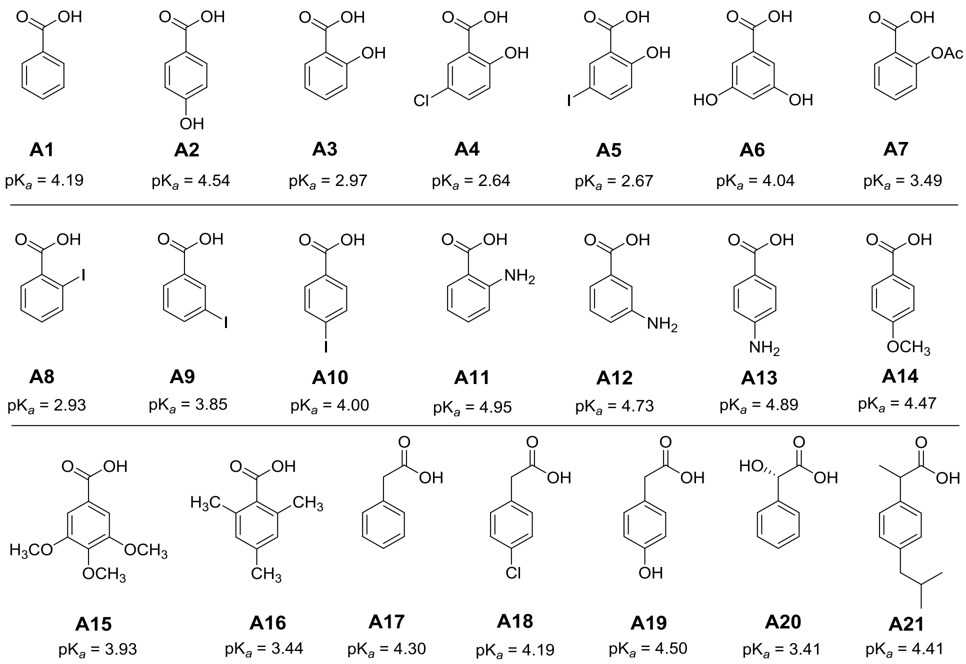

Figure 18. Structures and pK_a values of the investigated aromatic acids **A1-A21**.

Figure 19 shows the designed strategies of working combinations of different species. Totally, 27 combinations were designed and screened with various aromatic acids. The combinations are mainly divided into two types: (**1**) PAEs-alone, including cationic, anionic and neutral PAEs with highly fluorescent and non-fluorescent properties. (2) Complex types, formed from highly fluorescent PAE and a non-fluorescent PAE by electrostatic interactions. We titrated highly fluorescent PAEs (2.0 x 10^{-6} M) with the non-fluorescent PAEs in aqueous buffered solution and obtained their binding constants using a modified Stern-Volmer equation. All titrations were performed in KH_2PO_4/Na_2HPO_4 buffered solution (pH = 7). The emission spectra are shown in the inset of the following figures (details see Chapter 5.4.2 Figure 130). The molecular structure of the fluorophore, K_{sv} and log K_{sv} is shown on the right. As parts of the quenching data were already known in our previous study,[41] only new K_{sv} were reported here (Table 4). Similar to the previous study, most of the binding constants range from 10^5 to 10^8, which is sufficient for sensing application.

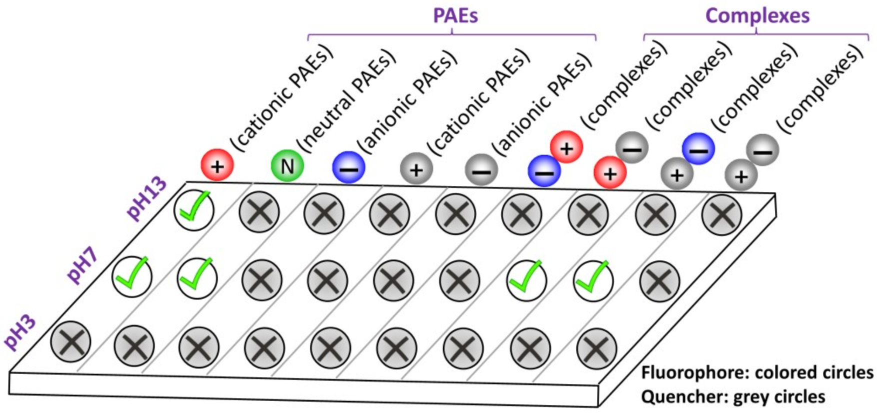

Figure 19. Systematic screening of PAEs and their complexes at different pH values (buffered) for aromatic acid sensing. The single cationic PAEs work well at pH7 and pH13, while neutral PAEs and fluorophore-quencher complexes are successful at pH7.

Table 4. Binding Constants (log K_{sv}) Obtained from Quenching Data by Mixing PAE^F with PAE^Q to Form **C1-C7** (Detailed Quenching Titrations see **Figure 130**, parts of the quenching data were already known in our previous study.[41])

Complex (PAE^F+PAE^Q)	**Complex 1 C1 (P5+P7)**	**Complex 2 C2 (P1+P6)**	**Complex 3 C3 (P1+P8)**	**Complex 4 C4 (P1+P9)**	**Complex 5 C5 (P1+P10)**	**Complex 6 C6 (P1+P11)**	**Complex 7 C7 (P1+P12)**
log *Ksv*	6.03±0.36	6.95±0.34	6.84±0.32	5.45±0.93	6.33±0.46	7.11±0.94	5.08±0.20

^{F} Fluorophore; ^{Q} Quencher.

2.2.2 Results and Discussions

2.2.2.1 Screening Process of PAEs Library and Their Complexes

Based on the design of the combinations of different species, we looked at single PAEs for aromatic acid discrimination and their complexes at pH3, pH7 and pH13 (all buffered). Because of the poor water solubility of aromatic acids at pH3, we worked at pH7 and pH13. Screening process of selected PAE-tongue at pH7 and pH13 are shown in Figure 20 -Figure 21, while results for the complex-tongue at pH7 and pH13 were shown in Figure 22 -Figure 23. Based on the results from the screening process (Figure 19), cationic fluorescent PAEs generated a signal at pH7 and pH13, while the neutral PAE generated a signal at pH7. Of the complexes, we found that cationic PAEs with anionic quenchers gave a signal, while the other combinations were unresponsive towards the carboxylic acids depicted in Figure 19. The sensor elements are employed in buffered solution. We screened single PAEs for aromatic acid discrimination and their complexes at pH3, pH7 and pH13 (all buffered). In our first experiment, we selected three positively charged, fluorescent PAEs (**P1-P3**, each at 2 μM, Figure 17), three negatively charged PAEs (**P5**, **P6**, **P13**, each at 2 μM) and one neutral PAE (**P4,** 2 μM) to react with aromatic acids **A1-A21** (5 mM, Figure 18) at pH7. Polymer concentrations are always given with respect to the molecular mass of their repeating unit. Only positively charged and neutral PAEs work

(Figure 19). Because of the poor water solubility of aromatic acids at pH3, we worked at pH7 and pH13. At pH13 positively charged PAEs generate a signal, being superior to the negatively charged PAEs. This is reasonable because positively charged PAEs form electrostatic complexes with carboxylates at high pH. Exposure of the less fluorescent, cationic PAE **P7** towards the tested carboxylic acids did not give any turn-on (Figure 21). Finally, complexes were investigated at pH7 (Figure 22) and pH13 (Figure 23). Only complexes formed from a fluorophore and a quencher at pH7 work well (used complexes see Table 4).

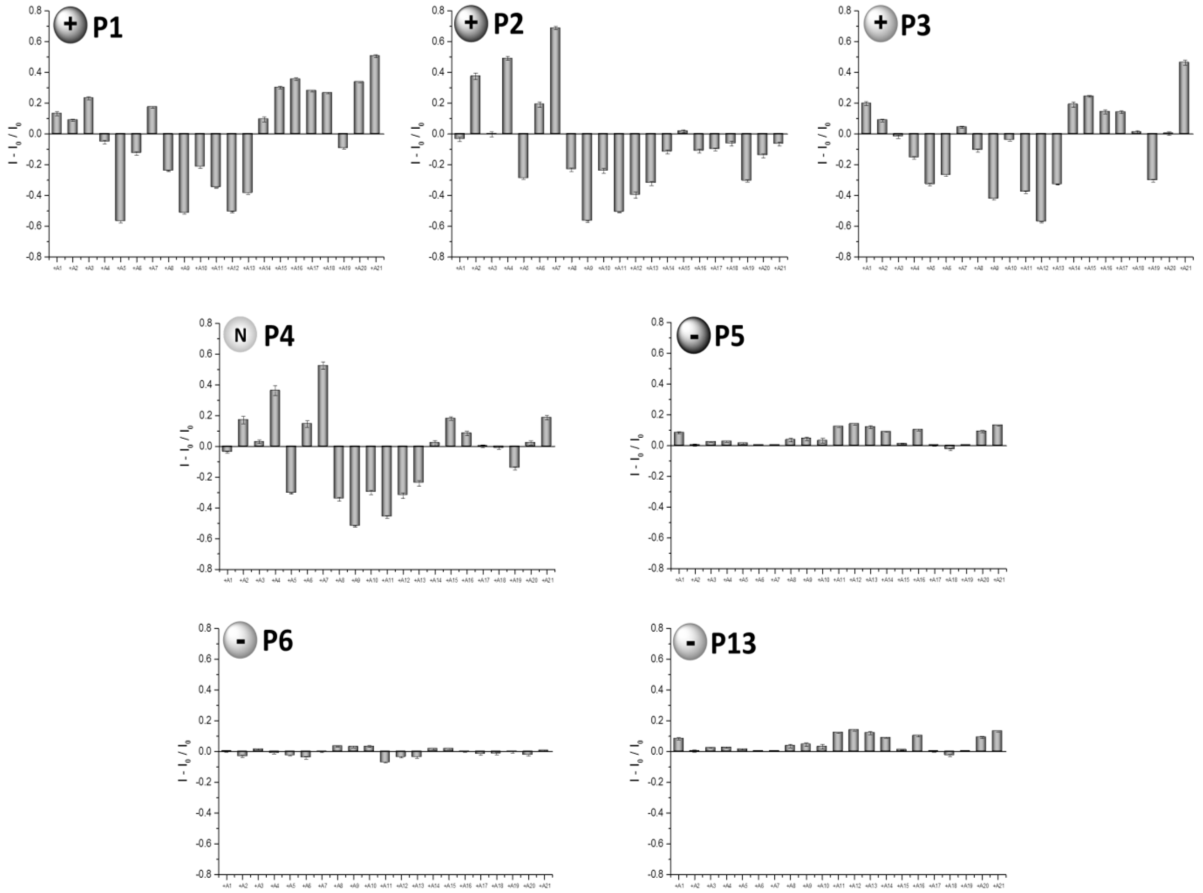

Figure 20. Screening of selected PAEs (pH7, buffered). Each value is the average of six independent measurements; each error bar shows the standard error of these measurements.

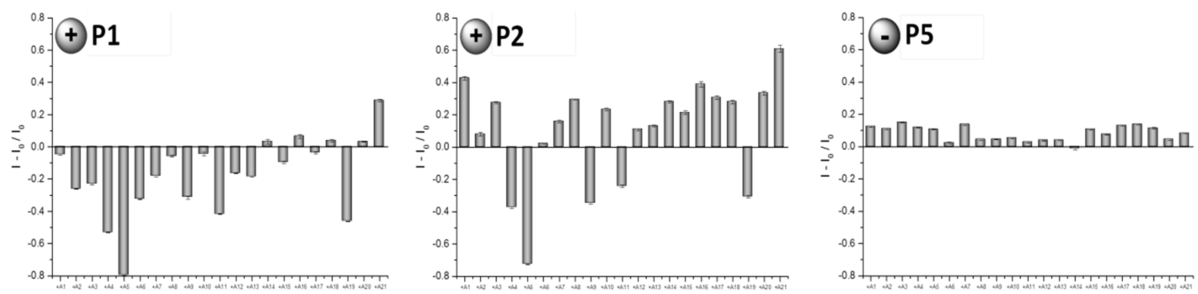

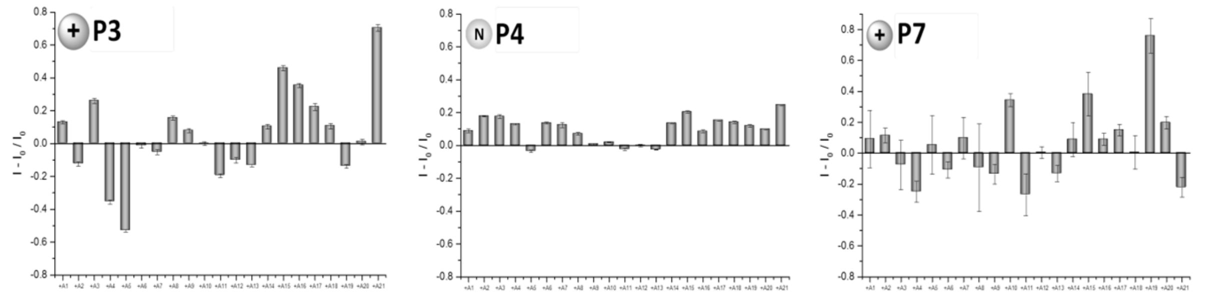

Figure 21. Screening of typical PAEs (pH13, buffered). Each value is the average of six independent measurements; each error bar shows the standard error of these measurements.

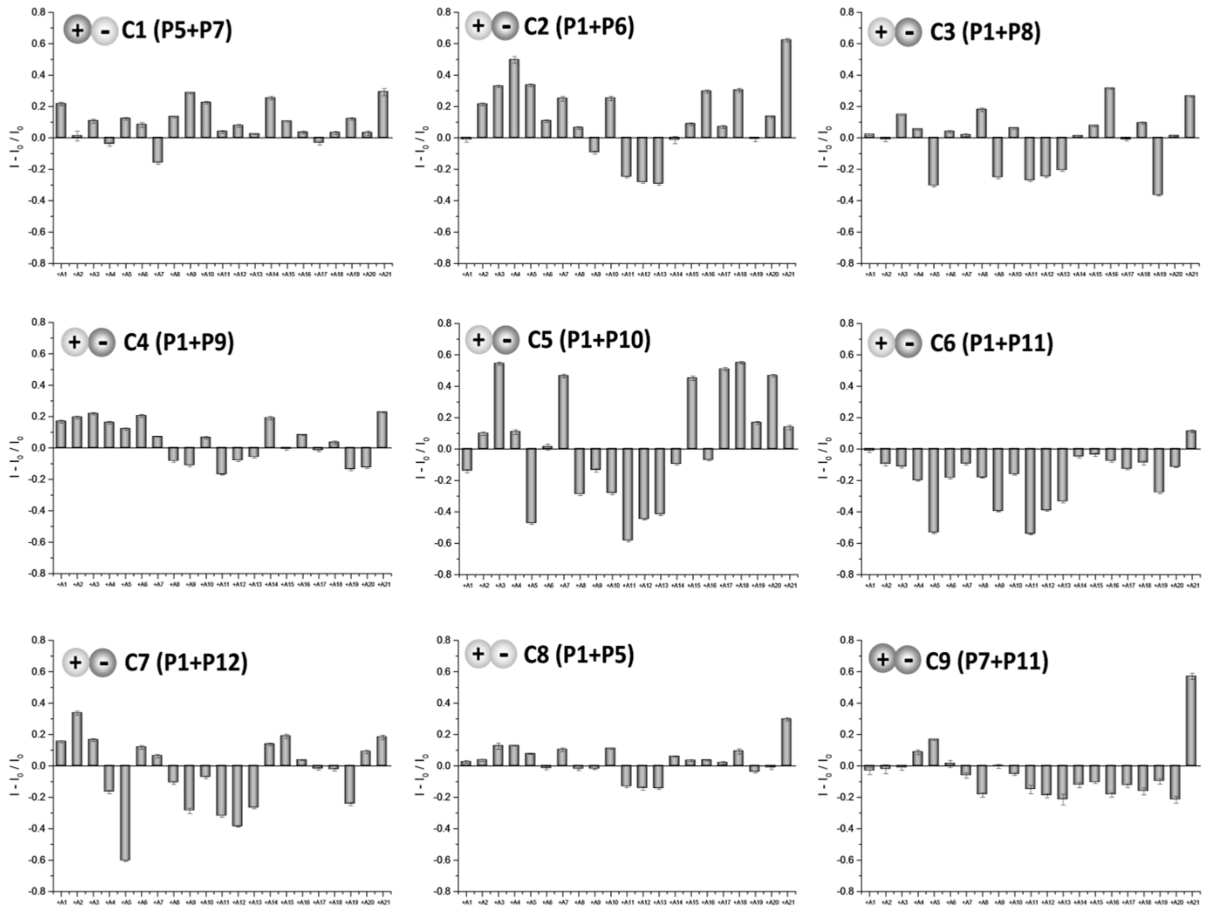

Figure 22. Screening of typical complexes (pH7, buffered). Each value is the average of six independent measurements; each error bar shows the standard error of these measurements.

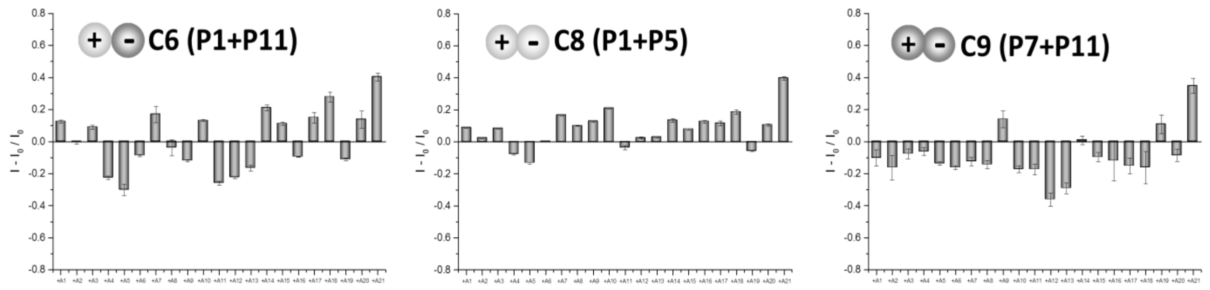

Figure 23. Screening of typical complexes (pH13, buffered). Each value is the average of six independent measurements; each error bar shows the standard error of these measurements.

2.2.2.2 Identification of Aromatic Acids with LDA

After this cursory evaluation, we employed the three most promising and reactive sensing elements for the discrimination experiments, including: (1) single PAEs at pH7, (2) single PAEs at pH13 and (3) fluorophore-quencher complexes at pH7. Figure 24 shows the modulation of the emission data of the single PAEs at pH7 and pH13 by the 21 different carboxylic acids. Figure 24A and b show the original fluorescence response data for the polymers at pH7 and pH13. In Figure 24C and d the linear discriminant analysis (LDA) of this data is shown. We note that iodo- (**A8**-**A10**, blue color) and amino-substituted (**A11**-**A13**, green color) benzoic acids quench the fluorescence, particularly at pH7, and are grouped to the left-top side of the LDA-plot in Figure 24C. The hydroxy-substituted derivatives (**A2**-**A7**, purple color) group in the lower part of the plot. Most of the other, chemically "non-functional" aromatic carboxylic acids, including benzoic acid and a number of the phenylacetic acids, group together quite tightly in the upper right quadrant of the graph. We note that at pH7 at least the influence of the pKa-value of the acids does not seem to play a large role as all of the acids are present as their carboxylate salts. At pH13 (Figure 24D) grouping according to the chemical structure is not retained anymore but the discriminative power of the small array is not reduced. Attempts to investigate the fluorescence response of our polymers towards the carboxylic acids at pH3 failed, as most of the acids are simply not soluble in an aqueous environment anymore. In the second part of our investigation, we prepared seven complexes from different PAEs and determined their formation constants. All of the complexes are fairly stable, their logK_{SV} constants range from 5.1 to 7.1, with an average value being around log K_{SV} = 6 (Table 4).

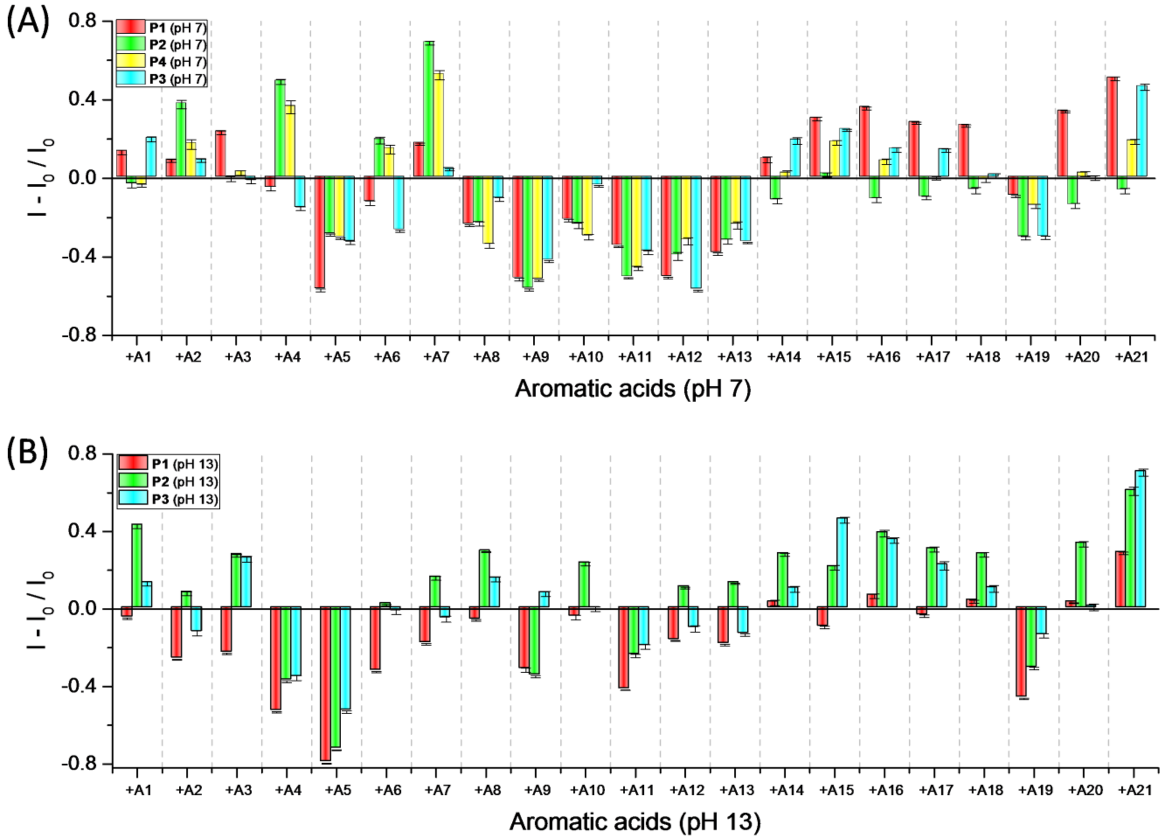

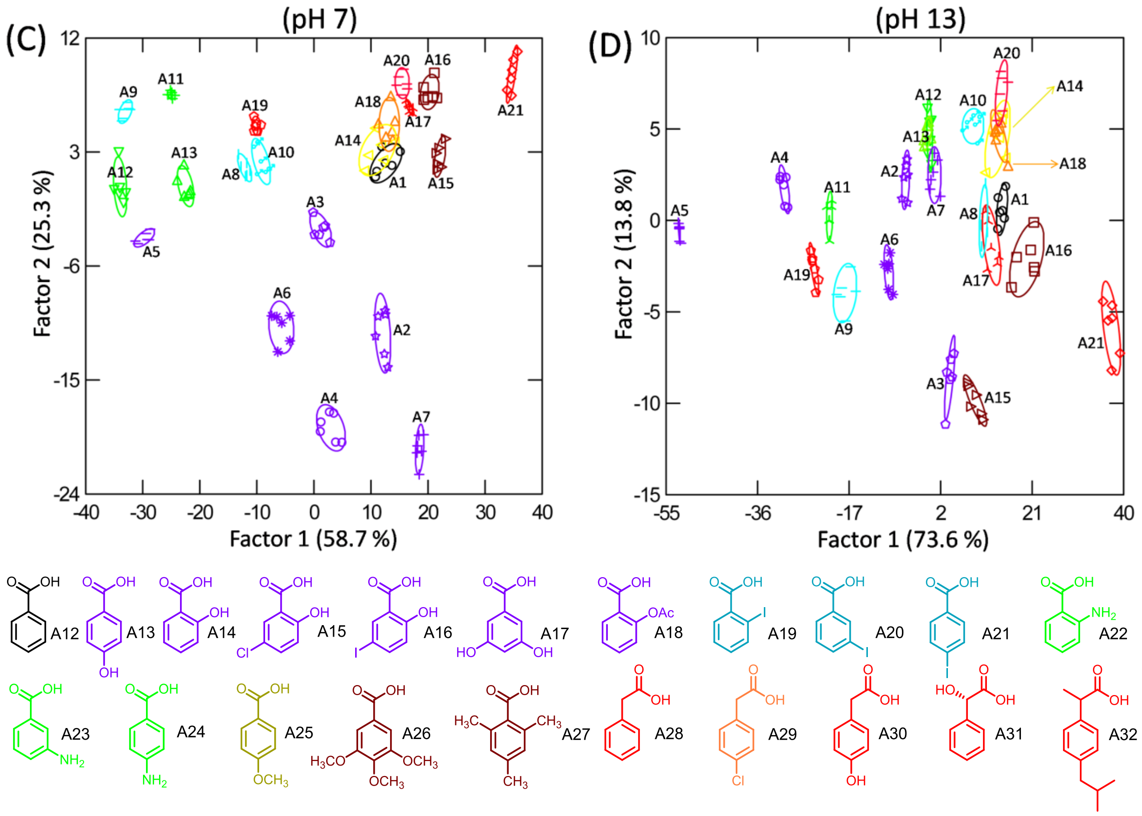

Figure 24. (A) Fluorescence response pattern (I - I_0 / I_0) obtained by PAEs **P1-P4** (2 µM, at pH7, buffered) treated with aromatic acids **A1-A21** (c = 5 mM). **(B)** Fluorescence response pattern (I - I_0 / I_0) obtained by PAEs **P1-P3** (2 µM, pH13, buffered) treated with aromatic acids **A1-A21** (c = 5 mM). Each value is the average of six independent measurements; each error bar shows the standard error of these measurements. **(C)** Canonical score plot for the first two factors of fluorescence response patterns obtained with an array of PAEs **P1-P4** (2 µM, pH7, buffered) with 95% confidence ellipses. **(D)** Canonical score plot for the first two factors of fluorescence response patterns obtained with an array of PAEs **P1-P3** (2 µM, pH13, buffered) with 95% confidence ellipses. Each point represents the response pattern for a single acid in the array. Iodine-substituted benzoic acids A8-A10 (blue) and amino-substituted benzoic acids A11-A13 (green) were located to the left-top side of the plot whereas hydroxyl-substituted benzoic acids **A2-A7** (purple) are located in the lower part of the plot.

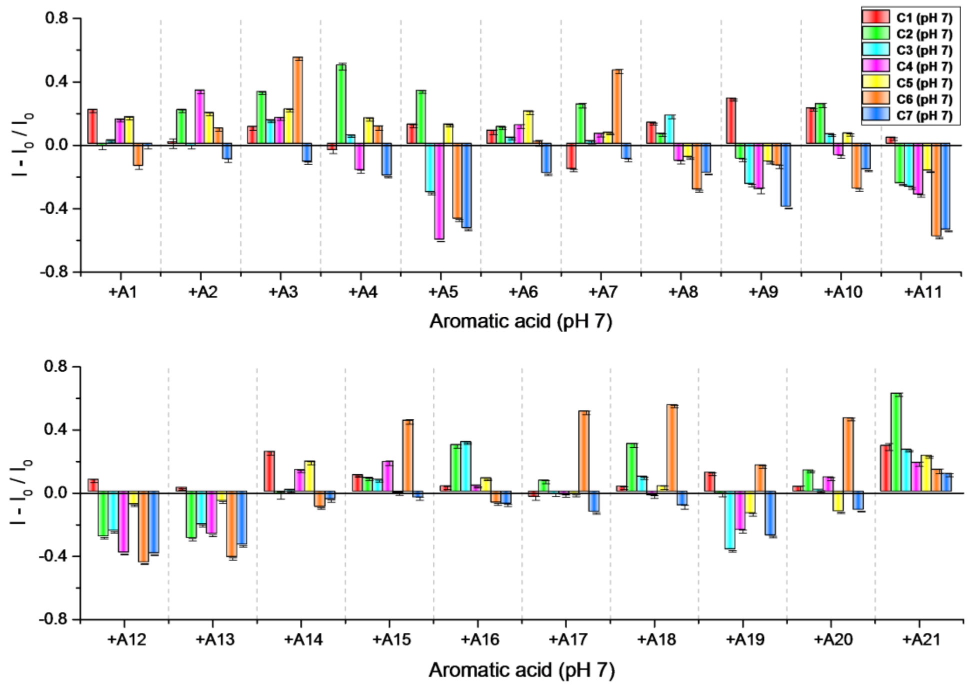

Figure 25. Fluorescence response pattern (I - I_0 / I_0) obtained by complexes **C1-C7** (2 µM, at pH7, buffered) treated with aromatic acids **A1-A21** (c = 5 mM). Each value is the average of six independent measurements; each error bar shows the standard error of these measurements.

Figure 25 shows the response pattern of the complexes **C1-C7** upon exposure towards the different carboxylic acids at pH7. All of the acids were discerned. Despite the strong binding of the complexes, the 5 mM solutions of the carboxylic acids lead to a fluorescence modulation. Performing LDA (Figure 26) gives the 3D-plot, as the discrimination needs three factors. The amino-substituted and the hydroxy-substituted benzoic acids cluster, while also most phenylacetic acids group together.

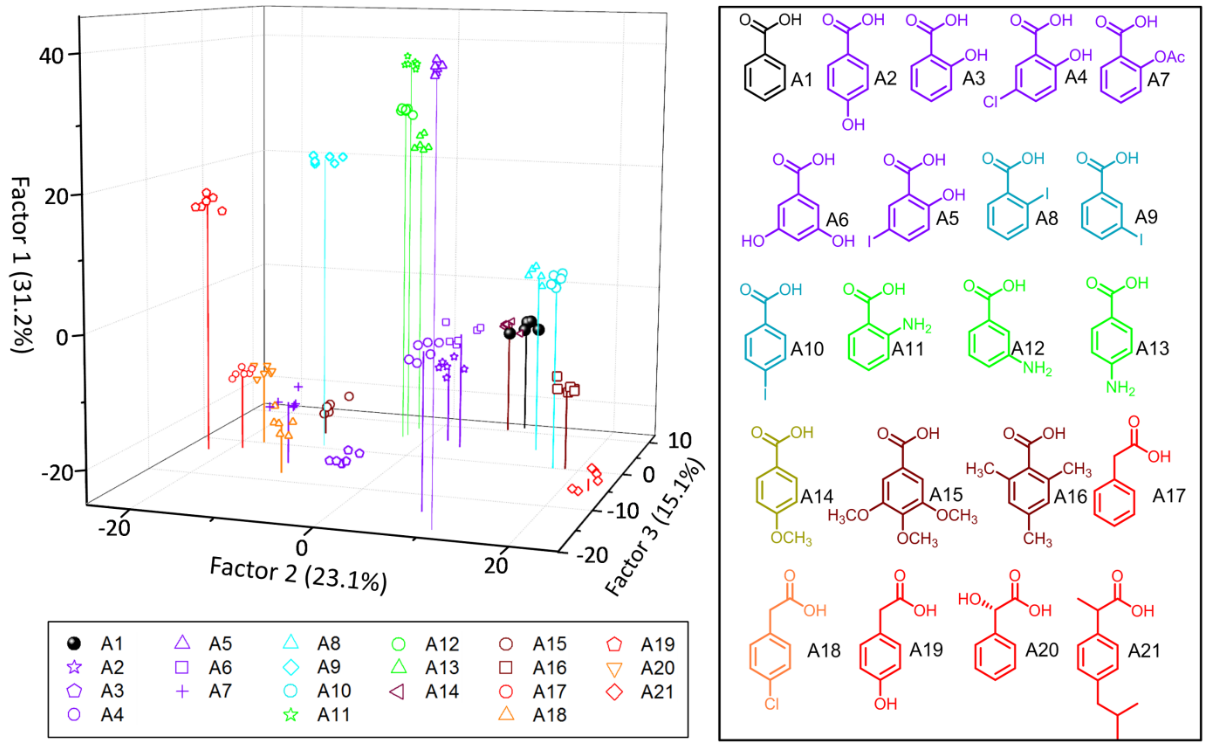

Figure 26. 3D Canonical score plot for the first three factors of simplified fluorescence response patterns obtained with an array of **C1-C7** (2 µM, pH7, buffered) with 95% confidence ellipses. Each point represents the response pattern for a single acid in the array.

As we have created three types of small arrays, we wanted to test their accuracy in identifying unknowns (Table 5). The array of four PAEs at pH7 recognized 93% of the samples, while a smaller array at pH13 did a somewhat better job. This is an interesting observation, as the intuitive chemical ordering is better in the array at pH7 but the discrimination is better with the smaller array at pH13. The best results are obtained by the 7-element array of the complexes. We note that the complexes **C2, C3** and **C5-7** are the most important contributors, while **C1** and **C4** seem to contribute less to the discrimination. The complexes discern almost 99% of all of the tested aromatic carboxylic acids but retain some of the intuitive qualities of the first array, consisting of PAEs at pH7. What happens if we combine the three sensor fields into a larger one? We can do that simply by re-processing the collected data. Figure 27 shows the canonical score plot for the first two factors of the enlarged sensor field. We treated these data using LDA (14 sensing elements x 21 acid-analytes x 6 replicates, quintuplet data sets), and discern *all* of the acids according to their Mahalanobis distances, employing two dimensionless factors. The jackknifed classification matrix with cross-validation reveals a 100% accuracy.

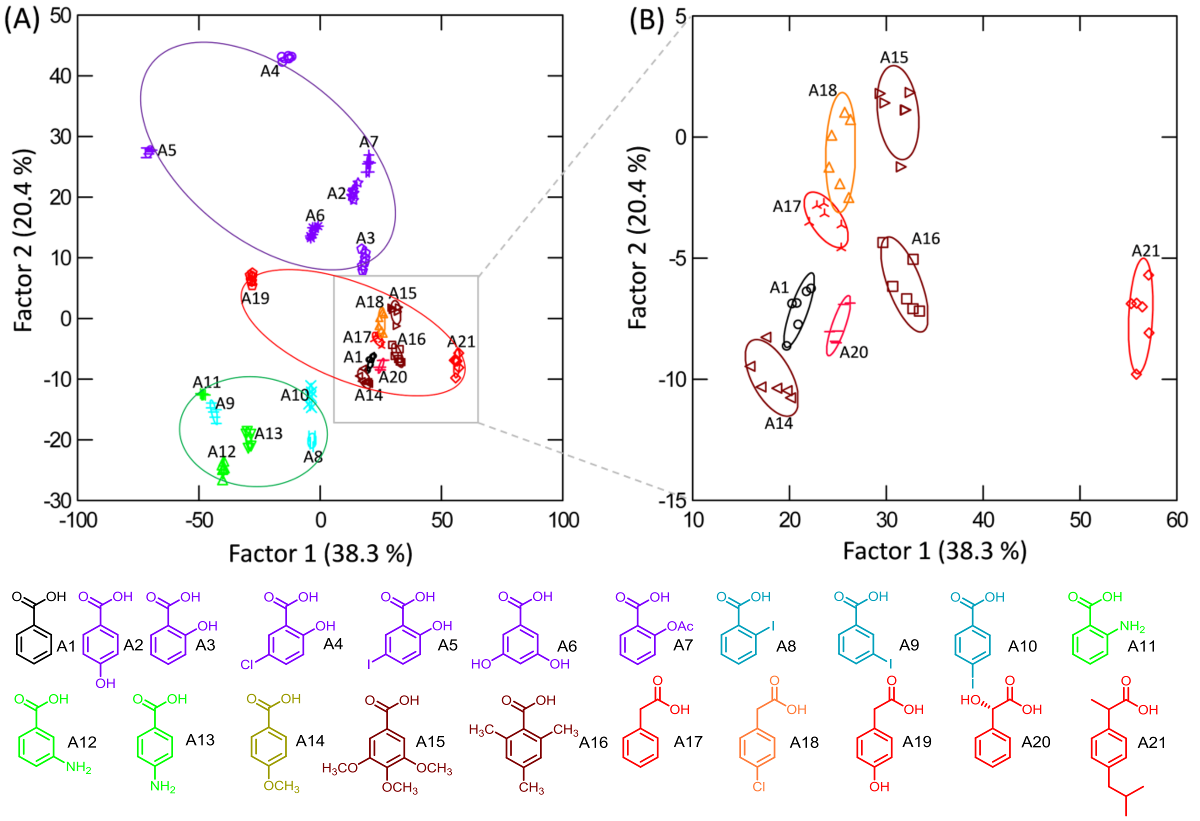

Figure 27. Canonical score plot for the first two factors obtained with an array of overall 14 sensing elements including single PAEs **P2-P4**, and **P14** (2 µM, pH7, buffered) **P2**, **P3**, and **P14** (2 µM, pH 13, buffered) and complexes **C1-C7** (2 µM, pH7, buffered) treated with aromatic acids **A1-A21** (c = 5 mM) with 95% confidence ellipses. Each point represents the response pattern for a single acid to the array. Iodine-substituted benzoic acid **A8-A10** (blue) and amino-substituted benzoic acid **A11-A13** (green) were located to the middle-bottom of the plot. Hydroxyl-containing benzoic acids **A2-A7** (purple) and **A19** (red) were located at the top side of the plot.

Also, the larger array gives results that are chemically intuitive and somewhat ordered, according to functional groups. All of the hydroxy-carrying benzoic acids **A2-A7** (including 4-hydroxyphenylacetic acid **A19**) group together, i.e. phenolic functional groups are recognized. Iodo- (**A8-A10**) and amino-containing (**A11-A13**) benzoic acids group together; all of them quench the fluorescence of the sensor elements. In the middle of the plot, we find the hydrophobic aromatic carboxylic acids including benzoic acid.

Table 5. Identification of Unknown Samples (Detailed Calculation see Table 22-Table 27)

No.	Sensing Elements	Sensing Factors	Total Unknown Samples	Correctly Identified	Accuracy
1	**PAEs** (pH7)	4 elements	84	78	92.9%
2	**PAEs** (pH13)	3 elements	84	80	95.2%
3	**Complexes** (pH7)	7 elements	84	83	98.8%

2.2.3 Conclusions

Overall, a focused sensor field comprised of 14 different elements (four PAEs at two different pH values, and seven different complexes prepared from a less emissive and a highly emissive PAE each) discerns 21 structurally related aromatic carboxylic acids with full accuracy. This chemical tongue weakly "orders" the carboxylic acids by their functional groups. Hydroxy-substituted species appear together in an LDA plot, while iodine- and amino-substituted benzoic acids as well as phenyl acetic acids also group respectively.

While this result is satisfying and the dimensionless factors in Figure 7 are weakly attributed to and correlated with chemical structure, *it is at the same time not clear what leads to the subtle discrimination* and the binding of the sensor elements to the carboxylate anions. Also, and that is one of the pressing questions, we still operate by trial and error, when selecting the correct elements of the sensor field. Why is that? Modulation of fluorescence occurs by interaction of the analytes with the excited state of the sensor elements, even if we talk about static quenching. There the analytes interact with the ground state of the PAEs; upon irradiation the excited states of the PAEs react differently to the presence of the benzoic acids. So the overall issue is the extreme sensitivity of the excited state of the sensor-field-elements towards the analytes.

When comparing colorimetric types of sensor arrays with fluorescence-based arrays, the former detect changes of ground state properties, color change, which is easily explained or rationalized. Fluorescence quenching and its extent, on the other hand, is currently not easily predicted and quantitatively correlated to the molecular structure of the sensor fluorophore. That makes fluorescent sensor fields uniquely challenging and exciting, as serendipity constantly raises its head. We need to extract –at least empirically– rules that connect molecular structure of the sensor elements with their planned use. Robust, bespoke sensors for tightly focused groups of analytes, un-perturbed by the presence of other compounds present in the analytical matrix are the goal.

2.3 PAE-Based Tongue Identifies Nonsteroidal Anti-Inflammatory Drugs in Water: A Test Case for Combating Counterfeit Drugs

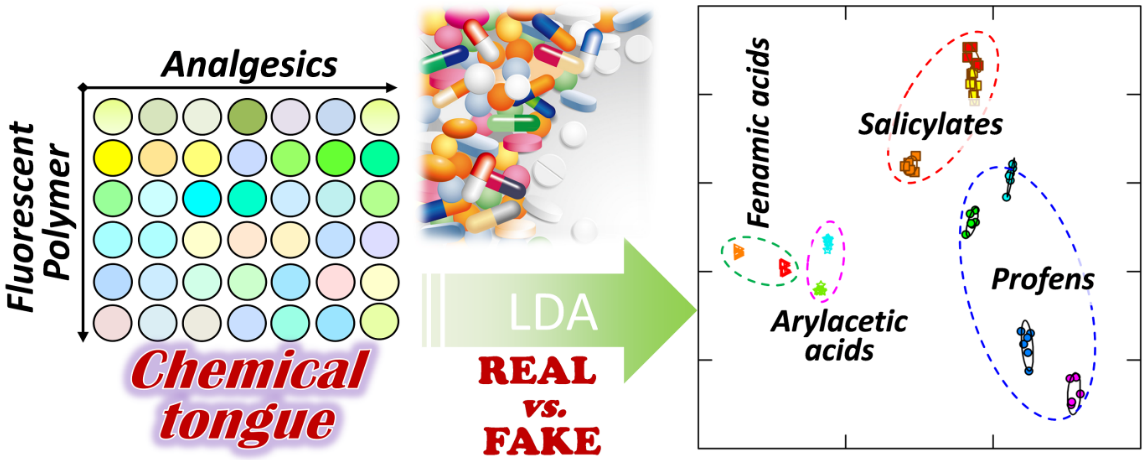

Figure 28. Systematic illustration of PAE-based sensor array for the identification of nonsteroidal anti-inflammatory drugs (NSAIDs).

Our previous work with PAE-based chemical tongue identifying various aliphatic organic acids and aromatic organic acids inspired us to extend our work to carboxylic acid drugs.[40-41] In this Chapter, we constructed a small sensor array composed of a highly fluorescent positively charged poly(*para*-phenyleneethynylene) **P1** and its complex **C** with a negatively charged pyridine-containing poly(*para*-aryleneethynylene) **P2** (quencher) at pH10 and pH13. A sensor field composed of four elements, **P1** (pH10), **P1** (pH13), **C** (pH10), and **C** (pH13) results. The elements of this small sensor field experience either fluorescence turn on or fluorescence quenching upon exposure towards eleven nonsteroidal anti-inflammatory drugs (NSAIDs), such as aspirin, ibuprofen, diclofenac or naproxen. The combined responses of the sensor field are analyzed by linear discriminant analysis (LDA). All of the NSAIDs were identified and discriminated and the sensing mechanism – hydrophobic vs. electrostatic – discussed.

2.3.1 Background and Screening Process

A sensor array formed from a highly fluorescent cationic poly(para-phenyleneethynylene) (PPE) **P1** and its electrostatic complex with the weakly fluorescent **P2** discerns eleven nonsteroidal anti-inflammatory drugs (NSAIDs) at pH10 and pH13.

Discrimination and identification of medications is a fundamentally important and interesting topic. Aspects that deal with falsified, stretched, filled or faked drugs are a serious health policy problem that does not only affect 3rd world countries (antimalarials, antibiotics, painkillers, HIV drugs etc.) but indirectly also Europe and North America, as resistant bacterial strains develop and spread.[171-177] As a consequence, quality control, identification and fingerprinting of the active compounds, but also of the whole processed drug formulation (tablet, drops, capsules, suppositories) is an important task. While the detection of counterfeits is a critical issue, it is not an ideal test bed to investigate the discriminative power of a new sensory system for drugs.

Several approaches and techniques (high-performance liquid chromatography, thin-layer chromatography, mass spectrometry, vibrational spectroscopies, nuclear magnetic resonance spectroscopy, colorimetric tests, NIR spectrometry, etc.) were reported to detect counterfeit drugs.[178-184] We present an alternative approach, in which we employ an array of charged fluorescent polymers[8-10, 148, 185-187] in water at two different pH values. Our four element sensor field acts as an efficient chemical tongue;[18,19] it discerns different NSAIDs but also discriminates between the various brands of ibuprofen and aspirin. We think this is a powerful, widely applicable concept; we have already shown that different versions (including conjugated polymer-gold nanoparticle complexes,[20] conjugated polymer-green fluorescent protein complexes,[48] and conjugated polymer-conjugated polymer complexes[40-41, 47]) of this concept successfully discriminated anions, white wines, proteins, cells, and cancer states in mammalian cells etc. Herein we discriminate 11 nonsteroidal anti-inflammatory drugs (NSAIDs, Figure 29). These analytes are sufficiently narrow in scope, yet have significant differences.

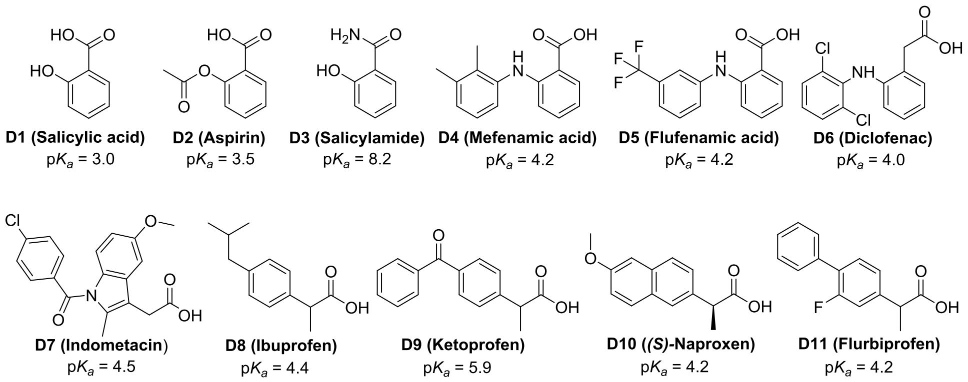

Figure 29. Structures and pK*a* values of widely used NSAIDs.

According to our recent work, a chemical tongue composed of PAEs and their polyelectrolyte complexes discriminates 21 aromatic acids in aqueous solution.[40] The structures of tested aromatic acids are similar to that of the NSAIDs. We thus pre-selected the optimal array for aromatic acids as a starting point for discrimination of the eleven NSAIDs (Figure 29). We finally found that two types of elements work well: (1) individual highly fluorescent PAEs and (2) complexes composed of a fluorophore and a quencher-PAE, the detailed screening process shown as follows.

2.3.1.1 Screening with Highly Fluorescent PAEs and pH Values.

Four highly fluorescent PAEs (positively-charged **P1**, **P3**, neutral **P4** and negatively-charged **P5**, Figure 30) were chosen for screening. The results showed that negatively charged **P5** works poorly, **P1**, **P3** and **P4** showed similar response (Figure 31). Therefore, **P1** with the highest quantum yield and best distinguishing ability according to PCA calculations (Figure 31 B-C) was finally selected as sensor element.

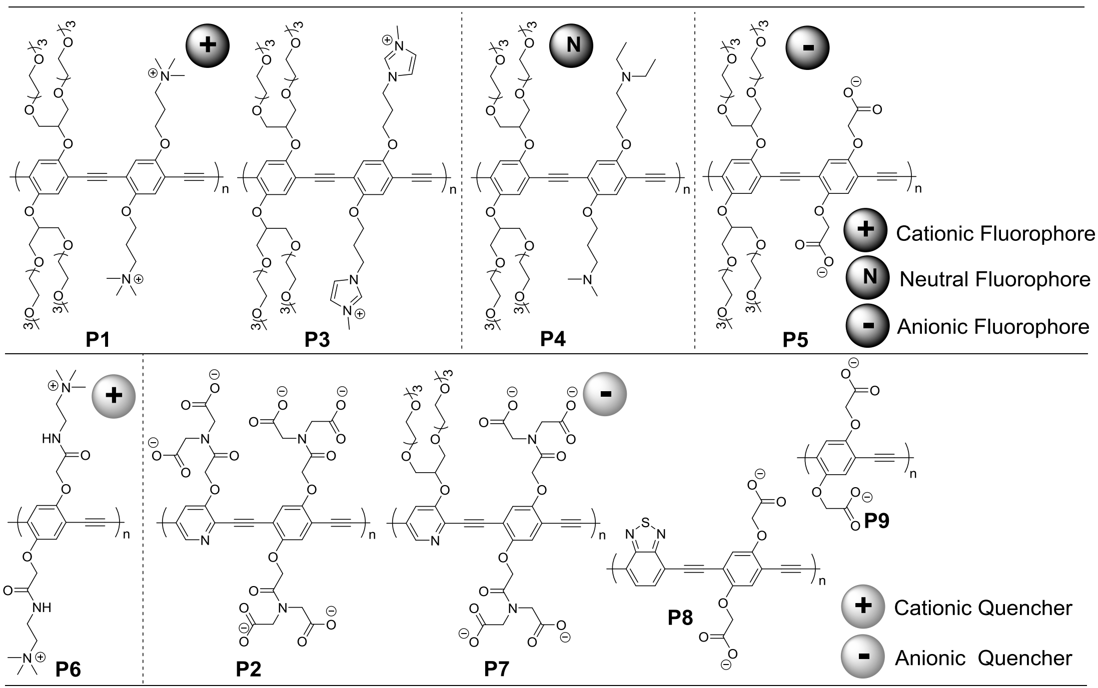

Figure 30. Structure of PAEs used in this study.

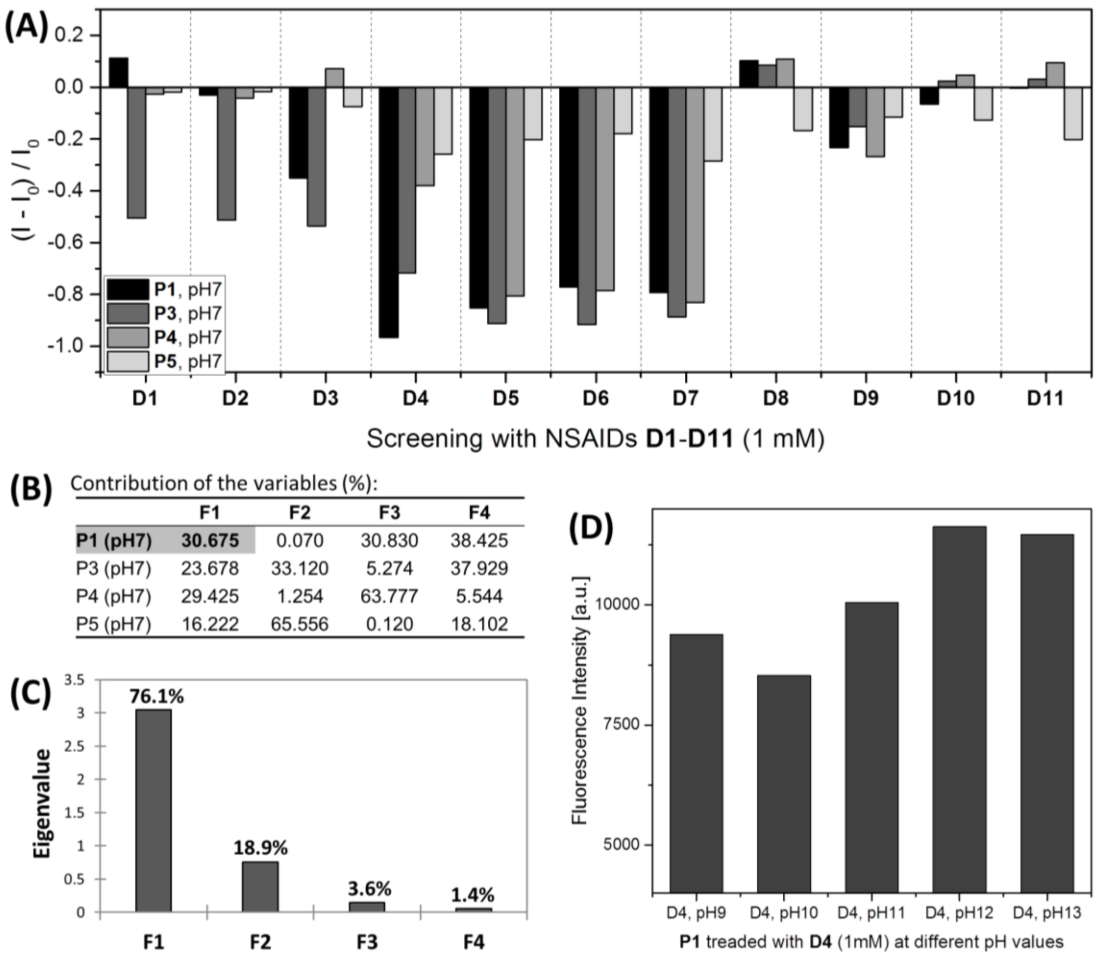

	F1	F2	F3	F4
P1 (pH7)	**30.675**	0.070	30.830	38.425
P3 (pH7)	23.678	33.120	5.274	37.929
P4 (pH7)	29.425	1.254	63.777	5.544
P5 (pH7)	16.222	65.556	0.120	18.102

Figure 31. (A) Fluorescence response pattern ((I - I_0) / I_0) obtained by **P1**, **P3**-**P5** (500 nM, at pH 7, buffered) treated with analgesics **D1**-**D11** (1 mM). Each value is the average of three independent measurements. **(B)** Contribution of each sensor elements to the resulted in four factor (**F1** - **F4**), sensor element of **P1** (pH 7) contributed most to the Factor 1 (**F1**). **(C)** Eigenvalue calculated from principal component analysis, factor 1 (**F1**) represent 76.1% of the total variation. (**D**) Fluorescence intensity obtained by **P1** (500 nM) treated with analgesics **D4** (1 mM) from pH 9 to pH 13.

Analgesic **D4** (1 mM) were selected as the initial drugs for the screening of best pH values. Because of the poor solubility of **D4** at pH 1 - pH 8, pH 9 to pH 13 were employed for screening. Finally, the best condition of pH 10 (strong quench) and pH 13 (weak quench) were selected (Figure 31D).

2.3.1.2 Screening with PAE/PAE complexes.

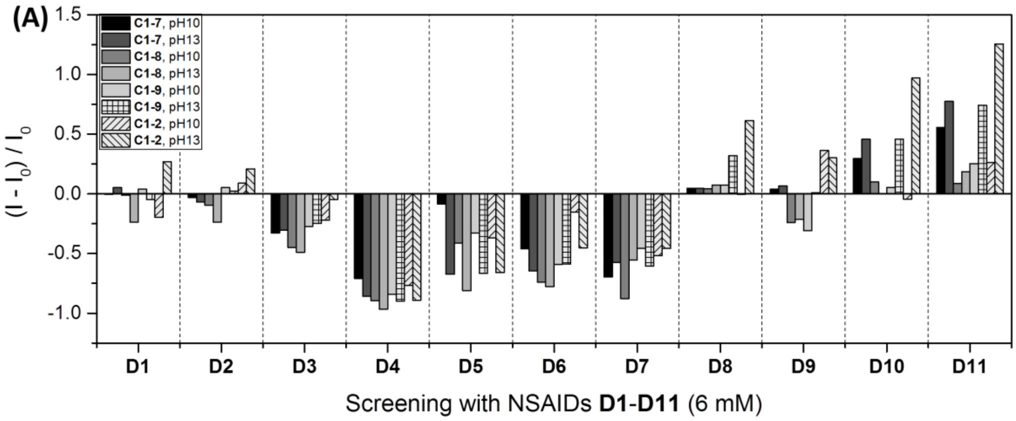

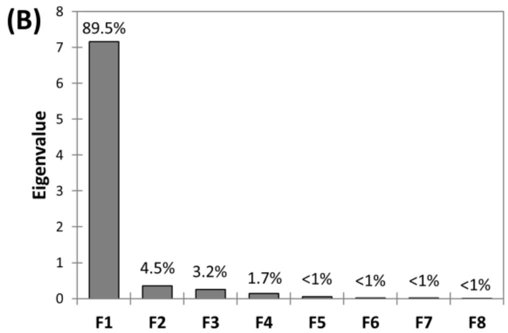

(C)

	F1	F2	F3
C1-7, pH10	12.438	0.279	20.708
C1-7, pH13	13.327	0.215	7.795
C1-8, pH10	12.544	3.520	24.708
C1-8, pH13	13.021	1.076	12.383
C1-9, pH10	12.276	10.821	10.956
C1-9, pH13	13.293	1.147	10.911
C1-2, pH10	9.685	82.435	0.572
C1-2, pH13	13.415	0.507	11.967

Figure 32. (A) Fluorescence response pattern (($I - I_0$) / I_0) obtained by eight complex (500 nM-250nM, at pH 10 and pH 13, buffered) treated with analgesics **D1-D11** (1 mM). Each value is the average of two or three independent measurements. **(B)** Eigenvalue calculated from principal component analysis, factor 1 and factor 2 represent 94% of the total variation. **(C)** Contribution of each sensor elements to the resulted factors (F1 – F8), **C1-2** (pH 13) contributed most to the factor 1 (F1) and C1-2 (PH 10) contributed most to the factor 2 (**F2**).

Four complexes (**C1-2**, **C1-7**, **C1-8**, **C1-9**) were used for the screening at pH 10 and pH 13. The complex **C1-2** with best distinguishing ability based on the PCA calculation was finally chose as sensor element for the further study (Figure 32).

2.3.2 Identification of Eleven NSAIDs

Figure 29 shows eleven NSAIDs chosen as a test bed. Structural similarity suggests separation into four groups, viz. salicylates, fenamic acids, profens and arylacetic acids. Figure 33A) shows the water solubility of the NSAIDs at 6 mM concentration at different pH values and the selected four-member array based on the previous screening process. For the construction of PAE/PAE complex, we titrated the highly fluorescent **P1** with quencher **P2** at different pH solution; all titrations were performed in buffered solution (pH = 7, 10, 13). The corresponding emission spectra are shown in the inset of the following figures (Figure 131). The molecular structure of the fluorophore, K_{SV} and log K_{SV} is shown on the right. The fitting of the quenching data was performed using the modified Stern-Volmer equation. As shown in Table 6, the quenching constants (log *Ksv*) of the complex at three different pHs were among 6.7 to 7.4; 22%-40% of the fluorescence was retained.

(A)

NSAIDs	pH7	pH10	pH13
D1	✔	✔	✔
D2	✔	✔	✔
D3	✔	✔	✔
D4	✖	✔	✔
D5	✖	✔	✔
D6	✔	✔	✔
D7	✖	✔	✔
D8	✔	✔	✔
D9	✔	✔	✔
D10	✔	✔	✔
D11	✔	✔	✔

✖ : bad water solubility

(B)

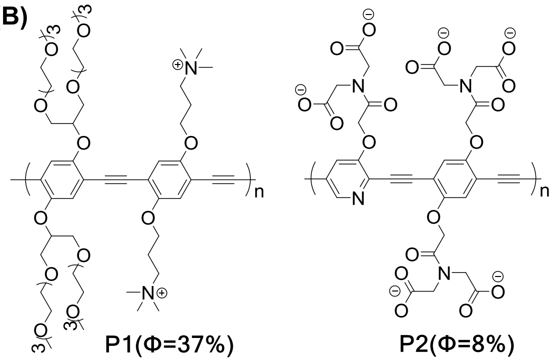

(C)

	P1	**C** (P1-P2)
pH10	Factor 1	Factor 3
pH13	Factor 2	Factor 4

Figure 33. (A) Water solubility of NSAIDs **D1**-**D11** (6 mM) at different pH values. **(B)** Structures of positively charged **P1** and negatively charged **P2**, used for analgesics sensing (φ = quantum yield). **(C)** Final selected four sensing factors by using single **P1** and its electrostatic complex **C** (**P1** + **P2**).

Table 6. Binding Constants (log *Ksv*) of Complex C Obtained from Quenching Data by Mixing **P1** (500 nM) with **P2** (500 nM) at pH7, pH10 and pH13 (Details see **Figure 131**).

Complex	**C (pH7)**	**C (pH10)**	**C (pH13)**
log *Ksv*	6.95±0.34	7.37±0.73	6.66±0.44
Residual fluorescence **C** (500nM-250nM)	37%	22%	40%

The 11 NSAIDs show varied responses towards this sensor field (Figure 34). Processing these data by linear discriminant analysis (LDA, sextuplet data sets), one discriminates all of the NSAIDs according to their Mahalanobis distances, employing two dimensionless factors. LDA converts the training matrix (4 factors x 11 NSAIDs x 6 replicates) into canonical scores. The first two canonical factors represent 80% of the total variation. We observed that Factor 1 represents the overall net quenching ability of the analytes towards the quencher – independent from any apparent structural features. The canonical scores are clustered into eleven different groups. The jackknifed classification matrix with cross-validation reveals 100% accuracy (details see Table 28, Table 30 and Figure 104), and the sensor system successfully discriminates the different analgesics.

To validate its efficiency, we performed tests with randomly chosen NSAID samples of our training set. The new cases are classified into groups, generated through the training matrix, based on their shortest Mahalanobis distance to the respective group. All of the 44 unknown NSAIDs samples were correctly identified (Table 29). In the 2D LDA plot (Figure 34C), results from eleven NSAIDs clustered independently in accordance to their structural similarity. Super groups form, i.e. all salicylates cluster differently from the profens, the fenamic acids and the arylacetic acids.

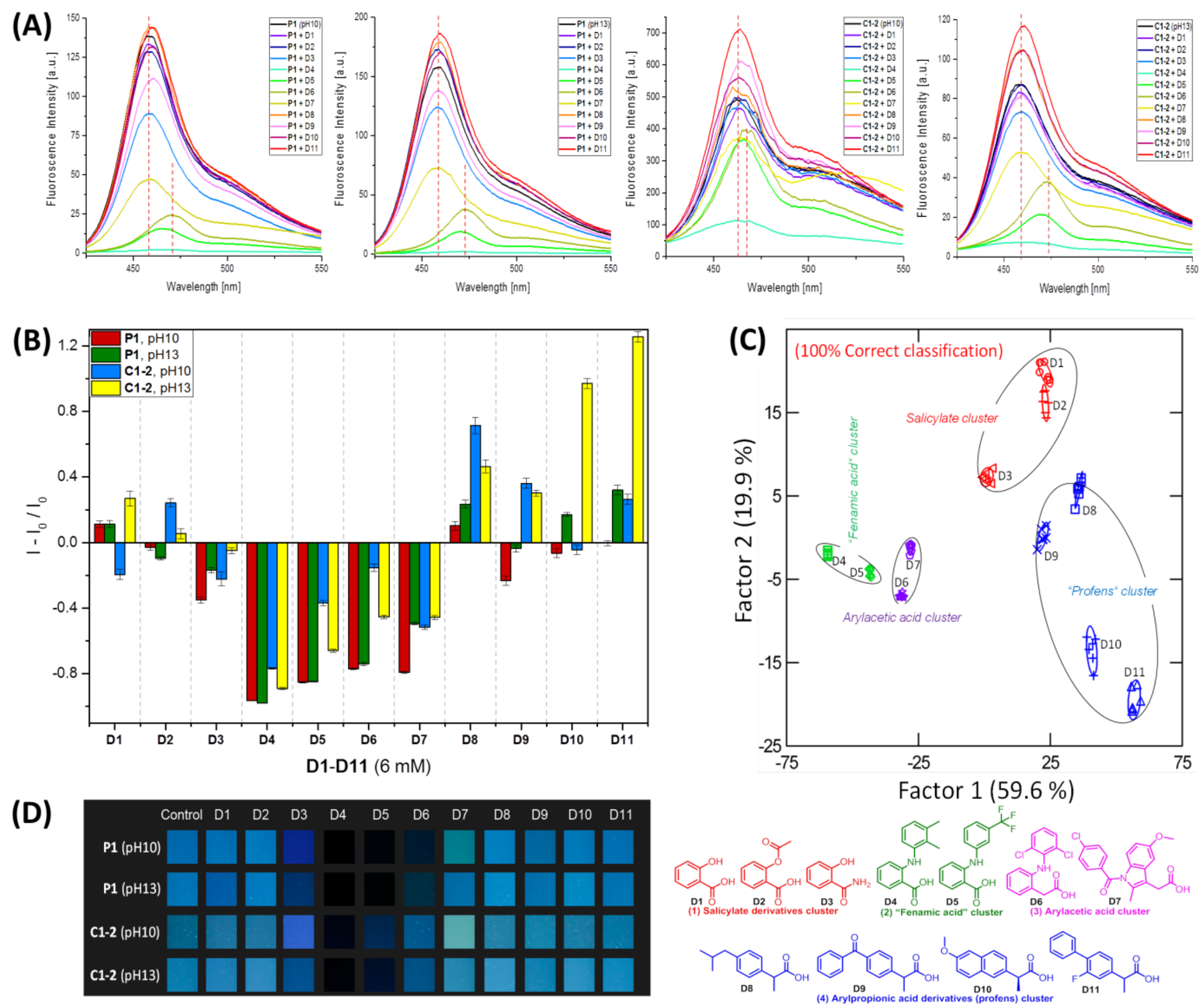

Figure 34. (A) Emission spectra obtained by **P1** (500 nM, at pH10 and 13, buffered) and its complex **C** (P1-P2 at 500 nM-250 nM, at pH10 and 13, buffered) treated with analgesics D1-D11 (6 mM). Redshift were found while adding D4, D5 and D6. **(B)** Fluorescence response pattern ((I - I_0) / I_0) obtained by **P1** (500 nM, at pH10 and 13, buffered) and its complex **C** (P1-P2 at 500 nM-250 nM, at pH10 and 13, buffered) treated with analgesics D1-D11 (6 mM). Each value is the average of six independent measurements; each error bar shows the standard deviation of these measurements. **(C)** 2D canonical score plot for the first two factors of simplified fluorescence response patterns obtained with an array of **P1**, **C** (each at pH10 and 13, buffered) with 95% confidence ellipses. Each point represents the response pattern for a single analgesic to the array. The canonical scores are clustered into eleven different groups. The jackknifed classification matrix with cross-validation reveals 100% accuracy. **(D)** Photograph of **P1** (at pH10 and 13, buffered) and its complex **C** (P1-P2, at pH10 and 13, buffered) treated with analgesics D1-D11.

2.3.3 Concentration Dependent Discrimination of 'Fenamic Acid'

We recorded the fluorescence modulation data for **D4** at concentrations from 0 mM to 1.8 mM. LDA (Figure 35A) converts the training matrix (4 factors x **D4**, nine concentrations x 6 replicates) into nine canonical scores. The first two canonical factors represent 94% of the total variation. The jackknifed classification matrix with cross-validation reveals 100% accuracy (Figure 35B). Eight different concentrations (without control, 0 mM) of **D4** from our training set were randomly chosen for blind testing. The new cases are classified into groups, generated through the training matrix, based on their shortest Mahalanobis distance to the respective group. Among 32 unknown concentration samples, all were classified correctly (Table 31 and Table 32).

The concentration is linearly mapped in the LDA plot, with the zero-point in the upper right-hand corner (Figure 35C). The same experiment was performed with **D7** and **D9**, and here also the concentration is linearly correlated with the response. This suggests that for every NSAID we have a slice of exclusion where one can identify NSAIDs at unknown concentrations without interference. There is a corollary to this: if two or more NSAIDs are on the same vector connecting to the origin, then their concentration dependent profiles cannot be discerned. However, in the other cases one should be able to obtain both structure and concentration from an unknown sample, even though at low concentrations this would become increasingly difficult. Figure 35D depicts the concentration dependent data in the context of all of the other NSAIDs. The cases that cannot be discerned when different concentrations are allowed are **D6**, **D3** or **D1**, and **D2**, **D8**, **D10**, or **D11**. In an ideal case, the concentration dependent slope would be significantly different for each and any NSAID.

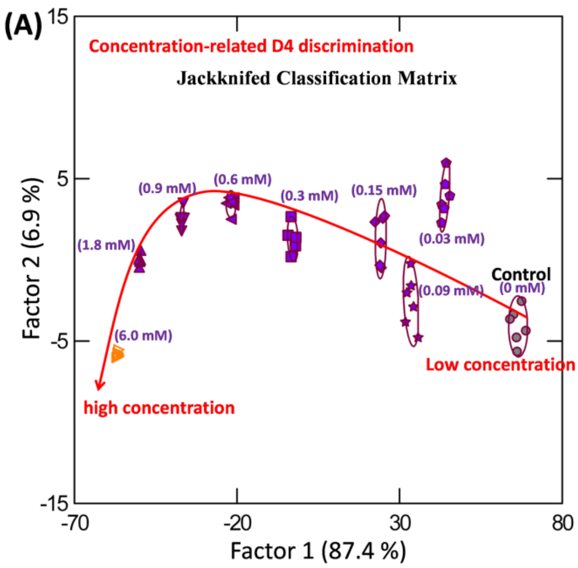

(B)

D4 (mM)	0.03	0.09	0.15	0.3	0.6	0.9	1.8	6.0	0	%correct
0.03	6	0	0	0	0	0	0	0	0	100
0.09	0	6	0	0	0	0	0	0	0	100
0.15	0	0	6	0	0	0	0	0	0	100
0.3	0	0	0	6	0	0	0	0	0	100
0.6	0	0	0	0	6	0	0	0	0	100
0.9	0	0	0	0	0	6	0	0	0	100
1.8	0	0	0	0	0	0	6	0	0	100
6.0	0	0	0	0	0	0	0	6	0	100
0	0	0	0	0	0	0	0	0	6	100
Total	6	6	6	6	6	6	6	6	6	100

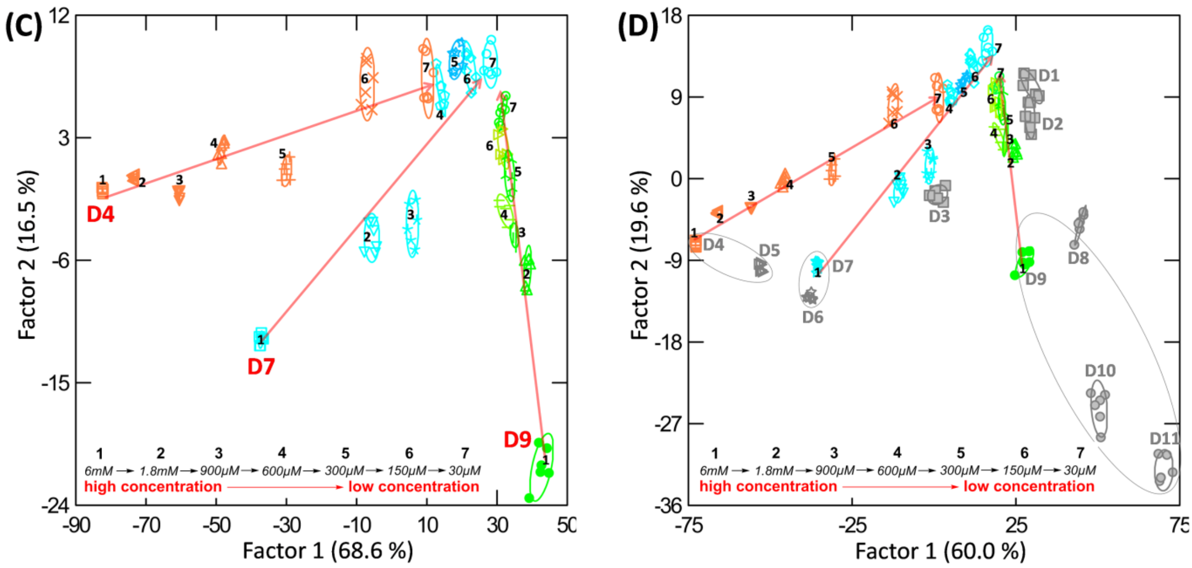

Figure 35. (A) 2D canonical score plot for the first two factors of simplified fluorescence response patterns obtained with an array of **P1**, **C1-2** (each at pH 10 and pH 13, buffered) treated with **D4** (from high concentration to low concentration) with 95% confidence ellipses. **(B)** LDA jackknifed classification matrix table obtained from an array of **P1**, **C1-2** (each at pH 10 and 13, buffered) against NSAIDs **D4** at different concentrations. The jackknifed classification matrix with cross-validation reveals a 100% accuracy. **(C)** 2D canonical score plot for the first two factors of simplified fluorescence response patterns

obtained with an array of **P1**, **C1-2** (each at pH10 and 13, buffered) treated with **D4**, **D7** and **D9** (from high concentration to low concentration) with 95% confidence ellipses, **(D)** 2D canonical score plot obtained with an array of **P1**, **C1-2** (each at pH10 and 13, buffered) treated with analgesics **D1-D11** (6 mM) and **D4**, **D7** and **D9** (from 30 µM to 1.8 mM). Each point represents the response pattern for a single concentration of analgesics to the array. The jackknifed classification matrix with cross-validation reveals 100% accuracy.

2.3.4 Sensing of Commercial OTC Samples and "Fakes" (Aspirin and Ibuprofen)

Can we identify and discriminate different, commercially available NSAIDs? Various fillers, super-disintegrants etc. are present in varying concentrations. We selected five commercially available samples of aspirin and five samples of ibuprofen. Table 7 shows the composition and the weight of all of the ingredients according to the package insert. Figure 36 shows the fluorescence responses of the different ibuprofen and aspirin samples. For aspirin, the sample **ASS2** is the least fitting in this series, probably due to the presence of carnauba wax, not too surprising, as it is colored (yellow/brown). The other ASS-samples cluster closely. In the case of the ibuprofens, samples **IBU2**, **3** cluster and are away from the data point for **D8**. **IBU2**, **3** contain titanium dioxide, another ingredient that will interfere with the fluorescence modulation of the chemical tongue by ibuprofen. The other IBU samples cluster more closely. The super cluster of the IBUs does not overlap with the super cluster of the ASS-species.

Table 7. Detailed Information of the Ten Over-the-Counter (OTC) NSAIDs* Used in This Study

Abbr.	*Brand name (Company)*	Main/total (mg) [a]	Side ingredients
ASS1	*ASS-ratiopharm® (Ratiopharm)*	500/620	corn starch, cellulose powder
ASS2	*Aspirin® (Bayer)*	500/670	Na_2CO_3, highly dispersed SiO_2, carnauba wax, hydroxypropylmethylcellulose (HPMC), Zn-stearate
ASS3	*ASS 500mg HEXAL® (Hexal AG)*	500/620	microcrystalline cellulose, corn starch
ASS4	*ASS 500-1A Pharma® (1A Pharma)*	500/620	microcrystalline cellulose, corn starch
ASS5	*ASS STADA® (STADA pharm)*	500/650	microcrystalline cellulose, corn starch
IBU1	*Ibuflam® akut (Winthrop)*	400/590	microcrystalline cellulose, corn starch, lactose monohydrate, E468, highly dispersed SiO_2, Mg-stearate, polyvinylalcohol, Macrogel 3350, talcum powder
IBU2	*IbuHEXAL® akut (Hexal AG)*	400/480	microcrystalline cellulose, E468, HPMC, Macrogel 400, Mg-stearate, highly dispersed SiO_2, talcum powder, TiO_2
IBU3	*Ibu 400 akut-1A Pharma® (1A Pharma)*	400/480	microcrystalline cellulose, E468, HPMC, Macrogel 400, Mg-stearate, highly dispersed SiO_2, talcum powder, TiO_2
IBU4	*Ibuprofen AL 400 (ALIUD PHARMA)*	400/680	Mg-stearate, corn starch, Macrogel 400, 6000, carboxymethyl starch sodium, HPMC
IBU5	*Dolormin® (McNeil)*	400/820	Microcrystalline celluloses, povidon, Mg-stearatete, TiO_2, hydroxypropyl cellulose, HPMC

Apart from the commercially available NSAIDs, we also tested two "counterfeit" tablet types, one containing aspirin **(ASS-Fake)** and the other containing ibuprofen (**IBU-Fake**). Both were manufactured at the Institute of Pharmacy and Molecular Biotechnology (IPMB, University of

Heidelberg) with an unknown concentration of the corresponding NSAID and other side ingredients (metal, salts, etc.). Not only that these drugs show different fluorescence responses (Figure 36A), their responses are also located far from the super clusters of the ASS- and IBU-species (Figure 36B), thus can be easily identified.

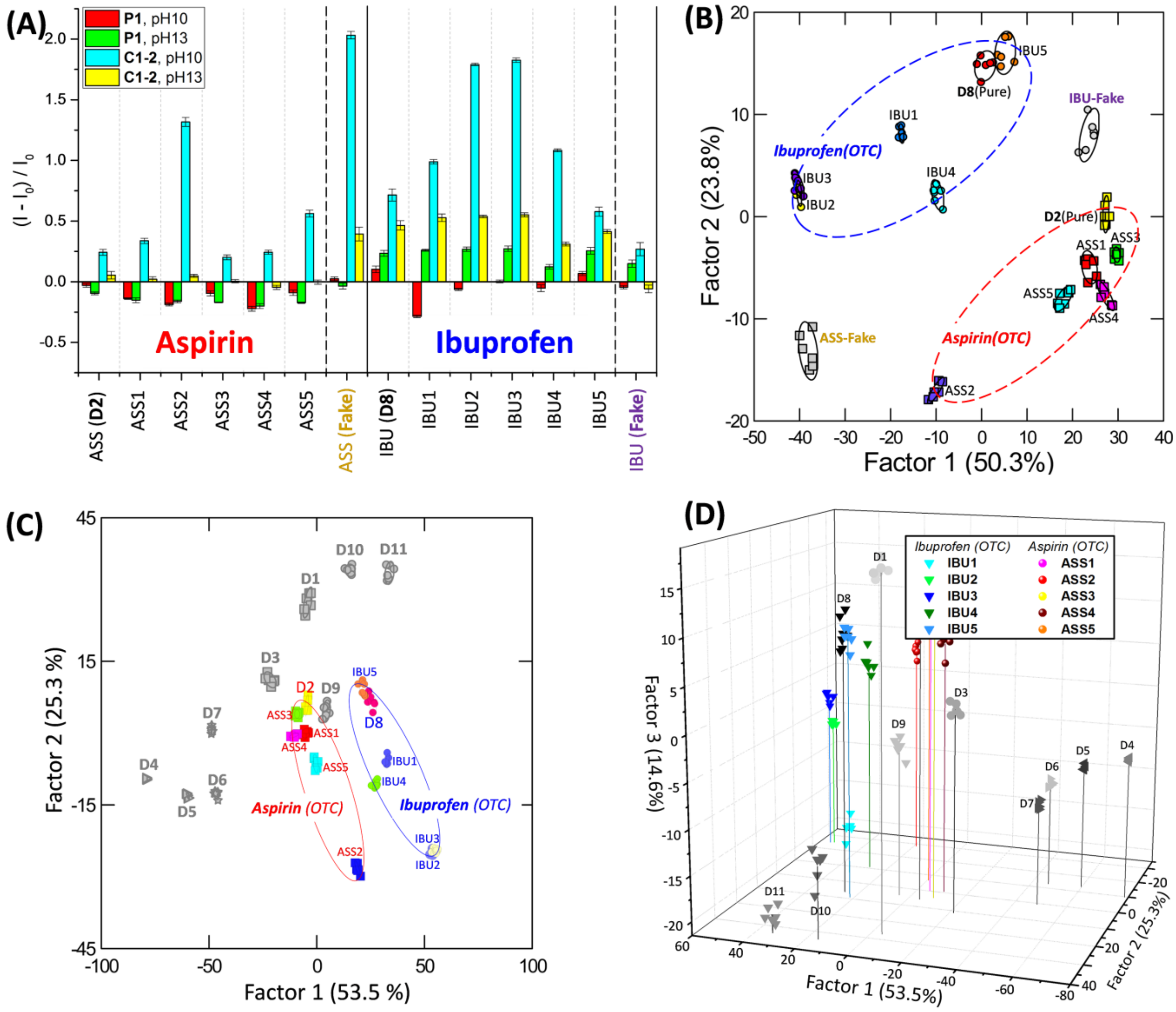

Figure 36. (A) Fluorescence response pattern ((I - I_0) / I_0) obtained by **P1** (500 nM, at pH10 and 13, buffered) and complex **C1-2** (**P1**-**P2** at 500 nM-250 nM, at pH10 and 13, buffered) treated with **D2** (aspirin, 6 mM, control), **D8** (ibuprofen, 6 mM, control), OTC tablet aspirin (**ASS1-ASS5**, 6 mM active compound), ibuprofen (**IBU1-IBU5**, 6 mM active compound) and "counterfeit" drug samples (**ASS-Fake** and **IBU-Fake**, same mass as used for the corresponding OTCs). **(B)** 2D canonical score plot for the first two factors of simplified fluorescence response patterns obtained with an array of **P1**, and **C1-2** (each at pH 10 and 13, buffered, 95% confidence ellipses) are shown. Each point represents the response pattern for a single analgesic to the array. **(C)** 2D canonical score plot and **(D)** 3D canonical score plot obtained with an array of **P1**, **C1-2** (each at pH10 and 13, buffered) treated with NSAIDs **D1-D11** and commercial available OTC tablet aspirin (**ASS1-ASS5**), ibuprofen (**IBU1-IBU5**). Each point represents the response pattern for a single analgesic to the array. The grey/black colors represent pure analgesics, the colorful shape represent the OTC aspirin and ibuprofen.

Once we co-process the data employed for Figure 36 with all of the data obtained for the other NSAIDs, we find that the IBU and the ASS samples form superclusters that do not overlap with any of the other NSAIDs (here shown in grey, Figure 36 C-D). The response to the sensor field, while modulated by the additives and formulations, is fundamentally determined by the active drug component. The selected sensor field - in combination with LDA - easily handles these discriminative tasks.

2.3.5 Sensing Mechanisms of the PAE Tongue

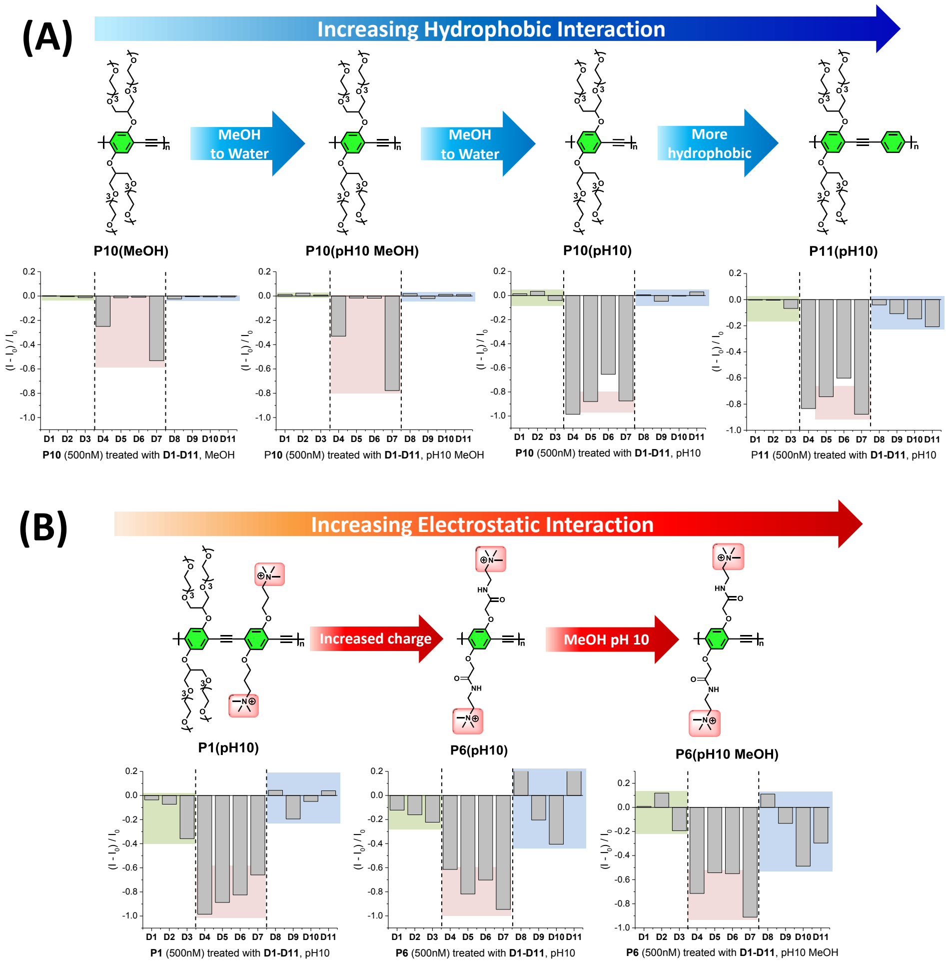

Figure 37. (A) Structure-activity relationship while increasing hydrophilic interaction. **(B)** Structure-activity relationship while enhancing electrostatic interaction.

To explain the reactivity and selectivity of our tongue, we investigated if uncharged water soluble PPEs would interact with the NSAIDs. Indeed, **P10** does not strongly react to the analytes, when dissolved in methanol. Only **D4** and **D7** show some quenching (Figure 37A). Upon going from methanol into water, the general hydrophobic interactions are turned on and **P10** interacts with the analytes **D4-D7**. If the aromatic sensor core is enlarged and an unsubstituted benzene ring is added, polymer **P11** results and is now fairly responsive towards the NSAIDs; quenching is now observed for **D8-D11**. The highly hydrophilic compounds **D1-D3** are generally not very responsive towards the neutral **P11**, as hydrophobic components seem to be less important for interactions. In the next experiment (Figure 37B) we investigated the cationic polymer **P1** in water at pH 10. All of the analytes react. Upon increasing the charge on a per repeat unit, the interaction increases somewhat but not dramatically. For **D8-D11** the interaction increases. If we then try to turn off the hydrophobic interaction by going into methanol, we also increase the electrostatic interactions. Interestingly there are no gross changes in the response profiles, yet the *differential* response changes are sufficiently developed to be useful for discrimination. To note, the increase in electrostatic interactions does not lead to a dramatic increase in binding. That could be due to the decrease in hydrophobic interactions but also due to tighter binding towards the non-analyte counteranions that are present in the solution. Overall, binding occurs both by hydrophobic effects but also by electrostatic interactions. The sensing act though, that is the transfer of "discriminative information" is probably due to interactions between the aromatic nuclei of the polymer and the analyte – yet it can be induced or magnified by electrostatic interactions. This picture is not very far from Swager's nitroarene sensors,[7, 188] with the exception that the quenching efficiency is modulated by the electron accepting nature of the nitroarenes, an effect which we do not observe in our overall donor-substituted analytes.

For further understanding of the mechanisms, emissive lifetimes were measured for selected tongue elements and sensor+analyte complexes (Figure 39 - Figure 42, collaboration with Soh Kushida). Based on the fluorescence response and selectivity (vide supra), the representative drugs **D1**, **D4**, and **D10** were selected. As shown in Table 8, the lifetime of the **P1**+**D4** complex is decreased compared with that of pure **P1** at both ph10 and pH13 (also see Figure 40). There are two possible mechanisms, which might explain the shortened lifetime; energy transfer to the exciplex state and charge separation (Figure 38).

Table 8. Selected Examples of Exponential Fitting Parameter of Lifetimes of the Emissive Lifetimes of the Polymers **P1**, **P2** and the Complex **C1-2** Alone and in the Presence of Selected NSAIDs **D1**, **D4** and **D10** as Model Analytes.

Sample	τ_1 / ns (f_1)	τ_2 / ns (f_2)	τ_3 / ns (f_3)	τ_{av} / ns ^{a}
P1 (pH10)	0.60 (1.00)	-	-	0.60
P1 (pH13)	0.61 (1.00)	-	-	0.61
P2 (pH10)	0.71 (1.00)	-	-	0.71
P2 (pH13)	0.71 (1.00)	-	-	0.71
C1-2 (pH10)	0.20 (0.20)	0.80 (0.72)	3.66 (0.08)	0.93
C1-2 (pH13)	0.31 (0.26)	0.77 (0.69)	3.69 (0.05)	0.79
P1+**D1** (pH10)	0.52 (0.81)	1.20 (0.19)	-	0.65
P1+**D1** (pH13)	0.30 (0.84)	1.07 (0.16)	-	0.60
P1+**D4** (pH10)	0.02 (0.67)	2.43 (0.33)	-	0.81
P1+**D4** (pH13)	0.03^b (1.00)	-	-	0.03
P1+**D10** (pH10)	0.58 (0.84)	1.48 (0.16)	-	0.73
P1+**D10** (pH13)	0.58 (0.84)	1.48 (0.16)	-	0.73
C1-2+**D1** (pH10)	0.25 (0.20)	0.81 (0.72)	2.48 (0.08)	0.91
C1-2+**D1** (pH13)	0.32 (0.26)	0.77 (0.70)	3.30 (0.04)	0.75
C1-2+**D4** (pH10)	0.02 (0.33)	0.60 (0.47)	2.48 (0.20)	0.79
C1-2+**D4** (pH13)	0.02 (0.42)	0.57 (0.46)	1.51 (0.12)	0.45
C1-2+**D10** (pH10)	0.23 (0.21)	0.82 (0.73)	3.86 (0.06)	0.87
C1-2+**D10** (pH13)	0.29 (0.19)	0.79 (0.79)	3.74 (0.02)	0.77

^{a} τ_{av} is defined as $(\tau_1 f_1 + \tau_2 f_2 + \tau_3 f_3)/(f_1 + f_2 + f_3)$. ^{b} The lifetime was under resolution.
τ_x and f_x indicate the lifetime and their ratio, respectively. Short and long lifetime are written in blue and red, respectively.

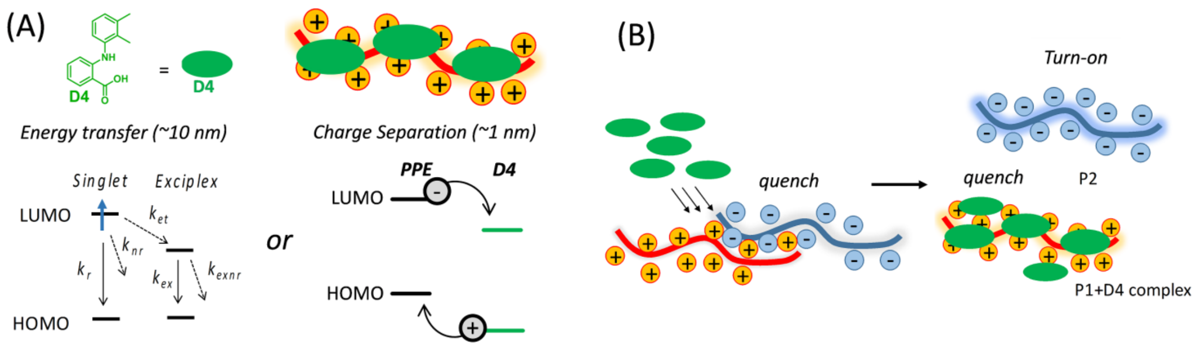

Figure 38. Schematic representations of involved electronic states and sensing mechanisms of **(A)** P1+D4 and **(B)** C1-2+D4.

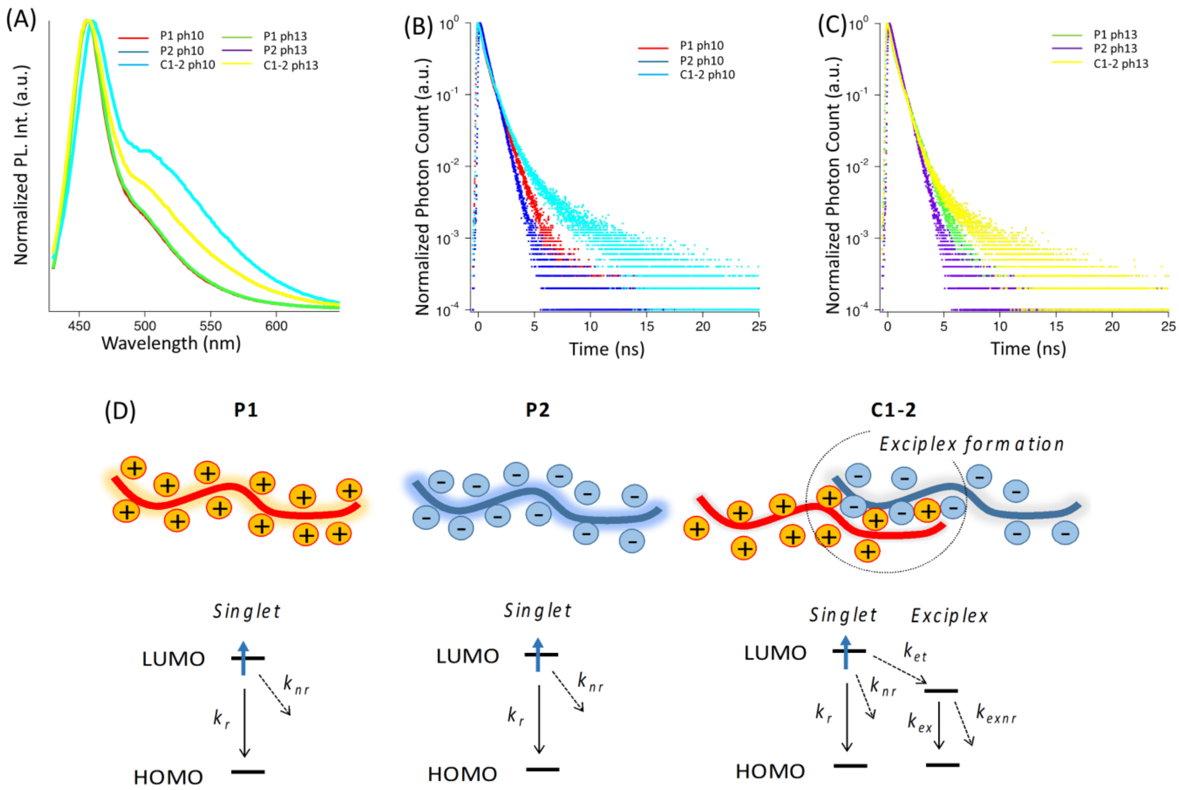

Figure 39. (A) PL spectra of **P1** at pH 10 (red), **P2** at pH 10 (dark blue), **C1-2** at pH 10 (clear blue), **P1** at pH 13 (green), **P2** at pH 13 (purple), and **C1-2** pH 13 (yellow). **(B-C)** Fluorescence decay profiles of of **P1** at pH 10 (red), **P2** at pH 10 (dark blue), **C1-2** at pH 10 (clear blue), **P1** at pH 13 (green), **P2** at pH 13 (purple), and **C1-2** at pH 13 (yellow). **(D)** Schematic representation of possible states of the polymers in water (top) and its electronic state (bottom).

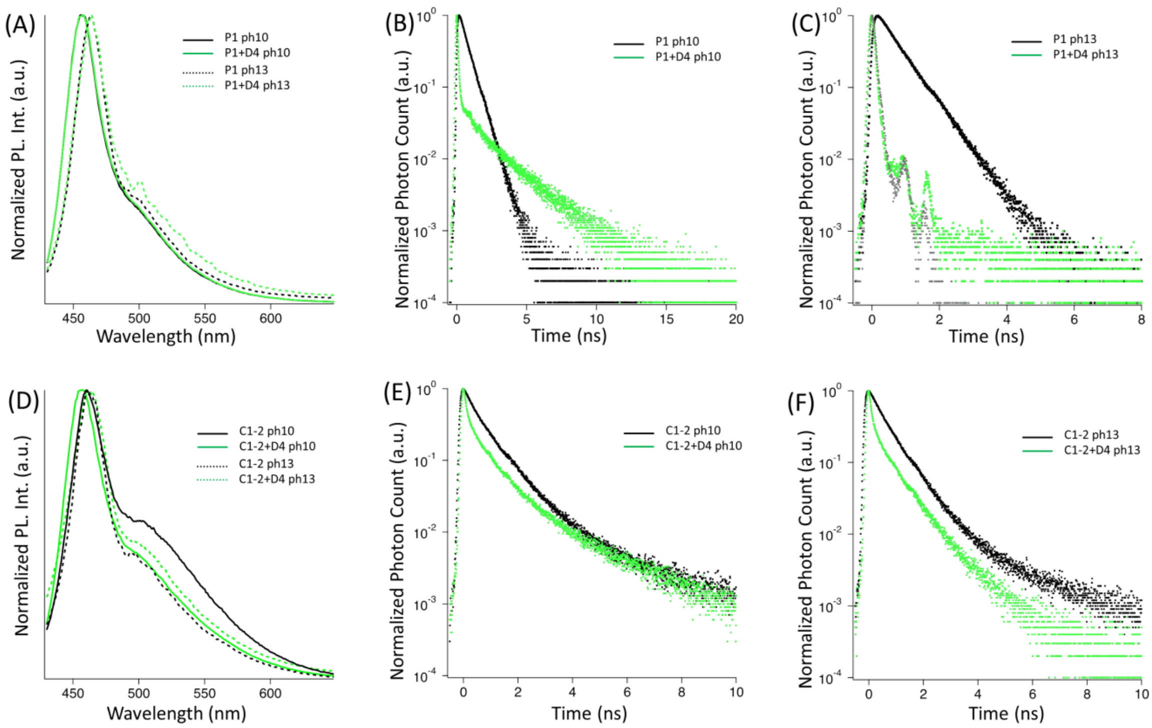

Figure 40. (A) PL spectra of **P1** at pH 10 (solid, black), **P1**+**D4** at pH 10 (solid, green), **P1** at pH 13 (dashed, black) and **P1**+**D4** at pH 13 (dashed, green). **(B)** Fluorescence decay profiles of **P1** at pH 10 (black) and **P1**+**D4** at pH 10 (solid, green) **(C)** Fluorescence decay profiles of **P1** at pH 13 (black) and **P1**+**D4** at pH 13 (solid, green) and prompt decay of excitation laser (gray). The shapes of **P1**+**D4** in pH 13 and prompt decay of excitation laser coincides, meaning that the lifetime of **P1**+**D4** in pH 13 is under resolution. **(D)** PL spectra of **C1-2** at pH 10 (solid, black), **C1-2**+**D4** at pH 10 (solid, green), **C1-2** at pH 13 (dashed, black) and **C1-2**+**D4** at pH 13 (dashed, green). **(E-F)** Fluorescence decay profiles of **C1-2** pH 10 and pH 13 (black), **C1-2**+**D4** pH 10 and pH 13 (solid, green).

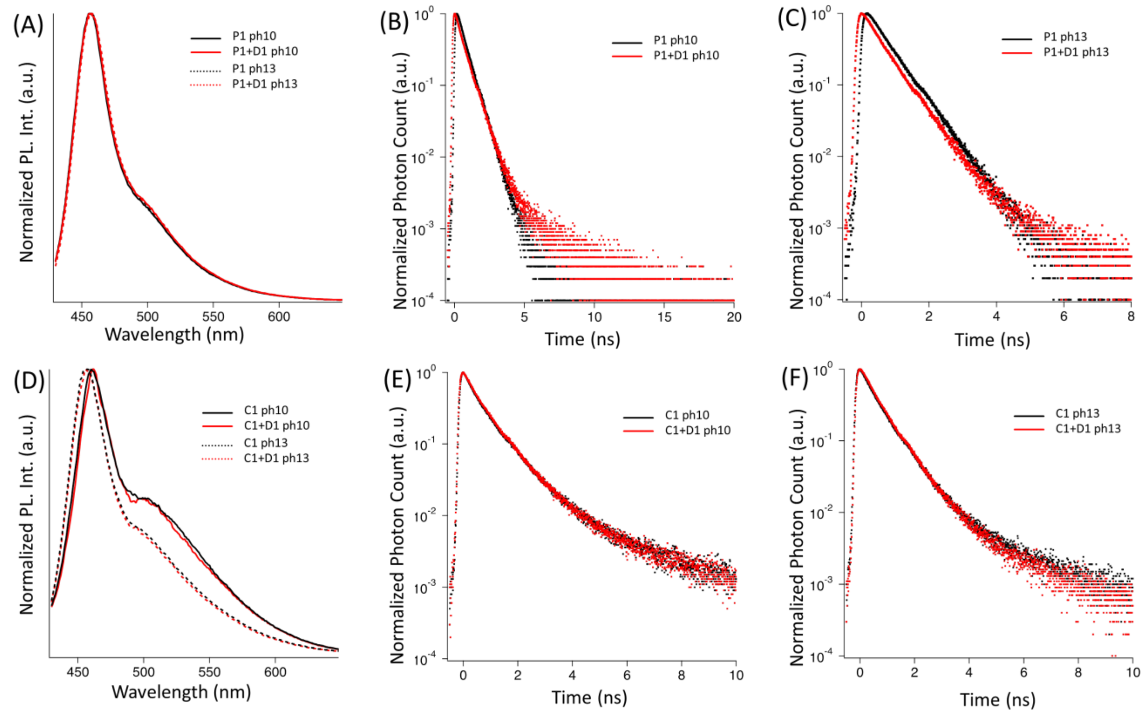

Figure 41. (A) PL spectra of **P1** at pH 10 (solid, black), **P1**+**D1** at pH 10 (solid, red), **P1** at pH 13 (dashed, black) and **P1**+**D1** at pH 13 (dashed, red). **(B-C)** Fluorescence decay profiles of **P1** at pH 10 and pH 13 (black), **P1**+**D1** at pH 10 and pH 13 (solid, red) **(D)** PL spectra of **C1-2** at pH 10 (solid, black), **C1-2**+**D1** pH 10 (solid, red), **C1-2** at pH 13 (dashed, black) and **C1-2**+**D1** at pH 13 (dashed, red). **(E-F)** Fluorescence decay profiles of **C1-2** at pH 10 and pH 13 (black) and **C1-2**+**D1** at pH 10 and pH 13 (solid, red).

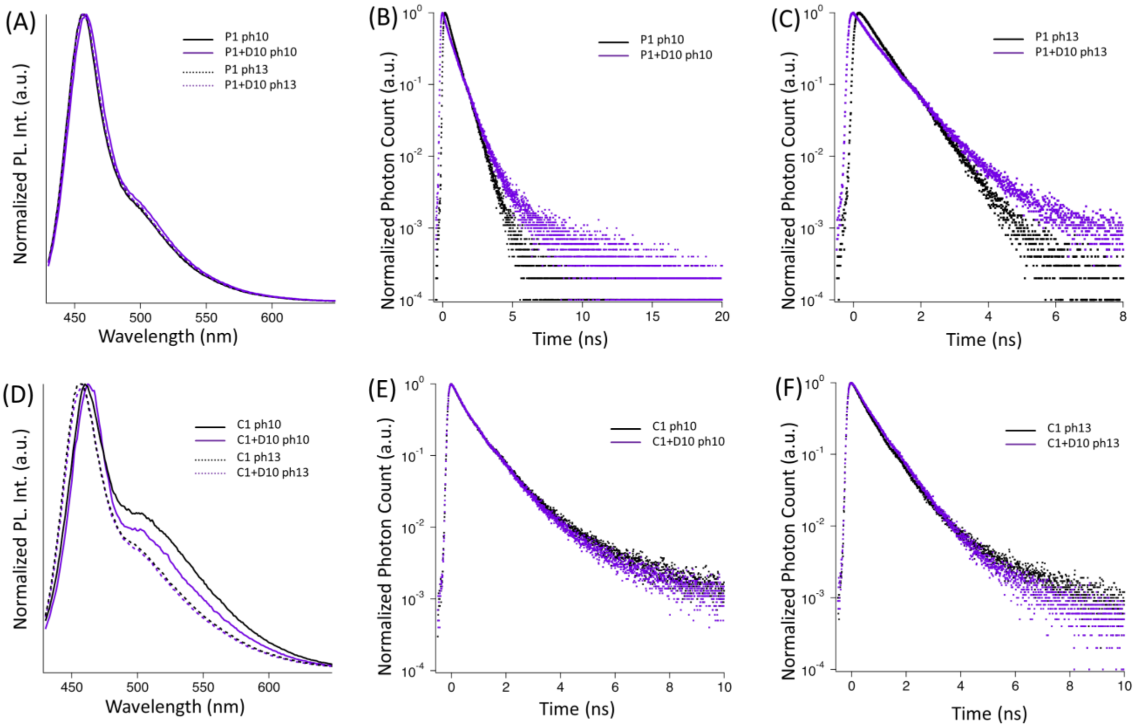

Figure 42. (A) PL spectra of **P1** at pH 10 (solid, black), **P1**+**D10** at pH 10 (solid, red), **P1** at pH 13 (dashed, black) and **P1**+**D10** at pH 13 (dashed, red). **(B-C)** Fluorescence decay profiles of **P1** at pH 10 and pH 13 (black), **P1**+**D10** at pH 10 and pH 13 (solid, red) **(D)** PL spectra of **C1-2** at pH 10 (solid, black), **C1-2**+**D10** pH 10 (solid, red), **C1-2** at pH 13 (dashed, black) and **C1-2**+**D10** at pH 13 (dashed, red). **(E-F)** Fluorescence decay profiles of **C1-2** at pH 10 and pH 13 (black) and **C1-2**+**D10** at pH 10 and pH 13 (solid, red).

The emissive lifetime (collaboration with Soh Kushida) of the complex of **P1**+**D4** (pH10) has two factors: one short (0.017 ns, 67.2%) and long lifetime (2.43 ns, 32.8%). The factors are considered as singlet state of **P1** and its exciplex state, respectively. However, the emission spectrum of the **P1+D4** complex is quite similar to that of **P1** (Figure 40), suggesting that the radiation rate constant of exciplex (k_{exr}) is too small to appear. Another explanation is that charge separation also takes place. The **P1**+**D4** complex at pH13 shows a short lifetime, below our resolution. At pH13, the interaction between **P1** and **D4** is fairly strong, possibly resulting in an ion pair. The effective distance of charge separation (~1 nm) is smaller than that of energy transfer (~10 nm). Therefore, we might consider here both energy transfer to the exciplex state and charge separation as possible mechanisms.

The lifetime of the **C1-2**+**D4** complex consists of three factors: short (~0.02 ns), normal (~0.6 ns) and one long lifetime component (1.5 ns or 2.5 ns), respectively (Figure 40). Charged analytes can separate electrolyte complexes such as **C1-2**.[41] Consequently, the factors of long and short lifetime are attributed to the **P1**+**D4** complex, whereas the factor of normal lifetime is attributed to **P2**. Contrary to the case of **D4**, the analytes **D1** and **D10** did not show obvious lifetime changes (Figure 41 and Figure 42), suggesting quenching/enhancing mechanisms with **D1** or **D10** are not related to energy transfer or charge separation phenomena, but - as we explained above (Figure 38) - hydrophobic and electrostatic interaction determine the selectivity.

2.3.6 Conclusions

We have developed a four-element sensor array consisting of a highly fluorescent cationic PPE and its complex with a weakly fluorescent anionic PAE. Both elements (at pH10 and pH13) discern 11 different NSAIDs, even at different concentrations. The tongue identifies and discriminates commercial NSAIDs (over-the-counter ibuprofen and aspirin) and their “counterfeits”. While the different ibuprofens and aspirins cluster together, it is possible to identify a tablet from a specific drug maker. This successful discrimination is a testament to the power of these small arrays composed of weakly selective elements.

What is the array’s secret? We do not know exactly, but the effect must be a combination of hydrophobic and electrostatic interaction of the analytes with the conjugated polymer(s) or with their formed complex(es). These effects are magnified as we employ fluorescence-based detection; the excited state is far more responsive towards external stimuli than the ground state. Our mechanistic investigations have corroborated this picture, yet the subtle effects that modulate the fluorescence response between closely related analytes are complex, and not easily unraveled. It does not escape our attention that the problems of differential selectivity might be best tackled by big data approaches to map out interactomes. What we have done here is just a tiny slice of possible combinations for NSAID-analytes; while our experiments cast a hard shadow on these problems, a general solution might lie on a level that is deeper than what we usually do employing physical organic principles. The complexity of the systems, their tremendous variability, combined with their discriminative stability makes application of big-data instruments, both with respect to data acquisition but also data processing a promising and perhaps necessary proposition.

A further thought is provocative: the more or less *ad hoc* and almost randomly selected sensory systems work eerily well and surpass in their flexibility and discriminatory power most specific sensors. Such sensors often do not exist (at any rate) for discrimination of even fairly simple or complex analytes we are interested in.[7-8] If transparent and easily applicable rules are developed that connect analyte class to ideal fluorophore and quencher type, these tongues will achieve great impact in quality control of drugs, beverages, etc.

2.4 Evolution of PAE-Based Fluorescent Sensor Arrays for Fingerprinting Antibiotics

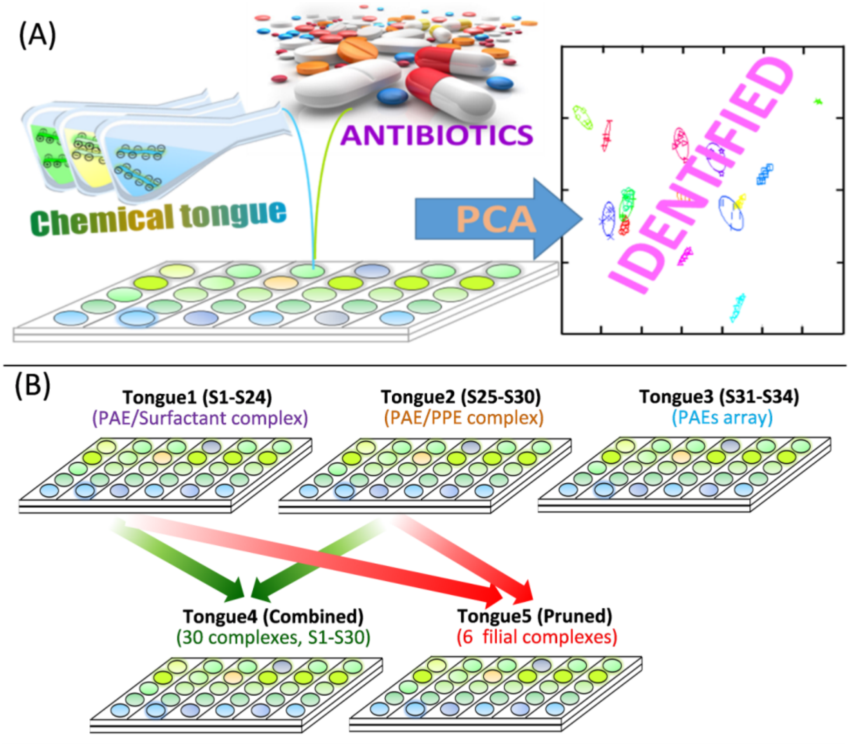

Figure 43. (A) Systematic illustration of PAE-based sensor array for the identification of antibiotics. **(B)** Construction and evolution of chemical tongues.

In this chapter, we outline an evolution process for tongue elements composed of poly(*para*-aryleneethynylene)s (PAEs) and detergents, resulting in a chemical tongue (24 elements, tongue #1) that discerns antibiotics. Cross-breeding of this new tongue (tongue #2) with tongue elements that consist of simple poly(*para*-phenyleneethynylene)s (PPEs) at different pH-values leads to an enlarged sensor array, composed of 30 elements (tongue #4). This tongue was pruned, employing principal component analysis. We find that a filial tongue (tongue #5) featuring three elements from each original array (i.e. a six element tongue) is superior to either of the prior tongues and the composite tongue is superior in the discrimination of structurally different antibiotics. Such a selection processes should be general and give an idea how to successfully generate powerful low-selectivity sensor elements and configure them into discriminative chemical tongues.

2.4.1 Construction and Comparison of Various Chemical Tongues

We describe the evolution of an efficient six-element, fluorescence-based optoelectronic tongue that discriminates antibiotics. This superior "filial tongue" results from combination of two starting tongues, followed by productive pruning of non-performing elements.

Sensing, detecting and discriminating of simple but also of complex analytes is an ever attractive and important issue for quality control of food,[117-118] beverages[47, 123-125, 189] and drugs;[190-192] it is also critical for detecting fake malaria tablets,[172] and generally adulteration of prescription drugs. While complex instrumental analytical tools, such as mass spectrometry, handle such tasks-if the analyte under consideration can be brought into the gas phase-there is still a great need for simple, “low tech” methods of discrimination and sensing, quality control, or fraud detection. A promising approach for the discrimination of complex (or simple) analytes is chemical tongues. These consist of 3-50 different sensor elements that are exposed towards an analyte of choice. Optical changes (color, fluorescence wavelength, or intensity etc.) are recorded, and the formed pattern is analyzed by statistical methods, including multivariate analysis of variance (MANOVA),[164, 193] principal component analysis (PCA), or linear discriminant analysis (LDA).[61] The discrimination rests in the uniqueness of the formed pattern and *not* in the response of a single sensing element, which might display a rather low selectivity for any given analyte.

An important and not well understood aspect of this approach are the principles that guide the construction of such tongues, including what would be the minimum number of necessary tongue elements to identify a specific analyte or sample. In most of these problems, the classic issue of sensitivity is in-operative, as the analytes or samples for quality control are available on multi-gram or at least on a multi-100-mg scale. That is for sure true for (alcoholic) beverages and food-stuffs, but mostly also for prescription and non-prescription drugs. Which concepts are currently available for the construction of successful tongues? (**1**) General-poorly fitting receptors that interact with the analytes of choice. This elegant concept, developed by Anslyn et al. as a variation of Fischer’s lock-and-key principle,[37, 129-130, 159, 194] discriminates a variety of analytes with tongue elements of suitable shape/cavity/binding characteristic. (**2**) Suslick et al. developed a colorimetric assay, in which chemically different types of dyes (typically 16-36) are printed on a substrate and exposed towards gaseous or solution-phase analytes. Suslick stresses, that the chemical diversity of the elements of his tongue or nose (he calls the process smell-seeing) are critical for the success of the concept.[36, 70-71, 128] (**3**) Rotello et al. discovered that binary complexes of positively charged gold nanoparticles and negatively charged conjugated polymers of the poly(*para*-phenyleneethynylene) (PPE) type make for powerful chemical tongues that discriminate proteins, bacteria, but also cells and cell lysates.[49, 51, 53, 57] The functionalized gold nanoparticle is the protein-like recognition element but also a powerful quencher of the PPEs’ fluorescence. Addition of the analytes releases the gold nanoparticle, and PPE fluorescence turn-on is observed. Yet, Bunz and Rotello found also that a library of simple charged PPEs *alone* discriminates proteins, a critical discovery.[58]

The above concepts state rules *sufficient* for the construction of tongues; do these rules formulate conditions that are *necessary* for the construction of a successful tongue? We found simple, ionic, PPE-based chemical tongues without any discernable sensory properties to recognize useful analytes. A small PPE-based tongue easily discriminates white wines[47] but also aliphatic and aromatic acids.[40-41]

An important aspect of this approach is the combination of different tongue elements into new complexes that work as sensor elements. Additionally, the change of the pH value empowers one PPE to act in several independent sensor elements with modulated responses. Complex formation and pH-control are powerful yet simple strategies as they do not entail the (work intensive) synthesis of new tongue elements. As a consequence, an efficient approach towards development of tongues will include complexation and pH-changes. The modulation of the inherent fluorescence response by (commercially available) adjuvants such as cationic or anionic surfactants should also modulate the fluorescence response of tongue elements towards analytes.

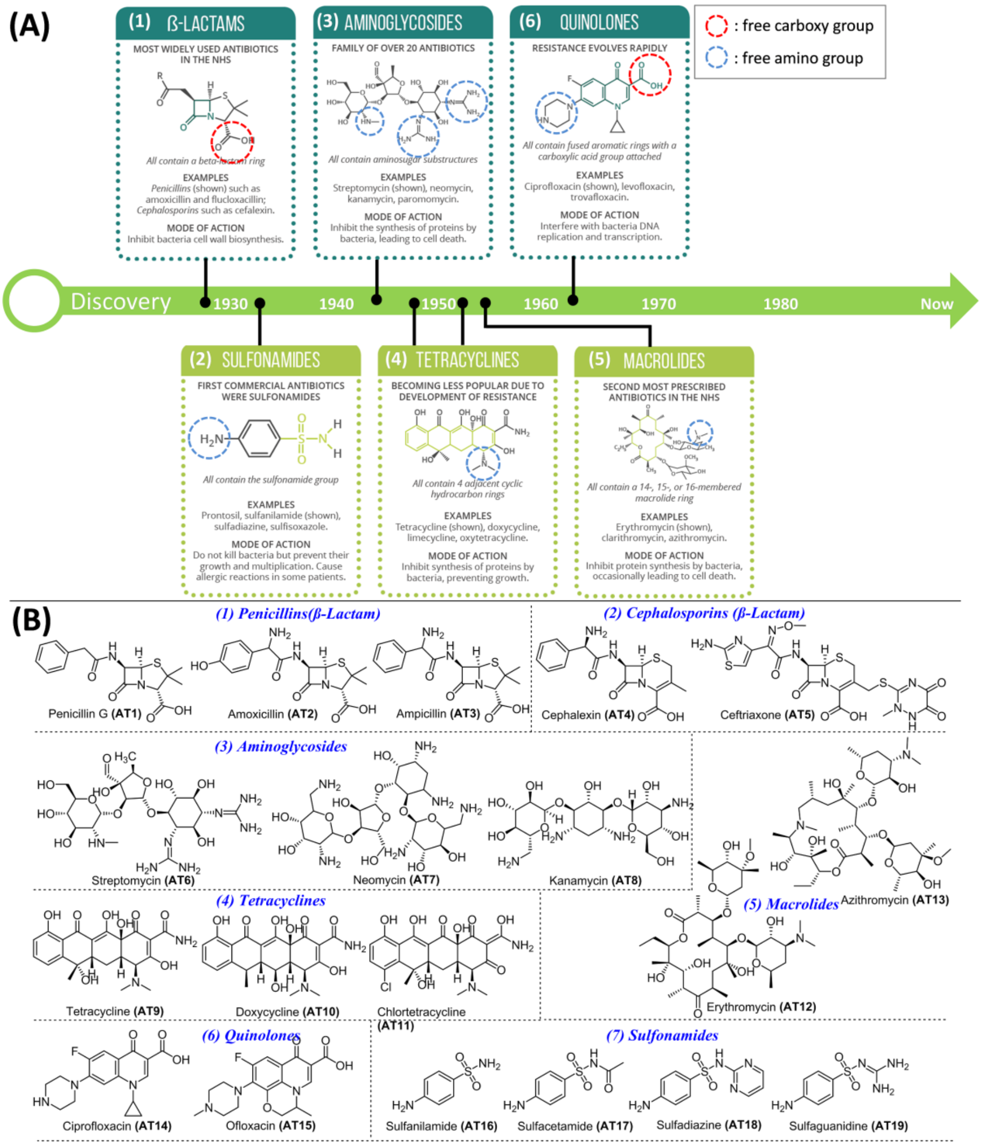

Figure 44. **(A)** Timeline, classification, and structural properties of antibiotics and **(B)** structures, classification of the investigated antibiotics (AT1-AT19).

In this contribution we discriminate 19 different antibiotics (seven different families) as test-bed to train and develop our tongues; antibiotics belong to different structure types for the different families, yet are structurally similar within their families, an ideal test bed. There are aromatic (sulfonamides, quinolones, tetracyclines) antibiotics, then, antibiotics that have at least one aromatic substituent (ß-lactams) and sugar-based antibiotics, such as the macrolides and the aminoglycosides. The desired antibiotic-sensitive tongue could help to uncover potential drug fraud or falsification, as the price differences in penicillin can reach a factor of >300 per prescribed unit (amoxicillin as tablet is cheap, vs. penicillin G benzathin-complex as injectable solution); that, even though the penicillinG-benzathin complex is not patent-protected anymore. A working optical tongue for antibiotics is also of potential interest if one wishes to perform quality and activity control of these antibiotics as tablet or any other formulation, some of which are quite sensitive towards degradation.

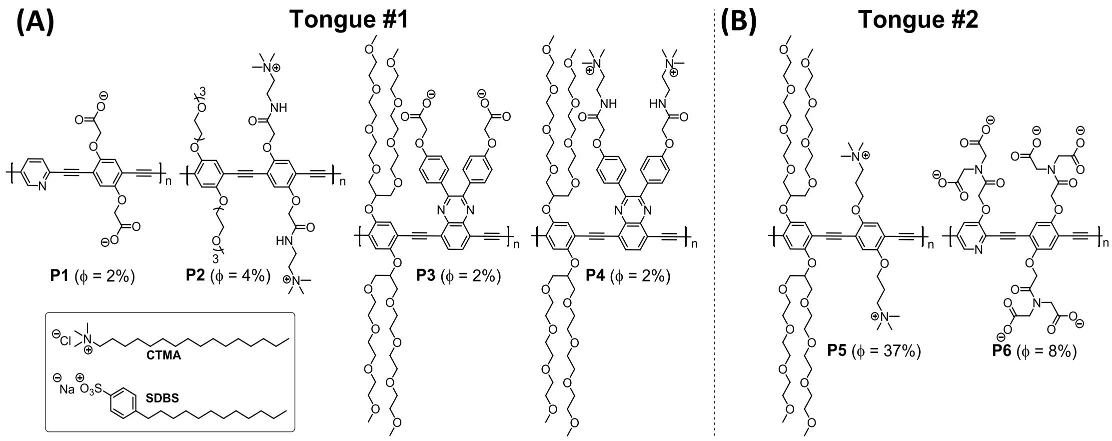

Figure 45. (**A**) Structures and quantum yields (ϕ) of the poly(*para*-aryleneeethynylene)s (PAE) **P1**-**P4** and surfactants CTMA and SDBS employed for construct PAE/surfactant tongue. (**B**) Structures and quantum yields (ϕ) of the poly(*para*-phenyleneethynylene)s PAEs **P5**-**P6** used for construct PAE/PAE tongue.

Table 9. Additional analytical data of **P1**-**P6**.

No.	M_n[a] [g/mol]	M_w[a] [g/mol]	PDI[a]	P_n	$\lambda_{max,abs.}$[b] [nm]	$\lambda_{max,em.}$[b] [nm]	Φ[b] [%]
P1	6.9 x 10^3	1.3 x 10^4	1.9	17	415	536	2
P2	1.1 x 10^4	1.7 x 10^4	1.5	15	404	460	4
P3	2.1 x 10^4	3.2 x 10^4	1.5	13	477	546	2
P4	2.1 x 10^4	3.2 x 10^4	1.5	13	403	550	4
P5	1.4 x 10^4	5.5 x 10^4	3.9	11	410	459	37
P6	1.1 x 10^4	1.8 x 10^4	1.5	12	390	443	8

[a] determined by gel permeation chromatography of the corresponding organosoluble precursors; [b] measured in KH_2PO_4/Na_2HPO_4 buffer solution.

Figure 43B shows the five types of chemical tongues we designed, tongue #1 is a fluorescence turn-on sensor array with 24 sensing elements composed of PAEs and surfactants according to the electrostatic interaction (Figure 45A); tongue #2 is a fluorescence turn-off sensor array with 6 sensing elements, which is composed of a highly fluorescent PAE and a quencher PAE according to the electrostatic interaction (Figure 45B); tongue #3, a combination of tongue #1 and #2; and tongue #4, the most responsive elements of tongue #1 and #2; tongue #5 are the sensor array composed of all PAEs we used. Figure 45A shows the selection of the four conjugated polymers employed in the construction of the tongue #1. Their fluorescence quantum yield is fairly low. The additional analytical data of **P1**-**P6** were shown in Table 9. For the construction of working tongue elements consisting of a polymer/surfactant combination (tongue #1), we screened seven kinds of surfactants with different properties (such as small molecular surfactant, biomolecular surfactants, and cationic surfactants, neutral and anionic surfactants). As shown in Figure 46A, we applied different surfactants in excess concentration to our fluorescent polymers in this study. The surfactant with the highest fluorescence enhancement was selected for the construction of our tongue. Finally, CTMA and SDB-sodium were employed for our complexes.

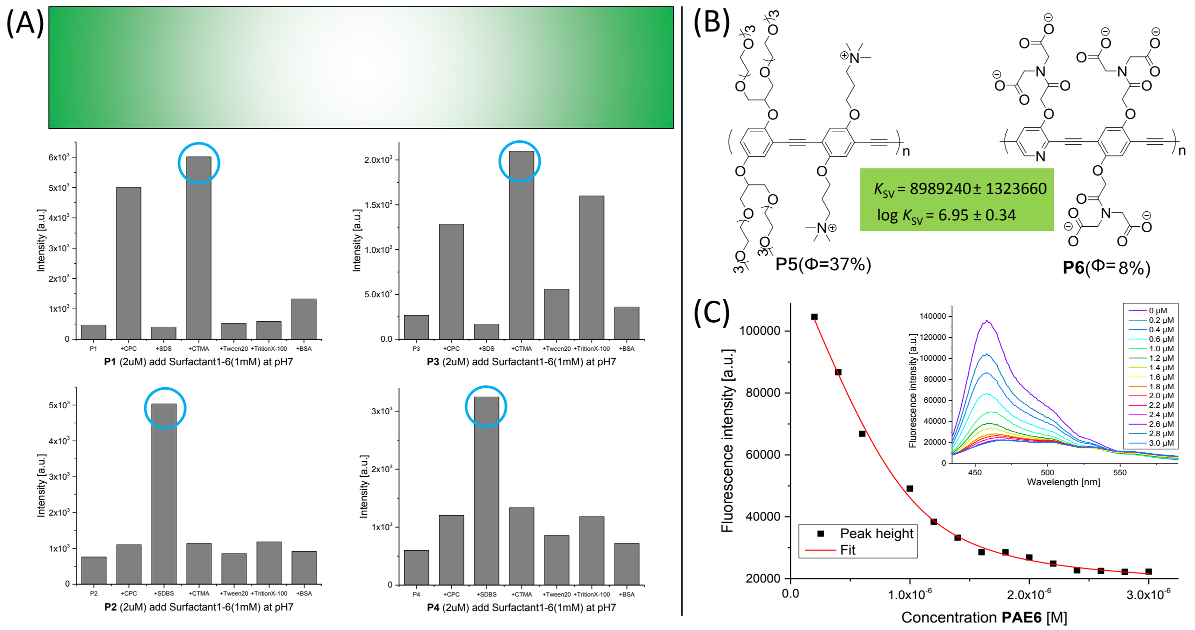

Figure 46. (A) Screening with seven kinds of surfactants for the construction of PAE/surfactant tongue (tongue #1), the fluorescence of PAE strongly enhanced after complexing with oppositely charged surfactants. (**B**) Structure of PAEs for tongue #2. **(C)** Titration of highly fluorescent PAE **P5** with quencher **P6** for the construction of PAE/PAE tongue (tongue #2).

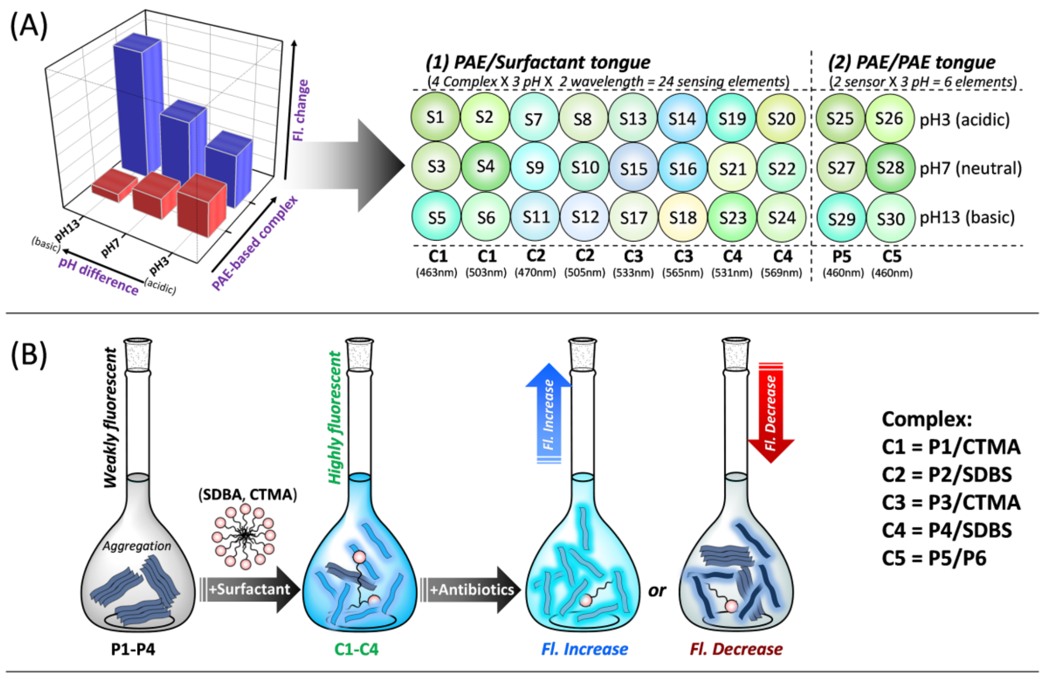

Figure 47. (**A**) Components of PAE/surfactant tongue and PAE/PAE tongue. (**B**) Systematic illustration of PAE/surfactant tongue and fluorescence modulation after adding antibiotics. The contents of the polymer and surfactant are: **C1** = **P1** (2μM) + CTMA (200 μM), **C2** = **P2** (2μM) + SDBS (300 μM), **C3** = **P3** (2μM) + CTMA (100 μM); **C4** = **P4** (2μM) + SDBS (200 μM), **C5** = **P5** (0.5 M) + **P6** (0.25 μM).

The analytes we selected for sensing consist of seven families of commercially available antibiotics. Of each type two or three examples, structurally similar to one another, were selected as member of the analyte pool for discrimination (Figure 44). Figure 47A highlights the construction of the fluorescent chemical tongues. Tongue #1, consisted with four complexes (**C1-C4**), was prepared by treating the almost non-fluorescent solutions of the PAEs **P1-P4** with counter charged surfactants, C1 = P1 (2μM) + CTMA (200 μM), C2 = P2 (2μM) + SDBS (300 μM), C3 = P3 (2μM) + CTMA (100 μM); C4 = P4 (2μM) + SDBS (200 μM); a significant fluorescence increase is observed with the addition of surfactants. Tongue #2 was constructed by one highly fluorescent **P5** and weakly fluorescent **P6** (act as quencher). Systematic illustration of possible mechanism were shown in Figure 47B, the addition of charged antibiotics disrupted the PAE-surfactant complexes and lead to the fluorescence change.

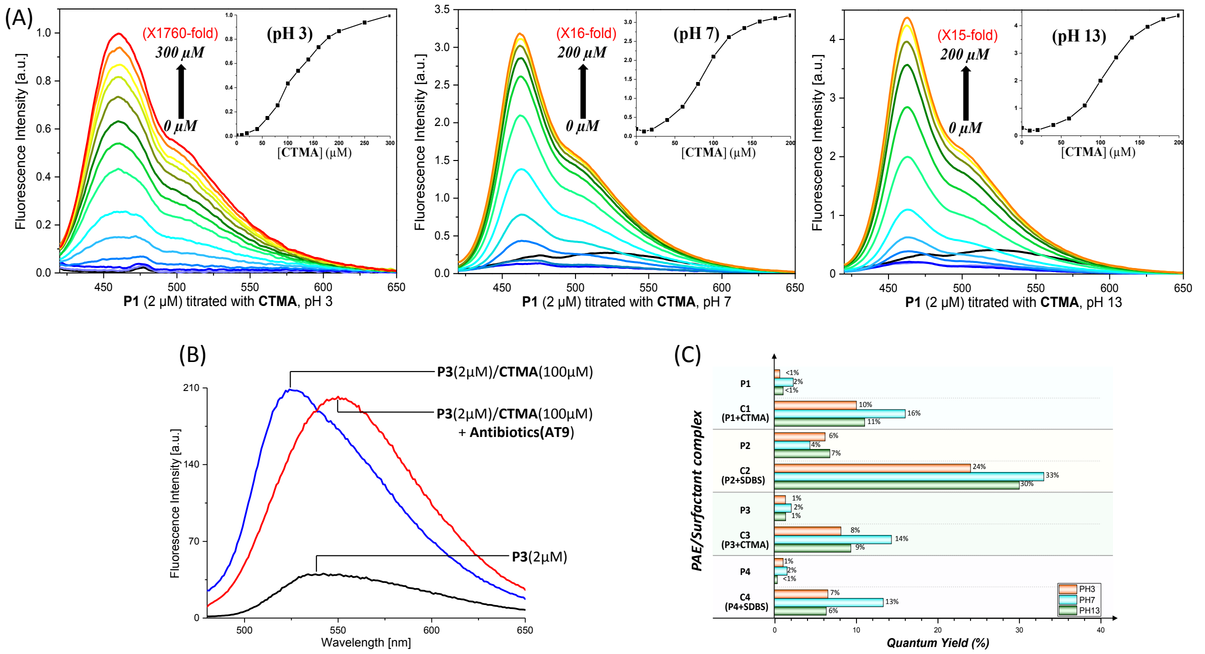

Figure 48. (A) P1 (2 μM, black line) titrated with CTMA at pH 3, pH 7, and pH 13. Inserted graph shows the change of I_{Fl} (463 nm) with increasing CTMA concentration (similar titrations of the other PAE P2-P4 can be found in the ESI†). Applying higher concentrations of surfactant than indicated did not elevate the fluorescence further. **(B)** Fluorescence intensity properties of PAE, PAE/surfactant and PAE/surfactant + antibiotics are shown; two wavelengths for detection were selected (pH 13). **(C)** Quantum yield of P1-P4 before and after adding the surfactant (pH 3, pH 7, pH 13), each value is from the average of two measurements.

Figure 48A shows an example titration of **P1** (concentration 2 μM) with cetyltrimethylammonium chloride (**CTMA**) at different pH values. Upon addition of the 100-fold amount of the **CTMA** at pH 7 (concentration 200 μM, below the critical micelle concentration (CMC) of **CTMA** (1.85 mM), the fluorescence intensity of **P1** increased by a factor of 16. The fluorescence increase is observed at pH 3, pH 7 and pH 13, even though the end quantum yields are lower, particularly when working at pH 3. That is not surprising, as the carboxylate units of **P1** must be protonated at pH 3, and the positively charged CTMA can not interact as strongly with the carboxylic acid as it does with the carboxylate. For the other polymers, **P2-P4** (at pH 3, pH 7, and pH 13) a similar increase in fluorescence intensity is observed (details see Figure 132). **P4**´s fluorescence quantum yield is vanishingly small in aqueous solution at pH 13. Upon addition of a 100 fold excess of sodium dodecylbenzenesulfonate (SDBS), the quantum yield is significant. Surfactochromic behavior, an effect described by Lavigne et al., is operative.[195]

2.4.2 Results and Discussions

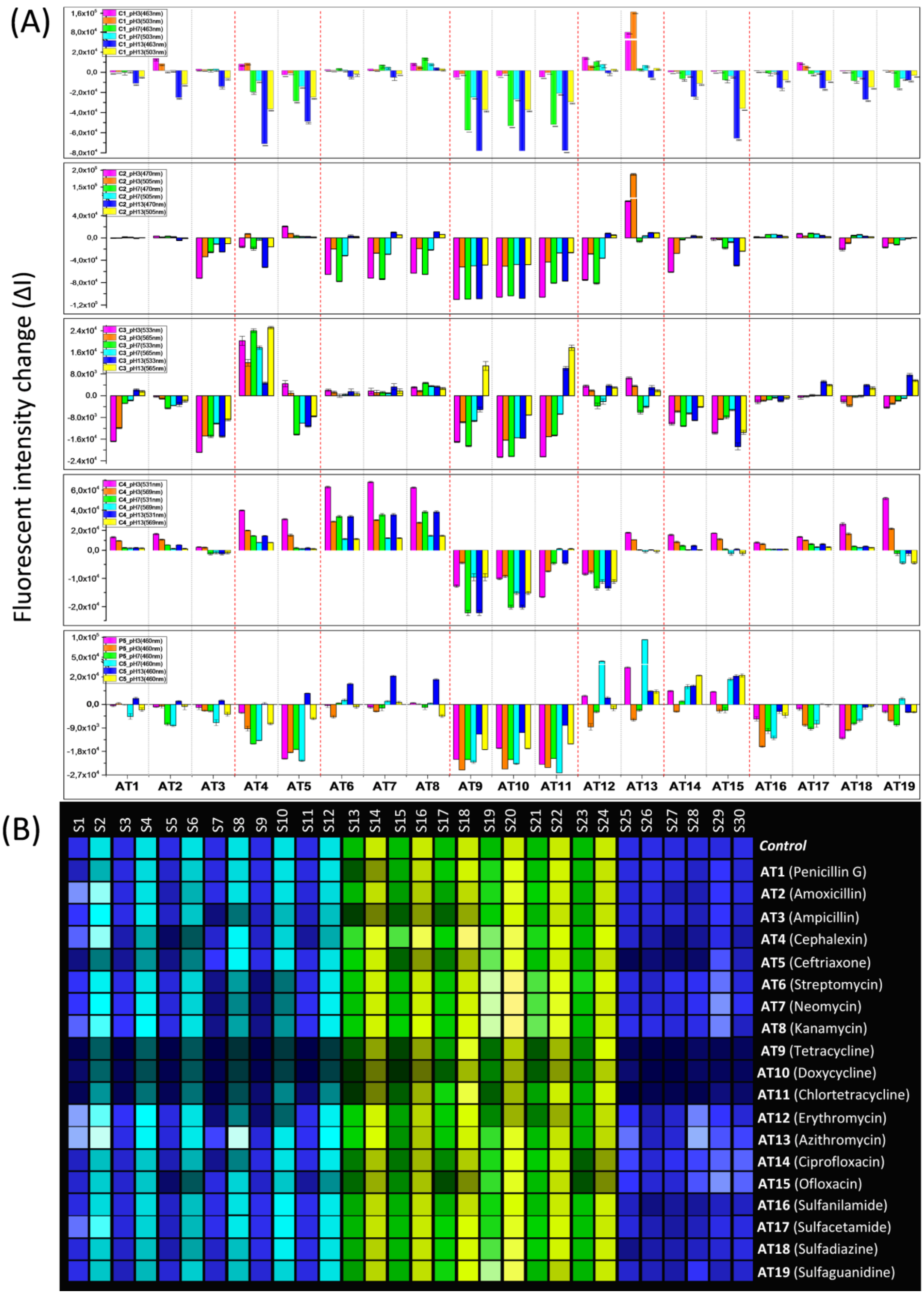

Figure 49. (A) Fluorescence response pattern ΔI obtained by C1-C4 (2 µM, at pH3, pH7 and pH13, buffered) and P5, C5 (0.5 µM, at pH 3, pH 7 and pH 13, buffered) treated with antibiotics AT1-AT19 (c = 5 mM). Each value is the average of six independent measurements; each error bar shows the standard error of these measurements. The black dotted line shows the type of each antibiotic, red dotted line shows the seven families of antibiotics. (**B**) The visual map (heatmap) for the fingerprint the 19 antibiotics with 30 sensor elements.

In the following experiments, we treated the surfactant-PAE-complexes with the different antibiotics (AT1-AT19, 5 mM), a response pattern (Figure 49A) and a visual map (heatmap, Figure 49B) were obtained. We measured the fluorescence intensity upon addition of the analytes at two different wavelengths (463 and 503 nm for C1, 470 and 505 nm for C2, 533 and 565 nm for C3, 531 and 569 nm for C4, typical example see Figure 48B), as the addition of the 5 mM solution of the antibiotics does not only modulate the fluorescence intensity but also has ratiometric elements.

We found that differential quenching results at different wavelengths. In the bottom panel we employed a second tongue, consisting of **P5** and its complex **C5** at three different pH-values, a simple six-element control tongue that does not have any surfactants added. The red dotted line classified the antibiotics into seven families. Similar fluorescence responses result for structurally similar antibiotics within each family. Particularly for tetracyclines (**AT9-AT11**), strong fluorescence quenching was found for *all* of the sensor elements (S1-S30). That is reasonable because the extended aromatic system made these species yellow and nonfluorescent in water and quenched the fluorescence of *all* of the sensor polymers.

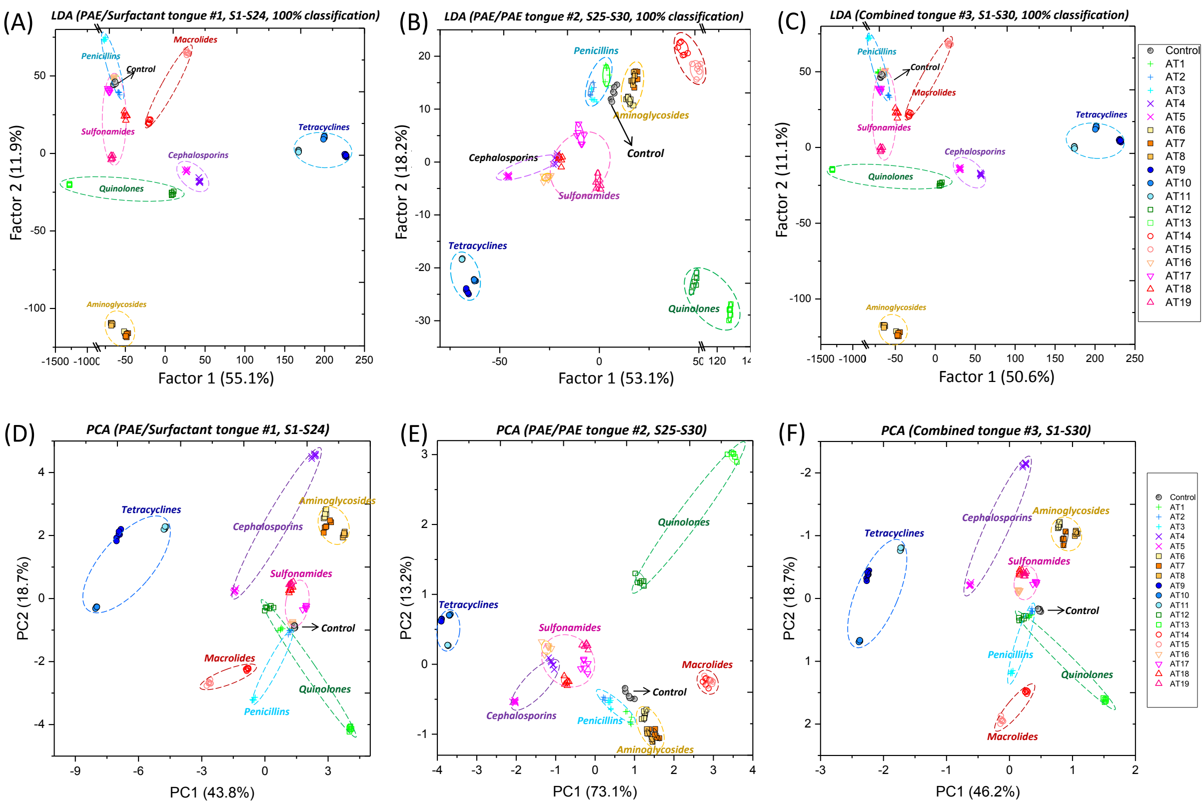

Figure 50. 2D LDA canonical score plot for the first two factors obtained with an array of (**A**) S1-S24 (left, PAE/surfactant tongue #1), (**B**) S25-S30 (right, PAE/PAE tongue #2) and (**C**) the combined tongue of S1-S30 (bottom, tongue #3) treated with antibiotics AT1-AT19 (c = 5 mM) with 95% confidence ellipses. 2D PCA plot for the first two principal component obtained with an array of (**D**) S1-S24 (left, PAE/surfactant tongue #1), (**E**) S25-S30 (right, PAE/PAE tongue #2) and (**F**) combined tongue of S1-S30 (down, tongue #3) treated with antibiotics AT1-AT19 (c = 5 mM) with 95% confidence ellipses. Each point represents the response pattern for a single antibiotic to the array. Each antibiotic was shown with their individual shape (triangle, square, circle etc.) and similar color. Each point represents the response pattern for a single antibiotic to the array. After combining the two tongues, the result looks similar to the result gathered from the first tongue (left), and inefficient but somewhat improved discrimination endures.

The raw fluorescence intensity change data were evaluated by the statistical method of linear discriminant analysis (LDA) and by principal component analysis (PCA). Both methods are widely used for the workup of data from sensor-fields. Figure 50 A-C shows the LDA plots of the two different tongues (top) when the data from Figure 49 are processed.

Depicted in grey is the control (Figure 50 A-F), i.e. if only water is added as analyte. Either of the two tongues is reasonably well capable of discriminating the antibiotics, even though they result in different LDA-plots. Surprisingly, the quality of the separation and discrimination does not change much upon the combination of the two different tongues into a larger tongue containing 30 elements. We performed principal component analysis (Figure 50 D-F) on the data and also find a reasonable separation with the single tongues but also with the combined tongue, even though the result seems more like the one gleaned from the first tongue (left); both PCA and LDA work well.

(1) *PAE/Surfactant tongue*

PCA sensor element		PC1 (43.8%)	PC2 (18.7%)	PC3 (11.9%)
S1	(C1_Ph3_463nm)	2.111	3.903	14.046
S2	***(C1_pH3_503nm)***	1.082	4.117	***15.746***
S3	(C1_pH7_463nm)	7.035	1.907	2.759
S4	(C1_pH7_503nm)	7.120	1.972	1.290
S5	(C1_pH13_463nm)	6.113	1.537	2.356
S6	(C1_pH13_503nm)	5.413	1.568	1.041
S7	(C2_pH3_470nm)	3.357	7.736	2.720
S8	(C2_pH3_505nm)	2.482	5.912	12.734
S9	(C2_pH7_470nm)	2.398	6.204	0.026
S10	(C2_pH7_505nm)	2.999	4.895	0.197
S11	(C2_pH13_470nm)	7.266	1.913	2.530
S12	***(C2_pH13_505nm)***	***7.746***	1.350	1.124
S13	(C3_pH3_533nm)	5.179	2.142	2.577
S14	(C3_pH3_565nm)	5.145	2.251	2.411
S15	(C3_pH7_533nm)	5.372	4.275	0.854
S16	(C3_pH7_565nm)	4.495	5.864	1.494
S17	(C3_pH13_533nm)	2.429	5.127	4.650
S18	***(C3_pH13_565nm)***	0.078	***10.948***	11.670
S19	(C4_pH3_531nm)	4.212	3.326	4.123
S20	(C4_pH3_569nm)	4.772	2.336	3.334
S21	(C4_pH7_531nm)	4.938	3.119	5.416
S22	(C4_pH7_569nm)	4.698	3.169	2.535
S23	(C4_pH13_531nm)	3.079	4.722	0.183
S24	(C4_pH13_569nm)	0.480	9.707	4.184

Contribution of the variables (%)

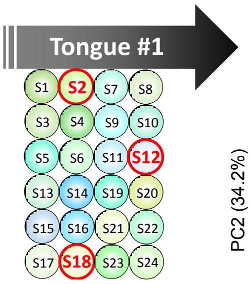

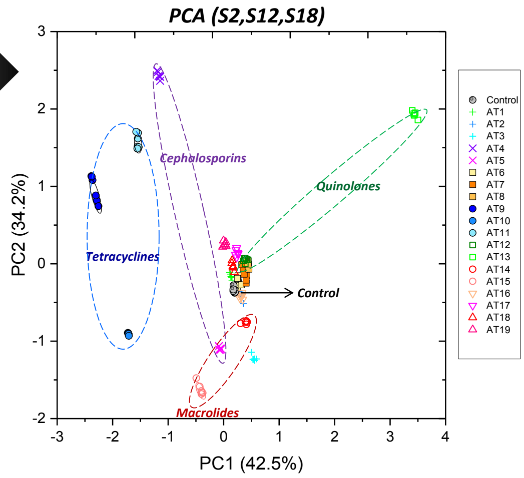

(2) *PAE/PAE tongue*

PCA sensor element		PC1 (73.1%)	PC2 (13.2%)	PC3 (7.1%)
S25	***(P5_pH3_560nm)***	***19.35***	12.82	3.16
S26	(P5_pH7_560nm)	16.72	15.76	26.73
S27	(P5_pH13_560nm)	19.30	6.35	10.39
S28	***(C5_pH3_560nm)***	12.51	***52.77***	0.00
S29	***(C5_pH7_560nm)***	14.88	12.27	***38.79***
S30	(C5_pH13_560nm)	17.23	0.02	20.93

Contribution of the variables (%)

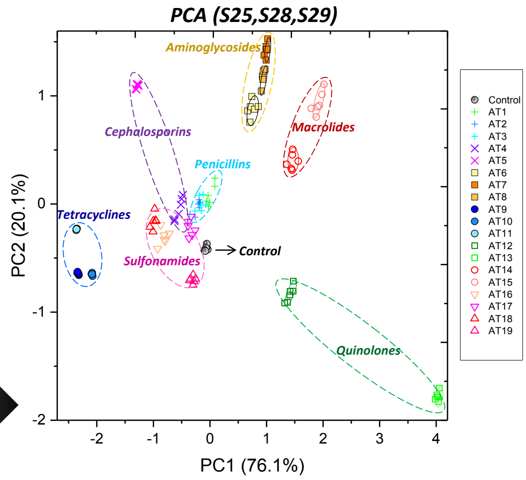

Figure 51. Optimization and selection of the best three sensing elements from the PAE/surfactant tongue (S1-S24) and PAE/PAE tongue (S25-S30) based on the contribution of the variables of PCA. The resulting PCA plots were shown.

Contrary to LDA, PCA allows analysis of the discriminating factors, which in this heterogeneous yet well-defined analyte library does not correspond to an easily explainable physicochemical property. Some of the sensor elements are much better at discriminating the analytes than others. The fluorescence response of the antibiotic analytes towards 24 sensing elements (S1-S24, tongue #1) was evaluated using PCA (Figure 51, top); the first three principal components (PC1-PC3) represent 74%

(43.8%+18.7%+11.9%) of the total variance. For each principal component (PC1-PC3), S12 contributes the most to PC1, S18 contributes the most to PC2, and S2 contributes the most to PC3. Thus, S2, S12 and S18 of the new tongue are the most responsive elements. Similarly, for tongue #2 (Figure 51, bottom, S25-S30), PCA was applied, S25, S28 and S29 make the most contribution to the first three PCs, respectively, which are also selected into the new, pruned tongue. Both pruned tongues give a somewhat reasonable discrimination, tongue #2 more so than tongue #1.

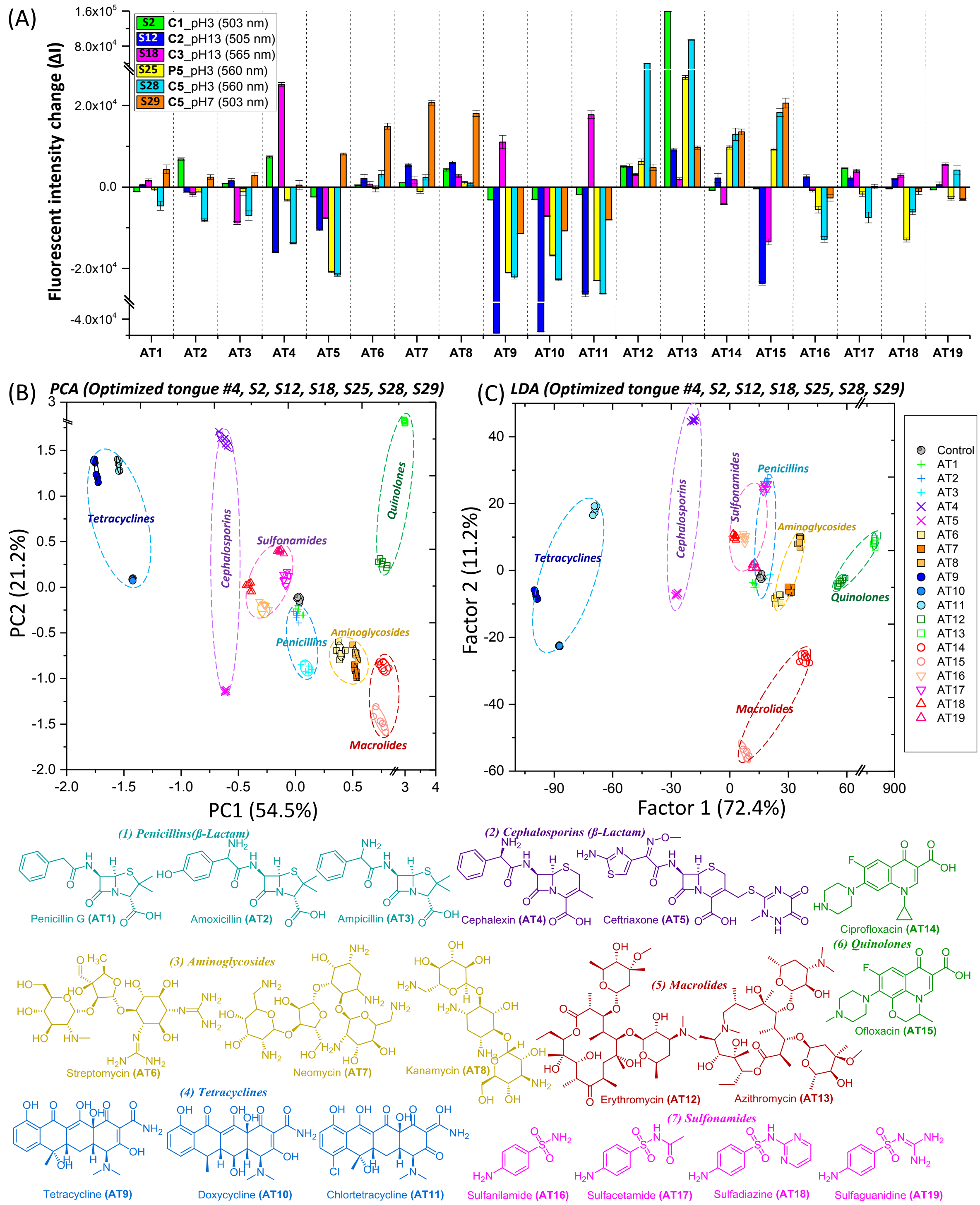

Figure 52. **(A)** Fluorescence response pattern ΔI obtained by the pruned tongue (S2, S12, S18, S25, S28, S29) **(B)** Combined PCA plot from the optimized six sensing factor (see Figure 9). **(C)** Combined LDA plot from the optimized six sensing factor, all antibiotics can be classified and clustered depend on the antibiotics types. Cross-validated LDA showed 100% correct accuracy for all antibiotics.

Once we performed data analysis (PCA) with the six best elements from both parental tongues we see (Figure 52) that all of the antibiotics are discriminated. When the same data are processed using LDA, the result is a bit different (Figure 52C). The penicillins and the sulfonamides are not well separated, particularly amoxicillin and sulfacetamide are almost non-separable, and sulfaguanidine is in the area where one would expect penicillins. PCA resolves the data. The pruned tongue is better than the tongue in which *all* elements of both of the original tongues are present. Removal of the low responding sensor elements improves the quality of the overall tongue by weeding out elements that contribute to the noise but not to the signal.

Which of the elements are the most successful for the construction of the pruned tongue? From tongue #1 S2 (**P1** complexed with CTMA, pH 3), S12 (**P2** complexed with SDBS, pH 13) and S18 (**P3** complexed with CTMA, pH 13). From the tongue#2 S25 (**P5**, pH 3), S28 (**P5**, pH 13) and S29 (C5 from **P5**/**P6**, pH 7) are the elements with the most discriminatory power. We observe that the anionic polymers unfold their discriminatory prowess at strongly basic conditions. Under those conditions some of the analytes might be not stable but hydrolyze, such as the lactam antibiotics. That, however, is not an issue; the hydrolyzed species are discriminated. As we have no problems with reproducibility, the hydrolysis is either very fast or too slow to interfere with the measurements.

Based on the successful selection process of pruned tongue #4 and positive results of antibiotics discrimination with such sensor array, we further carried out a semi-quantitative assay to identify antibiotics with various concentrations (from 0.05 mM to 5 mM). The fluorescence modulation data of AT11, AT12 and AT15 were recorded and calculated with LDA, which converts the training matrix (6 factors × 7 concentrations × 3 replicates) into canonical scores. The first three canonical factors represent 93% of the total variation. The jackknifed classification matrix with cross-validation reveals 100% accuracy. As shown in Figure 53 - Figure 54, the concentration is linearly mapped in the LDA plot, clear discrimination dependence on the concentration of AT11, AT12 and AT14 were observed. The results suggesting that the array should allow for a rigorous quantitative detection.

So far, we have established different tongues (tongue #1 with 24 sensing elements; tongue #2 with 6 sensing elements; tongue #3, combination of tongue #1 and #2; and tongue #4, the most responsive elements of tongue #1 and #2), each of which generates unique responses for the studied antibiotics. Effectively, combination of these responses in each data set (i.e order of entry into the data matrix) represents the structure of data used to generate the desired classifications. Within each tongue, a large number of unique responses (i.e., diverse data orderings) are possible.[196] The small number of replicates in these data sets, coupled with the possibility of having significant distortions caused by potential outliers and different data orders, raises questions about the robustness of the LDA classification results. Bootstrapping[197] is a statistical re-sampling method that can be used to explore these concerns by measuring the variability of the LDA solution spaces. In bootstrapping analyses, each data set is randomly sampled (with replacement) numerous times; each resulting sample is treated as another data set that could reasonably be obtained in the experiment. Overall, this statistical technique provides insights into the robustness of the LDA results from different combinations of observations in the dataset.

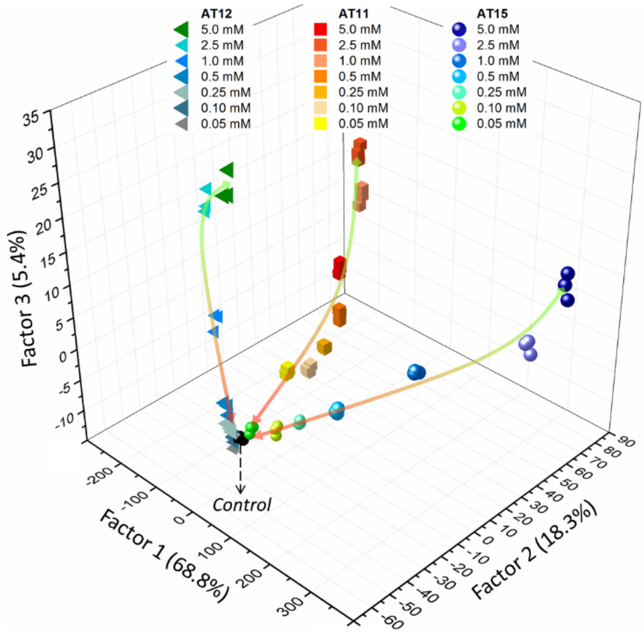

Figure 53. 3D canonical score plot for the semi-quantitative assay of antibiotics (AT11, AT12 and AT15) with the pruned tongue #4, cross-validated LDA showed 100% accuracy.

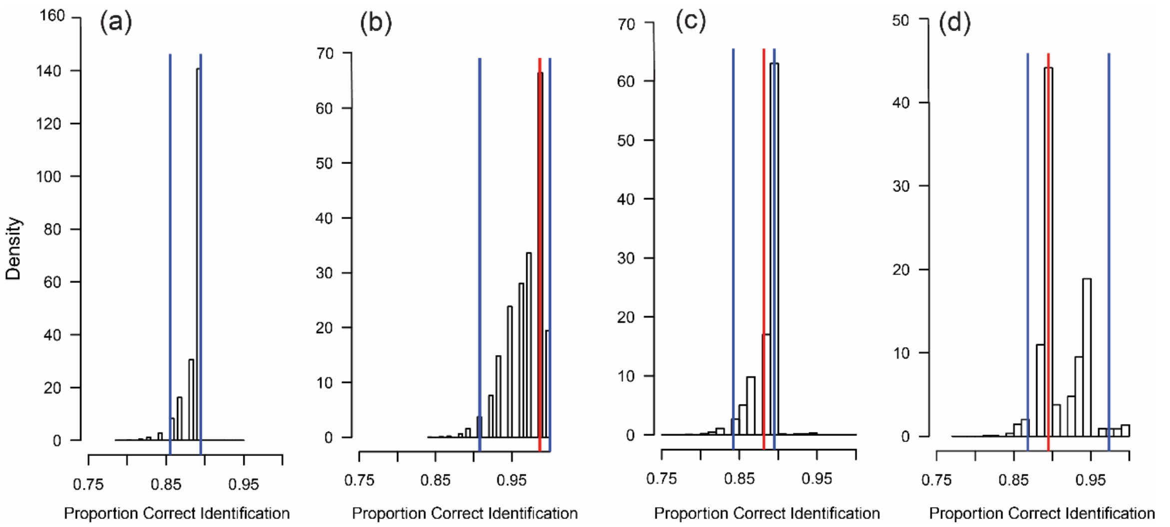

Figure 54. Distribution of proportion of correctly identified unknowns (CIU) obtained through the analysis of 20,000 bootstrapped samples of each data set from different tongues. (a) Tongue #1; (b) Tongue #2; (c) Tongue #3 (Tongue #1 & #2); (d) Tongue #4 (most responsive elements of tongue #3). The red line shows the CIU for the original data set without bootstrapping. The blue lines represent the CIUs of the 2.5th and 97.5th percentile of the data.

Table 10. Proportion of CIU of the 2.5th and 97.5th Percentile of the Bootstrapped Results Along with the CIU of the Original Data Set (Without Bootstrapping).

	Original data set	2.5th percentile	97.5th percentile
Tongue #1	89.47	85.53	89.47
Tongue #2	98.68	90.79	100
Tongue #3	88.16	84.21	89.47
Tongue #4	89.47	86.84	97.37

An analysis of 20,000 stratified bootstrapped samples was conducted for each separate tongue (collaboration with Prof. Vincent M. Rotello and Prof. Caren M. Rotello). With stratified sampling, each sample has the same size as the original data, as well as the same number of samples within each training class. For each bootstrapped sample, the best-fitting LDA solution was obtained and the proportion of correctly identified unknowns (CIU) was calculated using a specially written R script. When identifying the unknowns, we used only the first three discriminants because they account for more than 95% of the variance in our original data sets. Figure 54 shows the histograms of the classification accuracies of the unknowns across the 20,000 bootstrapped samples for each different tongue. The red line represents the CIU for the original dataset and the blue lines represent the CIUs of the 2.5th and 97.5th percentile for which 95% of the bootstrapped data is covered. These values have been tabulated in Table 10.

The bootstrapping results reveal that the accuracy of unknown identification is highly dependent on the structure of the training set. In effect, bootstrapped data sets can be obtained across all tongues with substantial variability in the CIU values. The probability of obtaining specific CIU values varies across the 20,000 bootstrapped samples, as shown by the heights of the bars in Figure 54. Therefore, the bars with the highest density reflect the most frequent outcomes of the system and thus they can provide a test bed for recognizing the most reliable and consistent combinations. Accordingly, original CIU values that fall in high-density regions of the histogram are results similar to those that would be expected in replication studies; original CIU values that fall in low-density regions would not necessarily replicate. The effect of noise in the measurements is to increase the range of possible CIU values, resulting in wide histograms. Overall, this strategy could be considered as a potential route for substantially improving the classification performance reliability of array-based sensors.

2.4.3 Conclusions

Simple surfactants modulate and increase the fluorescence of ionic PAEs and PPEs. The formed constructs are sensor elements for opto-electronic tongues and discriminate antibiotics. Important is **a**) five different polymers create a library of 30 different elements. Changing the investigated emission wavelength, the pH-value, and the addition of oppositely charged surfactants modulates the response of the sensor elements into an efficient tongue. **b**) Using PCA, the six most important contributing elements were selected to give a pruned filial tongue with an improved overall response towards all of the investigated antibiotics.

Quo vadis lingua optoelectronica? Manipulation and modulation of the response of tongue elements reaches far beyond changes in chemical structure and sequence of the employed polymers. Changes of pH, observation wavelength, and addition of surfactants modulate the response of the sensor elements towards analytes, here, antibiotics. The "naive" tongue, i.e. one where the polymers **P1**-**P5** are employed at physiological pH (Figure 55) displays large error bars and (Figure 55 B-C) does not reliably discriminate the antibiotics; *modulation unlocks the full potential of the sensor elements*. We have only started to scratch at the surface of a multidimensional space, where observation wavelength, temperature, pressure, pH, simple additives and change of solvents and/or a combination of all of the above render small libraries of conjugated polymers all-powerful and omni-capable of discerning and discriminating any analyte available in more than mg-quantities. Questions of sparse data and big data as well as data processing are increasingly critical to answer the question of the definition of minimally necessary structural changes of the sensor elements to discriminate analytes. Prediction of the pattern observed in LDA is currently not possible, and the axes of variation cannot be attributed to simple properties (electrostatic interactions + hydrogen bonding + hydrophobicity + nucleophilicity + Pi-Pi stacking +….+…) that are operative. Consequently, construction of suitable minimalist tongues is purely empirical. When larger data amounts are amassed and different concepts are explored, further analysis shall allow formulating rules for construction of these highly interesting and ultimately powerful optoelectronic tongues.

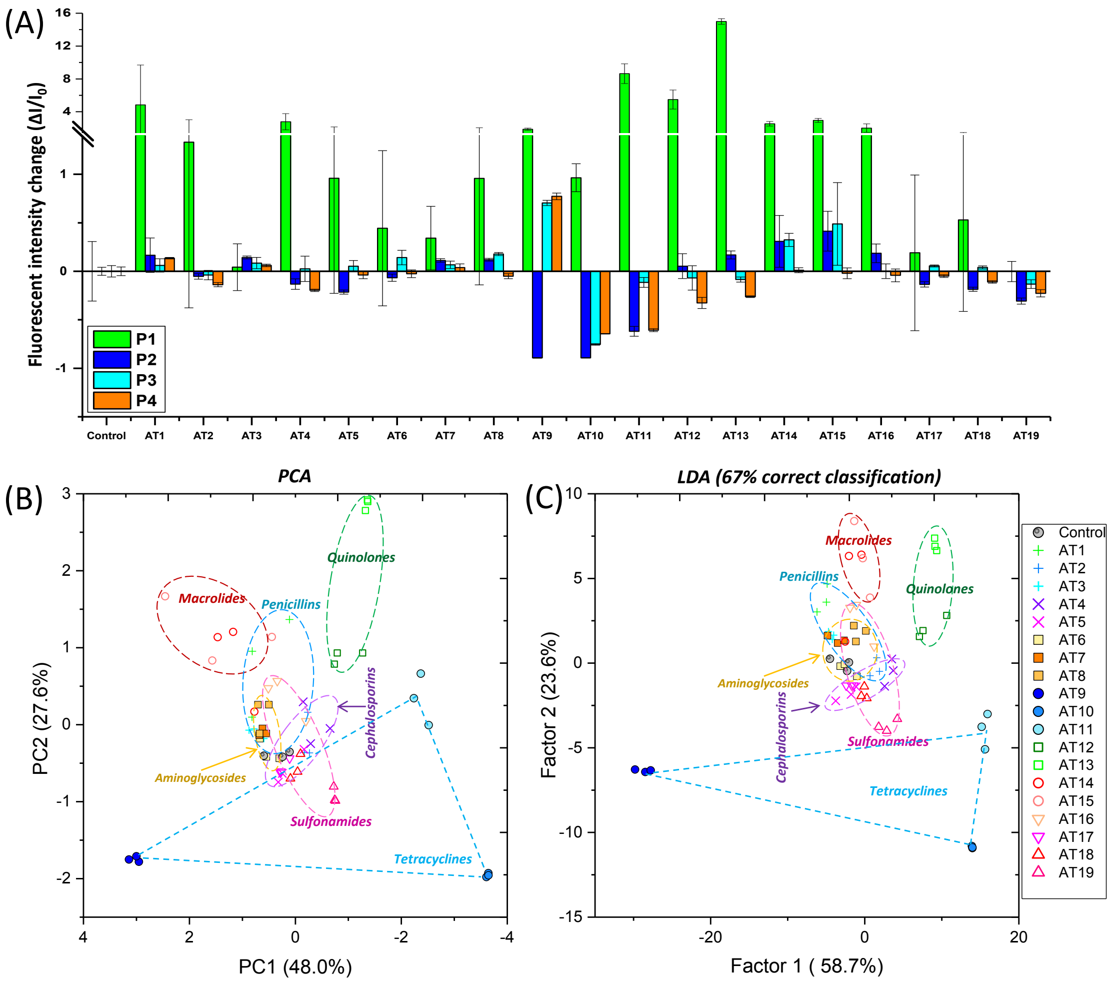

Figure 55. (A) Fluorescence intensity change $\Delta I/I_0$ obtained by weakly florescent **P1-P4** (2 µM, at pH7, buffered) treated with antibiotics AT1-AT19 (c = 5 mM). Each value is the average of three independent measurements; each error bar shows the standard error (SD) of these measurements. **(B)** PCA plot and **(C)** LDA plot from first the first two factors obtained with P1-P4 (2 µM, at pH7, buffered) treated with antibiotics AT1-AT19 (c = 5 mM). Cross-validated LDA showed 67% correct accuracy for all antibiotics.

Chapter 3. PAE-Based Chemical Tongue for the Identification of Complex Analytes

3.1 Discrimination of White Wines with Two Oppositely Charged Poly(*p*-phenyleneethynylene)s and Their Complex

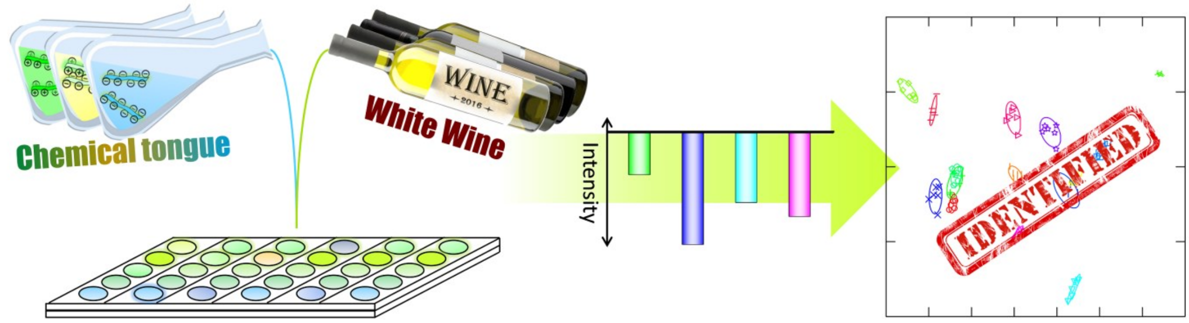

Figure 56. Systematic illustration of PAE-based chemical tongue for fingerprinting white wine.

In this Chapter, we present a simple array composed of an anionic and a cationic poly(*para*-phenyleneethynylene) (PPE) together with their electrostatic complex. The PPEs and their complex are employed in the sensing of white wines at pH 13; the complex is also successfully employed as a sensor element at pH 3. The sensing mechanism is fluorescence quenching. We discriminate thirteen different wines by this chemical tongue, consisting of four elements. The fluorescence quenching is not induced by the major components of the wines. Acids, sugars, alcohols, etc. alone do not quench the fluorescence, but the colored tannins and other polyphenols contained in wine are the main quenchers. The major constituents of wine significantly modulate the quenching of the PPEs by the tannins though.

3.1.1 Construction of Chemical Tongue

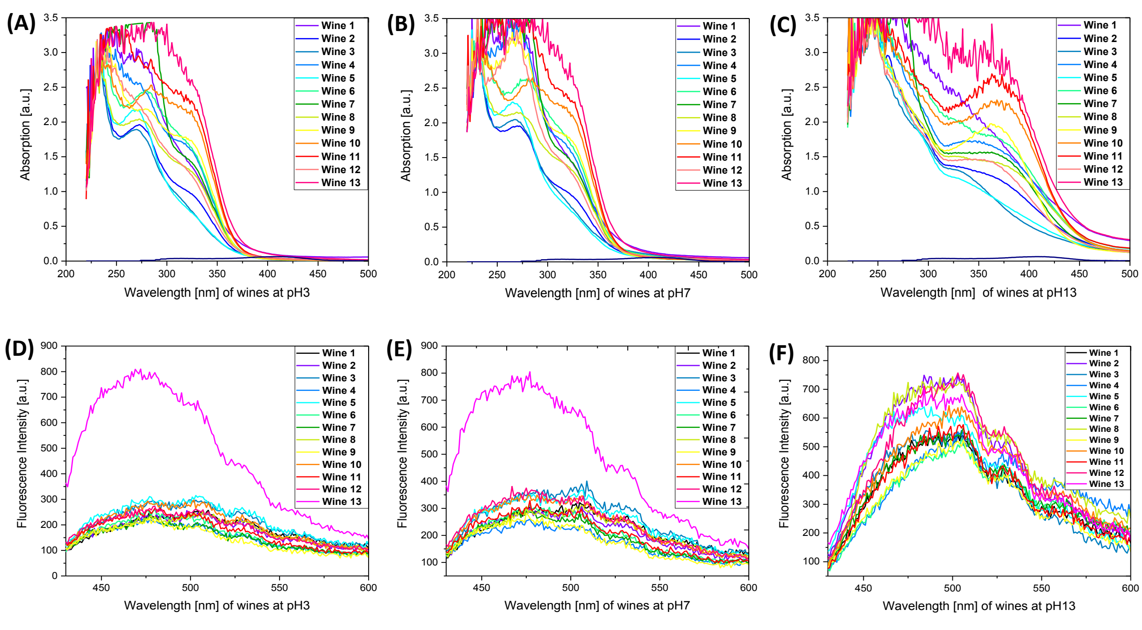

Figure 57. Absorption spectra of white wine samples **Wine 1-13** at pH 3 **(A)**, pH 7 **(B)** and pH 13 **(C)**. Emission spectra of white wine samples **Wine 1-13** at pH 3 **(D)**, pH 7 **(E)** and pH 13 **(F)**.

In this contribution we disclose a simple array formed from two conjugated polyelectrolytes (one polyanionic, one polycationic) and its electrostatic complex; these three elements discern white wines at pH 13 and pH 3 in a fluorescence quenching-based assay. Wine, fermented grape juice, is a complex mixture of sugars, acids, minerals, proteins and natural dyes in a composition that varies but resembles the values shown in Figure 58D. Alcohol (10-16.5 vol%) and sugar content vary greatly, so do the amount and type of acids present in wines. Typical white wines are acidic with a pH range of 3.0-3.3.

Wines are perfect test beds for the power of small arrays of colorimetric or fluorescence sensor arrays. **a)** There are thousands of different wines **b)** wine as an analyte is available in abundance (0.75 L/unit) **c)** wines can be grouped by grape varietal/blends of grapes, country and area of origin, producer, used (designer) yeast, vintage, cooperage, etc. **d)** wine is a complex mixture of compounds, a significant number of which are present in trace amounts – perhaps not even known. They are metabolites of the yeast and probably reach into the thousands, giving the specific body, taste and smell to the wine.

This complexity renders wines different from each other, consequently one should be able to "fingerprint" wines with respect to their composition. High priced wines have been counterfeit and re-labeled, an annoying problem, particularly for cult-wines. An example for fakes are the Jefferson bottles of Bordeaux wines, purportedly produced for the third president of the US.[198] Addition of cheaper wines or also juice from non-allowed grape varietals to fermenting wines of the Brunello or Burgundy type are tricks of the trade to increase the profit (Brunellopoli scandal, or Brunellogate)[199] of the producers and gouge unsuspecting consumers; consequently, simple fingerprint tests that use small amounts of wine (less than 5 mL) would be attractive.

Table 11. Detailed information of the thirteen different white wines used in this study.

Wine	White Wine	Origin	Vintage	pH	Sugar	EtOH content [%]
1	Spätburgunder	Baden, Germany	2014	3.3	semidry	11.5
2	Pinot Grigio	Valdadige, Italy	2014	3.2	dry	12.0
3	Müller Thurgau	Baden, Germany	2014	3.3	semidry	11.0
4	Sauvignon blanc	Western Cape, South Africa	2015	3.1	dry	12.5
5	Chardonnay	Valdadige, Italy	2014	3.0	dry	12.0
6	Grüner Veltliner	Burgenland, Austria	2015	3.1	dry	11.5
7	Riesling	Pfalz, Germany	2014	3.0	dry	11.5
8	Weißburgunder	Baden, Germany	2014	3.2	dry	12.5
9	Riesling	Rheinhessen, Germany	2014	3.0	dry	11.5
10	Riesling	Pfalz, Germany	2014	3.1	semidry	11.5
11	Riesling	Baden, Germany	2014	3.2	dry	12.0
12	Riesling	Baden, Germany	2014	3.1	dry	11.5
13	Riesling	Pfalz, Germany	2012	3.1	smooth/sweet	10.0

Anslyn et al.[123] have developed a ternary colorimetric wine-sensor array, consisting of copper (II) and pyrocatechol violet (CPV) in the presence of different oligopeptides. The addition of flavonoids to these ternary complexes led to a change of absorbance at 444 nm; a handful of the histidine-rich peptide/CPV complexes discern the flavonoids. The same complexes discriminate different red wines, depending upon their grape varietals. In a newer publication Anslyn et al. have even developed a protocol to make predictions about composition of binary blends of grapes in wines.[200]

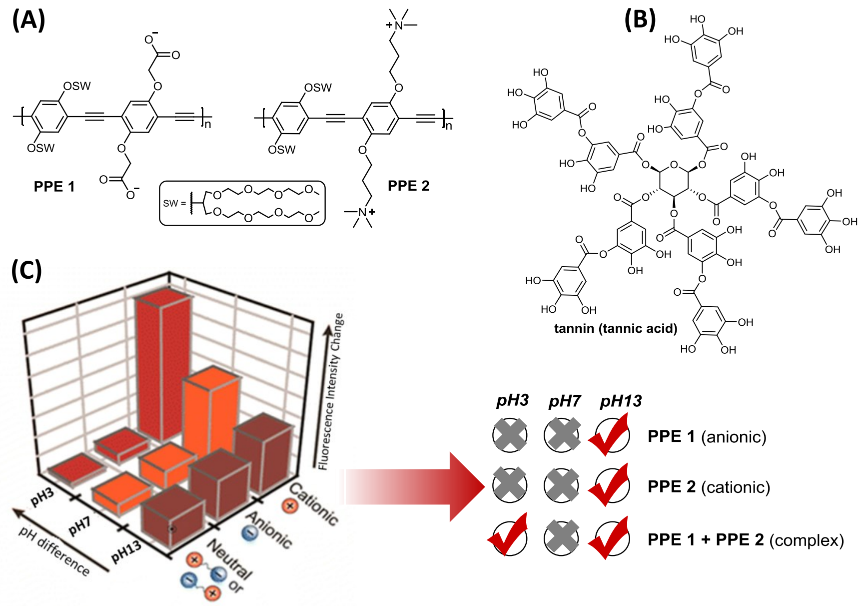

(D)

Type	Ingredient	Content
alcohols	ethanol	11.5 %
	methanol	0.01 %
saccharides:	fructose	7 g/L
	glucose	3 g/L
	glycerol	7 g/L
acids:	malic acid	2 g/L
	tartaric acid	3 g/L
	lactic acid	1 g/L
	citric acid	1 g/L
	acetic acid	1 g/L
vitamins:	vitamin C	0.05 g/L
mineral nutrients:	K^+	1 g/L
	Ca^{2+}	0.1 g/L
	Mg^{2+}	0.1 g/L

Figure 58. (A) Structures of negatively charged **PPE 1** and positively charged **PPE 2**, used for white wine sensing. **(B)** Structure of used tannin (tannic acid). **(C)** Screening of the previously selected PPEs at different pH values. The single PPEs **PPE 1** and **PPE 2** work best at pH13, while the electrostatic complex (**PPE 1** + **PPE 2**) is successful at pH3 and pH13. **(D)** Composition of the Used Artificial Wine.

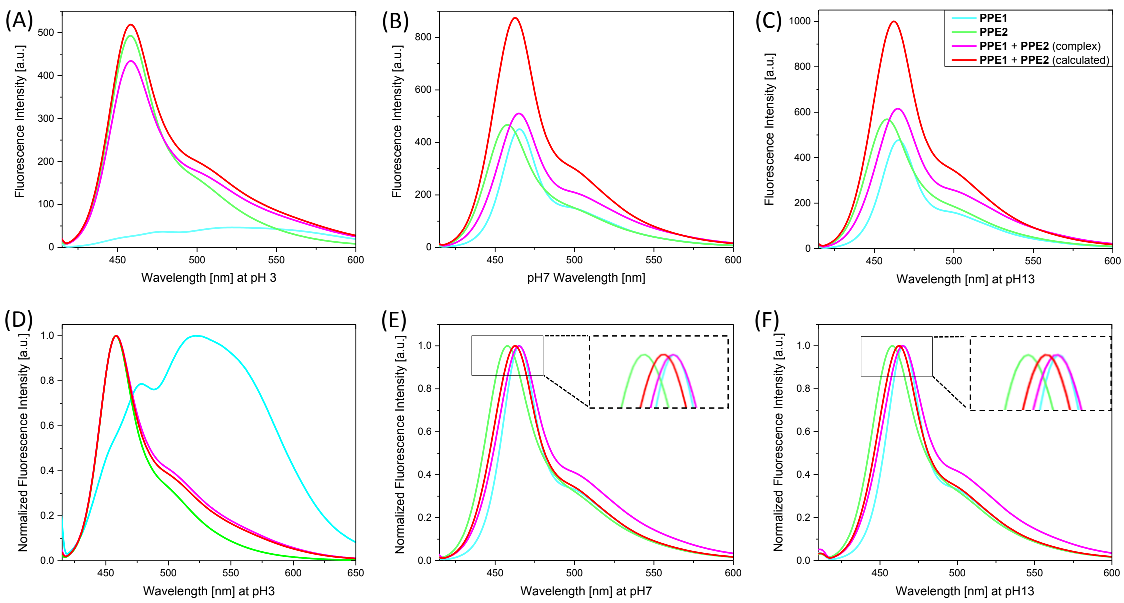

Figure 59. Emission spectra of **PPE 1**, **PPE 2**, **PPE 1 - PPE 2** complex and calculated sum of **PPE 1+PPE 2** at pH3 **(A)**, pH7 **(B)** and pH13 **(C)**. Normalized emission spectra of **PPE 1**, **PPE 2**, **PPE 1 - PPE 2** complex and calculated sum of **PPE 1+PPE 2** at pH3 **(D)**, pH7 **(E)** and pH13 **(F)**.

Table 11 shown the detailed information of the thirteen different white wines used in this study. Figure 57 shown the absorption and emission of thirteen wines, both the absorption (A-C) and emission (D-F) spectra at different pH values (pH 3, pH 7, pH 13) of most wines are quite similar and close to each other, some of them are even overlapped. However, smooth curve of absorption and emission spectra can not be obtained owing to the physical properties low fluorescence of the whiskies, imply the significant error of intensity among wines. Therefore, it is impossible to fingerprint wines only depend on the absorption and emission.

We are interested in conjugated, charged, water-soluble polymers of the PPE-type[9, 148] and their use in sensory applications for bio-species, metal ions and other analytes.[10, 43-44, 51, 53, 170, 201-203] Very recently, we demonstrated that simple polyelectrolyte complexes formed from a cationic and an anionic PPE could discern and detect the anions of carboxylic acids, diacids and hydroxy acids.[40-41] The tested carboxylic acids are major components in (white) wines. As a consequence, we set out to test, if PPEs or their complexes could also discern white wines. In a first experiment, we employed the same set of complexes as we did for the sensing of carboxylic acids, but found that only the PPEs and their complexes, as shown in Figure 58A, were reactive towards wine 3 (Table 11), which we used as preliminary test bed. Figure 59 shows the (normalized) emission spectra of **PPE 1**, **PPE 2**, **PPE 1 - PPE 2** complex and calculated **PPE 1** + **PPE 2** at different pH solutions (pH 3, pH 7, pH 13), the difference between the **PPE 1 - PPE 2** complex and calculated **PPE 1** + **PPE 2** indicate the complexes formed between **PPE 1** and **PPE 2**. We checked the pH-dependence of the fluorescence responses of the three sensor species and found that **PPE 1** and **PPE 2** were best used at pH 13, while the complex worked both at pH 3 and pH 13. Consequently, we have a small sensor field consisting of four elements. In all cases we observed fluorescence quenching. Fluorescence enhancements were not observed with white wines, contrary to our experience when sensing carboxylic acids.

3.1.2 Results and Discussions

Figure 60 shows the results of the fluorescence quenching of the wines 1-13. Furthermore we successfully tested 6 different bottles of the same wine (wine 10) to ensure that the quenching behavior to exclude artifacts (Figure 63). The fluorescence of the sensor elements is most strongly quenched by the red wine 1. However, the white wines also show quenching. In the case of the anions of lactic acid, mandelic acid, and tartaric acid (principal components of wine) fluorescence turn-on of PPEs was observed for most of the employed sensor-elements. As a consequence, we were surprised that there was no fluorescence turn-on of the sensor elements in any of the white wines. To find out, if the major components of the white wines would elicit any response towards the sensor elements, we created an artificial, colorless test wine, with a composition described in Figure 58D. Exposure of this test wine towards our sensor elements (Figure 60) shows that a combination of the major components gives a small turn on for three of the four sensor elements.

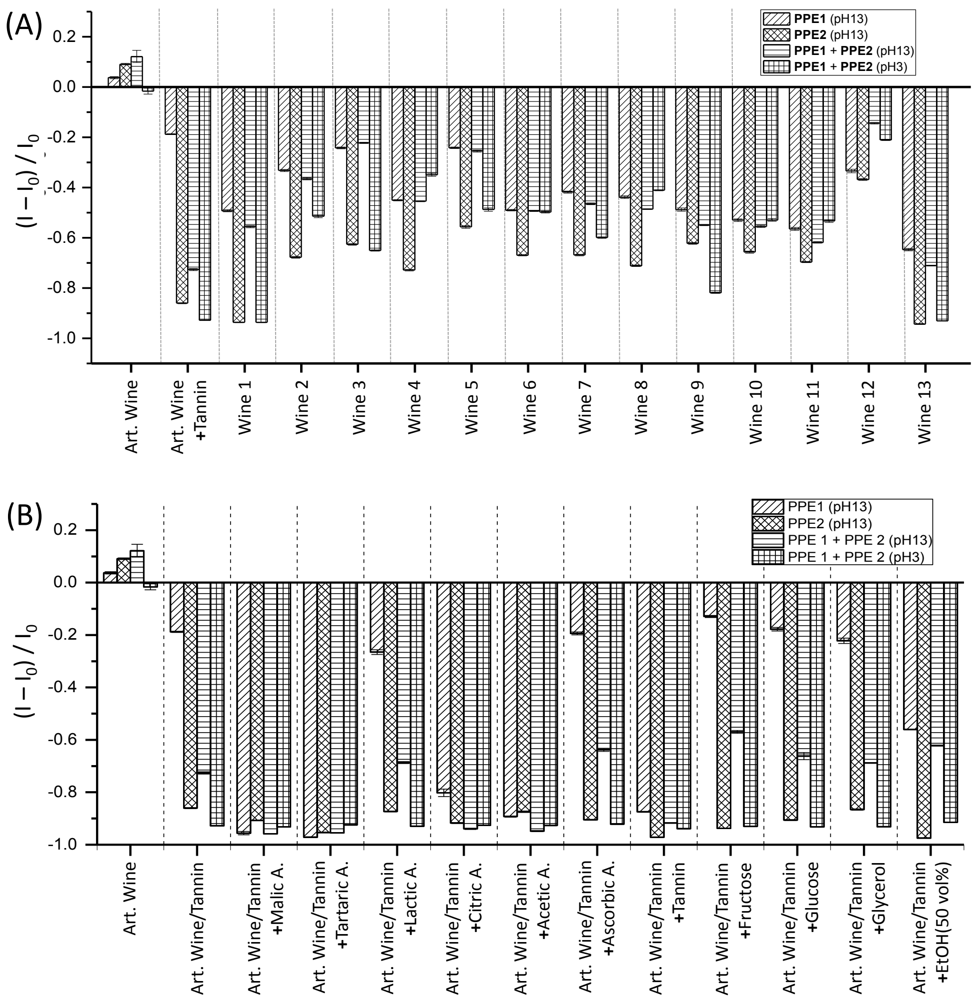

Figure 60. (A) Fluorescence response pattern (I - I_0 / I_0) obtained by **PPE 1**, **PPE 2** (2 µM, each at pH 13, buffered) and their complexes (each PPE 2 µM, at pH 3 and 13, buffered) treated with artificial (art.) wine (7 vol% for **PPE 2**, 33 vol% for the others, ingredients see Figure 58D), artificial wine plus tannin (0.1 mg/mL) and thirteen different, commercial available white wines (7 vol% for **PPE 2**, 33 vol% for the others, composition of the artificial wine see Table 11). **(B)** Fluorescence response pattern (I – I_0) / I_0 obtained by **PPE 1**, **PPE 2** and PPE-complex (each at 2 µM, pH 3 or pH 13 buffer) treated with artificial wine, artificial wine plus tannin, and then the quenched mixture treated with different wine ingredients (added at ten-folds concentration of each ingredient shown in Figure 58D). Each value is the average of three measurements; each error bar is the standard error (SE) of six measurements.

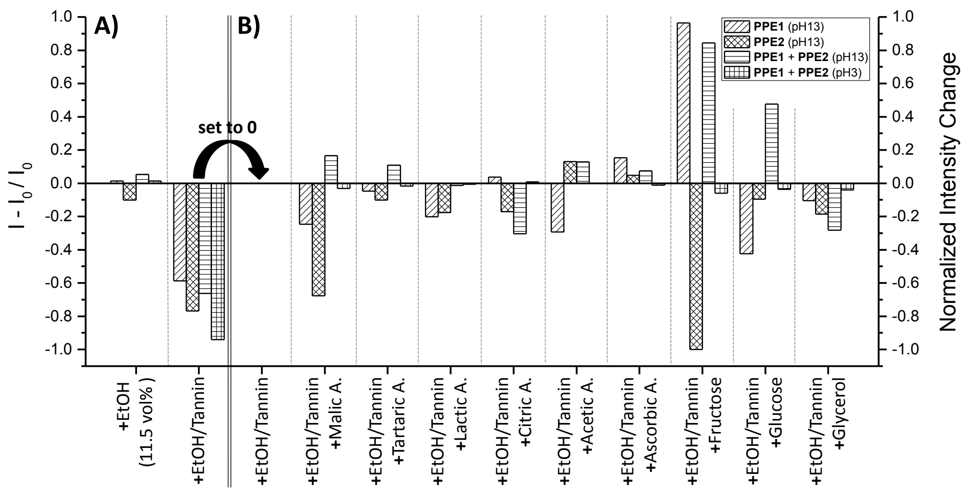

Figure 61. (A) Fluorescence response pattern (I - I_0 / I_0) obtained by **PPE 1**, **PPE 2** (2 µM, each at pH13, buffered) and their complexes (each PPE 2 µM, at pH 3 and 13, buffered) treated with EtOH (11.5 vol%; first array). To this solution tannin (0.1 mg/mL, second array) was added. **(B)** First array: the results from picture A), second array were set to 0. Remaining arrays: additional indicated ingredients (final concentrations see Figure 58D), acid = A) were added and the shown data (normalized) are the raw results minus the results from A), second array. Each value is the average of three independent measurements.

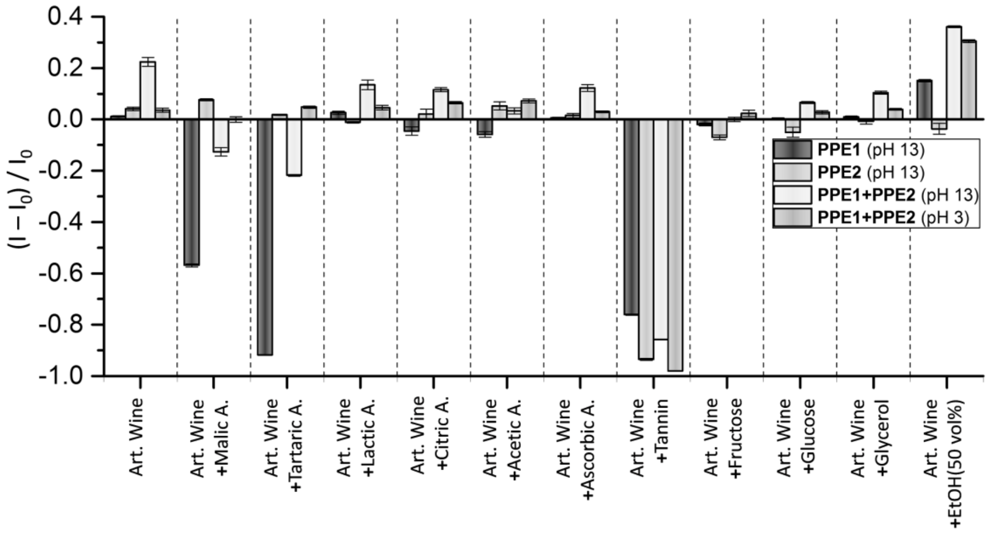

Figure 62. Fluorescence response pattern (I – I_0) / I_0 obtained by **PPE 1**, **PPE 2** and **PPE-complex** (each at 2 μM, pH 3 or pH 13 buffer) treated with artificial wine, and then the artificial wine treated with different wine ingredients (added at ten-folds concentration of each ingredient shown in Table 1). Each value is the average of three measurements; each error bar is the standard error (SE) of three measurements.

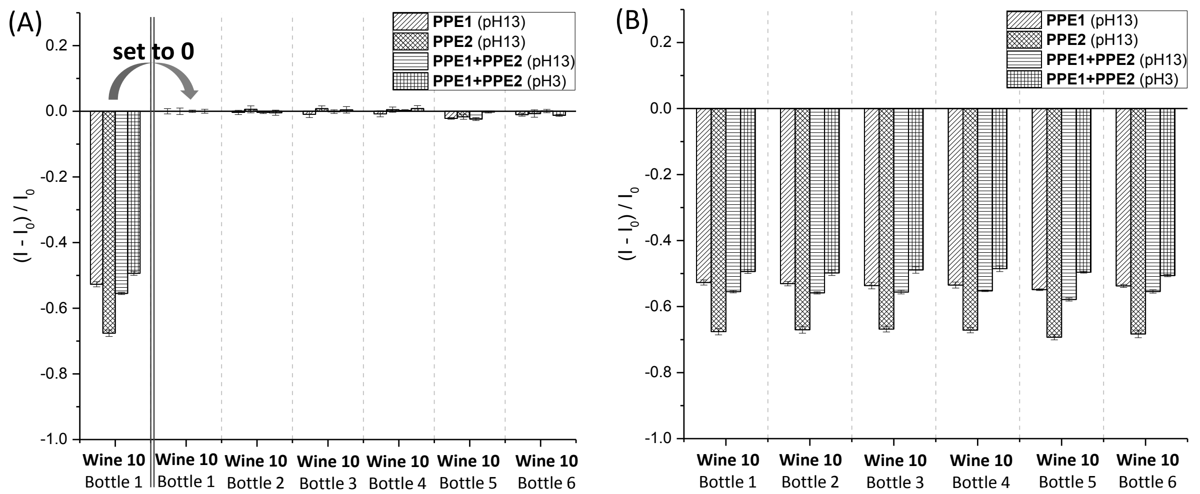

Figure 63. (A) Fluorescence response pattern (I – I_0) / I_0 obtained by **PPE 1**, **PPE 2** and **PPE-complex** (each at 2 μM, pH 3 or pH 13 buffer) treated with six different bottles (Bottle 1 to 6) of Wine 10. Second array: the results from first array (bottle 1) was set to 0. Remaining arrays: the results (from subtraction) of Bottles **2-6**. **(B)** Fluorescence response pattern (I – I_0) / I_0 obtained by **PPE 1**, **PPE 2** and **PPE-complex** (each at 2 μM, pH 3 or pH 13 buffer) treated with six different bottles of Wine 10. Each value is the average of six measurements; each error bar is the standard deviation (SD) of six measurements.

Artificial colorants for wines are commercially available. Once we spiked our artificial wine with commercial tannins (tannic acid, 0.1 mg/mL), the artificial wine showed fluorescence quenching on a level quite similar to that observed for the tested red wine 1 (Figure 60, Figure 62). Our artificial wine resembles real wine in terms of sensory response, once the tannin was added. We were interested, if the major components of the wine, shown in Figure 58D, would modulate the fluorescence response of the tannin-containing artificial wine. One can see from Figure 61, that the fundamental quenching of the fluorescence of the PPEs in a simple water/ethanol/tannic acid mixture by the tannic acid is modulated by the added components, present in white wines. If we look at Figure 60, we see similar patterns in the commercially available white wines. Even if we assume that the tannins and their related flavones etc. all lead to fairly similar quenching, then differentiation in the major components modulates the quenching properties of the white wines. Glucose, fructose and malic acid are the most potent modifiers of the fluorescence quenching properties of the water/ethanol/tannic acid solution in the presence of the PPEs.

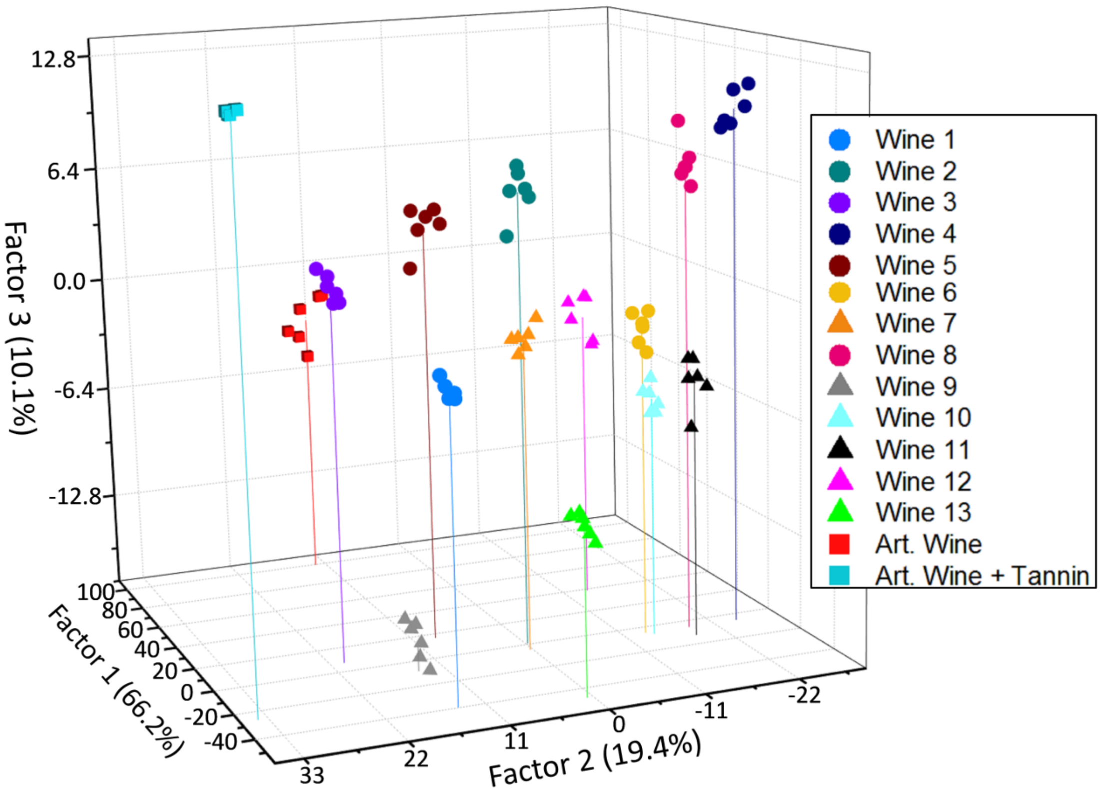

Figure 64. 3D canonical score plot for the first three factors of simplified fluorescence response patterns obtained with an array of **PPE 1**, **PPE 2** (each at pH 13, buffered) and their complex (at pH 3 and 13, buffered). Each point represents the response pattern for a single wine to the array. The blue/green triangles represent the Riesling wines, the circles correspond to the other wines and the artificial wine (with or without tannin) are given in squares.

Figure 64 contains the linear discriminant analysis (LDA) plots of all of the investigated wines 1-13; LDA converts the training matrix (4 sensor elements X 13 wines X 6 replicates) into canonical scores according to their Mahalanobis distance (Table 38, Figure 109). The jackknifed classification matrix with cross-validation reveals a 100% accuracy. As a result, all of the wines are reliably discerned using this simple four-element sensory array.

To further validate the efficiency of our sensing system, we established tests with randomly chosen white wines of our training set. The new cases were classified into groups, generated from the training matrix, based on the shortest Mahalanobis distance to the respective group. Only 1 of 52 unknown wines was misclassified, representing an accuracy of 98% (Table 39). The 3D LDA-results from wines made from identical grape varietals (in this case the family of Riesling wines) weakly group together, as visualized by the Factor 2 and particularly Factor 3 (Figure 64). That is consistent with the results from Anslyn et al., who could show that LDA-analysis for discrimination of red wines would cluster, depending upon the grape varietals.[125]

In our case the varietals only cluster to a moderate extent (wine 6 is similar to the Riesling wines). This could be due to a number of reasons. The most probable one being that the metabolome of the yeast and the cooperage change the composition of the white wines, such that the nature of the grape varietal loses importance in white wines and is "washed out" in the sensing results.

3.1.3 Conclusions

In conclusion, we discriminate and differentiate white wines using a small array of two ionic PPEs and a complex between the two ionic PPEs. The PPEs function best at pH13, while the complex generates response at pH 3 and at pH 13. The fluorescence response of the sensor elements to the wines is primarily due to the wine colorant, as demonstrated by the quenching behavior of a water/ethanol /tannic acid mixture. The mixture quenches the sensor elements' fluorescence like real wines do. The fluorescence quenching is modulated by the presence of the major components of the wines, such as sugars and acids. Particularly fructose and malic acid are active, even though – on their own – they do not modulate the fluorescence of the PPEs to any significant amount.

Our continuing commitment to conjugated polymers and their electrostatic complexes as sensory systems stems from their powerful sensing performance, facile and highly modular and scale-able synthesis, their great stability and their relatively low cost.

3.2 PAE-Based Tongues Discriminate Fruit Juices

Figure 65. Systematic illustration of PAE-based tongues discriminate fruit juices.

In this Chapter, we describe a simple promiscuous tongue, consisting of a positively charged, fluorescent poly(*para*-phenyleneethynylene), **P2**, that discriminates commercially available fruit juices, when employed at different pH-values (pH 3, 7, 13). This minimal tongue identifies 14 different apple juices, 6 different grape juices and 5 different black currant juices from each other (Figure 65). All of the examined commercial samples were discriminated by this simple non-specific tongue. When a similar, negatively charged fluorescent polymer, **P1**, was used, discrimination was also achieved, but the analyte concentration had to be increased by a factor of 50. Mixture of black currant juice and red grape juice are identified as red grape juice, if suitable combinations of grape juice and black currant juice are employed. A mixture of red and green grape juice passes as red grape juice in our sensing system when it contains more than 70% of red grape juice. The data were obtained by fluorescence quenching of the conjugated polymers and processed by linear discriminant analysis of the collected data.

3.2.1 Screening and Construction of PAE Tongue

Quality control of food, medications and other complex analytes is a practical, important, yet intellectually ambitious task. Different analytical methods have been exploited, including mass spectrometry,[106-110] electrochemical tongues and noses,[111-113] but also biological methods (antibodies, genetics),[114-115] One specific method are chemo-optical tongues.[36, 116] These indicate the spoiling of fish,[117-118] fingerprint coffees,[119] whiskeys,[120] beers,[121] soft drinks,[122] red wines[123-125] and white wines,[47] to highlight applications of tongues that react by color change or fluorescence intensity modulation. These tongues consist of arrays of different receptors that are bound to colored or fluorescent indicator-dyes that are replaced by the analytes. Their action principle is different from that of classic sensors but also of that of instrumental analytical methods. Suslick described in his superb review[36] some of the features that are presumably necessary to achieve successful discrimination for complex analytes and stressed that "*…in general, an optimal sensor array for general sensing purposes will incorporate as much chemical diversity as possible…*".[36] This statement guided the development of arrays in which a wide variety of different colorimetric indicator molecules are employed to identify analytes. Suslick's (printed) sensor libraries typically consist of 16-36 elements for successful identification of different classes of analytes.

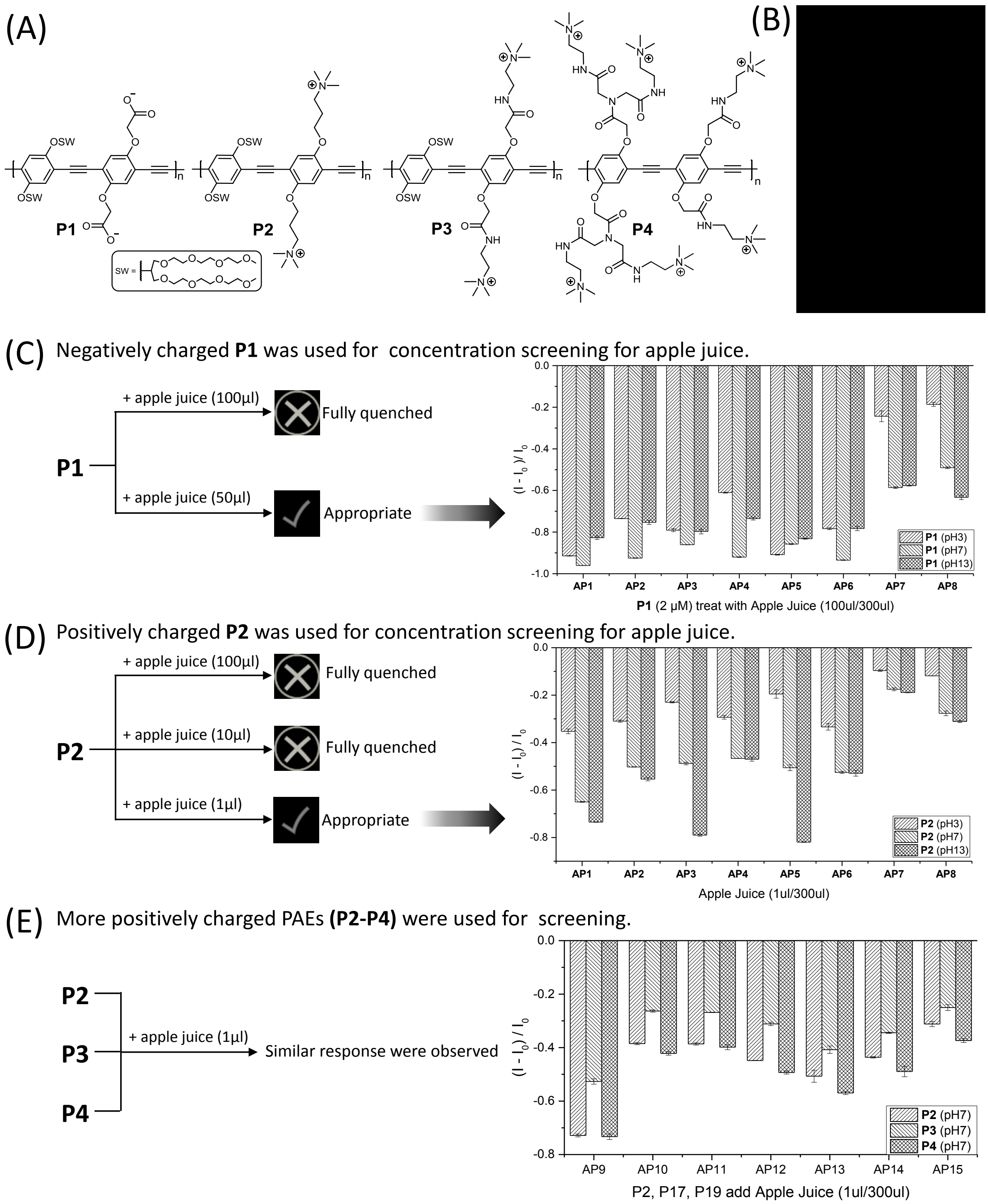

Figure 66. **(A)** Structure of highly fluorescent charged PAE (**P1-P4**) employed for screening. **(B)** Selected apple juice sample used for screening. **(C)** Concentration-dependent screening process of ample juice with **P1**. **(D)** Concentration-dependent screening process of ample juice with **P2**. **(E)** Screening of PAEs for ample juice sensing.

A second accepted tenet of these chemo-optical tongues was formulated by Anslyn, and is a weakened variation of the lock and key principle of Fischer as nicely shown in Figure 1 of ref.[129] In this picture molecular keys fit into many locks with a varying degree of fit. Several of such partially fitting receptors identify and discriminate groups of analytes by the unique signal patterns of the sum of the sensor elements. Here the most practical approach is to offer small libraries of receptors that are "filled" with dyes to be replaced by the analytes with differential efficiency.[130]

Both of these approaches stress that cross-reactivity, structural differentiation and structural variation of the sensor elements are important, as expressed by the wish to obtain high dimensionality sensor arrays that differentiate a broad variety of similar but complex analytes, including soft drinks, coffees, beers, whiskeys, etc.

Both approaches, i.e. the weakened lock and key principle but also the chemical diversity of the sensors are *sufficient* to guide the production of useful sensor arrays. Are they necessary though? Both concepts have generated in the past an arbitrary and large number of exceptionally well-working tongues and sensors, but neither predicts or defines the minimum structural variation in sensor elements necessary to discriminate complex analytes; a non-trivial puzzle. As optical tongues are constructed in a glass-bead game of nature, there must be rules that guide the arrays' rational and minimalist construction. What are the rules of this game and are the rules defined, to construct minimalist tongues, the simplest systems discriminating a given set of analytes? The overall chemical tongue is not only defined by the selection of the cross-reactive or promiscuous sensor elements (ProSE) but also by the mathematical workup of the collected raw data. Common methods for data workup include MANOVA-types,[164] hierarchical cluster analysis,[36] principal component analysis,[36] and linear discriminant analysis (LDA).[36, 51] LDA is the most useful mathematical tool to us, with which we now almost exclusively analyse our results.

In this contribution, we demonstrate that a minimalist tongue, the cationic poly(*para*-phenyleneethynylene) (PPE) **P2** successfully discerns different brands of apple, black currant and red grape juice. This chemical tongue, based upon fluorescence quenching of conjugated polymers **P1** and **P2** in water, allows the assessment and discrimination of commercially available fruit juices and their mixtures.

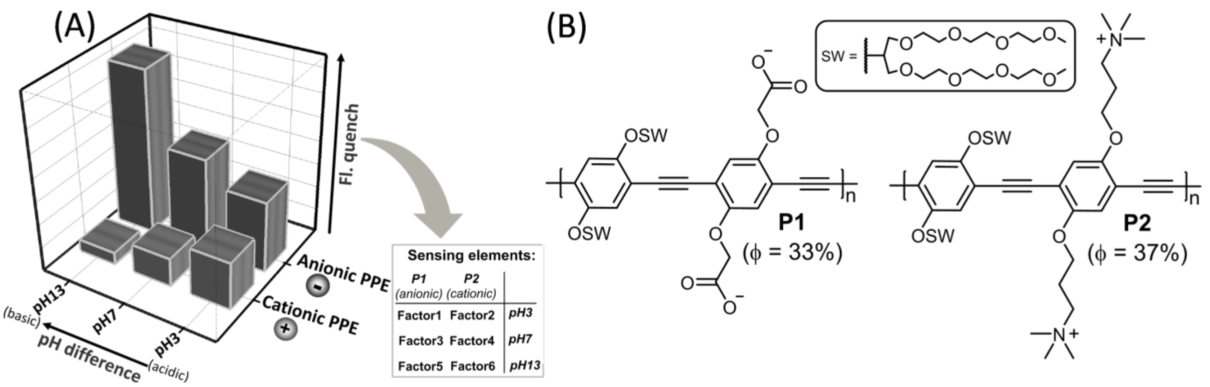

Figure 67. (A) Systematic evaluation and selection of the successful tongue elements for the juice sensing. **(B)** Chemical structures of selected **P1**–**P2**.

For the investigation and discrimination of fruit juices we set out for a suitable minimal sensor field that would react towards all of the different juices. The selection of a suitable tongue with **P1**-**P4** for the discrimination of the fruit juices is described (Figure 66). Preliminary screening of various PAEs treated with randomly selected apple juices at different concentrations (1, 10, 50, 100 µL) and pH solutions (pH 3, pH 7 and pH 13) arrived at a workable tongue showing six elements, consisting of **P1** and **P2** at different pH values (pH 3, pH 7 and pH 13). **P1** is anionic while **P2** is positively charged; both are highly fluorescent in water (Figure 67).

3.2.2 Results and Discussions

Table 12. Detailed Information of the Investigated Juices (14 Apple Juices AJ1-AJ14, 5 Black Currant Juices BJ1-BJ5 and 6 Red Grape Juices GJ1-GJ6) Used in This Study.

Abbr.	Commercial Juice Name	pH[a]	*Conc.*	Fat/Fatty acids[b]	Carbohydrates /Sugar[b]	Proteins[b]	Salts[b]
AJ1	Apple Juice*Bio*	3.47	100%	<0.5g /0.5g	11.0g/10.0g	<0.5g	<0.01g
AJ2	Apple Juice	3.40	100%	0.1g/0.02g	11.0g/10.5g	0.1g	0.005g
AJ3	Riod'oro Apple Juice	3.49	100%	<0.1g/0.1g	10.3g/9.9g	0.1g	<0.01g
AJ4	Riod'oro Premium Apple Juice	3.41	100%	0g/0g	11.0g/11.0g	0g	0g
AJ5	REWE Apple Juice	3.50	100%	0g/0g	11.2g/10.7g	0g	0g
AJ6	Albi Apple Juice	3.60	100%	<0.5g/<0.1g	11.0g/10.0g	<0.5g	<0.01g
AJ7	Solevita Bio Apple Juice*Bio*	3.56	100%	0.1g/<0.1g	11.0g/10.5g	0.1g	<0.01g
AJ8	VITAFIT Apple Juice	3.60	100%	0.1g/0.02g	10.5g/10.0g	0.1g	<0.01g
AJ9	VITAFIT Premium Apple Juice	3.63	100%	0.1g/0.02g	11.0g/10.5g	0.1g	<0.01g
AJ10	Amecke Apple Juice	3.65	100%	0.1g/<0.1g	11.1g/10.6g	0.5g	0.01g
AJ11	Ja Apple Juice	3.56	100%	0g/0g	10.2g/9.8g	0g	0.01g
AJ12	EDEKA Apple Juice	3.73	100%	0.1g/0.02g	10.5g/10.0g	0.1g	0.008g
AJ13	Lift Apple spritzer	3.53	55%	0g/0g	6.0g/5.8g	0g	0g
AJ14[c]	Hessischer Apple Wine	3.76	5.5% Alcohol	-	-	-	-
BJ1	Cassis Black Currant juice*Bio*	3.10	30%	0g/0g	82g/82g	0g	0g
BJ2	Nektar Black Currant juice*Bio*	3.60	25%	0.1g/0.02g	13g/13g	0.1g	0.001g
BJ3	Heimishe Black Currant juice	3.60	25%	<0.5g/<0.1g	12g/12g	0.1g	<0.01g
BJ4	REWE Black Currant juice	3.54	25%	0g/0g	12.9g/12.9g	0.3g	0.01g
BJ5	Jacoby Black Currant juice	3.57	25%	<0.5g/<0.1g	8.4g/8.4g	<0.5g	<0.01g
GJ1	Grape juice*Bio*	4.06	100%	0.01g/0.002g	17g/17g	0.2g	0.003g
GJ2	REWE Red Grape juice*Bio*	4.07	100%	0g/0g	16.6g/16.6g	0g	0g
GJ3	REWE Grape juice	3.92	100%	0g/0g	16.9g/16.9g	0g	0g
GJ4	Riod'oro Premium Grape juice	3.68	100%	0g/0g	16.6g/16.6g	0g	0g
GJ5	Jacoby Grape juice	3.77	100%	<0.5g/<0.1g	16g/16g	<0.5g	<0.01g
GJ6	REWE Merlot Grape juice	3.63	100%	0g/0g	17g/17g	0.3g	0.01g

Table 12 informs about the different apple, grape and black currant juices in this study. Juices, complex mixtures of different compounds, the number of which probably ranges in the hundreds, are 8-17% aqueous solutions of sugar at a pH between pH 3.1-4.1. Their low pH prevents fast microbial spoiling. As a first experiment we exposed all of the juices towards PPEs **P1** and **P2**. Figure 68 and Figure 69 show the quenching results of the PPEs when the juices are added at different pH values.

The fluorescence quenching of the cationic polymer **P2** is much more efficiently quenched (1 µL analyte vs. 50 µL analyte per 300 µL buffer/PPE solution) than that of the anionic **P1**.

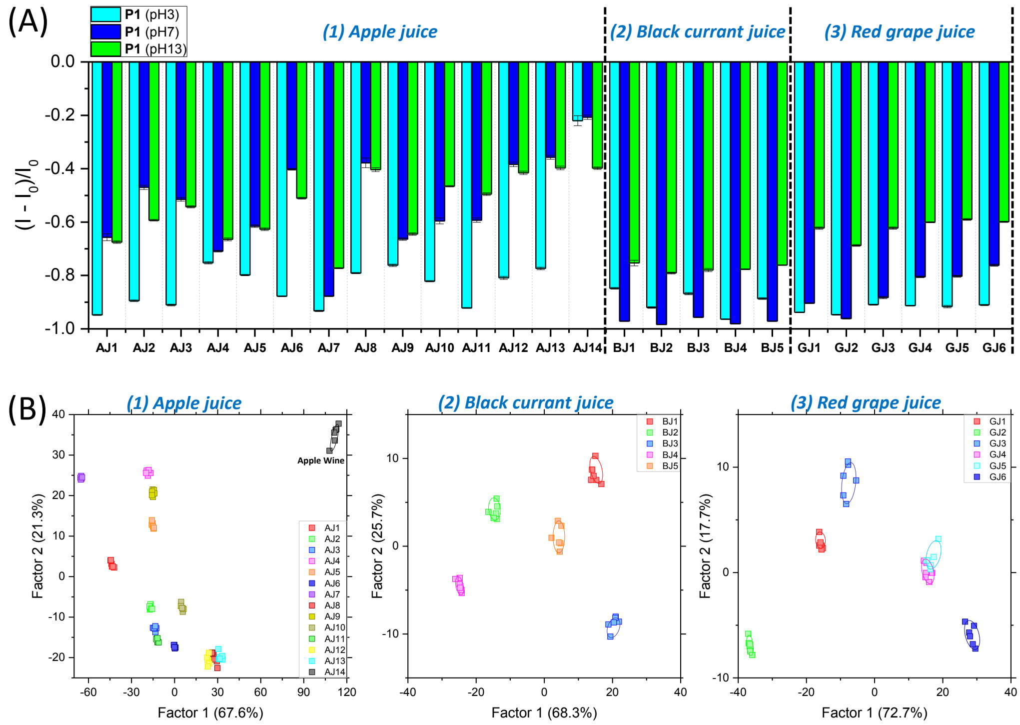

Figure 68. (A) Fluorescence response pattern ($(I - I_0) / I_0$) obtained by **P1** (2 µM, at pH 3, 7 and 13, buffered) treated with commercial apple juice (1), black current juice (2) and red grape juice (3) samples (50 µL per 300 µL). Each value is the average of six independent measurements; each error bar shows the standard deviation of these measurements. **(B)** 2D canonical score plots for the first two factors of simplified fluorescence response patterns obtained with an array of **P1** with 95% confidence ellipses. Each point represents the response pattern for a single juice sample to the array.

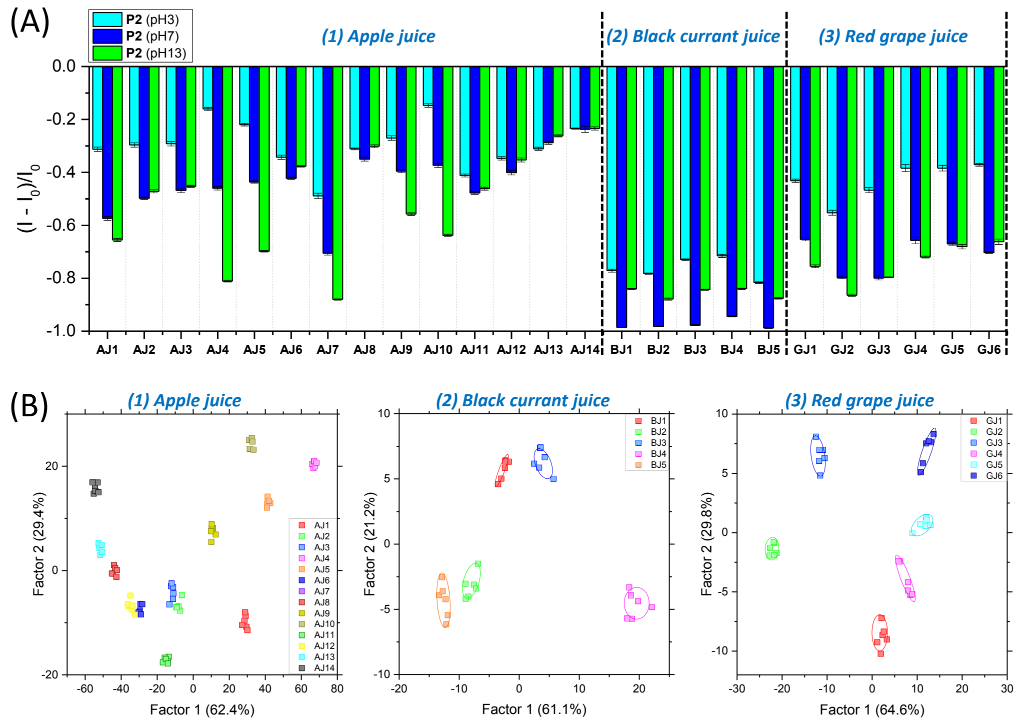

Figure 69. (A) Fluorescence response pattern ($(I - I_0) / I_0$) obtained by **P2** (2 µM, at pH3, 7 and 13, buffered) treated with commercial apple juice (1), black current juice (2) and red grape juice (3) samples (1 µL per 300 µL). Each value is the average of six independent measurements; each error bar shows the standard deviation of these measurements. **(B)** 2D canonical score plots for the first two factors of simplified fluorescence response patterns obtained with an array of **P2** with 95% confidence ellipses. Each point represents the response pattern for a single juice sample to the array.

This behavior suggests electrostatic effects to play a role in the discrimination of fruit juices; the major fluorescence quenching “interactome” of the fruit juices with the PPEs is negatively charged, allowing a strong interaction with the positively charged PPE **P2**. All of the juices are discriminated either by **P1** or by **P2** when working at 3 different pH-values. Discrimination is possible when inspecting the raw data but it is much better visualized after linear discriminant analysis (LDA).

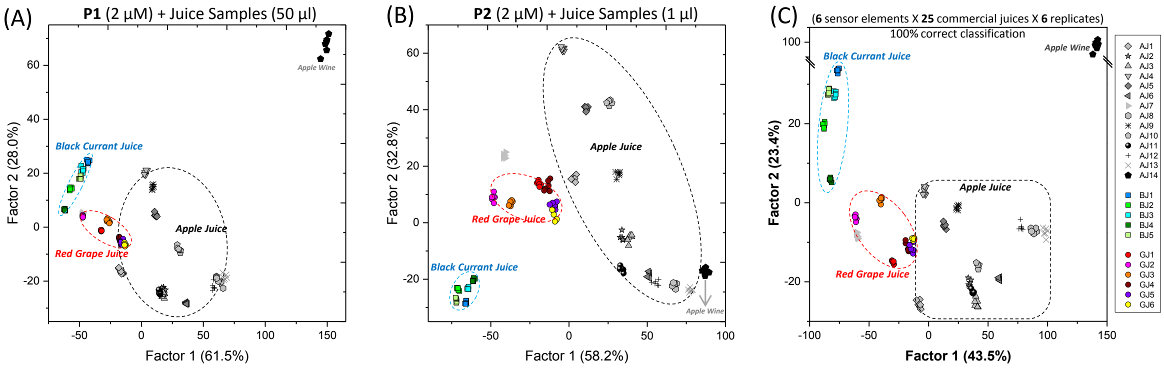

Figure 70. **(A)** Combined 2D canonical score plot obtained with an array of **P1** (2 µM, at pH 3, 7 and 13, buffered) treated with apple, black currant and red grape juices (50 µL). **(B)** Combined 2D canonical score plot obtained with an array of **P2** (2 µM, at pH 3, 7 and 13, buffered) under the same conditions using 1 µL of juice. **(C)** Combined 2D LDA plot for the first two factors of simplified fluorescence response patterns from six sensing elements obtained from both **P1** and **P2** (each at pH 3, 7 and 13, buffered) using the same selection of 25 juices.

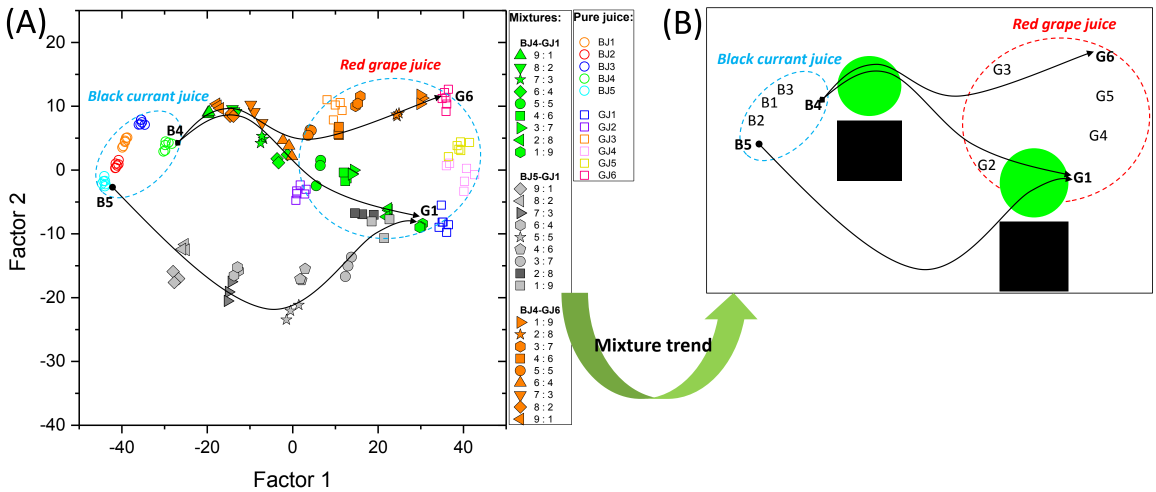

Figure 71. 2D canonical score plot obtained from **P2** (2 µM, at pH 3, 7 and 13, buffered) treated with the mixture of black currant juice and red grape juice (mixture samples of BJ4-GJ1, BJ5-GJ1 and BJ4-GJ6 in different ratios, 1 µL juice(s) per 300 µL for each well); each point represents the response pattern for a single juice sample to the array.

Figure 70 combines the response results from all juices after LDA. Both **P1** as well as **P2** discriminate all of the juices. **P2** does a better job at it, as all of the red grape juice and the black currant juices are discriminated. For unknowns, **P2** is not perfect for apple juice, while **P1** is not optimal for grape juice. Black currant juices are discriminated by both. LDA of the combination of data extracted from **P1** and **P2** (Figure 70C, totally six sensing elements), results in improved discrimination. The jackknifed classification matrix with cross-validation reveals a 100% accuracy, the randomly chosen 100 unknown juice samples using combined six elements were calculated with the training matrix. The accuracy increased to 100%. A more detailed fingerprint is conferred on each juice with the growth of sensing elements (Table 13). While the combined tongue is more discriminating for single juice elements, the inter group differentiation between apple juice and red grape juice is less pronounced than for **P2** alone (Table 13).

Table 13. Jackknifed Classification Matrix and unknown sample identification Obtained from LDA of **P1** and **P2** at Three Different pH-Values[a]

Sensing elements		P1			P2			Total
	Juice types	AJ	BJ	GJ	AJ	BJ	GJ	
Jackknifed classification matrix	Number of samples	84	30	36	84	30	36	150
	Correctly classified	83	30	35	84	30	36	150
	Accuracy (%)	**99**	**100**	**97**	**100**	**100**	**100**	**100**
Blind test	Unknown samples	56	20	24	56	20	24	100
	Correctly identified	56	20	22	54	20	24	**100**
	Accuracy (%)	**100**	**100**	**92**	**96**	**100**	**100**	**100**

[a] Measured at pH 3 (acidic), pH 7 (neutral),and p H 13 (basic), for detailed calculation see Table 40 - Table 51.

Are all of the claimed grape juices pure grape juices? They might be mixtures of red grape juice with black currant juice. Could we distinguish such mixtures? Admixing black currant juice deepens the color of red grape juice if that is desired. To test this hypothesis, we selected the **P2** tongue at pH 3, 7 and 13 under standard conditions (1 µL juice /300 µL matrix, Figure 71). We added black currant juice **B4** or **B5** to either **G6** or **G1**. If one does this, **B4** can substitute up to 50% of **G6** or **G1** and the mixture is yet identified as red grape juice. The alternative does not work, i.e. if one adds grape juice towards black currant juice, **P2** indicates leaving the area that is assigned by LDA to the black currant juice. To obtain more insight we tested fruit juices we prepared in our laboratory from commercially available green and red grapes, and black currants.

Figure 72A shows the fluorescence response of our self-made juices (black currant, green grapes, red grapes) and mixtures of red and green grape juices. After LDA (Table 52 - Table 53) from the data obtained for the self-prepared juices, we find that mixing of the red and green grape juices is an additive process with respect to their properties expressed by LDA. Our hot extracted black currant juice does not group with the commercial black currant juices (added to the training matrix), suggesting that commercial black currant juice is processed differently. The main discriminating factor in Figure 72 (x-axis, Factor 1) expresses color and the quenching ability of the juices. Green grape juice, the least colored juice is placed on the left-hand side, while black currant juice samples are placed on the right-hand side. The red grape juices locate in the middle. The same applies for Figure 70, where the response of all of the juices are displayed. The x-axis approximates the color depth of the juices, just mirror-symmetrical from the ordering seen in Figure 72. The y-axis is currently not ascribed to a simple physicochemical property and can neither be correlated with sugar content nor with acidity. It must represent a complex property or properties; it could be a combination of fruit acids (mandelic acid, citric acid, tartaric acid etc.) and/or sugar plus other complex colored species present in these fruit juices.

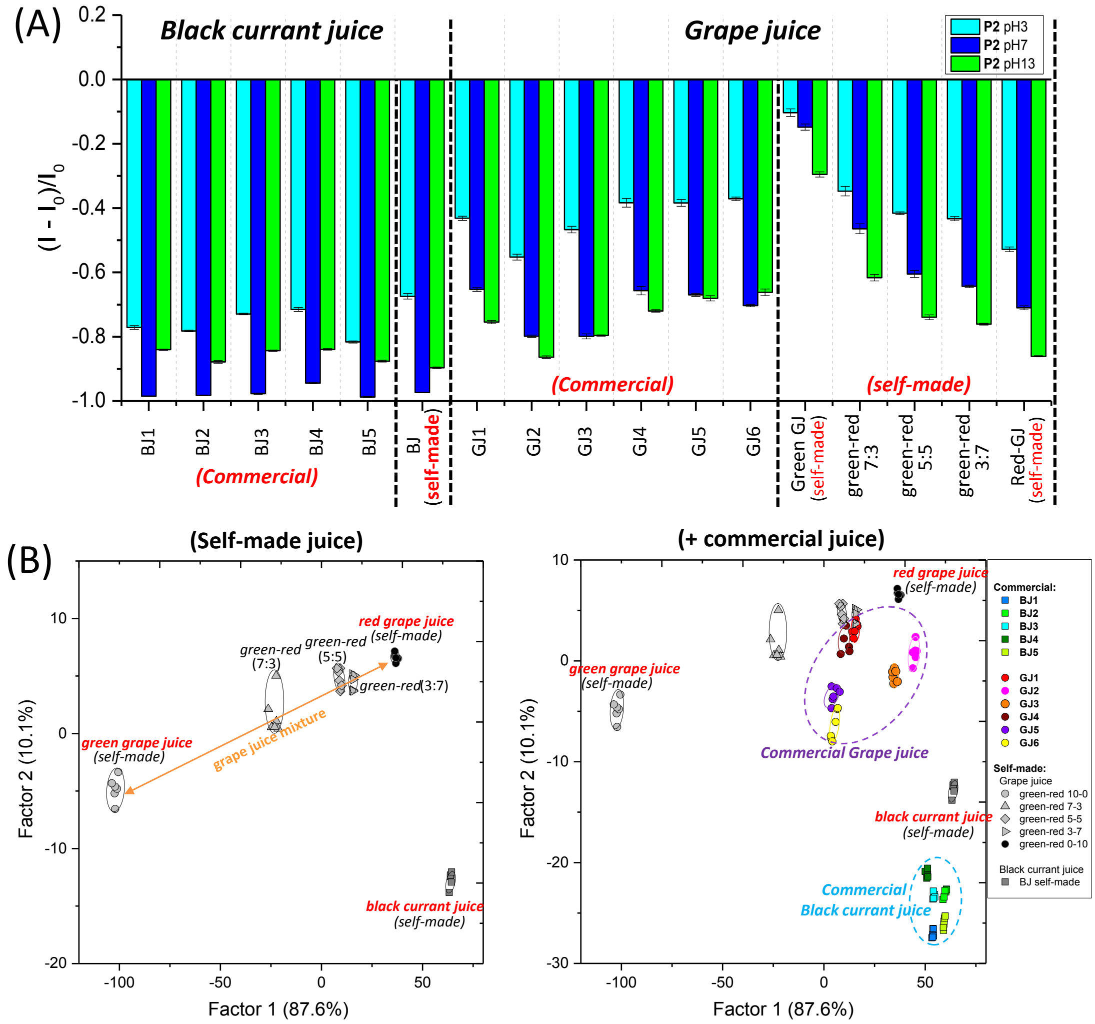

Figure 72. (A) Fluorescence response pattern ((I - I_0) / I_0) obtained by **P2** (2 µM, at pH 3, 7 and 13, buffered) treated with self-made and commercial juice samples (1 µL/300 µL). Each value is the average of six independent measurements; each error bar shows the standard deviation of these measurements. **(B) Left**: 2D canonical score plot for the first two factors of simplified fluorescence response patterns obtained with an array of **P2** (2 µM, at pH 3, 7 and 13, buffered) treated with self-made black currant juice, self-made green and red grape juices, and mixtures of green and red grape juices. **(B) Right**: The commercial juice samples were added as blind to the training matrix of the self-made juices. Each point represents the response pattern for a single juice sample to the array (a water control is located as a zero point).

3.2.3 Conclusions

A single positively charged, water-soluble conjugated polymer, **P2**, discriminates apple juices, black currant juices and grape juices. We established that red grape juice can be mixed with black currant juice into a zone where the LDA-processed responses of a significant number of commercially available (pure) grape juices are located. The result poses several questions. **a)** Some of the commercial red grape juices might contain small to moderate amounts of black currant juice or **b)** the variation of the response of grape juices is due to the multiple dozens of different grape varietals and therefore is to be expected, or **c)** our tongue is not sufficiently developed to discriminate mixtures, or all of the above.

The power of this minimalist tongue is surprising, as the discriminative power of **P2** is brought out by its employ at different pH-values, i.e. only change of the sensing conditions. This one polymer acts therefore as an efficient three-element-tongue, where the change of the analytes with the pH-value must significantly contribute towards the successful recognition strategy. Why are **P1** and **P2** successful in discriminating complex analytes such as fruit juices? **P1** and **P2** display a fairly rigid backbone, and -depending upon their conformation could either be viewed as a “sticky” molecular board (phenyl rings parallel to each other) or a “sticky” molecular rod (phenyl rings twisted with respect to each other). The stickiness or non-specific affinity towards arbitrary analytes comes from hydrophobic interactions, hydrogen bonding, and electrostatic interactions. All of these interactions must be promiscuous and non-specific as our sticky boards/rods have no inbuilt shape recognition elements and neither do they show significant variations in their chemical structure, not even upon protonation. These results shed a different light on both the lock-and-key principle (first stated by Emil Fischer and subsequently elegantly adapted for sensor arrays by Anslyn et al.) but also on the professed need to employ chemically different tongue elements (Suslick) to reach recognition. Neither of these constraints are active in our boards or rods, just the presence of a molecular surface with varying “stickiness” or non-specific affinity for interactions with complex analytes.

Sticky linear molecular surfaces such as in our PPEs are powerful as they allow the sensing and the discrimination of almost all and any conceivable analytes because of the complete lack of shape requirements for either analytes or tongue elements. The weakness of the method is that the discriminative axes that show up in the LDA plots of the processed data often do not correlate well with an easily recognized chemical or physical property. That however is also advantage. If one looks into the identification of counterfeit products, drugs, or consumer goods, the absence of a clearly identifiable signal molecule means that counterfeit and adulterated products are more easily recognized as the signal generation and identification process is complex and unknown to both the counterfeiter but also the legal producer of the analyzed product, making potential protection stronger. Over all, we have created a minimalist chemical tongue made from **P2** that discriminates fruit juices at different pH-values without any problem.

3.3 A Hypothesis-Free Sensor Array Discriminates Whiskies for Brand, Age and Taste

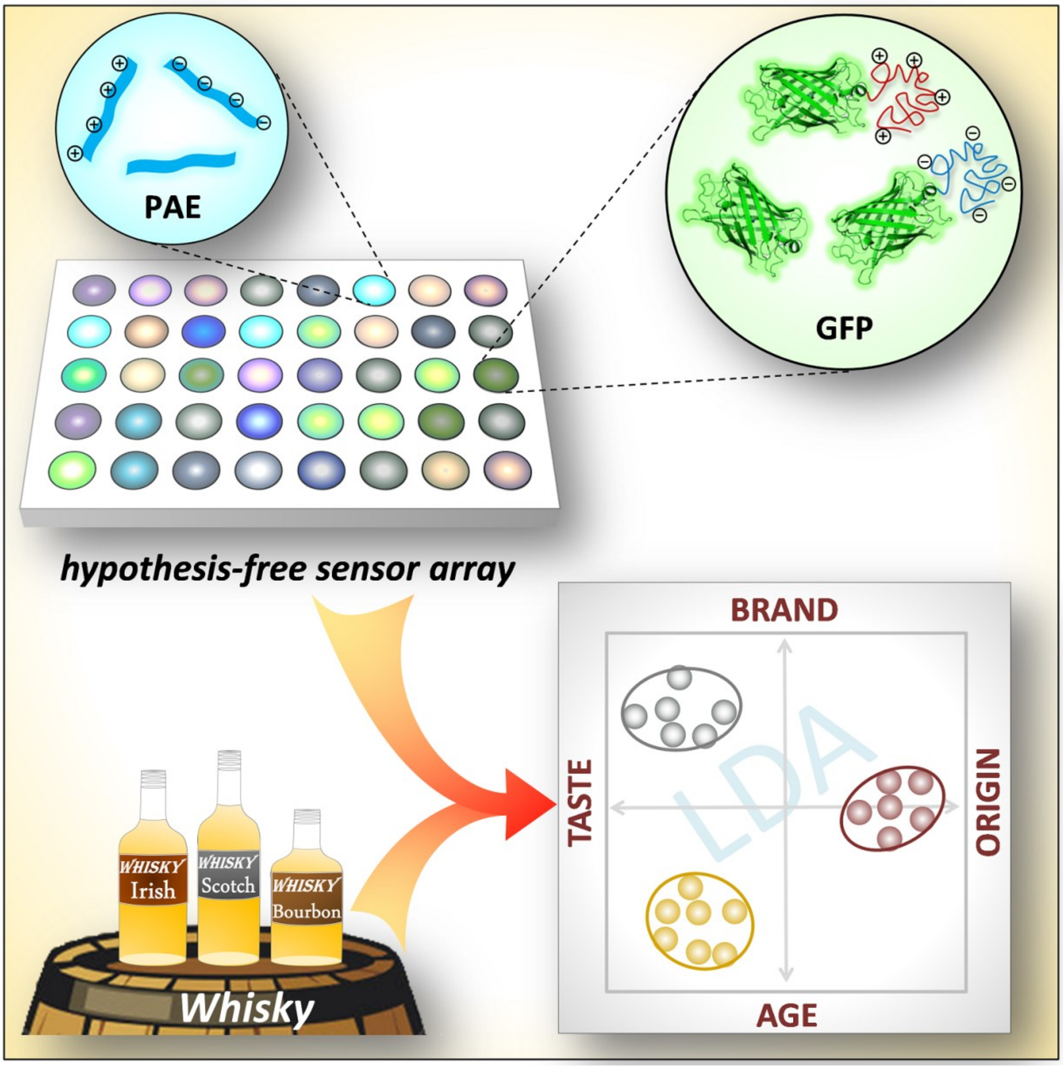

Figure 73. Systematic illustration of hypothesis-free sensor array discriminates whiskies for brand, age and taste.

In biology, non-specific interactions are ubiquitous and essential, while in chemistry non-specificity/non-selectivity is somewhat suspect. We present simple tongues consisting of fluorescent polyelectrolytes or chimeric green fluorescent proteins (GFP, collaborated with Prof. Andreas Herrmann, from Zernike Institute for Advanced Materials, University of Groningen), discriminating 33 different whiskies according to their country of origin (Ireland, US, Scotland), brand, blend status (blend/single malt), age and taste (rich/light). The mechanism of action for these tongues is differential quenching of the fluorescence of the poly(aryleneethynylene)s or the GFPs by the complex mixture of colorants in the whiskies (the interactome), extracted into the whiskies from the oak barrels and added coloring. The differential binding and signal generation of the interactomes to the polymers and proteins results from hydrophobic and electrostatic interactions. The collected quenching data, i.e. the response patterns are analyzed by linear discriminant analysis (LDA). Our tongues do not need any sample preparation and are equal or superior to state-of-the-art mass spectrometric methods with respect to speed, resolution and efficiency of discrimination.

3.3.1 Introduction and Screening Process

Whisky was first produced in Scotland, and there the oldest distillery was licensed 1775. Ever since then, Scotch (and other whiskies) have been popular; expensive, specialized varieties have increased in demand during the last decades. Today countless whiskies of different origin, age, brand, blend status, taste and price range are available. For high-end whiskies, asking prices range from 10,000 up to 135,000 € per bottle. For this type of price segment one might worry about counterfeits, but also at the low end of the quality spectrum, where large amounts of cheap alcoholic beverages, low quality counterfeits, are sold as branded Scotch. As it is difficult to obtain bona fide counterfeit whiskies, discriminating different whisky brands and sub-brands is a closely related and perhaps even more challenging and important task. We demonstrate discrimination of *any* whisky with ease, employing a hypothesis-free ad-hoc tongue, based on conjugated fluorescent polyelectrolytes or on green fluorescent proteins (GFP), fused to a supercharged polypeptide chains.

A "whisky sensor" based on a dye-replacement assay has been reported by Anslyn et al.[120] The age of different whiskies was determined by detecting the concentration of gallate and other phenolic species, the concentration of which increase with age. The most common way to discriminate whiskies though employs mass spectrometric methods,[204-206] but also simple quantitative UV-Vis[207] or mid-IR-spectroscopy[208] have been employed with reasonable success, but less than spectacular discriminative power.

Optoelectronic noses and tongues discriminate complex analytes and were popularized by Suslick et al.[36, 69, 71] and by Anslyn et al.,[37, 129, 151] even though now more groups start working in this area.[10, 54, 62, 116, 152-153] The concepts of the two pioneers to construct functional sensor arrays differ. While Suslick states that chemical diversity is necessary in his tongues,[36] Anslyn supported the idea that a relaxed lock and key principle is a powerful concept to create sensor arrays for the discrimination of complex analytes.[37] Both concepts formulate sufficient but not necessary requisites for the construction of optoelectronic arrays. Rotello et al.[51, 152] posed that for certain arrays the structural pre-requisites can be much more relaxed favoring a concept of hypothesis-free sensor arrays.

A hypothesis-free sensor array would fundamentally allow to sense "everything" with any fluorescent dye. Conjugated polyelectrolytes may represent such hypothesis-free arrays; they discriminate white wines,[47] fruit juices,[46] non-steroidal anti-inflammatories[39] and proteins[58] with small selected sensor arrays, based upon fluorescence modulation, i.e. either quenching or fluorescence enhancement. The excited state of conjugated polymers lives for about 0.5-1 ns and is exquisitely sensitive towards environmental change, be it solvent but also any type of analyte that interacts either via hydrophobic or electrostatic interactions or other forces. The magnitude of the effect, the analyte has on the fluorescence intensity is not predictable. A sensor arrays' fluorescence response towards complex analytes such as whiskies can neither be predicted nor modeled, due to its large interactome. If the complex analyte is colored (such as whisky etc.), differential quenching of all of the sensor elements' fluorescence is observed. Here we exploit arrays to discriminate whiskies according to their region of origin, brand, age and taste.

Table 14 (Figure 74 and Figure 75) shows the properties of the selected, studied whiskies. Totally, 36 whiskies with different brand, origin (America, Scotland and Ireland), Type (single malt or blended) and Storage Age (4-18 years) were selected for our study.

Table 14. 36 Tested Whiskies and Their Origin, Type and Storage Age

Abbre.	Whiskey Brand	Oringin	Type	Alcohol content	Storage age
B-1	Jim Beam	Bourbon Whisky	Bourbon	40% vol	4 years
B-2	Jack Daniel's	Bourbon Whisky	Bourbon	40% vol	4 years
Ib-1	Jameson, John	Irish Whiskey	Blended	40% vol	7 years
Ib-2	Kilbeggan	Irish Whiskey	Blended	40% vol	NAS
Is-1	Kilbeggan	Irish Whiskey	Single Malt	40% vol	8 years
Is-2	Connemara	Irish Whiskey	Single Malt	40% vol	NAS
Is-3	Tyrconnell	Irish Whiskey	Single Malt	40% vol	NAS
Is-4	Tullamore Dew	Irish Whiskey	Single Malt	40% vol	NAS
Sb-1	Mac Namara	Scotch Whisky	Blended	40% vol	6 years
Sb-2	Ballantine's Finest	Scotch Whisky	Blended	40% vol	NAS
Sb-3	Té Bheag Nan Eilean	Scotch Whisky	Blended	40% vol	NAS
Sb-4	Dean's	Scotch Whisky	Blended	40% vol	NAS
Sb-5	Grant's	Scotch Whisky	Blended	40% vol	NAS
Sb-6	Johnnie Walker Red Label	Scotch Whisky	Blended	40% vol	NAS
Sb-Y8 [a]	Poit Dhubh	Scotch Whisky	Blended	43% vol	8 years
Sb-Y12 [a]	Poit Dhubh	Scotch Whisky	Blended	43% vol	12 years
Sb-Y21 [a]	Poit Dhubh	Scotch Whisky	Blended	43% vol	21 years
Ss-1	Laphroaig Quarter Cask	Scotch Whisky	Single Malt	48% vol	7 years
Ss-2	Talisker isle of skye	Scotch Whisky	Single Malt	46% vol	10 years
Ss-3	Laphroaig	Scotch Whisky	Single Malt	40% vol	10 years
Ss-4	Cragganmore	Scotch Whisky	Single Malt	40% vol	12 years
Ss-5	Glenfiddich	Scotch Whisky	Single Malt	40% vol	12 years
Ss-6	GlenDronach	Scotch Whisky	Single Malt	43% vol	12 years
Ss-7	Glenfarclas	Scotch Whisky	Single Malt	43% vol	15 years
Ss-8	Dalwhinnie	Scotch Whisky	Single Malt	43% vol	15 years
Ss-9	Ardmore Legacy	Scotch Whisky	Single Malt	40% vol	NAS
Ss-10	Bowmore	Scotch Whisky	Single Malt	40% vol	NAS
Ss-11	Highland Park	Scotch Whisky	Single Malt	40% vol	12 years
Ss-12	Balvenie Double Wood	Scotch Whisky	Single Malt	40% vol	12 years
Ss-13	Glenlivet	Scotch Whisky	Single Malt	43% vol	18 years
Ss-Y12 [a]	Bowmore	Scotch Whisky	Single Malt	40% vol	12 years
Ss-Y15 [a]	Bowmore	Scotch Whisky	Single Malt	43% vol	15 years
Ss-Y18 [a]	Bowmore	Scotch Whisky	Single Malt	43% vol	18 years
New-1	Ardbeg	Scotch Whisky	Single Malt	46% vol	10 years
New-2	Glenmorangie Original	Scotch Whisky	Single Malt	40% vol	10 years
Fake-1	Old Keeper	Scotch Whisky	Blended	40% vol	NAS

NAS – No age statement
[a]"Y" – "year"

Since most of the whiskies possess a similar color, we checked the absorption and emission of pure whiskeys without adding any fluorophores to see if we can distinguish them solely depend on their own properties. Figure 74A shows the absorption spectra of all whiskies investigated, the absorption spectra of the whiskies are quite similar and close to each other with some of them even being overlapped. The absorption at 410 nm was further selected for comparison among the whiskies. As shown in Figure 74B, several whisky are still similar to each other, partial examples are Ib-2, Is-1, Ss-1, Ss-5, Ss-7 (yellow), B-1, Is-2, Sb-Y8 (orange), Is-3, Sb-5, Ss-3, Ss-11 (green) and Sb-4, Sb-Y12, Sb-Y21 (blue). In conclusion, an identification of the different whisky samples, solely based on their absorption is impossible.

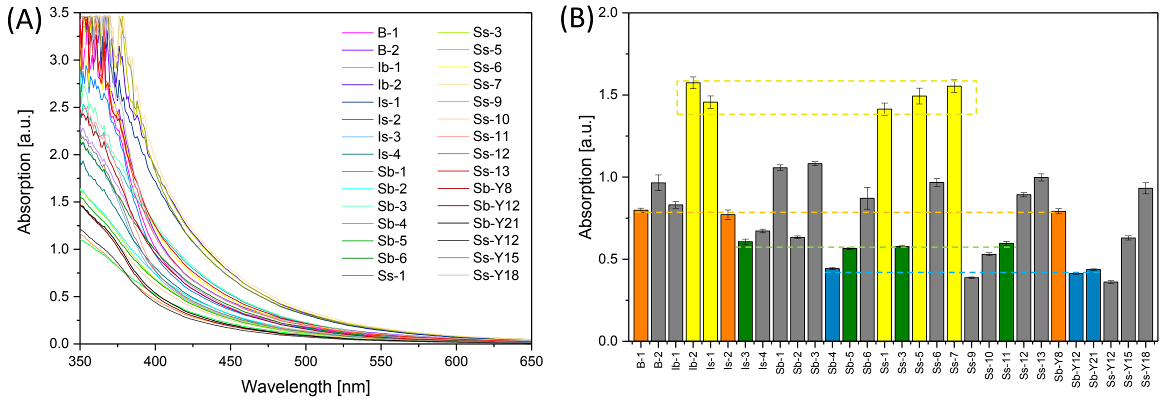

Figure 74. (A) Absorption spectra of whiskies in this study. **(B)** Absorption of the whisky at 410 nm, each value is the average of three measurements.

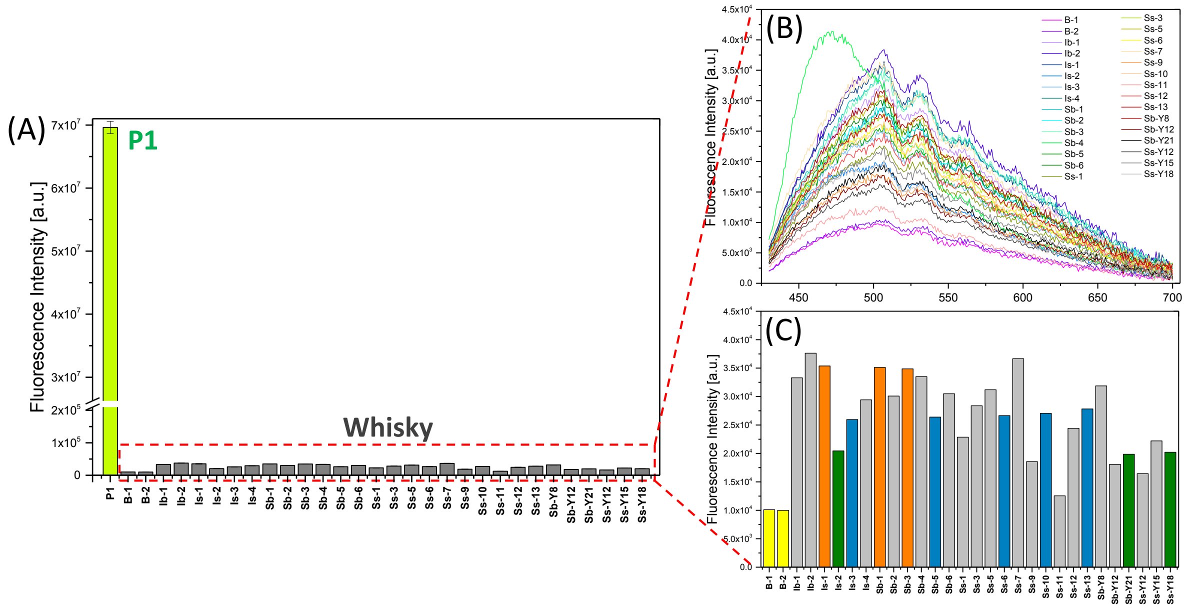

Figure 75. (A) Fluorescence intensity of **P1** (2 µM, at 460nm) and whisky (at 507nm) in this study. **(B)** Fluorescence spectra of the whisky. **(C)** Fluorescence of the whisky at 507nm, each value is the average of three measurements.

To check the fluorescence of the pure whiskies we selected 410 nm as excitation wavelength and recorded their fluorescence intensity. Apparently, when compared with pure **P1**, whiskies show almost no fluorescence (Figure 75A). Figure 75B and Figure 75C show the detailed emission spectra and fluorescence intensity of all whiskies. Testament to the low fluorescence of the whiskies, only noisy emission spectra can be recorded, implying a large error in the measurements. Several whiskies show similar emission intensity (Figure 75C, partial examples are colored in yellow, orange, blue and green) and thus an identification is also impossible.

Next, a library of 22 PAEs (structures see Figure 76) were used for our study. Of these, 9 are positively charged (red color), 4 are neutral (green color) and 9 are negatively charged (blue color). We checked all of them against a sub-section of the tested whiskies (Table 14) using a plate reader. From the recorded fluorescence response patterns we conclude that positively charged PAEs (0.3mL, 2 µM) give an optical signal with 3 µL of whisky, while for neutral PAEs and for negatively charged PAEs we need 30 µL or 60 µL of the whiskies to elicit a similar fluorescence response, respectively (see Figure 77 and Figure 78). While for all of the different PAEs there is significant selectivity/cross-reactivity for the whiskies, the positively charged PAEs react strongest, suggesting that the "whisky interactome" i.e. the compounds or compound mixtures that are responsible for the generation of signal are mostly negatively charged, which indicating that hydrophobic and electrostatic interactions should paly the key role in the sensing process. Initial screenings with PAEs of diverse hydrophobicity and charge density show that neither of these interactions alone, but a combination of both is required to create distinct response patterns (Figure 79).

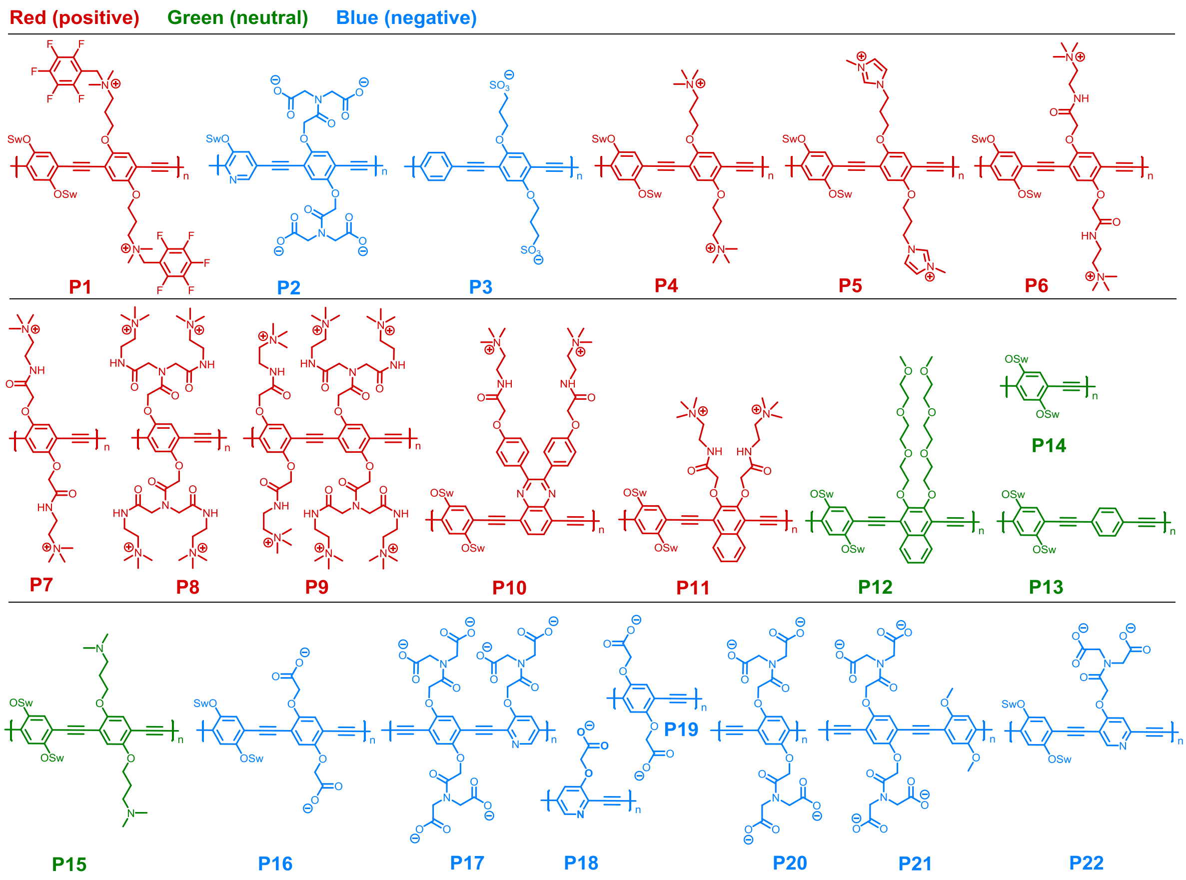

Figure 76. The structure of 22 PAEs used in this study, of these 9 are positively charged (red color), 4 are neutral (green color) and 9 are negatively charged (blue color).

To prove and explain the non-specific interactions (hydrophobic and electrostatic interactions) did make the most contribution to the whisky sensing, we selected PAEs (in MeOH or pH7 buffer) with increasing hydrophilic interaction (Figure 79A) and increasing electrostatic interaction (Figure 79B) to react with 13 randomly selected whiskies. The PAEs are: **P14** (only with hydrophilic swallowtail and hydrophobic backbone), **P13** (extended hydrophobic backbone), **P4** (positively charged and hydrophilic swallowtail) and **P6** (positively charged and without hydrophilic swallowtail).

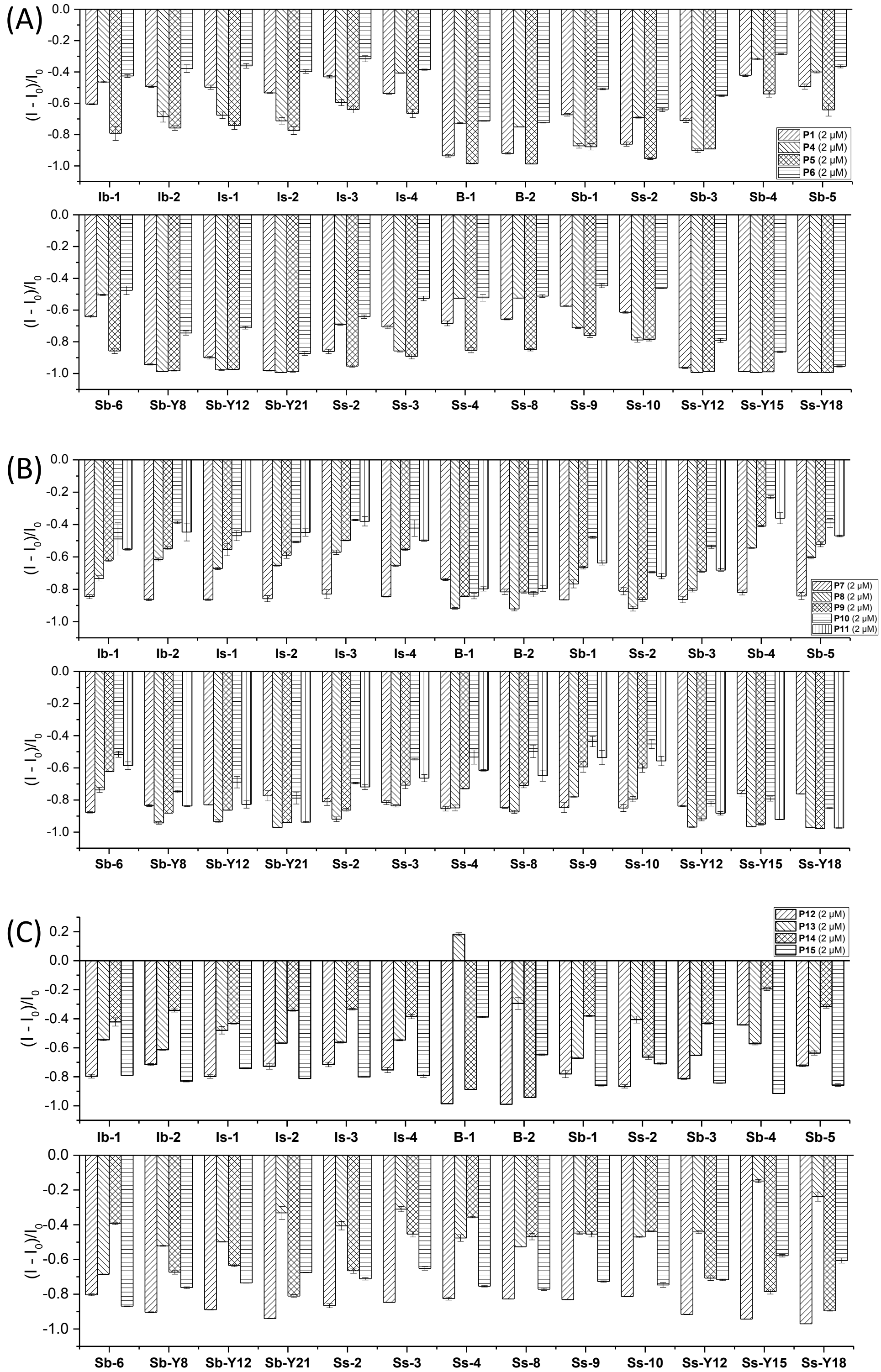

Figure 77. Fluorescence response pattern $(I - I_0) / I_0$ obtained by positively charged PAE **P1**, **P4-P6 (A)** and **P7**-**P11 (B)** (each at 2 µM, pH 7 buffered) treated with whisky samples (3 µL, 0.5%vol). **(C)** Fluorescence response pattern $(I - I_0) / I_0$ obtained by neutral PAE **P12**-**P15** (each at 2 µM, pH 7 buffered) treated with whisky samples (30 µL, 5%vol). Each value is the average of two measurements; each error bar is the standard deviation (SD) of two measurements.

As can be seen (Figure 79A), the increase of hydrophobicity of the used PAEs leads to a stronger quenching in two of the 13 whiskey samples, but the remaining whiskies still display a similar quenching behavior. The same behavior is observed, when increasing the electrostatic interaction of the applied PAEs. When the hydrophobicity and electrostatic interaction is well-balanced as **P4** at pH7 (Figure 79B) the highest diversity in quenching behavior of the investigated whiskies is observed.

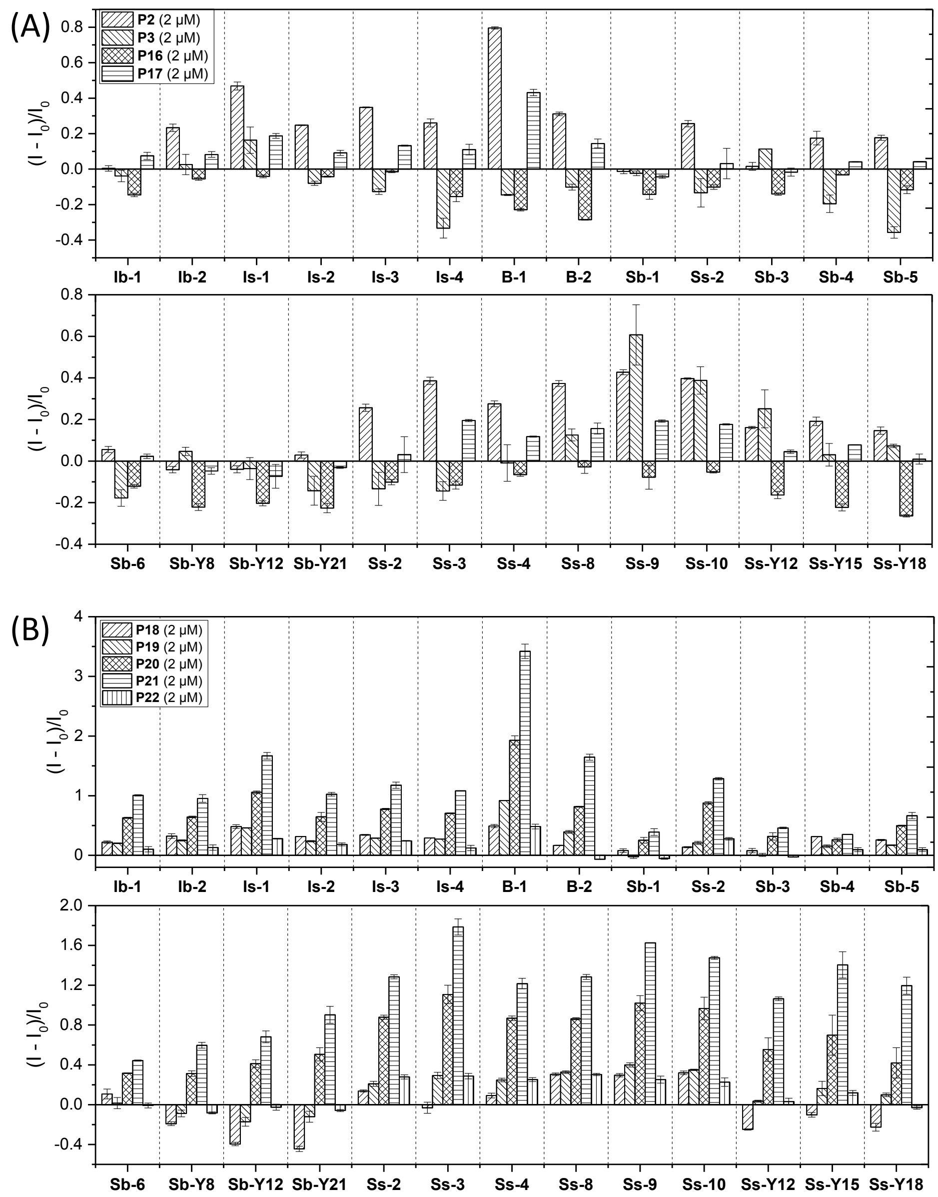

Figure 78. Fluorescence response pattern $(I - I_0) / I_0$ obtained by negatively charged PAE **P2-P3**, **P16-P17 (A)** and **P18-P22 (B)** (each at 2 µM, pH 7 buffered) treated with whisky samples (60 µL, 10%vol). Each value is the average of two measurements; each error bar is the standard deviation (SD) of two measurements.

Apparently, two oligoethylenglycol substituents and two charged side chains are required to assure distinctive interactions between the PAEs and the whiskies. Thus the sensory mechanism of our tongue is not based solely on one type of interaction, but relies on both: electrostatic and hydrophobic/hydrophilic interactions. As a consequence two PAEs of our finalized tongue have both oligoethylenglycol and charged side chains. We thus can conclude from the results that non-specific interactions (hydrophobic and electrostatic interactions) caused the signal generation and played a vital role in our tongue.

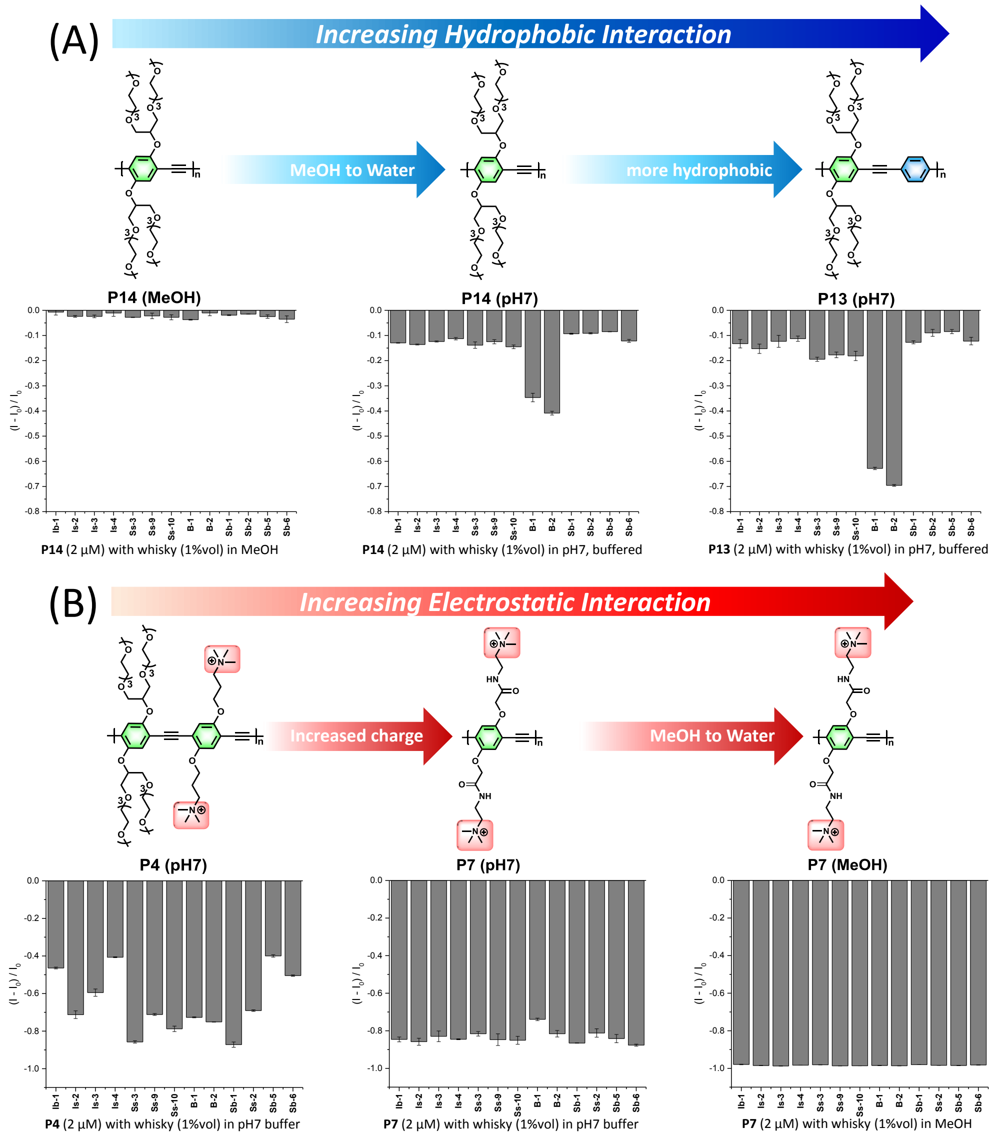

Figure 79. (A) PAEs with increasing hydrophilic interaction treated with 13 randomly selected whiskies (1%vol). **(B)** PAEs with increasing electrostatic interaction treated with 13 randomly selected whiskies (1%vol). Each value is the average of two measurements.

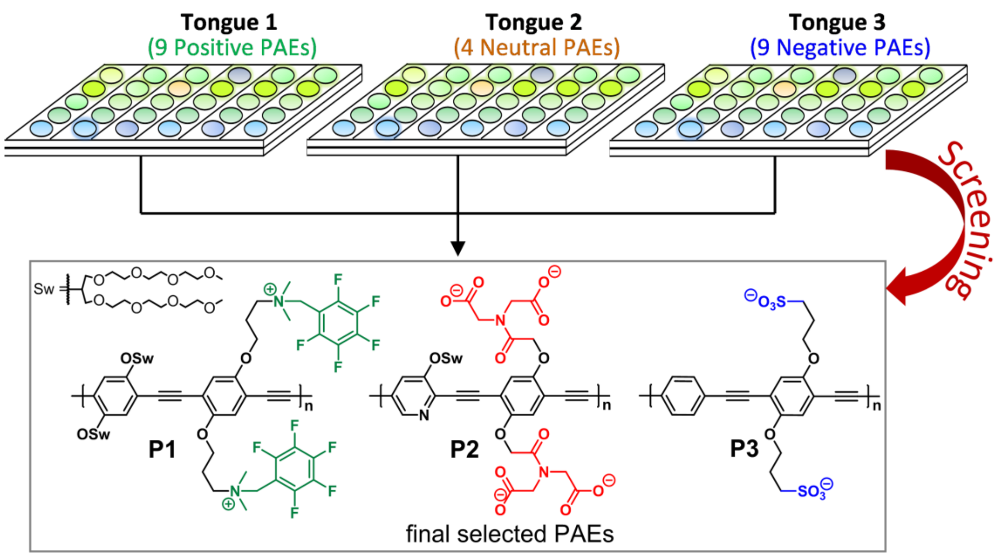

Figure 80. Screening process of PAE-based Tongue. Selection of the three most discriminating elements for the formation of a functional sensor array (for the details of the selection process see Figure 81)

Contribution of the Variables (%):

	Sensor elements	PC1 (52.9%)	PC2 (30.7%)	PC3 (6.4%)
Tongue 1 (9 Positive PAEs)	**P1** (2μM)	**8.268**	0.187	0.014
	P4 (2μM)	5.181	0.829	10.715
	P5 (2μM)	7.393	0.151	1.348
	P6 (2μM)	8.181	0.355	0.001
	P7 (2μM)	3.693	1.552	10.603
	P8 (2μM)	7.672	0.043	2.138
	P9 (2μM)	8.005	0.207	0.295
	P10 (2μM)	8.047	0.001	0.183
	P11 (2μM)	8.085	0.468	0.061
Tongue 2 (4 Neutral PAEs)	**P12** (2μM)	6.842	0.266	0.354
	P13 (2μM)	4.505	5.617	1.339
	P14 (2μM)	7.580	0.220	1.368
	P15 (2μM)	5.339	5.141	0.239
Tongue 3 (9 Negative PAEs)	**P2** (2μM)	0.036	**13.880**	0.248
	P3 (2μM)	0.246	0.060	**59.114**
	P16 (2μM)	5.363	0.455	9.709
	P17 (2μM)	0.053	13.468	0.015
	P18 (2μM)	3.754	6.056	0.000
	P19 (2μM)	0.106	13.849	0.116
	P20 (2μM)	0.218	13.537	0.402
	P21 (2μM)	1.081	12.665	0.022
	P22 (2μM)	0.351	10.996	1.714

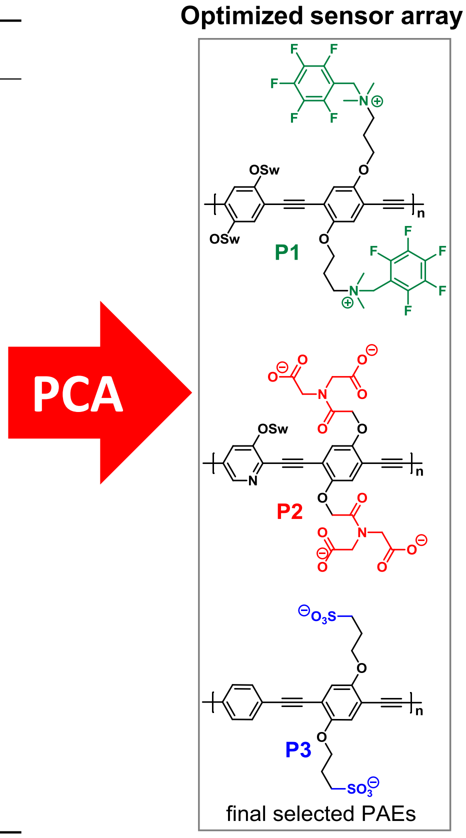

Figure 81. Optimization and selection of the best three sensing elements from Tongue 1 (positively charged PAEs), Tongue 2 (neutral PAEs) and Tongue 3 (negatively charged PAEs) based on the contribution of the variables of PCA.

Principal component analysis (PCA) of the responses (for the details of the selection process see Figure 81) selected three tongue elements (Figure 80) with the highest discriminative power; a positively charged PAE with a perfluorobenzylammonium group (**P1**) and two negatively charge PAEs (**P2** and **P3**), one carrying carboxylic acid groups and the other equipped with sulfonate groups.

3.3.2 Results and Discussions

Figure 82 depicts the overall results of the discrimination experiments. All of the whiskies are easily discriminated using the data from the small conjugated polymer assay. The three factors suffice to uniquely discriminate all of the samples (the jackknifed classification matrix with cross-validation reveals 99% accuracy, Table 55 and Figure 116). Blind tests were performed with randomly chosen whiskies of our training set. The new cases were classified into groups generated from the training matrix, based on the shortest Mahalanobis distance to the respective group. 4 of 120 unknown whiskies were misclassified, representing an accuracy of 96.7 % (Table 56). To explore the reproducibility of our sensing system, the 3D score plots have been reproduced from scratch by using a freshly made array of the PAE fluorophores (**P1**-**P3**) exhibiting similar results. More interestingly, two new single malt scotch whiskies (New-1, New-2 in Table 14) were selected and applied to our tongue. The fluorescence response was recorded and treated as blind sample in the LDA based on the initial training set. As a result the new whiskies, not being part of the initial training set were correctly identified as single malt scotch whiskies (Figure 83). In the next step, the data of the linear discriminant analysis (LDA) were analyzed with respect to specific properties (Figure 84 top).

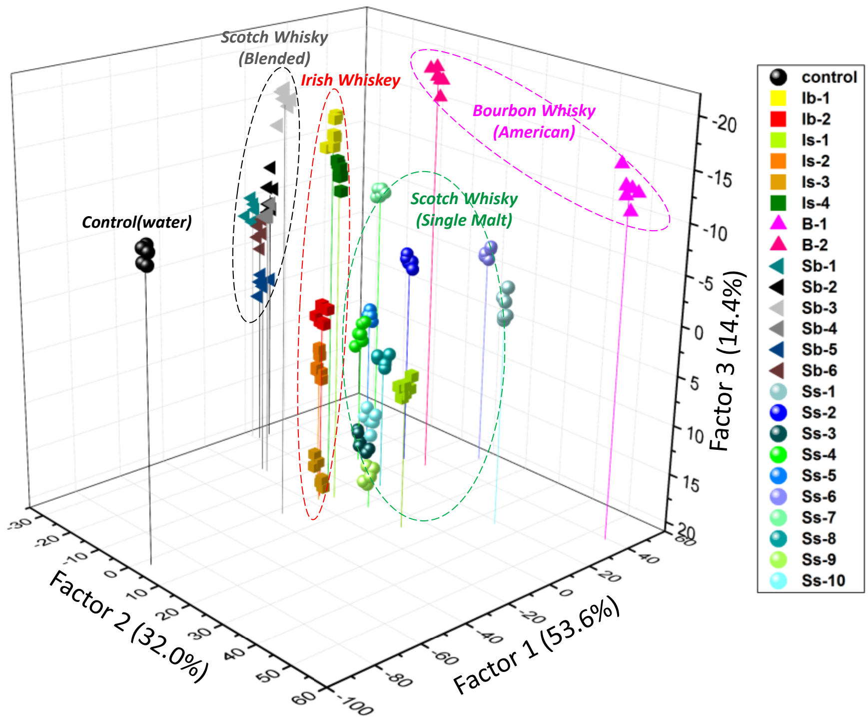

Figure 82. Discrimination of Whisky with PAE-based Tongue. 3D Linear discriminant analysis (LDA) plot of the fluorescence modulation data obtained with an array of final selected PAEs treated with all investigated whiskies. Each point represents the response pattern for a single whisky to the array. The jackknifed classification matrix with cross-validation reveals 99% accuracy.

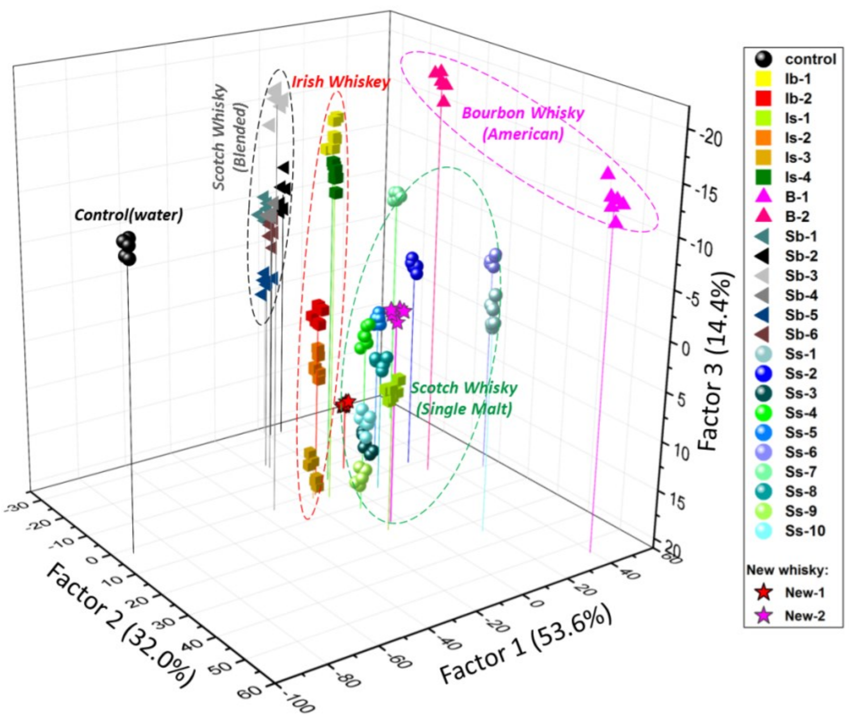

Figure 83. Two single malt scotch whiskies (details of New-1, New-2 were added in Table 1) which not used as part of the training set, were tested and calculated as blind with LDA, the results of 3D LDA plot shown that two new whiskies were located into the cluster of single malt Scotch Whisky (show as pentagram).

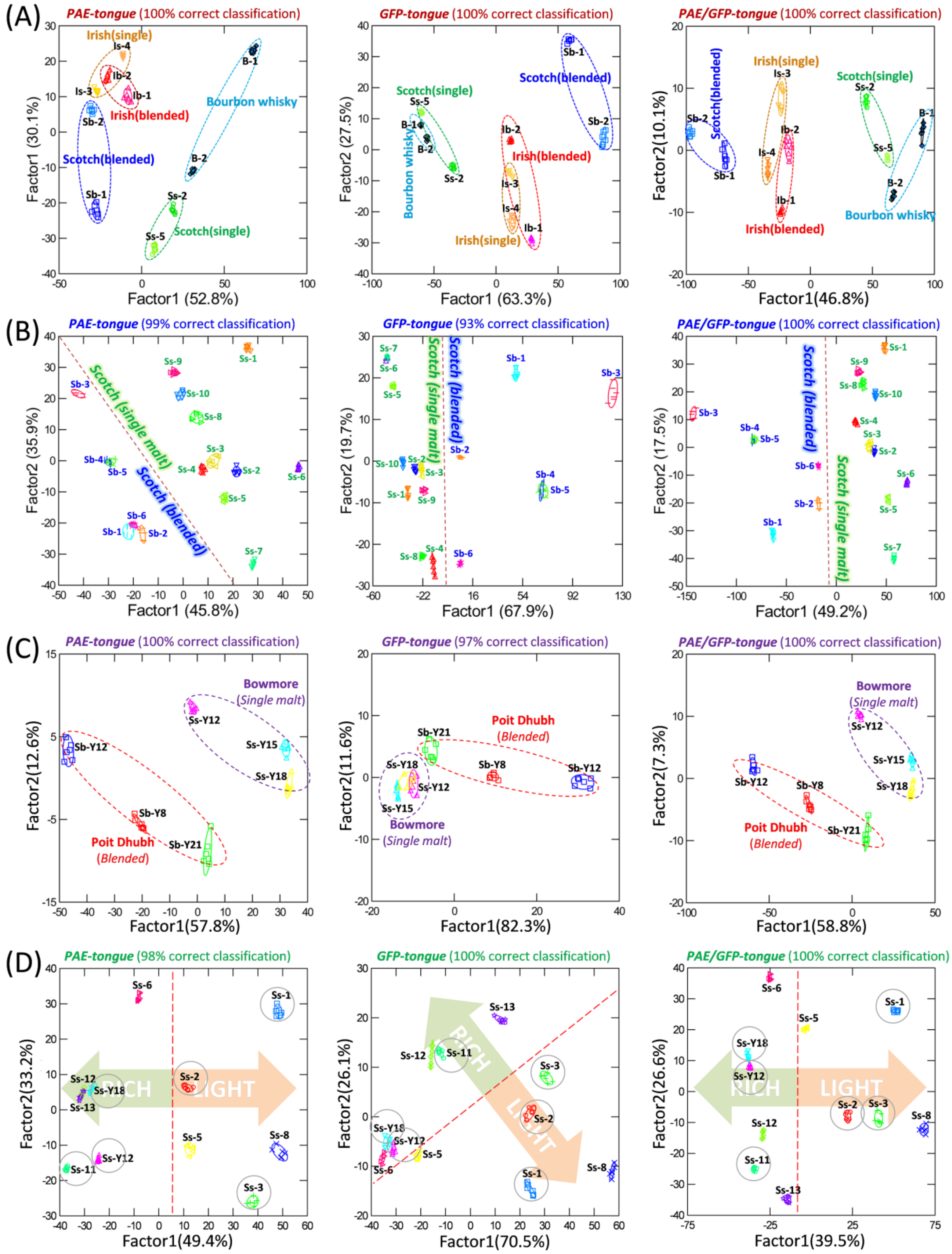

Figure 84. Discrimination of Whisky for Brand, Origin, Age and Taste. Discrimination of the whiskies for **(A)** origin, **(B)** blending status, **(C)** age, and **(D)** taste for **(left)** a pure PAE-tongue, **(middle)** a GFP-based tongue and **(right)** a joint GFP-PAE-tongue based on linear discriminant analysis (LDA), with 95% confidence ellipses. The published richness->lightness gradation is Ss-13, Ss-12, Ss-6, Ss-Y18, Ss-11, Ss-Y12 (rich) Ss-2, Ss-5, Ss-1, Ss-8, Ss-3. The grey rings in the bottom row (D) denote whiskies that are labeled "smoky". (Details see Table 57 - Table 68, Figure 117 - Figure 128)

We discriminate different types of whiskies, and distinguish between blended and single malt whiskies in all of the Scotch examples. We also investigated samples of whiskies of different age. For Bowmore single malt we find a linear relationship between age and response when looking at the LDA-sub-plot

(Figure 84C). In the blended whiskies, this relationship does not hold true anymore, but that is not too surprising, as in blends the ages of the constituent whiskies can and will vary to achieve a consistent taste and look. The last and perhaps most important quality is taste. Scotch is grouped along two different "taste" axes. The first axis is "smoky" and "delicate", while the second axis is "light" and "rich".[209-211] Surprisingly, we can not discriminate whiskies according to their peatiness i.e. smoky character but the array discriminates light from rich, very malty whiskies (Figure 84D).

Are PAEs the only fluorescent systems that discriminate whiskies? We investigated GFPs (collaboration with Prof. Andreas Herrmann, from Zernike Institute for Advanced Materials, University of Groningen), fused to unfolded, supercharged polypeptide chains.[212-213] These genetically engineered tags consist mainly of the pentapeptide repeat [GVGXP]$_n$, with X being either a positively charged lysine (K) residue or a negatively charged glutamic acid (E).[214] These motifs were multimerized to exhibit 36 charged amino acids. The fluorescent protein tongue consisted of three elements: Conventional GFP with a net charge of -7, a highly positively charged variant (GFP-K36) and a highly negatively charged one (GFP-E36, Figure 85C). The amount of whisky necessary for a useful signal generation was lower than for the PAEs: 0.5 µL for GFP-K36, 1.5 µL for GFP and 15 µL for GFP-E36 (for the details of the concentration and pH selection process see Figure 85).

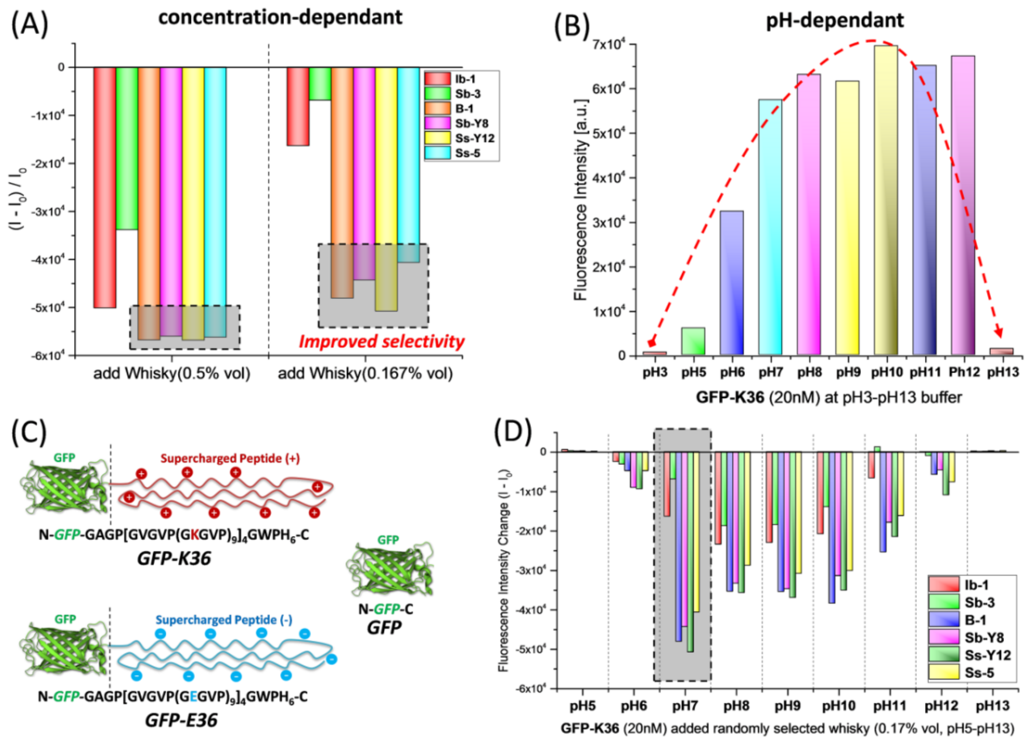

Figure 85. (A). GFP-K36 (20nM, pH7) treated with randomly selected six whiskies at different concentration (0.5% vol and 0.167% vol) for screening. Whisky concentration (0.167% vol) was selected for the further pH-dependant screening. **(B).** GFP-K36 (20nM, pH7) at different pH condition (pH3 to pH13). The fluorescence of GFP-K36 was strongly quenched at acid or base condition, similar results were also observed for GFP and GFP-E36. **(C).** Different GFP variants (GFP, GFP-K36 and GFP-E36) employed for sensing. **(D).** GFP-K36 (20nM, pH7 buffered) treated with whiskies at different pH condition (pH3 to pH13). Condition at pH7 was selected for sensing. The similar screening process also applied for GFP and GFP-E36.

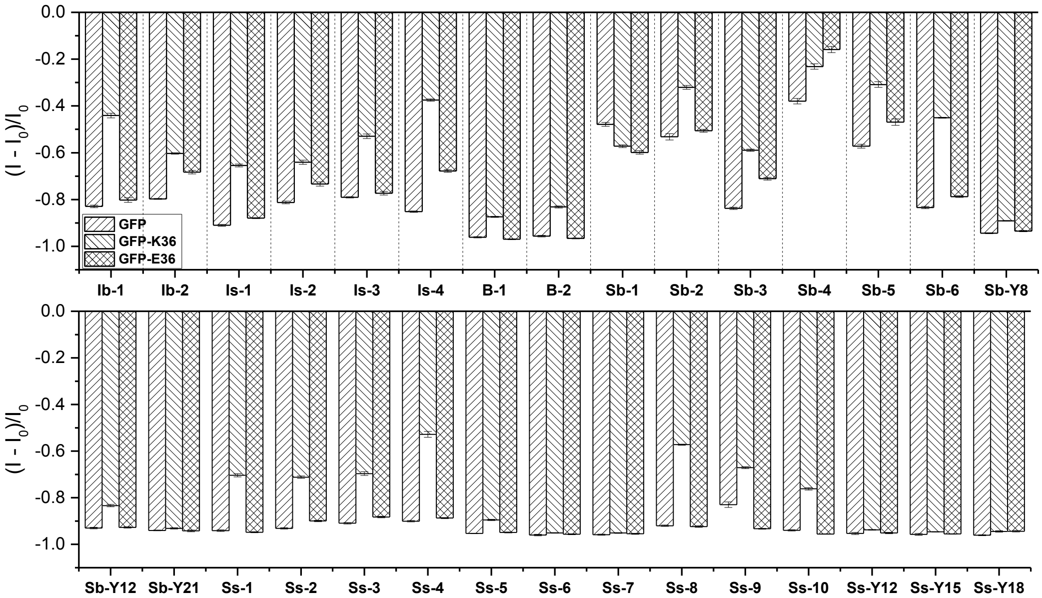

Figure 86. Fluorescence response pattern $(I - I_0) / I_0$ obtained by **GFP**, **GFP-K36** and **GFP-E36** (each at 20 nM, pH 7 buffered) treated with whisky samples (0.5%vol, 0.17%vol, 2%vol). Each value is the average of six measurements; each error bar is the standard deviation (SD) of six measurements.

Figure 84 (middle) shows the overall sensing outcome for a GFP-based tongue. The results compare to those obtained by the PAE array. The analytes are differentiated a bit worse than in the case of the PAEs, but considering that the direct protein environment close to the chromophore of GFP is very similar and structural differences are located at the rim of the folded scaffold, the result is remarkable. The positively charged GFP, similar to **P1**, reacts most sensitively towards the whisky, as its interactome must be negatively charged. A combined PAE/GFP tongue (Figure 84 right) is even better than each of the single tongues, particularly with respect to discriminate blends from single malt whiskies. It is surprising that two chemically so different tongues are supremely successful in differentiating whiskies.

3.3.3 Fingerprinting Whiskey with GC-MS

The arrays do not need *any* sample preparation; the analyte is pipetted to the solution of the fluorescent dyes. The analysis is performed with a standard plate reader on a 96 well plate. Multiple analytes are measured in one run, and data workup is performed by LDA with a commercial statistics software. Alternative methods to investigate whiskies (mid-IR, simple UV-vis spectroscopy) either do show a considerably lower “resolving power”, with respect to the analytes (UV-VIS spectroscopy or mid-IR spectroscopy) or they need a significant amount of sample preparation and fairly specialized equipment when performing MS and GC-MS.[215]

We performed an analysis of whiskies using a standard GC-MS combination with optimized methods (Figure 87), the three most important peaks of GC-MS was selected, transformed and calculated with PCA (Table 54 and Figure 88), but the final results (see Figure 89) were worse compared to that of our chemical tongues. Here, we need around 6 mL of sample and a significant amount of preparation time (each sample, 30 min for liquid-liquid extraction and mini silica gel column drying process, 30 min for a GC-MS run. The relatively low resolution is disappointing. While more specialized, electrospray-based MS approaches[216] do not need sample preparation and show improved discrimination, they still require a large investment in hardware and do not seem to quite reach the "resolution" we obtain with simple fluorescence-based arrays.

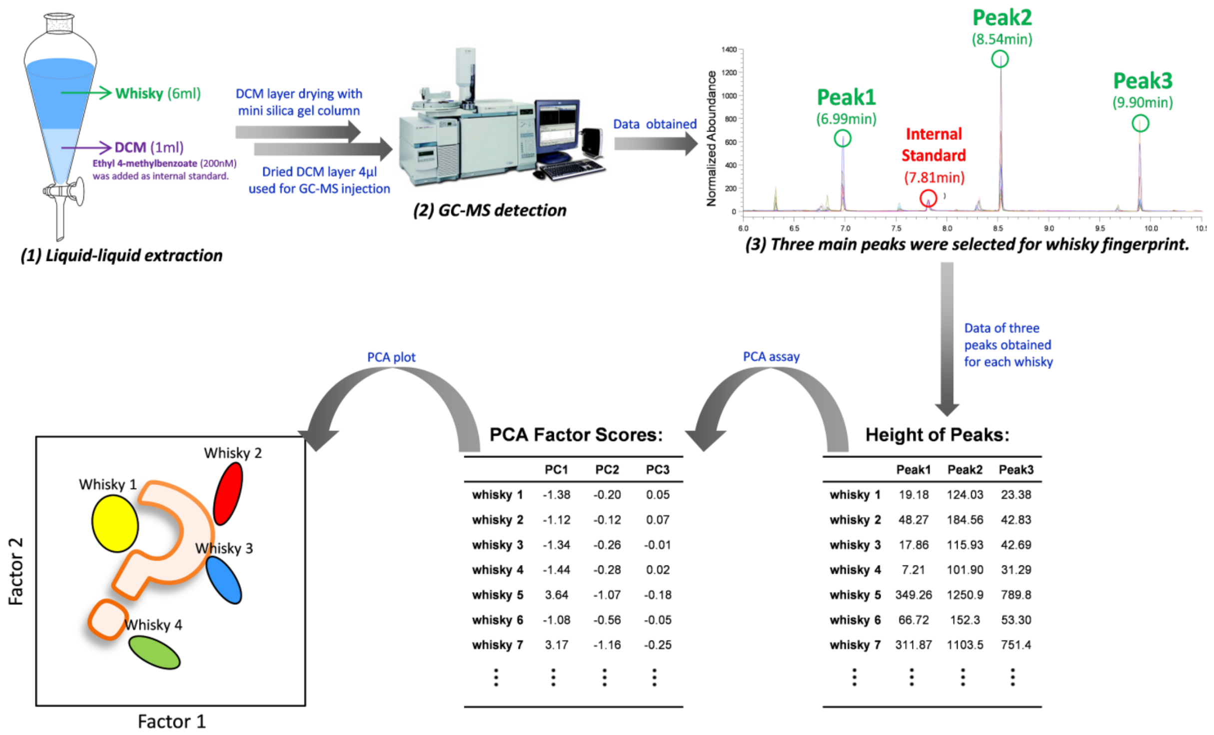

Figure 87. Final optimized methods and procedures for whiskey fingerprint.

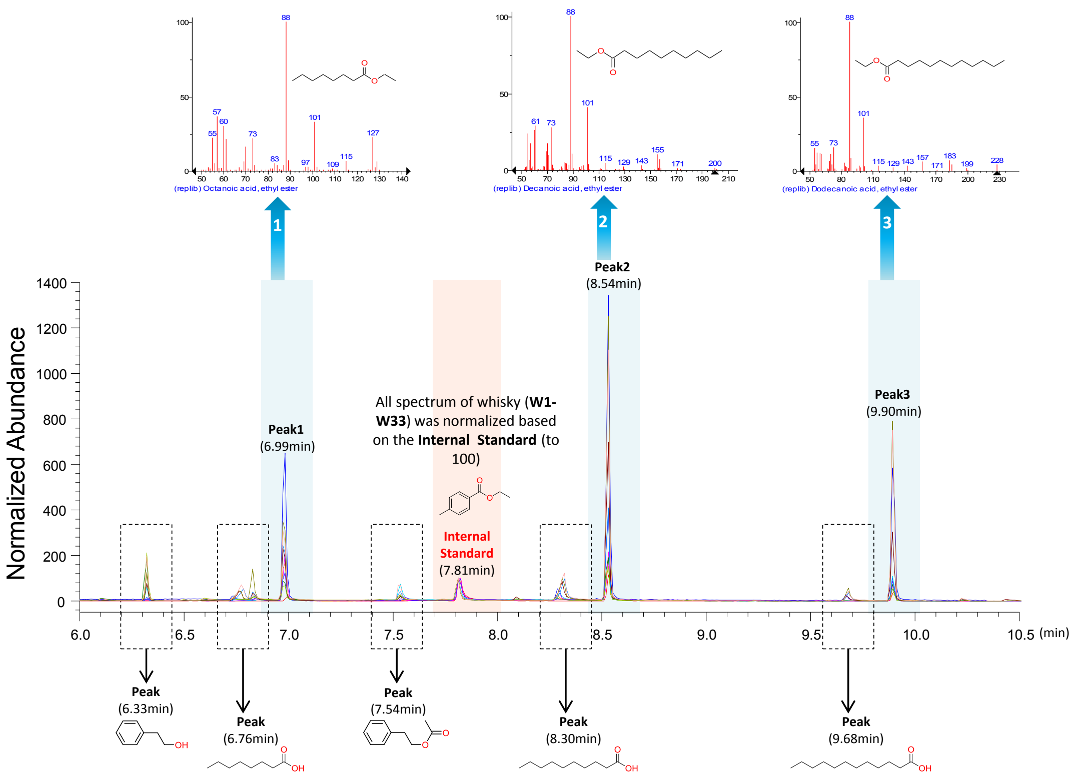

Figure 88. Chemical structure of each peak obtained from GC-MS data of whiskies (structure were obtained from Mass matched by NIST Standard Reference Database 1A Version 2005, with over 90% accuracy).

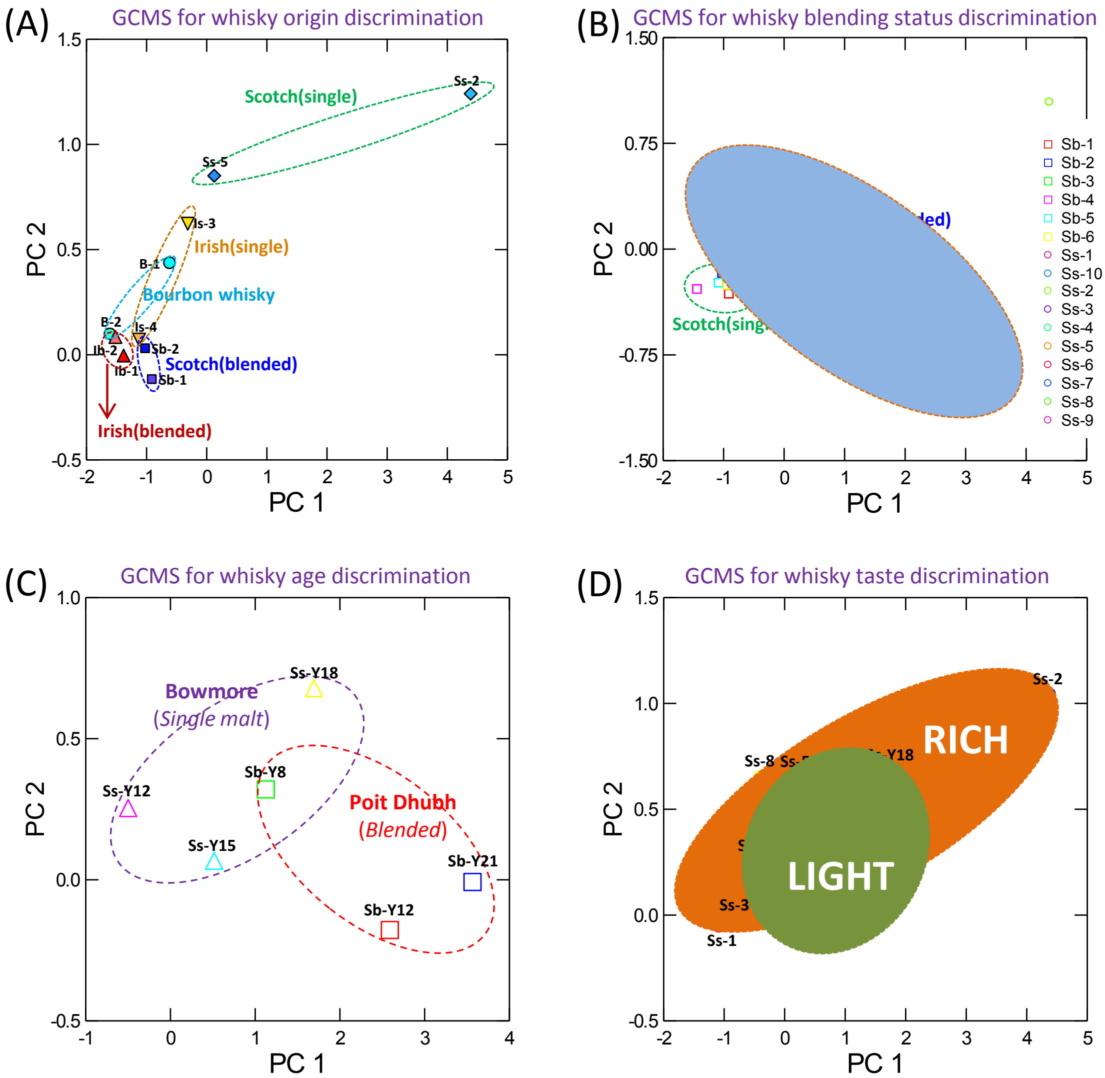

Figure 89. Discrimination of the whiskies with GCMS for (a) origin, (b) blending status, (c) age, and (d) taste by sing GC-MS based on principal components analysis (PCA).

3.3.4 Conclusions

In conclusion, two different, hypothesis-free sensor arrays based upon three fluorophores each, successfully discriminate Whisky samples for brand, origin, blending state, age and taste. Both tongues create patterns based upon fluorescence modulation, exquisitely sensitive, here, for whiskies. Signal generation depends on fluorescence intensity modulation of the dyes; the nature of the excited state and its interaction with the analytes plays a critical role. In conventional sensor applications, nonspecific interactions are troublesome reducing fluorescence quantum yields and/or fluorescence lifetimes. Nonspecific interactions exert undesired and unpredictable effects that one can neither calculate nor model, however, when parallelized in sensor arrays such interactions are the basis for discrimination and deliver spectacular power in hypothesis-free setups. In the end, small sensor arrays based on charged fluorophore systems are powerful tools that discriminate any soluble analyte, apparently regardless of its structure, function or origin.

Chapter 4. PAE-Based Chemical Tongue for Sensing of Bioanalytes

4.1 Polymer/Peptide Complex-Based Tongues Discriminate Bacteria in Complex Biological Milieu

In this contribution, we disclose a fluorescent sensor array of four electrostatic complexes, comprised of one negatively charged poly(*para*-phenyleneethynylene **PPE 1** and four positively charged antimicrobial peptides AMPs **1**-**4**. The AMPs quench the PPE's fluorescence. The four partially quenched complexes identify fourteen different bacteria in water and in human urine by pattern based fluorescence recognition (i.e. turn on or further fluorescence turn off), owing to the differential binding of the AMPs and PPEs to the components of the bacterial surface (Figure 90). The bacterial types form clusters according to staining properties (Gram-positive and Gram-negative) or genetic similarity (genus, species and strain). The identification and data treatment is performed by pattern evaluation with linear discriminant analysis (LDA) of the collected fluorescence intensity data. Experiments were performed in collaboration with Prof. Michael Wink and Haoran Cheng, from Institute of Pharmacy and Molecular Biotechnology (IPMB, Heidelberg University).

4.1.1 Introduction and Construction of PAE/AMP Tongue

Bacterial infections are still one of the leading causes of human death (40%); at the same time antibiotic resistance of microbes (AMR) has increased to levels that make some infections difficult to treat[217-218]. Around 6k humans die in Germany and around 0.7 M humans in the whole world as a consequence of AMR, as a growing number of microbes is un-responsive towards antibiotics[144]; multidrug resistant strains (MDR) have developed. The reason for this situation is multifaceted and includes antibiotics use in livestock, uncontrolled sales in second world countries and over-prescription in first world countries. This situation makes the rapid and efficient identification and classification of bacteria a vital issue. Planting and culturing are[131] the gold standard of bacteriology but take 24 – 72 h, and some bacteria are only cultured on specific substrates. Yet, the high sensitivity and at the same time the fairly facile screening for AMR leaves this method without serious competition in most clinical settings. The time lag, however, can be a problem for patients with any serious infection.

More recently, polymerase chain reaction (PCR),[132-133] antibodies, gene microarrays,[134-135] mass spectrometry[136] and surface-enhanced Raman spectroscopy (SERS)[137] as well as bio- and chemo-materials functionalized with recognition elements, such as antibodies (IgG),[138-139] aptamers,[140] phage display[141-142] and carbohydrates,[143] have been[144] developed as alternatives, which, however, have other disadvantages such as their non-generality, high cost for purchase and maintenance of expensive and highly complex instrumentation, complex procedures etc. Bazan et al.[146] employed electrostatic complexes, containing a cationic conjugated oligoelectrolyte and fluorescein (FAM)-labeled single-stranded DNA (ssDNA), identified seven bacteria. Jiang et al.[147] designed a fluorescent turn-on sensor array with five small molecular aggregation-induced emission (AIE) probes and eight different types of bacteria were identified successfully.

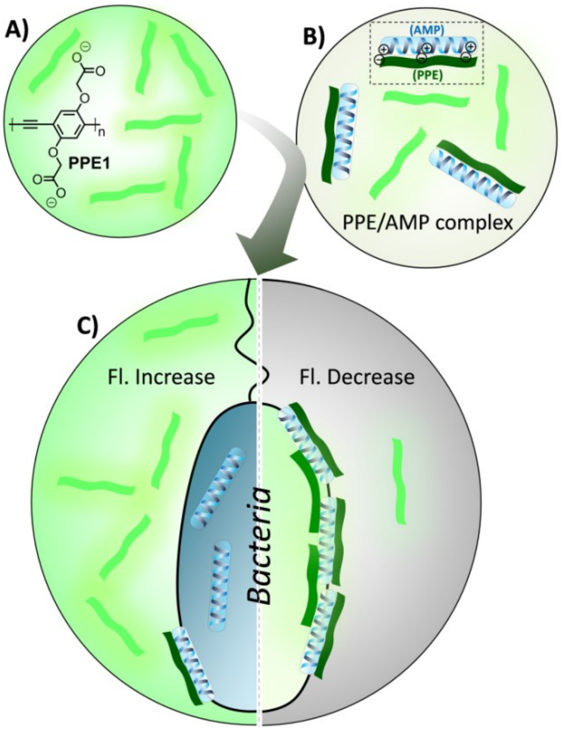

Figure 90. Schematic representation of PPE/AMP complex sensor array for the discrimination of bacteria. (**A**) Structure of fluorescent polymer **PPE 1**. (**B**) Electrostatic complex formed between negatively charged **PPE 1** and positively charged AMP, AMP quench the PPE's fluorescence. (**C**) The addition of bacteria to the complex, leads to the fluorescence increase by indicator displacement (**left**) or results in the fluorescence decrease by the aggregation of PPEs and AMPs on the surface of bacteria (**right**).

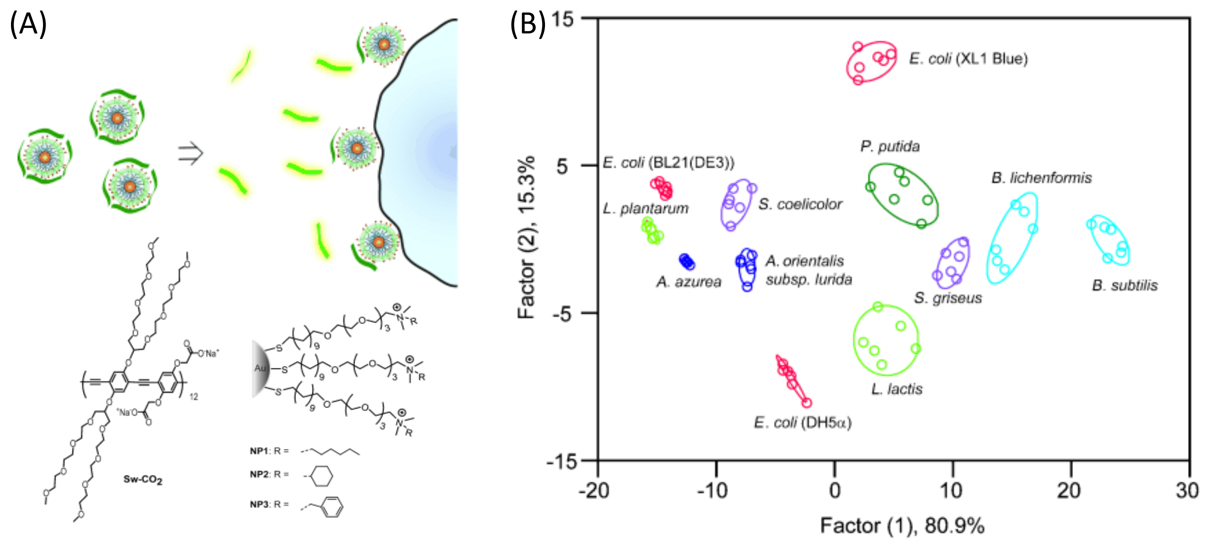

Figure 91. (A) Schematic representation of the displacement of anionic conjugated polymers from cationic nanoparticles by negatively charged bacterial surfaces. Receptor and transducer components of the bacterial sensors. Structural representation of three cationic gold nanoparticles (**NP1–NP3**) with various hydrophobic tails and one conjugated polymer (Sw-CO2) featuring a branched oligo(ethyleneglycol) side chain. **(B)** Canonical score plot for the fluorescence response patterns as determined with LDA. The first two factors collate 96.2% of the variance. 95% confidence ellipses for the individual bacteria are depicted. Figure reproduced with permission from reference [56] © 2010, Wiley VCH.

We have recently developed a simple array composed of an anionic PPE and three different cationic gold nanoparticles (Figure 91).[56] The three electrostatic complexes formed from the nanoparticles and the PPE are greatly reduced in their fluorescence and form a small array. The addition of different bacteria to this small array led to fluorescence intensity modulation that, upon linear discriminant analysis (LDA), identifies the microbes. Even several *E. coli* strains were distinguished, however, the microbes did not group with respect to their genetic or gram relationship to each other[145], and application to complex biological fluids (serum, urine) has not been reported for this system.

Table 15. Detailed information of the positively charged AMPs used in this study.

Nr.	Name	Source	Sequence	Net Charge	Length	Hydrophobic Residue	Mass (kDa)	Activity
AMP1	Protamine	*Salmon*	MPRRRRSSSRPVRRRRR PRVSRRRRRRGGRRRR	21	33	9%	5.1	anti-Gram+ and Gram-
AMP2	Ib-AMP4	*Seeds, Impatiens balsamina (Ib)*	QWGRRCCGWG PGRRYCRRWC	6	20	35%	2.55	anti-Gram+
AMP3	PAF26	*Synthetic*	**RKKWFW**	3	6	50%	0.95	anti-Gram+ and Gram-
AMP4	Jelleine-I	*Honeybees, Apis mellifera*	**PFKLSLHL**	2	8	50%	0.96	anti-Gram+ and Gram-

Here we employ a four-element tongue, consisting of four cationic antimicrobial peptides (AMPs **1-4**, Table 15) and the negatively charged **PPE 1** as sensor array that identifies and classifies different types of bacteria. AMPs are small oligopeptides with cationic and hydrophobic amino acid residues of natural origin[219-221], stable and easily available. They form tight complexes with the PPEs, the fluorescence of which is quenched. AMPs bind to different bacterial species due to their positive charge.[222-224] With the four sensor elements formed from **PPE 1** and AMPs **1-4**, we investigated 14 different bacteria, including six Gram-negative and eight Gram-positive ones. Especially, to validate the efficiency of our designed AMP-based sensing system, we selected five different species of *Kocuria* and four different strains of *Escherichia coli (E.coli)* with increasing biochemical and genetic similarity (Table 17).

Table 16. Binding constants (log K_{SV}) obtained from quenching data by mixing PPE1 with AMPs 1-4 to form M1-M4 (details see the Supporting Information).

M1	M2	M3	M4
PPE1 +AMP1	PPE1 +AMP2	PPE1 +AMP3	PPE1 +AMP4
10.4 ± 0.2	9.43 ± 0.9	7.38 ± 0.9	5.4 ± 0.2

Table 17. Details of bacteria used in this study.

Nr.	Abbreviation	Gram	Nomenclature		
			Genus	Species	Strain
1	*B. megaterium*	positive	Bacillus	megaterium	-
2	*S. auricularis*	positive	Staphylococcus	auricularis	-
3	*M. leteus*	positive	Micrococcus	leteus	-
4	*K. kristinae*	positive	Kocuria	kristinae	-
5	*K. marina*	positive	Kocuria	marina	-
6	*K. rhizophilia*	positive	Kocuria	rhizophilia	-
7	*K. salsicia*	positive	Kocuria	salsicia	-
8	*K. varians*	positive	Kocuria	varians	-
9	*P. fluorescens*	negative	Pseudomonas	fluorescens	-
10	*Y. mollaretii*	negative	Yersinia	mollaretii	-
11	*E. coli K12*	negative	Escherichia	coli	K12
12	*E. coli HT115*	negative	Escherichia	coli	HT115
13	*E. coli OP50*	negative	Escherichia	coli	OP50
14	*E. coli DH5α*	negative	Escherichia	coli	DH5α

4.1.2 PAE/AMP Tongue Discriminates Bacteria in Water

The negatively charged, fluorescent polymer **PPE 1** were titrated with four positively charged antimicrobial peptides AMPs **1-4** (Table 15) in aqueous solution (details of the titration see Chapter 5.4.5 Figure 133). Binding constants of the formed complexes **M1-M4** of up to log K_{sv} = 10 were obtained by using a modified Stern–Volmer equation (Table 16). Binding constants rise - as expected - with the increase of net charge of AMPs (Table 15). To note, the log K_{sv} values of the PAE/AMP complexes are bigger than those of PAE/PAE complexes (log K_{sv} 5–7),[40-41, 47, 225] indicating a more sensitive method while detecting analytes. After having established the binding constants of **M1-M4**, we investigated the four complexes (approximately 40% of the fluorescence intensity retained) for their sensing application by detecting the bacteria. Fourteen different bacteria with increasing biochemical and genetic similarity were investigated, including six Gram-negative and eight Gram-positive ones.

For the first model study to test our methodology, we exposed the suspensions of 14 bacteria (OD_{600} = 0.1) to the solutions of the complexes in water. Figure 92A showeded the fluorescence modulation, while Figure 92B displays the LDA[61, 63] plots of all of the investigated bacteria with the four complexes; LDA converts the training matrix (4 complexes X 14 bacteria X 6 replicates) into canonical scores, prepared according to their Mahalanobis distance. The jackknifed classification matrix with cross-validation reveals 100% accuracy for PPE/AMP complex sensor array. As a result, all of the bacteria are reliably discerned. Interestingly, Gram-positive bacteria were observed that located to the left-hand side of the plot, while Gram-negative bacteria located on the right-hand side of the plot (Figure 92B, factor 1). This result could be explained by the significant structural difference between Gram-positive and Gram-negative bacteria, especially, AMPs differentially bind to the lipopolysaccharide (LPS)[222]. LPS is the main component of cell walls of Gram-negative bacteria, which is not existting in Gram-positive bacteria. This result indicates a potential and useful tool to for the discrimination of Gram-positive and Gram-negative bacteria.

To further validate the efficiency of our sensing system, we established blind test with randomly chosen bacteria of our training set. The new cases were classified into groups, generated from the training matrix mentioned above, based on the shortest Mahalanobis distance to the respective group. For PPE/AMP sensor array, 72 unknown sample solutions were studied, 66 were correctly identified, representing an accuracy of 92%.

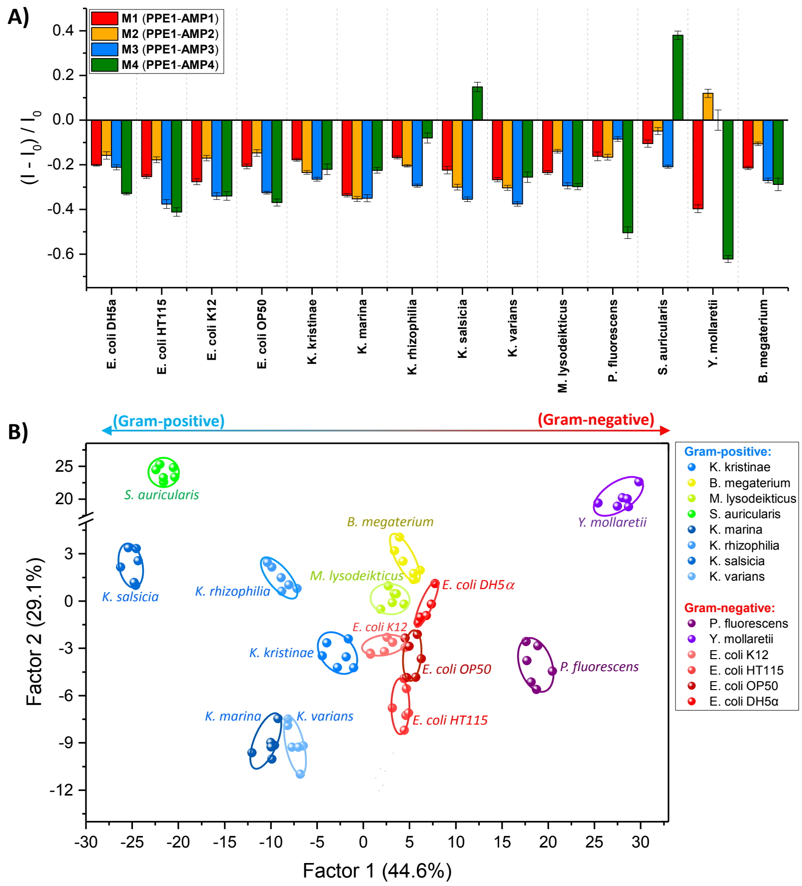

Figure 92. **(A)** Fluorescence response pattern (I - I_0) / I_0 obtained by PPE/AMP complexes **M1-M4** (1 µM in water) treated with different bacteria in water (OD_{600} = 0.1, incubation for 30 min). Each value is the average of six independent measurements; each error bar shows the standard deviation (SD) of these measurements. **(B)** 2D canonical score plot for the first two factors of simplified fluorescence response patterns obtained with an array of PPE/AMP complexes M1-M4 (1 µM) treated with different bacteria in water (OD_{600} = 0.1, incubation for 30 min). 95 % confidence ellipses for the individual bacteria are depicted. Each point represents the response pattern for a single bacteria to the array. (Five different species of *Kocuria* were shown as blue color; four different strains of *Escherichia coli* were shown as red color). The jackknifed classification matrix with cross-validation reveals 100% accuracy; blind test shows 91.7% accuracy (66/72).

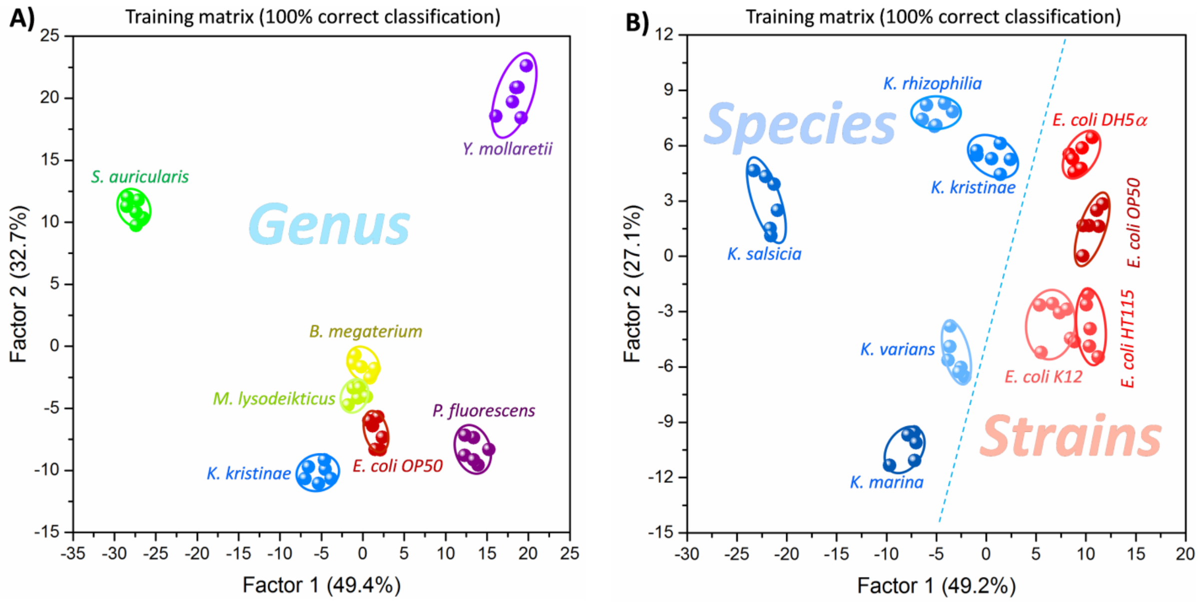

Figure 93. 2D canonical score plot of bacteria with **(A)** different genera and **(B)** different species and strains, obtained with an array of PPE/AMP complexes **M1-M4** (1 µM) treated with different bacteria in water (OD_{600} = 0.1, incubation for 30 min). 95 % confidence ellipses for the individual bacteria are depicted. Each point represents the response pattern for single bacteria to the array.

In the next step, the data of the linear discriminant analysis (LDA) were analyzed with respect to specific types of bacteria (genus, species and strains). Figure 93A show the identification of bacteria from seven genus in water, and similarly, the results of five species of *Kocuria* and four strains of *Escherichia coli (E. coli)* were shown in Figure 93B. The accuracy of blind test was shown in Table 18. LDA discriminated seven genera of bacteria, five species of *Kocuria* and four strains of *E. coli*, Blind tests show 85% and 96% accuracy, respectively.

4.1.3 PAE/AMP Tongue Discriminates Bacteria in Urine

The ultimate purpose of developing sensors for bio-analytes is to create a simple technique for the rapid detection and diagnosis of disease according to the analysis of clinical specimens (blood, urine, swab, saliva, etc.). Thus, it would be more interesting, challenging and clinically demanding if we can apply our sensing system to complex biological fluids, instead of water solution. Saliva is hard to detect because of its substantial viscosity. Blood serum is a complicated mixture solution with more than 20,000 proteins, and overall protein content is greater than 1 mM, and human urine is a more complex biological milieu contains urea, uric acid, inorganic salts, amino acids, proteins, hormones, and metabolites, etc.

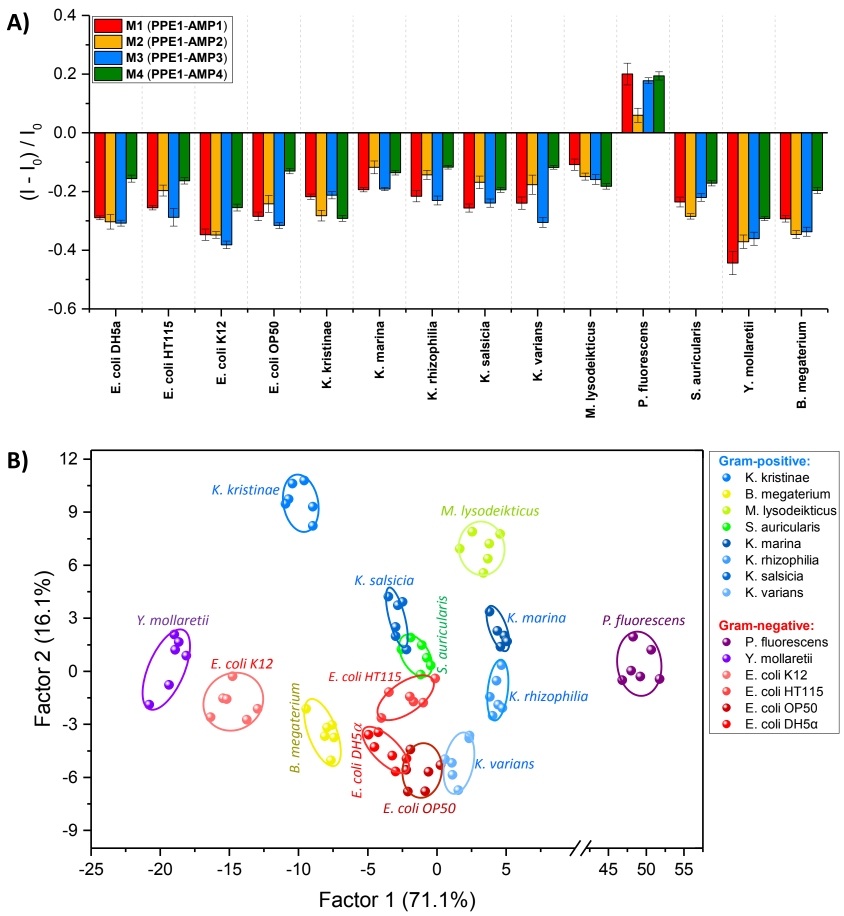

Figure 94. (A) Fluorescence response pattern $(I - I_0) / I_0$ obtained by PPE/AMP complexes **M1-M4** (1 μM in water) treated with 14 bacteria in urine (OD_{600} = 0.1, incubation for 30 min). Each value is the average of six independent measurements; each error bar shows the standard deviation (SD) of these measurements. **(B)** 2D canonical score plot for the first two factors of simplified fluorescence response patterns obtained with an array of PPE/AMP complexes **M1-M4** (1 μM) treated with different bacteria in urine (OD_{600} = 0.1, incubation for 30 min). 95 % confidence ellipses for the individual bacteria are

depicted. Each point represents the response pattern for a single bacteria to the array. (Five different species of *Kocuria* were shown as blue color; four different strains of *Escherichia coli* were shown as red color). The jackknifed classification matrix with cross-validation reveals 98% accuracy; blind test shows 88% accuracy (49/56).

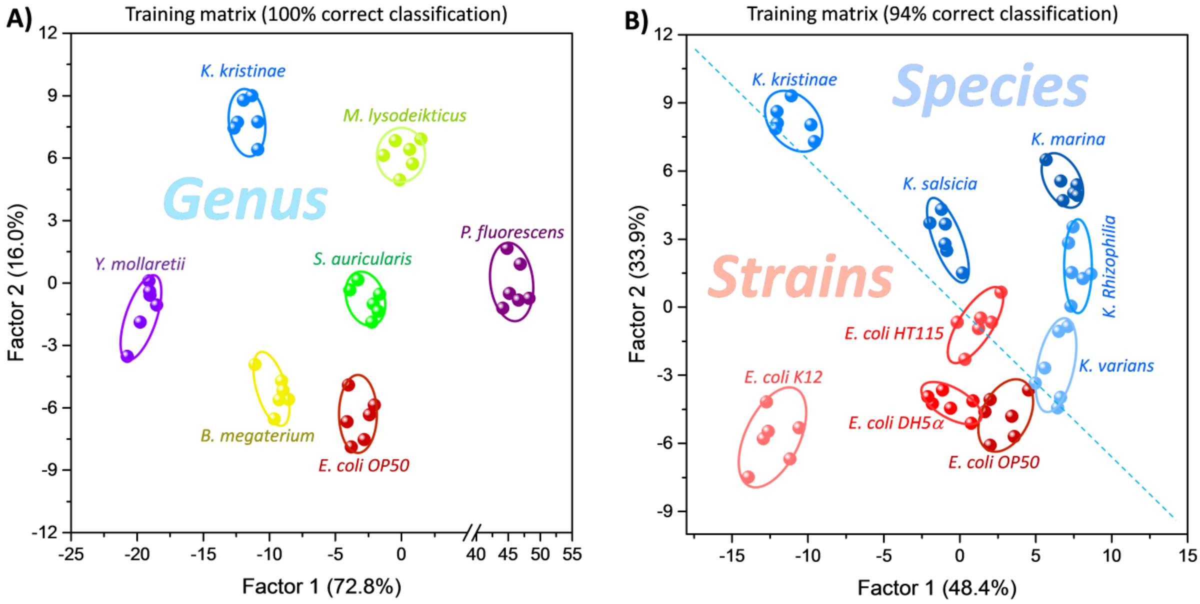

Figure 95. **(A)** 2D canonical score plot of bacteria with different genus and **(B)** 2D canonical score plot of bacteria with different species and strain obtained with an array of PPE/AMP complexes **M1**-**M4** (1 µM) treated with different bacteria in urine (OD_{600} = 0.1, incubation for 30 min). 95 % confidence ellipses for the individual bacteria are depicted. Each point represents the response pattern for single bacteria to the array.

Table 18. Accuracy of the blind test obtained from PAE/AMP complex with bacteria in water and in urine.

Bacteria	genus	species and strains	genus	species and strains	genus	species and strains
Milieu	water	water	urine	urine	urine	urine
Concentration (OD_{600})	0.1	0.1	0.1	0.1	0.01	0.01
Number of samples	28	42	28	33	24	28
Correctly identified	33	44	28	36	28	36
Accuracy (%)	84.8	95.5	100	94	85.7	77.8

Detection of bacteria in urine is non-invasive but important in clinical settings. We employed our system in human urine (four complexes with 14 bacteria at a concentration of OD_{600}= 0.1). Figure 94 - Figure 95 show the corresponding LDA results, all bacteria were successfully discriminated in urine. The results are as reliable as in water, as the contents of urine do not seem to interfere. Especially, seven genera of bacteria (Figure 95A), as well as four species of *Kocuria* (Gram+) and five strains of *E.coli* (Gram-) in Figure 95B have been successfully discriminated and grouped according to their biochemical and genetic similarity. Blind test (Table 18) showed 100% and 94% accuracy, respectively, allowing for higher accuracy in discrimination of the genera in urine (100%) than that in water (85%).

After the successful detection of bacteria in human urine, the next challenge was to detect the bacteria at a clinically relevant concentration levels. Typically, the disease related concentration in urine is 10^5-10^7 bacteria/mL,[226] based on our counting experiment of all used bacteria (Table 19), which is approach to OD_{600} values of 0.001 – 0.1. Thus, we further decreased the concentration of bacteria to

OD_{600} 0.01 (Figure 96 - Figure 97). From the 2D LDA results for bacteria of different genus (7 types, Figure 97A), species and strains (nine kinds, Figure 97B), most of the bacteria were successfully discriminated. Although the decreased concentration lead to slightly decreased accuracy when compared to the concentration of OD_{600} = 0.1, and few samples showed some overlap (*B. megaterium* and *S. auricularis*, as well as two species of *K. rhizophilia* and *K. salsicia*), most of the bacteria were successfully identified in urine.

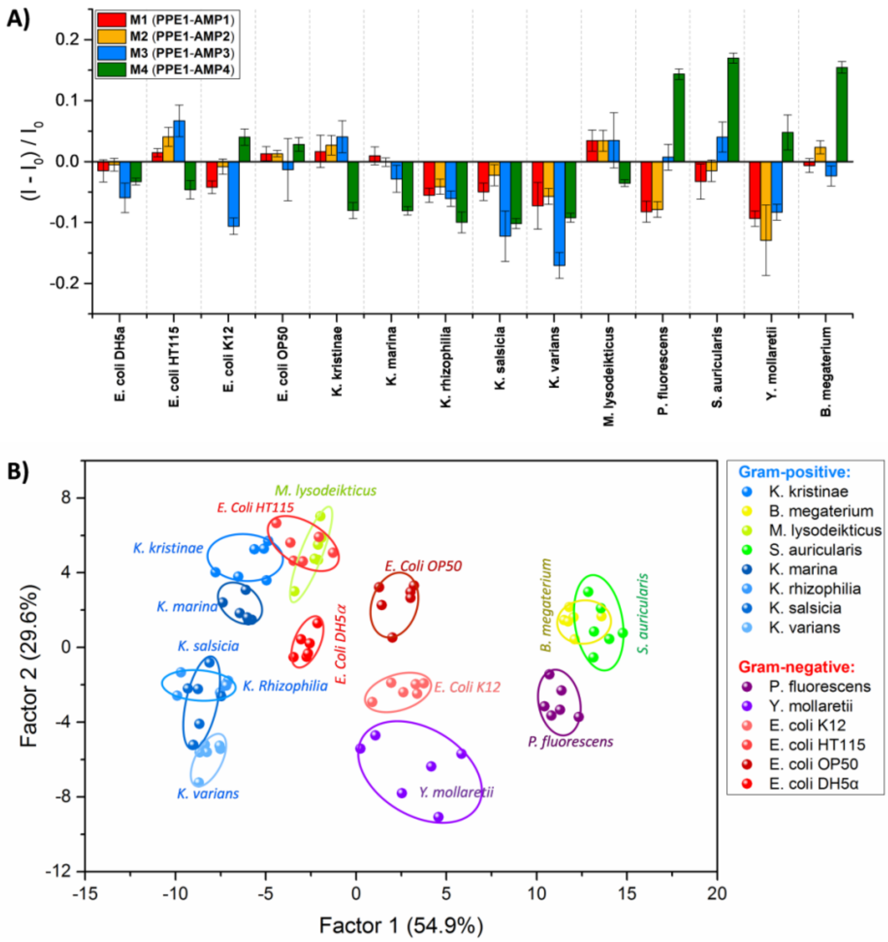

Figure 96. (A) Fluorescence response pattern (I - I_0) / I_0 obtained by PPE/AMP complexes **M1-M4** (1 µM in water) treated with 14 bacteria in urine (OD_{600} = 0.01, incubation for 30 min). Each value is the average of six independent measurements; each error bar shows the standard deviation (SD) of these measurements. **(B)** 2D canonical score plot for the first two factors of simplified fluorescence response patterns obtained with an array of PPE/AMP complexes **M1-M4** (1 µM) treated with different bacteria in urine (OD_{600} = 0.1, incubation for 30 min). 95 % confidence ellipses for the individual bacteria are depicted. Each point represents the response pattern for a single bacteria to the array. (Five different species of *Kocuria* were shown as blue color; four different strains of *Escherichia coli* were shown as red color). The jackknifed classification matrix with cross-validation reveals 98% accuracy; blind test shows 62.5% accuracy (35/56).

Table 19. Numbers of bacteria (/ml) at OD_{600}=0.01, counted under microscope.

Nr.	*Abbreviation of Bacteria*	OD_{600}	**Corresponding Numbers of Bacteria** (numbers/ml)
1	*B. megaterium*	0.01	4.7 X 10^6
2	*S. auricularis*	0.01	5.2 X 10^6
3	*M. leteus*	0.01	7.3 X 10^6
4	*K. kristinae*	0.01	2.2 X 10^6
5	*K. marina*	0.01	1.6 X 10^6
6	*K. rhizophilia*	0.01	2.4 X 10^6
7	*K. salsicia*	0.01	2.8 X 10^6
8	*K. varians*	0.01	2.0 X 10^6

9	*P. fluorescens*	0.01	3.1 X 10^6
10	*Y. mollaretii*	0.01	6.2 X 10^6
11	*E. coli K12*	0.01	3.3 X 10^6
12	*E. coli HT115*	0.01	5.4 X 10^6
13	*E. coli OP50*	0.01	7.7 X 10^6
14	*E. coli DH5α*	0.01	3.7 X 10^6

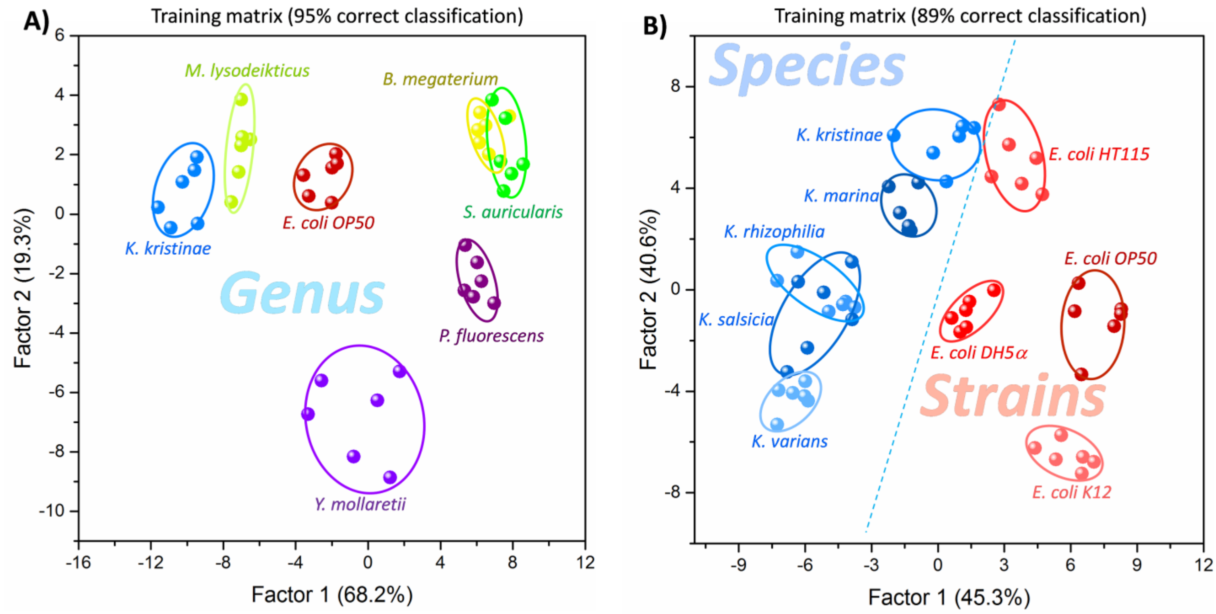

Figure 97. **(A)** 2D canonical score plot of bacteria with different genus and **(B)** 2D canonical score plot of bacteria with different species and strain obtained with an array of PPE/AMP complexes M1-M4 (1 µM) treated with different bacteria in urine (OD_{600} = 0.01, incubation for 30 min). 95 % confidence ellipses for the individual bacteria are depicted. Each point represents the response pattern for single bacteria to the array.

4.1.4 Quantitative Detection of Bacteria in Urine and Serum

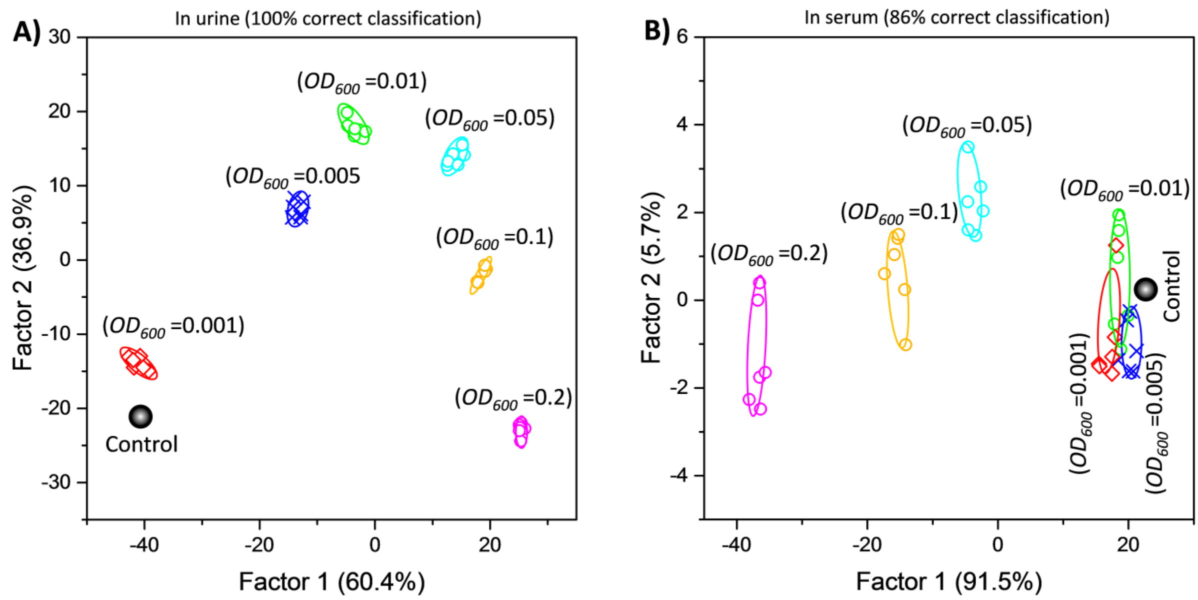

Figure 98. 2D canonical score obtained with an array of PPE/AMP complex **M1-M4** (1 µM) treated *B. megaterium* in urine **(A)** and in serum **(B)** at different concentrations (OD_{600} from 0.2 to 0.001). 95 % confidence ellipses for the individual bacteria are depicted. Each point represents the response pattern for single bacteria to the array.

With these data in hand, next step, we asked if we can further decrease the concentration of bacteria in urine, and if we can also apply this system in serum. Thus, we randomly selected *B. megaterium* as an example and performed the quantitative analysis of bacteria (OD_{600} from 0.2 to 0.001) in human urine and serum. Intriguingly, all of the six concentrations have been clearly discriminated in urine with a 100% accuracy (Figure 97), even at the lowest concentration of OD_{600} 0.001. However, for the LDA results in serum, partial overlap was observed at lower concentrations, as the results of the score plot are fairly close to that of the control.

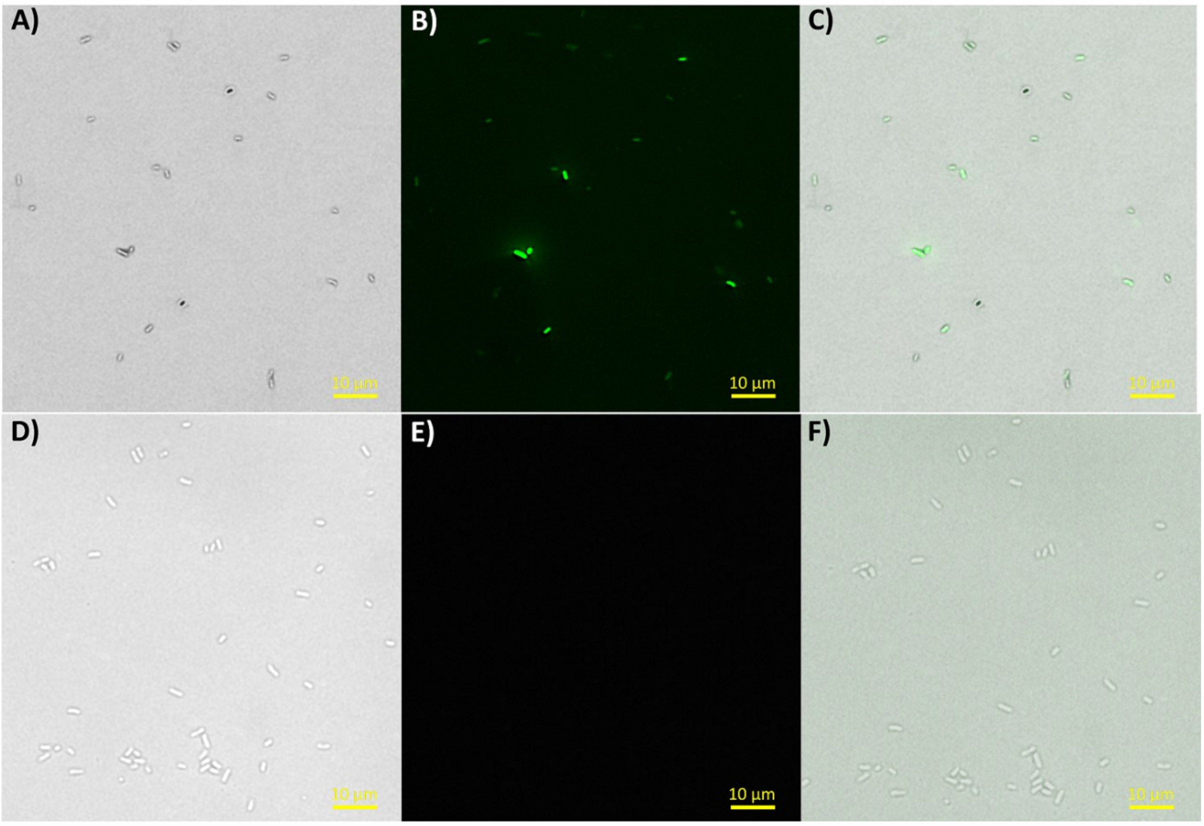

Figure 99. Microscopy images of complex **PPE 1**/**AMP 1** treated with *E. coli OP50* in water, **(A)** bright-field image, **(B)** fluorescence image, and **(C)** merged image; Microscopy images of complex **PPE 1** alone treated with *E. coli OP50* in water, **(D)** bright-field image, **(E)** fluorescence image, and **(F)** merged image (Scale bars: 10 µm).

What is the working principle of the system? The addition of bacteria to the complexes **C1**-**C4** leads to the fluorescence intensity change of the complexes (Figure 92). The fluorescence turn-on is caused by displacement; PPE is released as the AMP binds to pili, immunity proteins, M proteins on the bacterial surface. In most cases, surprisingly, we observe further fluorescence decrease (Figure 92), probably due to differential binding of **C1**-**C4** to the components of the bacterial surface forming ternary complexes. Non-specific interactions (hydrophobic/hydrophilic and electrostatic) between the intact complexes **C1**-**C4** and bacterial surface (negative) lead to aggregation of these complexes on the surface of the bacteria demonstrate by fluorescence microscopy (Figure 99). Gram-positive bacteria have only one layer membrane with specific anionic components (lipoteichoic acids and teichoic acids) on the surface, promoting strong binding efficiency between AMP and bacteria; However, Gram-negative bacteria are enclosed by a two layered membrane coupled with LPS, which promote a weaker interaction between AMPs and the cell membrane. The structural difference of bacteria leads to the differential fluorescence response. **C1** is exposed to E. coli, and increased fluorescence of the bacteria was observed (Figure 99A-C), indicating that PPE or the complex was attached to the surface of bacteria because of the electrostatic interactions between PPE (negative), AMP (positive) and bacteria (negative). With an increasing amount of PPE attached to the surface of bacteria, the concentration of PPE and **C1** in solution decreases. Decline of the fluorescence intensity is detected by a plate reader. As control experiment, **PPE 1** alone (without AMP) was treated with E. coli in water, but negligible fluorescence was observed on the surface of bacteria (Figure 99D-F). Consequently, C1 stains the bacteria.

4.1.5 Conclusions

In conclusion, we have developed a sensor array composed of four electrostatic complexes (**C1**-**C4**), formed from one negatively charged PPE and four AMPs **1-4**. The array identifies 14 different types of bacteria according to Gram status and their genetic relationship, including different strains of E. coli. This chemical tongue was further applied to sense microbes in urine and serum; for urine this tongue successfully discriminated all bacteria in the upper ranges of clinically relevant bacterial concentrations, indicating a potential application of such a tongue in clinical settings. The approach allows for identification of different bacteria but also gives their genetic relationship by their respective distance in the score plot. Even an unknown bacterium can be potentially identified with respect to its relationship to the known ones. Over all, this system has vastly improved recognition ability over that of the one reported by Rotello et al.; it shows a higher sensitivity as it can be used at an OD_{600} of 0.01 (instead of 0.1) and discriminates bacteria in urine without any problems.

In this system the AMPs perform some of the recognition, while the PPEs are primarily the elements reporting the signal, yet from the observations, we can conclude that the PPE forms ternary complexes with the bacteria and the AMPs, these are responsible for the recognition/discrimination of the bacteria. In future we will aim to increase the sensitivity of this attractive system.

Chapter 5. Experimental Section

5.1 General Remarks

Chemicals: All chemicals were either purchased from the chemical store at the Organisch-Chemisches Institut of the University of Heidelberg or from commercial laboratory suppliers. Reagents were used without further purification unless otherwise noted. Human urine (Surine™ Negative Urine Control) was purchased directly from Sigma-Aldrich®. Reagents were used without further purification unless otherwise noted. *Acinetobacter pakistanensis* (*A. pakistanensis*, DSM 100419), *Bacillus megaterium* (*B. megaterium*, DSM 32), *Escherichia coli DH5α* (*E. coli DH5α*, DSM 6897), *Escherichia coli K12* (*E. coli K12*, DSM 498), *Kocuria kristinae* (*K. kristinae*, DSM-20032), *Kocuria marina* (*K. marina*, DSM 16420), *Kocuria rhizophilia* (*K. rhizophilia*, DSM 11926), *Kocuria salsicia* (*K. salsicia*, DSM 24776), *Kocuria varians* (*K. varians*, DSM 20033), *Pseudomonas fluorescens* (*P. fluorescens*, DSM 50090), *Staphylococcus auricularis* (*S. auricularis*, DSM 20609), *Yersinia mollaretii* (*Y. mollaretii*, DSM 18520) were provided by the German Collection of Microorganisms and Cell Cultures (DSMZ). *Escherichia coli HT115* (*E. coli HT115*), *Escherichia coli OP50* (*E. coli OP50*) was purchased from Caenorhabditis Genetics Center (CGC). Protamine was purchased from Sigma-Aldrich®.

Solvents: All solvents were purchased from the store of the Theoretikum or chemical store at the Organisch-Chemisches Institut of the University of Heidelberg and if necessary distilled prior use. All of the other absolute solvents were dried by a MB SPS-800 using drying columns.

Analytical thin layer chromatography (TLC): TLC was performed on Macherey & Nagel Polygram® SIL G/UV254 precoated plastic sheets. Components were visualized by observation under UV light (254 nm or 365 nm) or in the case of UV-inactive substances by using the suitably coloring solutions. The following coloring solutions were used for the visualization of UV-inactive substances:

> $KMnO_4$ solution: 2.0 g $KMnO_4$, 10.0 g K_2CO_3, 0.3 g NaOH, 200 mL distilled water.
>
> Cer solution: 10.0 g $Ce_2(SO)_3$, 25 g phosphomolybdic acid hydrate, 1 L distilled water, 50 mL conc. H_2SO_4.

Flash column chromatography was carried out using silica gel S (0.032 mm-0.062 mm), purchased from Sigma Aldrich, according to G. Nill, unless otherwise stated.[227]

^{1}H NMR spectra were recorded at room temperature on the following spectrometers: Bruker Avance III 300 (300 MHz), Bruker Avance III 400 (400 MHz) and Bruker Avance III 600 (600 MHz). The data were interpreted in first order spectra. The spectra were recorded in $CDCl_3$ or MeOD as indicated in each case. Chemical shifts are reported in δ units relative to the solvent residual peak ($CHCl_3$ in $CDCl_3$ at δ_H = 7.26 ppm, HDO in D_2O at δ_H = 4.74 ppm, HCD_2OD in MeOD at δ_H = 3.21 ppm) or

TMS (δ_H = 0.00 ppm).[228] The following abbreviations are used to indicate the signal multiplicity: s (singlet), d (doublet), t (triplet), q (quartet), quin (quintet), sext (sextet), dd (doublet of doublet), dt (doublet of triplet), ddd (doublet of doublet of doublet), etc., bs (broad signal), m (multiplet).

^{13}C NMR spectra were recorded at room temperature on the following spectrometers: Bruker Avance III 300 (75 MHz), Bruker Avance III 400 (100 MHz) and Bruker Avance III 600 (150 MHz). The spectra were recorded in $CDCl_3$ or D_2O as indicated in each case. Chemical shifts are reported in δ units relative to the solvent signal: $CDCl_3$ [δ_C = 77.16 ppm (central line of the triplet)] or TMS (δ_C = 0.00 ppm).

High-resolution mass spectra (HR-MS) were either recorded on a Bruker ApexQehybrid 9.4 T FT-ICR-MS (ESI^+, $DART^+$) , a Finnigan LCQ (ESI^+) or a JEOL JMS-700 (EI^+) mass spectrometer at the Organisch-Chemisches Institut der Universität Heidelberg.

A**bsorption and emission spectra** were recorded using a Jasco V660 and Jasco FP6500 spectrometer.

IR spectra were recorded on a JASCO FT/IR-4100. Substances were applied as a film, solid or in solution. The obtained data was processed with the software JASCO Spectra anager™ II.

Fluorescence lifetimes τ were acquired by an exponential fit according to the least mean square with commercially available software HORIBA Scientific Decay Data Analyses 6 (DAS6) version 6.4.4. The luminescence decays were recorded with a HORIBA Scientific Fluorocube single photon counting system operated with HORIBA Scientific DataStation version 2.2.

Quantum yields (Φ): Quantum yields were measured by using the comparative method with quinine sulfate in 0.1 N sulfuric acid as a reference (Φ = 0.54) according to the literature, the average values of three measurements were calculated for each sample.[229]

Dialysis was realized with regenerated cellulose tubular membranes (ZelluTrans, Carl Roth®) with a molecular weight cut-off of 3500 Da against deionized (DI) water.

Gel Permeation Chromatography (GPC): Number- (M_n) and weight average (M_w) molecular weights and polydispersities (PDI, M_w/M_n) were determined by GPC versus polystyrene standards. Measurements were carried out at room temperature in chloroform with PSS-SDV columns (8.0 mm x 30.0 mm, 5 µm particles, 10^2-, 10^3- and 10^5- Å pore size) on a Jasco PU-2050 GPC unit equipped with a Jasco UV-2075 UV- and a Jasco RI-2031 RI-detector.

Linear discriminant analysis was carried out using using classical linear discriminant analysis (LDA) in SYSTAT (version 13.0). In LDA, all variables were used in the model (complete mode) and the tolerance was set as 0.001. The fluorescence response patterns were transformed to canonical patterns. The Mahalanobis distances of each individual pattern to the centroid of each group in a multidimensional space were calculated and the assignment of the case was based on the shortest Mahalanobis distance.

Principal component analysis (PCA) is a mathematical transformation used to extract variance between entries in a data matrix by reducing the redundancy in the dimensionality of the data. It takes the data points for all analytes and generates a set of orthogonal eigenvectors (principal components, PCs) for maximum variance. PCA was carried out using using classical linear discriminant analysis (LDA) in SYSTAT (version 13.0).

Fluorescence Response Patterns. Emission spectra were recorded and analyzed on a CLARIO¬star (firmware version 1.13) Platereader (BMG Labtech, built in software, version 5.20 R5). Data were analyzed by CLARIOstar MARS Data Analysis Software (version 3.10 R5) from BMG Labtech. The specific response for each analyte was measured six times, the peak values acquired. These were used as the observables for the subsequent linear discriminant analysis (LDA).

Method for Microscopy.

An inverted type fluorescence phase-contrast microscope, fluorescence microscope BZ-9000 (BIOREVO), carry the objective lens of Nikon CF160 Series was used for our image. Magnification for final image was 10× ocular combined with a 100× objective of. Fluorescence exposure time was 1/4 s. Three stock solutions were first prepared, including: **PPE 1** (100 µM), **AMP 1** (10 µM) and fresh *E. coli OP50* (OD_{600}=0.4). Then, **PPE 1** (0.3 mL) was mixed with **AMP 1** (0.3 mL), the mixed solution was shake for 20 min to form the complex **C1**, 1.4 mL of bacteria *E. coli* (1.4 mL) was added to the mixed solution (total volume = 2 mL), and incubated for 10min. The prepared sample solution was used for microscopy experiment (Fig. 5). As a control experiment, **PPE 1** alone (0.3 mL) was added with DI water (0.3 mL, instead of **AMP 1**), then treated with *E. coli OP50* (1.4 mL), incubated for 10min. The prepared control solution was used for microscopy experiment.

5.2 Experiment Details of PAE Synthesis

5.2.1 Synthesis of PAEs (Chapter 2.1)

Synthesis of PAE 1

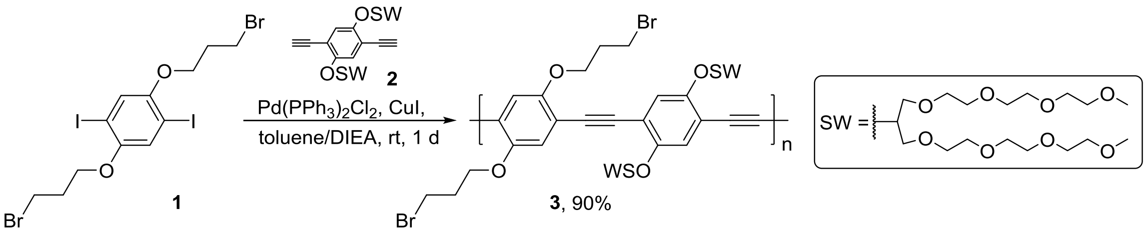

*Compounds **1** was synthesized according to the literature.*[230-231]

*Compounds **2** was synthesized according to the literature.*[156]

Synthesis of 3. Monomer **1** (1.04 g, 2.35 mmol) and monomer **2** (2.09 g, 2.35 mmol) were dissolved in degassed toluene/DIEA (7.2 mL/4.9 mL). $Pd(PPh_3)_2Cl_2$ (4.95 mg, 7.05 µmol) and CuI (2.69 mg, 14.10 µmol) were added and the mixture was stirred at ambient temperature for 24 h. Saturated NH_4Cl solution and $CHCl_3$ were added, the aqueous layer was separated and extracted with $CHCl_3$. The combined organic layers were dried over $MgSO_4$, filtered and concentrated in vacuo. The crude product was dissolved in small amounts of $CHCl_3$ and slowly added to an excess of *n*-hexane for precipitating, repeated the precipitate process for three times to gave **3** as oil-like, yellow-brownish solid (2.63 g, 90%). The M_n was estimated to be 1.4 x 10^4 with a PDI of 3.9. ^{1}H NMR (300 MHz, $CDCl_3$) δ = 7.12-7.24 (m, 2 H), 6.94-7.10 (m, 2 H), 4.40-4.64 (m, 2 H), 4.02-4.34 (m, 4 H), 3.48-3.87 (m, 60 H), 3.30-3.40 (m, 12 H), 2.25-2.47 (m, 4 H). IR (cm^{-1}): ν 2912, 2870, 1508, 1489, 1469, 1420, 1389, 1351, 1271, 1200, 1096, 1026, 943, 849, 719, 650. Due to low solubility, ^{13}C NMR spectrum could not be obtained.

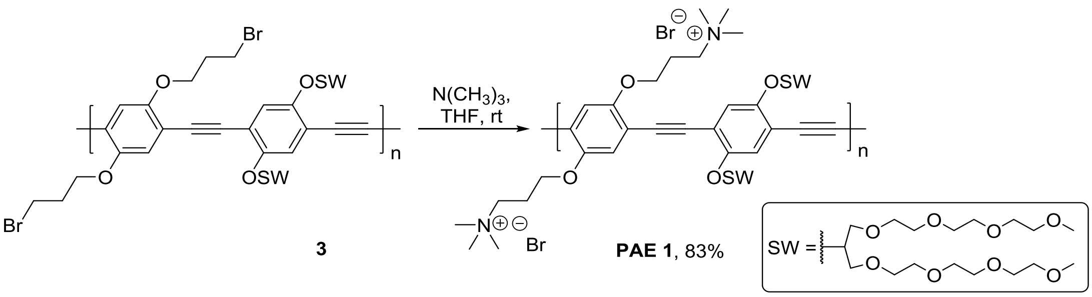

Synthesis of PAE 1. Polymer **3** (100 mg, 0.083 mmol) was dissolved in degassed THF/EtOH (10 mL/5 mL). $N(CH_3)_3$ (2 mL) was added slowly and stirred at rt for 2 d under N_2 atmosphere. Additional $N(CH_3)_3$ (2 mL) was added and stirred for another 6 d. After evaporation of the solvents **PAE 1** was redissolved in distilled water and then dialyzed against DI water for 7days. Freeze-drying gave polymer 4 as yellow solid (90 mg, 83%). The M_n and PDI result from **3**. ^{1}H NMR (300 MHz, MeOD) δ = 7.21-7.45 (m, 4 H), 4.54-4.65 (m, 2H), 4.16-4.38 (m, 4 H), 3.47-3.89 (m, 60 H), 3.32-3.37 (m, 12 H), 3.12-3.25 (m, 18 H), 2.31-2.46 (m, 4 H) ppm. IR (cm^{-1}): ν 3421, 2871, 2359, 1649, 1600, 1508, 1489, 1419, 1350, 1272, 1200, 1091, 1049, 944, 849. Due to low solubility, ^{13}C NMR spectrum could not be obtained.

Synthesis of PAE 2

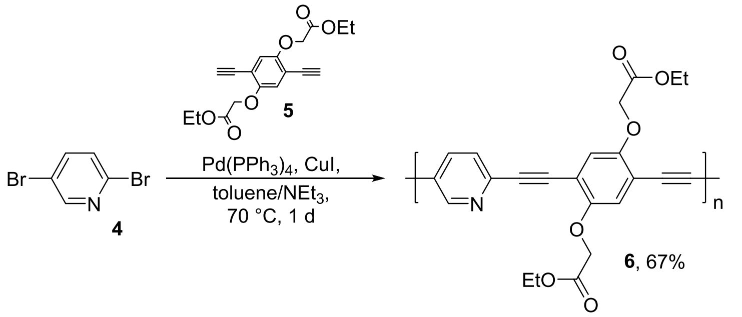

Synthesis of 6. Monomer **4** (359 mg, 1.51 mmol) and monomer **16** (500 mg, 1.51 mmol) were dissolved in a mixture of degassed toluene/NEt_3 (1.5:1, 30 mL/30 mL). $Pd(PPh_3)_4$ (87 mg, 76 µmol) and CuI (14 mg, 76 µmol) were added and the mixture was stirred at 70 °C for 24 h. Saturated aqueous NH_4Cl and CH_2Cl_2 were added, the aqueous layer was separated and extracted with CH_2Cl_2. The combined organic layers were dried over $MgSO_4$, filtered and concentrated in vacuo. Two times, the crude product was dissolved in a small amount of $CHCl_3$ and slowly added to an excess of MeOH to give **6** as orange solid (413 mg, 67%). The M_n was estimated to be 6.9 x 10^3 with a PDI of 1.9. ^1H NMR (600 MHz, $CDCl_3$): δ = 8.65-8.83 (m, 1 H), 7.79-7.88 (m, 1 H), 7.46-7.63 (m, 2 H), 6.94-7.09 (m, 4 H), 4.64-4.84 (m, 4 H), 4.20-4.39, 1.09-1.46 ppm. IR (cm^{-1}): ν 2979, 2964, 2934, 2906, 2212, 1749, 1730, 1606, 1580, 1565, 1541, 1502, 1462, 1440, 1409, 1377, 1364, 1279, 1261, 1183, 1069, 1017, 950, 853, 843, 798, 751, 720, 705, 693, 663, 653, 639, 601, 582, 534, 510, 497, 404. Due to low solubility, ^{13}C NMR spectrum could not be obtained.

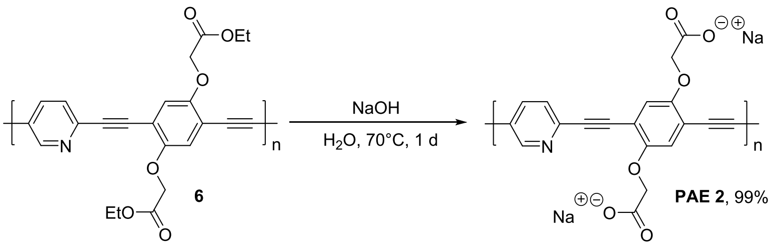

Synthesis of PAE 2. To a mixture of **6** (150 mg, 0.37 mmol) and water (20 mL), NaOH (296 mg, 7.40 mmol) was added and the resulting mixture was stirred at 70 °C for 2 d. After adjusting a pH of 7 (HCl) the aqueous mixture was dialyzed against DI H_2O for 3 d. Freeze-drying gave **PAE 2** as spongy, orange solid (129 mg, 99%). The M_n and PDI result from **6**. ^1H NMR (600 MHz, D_2O): δ = 6.65-8.77 (m, 5 H), 4.46-4.65 (m, 4 H) ppm. IR (cm^{-1}): ν 3348, 3226, 3071, 2935, 2639, 2214, 2168, 1606, 1504, 1467, 1405, 1366, 1327, 1285, 1085, 1057, 965, 849, 792, 751, 721, 703, 693, 674, 656, 595, 581, 572, 566, 548, 459, 447, 437, 429, 408. Due to low solubility, ^{13}C NMR spectrum could not be obtained.

Synthesis of PAE 3

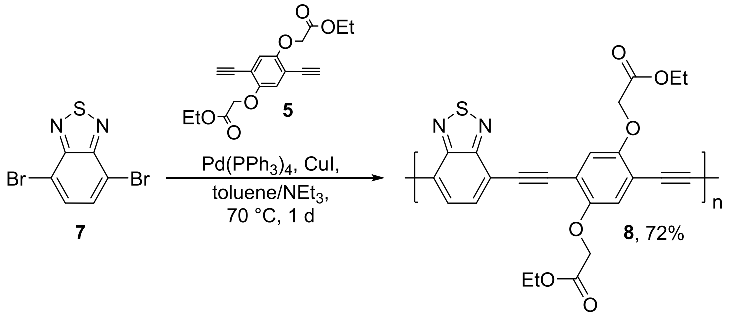

Compound 7 was synthesized according to the literature.[232]

Synthesis of 8. Monomer **7** (712 mg, 2.42 mmol) and monomer **5** (800 mg, 2.42 mmol) were dissolved in a mixture of degassed THF/$CHCl_3$/NEt_3 (1:1:1, 7.5 mL/7.5 mL/7.5 mL). $Pd(PPh_3)_4$ (140 mg, 121 µmol) and CuI (23 mg, 121 µmol) were added and the mixture was stirred at 70 °C for 3 d. Saturated aqueous NH_4Cl and CH_2Cl_2 were added, the aqueous layer was separated and extracted with CH_2Cl_2. The combined organic layers were dried over $MgSO_4$, filtered and concentrated in vacuo. The crude product was dissolved in a small amount of $CHCl_3$ and slowly added to an excess of n-pentane to give **8** as red solid (810 mg, 72%). The M_n was estimated to be 1.8 x 10^3 with a PDI of 3.1. ^{1}H NMR (600 MHz, $CDCl_3$): δ = 7.71-7.90 (m, 2 H), 7.68-7.78 (m, 1 H), 7.33-7.49 (m, 1 H), 7.16-7.22 (m, 1 H), 4.72-4.86 (m, 4 H), 4.25-4.37 (m, 4H), 1.12-1.47 (m, 8 H) ppm. IR (cm^{-1}): ν 2981, 2934, 2906, 2212, 2206, 2199, 1754, 1733, 1506, 1486, 1438, 1408, 1279, 1183, 1071, 1029, 844, 693, 634, 521, 510. Due to low solubility, ^{13}C NMR spectrum could not be obtained.

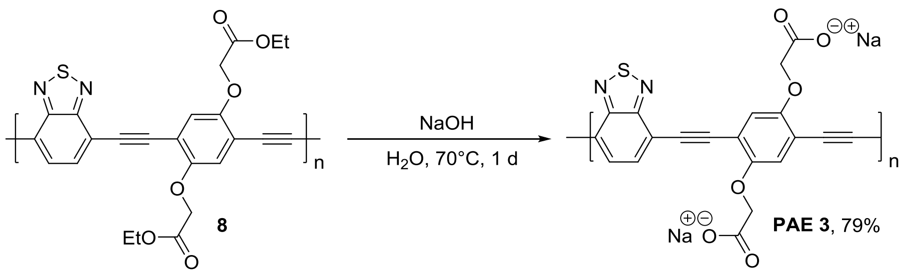

Synthesis of PAE 3. To a mixture of **8** (616 mg, 1.33 mmol) and water (20 mL), NaOH (1.06 g, 26.6 mmol) was added and the resulting mixture was stirred at 70 °C for 2 d. After adjusting a pH of 7 (HCl) the aqueous mixture was dialyzed against DI H_2O for 3 d. Freeze-drying gave **PAE 3** as spongy, orange solid (425 mg, 79%). The M_n and PDI result from **8**. ^{1}H NMR (600 MHz, D_2O): δ = 5.37-8.80 (m, 4 H), 3.65-3.78 (m, 4 H) ppm. IR (cm^{-1}): ν 3343, 3032, 2917, 2834, 2352, 2324, 2200, 2190, 2163, 2114, 2020, 1991, 1586, 1495, 1398, 1323, 1282, 1198, 1096, 1043, 944, 915, 893, 849, 695, 419. Due to low solubility, ^{13}C NMR spectrum could not be obtained.

Synthesis of PAE 4

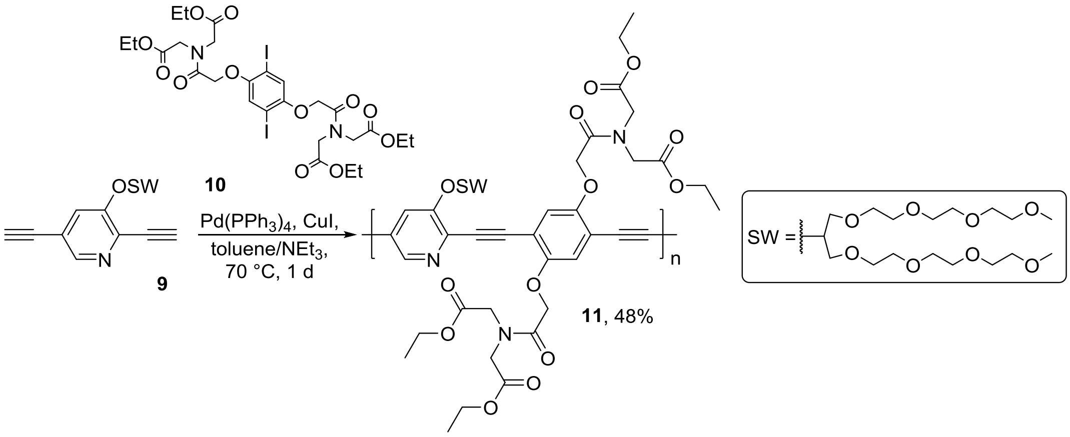

*Compound **9** was synthesized according to the literature.*[155]
*Compound **10** was synthesized according to the literature.*[156]

Synthesis of 11. Monomer **9** (114 mg, 0.22 mmol) and monomer **10** (180 mg, 0.22 mmol) were dissolved in a mixture of degassed toluene/NEt_3 (1:1, 4 mL/4 mL). $Pd(PPh_3)_4$ (13 mg, 11 µmol) and CuI (2.0 mg, 11 µmol) were added and the mixture was stirred at 70 °C for 24 h. Saturated aqueous NH_4Cl and CH_2Cl_2 were added, the aqueous layer was separated and extracted with CH_2Cl_2. The combined organic layers were dried over $MgSO_4$, filtered and concentrated in vacuo. Two times, the crude product was dissolved in a small amount of $CHCl_3$ and slowly added to an excess of n-pentane to give **11** as brown-orange solid (111 mg, 48%). The M_n was estimated to be 1.9 x 10^4 with a PDI of 6.5. ^1H NMR (600 MHz, $CDCl_3$): δ = 8.30-8.50, (m, 1 H), 7.46-7.71 (m, 1 H), 6.99-7.25 (m, 2 H), 4.67-4.91 (m, 4 H), 4.12-4.39 (m, 16 H), 3.47-3.90 (m, 28 H), 3.28-3.37 (m, 6 H), 1.13-1.33 (m, 12 H) ppm. IR (cm^{-1}): ν 2978, 2939, 2874, 1738, 1680, 1578, 1503, 1464, 1405, 1373, 1350, 1298, 1255, 1191, 1092, 1020, 971, 938, 856, 738, 508. Due to low solubility, ^{13}C NMR spectrum could not be obtained.

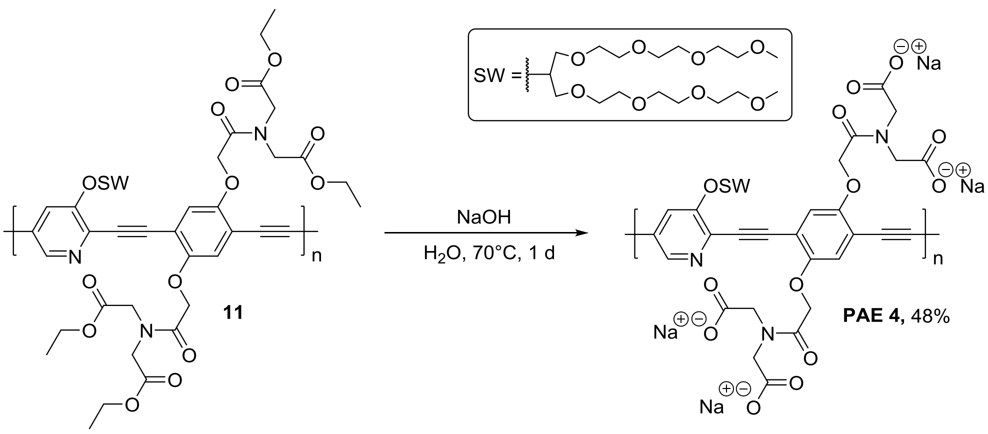

Synthesis of PAE 4. To a mixture of **11** (61 mg, 57 µmol) and water (20 mL), NaOH (46.0 mg, 1.14 mmol) was added and the resulting mixture was stirred at 70 °C for 2 d. After adjusting a pH of 7 (HCl) the aqueous mixture was dialyzed against DI H_2O for 3 d. Freeze-drying gave **PAE 4** as spongy, yellow solid (43 mg, 77%). The M_n and PDI result from **11**. ^{1}H NMR (600 MHz, D_2O): δ = 7.09-8.18 (m, 4 H), 4.76-5.29 (m, 5 H), 3.99-4.48 (m, 8 H), 3.12-3.87 (m, 34 H) ppm. IR (cm^{-1}): ν 2933, 2882, 2832, 1724, 1667, 1581, 1504, 1460, 1407, 1352, 1297, 1236, 1195, 1085, 1037, 973, 948, 914, 882, 843, 699, 638, 606, 576, 537, 498. Due to low solubility, ^{13}C NMR spectrum could not be obtained.

Synthesis of PAE 5

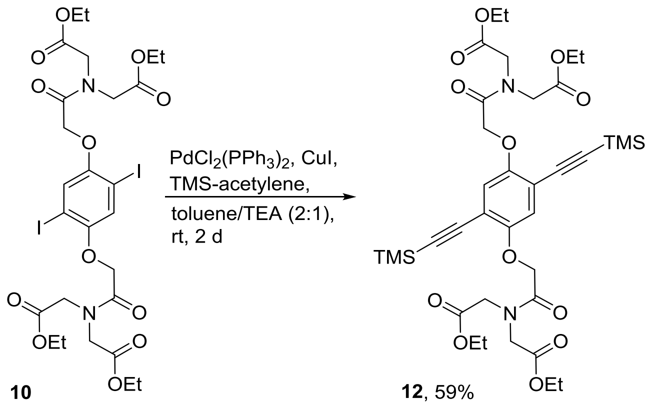

10 **12**, 59%

*Compound **10** was synthesized according to the literature.*[156]

Synthesis of 12. Compound **10** (2.00 g, 2.44 mmol) was dissolved in a degassed mixture of toluene/NEt_3 (2:1, 15 mL/7.5 mL). $PdCl_2(PPh_3)_2$ (86 mg, 122 µmol) and CuI (23 mg, 122 µmol) were added, then TMS-acetylene (867 µL, 2.60 mmol) was and dropwise and the resulting mixture was stirred for 2 d at room temperature. Saturated aqueous NH_4Cl and CH_2Cl_2 were added, the aqueous layer was separated and extracted with CH_2Cl_2. The combined organic layers were dried over $MgSO_4$, filtered and concentrated in vacuo. The crude product was purified by flash chromatography on silica gel [petroleum ether/ethyl acetate (5/2)] to give compound **12** (1.10 g, 1.45 mmol, 59%) as grizzly solid (m. p. 120 – 122 °C). ^{1}H NMR (400 MHz, $CDCl_3$): δ = 6.98 (s, 2 H), 4.76 (s, 4 H), 4.39 (s, 4 H), 4.13-4.21 (m, 12 H), 1.19-1.27 (m, 12 H), 0.26 (s, 18 H) ppm. ^{13}C NMR (100 MHz, $CDCl_3$): δ = 168.81, 168.79, 168.49, 153.51, 118.76, 114.82, 101.71, 99.97, 69.41, 61.87, 49.98, 48.75, 14.27, 14.26, -0.01 ppm. IR (cm^{-1}): ν 2987, 2960, 2900, 2160, 2153, 1741, 1666, 1502, 1491, 1464, 1446, 1433, 1407, 1374, 1351, 1291, 1248, 1183, 1117, 1088, 1046, 1021, 1013, 973, 876, 858, 840, 762, 731, 704. HR-MS (DART$^+$): *m/z* calcd. for $C_{36}H_{56}N_3O_{12}Si_2^+$ 778.3397 $[M+NH_4]^+$; found 778.3402. $C_{36}H_{52}N_2O_{12}Si_2$ (760.98): calcd. C 56.82, H 6.89, N 3.68; found C 56.80, H 6.59, N 3.54.

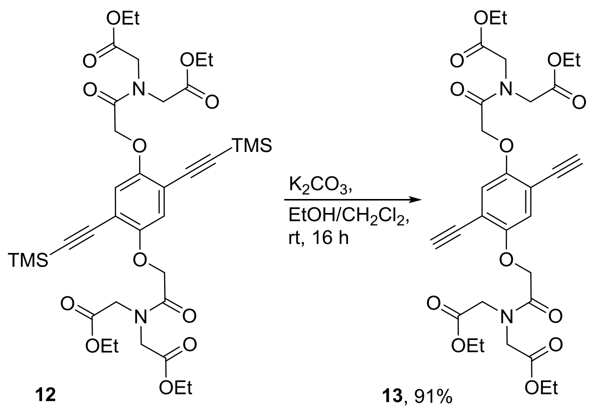

Synthesis of 13. Compound **12** (1.10 g, 1.45 mmol) was dissolved in a mixture of EtOH/CH_2Cl_2 (1:1, 15 mL/15 mL). K_2CO_3 (2.00 g, 14.5 mmol) was added and the resulting mixture was stirred for 16 h at ambient temperature. Water and CH_2Cl_2 were added, the aqueous layer was separated and extracted with CH_2Cl_2. The combined organic layers were dried over $MgSO_4$, filtered and concentrated in vacuo. The crude product was dissolved in CH_2Cl_2 and filtered again and concentrated in vacuo to give compound **13** (812 mg, 1.32 mmol, 91%) as yellowish solid (m. p. 190 °C decomposition). ^{1}H NMR (400 MHz, $CDCl_3$): δ = 7.03 (s, 2 H), 4.78 (s, 4 H), 4.34 (s, 4 H), 4.13-4.23 (m, 12 H), 3.34 (s, 2 H), 1.21-1.30 (m, 12 H) ppm. ^{13}C NMR (100 MHz, $CDCl_3$): δ = 168.85, 168.69, 168.31, 153.77, 118.78, 114.01, 83.81, 78.92, 69.18, 61.95, 61.55, 49.93, 48.64, 14.28, 14.25 ppm. IR (cm^{-1}): ν 3242, 2982, 2942, 1743, 1658, 1506, 1472, 1431, 1403, 1373, 1354, 1311, 1292, 1274, 1249, 1193, 1118, 1094, 1046, 1022, 1010, 971, 927, 889, 872, 821, 796, 762, 731, 633. HR-MS (DART$^+$): *m*/*z* calcd. for $C_{30}H_{40}N_3O_{12}^+$ 634.2607 $[M+NH_4]^+$; found 634.2583. $C_{30}H_{36}N_2O_{12}$ (616.62): calcd. C 58.44, H 5.88, N 4.54, found C 57.94, H 5.84, N 4.50.

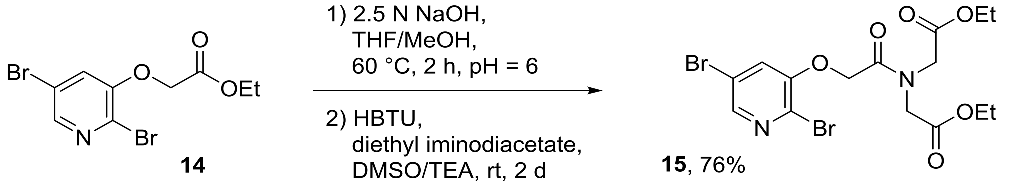

*Compound **14** was synthesized according to the literature.*[155]

Synthesis of 15. To a solution of **14** (3.00 g, 8.85 mmol) in mixture of THF/MeOH (2:1, 60 mL/30 mL) was added 2.5 N $NaOH_{aq}$ (33 mL) and heated at 60 °C for 2 h. After cooling down to ambient temperature, the pH value was adjusted to 6.0. The solution was filtered and the solvent was removed under reduced pressure. The resulting white solid was solved in DMSO (30 mL) and TEA (5 mL), before diethyliminodiacetate (2.0 mL, 10.6 mmol) was added. The reaction was stirred for 2 d at room temperature. The solution was diluted with ethyl acetate, washed with H_2O and $NaCl_{aq}$. The organic layer was dried over $MgSO_4$, filtered and the solvent was evaporated in vacuo. The resulting yellow oil was purified by flash chromatography on silica gel [petroleum ether/ethyl acetate (1/1)] to give compound **15** (3.24 g, 6.72 mmol, 76%) as colorless solid (m. p. 100-102 °C). ^{1}H NMR (600 MHz, $CDCl_3$):

δ = 8.11 (d, J = 1.9 Hz, 1 H), 7.39 (d, J = 1.9 Hz, 1 H), 4.88 (s, 2 H), 4.28 (s, 2 H), 4.19-4.25 (m, 4 H), 4.18 (s, 2 H), 1.25-1.30 (m, 6 H) ppm. ^{13}C NMR (150 MHz, $CDCl_3$): δ = 168.44, 168.30, 167.04, 151.74, 143.10, 130.99, 123.53, 119.66, 67.97, 62.18, 61.61, 49.74, 48.48, 14.10 ppm. IR (cm^{-1}): ν 2964, 1736, 1665, 1561, 1546, 1475, 1450, 1417, 1398, 1372, 1351, 1299, 1271, 1248, 1214, 1190, 1124, 1088, 1051, 1024, 960, 867, 826, 743, 713, 687, 602, 576, 502, 425. HR-MS (EI^+): m/z calcd. for $C_{15}H_{19}N_2O_6Br_2^+$ 482.5989 $[M+H]^+$; found 482.9577. $C_{15}H_{18}N_2O_6Br_2$ (482.13): calcd. C 37.37, H 3.76, N 5.81, Br 33.15, found C 37.13, H 3.74, N 5.65, Br 32.96.

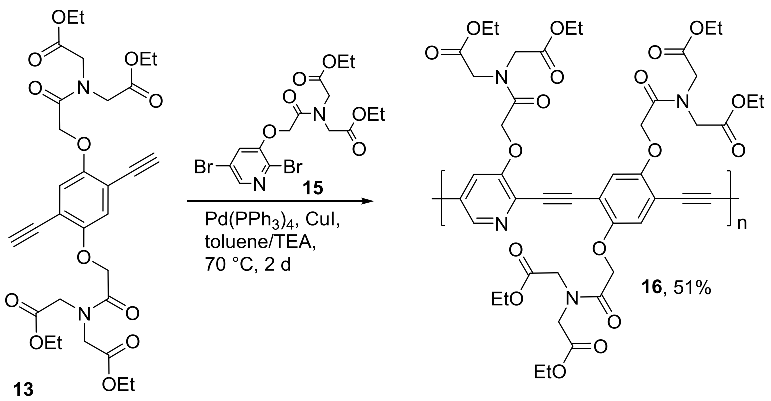

Synthesis of 16. Monomer **13** (250 mg, 0.52 mmol) and monomer **15** (320 mg, 0.52 mmol) were dissolved in a mixture of degassed toluene/NEt_3 (1.5:1, 9 mL/7 mL). $Pd(PPh_3)_4$ (30 mg, 26 µmol) and CuI (5.0 mg, 26 µmol) were added and the mixture was stirred at 70 °C for 2 d. Saturated aqueous NH_4Cl and CH_2Cl_2 were added, the aqueous layer was separated and extracted with CH_2Cl_2. The combined organic layers were dried over $MgSO_4$, filtered and concentrated in vacuo. The residue was dissolved in CH_2Cl_2, filtered again and concentrated in vacuo. Two times, the crude product was dissolved in a small amount of CH_2Cl_2 and slowly added to an excess of pentene to give **16** as yellow solid (256 mg, 51%). The M_n was estimated to be 1.1 x 10^4 with a PDI of 1.5. ^{1}H NMR (600 MHz, $CDCl_3$): δ = 8.28-8.47 (m, 1 H), 7.46-7.60 (m, 1 H), 7.02-7.24 (m, 2 H), 4.75-5.12 (m, 6 H), 4.06-4.45 (m, 24 H), 1.10-1.32 (m, 18 H) ppm. IR (cm^{-1}): ν 2983, 2939, 2905, 2875, 1738, 1661, 1575, 1560, 1503, 1464, 1402, 1373, 1352, 1260, 1094, 1021, 970, 863, 752, 698, 651, 623, 589, 520. Due to low solubility, ^{13}C NMR spectrum could not be obtained.

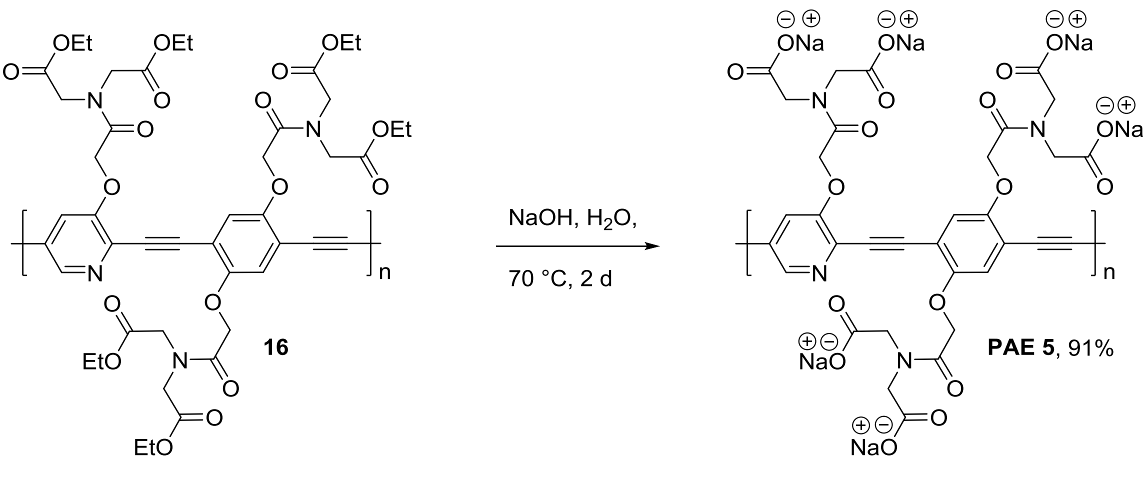

Synthesis of PAE 5. To a mixture of **15** (100 mg, 0.11 mmol) and water (20 mL), NaOH (88 mg, 2.2 mmol) was added and the resulting mixture was stirred at 70 °C for 2 d. After adjusting a pH of 7 (HCl) the aqueous mixture was dialyzed against DI H_2O for 3 d. Freeze-drying gave **PAE 5** as spongy, orange solid (77 mg, 91%). The M_n and PDI result from **15**. ^{1}H NMR (600 MHz, D_2O): δ = 8.22-8.30 (m, 1 H), 7.63-7.75 (m, 1 H), 7.04-7.33 (m, 2 H), 4.95-5.10 (m, 4 H), 3.96-4.14 (m, 14 H) ppm. IR (cm^{-1}): ν 3384, 3263, 3068, 2996, 2950, 2643, 1715, 1642, 1598, 1502, 1478, 1396, 1319, 1294, 1193, 1140, 1091, 1038, 974, 915, 877, 844, 658, 548, 519, 457, 428, 413 Due to low solubility, ^{13}C NMR spectrum could not be obtained.

Synthesis of PAE 6

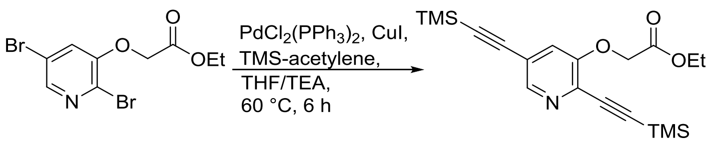

14 **17**, 99%

*Compound **14** was synthesized according to the literature.*[155]

Synthesis of 17. Compound **14** (350 mg, 1.03 mmol) was dissolved in a degassed mixture of THF/NEt_3 (2:1, 4 mL/2 mL). $PdCl_2(PPh_3)_2$ (36 mg, 52 µmol) and CuI (10 mg, 52 µmol) were added, then TMS-acetylene (370 µL, 2.60 mmol) was and dropwise and the resulting mixture was stirred for 6 h at 60 °C. Saturated aqueous NH_4Cl and CH_2Cl_2 were added, the aqueous layer was separated and extracted with CH_2Cl_2. The combined organic layers were dried over $MgSO_4$, filtered and concentrated in vacuo. The crude product was purified by flash chromatography on silica gel [petroleum ether/ethyl acetate (10/1)] to give compound **17** (380 mg, 1.02 mmol, 99%) as colorless solid (m. p. 77 °C). ^{1}H NMR (400 MHz, $CDCl_3$): δ = 8.29 (d, J = 1.6 Hz, 1 H), 7.16 (d, J = 1.6 Hz, 1 H), 4.70 (s, 2 H), 4.29 (q, J = 7.1 Hz, 2 H), 1.31 (t, J = 7.1 Hz, 3 H), 0.29 (s, 9 H), 0.26 (s, 9 H) ppm. ^{13}C NMR (100 MHz, $CDCl_3$): δ = 167.96, 155.04, 146.15, 133.38, 123.16, 120.21, 102.47, 101.03, 100.47, 99.28, 66.43, 61.78, 14.30, -0.11, -0.13 ppm. IR (cm^{-1}): ν 2957, 2898, 2163, 1769, 1581, 1454, 1403, 1270, 1246 ,1212 , 1157, 1113, 1078, 1024, 996, 861, 835, 755, 697, 627, 594, 575, 543, 502, 485, 459, 417. HR-MS (DART$^+$): m/z calcd. for $C_{38}H_{55}N_2O_6Si_4^+$ 747.3132 $[M_2+H]^+$; found 747.3188. $C_{19}H_{27}NO_3Si_2$ (373.60): calcd. C 61.08, H 7.28, N 3.75, found C 60.61, H 7.29, N 3.60.

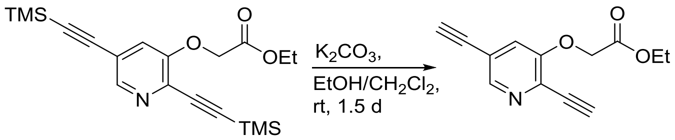

17 **18**, 52%

Synthesis of 18. Compound **17** (380 mg, 1.02 mmol) was dissolved in a mixture of EtOH/CH_2Cl_2 (1:1, 10 mL/10 mL). K_2CO_3 (1.41 g, 10.2 mmol) was added and the resulting mixture was stirred for 1.5 d at ambient temperature. Water and CH_2Cl_2 were added, the aqueous layer was separated and extracted with CH_2Cl_2. The combined organic layers were dried over $MgSO_4$, filtered and concentrated in vacuo. The crude product was purified by flash chromatography on silica gel [petroleum ether/ethyl acetate (3/1)] to give compound **18** (122 mg, 0.53 mmol, 52%) as colorless solid (m. p. 122 °C). ^{1}H NMR (600 MHz, $CDCl_3$): δ = 8.34 (d, *J* = 1.5 Hz, 1 H), 7.18 (d, *J* = 1.4 Hz, 1 H), 4.74 (s, 2 H), 4.28 (q, *J* = 7.1 Hz, 2 H), 3.51 (s, 1 H), 3.30 (s, 1 H), 1.30 (t, *J* = 7.1 Hz, 3 H) ppm. ^{13}C NMR (150 MHz, $CDCl_3$): δ = 167.77, 155.21, 146.08, 132.88, 122.58, 119.70, 83.86, 82.53, 79.83, 79.02, 65.99, 61.96, 14.26 ppm. IR (cm^{-1}): ν 3249, 3167, 2982, 2107, 1753, 1582, 1541, 1465, 1455, 1409, 1382, 1297, 1242, 1213, 1143, 1097, 1059, 1013, 980, 905, 877, 861, 810, 754, 712, 695, 680, 626, 604, 557, 484, 473, 418. HR-MS (DART$^+$): *m/z* calcd. for $C_{26}H_{23}N_2O_6^+$ 459.1551 $[M_2+H]^+$; found 459.1547. $C_{13}H_{11}NO_3$ (229.24): calcd. C 68.11, H 4.84, N 6.11, found C 67.93, H 5.03, N 5.93.

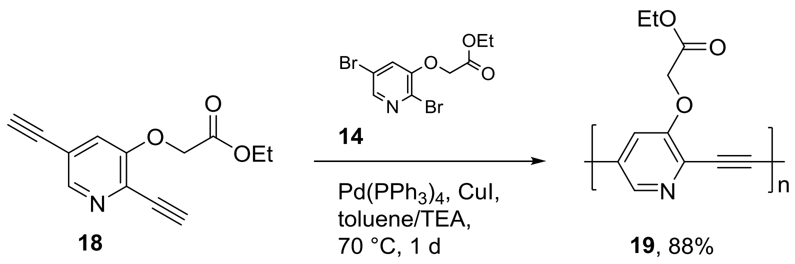

*Compound **14** was synthesized according to the literature.*[155]

Synthesis of 19. Monomer **18** (172 mg, 0.51 mmol) and monomer **14** (116 mg, 0.51 mmol) were dissolved in a mixture of degassed toluene/NEt_3 (1.5:1, 9 mL/6 mL). $Pd(PPh_3)_4$ (29 mg, 25 µmol) and CuI (4.8 mg, 25 µmol) were added and the mixture was stirred at 70 °C for 24 h. Saturated aqueous NH_4Cl and CH_2Cl_2 were added, the aqueous layer was separated and extracted with CH_2Cl_2. The combined organic layers were dried over $MgSO_4$, filtered and concentrated in vacuo. Two times, the crude product was dissolved in a small amount of $CHCl_3$ and slowly added to an excess of MeOH to give **19** as orange solid (178 mg, 88%). The M_n was estimated to be 3.2 x 10^3 with a PDI of 1.2. ^{1}H NMR (600 MHz, $CDCl_3$): δ = 8.17-8.60 (m, 1 H), 7.29-7.75 (m, 1 H), 4.63-5.05 (m, 2 H), 4.17-4.43 (m, 2 H), 1.23-1.29 (m, 3 H) ppm. IR (cm^{-1}): ν 3060, 2979, 2931, 2364, 2194, 2159, 2033, 1746, 1577, 1560, 1532, 1478, 1434, 1401, 1296, 1194, 1111, 1096, 1061, 1018, 895, 857, 753, 694, 620, 589, 566, 542, 534, 518, 509, 499, 493, 485, 476, 466, 457, 453, 435, 426, 419, 407. Due to low solubility, ^{13}C NMR spectrum could not be obtained.

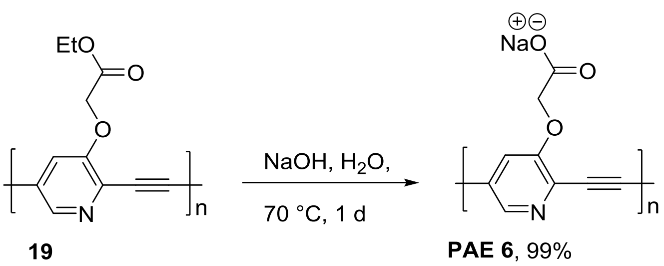

Synthesis of PAE 6. To a mixture of **19** (70.0 mg, 0.34 mmol) and water (20 mL), NaOH (272 mg, 6.80 mmol) was added and the resulting mixture was stirred at 70 °C for 24 h. After adjusting a pH of 7 (HCl) the aqueous mixture was dialyzed against DI H_2O for 3 d. Freeze-drying gave **PAE 6** as spongy, dark orange solid (59 mg, 99%). The M_n and PDI result from **19**. ^{1}H NMR (600 MHz, D_2O): δ 6.80-8.38 (m, 2 H), 3.81-3.88 (s, 2 H) ppm. IR (cm^{-1}): ν 3361, 3243, 3007, 2852, 1606, 1481, 1393, 1357, 1322, 1275, 1229, 1204, 1093, 1048, 955, 911, 862, 806, 687, 621, 527, 476, 464, 432, 413. Due to low solubility, ^{13}C NMR spectrum could not be obtained.

5.2.2 Synthesis of PAEs (Chapter 2.2)

In this chapter, the synthesis of **P1**[41], **P3**[48], **P5**[156], **P6**[41], **P7**[48], **P8**[170], **P10**[41], **P11**[45], **P12**[41], **P13**[41] were reported previously. The synthesis of **P2**, **P4** and **P9** is reported here.

Synthesis of P2

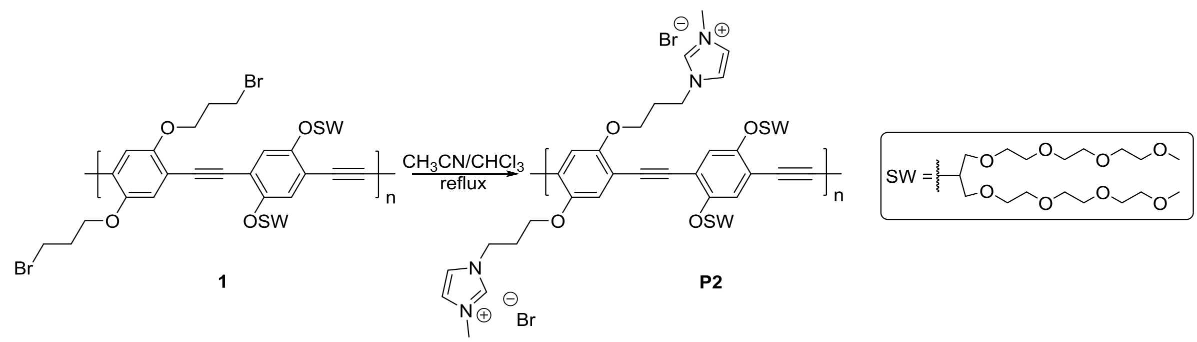

*Compounds **1** was synthesized according to the literature [41].*

Synthesis of P2. Polymer **1** (100 mg, 0.083 mmol) was dissolved in degassed $CH_3CN/CHCl_3$ (5 mL/2 mL). 1-methyl-imidazole (1 mL) was added slowly and refluxed for 8 days under N_2 atmosphere. After evaporation of the solvents, the mixture was redissolved in distilled water and then dialyzed against DI water for 7days. Freeze-drying gave **P2** as yellow solid (99 mg, 86.2%). The M_n and PDI result from **1**. ^{1}H NMR (300 MHz, MeOD) δ = 8.32-8.93 (d, 2 H), 7.41-7.60 (m, 4 H), 7.31-7.10 (m, 4 H), 4.58-4.34 (m, 6H), 4.01-4.28 (m, 4 H), 3.76-3.84 (m, 6 H), 3.32-3.75 (m, 56 H), 3.11-3.25 (m, 12 H), 2.31-2.46 (m, 4 H) ppm. Due to low solubility, ^{13}C NMR spectrum could not be obtained. IR (cm^{-1}): ν 3410, 2871, 2359, 1647, 1575, 1508, 1490, 1470, 1420, 1350, 1272, 1200, 1088, 1042, 949, 849, 623. Quantum yields (Φ = 0.29).

Synthesis of P4

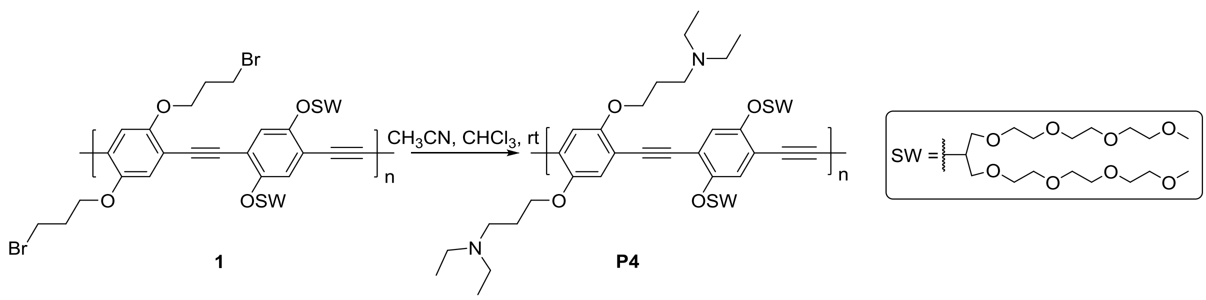

*Compounds **1** was synthesized according to the literature [41].*

Synthesis of P4. Polymer **1** (275 mg, 0.228 mmol) was dissolved in degassed $CH_3CN/CHCl_3$ (8 mL/8 mL). Diethylamine (8 mL) was added slowly and reacted for 7 days under N_2 atmosphere at room temperature. After evaporation of the solvents, the mixture was redissolved in distilled water and then dialyzed against DI water for 7days. Freeze-drying gave **P4** as yellow solid (220 mg, 81.5%). The M_n and PDI result from **1**. ^{1}H NMR (300 MHz, $CDCl_3$) δ = 7.17-7.08 (m, 2 H), 7.03-6.88 (m, 2 H), 4.56-4.32 (m, 2H), 4.18-3.92 (m, 4 H), 3.87-3.38 (m, 56 H), 3.36-3.17 (m, 12 H), 2.91-2.32 (m, 12 H), 2.12-1.74 (m, 4 H), 1.17-0.86 (m, 4 H) ppm. Due to low solubility, ^{13}C NMR spectrum could not be obtained. IR (cm^{-1}): ν 2870, 2817, 2361, 1508, 1489, 1469, 1420, 1380, 1350, 1272, 1200, 1101, 1041, 953, 850, 718. Quantum yield (Φ = 0.21).

Synthesis of P9.

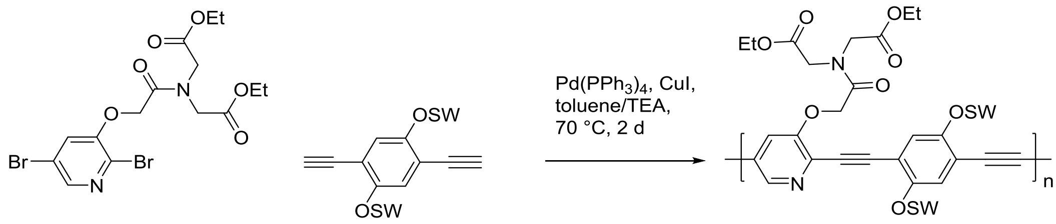

2 **3** **4**

Compounds 2[6] and compounds 3[7] were synthesized according to the literature.

Synthesis of 4. Under a nitrogen atmosphere, **2** (193 mg, 400 µmol, 1.0 eq) and **3** (356 mg, 400 µmol, 1.0 eq) were solved in degassed toluene (3.9 mL) and TEA (2.6 mL). Then CuI (4 mg, 20 µmol, 0.05 eq) and $Pd(PPh_3)_4Cl_2$ (23 mg, 20 µmol, 0.05 eq) were added, before the reaction was heated to 60 °C in a closed flask. After stirring for 24 h, the solution was allowed to reach ambient temperature. The gelatinous solution was solved in chloroform and THF (1:1, 50 mL), before it was washed with NH4Claq (50 mL). The two layers were separated, the aqueous layer was extracted with DCM (3 x 50 mL) and the combined organic layers were dried over MgSO4 and filtered before the solvent was removed under reduced pressure. The resulting residue was dissolved in chloroform (5 mL) and precipitated in pentane (400 mL) and stirred for one hour. The suspension was filtered and the precipitate was dried in vacuo to give **4** as a brown solid (348 mg, 72%). The M_n was estimated to be 2.4×10^3 with a PDI of 14. ^{1}H NMR (600 MHz, $CDCl_3$): δ = 7.12-7.62 (m, 3 H), 4.97 (br. s, 2 H), 4.50-4.54 (m, 2 H), 4.06-4.30 (m, 8 H), 3.46-3.75 (m, 56 H), 3.29 (br. s, 12 H), 1.18 (br. s, 6 H) ppm. Due to low solubility, ^{13}C NMR spectrum could not be obtained. IR (cm^{-1}): ν 2871, 1743, 1684, 1498, 1455, 1398, 1350, 1259, 1193, 1024, 850, 804, 697, 611, 541, 500, 418 cm^{-1}.

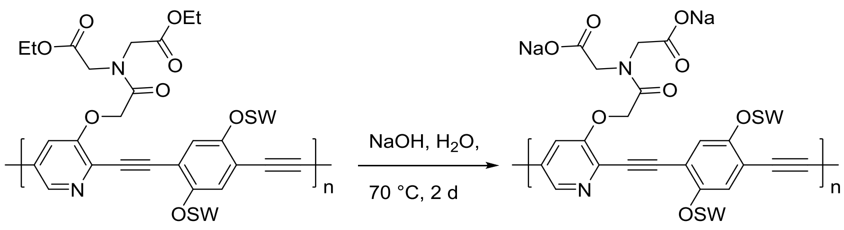

4 **P9**

Synthesis of P9. **4** (148 mg, 122 µmol, 1.0 eq) was suspended in 2.5 N NaOH (1.5 mL, 50 eq) and refluxed at 50 °C for 24 h. After cooling down to room temperature, the pH-value was adjusted to 7.0 (HCl). The solution was filled into a membrane and was dialyzed for three days, before the water was removed by freeze-drying to give **P9** as a rubber-like yellow solid (131 mg, 89%). ^{1}H NMR (600 MHz, D_2O): δ = 8.28-8.37 (m, 1 H), 7.74-7.79 (m, 1 H), 5.04-5.06 (m, 2 H), 3.93-3.96 (m, 4 H), 3.46-3.84 (m, 60 H), 3.25 (br. s, 12 H) ppm. Due to low solubility, ^{13}C NMR spectrum could not be obtained. IR (cm^{-1}): ν 3382, 2872, 2362, 1597, 1499, 1453, 1397, 1198, 1094, 1031, 934, 845, 718, 539, 427, 416 cm^{-1}. Quantum yield (Φ = 0.16).

5.2.3 Synthesis of PAEs (Chapter 3.3)

Synthesis of P1

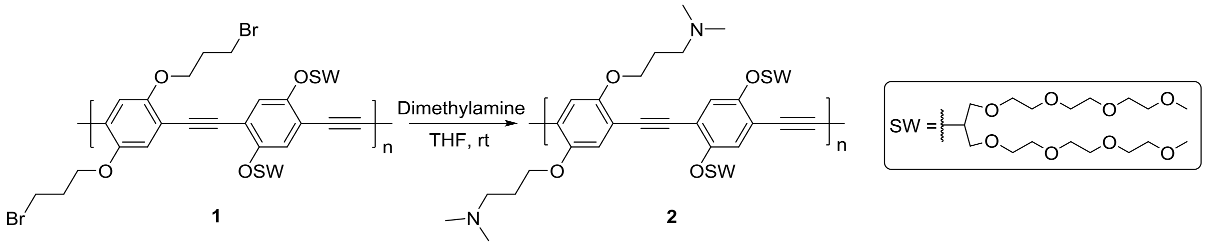

1 **2**

*Compounds **1** was synthesized according to the literature.*[41]

Synthesis of 2. Polymer **1** (400 mg) was dissolved in degassed THF (10 mL). Dimethylamine (33% in absolute ethanol, 5 mL) was added and reacted for 7 days under N_2 atmosphere at room temperature. After evaporation of the solvents, polymer **2** was obtained as yellow solid (387 mg, 98% yield). The M_n and PDI result from **1**[41] (Mn = 1.48 X 10^4, Mw = 5.7 X 10^4), ^{1}H NMR (300 MHz, $CDCl_3$) δ = 7.17 (s, 2H), 7.01 (s, 2H), 4.47 (d, J = 4.4 Hz, 2H), 4.14 (s, 4H), 3.55 (m, 56H), 3.29 (s, 12H), 3.17 (s, 4H), 2.63 (m, 12H), 2.26 (s, 4H) ppm. Due to low solubility, ^{13}C NMR spectrum could not be obtained.

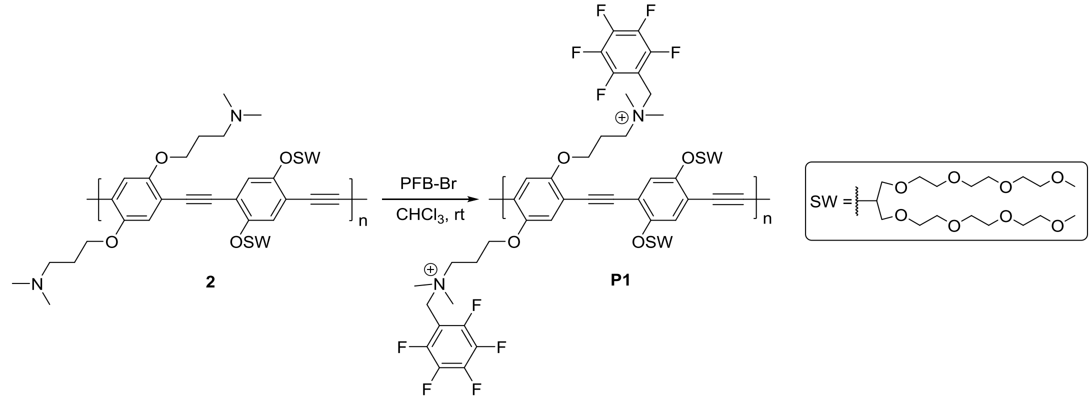

Synthesis of P1. Polymer **2** (180 mg) was dissolved in degassed $CHCl_3$ (5 mL). Pentafluorobenzyl bromide (PFB-Br, 780 mg, 3.0 mmol) was added and reacted for 7 days at room temperature. After evaporation of the solvents, the polymer was redissolved in small amount of MeOH and precipitated in n-Hexane for two times, and then dialyzed against DI water for 7 days. Freeze-drying gave polymer **P1** as yellow solid (163 mg, 91%). The M_n and PDI result from polymer **1**. ^{1}H NMR (300 MHz, MeOD) δ = 7.26 (s, 2H), 7.14 (s, 2H), 4.52 (s, 2H), 4.14 (s, 4H), 3.53 (m, 60H), 3.21 (m, 12H), 3.04 (m, 4H), 2.57 (s, 12H), 2.11 (s, 4H) ppm. Due to low solubility, ^{13}C NMR spectrum could not be obtained. IR (cm^{-1}): ν 2870, 2818, 1732, 1649, 1524, 1508, 1472, 1418, 1372, 1351, 1253, 1200, 1106, 1090, 1039, 950, 853, 788, 720, 677, 585.

5.3 Experiment Details of LDA Calculation

5.3.1 LDA Calculation (Chapter 2.1)

Table 20. Training matrix of fluorescence response pattern from PPE-complexes (**C1-C5**) sensor array against 13 acids analytes at a concentration of 50 mM. LDA was carried out as described above resulting in the five factors of the canonical scores and group generation.

Analyte	Fluorescence response pattern					Results LDA (Factor 1-5)					
Acids	**C1**	**C2**	**C3**	**C4**	**C5**	**F1**	**F2**	**F 3**	**F4**	**F5**	**Group**
A1	9.855	32.522	-28.644	-39.988	23.038	-0.686	3.907	-3.114	-0.396	-1.843	1
A1	3.973	18.211	-30.277	-41.112	20.645	-1.677	2.485	-3.349	-0.414	-0.880	1
A1	-0.694	13.441	-30.287	-42.852	0.159	-3.772	-0.569	-2.079	-0.135	-1.501	1
A1	-5.124	11.405	-30.608	-41.803	20.560	-2.450	1.704	-4.290	-0.633	-0.424	1
A1	-11.237	9.505	-30.227	-43.574	23.827	-2.860	1.914	-5.353	-0.598	-0.146	1
A2	16.840	14.798	-20.853	-31.766	17.993	0.381	1.111	-1.598	0.357	-0.595	6
A2	21.994	17.904	-24.153	-26.364	15.161	1.271	0.779	-0.362	-0.669	-1.049	6
A2	20.175	18.344	-22.589	-33.816	15.415	0.119	1.426	-1.065	0.479	-0.967	6
A2	15.765	20.243	-16.576	-36.914	15.542	-0.429	1.473	-2.057	1.527	-1.026	6
A2	17.477	17.168	-20.876	-35.964	13.596	-0.475	1.135	-1.388	0.936	-0.933	6
A3	8.295	-5.894	-42.821	-49.590	40.500	-1.979	4.785	-4.134	-0.490	1.968	7
A3	7.174	18.858	-7.613	-43.513	37.021	-0.206	4.141	-5.702	3.203	0.248	7
A3	31.101	20.605	-38.041	-45.438	34.636	0.144	6.254	-1.427	0.136	-0.194	7
A3	29.327	-11.360	-36.115	-52.753	32.031	-1.820	4.111	-1.450	2.055	2.345	7
A3	23.594	20.231	-35.954	-51.225	31.199	-1.360	5.960	-2.367	0.918	-0.294	7
A4	55.503	33.454	226.502	227.601	53.345	48.924	-25.937	0.802	1.857	0.159	8
A4	54.991	40.734	225.076	232.644	50.563	49.557	-26.211	1.232	0.800	-0.649	8
A4	54.834	34.111	222.597	225.429	51.888	48.393	-25.744	0.927	1.554	0.002	8
A4	61.466	36.767	207.284	217.039	53.038	47.361	-23.738	1.847	0.719	-0.204	8
A4	59.577	29.267	194.387	209.375	55.515	45.889	-22.797	1.749	-0.040	0.409	8
A5	89.195	37.717	-56.735	-54.627	87.499	5.897	18.292	0.600	0.571	1.381	9
A5	87.310	50.434	-51.893	-49.520	69.070	5.566	16.059	1.886	0.345	-0.533	9
A5	99.370	46.084	-57.254	-56.592	66.059	4.803	16.690	3.456	1.203	-0.196	9
A5	97.977	44.565	-58.126	-55.924	65.073	4.704	16.366	3.486	0.963	-0.157	9
A5	96.320	58.282	-59.569	-53.634	60.196	4.837	16.512	3.743	0.100	-1.555	9
A6	17.923	1.314	-54.865	-64.615	44.681	-3.451	8.144	-3.720	0.067	1.709	10
A6	7.983	27.912	-35.577	-61.639	33.590	-3.475	7.224	-5.000	1.493	-0.802	10
A6	34.430	26.541	-37.926	-58.457	38.235	-1.218	8.532	-2.146	1.923	-0.289	10
A6	34.089	10.874	-51.405	-67.578	38.028	-3.181	8.739	-1.772	1.549	0.874	10
A6	35.598	31.638	-39.573	-55.138	34.886	-0.832	8.260	-1.529	1.198	-0.914	10
A7	78.033	31.143	-53.420	-55.949	45.540	1.975	11.866	2.930	1.176	-0.143	11
A7	71.222	40.099	-53.570	-52.887	50.180	2.543	12.589	1.804	0.194	-0.747	11
A7	70.483	37.803	-53.348	-52.990	57.529	2.974	13.358	1.083	0.203	-0.214	11
A7	70.699	36.172	-51.270	-58.382	52.553	1.838	13.026	1.183	1.321	-0.218	11
A7	73.367	31.958	-56.016	-56.717	53.700	2.144	12.996	1.759	0.614	0.108	11
A8	94.359	51.781	-41.406	-22.326	83.045	11.247	15.250	2.334	-1.658	-0.112	12
A8	88.000	52.790	-31.686	-8.066	81.052	13.066	13.074	2.057	-2.495	-0.397	12
A8	93.443	52.066	-32.528	-6.301	87.817	14.098	13.981	2.210	-2.643	0.002	12
A8	84.508	61.675	-33.454	-8.247	84.189	13.203	14.095	1.346	-3.105	-1.015	12
A8	79.985	53.587	-43.153	-14.229	83.972	11.687	14.251	1.130	-3.719	-0.485	12
A9	-23.923	-74.518	-73.066	-75.944	-62.930	-17.137	-11.378	2.464	-0.466	2.100	13
A9	-36.361	-49.878	-44.971	-75.573	-80.550	-18.024	-13.493	0.937	2.567	-0.427	13
A9	-29.334	-48.963	-66.803	-84.075	-74.325	-18.849	-10.667	1.791	0.823	-0.341	13
A9	-29.469	-70.105	-75.383	-84.391	-76.574	-19.652	-12.157	2.665	0.101	1.119	13
A9	-34.482	-53.319	-78.273	-88.389	-77.545	-20.332	-10.743	1.897	-0.363	-0.308	13
A10	-26.371	-40.861	6.233	26.291	1.546	4.768	-13.419	-2.513	-4.269	2.272	2
A10	-38.683	-16.955	10.058	23.292	-18.771	2.696	-14.659	-2.754	-4.246	-0.635	2
A10	-25.882	-20.968	16.515	8.220	-12.288	1.714	-12.429	-2.957	-0.631	0.416	2
A10	-20.327	-41.283	11.667	13.074	-7.217	2.625	-13.322	-2.018	-1.330	2.201	2
A10	-21.809	-12.081	17.942	18.309	-11.876	3.678	-12.585	-2.194	-1.813	-0.348	2
A11	67.202	-1.081	-68.355	-59.546	61.735	1.053	12.137	1.256	-0.398	2.931	3
A11	46.599	25.717	-68.405	-53.132	54.755	0.840	11.798	-0.450	-2.761	0.167	3
A11	72.110	28.173	-62.718	-65.231	54.284	0.642	13.823	1.499	0.827	0.442	3
A11	78.782	-9.791	-65.360	-62.618	55.045	0.672	11.233	2.954	1.225	3.505	3
A11	65.925	28.990	-61.869	-66.099	52.632	0.071	13.480	0.854	0.780	0.261	3
A12	-80.178	-114.695	-114.344	-136.453	-129.073	-35.726	-17.764	1.419	0.621	1.800	4
A12	-90.416	-91.574	-117.830	-134.139	-158.444	-37.702	-20.392	2.867	-0.960	-1.636	4
A12	-86.591	-88.509	-116.083	-139.800	-148.394	-37.504	-18.228	1.977	0.098	-1.262	4
A12	-91.657	-110.036	-121.895	-142.609	-146.159	-38.590	-19.217	1.637	-0.133	0.469	4

A12	-89.150	-99.284	-120.528	-142.617	-145.045	-38.128	-18.235	1.607	-0.065	-0.293	4
A13	0.469	-5.758	-48.075	-64.137	-29.677	-9.740	-3.123	0.714	0.892	-1.360	5
A13	-2.428	-8.160	-48.888	-62.093	-28.535	-9.585	-3.424	0.468	0.408	-1.180	5
A13	-3.387	-18.455	-50.162	-61.020	-26.205	-9.541	-3.966	0.411	0.243	-0.288	5
A13	-3.096	-23.125	-60.614	-62.767	-27.779	-10.196	-3.927	1.070	-0.903	-0.117	5
A13	-8.337	-24.515	-58.249	-62.976	-31.854	-10.803	-4.838	0.735	-0.711	-0.215	5

Table 21. Detection and Identification of unknown organic acids samples using LDA training matrix. All unknown samples could be assigned to the corresponding acids group defined by the training matrix according to the shortest Mahalanobis distance.

Sample	Fluorescence response pattern					Results LDA (Factor 1-5)					Analyte	
#	C1	C2	C3	C4	C5	F1	F 2	F3	F4	Group	Identification	Verification
1	34.77	23.01	-48.09	-51.14	33.22	-0.75	7.33	-0.73	-0.42	10	A6	A6
2	19.68	7.84	-38.09	-53.50	42.69	-1.38	6.71	-3.68	0.93	7	A3	A3
3	73.74	38.88	-55.67	-54.17	56.34	2.88	13.61	1.59	0.16	11	A7	A7
4	-8.66	-39.89	-21.75	-59.10	-63.62	-12.11	-11.97	2.13	4.60	13	A9	A9
5	47.07	23.42	200.75	211.62	39.07	44.33	-26.33	1.69	0.25	8	A4	A4
6	11.27	11.04	-27.26	-37.27	11.86	-1.40	0.60	-1.60	0.05	1	A1	A2
7	104.63	41.43	-58.92	-41.85	71.24	7.54	15.89	4.51	-0.74	9	A5	A5
8	62.36	7.31	-57.57	-58.18	67.34	1.76	12.75	-0.36	0.53	3	A11	A11
9	17.16	10.22	-36.48	-56.32	37.76	-2.22	6.34	-3.78	1.42	7	A3	A3
10	-7.84	-41.52	-30.02	-56.22	-57.50	-11.39	-11.20	2.26	3.04	13	A9	A9
11	-12.01	-18.39	-50.57	-70.87	-31.33	-11.88	-4.01	-0.60	1.17	5	A13	A13
12	-10.78	-41.13	-17.10	-53.67	-59.95	-11.09	-12.36	1.64	4.44	13	A9	A9
13	-8.73	-20.89	-56.23	-79.89	-48.20	-14.40	-5.20	1.10	1.91	5	A13	A13
14	79.81	37.82	-54.55	-51.56	65.31	4.26	14.65	1.57	0.20	9	A5	A5
15	63.87	32.80	-60.44	-50.97	54.96	2.47	12.49	1.09	-1.27	11	A7	A7
16	17.00	12.86	-26.78	-45.87	4.33	-2.84	0.76	-0.79	1.57	6	A2	A2
17	18.85	8.50	-33.92	-47.61	40.98	-0.58	5.77	-3.52	0.69	7	A3	A3
18	72.08	37.16	-53.69	-48.49	54.65	3.51	12.58	1.78	-0.35	11	A7	A7
19	71.37	13.16	-60.60	-57.46	70.17	2.64	13.95	0.51	0.25	3	A11	A11
20	45.16	26.42	196.22	218.58	37.00	45.07	-26.94	2.21	-1.49	8	A4	A4
21	-28.10	-12.93	24.19	34.26	-12.80	5.72	-14.78	-2.27	-3.35	2	A10	A10
22	64.68	16.71	-57.70	-54.79	59.97	2.05	12.25	0.62	0.00	3	A11	A11
23	-11.10	-20.23	-49.92	-75.08	-32.19	-12.53	-3.84	-0.65	1.93	5	A13	A13
24	44.74	17.66	193.26	217.36	29.87	44.12	-28.31	3.00	-1.53	8	A4	A4
25	-66.35	-75.46	-97.34	-121.11	-126.10	-31.33	-16.09	2.15	0.73	4	A12	A12
26	17.93	16.89	-30.56	-41.97	8.90	-1.88	1.47	-0.76	0.42	6	A2	A2
27	-11.61	-8.52	22.58	33.11	-9.51	6.80	-13.22	-0.76	-2.79	2	A10	A10
28	-67.07	-73.97	-103.73	-118.47	-119.50	-30.60	-15.14	1.92	-0.67	4	A12	A12
29	90.18	46.86	-48.92	-24.60	67.36	9.29	13.18	3.58	-2.40	12	A8	A8
30	-63.45	-74.85	-95.42	-111.66	-124.76	-29.62	-16.74	2.75	-0.17	4	A12	A12
31	24.85	10.43	-28.84	-39.36	6.38	-1.37	0.61	0.39	0.79	6	A2	A2
32	34.83	25.65	-48.36	-59.54	33.54	-1.92	8.38	-1.21	0.64	10	A6	A6
33	10.12	12.90	-29.08	-44.28	12.28	-2.47	1.49	-2.07	0.65	1	A1	A1
34	76.90	43.24	-53.95	-20.85	67.10	8.90	12.21	2.61	-4.17	12	A8	A8
35	-8.06	-10.67	18.08	29.63	-8.36	6.44	-12.58	-0.39	-2.77	2	A10	A10
36	88.24	43.29	-48.02	-21.16	64.47	9.43	12.10	3.80	-2.73	12	A8	A8
37	22.06	24.67	-49.29	-56.10	37.56	-1.89	8.06	-2.76	-0.56	10	A6	A6
38	3.21	8.35	-32.92	-43.49	10.29	-3.06	0.70	-2.38	-0.21	1	A1	A1
39	89.57	43.10	-56.11	-49.34	63.92	5.13	15.08	2.91	0.01	9	A5	A5

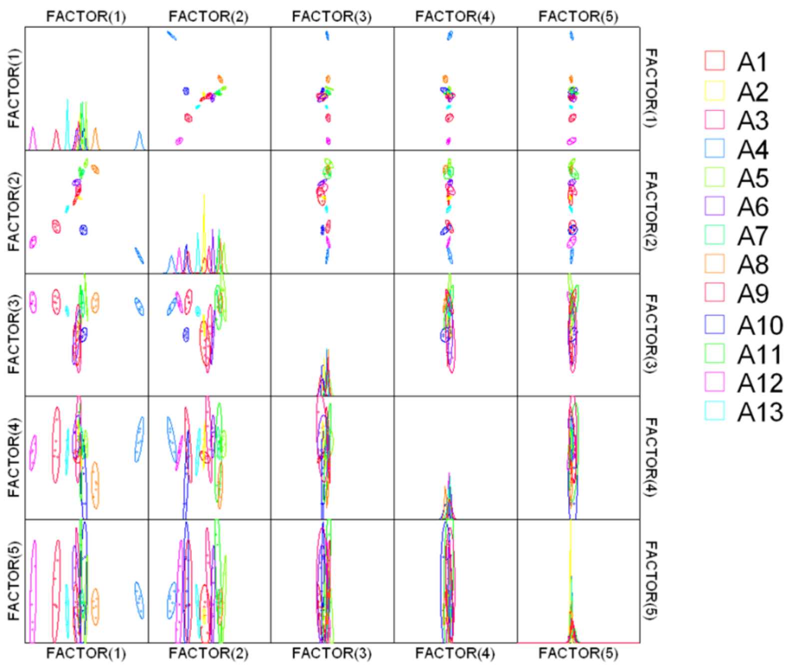

Figure 100. Correlations of canonical fluorescence response patterns.The 90% confidence ellipses for the individual acids are also shown.

5.3.2 LDA Calculation (Chapter 2.2)

5.3.2.1 Linear Discriminant Analysis Results of PAEs at pH 7

Table 22. Training matrix of fluorescence response pattern from water-soluble PAEs sensor array **P1-P4** (2 µM, at pH 7, buffered) against 21 aromatic acids analytes (A1-A21) at a concentration of 5 mM. LDA was carried out as described above resulting in the four factors of the canonical scores and group generation.

Analytes	Fluorescence Response Pattern				Results LDA				
Acids	**P1**	**P2**	**P4**	**P3**	Factor 1	Factor 2	Factor 3	Factor 4	Group
A1	0.14	-0.03	-0.02	0.17	12.64	2.07	-3.72	0.92	1
A1	0.11	-0.03	-0.03	0.17	11.14	1.42	-4.52	1.01	1
A1	0.11	-0.10	-0.02	0.22	12.02	3.37	-6.33	-0.67	6
A1	0.15	-0.01	-0.06	0.22	13.79	1.88	-5.45	2.16	1
A1	0.10	-0.01	-0.05	0.17	10.91	0.98	-4.88	1.60	1
A1	0.18	-0.02	-0.06	0.23	15.26	2.98	-4.82	2.26	1
A2	0.10	0.43	0.22	0.05	12.36	-12.94	-0.56	2.76	12
A2	0.08	0.45	0.26	0.09	12.95	-13.99	-2.26	1.73	12
A2	0.08	0.33	0.14	0.08	11.25	-9.98	-2.25	2.70	12
A2	0.10	0.33	0.17	0.10	12.53	-9.82	-2.30	2.18	12
A2	0.06	0.37	0.15	0.10	10.81	-11.53	-3.34	2.69	12
A2	0.10	0.34	0.09	0.11	12.44	-9.53	-2.72	4.35	12
A3	-0.02	0.01	0.04	-0.04	1.98	-2.82	-0.78	-0.63	15
A3	-0.05	0.02	0.00	-0.02	0.93	-3.52	-2.24	0.17	15
A3	-0.06	-0.03	0.08	0.00	1.65	-2.94	-3.07	-2.75	15
A3	-0.05	0.05	0.02	0.03	2.82	-4.15	-4.08	0.01	15
A3	-0.07	0.00	0.01	-0.04	0.11	-3.53	-2.13	-0.54	15
A3	-0.07	-0.07	0.03	-0.03	-0.13	-1.77	-2.29	-2.05	15
A4	-0.02	0.53	0.48	-0.17	5.02	-19.97	3.89	-2.76	16
A4	-0.02	0.45	0.42	-0.19	3.59	-17.66	4.37	-2.28	16
A4	-0.04	0.48	0.26	-0.14	2.84	-17.57	2.03	1.78	16
A4	-0.06	0.53	0.37	-0.12	3.92	-19.95	1.27	-0.40	16
A4	-0.08	0.49	0.33	-0.17	1.25	-19.12	2.09	-0.16	16
A4	-0.09	0.46	0.31	-0.15	1.35	-18.37	1.22	-0.18	16
A5	-0.56	-0.28	-0.30	-0.31	-28.88	-3.93	-6.19	-1.40	17
A5	-0.56	-0.28	-0.30	-0.33	-29.18	-3.92	-5.17	-1.17	17
A5	-0.56	-0.29	-0.32	-0.33	-29.41	-3.44	-5.39	-1.04	17
A5	-0.59	-0.28	-0.32	-0.35	-30.83	-4.24	-5.37	-0.98	17
A5	-0.59	-0.30	-0.30	-0.35	-31.27	-4.04	-5.48	-1.80	17
A5	-0.56	-0.31	-0.29	-0.30	-28.68	-3.09	-6.48	-2.07	17

A6	-0.10	0.16	0.21	-0.26	-4.21	-9.92	4.87	-2.53	18
A6	-0.10	0.24	0.17	-0.26	-4.20	-11.91	4.90	-0.11	18
A6	-0.17	0.13	0.13	-0.26	-7.39	-9.93	2.84	-1.48	18
A6	-0.16	0.23	0.18	-0.27	-6.33	-12.77	3.65	-1.14	18
A6	-0.11	0.20	0.11	-0.27	-5.63	-10.49	4.94	0.53	18
A6	-0.11	0.19	0.07	-0.29	-6.50	-10.01	5.52	1.60	18
A7	0.18	0.67	0.47	0.04	18.40	-19.37	1.99	1.36	19
A7	0.16	0.68	0.58	0.02	18.07	-20.74	2.18	-1.51	19
A7	0.16	0.74	0.58	0.03	18.46	-22.45	1.66	-0.78	19
A7	0.18	0.69	0.56	0.04	18.87	-20.62	1.80	-0.92	19
A7	0.17	0.68	0.50	0.05	18.16	-20.20	1.47	0.48	19
A7	0.19	0.68	0.46	0.07	19.24	-19.32	1.25	1.70	19
A8	-0.23	-0.21	-0.30	-0.14	-11.98	1.09	-3.07	2.35	20
A8	-0.23	-0.21	-0.37	-0.08	-11.20	1.52	-5.13	4.17	20
A8	-0.24	-0.21	-0.35	-0.10	-11.75	1.17	-4.67	3.55	20
A8	-0.25	-0.24	-0.34	-0.12	-12.77	1.86	-4.04	2.83	20
A8	-0.25	-0.27	-0.38	-0.12	-13.22	2.82	-4.31	3.14	20
A8	-0.25	-0.26	-0.32	-0.08	-11.77	2.12	-5.48	1.96	20
A9	-0.52	-0.55	-0.51	-0.44	-33.65	5.45	-0.59	0.36	21
A9	-0.50	-0.56	-0.52	-0.42	-32.44	6.43	-0.40	0.55	21
A9	-0.50	-0.56	-0.52	-0.42	-32.18	6.35	-0.65	0.49	21
A9	-0.53	-0.58	-0.54	-0.43	-34.05	6.35	-0.94	0.42	21
A9	-0.51	-0.59	-0.52	-0.41	-32.64	6.92	-1.10	-0.12	21
A9	-0.53	-0.56	-0.51	-0.41	-33.29	5.65	-1.71	-0.07	21
A10	-0.21	-0.21	-0.25	-0.04	-8.33	1.36	-5.89	1.02	2
A10	-0.20	-0.21	-0.27	-0.02	-7.78	1.62	-6.23	1.53	2
A10	-0.24	-0.22	-0.30	-0.04	-9.84	1.21	-6.68	1.95	2
A10	-0.22	-0.29	-0.32	-0.04	-9.78	3.73	-6.40	1.32	2
A10	-0.23	-0.29	-0.34	-0.04	-10.41	3.36	-6.60	1.82	2
A10	-0.20	-0.22	-0.32	-0.06	-9.17	2.20	-4.87	2.90	2
A11	-0.34	-0.51	-0.44	-0.40	-24.89	7.69	2.93	0.80	3
A11	-0.34	-0.51	-0.43	-0.39	-25.02	7.50	2.76	0.57	3
A11	-0.35	-0.50	-0.47	-0.36	-24.36	7.47	1.35	1.59	3
A11	-0.35	-0.51	-0.46	-0.40	-25.61	7.53	2.65	1.37	3
A11	-0.36	-0.50	-0.49	-0.34	-24.78	7.21	0.40	1.80	3
A11	-0.35	-0.52	-0.47	-0.38	-25.14	7.88	2.31	1.37	3
A12	-0.49	-0.38	-0.29	-0.57	-32.96	-0.26	4.99	-1.67	4
A12	-0.50	-0.38	-0.36	-0.58	-34.00	0.15	4.91	-0.06	4
A12	-0.52	-0.37	-0.26	-0.56	-33.36	-1.03	3.77	-2.55	4
A12	-0.52	-0.39	-0.36	-0.59	-34.99	0.00	4.65	-0.37	4
A12	-0.51	-0.37	-0.37	-0.56	-34.13	-0.30	4.05	0.25	4
A12	-0.50	-0.50	-0.30	-0.58	-34.19	2.97	5.07	-3.42	4
A13	-0.37	-0.30	-0.19	-0.34	-21.78	-0.21	0.04	-2.44	5
A13	-0.37	-0.31	-0.21	-0.33	-21.64	0.00	-0.30	-2.28	5
A13	-0.38	-0.29	-0.26	-0.33	-22.04	-0.32	-0.38	-0.67	5
A13	-0.41	-0.32	-0.21	-0.31	-22.72	-0.45	-1.77	-2.61	5
A13	-0.40	-0.33	-0.32	-0.34	-23.95	0.81	-0.74	-0.09	5
A13	-0.38	-0.38	-0.25	-0.33	-22.78	2.03	-0.56	-2.30	5
A14	0.13	-0.08	0.08	0.15	12.13	2.36	-3.32	-2.19	6
A14	0.05	-0.10	0.06	0.15	8.81	1.53	-5.67	-3.12	6
A14	0.10	-0.18	0.03	0.17	10.71	4.88	-4.84	-2.98	6
A14	0.10	-0.12	-0.01	0.21	11.74	3.56	-6.21	-1.27	6
A14	0.13	-0.10	-0.02	0.26	14.11	3.81	-7.08	-0.35	1
A14	0.06	-0.12	-0.01	0.19	9.49	2.74	-6.83	-1.63	6
A15	0.29	0.01	0.16	0.24	21.54	2.92	-2.16	-1.56	7
A15	0.31	0.04	0.22	0.22	22.45	1.81	-0.93	-2.33	7
A15	0.30	0.05	0.18	0.23	21.71	1.62	-1.50	-1.36	7
A15	0.29	-0.02	0.20	0.25	22.03	3.32	-2.42	-2.96	7
A15	0.28	0.02	0.18	0.27	21.74	2.08	-3.37	-2.17	7
A15	0.34	0.00	0.14	0.25	23.17	4.05	-0.90	-0.63	7
A16	0.37	-0.09	0.10	0.10	19.96	7.28	4.95	-0.48	8
A16	0.37	-0.10	0.12	0.14	20.80	7.39	3.63	-1.10	8
A16	0.37	-0.17	0.11	0.16	21.11	9.25	2.71	-2.09	8
A16	0.37	-0.08	0.09	0.17	21.55	7.26	2.47	-0.24	8
A16	0.35	-0.09	0.07	0.12	19.25	7.13	3.82	0.02	8
A16	0.32	-0.13	0.02	0.17	19.23	8.10	1.15	0.15	8
A17	0.28	-0.10	0.01	0.16	17.35	6.44	0.71	0.69	9
A17	0.30	-0.08	-0.04	0.10	16.53	6.74	3.19	2.48	9
A17	0.27	-0.13	0.01	0.14	16.19	7.04	0.80	-0.10	9
A17	0.28	-0.09	0.03	0.14	17.25	6.02	1.09	0.51	9
A17	0.27	-0.09	0.00	0.15	16.74	6.17	0.75	0.89	9
A17	0.27	-0.11	-0.01	0.16	16.74	6.63	0.22	0.82	9
A18	0.27	-0.02	0.01	0.02	13.83	3.99	5.09	2.12	10
A18	0.25	-0.08	-0.03	-0.03	11.32	5.27	6.16	2.45	10
A18	0.27	-0.02	-0.03	-0.01	12.63	4.22	6.19	3.28	10
A18	0.26	-0.05	0.00	0.04	13.72	4.67	4.00	1.69	10
A18	0.27	-0.07	0.00	0.04	14.21	5.46	4.37	1.61	10

A18	0.29	-0.13	-0.03	0.01	13.48	7.43	5.92	1.77	10
A19	-0.07	-0.29	-0.17	-0.30	-9.25	5.14	6.81	0.08	11
A19	-0.11	-0.30	-0.12	-0.28	-9.88	4.61	5.37	-1.65	11
A19	-0.09	-0.29	-0.11	-0.34	-10.50	4.65	8.13	-1.42	11
A19	-0.10	-0.30	-0.17	-0.29	-10.26	5.01	5.66	-0.49	11
A19	-0.09	-0.30	-0.17	-0.29	-10.08	5.20	6.15	-0.49	11
A19	-0.10	-0.34	-0.12	-0.31	-10.52	5.81	6.64	-2.21	11
A20	0.34	-0.14	0.03	-0.05	14.50	8.27	9.57	0.85	13
A20	0.33	-0.10	0.00	0.00	15.32	7.51	7.60	1.87	13
A20	0.35	-0.11	0.00	0.02	16.34	7.98	7.06	1.85	13
A20	0.35	-0.14	0.07	0.00	16.30	8.37	7.99	-0.31	13
A20	0.31	-0.18	0.04	0.01	14.84	8.93	6.61	-0.49	13
A20	0.34	-0.17	-0.01	0.03	15.72	9.53	6.63	0.92	13
A21	0.51	-0.09	0.22	0.45	34.74	9.47	-3.59	-3.25	14
A21	0.50	-0.03	0.21	0.42	33.86	7.89	-2.43	-1.82	14
A21	0.52	-0.11	0.14	0.51	35.69	10.93	-5.18	-1.63	14
A21	0.54	-0.08	0.16	0.43	34.95	10.28	-1.64	-1.11	14
A21	0.49	-0.07	0.21	0.47	34.54	8.78	-4.41	-2.87	14
A21	0.47	-0.03	0.18	0.51	34.65	7.46	-6.41	-1.86	14

Total samples: 126

Table 23. Detection and Identification of 84 unknown acids samples using LDA training matrix from PAEs sensor array P1-P4 (2 µM, at pH 7, buffered). All unknown samples could be assigned to the corresponding acids group defined by the training matrix according to the shortest Mahalanobis distance. According to the verification, 6 of 84 unknown acids was misclassified, representing an accuracy of 92.9%.

Sample	Fluorescence Response Pattern				Results LDA					Analyte	
#	**P1**	**P2**	**P4**	**P3**	Factor 1	Factor 2	Factor 3	Factor 4	Group	Identification	Verification
1	-0.09	0.48	0.42	-0.14	2.41	-19.74	0.92	-2.81	16	A4	A4
2	0.17	0.70	0.46	0.03	17.54	-20.52	2.15	1.85	19	A7	A7
3	0.50	-0.09	0.20	0.50	35.37	9.75	-5.26	-2.92	14	A21	A21
4	0.09	-0.08	-0.01	0.19	11.15	2.43	-5.72	-0.71	6	A14	A14
5	-0.20	-0.25	-0.28	-0.02	-8.11	2.59	-6.26	1.29	2	A10	A10
6	-0.50	-0.43	-0.36	-0.59	-34.66	1.62	5.48	-0.63	4	A12	A12
7	-0.12	0.18	0.22	-0.28	-5.08	-10.90	4.89	-2.39	18	A6	A6
8	-0.09	-0.29	-0.16	-0.32	-10.39	4.92	7.41	-0.08	11	A19	A19
9	0.25	-0.10	0.07	-0.01	12.42	5.29	5.58	-0.76	10	A3	**A18**
10	0.10	0.40	0.24	0.09	13.08	-12.17	-1.89	1.44	12	A2	A2
11	0.09	-0.09	-0.09	0.15	9.17	3.04	-4.65	1.28	1	A14	**A1**
12	0.32	-0.12	0.01	0.01	15.10	7.54	6.99	1.20	13	A20	A20
13	0.31	-0.16	0.00	-0.03	13.50	8.61	8.07	0.93	13	A20	A20
14	-0.57	-0.28	-0.31	-0.32	-29.53	-3.88	-6.09	-1.25	17	A5	A5
15	0.18	0.70	0.56	0.07	19.66	-20.85	1.07	-0.72	19	A7	A7
16	0.33	-0.12	0.08	0.16	19.56	7.56	1.94	-0.99	8	A16	A16
17	0.31	-0.12	0.05	0.14	17.92	7.27	2.07	-0.36	9	A17	A17
18	-0.52	-0.54	-0.49	-0.42	-32.94	5.18	-1.27	-0.12	21	A9	A9
19	-0.37	-0.53	-0.45	-0.35	-24.98	7.80	0.66	0.38	3	A11	A11
20	-0.57	-0.29	-0.32	-0.35	-30.25	-3.75	-5.07	-0.98	17	A5	A5
21	-0.56	-0.28	-0.31	-0.36	-30.08	-3.72	-4.46	-1.01	17	A5	A5
22	0.34	0.02	0.20	0.24	23.46	3.13	-0.77	-1.92	7	A15	A15
23	-0.23	-0.22	-0.28	-0.12	-11.50	1.25	-3.79	1.78	20	A8	A8
24	0.24	-0.02	0.11	0.01	13.18	2.47	4.65	-0.53	10	A3	**A18**
25	0.25	-0.14	-0.01	0.12	15.06	7.21	1.02	0.30	9	A17	A17
26	0.33	-0.11	0.02	0.00	15.30	7.29	7.14	1.23	13	A20	A20
27	-0.35	-0.52	-0.45	-0.38	-24.89	7.89	2.13	0.78	3	A11	A11
28	0.28	-0.05	0.01	0.00	13.55	4.96	5.92	1.88	10	A18	A18
29	0.33	-0.10	0.03	-0.06	13.83	7.14	9.52	1.41	13	A20	A20
30	-0.51	-0.42	-0.33	-0.57	-33.95	1.05	4.46	-1.55	4	A12	A12
31	-0.52	-0.42	-0.35	-0.57	-34.53	0.72	4.17	-1.11	4	A12	A12
32	0.07	0.38	0.26	0.04	10.90	-12.43	-1.16	0.40	12	A2	A2
33	0.19	-0.03	-0.04	0.20	14.58	3.06	-3.39	2.00	1	A1	A1
34	0.28	-0.08	-0.05	0.00	13.19	6.26	6.12	3.08	10	A18	A18
35	0.21	0.67	0.61	0.06	20.93	-19.60	2.37	-2.00	19	A7	A7
36	0.20	0.71	0.51	0.07	20.21	-20.34	1.54	1.07	19	A7	A7
37	0.38	-0.12	0.07	0.10	20.17	8.69	5.32	-0.13	8	A16	A16
38	-0.22	-0.25	-0.29	-0.12	-11.46	2.17	-3.53	1.60	20	A8	A8
39	-0.23	-0.22	-0.32	-0.04	-9.75	1.70	-6.39	2.33	2	A10	A10
40	0.29	-0.14	0.01	0.15	17.21	7.57	0.81	-0.10	9	A17	A17
41	0.30	-0.15	0.04	0.15	17.99	7.94	1.35	-0.72	9	A17	A17
42	0.31	-0.01	0.17	0.26	22.57	3.69	-2.06	-2.05	7	A15	A15
43	0.29	-0.04	-0.01	0.00	13.95	5.14	6.39	2.68	10	A18	A18

44	-0.15	0.16	0.23	-0.27	-6.06	-11.02	3.74	-3.33	18	A6	A6
45	-0.11	-0.30	-0.19	-0.33	-11.69	4.99	7.18	0.20	11	A19	A19
46	-0.52	-0.55	-0.48	-0.41	-32.72	5.37	-1.49	-0.54	21	A9	A9
47	-0.40	-0.37	-0.29	-0.33	-23.55	1.70	-0.97	-1.39	5	A13	A13
48	-0.50	-0.58	-0.52	-0.44	-33.00	6.66	0.06	0.19	21	A9	A9
49	0.26	-0.11	0.00	0.02	12.99	6.28	5.02	0.96	10	A18	A18
50	0.24	-0.03	0.12	0.03	14.01	2.91	4.07	-0.96	10	A3	**A18**
51	-0.60	-0.30	-0.32	-0.34	-31.35	-3.86	-5.93	-1.41	17	A5	A5
52	0.34	0.05	0.18	0.27	24.22	2.66	-1.52	-0.91	7	A15	A15
53	0.18	-0.07	-0.01	0.22	14.94	3.74	-4.63	0.38	1	A1	A1
54	0.33	-0.15	0.02	0.16	18.94	8.53	1.60	0.01	8	A16	A16
55	0.10	-0.11	0.00	0.16	10.49	3.33	-4.20	-1.09	6	A14	A14
56	-0.08	-0.35	-0.15	-0.33	-10.69	6.53	7.86	-1.55	11	A19	A19
57	-0.52	-0.44	-0.36	-0.57	-34.80	1.25	3.95	-1.09	4	A12	A12
58	0.32	0.01	0.22	0.27	23.85	3.12	-2.16	-2.76	7	A15	A15
59	-0.36	-0.34	-0.32	-0.32	-22.08	1.81	-0.36	0.14	5	A13	A13
60	0.08	-0.10	-0.09	0.17	9.53	3.06	-5.46	1.07	1	A14	**A1**
61	0.13	-0.01	-0.04	0.18	12.27	1.44	-4.58	1.51	1	A1	A1
62	0.08	0.40	0.27	0.10	13.10	-12.63	-2.81	0.38	12	A2	A2
63	-0.24	-0.27	-0.32	-0.11	-12.39	2.66	-4.34	1.70	20	A8	A8
64	-0.11	-0.28	-0.18	-0.31	-11.35	4.34	6.27	0.20	11	A19	A19
65	-0.07	0.47	0.28	-0.17	1.20	-18.04	2.38	0.83	16	A4	A4
66	-0.11	0.22	0.23	-0.29	-4.70	-11.87	5.66	-1.90	18	A6	A6
67	-0.51	-0.58	-0.52	-0.43	-33.07	6.59	-0.75	0.17	21	A9	A9
68	-0.23	-0.22	-0.28	-0.02	-9.05	1.28	-7.32	1.35	2	A10	A10
69	-0.39	-0.37	-0.28	-0.33	-23.16	1.77	-0.68	-1.60	5	A13	A13
70	-0.34	-0.49	-0.46	-0.38	-24.55	7.24	2.20	1.48	3	A11	A11
71	0.48	-0.06	0.19	0.42	32.75	8.22	-3.27	-2.19	14	A21	A21
72	-0.09	0.50	0.48	-0.15	2.53	-20.67	1.23	-3.90	16	A4	A4
73	-0.16	0.19	0.24	-0.26	-6.04	-11.96	3.21	-3.25	18	A6	A6
74	0.48	-0.03	0.16	0.45	33.38	7.92	-4.15	-0.98	14	A21	A21
75	0.36	-0.11	0.08	0.17	21.12	7.86	2.27	-0.44	8	A16	A16
76	0.14	-0.05	-0.04	0.21	13.20	2.71	-5.09	1.05	1	A1	A1
77	0.06	0.35	0.27	0.07	11.33	-11.76	-2.42	-0.46	12	A2	A2
78	-0.07	0.49	0.22	-0.18	0.79	-18.04	2.83	2.66	16	A4	A4
79	0.26	0.01	0.02	0.00	13.41	3.05	5.69	2.58	10	A3	**A18**
80	0.49	-0.05	0.22	0.50	35.22	8.24	-5.68	-3.18	14	A21	A21
81	-0.24	-0.22	-0.31	-0.13	-12.45	1.31	-3.52	2.52	20	A8	A8
82	-0.40	-0.37	-0.28	-0.35	-24.12	1.53	-0.51	-1.75	5	A13	A13
83	-0.36	-0.54	-0.46	-0.36	-25.02	8.17	1.38	0.79	3	A11	A11
84	-0.20	-0.27	-0.31	-0.04	-8.90	3.40	-5.49	1.70	2	A10	A10

78/84
Accuracy 92.9%

Canonical Scores Plot

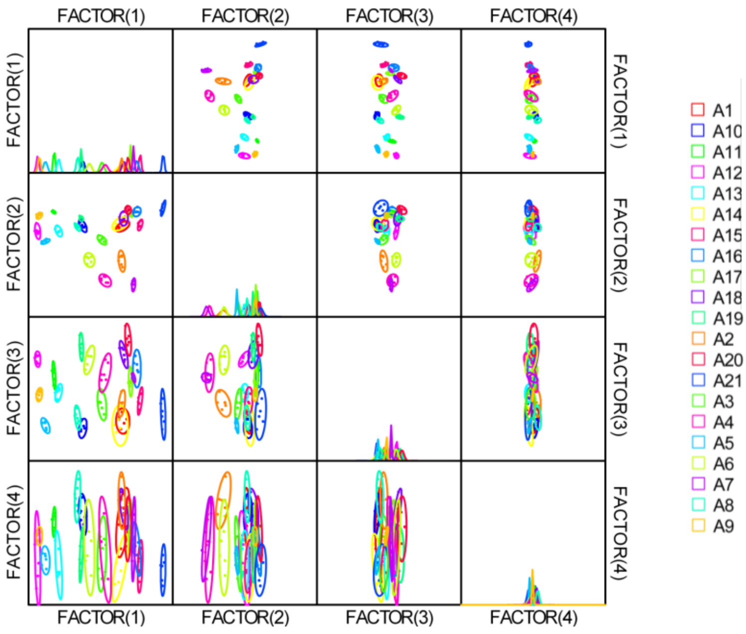

Figure 101. Correlations of canonical fluorescence response patterns from PAEs sensor array **P1**-**P4** (2 µM, at pH 7, buffered) against 21 aromatic acids analytes (A1-A21, 5 mM).The 95% confidence ellipses for the individual acids are also shown.

5.3.2.2 Linear Discriminant Analysis Results of PAEs at pH 13

Table 24. Training matrix of fluorescence response pattern from water-soluble PAEs sensor array P1-P3 (2 µM, at pH 13, buffered) against 21 aromatic acids analytes (A1-A21) at a concentration of 5 mM. LDA was carried out as described above resulting in the three factors of the canonical scores and group generation.

Analytes	Fluorescence Response Pattern			Results LDA			
Acids	**P1**	**P2**	**P3**	Factor 1	Factor 2	Factor 3	Group
A1	-0.05	0.46	0.14	15.37	0.09	-5.97	1
A1	-0.05	0.47	0.09	15.65	1.83	-6.08	1
A1	-0.06	0.43	0.13	14.40	0.41	-5.16	1
A1	-0.04	0.40	0.12	14.09	1.21	-3.88	1
A1	-0.03	0.41	0.15	14.98	0.51	-3.64	1
A1	-0.06	0.41	0.16	14.01	-0.50	-4.58	1
A2	-0.26	0.09	-0.15	-5.10	2.98	-3.67	12
A2	-0.25	0.09	-0.15	-4.96	3.35	-3.08	12
A2	-0.26	0.03	-0.08	-6.07	1.19	-1.22	12
A2	-0.27	0.08	-0.14	-5.61	2.36	-3.37	12
A2	-0.26	0.10	-0.13	-4.80	2.50	-3.62	12
A2	-0.26	0.09	-0.09	-4.84	0.97	-3.37	12
A3	-0.21	0.29	0.23	4.76	-7.28	-6.51	15
A3	-0.23	0.29	0.26	4.37	-8.56	-7.20	15
A3	-0.24	0.28	0.24	3.31	-8.30	-7.19	15
A3	-0.22	0.26	0.27	3.97	-8.70	-6.01	15
A3	-0.25	0.25	0.33	3.01	-11.15	-6.40	15
A3	-0.22	0.28	0.23	4.10	-7.60	-6.61	15
A4	-0.52	-0.39	-0.35	-30.42	1.91	0.65	16
A4	-0.53	-0.36	-0.37	-29.96	2.33	-0.32	16
A4	-0.53	-0.37	-0.32	-30.20	0.74	-0.08	16
A4	-0.53	-0.36	-0.32	-29.56	0.68	-0.13	16
A4	-0.54	-0.39	-0.38	-31.22	2.19	0.08	16
A4	-0.54	-0.37	-0.39	-31.16	2.37	-0.73	16
A5	-0.79	-0.73	-0.51	-51.89	-1.25	0.35	17
A5	-0.79	-0.73	-0.53	-52.25	-0.41	0.48	17
A5	-0.80	-0.73	-0.54	-52.25	-0.45	0.24	17
A5	-0.80	-0.73	-0.55	-52.40	-0.16	0.15	17
A5	-0.80	-0.73	-0.51	-52.22	-1.14	0.29	17
A5	-0.80	-0.72	-0.55	-52.21	-0.35	-0.26	17
A6	-0.32	0.01	-0.01	-8.98	-2.64	-2.63	18
A6	-0.31	0.02	0.04	-7.89	-4.05	-2.74	18
A6	-0.32	0.03	-0.03	-8.73	-2.37	-3.47	18
A6	-0.32	0.03	-0.05	-8.47	-1.77	-3.56	18
A6	-0.34	0.01	-0.04	-9.70	-2.40	-3.55	18
A6	-0.33	0.03	0.01	-8.80	-3.77	-3.71	18
A7	-0.17	0.17	0.00	1.95	1.32	-1.73	19
A7	-0.18	0.19	-0.08	1.36	3.30	-3.13	19
A7	-0.18	0.14	-0.05	0.48	2.65	-1.60	19
A7	-0.18	0.14	-0.04	0.00	2.22	-1.62	19
A7	-0.19	0.18	-0.10	0.72	3.68	-3.40	19
A7	-0.19	0.14	-0.03	-0.18	1.71	-1.86	19
A8	-0.08	0.30	0.18	10.52	-1.42	-1.79	20
A8	-0.04	0.29	0.19	11.71	-0.63	-0.45	9
A8	-0.06	0.29	0.16	10.59	-0.34	-1.29	20
A8	-0.04	0.30	0.10	11.33	2.03	-0.94	20
A8	-0.06	0.29	0.14	10.76	0.41	-1.14	20
A8	-0.06	0.28	0.16	10.40	-0.24	-1.02	20
A9	-0.33	-0.35	0.05	-18.49	-3.69	8.19	21
A9	-0.28	-0.33	0.11	-15.62	-3.87	9.76	21
A9	-0.29	-0.34	0.06	-16.70	-2.53	9.32	21
A9	-0.32	-0.34	0.12	-17.72	-5.49	8.34	21
A9	-0.33	-0.37	0.07	-18.77	-4.17	8.76	21
A9	-0.34	-0.36	0.05	-19.57	-4.05	7.95	21
A10	-0.09	0.23	-0.04	6.69	4.89	-0.94	2
A10	-0.06	0.22	-0.02	7.64	5.33	0.82	2
A10	-0.04	0.24	-0.02	8.98	5.70	0.64	2
A10	0.00	0.21	0.03	10.22	5.63	3.04	2
A10	-0.02	0.22	0.02	9.30	5.21	2.06	2
A10	-0.05	0.28	0.02	9.78	4.18	-0.74	2

A11	-0.42	-0.25	-0.15	-21.03	-1.12	0.80	3
A11	-0.41	-0.22	-0.22	-20.57	1.08	0.17	3
A11	-0.42	-0.25	-0.18	-21.15	-0.02	1.18	3
A11	-0.42	-0.26	-0.21	-21.65	0.74	1.15	3
A11	-0.42	-0.25	-0.18	-21.12	0.01	1.13	3
A11	-0.42	-0.21	-0.22	-20.63	0.74	-0.57	3
A12	-0.17	0.09	-0.07	-0.68	3.65	0.10	4
A12	-0.16	0.10	-0.08	-0.16	4.35	0.44	4
A12	-0.16	0.10	-0.15	-0.71	6.11	-0.06	4
A12	-0.17	0.11	-0.05	0.14	3.03	-0.22	4
A12	-0.17	0.12	-0.13	-0.31	5.35	-1.06	5
A12	-0.16	0.12	-0.13	0.07	5.45	-0.58	4
A13	-0.20	0.12	-0.13	-1.48	4.40	-2.05	5
A13	-0.20	0.13	-0.12	-1.40	4.07	-2.12	5
A13	-0.18	0.13	-0.14	-0.51	5.18	-1.74	5
A13	-0.19	0.15	-0.16	-0.47	5.41	-2.45	5
A13	-0.18	0.12	-0.14	-0.84	5.20	-1.10	5
A13	-0.17	0.14	-0.11	0.03	4.50	-1.48	5
A14	0.06	0.27	0.18	15.44	3.43	4.38	10
A14	-0.03	0.27	0.10	11.24	2.62	0.48	20
A14	0.02	0.26	0.08	12.80	4.78	2.73	6
A14	0.02	0.31	0.08	14.10	4.52	1.04	6
A14	0.06	0.29	0.08	14.91	5.87	3.23	10
A14	0.05	0.28	0.09	14.67	5.54	3.21	10
A15	-0.08	0.23	0.50	10.63	-10.57	1.22	7
A15	-0.09	0.26	0.50	10.93	-10.89	-0.15	7
A15	-0.07	0.19	0.48	9.55	-9.54	2.54	7
A15	-0.11	0.21	0.45	8.39	-10.18	0.43	7
A15	-0.11	0.19	0.42	7.82	-9.05	1.01	7
A15	-0.11	0.19	0.41	7.70	-8.87	0.88	7
A16	0.01	0.35	0.35	16.72	-3.65	0.56	8
A16	0.09	0.39	0.41	21.51	-2.78	2.47	8
A16	0.07	0.43	0.37	21.41	-2.56	0.33	8
A16	0.06	0.43	0.33	20.72	-1.61	0.06	8
A16	0.09	0.41	0.31	21.35	-0.10	1.49	8
A16	0.06	0.33	0.35	17.78	-2.01	2.86	8
A17	-0.04	0.35	0.25	13.79	-2.36	-1.98	9
A17	-0.01	0.32	0.27	14.10	-1.99	0.26	9
A17	-0.04	0.27	0.26	11.69	-2.68	0.42	9
A17	-0.02	0.28	0.25	12.50	-1.50	1.13	9
A17	-0.05	0.32	0.16	11.93	-0.05	-1.72	20
A17	-0.05	0.29	0.15	11.40	0.49	-0.66	20
A18	0.05	0.26	0.10	14.04	5.03	3.62	10
A18	0.06	0.29	0.19	16.02	3.00	3.69	10
A18	0.04	0.25	0.10	13.32	4.87	3.49	10
A18	0.04	0.25	0.10	13.44	4.99	3.76	10
A18	0.01	0.30	0.08	13.47	4.44	1.17	6
A18	0.03	0.32	0.06	14.60	5.37	1.14	13
A19	-0.46	-0.28	-0.12	-23.32	-3.24	0.55	11
A19	-0.47	-0.29	-0.10	-23.92	-3.95	0.59	11
A19	-0.46	-0.33	-0.15	-24.63	-2.08	1.88	11
A19	-0.45	-0.32	-0.13	-24.13	-2.66	1.82	11
A19	-0.47	-0.31	-0.16	-24.67	-2.21	1.03	11
A19	-0.47	-0.32	-0.17	-24.94	-1.65	1.20	11
A20	0.03	0.33	0.04	14.80	5.99	0.71	13
A20	0.03	0.38	-0.01	16.00	7.56	-0.90	13
A20	0.03	0.31	0.02	14.33	6.92	1.35	13
A20	0.03	0.34	-0.02	14.69	7.78	0.21	13
A20	0.02	0.35	-0.04	14.51	8.15	-0.38	13
A20	0.03	0.28	0.07	13.64	5.46	2.26	6
A21	0.28	0.67	0.74	39.24	-7.26	2.15	14
A21	0.27	0.61	0.67	36.76	-5.47	3.21	14
A21	0.27	0.65	0.66	37.58	-5.33	1.91	14
A21	0.31	0.52	0.69	35.74	-4.43	7.47	14
A21	0.30	0.59	0.68	37.60	-4.65	5.07	14
A21	0.28	0.60	0.78	37.51	-8.20	4.56	14

Total samples: 126

Table 25. Detection and Identification of 84 unknown acids samples using LDA training matrix from PAEs sensor array P1-P3 (2 µM, at pH 13, buffered). All unknown samples could be assigned to the corresponding acids group defined by the training matrix according to the shortest Mahalanobis distance. According to the verification, 4 of 84 unknown acids were misclassified, representing an accuracy of 95.2%.

Sample	Fluorescence Response Pattern			Results LDA				Analyte	
#	P1	P2	P3	Factor 1	Factor 2	Factor 3	Group	Identification	Verification
1	-0.22	0.32	0.24	5.64	-7.91	-7.73	15	A3	A3
2	-0.17	0.18	-0.09	1.65	3.81	-2.69	19	A7	A7
3	0.32	0.65	0.79	40.57	-7.69	4.09	14	A21	A21
4	-0.08	0.24	-0.01	7.40	4.27	-0.91	2	A10	A10
5	-0.18	0.14	-0.16	-0.45	5.76	-1.93	5	A13	A13
6	-0.26	0.08	-0.11	-4.99	1.87	-3.09	12	A2	A2
7	0.09	0.28	0.16	16.61	4.59	4.65	10	A14	**A18**
8	0.02	0.34	0.00	14.63	6.93	0.07	13	A20	A20
9	-0.32	-0.01	-0.04	-9.70	-2.04	-2.45	18	A6	A6
10	-0.53	-0.37	-0.36	-30.16	1.80	-0.20	16	A4	A4
11	0.10	0.26	0.12	16.07	6.21	5.59	10	A14	**A18**
12	-0.06	0.27	0.14	10.04	0.45	-0.48	20	A8	A8
13	0.05	0.28	0.11	14.51	4.93	3.37	10	A18	A18
14	-0.79	-0.73	-0.54	-51.97	-0.15	0.54	17	A5	A5
15	0.07	0.34	0.38	19.08	-2.45	3.23	8	A16	A16
16	-0.07	0.25	0.49	11.15	-10.21	0.89	7	A15	A15
17	-0.24	0.08	-0.12	-4.63	2.78	-2.30	12	A2	A2
18	-0.04	0.42	0.11	14.87	1.51	-4.28	1	A1	A1
19	-0.08	0.23	0.47	10.05	-9.79	1.03	7	A15	A15
20	-0.01	0.31	0.27	14.06	-1.90	0.54	9	A17	A17
21	-0.47	-0.30	-0.12	-24.47	-3.46	0.79	11	A19	A19
22	0.27	0.61	0.78	37.22	-8.80	3.47	14	A21	A21
23	0.31	0.65	0.75	39.86	-6.59	3.64	14	A21	A21
24	-0.31	-0.33	0.07	-17.24	-3.46	8.49	21	A9	A9
25	-0.31	-0.34	0.10	-17.53	-4.53	8.67	21	A9	A9
26	-0.06	0.25	-0.02	8.51	5.35	-0.29	2	A10	A10
27	-0.15	0.08	-0.07	-0.32	4.17	1.23	4	A12	A12
28	-0.23	0.23	0.28	2.93	-8.91	-5.17	15	A3	A3
29	-0.15	0.17	-0.05	2.60	3.60	-1.40	19	A7	A7
30	0.05	0.29	0.16	15.37	3.34	3.33	10	A18	A18
31	-0.05	0.28	0.19	11.17	-0.78	-0.18	20	A8	A8
32	-0.30	-0.35	0.09	-17.05	-3.97	9.33	21	A9	A9
33	-0.42	-0.23	-0.18	-20.51	-0.15	0.47	3	A11	A11
34	0.28	0.60	0.75	37.21	-7.20	4.40	14	A21	A21
35	-0.79	-0.73	-0.54	-52.11	-0.15	0.20	17	A5	A5
36	0.09	0.40	0.36	21.14	-1.67	1.78	8	A16	A16
37	-0.52	-0.36	-0.39	-29.67	2.87	-0.36	16	A4	A4
38	-0.23	0.29	0.25	4.02	-8.40	-7.09	15	A3	A3
39	-0.53	-0.36	-0.38	-30.27	2.31	-0.66	16	A4	A4
40	0.04	0.34	0.04	15.35	6.30	0.49	13	A20	A20
41	0.07	0.40	0.40	20.77	-3.47	1.20	8	A16	A16
42	-0.06	0.27	0.14	9.88	0.43	-0.35	20	A8	A8
43	-0.26	0.09	-0.15	-5.20	3.09	-3.30	12	A2	A2
44	0.05	0.27	0.07	14.26	6.00	3.57	10	A14	**A18**
45	-0.05	0.41	0.14	14.44	0.31	-4.11	1	A1	A1
46	-0.08	0.21	0.46	9.74	-9.53	1.42	7	A15	A15
47	0.04	0.31	0.08	14.77	5.17	1.85	10	A18	A18
48	-0.53	-0.36	-0.33	-29.71	1.18	-0.12	16	A4	A4
49	-0.47	-0.32	-0.13	-24.64	-2.77	1.42	11	A19	A19
50	-0.31	-0.01	-0.01	-9.04	-2.26	-1.70	18	A6	A6
51	-0.80	-0.73	-0.54	-52.52	-0.56	0.24	17	A5	A5
52	-0.06	0.24	0.00	8.13	4.54	0.09	2	A10	A10
53	-0.42	-0.23	-0.17	-20.51	-0.44	0.42	3	A11	A11
54	-0.14	0.20	-0.05	3.56	3.65	-1.91	19	A7	A7
55	-0.20	0.12	-0.16	-1.72	5.39	-1.88	5	A13	A13
56	-0.04	0.31	0.20	12.43	-0.57	-0.41	9	A17	A17
57	-0.32	0.00	0.02	-8.83	-3.55	-2.29	18	A6	A6
58	-0.19	0.19	-0.09	1.06	3.06	-3.76	19	A7	A7
59	-0.02	0.29	0.27	13.23	-2.04	0.84	9	A17	A17
60	-0.46	-0.30	-0.12	-23.91	-3.13	1.26	11	A19	A19
61	-0.04	0.46	0.09	15.72	1.91	-5.53	1	A1	A1
62	-0.04	0.31	0.17	12.22	0.10	-0.89	20	A17	A17
63	-0.04	0.40	0.18	14.83	-0.35	-3.43	1	A1	A1
64	0.03	0.37	0.04	16.12	6.06	-0.35	13	A20	A20

65	0.04	0.30	0.12	14.72	4.08	2.23	10	A14	A18
66	-0.47	-0.30	-0.15	-24.26	-2.32	0.75	11	A19	A19
67	-0.41	-0.22	-0.16	-19.97	-0.72	0.29	3	A11	A11
68	-0.19	0.07	-0.07	-2.25	2.96	0.05	4	A12	A12
69	-0.25	0.10	-0.10	-4.10	1.85	-2.98	12	A2	A2
70	0.04	0.29	0.11	14.36	4.36	2.49	10	A18	A18
71	-0.17	0.14	-0.15	-0.03	5.67	-1.77	5	A13	A13
72	-0.32	-0.02	-0.05	-9.91	-1.49	-2.05	18	A6	A6
73	-0.79	-0.73	-0.55	-52.06	0.04	0.30	17	A5	A5
74	-0.08	0.24	0.50	10.80	-10.80	0.87	7	A15	A15
75	0.03	0.35	-0.01	15.26	7.60	0.01	13	A20	A20
76	-0.17	0.15	-0.13	0.59	5.18	-1.81	5	A13	A13
77	-0.23	0.24	0.31	3.35	-10.14	-5.45	15	A3	A3
78	0.10	0.37	0.35	20.76	-0.98	3.23	8	A16	A16
79	-0.33	-0.34	0.09	-17.83	-4.69	7.91	21	A9	A9
80	-0.07	0.23	0.03	7.98	3.59	0.09	2	A10	A10
81	-0.16	0.07	-0.13	-1.29	5.94	1.17	4	A12	A12
82	-0.06	0.31	0.10	10.60	1.32	-1.87	20	A8	A8
83	-0.41	-0.23	-0.18	-20.14	0.24	0.73	3	A11	A11
84	-0.17	0.09	-0.09	-0.89	4.29	0.15	4	A12	A12
									80/84 Accuracy 95.2%

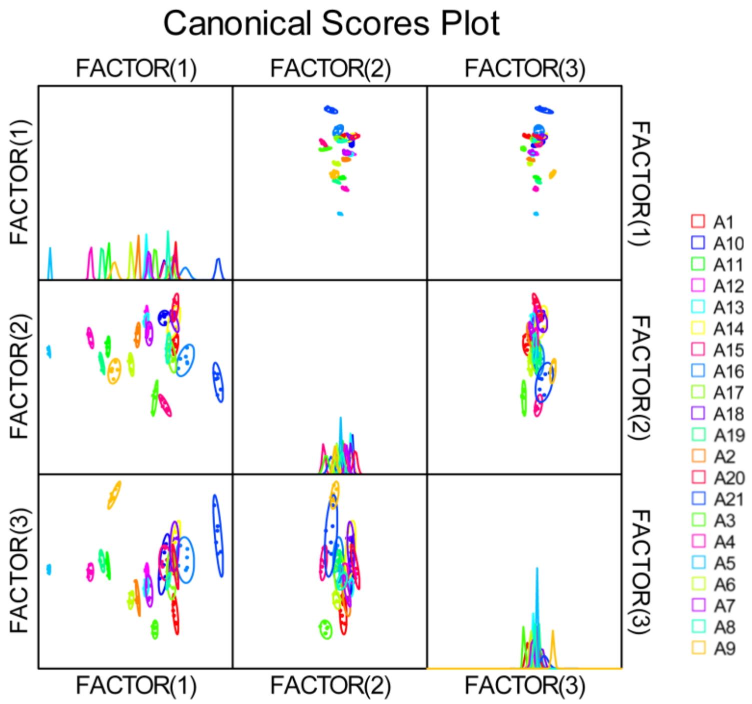

Figure 102. Correlations of canonical fluorescence response patterns from PAEs sensor array P1-P3 (2 µM, at pH 13, buffered) against 21 aromatic acids analytes (A1-A21, 5 mM).The 95% confidence ellipses for the individual acids are also shown.

5.3.2.3 Linear Discriminant Analysis Results of Complexes C1-C7 at pH 7

Table 26. Training matrix of fluorescence response pattern from complexes C1-C7 (2 µM, at pH 7, buffered) against 21 aromatic acids analytes (A1-A21) at a concentration of 5 mM. LDA was carried out as described above resulting in the seven factors of the canonical scores and group generation.

Analytes	Fluorescence response pattern							RESULTS LDA (SCORES)			
Acids	**C1**	**C2**	**C3**	**C4**	**C5**	**C6**	**C7**	**Factor 1**	**Factor 2**	**Factor 3**	**GROUP**
A1	0.24	-0.01	0	0.13	0.18	-0.09	0.02	-8.51	7.77	10.42	1
A1	0.25	-0.02	0.02	0.16	0.19	-0.15	0.02	-8.25	10.67	12.09	1
A1	0.19	0.05	0.02	0.18	0.18	-0.13	-0.05	-7.37	9.94	9.51	1
A1	0.21	-0.04	0.03	0.14	0.17	-0.16	-0.02	-6.9	9.72	12.02	1
A1	0.19	-0.03	0.03	0.16	0.13	-0.16	-0.01	-7.06	9.26	12.04	1
A1	0.21	-0.03	0.02	0.17	0.16	-0.15	-0.02	-7.23	9.29	12	1
A2	0.03	0.21	-0.02	0.36	0.2	0.13	-0.05	-14.86	1.87	6.19	12

A2	0.1	0.23	-0.03	0.35	0.17	0.07	-0.1	-11.06	2.93	5.81	12
A2	0.07	0.23	-0.02	0.35	0.21	0.11	-0.12	-12.49	2.39	5.12	12
A2	0.01	0.23	0.03	0.33	0.21	0.08	-0.13	-12.56	4.58	4.88	12
A2	-0.1	0.21	-0.03	0.36	0.21	0.11	-0.09	-12.85	1.29	5.35	12
A2	-0.05	0.18	0	0.28	0.17	0.09	-0.1	-11.7	1.91	4.95	12
A3	0.12	0.31	0.17	0.15	0.23	0.51	-0.13	-22.81	-3.31	-4.44	15
A3	0.13	0.33	0.15	0.16	0.18	0.52	-0.12	-22.42	-4.61	-4.52	15
A3	0.09	0.33	0.16	0.19	0.22	0.56	-0.11	-24.76	-5.42	-4.38	15
A3	0.11	0.34	0.13	0.14	0.22	0.56	-0.09	-23.65	-5.37	-5.64	15
A3	0.06	0.35	0.13	0.19	0.23	0.57	-0.14	-23.65	-6.14	-5.74	15
A3	0.13	0.31	0.15	0.16	0.22	0.55	-0.09	-24.28	-4.9	-4.39	15
A4	-0.02	0.44	0.06	-0.18	0.16	0.06	-0.19	-0.97	9.33	-12.23	16
A4	-0.02	0.55	0.05	-0.18	0.17	0.11	-0.19	-1.2	10	-15.61	16
A4	0	0.55	0.08	-0.16	0.15	0.15	-0.21	-2.65	8.55	-15.52	16
A4	-0.04	0.54	0.05	-0.12	0.13	0.15	-0.2	-2.75	7.15	-14.39	16
A4	-0.08	0.46	0.04	-0.19	0.19	0.1	-0.21	-0.7	7.98	-14.14	16
A4	-0.08	0.45	0.04	-0.17	0.18	0.08	-0.2	-0.65	8.54	-13.13	16
A5	0.14	0.31	-0.34	-0.61	0.12	-0.5	-0.52	40.11	11.01	-17.15	17
A5	0.15	0.33	-0.31	-0.6	0.13	-0.47	-0.53	38.88	11.33	-17.68	17
A5	0.13	0.32	-0.3	-0.61	0.13	-0.46	-0.54	38.34	11.15	-17.56	17
A5	0.1	0.36	-0.3	-0.61	0.13	-0.49	-0.55	39.51	12.39	-18.91	17
A5	0.13	0.36	-0.29	-0.61	0.09	-0.47	-0.54	39.32	11.46	-18.47	17
A5	0.09	0.33	-0.3	-0.61	0.13	-0.46	-0.52	38	11.29	-18.1	17
A6	0.11	0.14	0.05	0.09	0.21	0.06	-0.21	-6.8	4.15	1.8	18
A6	0.13	0.11	0.06	0.1	0.22	0.06	-0.18	-7.83	4.4	3.06	18
A6	0.09	0.12	0.05	0.1	0.22	0.04	-0.19	-6.92	4.81	2.57	18
A6	0.08	0.09	0.04	0.16	0.2	-0.03	-0.17	-6.33	5.72	5.66	18
A6	0.04	0.09	0.03	0.15	0.21	-0.05	-0.17	-5.79	6.22	5.49	18
A6	0.04	0.1	0.01	0.11	0.16	0	-0.19	-4.58	2.76	3.83	18
A7	-0.15	0.25	-0.01	0.03	0.08	0.41	-0.1	-12.56	-10.07	-5.34	19
A7	-0.13	0.22	0.04	0.04	0.07	0.47	-0.09	-16.02	-11.03	-4.52	19
A7	-0.16	0.22	0.03	0.1	0.07	0.47	-0.09	-16.9	-11.86	-3.28	19
A7	-0.17	0.27	0.02	0.07	0.06	0.45	-0.08	-15.44	-10.56	-5.04	19
A7	-0.17	0.23	0	0.04	0.08	0.48	-0.08	-15.27	-12.5	-5.29	19
A7	-0.17	0.32	0.02	0.08	0.06	0.51	-0.13	-15.17	-12.39	-7.11	19
A8	0.14	0.07	0.16	-0.15	-0.1	-0.31	-0.18	5.36	13.32	3.87	20
A8	0.14	0.03	0.16	-0.1	-0.1	-0.3	-0.18	4.17	12.1	5.88	20
A8	0.13	0.05	0.21	-0.09	-0.07	-0.27	-0.19	1.6	13.44	5.52	20
A8	0.15	0.08	0.18	-0.13	-0.07	-0.29	-0.19	3.78	13.91	3.93	20
A8	0.14	0.08	0.15	-0.09	-0.09	-0.27	-0.18	3.59	12.23	4.47	20
A8	0.11	0.07	0.21	-0.09	-0.08	-0.3	-0.17	1.87	14.95	5.23	20
A9	0.27	-0.08	-0.22	-0.35	-0.14	-0.11	-0.4	21.75	-10.42	-1.38	21
A9	0.28	-0.11	-0.27	-0.3	-0.12	-0.12	-0.4	22.16	-11.81	0.73	21
A9	0.29	-0.06	-0.26	-0.32	-0.1	-0.1	-0.39	21.3	-10.55	-1.07	21
A9	0.31	-0.12	-0.25	-0.24	-0.1	-0.14	-0.39	20.62	-10.18	2.46	21
A9	0.29	-0.11	-0.27	-0.25	-0.11	-0.15	-0.4	21.83	-10.48	1.91	21
A9	0.28	-0.09	-0.25	-0.26	-0.1	-0.18	-0.4	21.98	-8.59	1.39	21
A10	0.24	0.26	0.09	-0.06	0.04	-0.27	-0.17	3.84	16.88	0.33	2
A10	0.25	0.2	0.06	-0.08	0.04	-0.29	-0.15	4.9	16.21	1.53	2
A10	0.2	0.27	0.06	-0.06	0.08	-0.27	-0.15	3.63	17.19	-0.3	2
A10	0.22	0.29	0.06	-0.07	0.08	-0.26	-0.18	4.49	16.98	-1.23	2
A10	0.23	0.27	0.05	-0.07	0.08	-0.29	-0.16	5.17	17.76	-0.45	2
A10	0.21	0.23	0.06	-0.11	0.07	-0.31	-0.16	5.85	17.78	-0.04	2
A11	0.07	-0.25	-0.26	-0.34	-0.17	-0.57	-0.55	36.53	-2.92	5.51	3
A11	0.04	-0.25	-0.28	-0.31	-0.16	-0.57	-0.55	36.36	-3.5	5.94	3
A11	0.03	-0.26	-0.3	-0.32	-0.18	-0.6	-0.54	37.72	-3.34	6.27	3
A11	0.05	-0.26	-0.28	-0.33	-0.16	-0.59	-0.53	36.8	-2.33	6.09	3
A11	0.02	-0.23	-0.26	-0.32	-0.18	-0.6	-0.54	36.55	-1.96	5.8	3
A11	0.02	-0.25	-0.26	-0.29	-0.17	-0.58	-0.54	35.57	-2.53	6.65	3
A12	0.08	-0.28	-0.25	-0.39	-0.07	-0.45	-0.4	29.25	-2.85	4.92	4
A12	0.11	-0.28	-0.23	-0.39	-0.07	-0.44	-0.4	28.34	-2.19	5.34	4
A12	0.07	-0.28	-0.25	-0.39	-0.08	-0.46	-0.39	29.35	-2.78	5.26	4
A12	0.08	-0.29	-0.26	-0.38	-0.07	-0.45	-0.39	28.96	-3.14	5.5	4
A12	0.05	-0.31	-0.25	-0.38	-0.1	-0.45	-0.39	28.83	-3.99	6.04	4
A12	0.06	-0.28	-0.26	-0.4	-0.09	-0.45	-0.38	29.47	-3.26	4.86	4
A13	0.05	-0.32	-0.23	-0.28	-0.04	-0.44	-0.35	24.79	-2.41	8.71	5
A13	0.01	-0.3	-0.22	-0.28	-0.05	-0.43	-0.35	24.48	-2.5	7.83	5
A13	0.02	-0.27	-0.19	-0.26	-0.06	-0.42	-0.33	22.63	-1.53	8.04	5
A13	0.02	-0.29	-0.21	-0.26	-0.06	-0.41	-0.34	22.88	-2.6	8.1	5
A13	0.03	-0.31	-0.2	-0.25	-0.08	-0.39	-0.34	22.11	-3.83	9.27	5
A13	0.02	-0.28	-0.2	-0.27	-0.06	-0.4	-0.31	22.19	-2.06	7.88	5
A14	0.26	-0.06	0.01	0.1	0.2	-0.1	-0.02	-7.59	7.56	10.91	6

A14	0.28	-0.04	0.02	0.14	0.15	-0.08	-0.04	-7.85	6.55	11.54	6
A14	0.26	0.08	0.01	0.13	0.22	-0.09	-0.05	-7.19	10.19	7.56	6
A14	0.27	-0.07	0.01	0.14	0.21	-0.09	-0.07	-7.4	6.69	11.46	6
A14	0.25	-0.01	0.02	0.16	0.17	-0.12	-0.07	-6.59	7.87	10.83	6
A14	0.2	0.02	-0.01	0.14	0.2	-0.1	-0.05	-6.5	7.81	9.25	6
A15	0.11	0.06	0.07	0.21	-0.01	0.38	-0.02	-19.45	-10.42	6.48	7
A15	0.09	0.1	0.07	0.19	0.02	0.45	-0.04	-20.12	-11.7	3.7	7
A15	0.12	0.1	0.09	0.21	-0.01	0.47	-0.03	-21.48	-12	4.7	7
A15	0.11	0.11	0.09	0.22	-0.02	0.48	-0.02	-21.74	-12.48	4.51	7
A15	0.11	0.08	0.09	0.17	-0.01	0.44	-0.04	-19.9	-11.56	4.17	7
A15	0.1	0.06	0.05	0.13	-0.02	0.48	-0.08	-17.84	-15.27	2.92	7
A16	0.07	0.25	0.29	0.04	0.07	-0.08	-0.08	-11.04	16.87	1.48	8
A16	0.05	0.3	0.32	0.03	0.08	-0.08	-0.08	-11.79	18.96	-0.14	8
A16	0.01	0.3	0.32	0.05	0.1	-0.08	-0.07	-12.24	19.32	0.18	8
A16	0.02	0.32	0.31	0.03	0.09	-0.05	-0.09	-11.8	17.86	-1.08	8
A16	0.03	0.32	0.33	0.04	0.09	-0.08	-0.08	-12.32	19.47	-0.24	8
A16	0.02	0.28	0.32	0.03	0.08	-0.07	-0.05	-13.12	18.41	0.77	8
A17	-0.05	0.04	0.02	0	-0.02	0.5	-0.15	-13.31	-18.8	-0.7	9
A17	-0.02	0.08	-0.02	0	-0.01	0.55	-0.13	-13.68	-20	-2.18	9
A17	-0.02	0.07	-0.02	-0.05	0	0.5	-0.14	-11.29	-18.43	-2.81	9
A17	-0.05	0.06	-0.02	-0.03	-0.01	0.48	-0.11	-11.97	-17.86	-1.76	9
A17	0.01	0.06	-0.03	-0.01	-0.01	0.53	-0.12	-13.08	-19.87	-1.74	9
A17	-0.07	0.11	0	-0.04	-0.05	0.5	-0.12	-12.24	-17.93	-3.16	9
A18	0.06	0.26	0.07	-0.01	0.02	0.53	-0.13	-15.21	-12.07	-6.63	10
A18	0.06	0.33	0.08	0.01	0.05	0.56	-0.12	-17.05	-10.65	-8.24	10
A18	0.03	0.28	0.12	-0.05	0.04	0.52	-0.09	-17.03	-9.44	-7.51	10
A18	0.03	0.34	0.11	-0.03	0.06	0.56	-0.07	-18.38	-8.99	-9.13	10
A18	0.01	0.31	0.1	-0.04	0.04	0.57	-0.06	-18.54	-10.36	-8.48	10
A18	0.01	0.29	0.09	-0.02	-0.01	0.56	-0.06	-17.55	-11.86	-7.18	10
A19	0.11	-0.03	-0.36	-0.25	-0.17	0.14	-0.3	16.35	-22.7	-2.8	11
A19	0.11	-0.05	-0.37	-0.27	-0.11	0.14	-0.28	15.59	-21.92	-2.74	11
A19	0.12	-0.02	-0.37	-0.25	-0.13	0.17	-0.28	15.15	-22.37	-3.34	11
A19	0.14	-0.01	-0.36	-0.26	-0.14	0.19	-0.28	14.31	-22.76	-3.65	11
A19	0.09	0.02	-0.38	-0.22	-0.15	0.19	-0.27	14.28	-23.32	-3.89	11
A19	0.15	0.04	-0.36	-0.21	-0.13	0.16	-0.26	13.77	-20.31	-3.54	11
A20	0.02	0.12	0	0.08	-0.13	0.47	-0.12	-12.31	-18.69	0.03	13
A20	0.09	0.13	0.01	0.05	-0.13	0.45	-0.12	-12.03	-16.9	-0.21	13
A20	-0.01	0.13	0.02	0.08	-0.13	0.47	-0.11	-13.44	-17.37	-0.08	13
A20	0.04	0.16	0.01	0.11	-0.12	0.5	-0.11	-14.37	-18.07	-0.36	13
A20	0.04	0.13	0.01	0.11	-0.11	0.46	-0.12	-13.72	-17.08	0.86	13
A20	-0.01	0.15	0.02	0.11	-0.14	0.44	-0.11	-13.12	-16.6	0.33	13
A21	0.34	0.61	0.27	0.12	0.2	0.11	0.1	-21.21	23.4	-5.66	14
A21	0.29	0.59	0.28	0.21	0.23	0.11	0.07	-22.68	23.05	-3.69	14
A21	0.26	0.6	0.26	0.2	0.23	0.11	0.13	-23.02	23.4	-3.94	14
A21	0.37	0.64	0.26	0.2	0.24	0.14	0.11	-23.54	23.84	-4.86	14
A21	0.24	0.64	0.26	0.16	0.23	0.18	0.12	-24.06	21.65	-6.6	14
A21	0.24	0.66	0.25	0.19	0.24	0.18	0.14	-24.51	22.21	-6.33	14

Table 27. Detection and Identification of 84 unknown acids samples using LDA training matrix from complexes C1-C7 (2 μM, at pH 7, buffered). All unknown samples could be assigned to the corresponding acids group defined by the training matrix according to the shortest Mahalanobis distance. The first three among seven factor scores were shown According to the verification, 1 of 84 unknown acids was misclassified, representing an accuracy of 98.8%.

Sample	Fluorescence Response Pattern						Results LDA				Analyte	
#	C1	C2	C3	C4	C5	C6	Factor 1	Factor 2	Factor 3	Group	Identification	Verification
1	0.13	0.11	0.05	0.13	0.19	-0.02	-5.82	5.84	4.44	18	A6	A6
2	0.12	0.04	0.08	0.15	-0.04	0.44	-18.68	-13.39	4.97	7	A15	A15
3	-0.04	0.47	0.01	-0.12	0.19	0.11	-1.27	7.18	-12.7	16	A4	A4
4	-0.16	0.26	0	0.09	0.05	0.44	-13.5	-11.93	-4.89	19	A7	A7
5	-0.01	0.1	-0.04	-0.02	-0.04	0.53	-11.54	-20.18	-3.25	9	A17	A17
6	0.12	0.07	0.22	-0.1	-0.09	-0.3	2.87	14.68	4.9	20	A8	A8
7	0.13	0.05	0.17	-0.11	-0.11	-0.3	4.2	12.47	5.35	20	A8	A8
8	0.31	-0.11	-0.27	-0.3	-0.1	-0.13	22.34	-11.2	0.54	21	A9	A9
9	0.02	-0.25	-0.29	-0.31	-0.18	-0.57	36.91	-4.53	6.17	3	A11	A11
10	0.07	-0.29	-0.24	-0.37	-0.07	-0.45	28.52	-3.23	5.82	4	A12	A12
11	0.08	0.36	-0.31	-0.6	0.12	-0.46	38.74	11.22	-18.78	17	A5	A5
12	0.2	-0.05	0.03	0.12	0.17	-0.11	-7.29	7.43	10.9	6	A14	A14
13	0.07	0.17	-0.02	0.36	0.18	0.13	-14.33	0.7	7.44	12	A2	A2
14	0.11	0.06	0.07	0.22	0.01	0.38	-18.52	-10.49	5.97	7	A15	A15

15	0	0.17	-0.03	0.3	0.16	0.1	-11.97	0.86	6.09	12	A2	A2
16	0.12	0.13	0.03	0.14	0.17	0	-5.37	4.57	4	18	A6	A6
17	0.26	-0.05	0.02	0.13	0.15	-0.09	-8.06	6.88	11.33	6	A1	A14
18	0.21	0.01	-0.02	0.13	0.16	-0.12	-5.53	7.75	9.63	6	A14	A14
19	0.07	0.16	-0.01	0.29	0.18	0.07	-12.01	2.91	6.66	12	A2	A2
20	0.21	0.22	0.07	-0.09	0.08	-0.3	4.44	17.96	0.46	2	A10	A10
21	0.01	-0.26	-0.27	-0.31	-0.16	-0.57	35.94	-3.18	6.17	3	A11	A11
22	0	0.1	0.02	-0.02	-0.02	0.58	-15.04	-19.38	-3.13	9	A17	A17
23	0.3	0.64	0.22	0.15	0.23	0.13	-21.27	22.7	-6.31	14	A21	A21
24	0.28	-0.1	-0.24	-0.35	-0.12	-0.11	22.92	-11.82	-1.15	21	A9	A9
25	0.22	0.28	0.08	-0.1	0.04	-0.31	5.11	19.01	-0.75	2	A10	A10
26	0.11	0.33	-0.3	-0.62	0.14	-0.48	39.03	12.27	-18.3	17	A5	A5
27	-0.15	0.3	0	0.09	0.08	0.51	-15.87	-12.62	-6.35	19	A7	A7
28	0.05	0.31	0.04	0.01	0.04	0.53	-16.37	-10.68	-7.09	10	A18	A18
29	0.05	0.3	0.11	-0.03	0.03	0.55	-17.68	-10.21	-7.74	10	A18	A18
30	0.14	0.03	-0.38	-0.2	-0.15	0.13	15.1	-20.35	-2.79	11	A19	A19
31	0.13	0.05	0.22	-0.12	-0.1	-0.29	2.33	13.89	5.34	20	A8	A8
32	0.22	0.3	0.09	-0.05	0.05	-0.28	3.5	18.42	-0.68	2	A10	A10
33	0.1	0.1	0.07	0.17	-0.01	0.46	-18.24	-13.56	3.27	7	A15	A15
34	0.14	-0.05	-0.36	-0.27	-0.17	0.13	16.04	-21.91	-2.12	11	A19	A19
35	0.05	0.13	0.01	0.11	-0.14	0.46	-13.68	-17.46	1.07	13	A20	A20
36	-0.07	0.48	0.03	-0.12	0.14	0.07	-0.8	8.23	-12.42	16	A4	A4
37	-0.05	0.53	0.04	-0.1	0.14	0.06	-0.23	9.66	-13.47	16	A4	A4
38	0.11	0.37	-0.3	-0.6	0.09	-0.49	39.61	11.94	-18.58	17	A5	A5
39	0.01	0.27	0.28	0.03	0.06	-0.06	-11.62	16.49	0.94	8	A16	A16
40	0.11	0.06	0.21	-0.09	-0.09	-0.28	2.19	13.57	5.18	20	A8	A8
41	-0.15	0.26	-0.02	0.09	0.05	0.51	-15.33	-14.22	-5.12	19	A7	A7
42	0.16	0.01	-0.38	-0.2	-0.15	0.17	14.3	-22.19	-2.64	11	A19	A19
43	-0.16	0.3	-0.02	0.08	0.05	0.4	-13.01	-9.83	-5.18	19	A7	A7
44	0.15	0.33	0.11	0.12	0.18	0.52	-20.72	-5.86	-5.51	15	A3	A3
45	0.06	0.13	0.01	0.1	-0.11	0.46	-13.42	-16.78	0.5	13	A20	A20
46	0.07	0.13	0.02	0.08	0.14	0.01	-3.8	3.2	2.3	18	A6	A6
47	-0.03	0.08	0.02	-0.03	-0.03	0.53	-12.82	-19.21	-2.89	9	A17	A17
48	0.05	0.28	0.08	-0.02	0.02	0.52	-17.05	-10.34	-6.51	10	A18	A18
49	0.31	0.67	0.24	0.19	0.22	0.11	-21.76	24.25	-6.13	14	A21	A21
50	0.31	-0.06	-0.23	-0.25	-0.12	-0.13	21.52	-9.98	0.49	21	A9	A9
51	0.07	-0.29	-0.27	-0.38	-0.07	-0.47	29.9	-2.72	5.79	4	A12	A12
52	0	-0.29	-0.21	-0.26	-0.06	-0.4	22.6	-2.99	7.88	5	A13	A13
53	0.05	0.14	0	0.08	-0.12	0.44	-12.22	-16.44	-0.14	13	A20	A20
54	0.01	0.3	0.31	0.05	0.1	-0.07	-11.86	18.14	-0.02	8	A16	A16
55	0.1	0.32	0.17	0.16	0.2	0.54	-24.49	-4.42	-4.29	15	A3	A3
56	0.18	0.03	0	0.14	0.17	-0.12	-6.99	8.95	9.27	1	A1	A1
57	0.24	-0.05	0.02	0.12	0.17	-0.1	-7.03	6.98	11.07	6	A14	A14
58	0	0.3	0.33	0.03	0.09	-0.08	-12.05	19.29	-0.26	8	A16	A16
59	0.05	-0.3	-0.28	-0.37	-0.07	-0.47	29.63	-3.53	6.2	4	A12	A12
60	0.35	0.69	0.26	0.18	0.17	0.13	-22.65	23.95	-6.23	14	A21	A21
61	0.03	0.3	0.3	0.06	0.11	-0.04	-12.94	17.38	0.07	8	A16	A16
62	0	-0.26	-0.22	-0.26	-0.06	-0.41	22.97	-2.44	7.56	5	A13	A13
63	0.21	-0.06	0	0.15	0.18	-0.12	-7.55	7.36	11.83	1	A1	A1
64	0.04	0.13	0.01	0.11	-0.11	0.5	-14.62	-18.37	0.29	13	A20	A20
65	0.02	-0.29	-0.23	-0.27	-0.08	-0.44	24.88	-2.85	8.35	5	A13	A13
66	0.05	0.3	0.07	0.02	0.01	0.55	-17.32	-11.73	-6.67	10	A18	A18
67	-0.03	0.49	0.06	-0.16	0.12	0.11	-0.97	7.38	-13.92	16	A4	A4
68	0.26	0.61	0.22	0.14	0.18	0.11	-20	21.15	-5.53	14	A21	A21
69	0.02	-0.24	-0.29	-0.3	-0.16	-0.57	36.05	-3.47	5.89	3	A11	A11
70	0.07	0.1	0.01	0.13	0.15	-0.03	-4.55	3.92	4.85	18	A6	A6
71	0.17	0.35	0.17	0.17	0.22	0.51	-23.72	-2.57	-4.52	15	A3	A3
72	0.07	-0.3	-0.28	-0.37	-0.07	-0.45	29.76	-4.08	5.85	4	A12	A12
73	0.29	-0.06	-0.25	-0.32	-0.13	-0.14	23.65	-10.41	-1.25	21	A9	A9
74	0.02	-0.28	-0.22	-0.27	-0.08	-0.4	23.31	-3.39	7.77	5	A13	A13
75	0.23	-0.07	-0.01	0.11	0.19	-0.1	-6.08	6.24	10.85	6	A14	A14
76	0.2	0.06	-0.01	0.15	0.13	-0.1	-6.65	7.85	9.09	1	A1	A1
77	0.2	0.26	0.04	-0.09	0.02	-0.28	5.78	15.7	-0.64	2	A10	A10
78	0.15	0.32	0.13	0.13	0.19	0.56	-22.45	-6.45	-5.18	15	A3	A3
79	0.08	0.05	0.08	0.14	0.02	0.46	-19.06	-13.04	3.72	7	A15	A15
80	0.04	-0.24	-0.29	-0.31	-0.16	-0.57	36.72	-3.63	5.7	3	A11	A11
81	0.1	0.36	-0.31	-0.6	0.13	-0.46	38.37	11.66	-18.7	17	A5	A5
82	-0.01	0.08	0.02	-0.03	-0.05	0.55	-13.26	-20.05	-2.79	9	A17	A17
83	0.15	0.02	-0.37	-0.21	-0.17	0.14	15.1	-21.19	-2.57	11	A19	A19
84	0.07	0.2	0	0.31	0.16	0.08	-12.58	3.55	6.05	12	A2	A2

83/84 (Accuracy 98.8%)

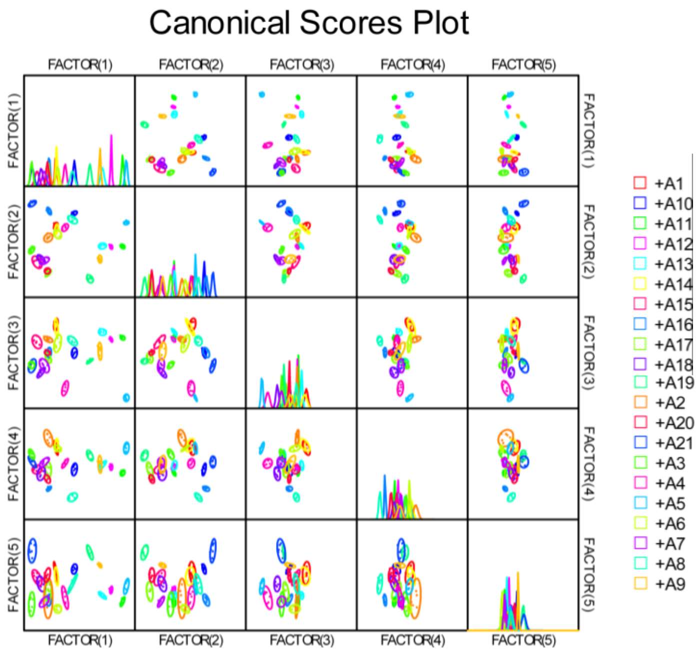

Figure 103. Correlations of canonical fluorescence response patterns from complexes C1-C7 (2 µM, at pH 7, buffered) against 21 aromatic acids analytes (A1-A21, 5 mM).The 95% confidence ellipses for the individual acids are also shown.

5.3.3 LDA Calculation (Chapter 2.3)

Table 28. Training matrix of fluorescence response pattern from an array of **P1**, **C1-2** (each at pH 10 and 13, buffered) against 11 nonsteroidal anti-inflammatory drugs (NSAIDs). LDA was carried out as described above resulting in the four factors of the canonical scores and group generation

Analyte	Fluorescence response pattern				Results LDA				
NSAIDs	P1 (pH10)	P1 (pH13)	C1-2 (pH10)	C1-2 (pH13)	Factor1	Factor2	Factor3	Factor4	Group
D1	0.128	0.121	-0.221	0.258	17.991	20.367	-6.569	5.622	1
D1	0.118	0.110	-0.157	0.293	19.178	18.321	-4.544	6.185	1
D1	0.109	0.143	-0.229	0.300	19.375	18.570	-7.507	3.939	1
D1	0.134	0.129	-0.208	0.324	20.020	18.266	-6.771	6.374	1
D1	0.101	0.087	-0.157	0.209	16.322	20.354	-3.619	5.504	1
D1	0.084	0.093	-0.197	0.228	16.285	19.186	-5.313	4.648	1
D2	0.016	0.099	0.061	0.240	19.363	16.002	3.425	0.312	4
D2	0.014	0.065	0.123	0.181	17.670	17.344	6.466	1.269	4
D2	-0.022	0.082	0.091	0.235	18.697	14.260	4.597	-0.725	4
D2	-0.031	0.087	0.076	0.180	17.288	16.193	4.492	-2.250	4
D2	0.032	0.081	0.055	0.208	18.110	17.413	3.713	1.773	4
D2	-0.026	0.075	0.130	0.209	18.321	14.923	6.261	-0.900	4
D3	-0.327	-0.140	-0.186	-0.038	-1.245	8.050	-1.140	-5.410	5
D3	-0.360	-0.176	-0.235	-0.058	-3.786	6.756	-2.381	-4.961	5
D3	-0.348	-0.158	-0.188	-0.022	-1.657	6.236	-1.203	-5.084	5
D3	-0.338	-0.175	-0.273	-0.047	-3.742	7.270	-3.763	-3.621	5
D3	-0.356	-0.183	-0.183	-0.051	-3.141	6.477	-0.518	-4.361	5
D3	-0.379	-0.176	-0.270	-0.079	-4.922	6.893	-3.495	-6.107	5
D4	-0.964	-0.976	-0.761	-0.896	-61.114	-2.464	-6.639	3.819	6
D4	-0.966	-0.980	-0.773	-0.886	-61.180	-3.007	-7.114	4.152	6
D4	-0.965	-0.978	-0.765	-0.899	-61.323	-2.419	-6.760	3.816	6
D4	-0.966	-0.980	-0.765	-0.890	-61.166	-2.898	-6.792	4.056	6
D4	-0.966	-0.983	-0.766	-0.884	-61.123	-3.155	-6.864	4.358	6
D4	-0.964	-0.980	-0.769	-0.891	-61.212	-2.758	-6.924	4.161	6
D5	-0.850	-0.847	-0.353	-0.671	-45.473	-4.084	4.653	3.622	7
D5	-0.857	-0.843	-0.389	-0.671	-45.883	-4.196	3.360	3.180	7
D5	-0.842	-0.848	-0.379	-0.657	-45.437	-4.321	3.657	4.424	7
D5	-0.855	-0.847	-0.369	-0.655	-45.334	-4.871	3.952	3.670	7
D5	-0.852	-0.851	-0.347	-0.649	-45.004	-5.077	4.733	4.128	7
D5	-0.853	-0.853	-0.379	-0.653	-45.581	-5.019	3.655	4.186	7

D6	-0.767	-0.742	-0.111	-0.464	-33.418	-6.570	10.472	3.601	8
D6	-0.774	-0.754	-0.171	-0.462	-34.592	-7.177	8.491	4.230	8
D6	-0.771	-0.727	-0.152	-0.440	-32.945	-7.248	8.673	2.964	8
D6	-0.772	-0.727	-0.150	-0.446	-33.073	-7.125	8.797	2.855	8
D6	-0.766	-0.748	-0.171	-0.449	-34.031	-7.241	8.311	4.450	8
D6	-0.776	-0.743	-0.163	-0.460	-34.094	-7.085	8.623	3.416	8
D7	-0.790	-0.489	-0.538	-0.442	-30.745	-2.095	-7.450	-11.820	9
D7	-0.788	-0.487	-0.527	-0.460	-30.927	-1.271	-6.909	-12.210	9
D7	-0.787	-0.490	-0.504	-0.458	-30.675	-1.407	-6.096	-12.016	9
D7	-0.792	-0.503	-0.502	-0.472	-31.436	-1.332	-5.786	-11.609	9
D7	-0.797	-0.506	-0.520	-0.447	-31.203	-2.563	-6.607	-11.253	9
D7	-0.801	-0.491	-0.512	-0.465	-31.123	-1.710	-6.337	-12.651	9
D8	0.074	0.215	0.023	0.614	31.858	6.585	-2.156	1.587	10
D8	0.032	0.210	0.027	0.604	31.045	5.228	-1.976	-0.325	10
D8	0.070	0.231	-0.002	0.608	31.831	7.047	-3.165	0.364	10
D8	0.050	0.218	-0.011	0.608	31.099	5.991	-3.394	0.249	10
D8	0.029	0.173	-0.031	0.630	29.751	3.323	-3.833	2.336	10
D8	0.055	0.205	-0.028	0.613	30.646	5.725	-3.896	1.374	10
D9	-0.211	0.000	0.331	0.313	19.131	1.859	12.808	-4.629	11
D9	-0.231	-0.033	0.343	0.314	18.105	0.264	13.531	-3.583	11
D9	-0.216	-0.042	0.341	0.293	17.428	1.443	13.788	-2.539	11
D9	-0.216	-0.034	0.405	0.322	19.193	0.492	15.692	-2.792	11
D9	-0.235	-0.049	0.386	0.297	17.702	0.368	15.349	-3.174	11
D9	-0.287	-0.061	0.365	0.271	15.938	-0.907	14.844	-5.304	11
D10	-0.018	0.183	-0.041	0.990	37.898	-12.063	-7.456	4.795	2
D10	-0.059	0.179	-0.022	0.958	36.857	-12.559	-6.568	2.425	2
D10	-0.100	0.175	-0.042	1.013	37.341	-16.320	-7.782	1.499	2
D10	-0.081	0.173	-0.013	0.976	36.995	-14.242	-6.386	1.940	2
D10	-0.073	0.169	-0.091	0.921	34.672	-11.840	-8.604	1.974	2
D10	-0.058	0.149	-0.057	0.961	35.578	-13.287	-7.494	4.510	2
D11	0.012	0.360	0.238	1.250	53.390	-17.028	-1.661	-1.789	3
D11	0.014	0.351	0.289	1.294	54.800	-18.910	-0.170	-0.610	3
D11	-0.014	0.319	0.283	1.202	51.290	-17.179	0.705	-1.335	3
D11	-0.011	0.292	0.292	1.257	51.889	-19.850	0.827	1.310	3
D11	-0.024	0.300	0.266	1.256	51.651	-20.117	-0.191	0.204	3
D11	0.002	0.303	0.217	1.277	51.877	-19.811	-2.040	1.775	3

Table 29. Detection and identification of unknown NSAIDs samples using LDA. All unknown samples could be assigned to the corresponding group defined by the training matrix according to the shortest Mahalanobis distance. According to the verification, all of the 44 unknown NSAIDs samples were correctly identified, representing an accuracy of 100%.

Sample	**Fluorescence response pattern**				Results LDA					Analyte	
#	**P1** (pH10)	**P1** (pH13)	**C1-2** (pH10)	**C1-2** (Ph13)	Factor1	Factor2	Factor3	Factor4	Group	Identification	Verification
1	-0.365	-0.181	-0.197	-0.055	-3.418	6.321	-1.033	-5.010	5	D3	D3
2	-0.775	-0.745	-0.157	-0.436	-33.508	-7.990	8.637	3.979	8	D6	D6
3	-0.790	-0.495	-0.515	-0.460	-31.066	-1.562	-6.423	-11.802	9	D7	D7
4	-0.053	0.159	-0.035	0.945	35.831	-12.252	-6.678	3.822	2	D10	D10
5	-0.965	-0.981	-0.762	-0.897	-61.297	-2.576	-6.628	4.073	6	D4	D4
6	0.025	0.136	-0.001	0.657	29.583	1.224	-2.639	4.798	10	D8	D8
7	-0.847	-0.842	-0.344	-0.655	-44.802	-4.484	4.788	3.740	7	D5	D5
8	-0.030	0.089	0.072	0.195	17.662	15.681	4.207	-2.053	4	D2	D2
9	-0.249	-0.052	0.392	0.309	17.813	-0.737	15.469	-3.482	11	D9	D9
10	-0.027	0.326	0.239	1.284	52.729	-20.673	-1.658	-1.052	3	D11	D11
11	0.141	0.127	-0.194	0.258	18.628	20.990	-5.674	5.840	1	D1	D1
12	-0.271	-0.036	0.359	0.285	17.081	-0.253	14.286	-5.861	11	D9	D9
13	-0.966	-0.977	-0.773	-0.890	-61.194	-2.778	-7.121	3.878	6	D4	D4
14	-0.791	-0.479	-0.517	-0.447	-30.288	-1.705	-6.757	-12.628	9	D7	D7
15	-0.360	-0.174	-0.217	-0.024	-2.695	5.522	-2.080	-4.666	5	D3	D3
16	-0.026	0.308	0.258	1.273	52.189	-20.648	-0.706	-0.136	3	D11	D11
17	-0.967	-0.982	-0.757	-0.883	-60.988	-3.237	-6.545	4.228	6	D4	D4
18	-0.772	-0.741	-0.136	-0.452	-33.489	-7.224	9.497	3.568	8	D6	D6
19	0.047	0.246	0.046	0.591	32.292	7.124	-1.543	-2.107	10	D8	D8
20	0.036	0.106	0.046	0.211	18.899	18.060	3.125	0.460	4	D2	D2
21	-0.244	-0.019	0.364	0.310	18.552	0.240	14.139	-5.239	11	D9	D9
22	-0.038	0.197	-0.043	0.966	37.559	-11.612	-7.531	2.509	2	D10	D10
23	-0.855	-0.853	-0.393	-0.662	-46.012	-4.705	3.238	4.040	7	D5	D5
24	0.135	0.136	-0.175	0.270	19.401	20.498	-5.220	5.074	1	D1	D1
25	0.034	0.228	0.022	0.595	31.372	6.098	-2.271	-1.519	10	D8	D8
26	-0.775	-0.743	-0.118	-0.465	-33.641	-6.898	10.243	3.355	8	D6	D6
27	-0.034	0.365	0.185	1.294	53.406	-20.366	-4.059	-3.546	3	D11	D11
28	-0.788	-0.498	-0.512	-0.432	-30.458	-2.609	-6.518	-11.084	9	D7	D7

29	0.097	0.100	-0.166	0.221	16.844	20.091	-4.180	4.684	1	D1	D1
30	-0.963	-0.982	-0.764	-0.890	-61.176	-2.793	-6.730	4.320	6	D4	D4
31	0.059	0.241	0.009	0.618	32.413	6.480	-3.012	-0.684	10	D8	D8
32	0.125	0.083	-0.150	0.256	17.625	19.363	-3.681	7.646	1	D1	D1
33	-0.024	0.154	-0.074	0.977	36.203	-12.481	-8.203	6.186	2	D10	D10
34	-0.789	-0.492	-0.519	-0.478	-31.430	-0.739	-6.453	-12.187	9	D7	D7
35	-0.037	0.314	0.268	1.273	52.376	-20.918	-0.455	-1.108	3	D11	D11
36	-0.383	-0.145	-0.190	-0.093	-3.299	7.873	-0.886	-8.699	5	D3	D3
37	-0.253	-0.042	0.398	0.286	17.624	0.265	15.742	-4.711	11	D9	D9
38	-0.054	0.173	-0.078	1.000	36.991	-14.058	-8.789	3.867	2	D10	D10
39	-0.845	-0.845	-0.366	-0.670	-45.494	-3.889	4.181	3.842	7	D5	D5
40	-0.771	-0.737	-0.120	-0.450	-33.077	-7.190	9.978	3.354	8	D6	D6
41	0.003	0.071	0.073	0.196	17.474	16.489	4.509	0.733	4	D2	D2
42	-0.329	-0.126	-0.210	-0.038	-1.139	8.355	-2.139	-6.276	5	D3	D3
43	0.002	0.086	0.071	0.210	18.237	16.285	4.129	-0.083	4	D2	D2
44	-0.841	-0.844	-0.391	-0.660	-45.518	-4.032	3.236	4.216	7	**D5**	**D5**

Table 30. LDA jackknifed classification matrix table obtained from an array of P1, C1-2 (each at pH10 and 13, buffered) against 11 nonsteroidal anti-inflammatory drugs (NSAIDs). The jackknifed classification matrix with cross-validation reveals a 100% accuracy.

Jackknifed Classification Matrix

	D1	D10	D11	D2	D3	D4	D5	D6	D7	D8	D9	%correct
D1	6	0	0	0	0	0	0	0	0	0	0	**100**
D10	0	6	0	0	0	0	0	0	0	0	0	**100**
D11	0	0	6	0	0	0	0	0	0	0	0	**100**
D2	0	0	0	6	0	0	0	0	0	0	0	**100**
D3	0	0	0	0	6	0	0	0	0	0	0	**100**
D4	0	0	0	0	0	6	0	0	0	0	0	**100**
D5	0	0	0	0	0	0	6	0	0	0	0	**100**
D6	0	0	0	0	0	0	0	6	0	0	0	**100**
D7	0	0	0	0	0	0	0	0	6	0	0	**100**
D8	0	0	0	0	0	0	0	0	0	6	0	**100**
D9	0	0	0	0	0	0	0	0	0	0	6	**100**
Total	6	6	6	6	6	6	6	6	6	6	6	**100**

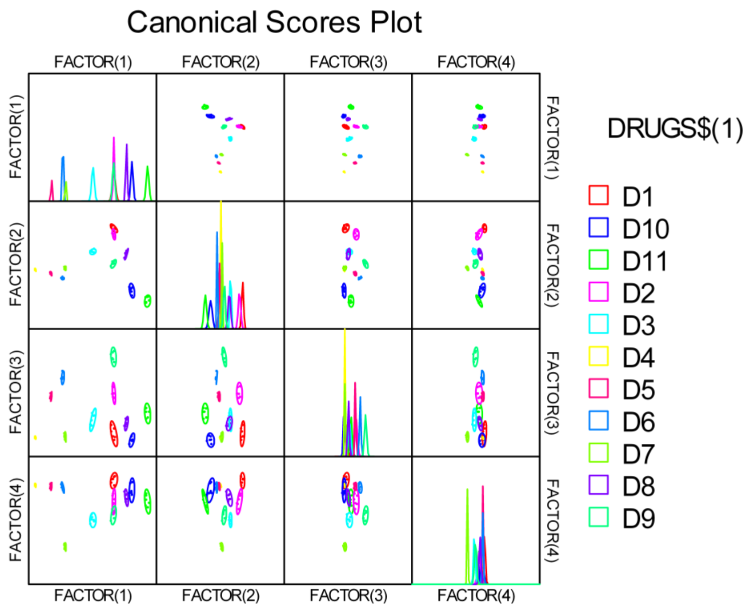

Figure 104. Correlations of canonical fluorescence response patterns. The 95% confidence ellipses for the individual acids are shown.

Table 31. Training matrix of fluorescence response pattern from an array of P1, C1-2 (each at pH 10 and 13, buffered) against D4 (from 0.03 mM to 6 mM). LDA was carried out as described above resulting in the four factors of the canonical scores and group generation

Analyte	Fluorescence response pattern				Results LDA				
NSAIDs **D4**	P1 (pH 10)	P1 (pH13)	C1-2 (pH10)	C1-2 (pH13)	Factor1	Factor2	Factor3	Factor4	Group
0.03 mM	-0.133	-0.253	-0.037	-0.137	65.388	1.498	2.515	0.032	1
0.03 mM	-0.122	-0.297	-0.047	-0.149	64.310	3.117	5.447	0.061	1
0.03 mM	-0.136	-0.273	-0.067	-0.176	61.883	0.631	3.454	1.878	1
0.03 mM	-0.162	-0.279	-0.051	-0.117	64.643	2.484	3.323	-2.964	1
0.03 mM	-0.178	-0.264	-0.087	-0.131	62.936	0.101	2.642	-2.291	1
0.03 mM	-0.168	-0.266	-0.070	-0.124	64.056	0.973	2.816	-2.441	1
0.09 mM	-0.263	-0.218	-0.148	-0.210	52.548	-6.180	-4.159	0.716	2
0.09 mM	-0.274	-0.245	-0.129	-0.210	51.260	-4.072	-4.021	-0.418	2
0.09 mM	-0.281	-0.276	-0.142	-0.228	48.900	-3.338	-2.795	-0.296	2
0.09 mM	-0.268	-0.255	-0.056	-0.229	49.898	-1.014	-6.327	0.556	2
0.09 mM	-0.263	-0.270	-0.129	-0.224	50.341	-3.041	-2.522	0.261	2
0.09 mM	-0.290	-0.276	-0.193	-0.228	48.420	-5.402	-1.430	-0.470	2
0.15 mM	-0.269	-0.403	-0.171	-0.326	39.480	0.233	2.940	3.243	3
0.15 mM	-0.274	-0.384	-0.134	-0.319	40.023	0.836	0.457	2.994	3
0.15 mM	-0.280	-0.386	-0.179	-0.338	38.285	-1.143	1.437	3.984	3
0.15 mM	-0.315	-0.354	-0.167	-0.310	38.871	-1.893	-1.800	1.638	3
0.15 mM	-0.320	-0.416	-0.181	-0.308	37.470	0.683	1.709	-0.196	3
0.15 mM	-0.310	-0.378	-0.204	-0.311	38.666	-2.180	0.996	1.439	3
0.30 mM	-0.525	-0.572	-0.285	-0.493	7.397	0.833	-2.277	-0.034	4
0.30 mM	-0.543	-0.584	-0.318	-0.462	8.468	0.626	-0.610	-2.917	4
0.30 mM	-0.548	-0.579	-0.316	-0.488	6.238	0.005	-1.907	-1.334	4
0.30 mM	-0.558	-0.599	-0.304	-0.484	5.495	1.511	-1.762	-2.495	4
0.30 mM	-0.533	-0.596	-0.272	-0.495	6.194	2.526	-2.034	-0.860	4
0.30 mM	-0.541	-0.577	-0.290	-0.465	8.402	1.354	-2.025	-2.502	4
0.60 mM	-0.639	-0.759	-0.394	-0.649	-15.484	3.023	1.168	1.035	5
0.60 mM	-0.640	-0.766	-0.393	-0.643	-15.177	3.488	1.546	0.431	5
0.60 mM	-0.665	-0.776	-0.402	-0.657	-17.994	3.387	0.724	0.113	5
0.60 mM	-0.659	-0.760	-0.415	-0.643	-16.174	2.295	1.053	-0.069	5
0.60 mM	-0.664	-0.771	-0.388	-0.644	-16.890	3.882	0.300	-0.525	5
0.60 mM	-0.648	-0.770	-0.403	-0.646	-15.969	3.241	1.688	0.272	5
0.90 mM	-0.780	-0.868	-0.452	-0.746	-33.887	4.244	-1.216	-0.829	6
0.90 mM	-0.781	-0.859	-0.466	-0.744	-33.590	3.259	-1.205	-0.752	6
0.90 mM	-0.788	-0.858	-0.468	-0.753	-34.716	2.982	-1.776	-0.430	6
0.90 mM	-0.793	-0.855	-0.449	-0.757	-35.275	3.500	-3.012	-0.354	6
0.90 mM	-0.789	-0.855	-0.476	-0.754	-34.742	2.495	-1.655	-0.306	6
0.90 mM	-0.790	-0.855	-0.450	-0.756	-35.020	3.534	-2.731	-0.274	6
1.80 mM	-0.870	-0.951	-0.578	-0.870	-50.532	1.187	-0.382	1.687	7
1.80 mM	-0.876	-0.948	-0.589	-0.867	-50.555	0.612	-0.348	1.426	7
1.80 mM	-0.879	-0.948	-0.599	-0.871	-51.072	0.123	-0.276	1.572	7
1.80 mM	-0.876	-0.950	-0.593	-0.870	-50.880	0.481	-0.237	1.574	7
1.80 mM	-0.878	-0.947	-0.580	-0.872	-51.084	0.840	-0.987	1.678	7
1.80 mM	-0.881	-0.949	-0.586	-0.871	-51.202	0.733	-0.775	1.428	7
6.00 mM	-0.964	-0.976	-0.761	-0.896	-58.480	-5.439	1.893	-0.437	8
6.00 mM	-0.966	-0.980	-0.773	-0.886	-57.884	-5.554	2.700	-1.211	8
6.00 mM	-0.965	-0.978	-0.765	-0.899	-58.863	-5.602	1.987	-0.301	8
6.00 mM	-0.966	-0.980	-0.765	-0.890	-58.215	-5.284	2.280	-1.027	8
6.00 mM	-0.966	-0.983	-0.766	-0.884	-57.760	-5.106	2.671	-1.429	8
6.00 mM	-0.964	-0.980	-0.769	-0.891	-58.129	-5.468	2.523	-0.857	8

Table 32. Detection and identification of D4 samples with unknown concentration. All unknown samples could be assigned to the corresponding group defined by the training matrix according to the shortest Mahalanobis distance. According to the verification, all of the 44 unknown concentration samples were correctly identified, representing an accuracy of 100%.

Sample	Fluorescence response pattern				Results LDA					Analyte	
#	**P1** (pH10)	**P1** (pH13)	**C1-2** (pH10)	**C1-2** (pH13)	Factor1	Factor2	Factor3	Factor4	Group	Identi fication	Verifi cation
1	-0.295	-0.399	-0.202	-0.309	39.299	-0.946	2.870	1.366	3	0.15 mM	0.15 mM
2	-0.781	-0.855	-0.460	-0.750	-33.990	3.228	-1.738	-0.290	6	0.90 mM	0.90 mM
3	-0.534	-0.585	-0.305	-0.479	7.657	0.906	-1.048	-1.523	4	0.30 mM	0.30 mM
4	-0.155	-0.246	-0.048	-0.131	64.648	0.752	1.519	-1.066	1	0.03 mM	0.03 mM
5	-0.303	-0.382	-0.264	-0.310	39.245	-4.302	3.834	1.659	3	0.15 mM	0.15 mM
6	-0.966	-0.977	-0.773	-0.890	-58.180	-5.797	2.420	-0.869	8	6.00 mM	6.00 mM
7	-0.878	-0.950	-0.588	-0.870	-50.967	0.693	-0.503	1.458	7	1.80 mM	1.80 mM
8	-0.965	-0.981	-0.762	-0.897	-58.664	-5.263	2.127	-0.539	8	6.00 mM	6.00 mM
9	-0.257	-0.258	-0.164	-0.206	52.419	-4.691	-1.082	-0.259	2	0.09 mM	0.09 mM

10	-0.654	-0.760	-0.389	-0.648	-16.283	3.249	0.267	0.378	5	0.60 mM	0.60 mM
11	-0.657	-0.772	-0.382	-0.639	-16.092	4.269	0.667	-0.652	5	0.60 mM	0.60 mM
12	-0.282	-0.380	-0.193	-0.323	39.436	-1.757	1.877	3.135	3	0.15 mM	0.15 mM
13	-0.878	-0.947	-0.618	-0.868	-50.683	-0.632	0.508	1.502	7	1.80 mM	1.80 mM
14	-0.141	-0.258	-0.047	-0.118	66.261	1.639	3.209	-1.615	1	0.03 mM	0.03 mM
15	-0.783	-0.858	-0.457	-0.755	-34.564	3.389	-1.942	-0.126	6	0.90 mM	0.90 mM
16	-0.308	-0.256	-0.112	-0.214	48.601	-2.960	-6.027	-1.795	2	0.09 mM	0.09 mM
17	-0.877	-0.948	-0.596	-0.866	-50.574	0.349	-0.162	1.311	7	1.80 mM	1.80 mM
18	-0.256	-0.244	-0.132	-0.233	50.647	-4.596	-3.597	1.740	2	0.09 mM	0.09 mM
19	-0.963	-0.982	-0.764	-0.890	-58.061	-5.163	2.501	-0.919	8	6.00 mM	6.00 mM
20	-0.541	-0.604	-0.285	-0.488	6.092	2.502	-1.344	-1.739	4	0.30 mM	0.30 mM
21	-0.151	-0.281	-0.050	-0.124	64.730	2.542	3.809	-2.155	1	0.03 mM	0.03 mM
22	-0.782	-0.863	-0.463	-0.759	-34.881	3.361	-1.487	0.051	6	0.90 mM	0.90 mM
23	-0.534	-0.562	-0.271	-0.470	8.767	1.235	-3.236	-1.621	4	0.30 mM	0.30 mM
24	-0.294	-0.401	-0.183	-0.325	38.061	-0.379	1.947	2.285	3	0.15 mM	0.15 mM
25	-0.180	-0.292	-0.097	-0.147	61.011	0.779	3.935	-1.976	1	0.03 mM	0.03 mM
26	-0.967	-0.982	-0.757	-0.883	-57.824	-4.749	2.227	-1.539	8	6.00 mM	6.00 mM
27	-0.652	-0.762	-0.384	-0.655	-16.787	3.441	0.122	0.819	5	0.60 mM	0.60 mM
28	-0.788	-0.856	-0.476	-0.756	-34.820	2.544	-1.607	-0.189	6	0.90 mM	0.90 mM
29	-0.272	-0.266	-0.178	-0.193	52.432	-4.661	-0.629	-1.808	2	0.09 mM	0.09 mM
30	-0.647	-0.763	-0.388	-0.656	-16.541	3.288	0.533	1.070	5	0.60 mM	0.60 mM
31	-0.544	-0.583	-0.296	-0.482	6.812	1.077	-2.042	-1.633	4	0.30 mM	0.30 mM
32	-0.871	-0.950	-0.607	-0.865	-50.115	0.079	0.707	1.432	7	1.80 mM	1.80 mM

5.3.4 LDA Calculation (Chapter 2.4)

Table 33. Training matrix of fluorescence response pattern from an array of sensor element S1-S24 against 19 antibiotics. LDA was carried out and resulting in 19 factors of the canonical scores (the first three scores were shown here) and group generation. Jackknifed classification matrix showed the 100% correct classification.

Analyte	Fluorescence response pattern													
Antibiotics	S1	S2	S3	S4	S5	S6	S7	S8	S9	S10	S11	S12	S13	S14
AT1	-1978	-1138	-3147	-852	-12974	-5802	-478	-763	2020	894	-1873	383	-17025	-11895
AT1	-1414	-1032	-860	-591	-12674	-6310	-1158	-859	2163	882	-653	715	-16658	-11588
AT1	-1704	-1264	-2708	661	-12415	-5408	-54	-295	1891	657	1101	456	-16716	-11915
AT1	-1744	-1163	193	56	-12440	-5172	-706	153	2030	1171	-864	834	-16795	-11790
AT1	-1468	-1098	-577	-308	-12601	-6145	-389	-677	-281	1066	11	568	-16967	-12106
AT1	-1755	-1045	-1528	-137	-13177	-5813	-495	-201	1981	1873	-236	467	-16785	-12167
AT2	12621	7187	-678	-3	-26056	-13329	3449	1404	3184	1382	-4639	-1467	-167	-809
AT2	13054	7289	-754	-170	-26577	-13268	3818	1070	3260	2145	-4664	-1212	-655	-1424
AT2	12826	7254	543	343	-26233	-13317	3903	1378	3625	2614	-3637	-1083	-310	-871
AT2	11062	6263	61	800	-26976	-13953	2903	1741	3123	2554	-3795	-966	-420	-799
AT2	11708	6848	170	220	-26645	-13500	3378	1824	1915	480	-5334	-992	-209	-1228
AT2	11915	6550	105	360	-27142	-13785	2982	1642	3435	2447	-4795	-998	207	-1142
AT3	1500	840	734	1785	-14289	-6495	19793	7555	5353	1445	2505	1016	-21005	-14776
AT3	1563	929	-560	-69	-16567	-8241	21265	8066	4204	3603	2483	2586	-20813	-14778
AT3	1712	857	1971	1507	-15759	-6708	21726	8582	1789	2075	3404	1665	-20914	-14760
AT3	1073	668	1243	2178	-14783	-7128	20968	7390	1361	1750	2493	1734	-20739	-14877
AT3	1188	803	1995	2172	-16526	-7477	19655	8251	4568	1696	2175	1175	-20718	-14711
AT3	1292	912	1487	1566	-15795	-6812	20665	7808	3370	2598	561	1015	-20682	-14731
AT4	6519	7336	-20663	-10137	-73121	-38539	-15709	7365	-23057	-1829	-53408	-15955	18937	11802
AT4	6494	7603	-20129	-9614	-72991	-38348	-17841	6360	-17047	-2607	-51784	-15792	21726	13427
AT4	5880	6900	-22452	-9987	-72791	-38386	-13532	8400	-17315	-2347	-52321	-15890	21655	13052
AT4	6792	7592	-21356	-10610	-72687	-38165	-15831	7029	-17396	-2604	-52842	-16202	19913	13335
AT4	6473	7580	-21474	-10315	-73038	-37900	-16121	8280	-17303	-5852	-52108	-15560	21844	10849
AT4	6481	7313	-20518	-10153	-72710	-37508	-17760	6825	-22971	-1726	-52827	-15874	17866	10773
AT5	-4248	-2458	-30020	-15836	-50939	-26853	-71485	-33688	-25936	-10046	-25706	-10820	5331	1586
AT5	-4251	-2335	-29619	-15426	-51898	-26924	-71617	-33770	-25105	-11210	-25199	-10103	4716	1178
AT5	-4184	-2472	-30371	-15879	-49739	-26329	-72174	-33686	-26864	-10854	-24389	-10265	4952	1716
AT5	-4127	-2378	-29840	-15436	-50329	-26598	-72344	-33993	-24964	-11339	-25293	-10646	5254	1020
AT5	-4326	-2411	-30620	-15600	-50067	-25908	-71968	-33451	-26658	-11169	-24878	-10539	4106	803
AT5	-4380	-2475	-30739	-15431	-49946	-25971	-72573	-33918	-24411	-10478	-25028	-9974	2279	-686
AT6	994	677	2866	395	-4776	-2633	-65263	-19632	-77862	-30707	1164	1146	1515	433
AT6	1021	454	2749	981	-5131	-3134	-65486	-19765	-77743	-31721	4809	2233	2298	1499
AT6	883	443	1866	815	-6143	-2885	-64914	-19743	-77331	-31400	4350	3405	2257	1602
AT6	832	401	602	1047	-5707	-2550	-65413	-19819	-78781	-32634	1537	835	1663	1435
AT6	763	403	2905	67	-6666	-3474	-64819	-19260	-76807	-31609	5782	2810	2581	1145

AT6	872	345	2311	379	-6808	-4737	-65282	-20052	-78336	-32014	4264	2336	1885	1630
AT7	1505	1088	5731	2870	-9549	-3084	-71719	-26916	-72982	-28312	10061	5202	359	83
AT7	1467	1137	7940	4688	-5628	-3553	-71846	-27713	-73802	-29571	10032	6192	2564	1289
AT7	1637	961	5697	3337	-7511	-3189	-72018	-27547	-75697	-29034	9595	5422	794	173
AT7	1569	1016	3909	3013	-4923	-3149	-71965	-27335	-73692	-29686	10372	5553	2163	1886
AT7	1362	996	4370	2965	-6147	-3186	-72035	-27404	-74141	-30211	11592	5265	2710	2138
AT7	1480	1058	5566	4390	-6044	-3286	-71210	-26591	-73106	-28391	9247	5118	2106	1537
AT8	8029	4642	11874	7249	3449	1720	-62799	-18987	-64549	-21200	10824	5776	2699	1306
AT8	8080	4478	13446	7140	2789	2046	-63044	-18987	-65047	-22419	10716	6348	3443	1989
AT8	7916	4403	11884	7553	3386	2837	-63041	-19204	-65097	-21423	11874	6173	3429	2002
AT8	6602	3907	13690	6819	2083	1803	-63005	-19310	-65438	-20750	10935	6221	2971	2169
AT8	6976	3927	13432	7913	2117	817	-63419	-19099	-65880	-22074	11038	5562	3508	1459
AT8	6874	4013	12409	6215	2964	1508	-63284	-18635	-64566	-20490	10499	6272	2822	1682
AT9	-6654	-3120	-59314	-26411	-84427	-39082	-110214	-51720	-109319	-49947	-108745	-48775	-16685	-9473
AT9	-6685	-3165	-59158	-26523	-84502	-39248	-110246	-51774	-109560	-50228	-108701	-48734	-17192	-9961
AT9	-6642	-3091	-59276	-26636	-84404	-39717	-110225	-51791	-109400	-49943	-108790	-48596	-16946	-9784
AT9	-6674	-3155	-59275	-26732	-84150	-38228	-110213	-51734	-109234	-49881	-108787	-48676	-17006	-9618
AT9	-6659	-3217	-59255	-26585	-84459	-38917	-110225	-51722	-109437	-49968	-108542	-48601	-17219	-9975
AT9	-6641	-3158	-59153	-26241	-84215	-38617	-110212	-51726	-109353	-49907	-108643	-48640	-16993	-9554
AT10	-5371	-3028	-54960	-28483	-82920	-38914	-105967	-50400	-102970	-47163	-107947	-47861	-22657	-16346
AT10	-5353	-3083	-55092	-28647	-82696	-39294	-105970	-50500	-103573	-47557	-107997	-47801	-22741	-16310
AT10	-5401	-3025	-55045	-28330	-82517	-38309	-105899	-50443	-103478	-47599	-107997	-48011	-22612	-16287
AT10	-5390	-3069	-54837	-28479	-82967	-39145	-105910	-50434	-103443	-47476	-107879	-47838	-22652	-16387
AT10	-5379	-2949	-54832	-28192	-82875	-39265	-105644	-50341	-103632	-47633	-107991	-47882	-22439	-16447
AT10	-5346	-2970	-54866	-28565	-82488	-38371	-105951	-50254	-103398	-47592	-107999	-47891	-22557	-16306
AT11	-6259	-1927	-53656	-22547	-79529	-31435	-105914	-43124	-80556	-26688	-77826	-26788	-22495	-15095
AT11	-6212	-1860	-53736	-22507	-79675	-31452	-105988	-42881	-81304	-26495	-77348	-26407	-22636	-15060
AT11	-6285	-1893	-54115	-22453	-79814	-31552	-105918	-42994	-80499	-26376	-77408	-25950	-22283	-15114
AT11	-6285	-1928	-53628	-22889	-79879	-31137	-106042	-43293	-81990	-27661	-77210	-27071	-22495	-15125
AT11	-6237	-1893	-53891	-22229	-79755	-30658	-105757	-42933	-80372	-26829	-76737	-25314	-22390	-14936
AT11	-6289	-1822	-53613	-22494	-79391	-31048	-105957	-43284	-80699	-27103	-76658	-26039	-22575	-15105
AT12	13858	5282	11707	8435	-3158	1175	-76292	-29020	-79390	-35691	9410	5412	3424	2326
AT12	13477	5135	10762	7045	-1248	1335	-74550	-28821	-82504	-36853	8459	5005	4034	1538
AT12	13476	5258	10335	6107	-1730	1916	-76474	-28887	-81885	-36606	8794	6041	4100	1679
AT12	13216	4861	7146	5225	-2130	2069	-75695	-28534	-82065	-36496	7298	4798	3962	1734
AT12	13419	4894	4736	3799	-1236	1363	-74986	-28011	-80574	-35776	7839	4181	3193	2098
AT12	12500	4620	7718	5787	-3817	693	-73880	-27347	-82563	-36768	7629	4755	3052	1886
AT13	72488	159089	804	4648	-6405	2087	66161	190957	-5696	3370	9905	8454	6429	3827
AT13	71906	159398	1513	6248	-6612	2019	65257	184846	-6804	3648	9786	9846	7409	3603
AT13	71708	158571	1181	4892	-7049	2127	67164	186315	-5575	3869	8601	9083	6522	3385
AT13	72472	159301	2796	5585	-7155	2930	64803	190909	-6164	3886	9153	8878	6364	3894
AT13	71889	159483	3038	6049	-6185	2701	66017	187189	-5828	2724	8835	9294	6077	3692
AT13	71568	158887	2191	4458	-7072	1965	66345	185299	-9309	4545	9281	8948	6662	3208
AT14	-1328	-648	-7385	-4168	-27132	-13326	-61586	-27739	-2690	1252	829	-76	-10907	-6198
AT14	-1506	-807	-7447	-4284	-25690	-12686	-60464	-27201	-4072	76	4651	2912	-10383	-5846
AT14	-1607	-744	-9526	-4214	-24833	-12074	-60689	-27745	-2431	-22	4380	2393	-10945	-5658
AT14	-1379	-929	-7321	-5064	-25938	-12585	-60666	-27352	-3619	-22	2851	3029	-9889	-5952
AT14	-1387	-824	-8381	-4247	-25502	-12968	-62015	-28324	-2979	-45	4587	2680	-10006	-5717
AT14	-1511	-878	-7684	-5402	-25364	-12263	-61283	-27635	-2099	-477	3625	2294	-9617	-5426
AT15	-725	-275	-7593	-4990	-67708	-37701	-5880	-3427	-16805	-6760	-50085	-24400	-13433	-8741
AT15	-805	-215	-7874	-5385	-67214	-37595	623	-3363	-20051	-6747	-48690	-23505	-13330	-8308
AT15	-1031	-458	-10918	-6338	-67127	-37935	-4971	-443	-16923	-8482	-49064	-22973	-14061	-8907
AT15	-759	-289	-10661	-5613	-66871	-37532	-840	-2956	-20347	-8037	-48376	-23743	-13798	-8428
AT15	-950	-501	-9161	-5295	-67676	-37542	-910	-1898	-16738	-6373	-49535	-23372	-14368	-8749
AT15	-1078	-437	-9534	-4472	-67925	-37557	-3188	-2650	-19174	-8035	-50994	-23648	-13743	-8691
AT16	130	-60	-2247	-1974	-15582	-9198	1205	1523	5490	6487	3598	1760	-1739	-2211
AT16	-390	9	-1687	-1001	-17219	-9607	1892	1317	6389	6873	4815	2130	-1963	-1794
AT16	-25	-45	-2514	-2028	-18004	-9494	2788	1468	6167	6280	6008	3115	-2082	-1343
AT16	-158	50	-3661	-889	-18541	-10338	2631	1261	6822	6885	4985	2269	-1802	-1418
AT16	-167	-100	-1073	-643	-17341	-9018	1753	1297	6149	6844	5027	2825	-2604	-1875
AT16	-229	-141	-3455	-1434	-15988	-8662	1155	277	5201	6205	3879	2859	-3585	-1839
AT17	7878	4642	-3805	-2403	-18112	-10304	7154	2475	7996	6057	3912	1710	-1535	-738
AT17	8286	4835	-3125	-1522	-17985	-9797	6775	3365	7565	7226	5166	2504	-755	-119
AT17	8080	4499	-3159	-2109	-17455	-9643	8479	3392	8642	6623	4214	2673	-265	-73
AT17	8019	4665	-3922	-1591	-17377	-9813	8591	3588	8557	8127	3666	2098	-23	130
AT17	8051	4578	-2298	-2216	-16475	-9605	7369	4290	9424	7618	4220	2694	-978	-471
AT17	7752	4412	-3019	-1633	-17648	-10003	7165	3715	7274	7084	2898	1525	262	-145
AT18	-831	-449	-10812	-6686	-29240	-16722	-20637	-9308	2629	5238	2489	2010	-1854	-3508
AT18	-636	-335	-10091	-6287	-28004	-16070	-17181	-8489	5610	6028	2752	1744	-2004	-4442
AT18	-392	-475	-9090	-6274	-28510	-16628	-22313	-7722	5139	5169	3655	2010	-2839	-3402
AT18	-391	-431	-11146	-7348	-29101	-16599	-23619	-10642	3049	6672	3427	1843	-1587	-3657
AT18	-314	-345	-9211	-6467	-28301	-16251	-21839	-11156	3605	5407	3165	2006	-3030	-3399

AT18	-593	-427	-10112	-5917	-28246	-16181	-18497	-8734	4561	5976	2632	2151	-1654	-3451
AT19	252	-553	-17891	-8172	-9913	-4610	-18460	-9965	-12168	-3576	-1574	-532	-4412	-2763
AT19	236	-631	-16658	-8050	-9593	-4528	-17960	-10181	-11781	-3555	-1445	279	-4114	-2959
AT19	105	-734	-16875	-7333	-8757	-4986	-17092	-9463	-12209	-3750	-1213	887	-4264	-2437
AT19	162	-736	-16456	-8504	-9185	-5080	-15440	-8689	-10765	-3169	-530	1312	-4704	-3027
AT19	109	-669	-16612	-7441	-9020	-4239	-17071	-9301	-11435	-3075	-1100	999	-3948	-3344
AT19	41	-762	-16823	-7762	-8622	-5054	-16212	-9324	-12997	-3751	-1441	490	-4703	-2732
Control	-9	4	175	477	905	853	-684	-691	-2154	-194	871	196	-21	28
Control	107	154	-1250	-390	1143	-17	542	161	1223	-143	363	126	-70	118
Control	-36	1	402	306	969	553	1427	667	-2340	-395	525	-41	203	136
Control	148	-157	298	157	518	86	-230	-22	-1431	225	35	186	67	136
Control	-99	10	-676	155	-536	-640	-578	256	-785	-484	-114	-422	202	-148
Control	-94	-2	-77	-279	1363	-1241	-498	-781	382	161	-48	-263	-45	73

(continued)

Fluorescence response pattern										Results LDA			
S15	S16	S17	S18	S19	S20	S21	S22	S23	S24	SCO RE1	SCO RE2	SCO RE3	Gr oup
-2740	-2057	2383	1586	12041	9164	1975	1289	-859	-591	67	68	44	1
-2867	-1597	2405	1623	13482	9470	2499	2106	-28	-10	68	70	42	1
-2786	-1759	1914	2160	12878	8976	3195	1873	-903	136	69	71	42	1
-2629	-1462	1472	1527	13036	10085	2688	2577	52	-70	68	71	42	1
-2958	-1653	2610	1101	12731	9356	2684	2158	-865	-377	68	70	42	1
-2750	-1654	2294	1911	14079	9772	2414	2209	-361	-299	66	71	42	1
-4912	-3551	-2773	-1412	15345	10486	5583	1943	-1300	-874	44	53	42	12
-4733	-3523	-4362	-2893	16648	10851	5315	869	-1352	-709	44	54	43	12
-4735	-3475	-3218	-1683	16548	10398	5249	2142	-1547	217	44	55	43	12
-4459	-3545	-2129	-1740	15987	10342	5611	1471	-1743	-435	46	54	42	12
-4631	-3749	-3424	-1929	16535	10719	5381	1881	-1398	-637	44	52	41	12
-4221	-3736	-3164	-1695	17366	11623	4996	1357	-1667	-1297	47	54	42	12
-15641	-10566	-15481	-8978	3088	2551	-905	-1385	-3403	-104	68	83	68	13
-15533	-10415	-14774	-8880	2827	3333	-1346	-983	-3422	-696	65	81	70	13
-14623	-10206	-15183	-8900	3461	3007	-1893	-1023	-3421	-598	66	83	68	13
-14779	-10051	-15062	-9077	3538	1898	-856	-503	-3144	-1364	66	82	67	13
-14443	-9989	-14496	-8977	3483	3103	-900	-77	-2748	-950	66	82	68	13
-14502	-10158	-15144	-8098	2954	3181	-1396	-1045	-2814	-674	65	80	69	13
23456	16602	4905	25615	39286	19354	13614	7575	1767	7228	-2	-72	6	14
23070	17714	4848	25022	39723	20277	14524	7605	823	6900	-2	-70	5	14
23953	18070	5122	25838	40272	19705	14001	8391	791	6510	0	-69	7	14
24739	17724	4229	25058	40720	20036	14824	7666	874	6357	-3	-70	5	14
24191	18726	5006	24966	39282	20073	14734	7754	985	6952	-3	-71	5	14
24671	17761	4001	24492	39212	19469	14601	7746	1087	6756	-2	-71	4	14
-14286	-10015	-11531	-7780	30484	16524	1632	904	-1519	-1346	90	-17	-17	15
-13973	-10162	-11709	-7598	31220	13921	2400	1001	-1250	-881	90	-17	-17	15
-14358	-9924	-11419	-7787	31574	14415	1517	2032	-1631	-1190	90	-16	-18	15
-14319	-10094	-10942	-7350	30246	16223	2778	1254	-486	-933	91	-16	-18	15
-14253	-10163	-11266	-7322	30595	14552	2922	1922	-1567	-1703	90	-16	-18	15
-14588	-9947	-10921	-7674	31889	14684	3081	1550	-1393	-1139	90	-14	-17	15
-455	488	1493	-33	63631	28713	34265	12151	12049	2749	50	44	-118	16
949	718	962	725	62162	29337	33311	10942	14011	3442	51	45	-118	16
-464	349	-137	494	62484	27958	34230	10974	13903	3413	51	44	-118	16
300	657	2719	300	64211	28275	32956	11638	14849	3705	50	43	-119	16
-499	-86	2339	1616	62230	28726	32626	10813	14672	3421	50	46	-117	16
226	535	1630	1278	63693	28983	34760	11481	15302	3915	50	44	-120	16
1008	767	2652	696	68692	29805	37551	12313	-438	-399	54	46	-120	17
1948	859	4864	1643	67645	30856	36201	13025	2293	1291	53	47	-122	17
1089	961	4111	2534	67500	29762	34757	11844	1528	-84	55	44	-120	17
1351	896	2149	1100	67202	29794	34013	12266	2314	1090	54	46	-120	17
1153	803	2179	1821	68236	30206	34806	11582	1313	438	54	46	-122	17
1179	1378	3837	3011	69030	30619	35435	12250	3107	1816	53	46	-122	17
4813	3802	3585	2407	61499	26350	39582	14098	177	531	41	59	-109	18
4568	3607	3042	3079	62635	27250	38153	14444	1216	1641	43	58	-111	18
4385	3328	3723	2694	62186	27635	37319	14995	1252	983	43	61	-110	18
4841	3363	3110	2120	63010	27384	37154	13983	1549	1201	42	60	-110	18
5162	3420	3684	3138	62449	27992	37656	14992	1796	1151	44	59	-110	18
4578	3928	3256	2755	63199	27935	39144	14798	1297	877	42	60	-111	18
-18419	-8848	-3803	12666	-12339	-4647	-21347	-8192	-11066	4722	116	-222	-2	19
-18617	-9313	-5792	9614	-12455	-4583	-23212	-10821	-11217	5065	116	-220	0	19
-18661	-9716	-6084	8898	-12650	-4308	-22686	-10267	-11033	3627	116	-220	0	19
-18818	-9393	-5537	10245	-13282	-3934	-21346	-8370	-10372	4592	117	-220	-2	19
-18579	-9234	-5029	12180	-13309	-4704	-21533	-8761	-10713	3989	117	-222	-1	19

-18224	-9154	-4382	12597	-12491	-4655	-23316	-10919	-10474	5414	116	-221	-1	19
-22266	-15506	-15723	-6991	-9633	-8577	-20129	-14898	-9538	-4631	120	-190	7	2
-22385	-15426	-15660	-7129	-10209	-9358	-19792	-14670	-9360	-4474	121	-191	7	2
-22364	-15457	-15679	-6975	-10480	-8961	-19967	-14847	-9334	-4367	120	-191	7	2
-22367	-15397	-15484	-7044	-10345	-9456	-21057	-15734	-9402	-4722	121	-191	8	2
-22381	-15385	-15614	-7112	-10029	-9296	-21213	-15923	-9467	-4667	120	-191	8	2
-22245	-15513	-15717	-7339	-9729	-9702	-19432	-14976	-9367	-4177	120	-190	6	2
-14623	-6714	9510	17022	-16630	-7457	-5094	1667	-1360	2094	91	-164	5	3
-14466	-6617	9437	16958	-16813	-7572	-4115	2143	-1998	2410	91	-165	4	3
-14826	-6835	9731	18069	-16331	-7781	-4406	1884	-1614	1769	91	-165	4	3
-14842	-6792	10069	16766	-16666	-7364	-4674	1429	-1277	1591	91	-164	3	3
-14515	-6465	11217	18795	-16731	-7177	-4908	1052	-1728	2081	91	-165	4	3
-14436	-6887	10757	18892	-16474	-7505	-4625	982	-1952	2461	90	-165	3	3
-2472	-783	4131	3129	-8258	-7229	-12275	-10519	-1830	-1648	81	-8	-26	4
-3609	-1162	3832	3316	-8543	-7870	-12980	-11328	-656	-694	81	-8	-27	4
-3624	-2871	3668	3116	-8418	-7161	-13923	-10311	-1519	-1114	80	-8	-28	4
-3515	-2295	4019	3294	-8471	-8219	-13530	-11809	-1330	-1379	82	-10	-27	4
-3602	-2277	3807	2966	-8223	-7959	-14097	-12091	-757	-1079	81	-8	-26	4
-5688	-3280	2657	2639	-9246	-8319	-13511	-10661	-1816	-634	82	-10	-25	4
-6233	-4067	2957	2384	17750	10265	136	-880	-2644	-2126	-1280	-19	3	5
-6792	-4211	2372	1193	17644	10661	130	-1135	-2683	-2917	-1281	-21	3	5
-5160	-3758	3276	1846	17916	10661	894	-330	-2281	-2231	-1275	-20	4	5
-5262	-3557	2149	1780	17763	10480	725	-168	-2594	-2289	-1282	-20	2	5
-6486	-4643	3552	2053	16715	10450	248	80	-2113	-2812	-1282	-20	4	5
-6380	-4268	4154	2011	17950	10996	326	124	-2405	-2915	-1279	-20	2	5
-11251	-6383	-9147	-4317	16075	9524	4004	568	-19463	-12945	89	32	14	6
-10935	-6265	-9273	-4032	16161	7999	5441	1277	-20089	-12921	89	34	11	6
-11079	-6483	-9066	-4336	14714	7666	3952	374	-19435	-13055	88	34	13	6
-11415	-6714	-9117	-4009	14822	8230	4131	38	-19056	-12816	91	32	13	6
-11270	-6245	-9125	-3888	15744	8633	5246	754	-19129	-13100	90	34	10	6
-11085	-6891	-8821	-4045	15177	7689	5202	227	-19195	-12563	90	34	11	6
-7913	-5174	-16840	-12122	17090	11633	146	-1601	-22042	-15960	80	-25	65	7
-7542	-5449	-19525	-13718	16916	10911	1080	-1440	-21305	-15781	78	-23	66	7
-8977	-5447	-19324	-13908	17382	12310	524	-1686	-22547	-16624	79	-25	64	7
-7966	-5655	-17442	-13152	16629	10192	1267	-776	-22357	-16410	79	-25	65	7
-7363	-4813	-19163	-13841	17615	11177	1970	-119	-22580	-16122	80	-23	67	7
-7803	-4980	-19973	-14075	16914	10516	1530	-1262	-21595	-15962	80	-27	65	7
-1514	-810	-1778	-1156	7006	5797	1255	286	1767	866	61	68	46	8
-1579	-296	-2070	-809	7104	6943	1196	1343	1427	1150	59	67	47	8
-1427	-861	-2043	-429	8588	5618	1446	905	1946	1151	60	68	46	8
-1395	-396	-1526	-1027	7854	5946	1287	1148	1628	1692	59	67	48	8
-1466	-762	-2424	-821	7907	6391	1175	380	2185	1618	61	69	47	8
-1460	-1001	-1825	-1273	8760	6949	1338	1177	2072	1172	61	68	45	8
-289	88	4917	3364	13549	9358	5873	3473	1203	224	43	66	43	9
148	88	4703	4541	12759	10145	6557	3124	1746	781	42	67	42	9
454	224	5531	3837	13707	10266	6847	3226	1424	-85	44	68	43	9
442	302	6050	4273	14032	10254	6405	2380	1467	1007	42	68	43	9
-6	241	5079	3993	12755	10371	5482	3301	1890	671	43	69	44	9
416	282	4990	3730	13476	9970	6663	3742	1486	1245	44	66	42	9
-467	-637	3905	2133	25899	15039	3557	2948	883	795	61	53	22	10
-103	-183	3592	3229	24699	16299	4637	3427	1177	1044	61	56	24	10
-358	-495	3827	2873	24533	15086	3272	2519	675	530	63	55	23	10
-10	286	4427	2700	27484	16663	4439	2074	988	715	62	54	18	10
-812	-329	3363	2735	25790	17270	4227	3068	188	1540	64	53	20	10
-461	305	4278	3622	28132	17546	4224	2523	722	1261	61	56	21	10
-1713	-1037	6948	5236	52838	21267	-2103	-4758	-637	421	59	70	-9	11
-1926	-815	7363	5442	50424	21707	-1999	-4989	472	791	60	70	-7	11
-1838	-814	8364	5614	52905	22895	-686	-4108	309	214	60	72	-10	11
-2064	-832	7233	5911	51073	21372	-309	-4458	-38	644	60	72	-7	11
-1630	-1103	7663	5358	50916	20322	-826	-4710	-24	-29	60	72	-7	11
-1910	-1038	8423	6079	52965	21632	-898	-3983	-813	206	60	71	-9	11
357	-326	723	-168	350	-295	-241	-77	-138	-309	64	68	41	20
-209	169	108	340	-652	251	333	134	68	302	64	67	43	20
-359	-245	-213	-567	581	387	-180	144	-7	6	64	68	42	20
-338	225	-472	-493	702	-310	-242	-29	-181	-214	66	67	42	20
676	292	449	-360	161	110	51	-23	-339	-103	64	65	42	20
429	188	122	-161	-47	-825	-238	137	199	217	64	67	43	20

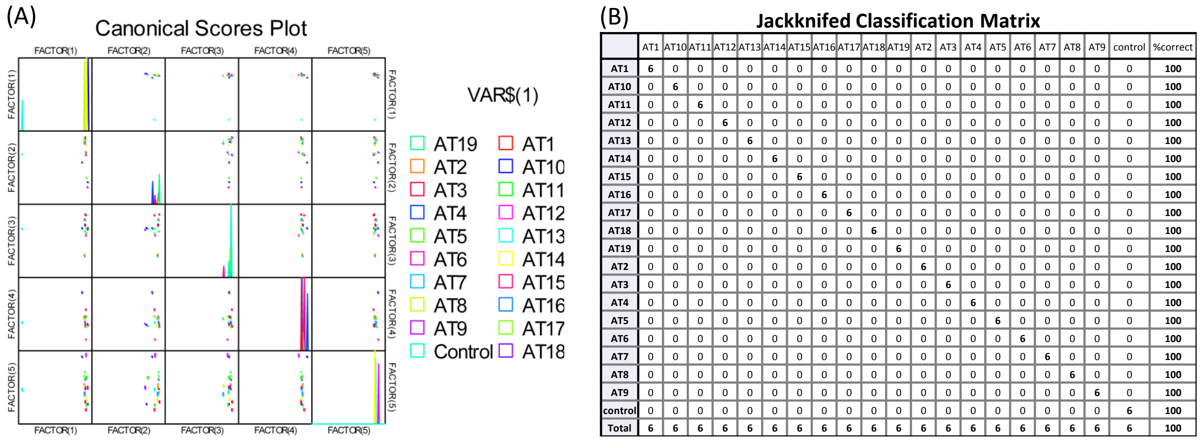

	AT1	AT10	AT11	AT12	AT13	AT14	AT15	AT16	AT17	AT18	AT19	AT2	AT3	AT4	AT5	AT6	AT7	AT8	AT9	control	%correct
AT1	6	0	0	0	0	0	0	0	0	0	0	0	0	0	0	0	0	0	0	0	100
AT10	0	6	0	0	0	0	0	0	0	0	0	0	0	0	0	0	0	0	0	0	100
AT11	0	0	6	0	0	0	0	0	0	0	0	0	0	0	0	0	0	0	0	0	100
AT12	0	0	0	6	0	0	0	0	0	0	0	0	0	0	0	0	0	0	0	0	100
AT13	0	0	0	0	6	0	0	0	0	0	0	0	0	0	0	0	0	0	0	0	100
AT14	0	0	0	0	0	6	0	0	0	0	0	0	0	0	0	0	0	0	0	0	100
AT15	0	0	0	0	0	0	6	0	0	0	0	0	0	0	0	0	0	0	0	0	100
AT16	0	0	0	0	0	0	0	6	0	0	0	0	0	0	0	0	0	0	0	0	100
AT17	0	0	0	0	0	0	0	0	6	0	0	0	0	0	0	0	0	0	0	0	100
AT18	0	0	0	0	0	0	0	0	0	6	0	0	0	0	0	0	0	0	0	0	100
AT19	0	0	0	0	0	0	0	0	0	0	6	0	0	0	0	0	0	0	0	0	100
AT2	0	0	0	0	0	0	0	0	0	0	0	6	0	0	0	0	0	0	0	0	100
AT3	0	0	0	0	0	0	0	0	0	0	0	0	6	0	0	0	0	0	0	0	100
AT4	0	0	0	0	0	0	0	0	0	0	0	0	0	6	0	0	0	0	0	0	100
AT5	0	0	0	0	0	0	0	0	0	0	0	0	0	0	6	0	0	0	0	0	100
AT6	0	0	0	0	0	0	0	0	0	0	0	0	0	0	0	6	0	0	0	0	100
AT7	0	0	0	0	0	0	0	0	0	0	0	0	0	0	0	0	6	0	0	0	100
AT8	0	0	0	0	0	0	0	0	0	0	0	0	0	0	0	0	0	6	0	0	100
AT9	0	0	0	0	0	0	0	0	0	0	0	0	0	0	0	0	0	0	6	0	100
control	0	0	0	0	0	0	0	0	0	0	0	0	0	0	0	0	0	0	0	6	100
Total	6	6	6	6	6	6	6	6	6	6	6	6	6	6	6	6	6	6	6	6	100

Figure 105. (A) Correlations of canonical fluorescence response patterns from an array of sensor element S1-S24 against 19 antibiotics. The 95% confidence ellipses for the individual acids are also shown. **(B)** Jackknifed classification matrix showed the 100% correct classification.

Table 34. Training matrix of fluorescence response pattern from an array of sensor element S25-S30 against 19 antibiotics. LDA was carried out and resulting in 6 factors of the canonical scores and group generation. Jackknifed classification matrix showed the 100% correct classification.

Analyte	Fluorescence response pattern						Results LDA						
Anti biotics	S25	S26	S27	S28	S29	S30	SCORE1	SCORE2	SCORE3	SCORE4	SCORE5	SCORE6	**GROUP**
AT1	-499	2101	113	-5638	3522	-2092	3.25	18.33	10.00	-10.02	-2.10	-1.26	**1**
AT1	-391	91	-135	-3984	5411	-1311	5.08	16.45	6.69	-8.17	-1.64	0.46	**1**
AT1	-145	822	236	-5652	5935	-3038	3.92	17.74	7.12	-10.09	0.04	0.95	**1**
AT1	-879	1386	-36	-5112	4125	-1460	3.53	17.76	8.37	-9.23	-2.59	-1.03	**1**
AT1	-161	-190	110	-4550	3270	-2765	2.95	15.18	10.10	-9.21	-1.68	1.50	**1**
AT1	-1118	133	-583	-2759	3861	-1656	4.55	14.43	7.25	-8.95	-2.99	-0.78	**1**
AT2	-530	18	-7396	-8613	2677	-80	-3.06	15.03	9.73	0.16	3.46	-7.02	**12**
AT2	-950	-106	-8217	-8268	2782	-1491	-3.80	13.33	8.67	-0.92	4.49	-7.76	**12**
AT2	-1159	-343	-8192	-8264	2528	-2286	-4.51	12.55	8.71	-1.71	4.58	-7.41	**12**
AT2	-1019	-1124	-6955	-7519	2333	1289	-2.68	14.09	9.13	1.33	1.27	-6.06	**12**
AT2	-1058	-238	-7736	-8043	1252	-1507	-4.48	12.74	10.61	-1.28	3.12	-7.28	**12**
AT2	-1358	-2021	-7206	-8259	2941	-575	-4.55	12.78	7.96	0.18	2.73	-4.86	**12**
AT3	-2496	-2597	-2690	-6382	1957	-2603	-3.84	11.87	8.33	-6.29	-2.19	0.12	**13**
AT3	-881	-2037	-2476	-6248	2322	-4450	-2.29	11.79	10.06	-7.61	0.70	1.07	**13**
AT3	-1737	-2225	-2438	-8080	3354	-3405	-4.03	13.76	8.19	-6.64	0.08	1.04	**13**
AT3	-422	-2474	-2618	-5828	3117	-4481	-1.33	11.40	9.35	-7.08	1.67	1.66	**13**
AT3	-407	-2355	-2284	-8803	3558	-4497	-3.84	13.97	9.95	-6.65	2.40	2.56	**13**
AT3	-1146	-2899	-3108	-6709	2667	-3342	-3.12	11.71	9.12	-5.51	0.60	1.09	**13**
AT4	-3110	-10304	-15118	-13579	970	-7484	-21.86	-0.33	6.88	5.34	12.13	-2.37	**14**
AT4	-3369	-9955	-14989	-13614	1912	-7395	-21.32	0.42	5.37	4.87	12.16	-2.73	**14**
AT4	-3420	-8995	-15114	-13877	-678	-6775	-22.39	0.74	8.95	5.13	10.55	-4.28	**14**
AT4	-3139	-8259	-15142	-14045	1459	-8066	-21.09	1.59	6.61	3.49	12.80	-4.52	**14**
AT4	-2823	-8248	-15198	-13814	26	-7674	-21.29	1.16	8.85	4.16	12.17	-4.65	**14**
AT4	-3386	-10154	-15071	-13827	-831	-7006	-23.12	-0.45	9.05	5.66	10.62	-2.83	**14**
AT5	-21026	-18490	-17327	-21688	8219	-5157	-46.05	-2.56	-25.20	4.08	-1.71	-4.07	**15**
AT5	-20837	-18357	-17145	-21333	8226	-5346	-45.45	-2.65	-25.02	3.70	-1.62	-3.94	**15**
AT5	-20861	-18538	-17113	-21321	7799	-5229	-45.76	-2.90	-24.50	3.91	-1.97	-3.77	**15**
AT5	-20878	-18130	-17247	-21521	8315	-5438	-45.56	-2.41	-25.13	3.55	-1.44	-4.27	**15**
AT5	-20534	-18615	-17263	-21410	8252	-5286	-45.41	-2.79	-24.70	4.25	-1.18	-3.59	**15**
AT5	-20671	-18216	-17319	-22210	7715	-6337	-46.76	-2.74	-23.83	3.13	-0.74	-3.82	**15**
AT6	-883	-5023	780	1868	15816	-1940	13.53	11.86	-10.36	-8.62	1.37	6.75	**16**
AT6	-1475	-4410	953	3159	14498	81	14.59	12.12	-9.72	-7.83	-1.68	5.06	**16**
AT6	-713	-4361	1137	2410	14916	-1206	14.43	12.37	-8.94	-8.59	0.21	6.13	**16**
AT6	334	-4704	557	2990	14976	-736	15.73	11.83	-8.06	-6.85	1.50	6.28	**16**
AT6	-350	-4583	1400	3972	13721	-1134	15.59	10.90	-7.38	-8.67	-0.67	6.46	**16**
AT6	480	-5708	1214	4298	15563	-697	17.13	10.70	-9.06	-6.94	1.06	8.01	**16**
AT7	-1284	-2497	36	2621	20688	2021	19.19	17.06	-17.58	-6.50	1.47	2.02	**17**
AT7	-1527	-2638	-3024	2889	20186	907	17.58	14.06	-18.21	-5.32	4.15	-1.15	**17**
AT7	-1542	-3170	-543	2569	21013	899	18.17	15.60	-18.58	-6.90	2.54	2.31	**17**
AT7	-663	-2439	-2209	3036	19872	2648	19.22	15.67	-16.45	-3.76	3.19	-0.44	**17**
AT7	-1192	-2590	-1914	1531	21631	2308	18.17	17.13	-18.90	-4.30	3.84	0.26	**17**
AT7	-590	-3065	-749	1540	20677	676	17.72	16.24	-16.55	-6.07	4.01	2.76	**17**
AT8	1147	-733	-1766	283	17978	-3719	16.06	15.36	-10.19	-9.52	8.35	1.04	**18**

AT8	700	-633	-1465	983	18620	-3951	16.81	15.14	-11.79	-10.60	7.88	0.95	**18**
AT8	832	635	204	527	18488	-4885	17.33	16.99	-10.63	-13.48	7.18	1.69	**18**
AT8	885	410	-540	1001	18793	-4637	17.75	16.28	-11.38	-12.60	7.77	1.03	**18**
AT8	1547	54	-1211	1303	16738	-4927	16.95	14.57	-8.10	-11.62	8.14	0.96	**18**
AT8	1298	657	-2083	705	17758	-4773	16.85	15.41	-9.76	-11.25	9.18	-0.69	**18**
AT9	-21055	-25075	-21046	-21269	-11381	-17265	-65.62	-24.98	-1.04	0.22	-1.46	0.88	**19**
AT9	-21017	-25094	-21052	-21906	-11381	-17311	-66.24	-24.57	-0.77	0.39	-1.23	1.06	**19**
AT9	-21052	-25101	-21125	-22337	-11385	-17251	-66.71	-24.29	-0.68	0.61	-1.13	1.04	**19**
AT9	-21033	-25066	-21097	-22482	-11398	-17398	-66.86	-24.22	-0.57	0.47	-1.01	1.11	**19**
AT9	-21029	-25073	-21054	-21688	-11323	-17353	-66.01	-24.71	-0.94	0.27	-1.24	0.99	**19**
AT9	-20949	-25049	-21120	-22658	-11309	-17124	-66.82	-23.89	-0.52	0.85	-0.97	1.09	**19**
AT10	-16704	-24673	-20957	-22235	-10843	-16685	-62.02	-22.48	4.39	3.75	3.57	3.14	**2**
AT10	-17020	-24689	-21056	-22536	-10749	-16801	-62.61	-22.43	3.92	3.58	3.49	2.97	**2**
AT10	-16732	-24699	-21123	-22820	-10722	-16890	-62.68	-22.26	4.35	3.82	4.01	3.15	**2**
AT10	-16670	-24760	-21098	-23063	-10669	-17019	-62.91	-22.17	4.45	3.82	4.23	3.37	**2**
AT10	-16927	-24677	-21129	-22620	-10769	-17033	-62.72	-22.53	4.08	3.48	3.81	3.00	**2**
AT10	-16642	-24715	-21129	-22971	-10788	-17045	-62.85	-22.27	4.61	3.79	4.22	3.28	**2**
AT11	-22944	-24028	-20673	-26199	-7999	-15097	-68.82	-18.24	-6.06	1.22	-2.22	-0.27	**3**
AT11	-22914	-24048	-20664	-26229	-7992	-15326	-68.90	-18.36	-6.02	1.02	-2.05	-0.16	**3**
AT11	-22962	-24124	-20694	-26178	-8142	-15182	-68.98	-18.46	-5.92	1.20	-2.25	-0.19	**3**
AT11	-22960	-24180	-20725	-26159	-8010	-15037	-68.88	-18.41	-6.11	1.40	-2.25	-0.19	**3**
AT11	-22922	-24164	-20576	-26174	-7979	-15011	-68.78	-18.26	-6.06	1.33	-2.33	-0.02	**3**
AT11	-22939	-24177	-20710	-26251	-8051	-15160	-69.01	-18.41	-5.99	1.30	-2.16	-0.12	**3**
AT12	6425	-8933	-3345	39209	6041	-2011	47.81	-22.62	-2.69	-7.20	-1.33	2.56	**4**
AT12	5821	-8692	-2435	40746	4820	-1513	48.69	-23.25	-2.11	-8.35	-4.12	2.41	**4**
AT12	7341	-7268	-2732	38968	5138	-2215	48.93	-20.92	0.20	-8.24	-1.13	1.87	**4**
AT12	5983	-8174	-2446	40468	4036	49	48.90	-21.98	-0.69	-6.89	-5.20	1.53	**4**
AT12	6319	-10940	-3407	39383	5013	-1427	46.33	-24.57	-1.79	-5.29	-2.28	4.52	**4**
AT12	5370	-7652	-3014	40196	3798	-2658	47.21	-23.44	-1.17	-9.85	-3.86	0.61	**4**
AT13	26105	-5703	-3141	94812	9814	7302	127.14	-48.37	-1.25	-1.53	2.90	-3.05	**5**
AT13	27342	-5829	-2452	94390	9293	8572	128.06	-46.99	1.40	0.29	2.80	-1.67	**5**
AT13	26974	-5110	-1885	93271	10373	9724	128.20	-44.25	0.12	0.51	2.04	-2.05	**5**
AT13	27266	-6593	-2084	93377	9513	10208	127.32	-45.70	1.37	2.36	1.81	-0.57	**5**
AT13	26417	-5853	-1716	94041	9284	10500	127.73	-45.41	0.52	1.11	0.06	-1.74	**5**
AT13	27142	-6321	-2226	93657	9571	10088	127.59	-45.82	1.03	2.01	1.81	-1.14	**5**
AT14	9635	-3123	2735	13897	12945	20665	41.97	20.18	3.78	15.56	-6.44	4.86	**6**
AT14	9428	-2973	3107	11930	14477	21234	41.09	22.78	2.28	16.04	-6.04	5.35	**6**
AT14	10519	-2478	2493	14684	14047	20594	44.42	20.58	3.20	15.60	-4.83	4.28	**6**
AT14	9181	-2903	1542	11756	12841	21702	39.48	21.64	3.77	17.66	-6.06	3.23	**6**
AT14	9824	-2575	2214	14252	12892	20958	42.70	20.28	3.89	15.94	-6.08	3.61	**6**
AT14	10221	-2822	2067	11162	13897	20816	40.33	22.54	4.10	17.14	-4.10	4.72	**6**
AT15	9528	-1978	-3122	18912	19306	19151	48.83	15.61	-8.19	16.13	1.33	-3.24	**7**
AT15	9371	-2888	-1614	18331	20203	21205	49.23	17.62	-9.08	17.60	-0.73	-0.91	**7**
AT15	9164	-2673	-1612	19304	20507	21051	50.26	17.09	-10.08	16.88	-0.97	-1.43	**7**
AT15	8595	-2276	-1538	16677	19545	20487	46.68	18.55	-8.53	16.35	-1.17	-1.52	**7**
AT15	9297	-1767	-3983	18739	21540	23218	50.89	18.52	-11.65	20.52	0.58	-5.32	**7**
AT15	9516	-3643	-1847	17720	22431	21350	49.56	18.20	-11.82	18.58	0.87	0.04	**7**
AT16	-4248	-16071	-9951	-12857	-2055	-5310	-24.87	-2.85	9.91	6.45	3.48	8.49	**8**
AT16	-5458	-16850	-9424	-12334	-2807	-3868	-25.66	-3.28	9.18	7.06	0.29	8.77	**8**
AT16	-5632	-16073	-10757	-12690	-2470	-3158	-25.71	-2.65	8.34	8.26	1.06	6.24	**8**
AT16	-5303	-15760	-9135	-11821	-2812	-3923	-24.32	-2.53	9.43	6.02	0.10	7.82	**8**
AT16	-5912	-16178	-11923	-13311	-4049	-3379	-27.96	-3.76	9.96	9.09	1.22	4.99	**8**
AT16	-6746	-16144	-9883	-13968	-1898	-5475	-28.14	-2.63	6.81	4.82	1.06	7.48	**8**
AT17	-1757	-7755	-10460	-8968	984	-1522	-11.30	5.06	8.64	5.65	4.91	-1.77	**9**
AT17	-1362	-8246	-9401	-6246	-257	-713	-8.66	3.42	10.08	5.56	2.64	-0.65	**9**
AT17	-2197	-8283	-8948	-8204	107	311	-10.67	5.60	9.32	6.18	1.38	-0.40	**9**
AT17	-686	-7593	-9286	-6721	245	70	-7.59	5.16	10.59	6.40	3.21	-0.93	**9**
AT17	-2223	-7382	-8526	-8763	389	481	-10.39	7.22	9.34	5.53	1.16	-0.90	**9**
AT17	-2063	-8728	-9247	-5980	-678	645	-9.04	3.39	9.61	6.58	0.62	-0.73	**9**
AT18	-12694	-10266	-6789	-5929	-884	-904	-19.03	0.36	-3.63	-3.36	-12.70	-2.09	**10**
AT18	-12722	-9846	-7497	-7000	-1179	-540	-20.14	1.15	-3.04	-2.43	-12.23	-3.26	**10**
AT18	-13768	-10204	-7494	-6199	42	4	-19.60	0.83	-6.38	-2.66	-13.31	-3.66	**10**
AT18	-13385	-9197	-7272	-6539	-1834	-1436	-20.49	0.62	-3.05	-4.49	-13.11	-4.08	**10**
AT18	-12890	-9886	-8199	-5103	-1917	-543	-19.07	-0.96	-3.15	-2.43	-12.69	-4.53	**10**
AT18	-12453	-9991	-6972	-6000	-935	-280	-18.61	0.92	-3.23	-2.58	-12.66	-2.61	**10**
AT19	-2399	-6060	-7815	4104	-3056	-2557	0.23	-3.40	9.50	-2.36	-2.94	-3.98	**11**
AT19	-3728	-6277	-8632	4243	-3209	-3390	-1.52	-4.98	7.65	-3.37	-3.36	-5.24	**11**
AT19	-3083	-6574	-7226	5569	-3268	-3260	0.63	-5.16	8.46	-4.05	-4.28	-3.29	**11**
AT19	-3075	-6866	-7508	3335	-3105	-3114	-1.69	-3.85	8.94	-2.89	-3.45	-2.81	**11**
AT19	-2534	-6068	-8335	4917	-2673	-3079	0.81	-4.48	8.37	-2.80	-2.35	-4.64	**11**
AT19	-2424	-5941	-7708	2782	-2678	-2498	-0.76	-2.13	9.48	-2.15	-2.56	-3.72	**11**
control	778	1567	408	177	4	929	8.88	14.61	14.32	-7.34	-6.00	-1.73	**20**

control	704	1429	-509	-599	82	278	7.52	14.14	14.11	-7.02	-4.67	-2.30	**20**
control	32	840	-121	198	442	-232	7.54	13.00	12.50	-8.15	-5.47	-1.61	**20**
control	508	687	-298	-423	-21	-16	7.01	13.25	13.90	-7.17	-4.98	-1.30	**20**
control	323	-611	-190	-457	-314	-317	5.84	11.90	13.92	-6.79	-5.22	0.28	**20**
control	296	-908	-934	108	-267	656	6.32	11.38	13.37	-5.20	-5.31	-0.55	**20**

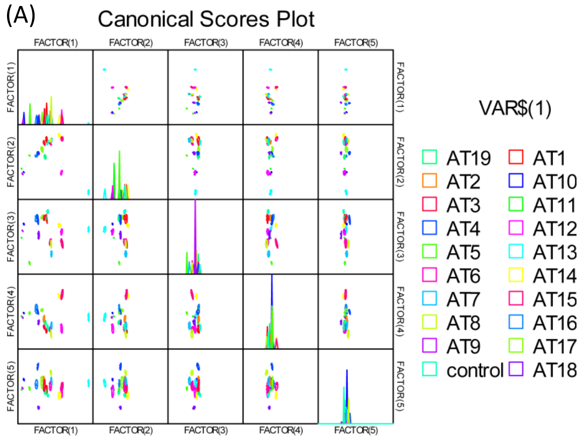

(B) **Jackknifed Classification Matrix**

	AT1	AT10	AT11	AT12	AT13	AT14	AT15	AT16	AT17	AT18	AT19	AT2	AT3	AT4	AT5	AT6	AT7	AT8	AT9	control	%correct
AT1	6	0	0	0	0	0	0	0	0	0	0	0	0	0	0	0	0	0	0	0	100
AT10	0	6	0	0	0	0	0	0	0	0	0	0	0	0	0	0	0	0	0	0	100
AT11	0	0	6	0	0	0	0	0	0	0	0	0	0	0	0	0	0	0	0	0	100
AT12	0	0	0	6	0	0	0	0	0	0	0	0	0	0	0	0	0	0	0	0	100
AT13	0	0	0	0	6	0	0	0	0	0	0	0	0	0	0	0	0	0	0	0	100
AT14	0	0	0	0	0	6	0	0	0	0	0	0	0	0	0	0	0	0	0	0	100
AT15	0	0	0	0	0	0	6	0	0	0	0	0	0	0	0	0	0	0	0	0	100
AT16	0	0	0	0	0	0	0	6	0	0	0	0	0	0	0	0	0	0	0	0	100
AT17	0	0	0	0	0	0	0	0	6	0	0	0	0	0	0	0	0	0	0	0	100
AT18	0	0	0	0	0	0	0	0	0	6	0	0	0	0	0	0	0	0	0	0	100
AT19	0	0	0	0	0	0	0	0	0	0	6	0	0	0	0	0	0	0	0	0	100
AT2	0	0	0	0	0	0	0	0	0	0	0	6	0	0	0	0	0	0	0	0	100
AT3	0	0	0	0	0	0	0	0	0	0	0	0	6	0	0	0	0	0	0	0	100
AT4	0	0	0	0	0	0	0	0	0	0	0	0	0	6	0	0	0	0	0	0	100
AT5	0	0	0	0	0	0	0	0	0	0	0	0	0	0	6	0	0	0	0	0	100
AT6	0	0	0	0	0	0	0	0	0	0	0	0	0	0	0	6	0	0	0	0	100
AT7	0	0	0	0	0	0	0	0	0	0	0	0	0	0	0	0	6	0	0	0	100
AT8	0	0	0	0	0	0	0	0	0	0	0	0	0	0	0	0	0	6	0	0	100
AT9	0	0	0	0	0	0	0	0	0	0	0	0	0	0	0	0	0	0	6	0	100
control	0	0	0	0	0	0	0	0	0	0	0	0	0	0	0	0	0	0	0	6	100
Total	6	6	6	6	6	6	6	6	6	6	6	6	6	6	6	6	6	6	6	6	100

Figure 106. (A) Correlations of canonical fluorescence response patterns from an array of sensor element S25-S30 against 19 antibiotics. The 95% confidence ellipses for the individual acids are also shown. **(B)** Jackknifed classification matrix showed the 100% correct classification.

Table 35. Training matrix of fluorescence response pattern from an array of sensor element S1-S30 against 19 antibiotics. Fluorescence response pattern LDA was carried out and resulting in 30 factors of the canonical scores (the first 8 scores were shown here) and group generation. Jackknifed classification matrix showed the 100% correct classification.

Analyte	Results LDA								
Antibiotics	SCORE1	SCORE2	SCORE3	SCORE4	SCORE5	SCORE6	SCORE7	SCORE8	GROUP
AT1	74.81	72.88	42.30	1.87	-11.33	-4.47	-17.15	-26.98	1
AT1	75.18	75.16	40.11	2.39	-10.75	-5.10	-15.70	-25.03	1
AT1	76.78	75.78	39.81	1.55	-12.03	-5.80	-16.80	-25.83	1
AT1	75.28	75.71	40.21	1.23	-11.54	-4.54	-17.25	-26.14	1
AT1	76.16	75.62	41.10	2.90	-12.20	-3.65	-17.59	-24.63	1
AT1	73.19	75.97	40.35	0.59	-11.65	-5.75	-15.70	-25.77	1
AT2	49.13	54.46	41.23	-11.22	15.10	3.45	-1.82	39.22	12
AT2	49.52	55.75	41.42	-12.60	15.69	3.10	-2.62	41.00	12
AT2	49.19	56.19	41.62	-13.56	13.48	4.36	-1.69	39.82	12
AT2	51.04	55.98	41.04	-12.17	13.74	2.36	-0.69	35.84	12
AT2	49.09	53.92	40.35	-12.54	14.85	4.16	-3.92	37.45	12
AT2	51.68	55.78	40.91	-14.30	15.55	2.45	-0.66	38.77	12
AT3	76.69	88.44	67.39	10.17	-7.97	-29.73	-30.15	6.13	13
AT3	74.36	86.71	69.70	8.90	-6.35	-27.00	-27.64	5.70	13
AT3	75.12	87.84	67.72	9.44	-6.34	-27.06	-30.22	6.20	13
AT3	76.02	88.22	67.13	11.59	-6.26	-26.56	-30.15	4.71	13
AT3	75.42	87.12	67.99	8.04	-6.43	-28.34	-29.67	5.33	13
AT3	74.41	85.67	68.63	9.42	-6.26	-26.80	-29.71	4.43	13
AT4	-2.38	-79.10	6.93	-77.31	55.37	75.34	13.19	-5.91	14
AT4	-2.42	-77.88	6.22	-78.23	54.08	75.22	16.63	-6.10	14
AT4	0.10	-76.88	9.03	-80.62	55.71	77.76	14.65	-7.83	14
AT4	-2.47	-77.46	6.83	-78.91	57.60	77.97	13.91	-8.05	14
AT4	-2.92	-78.67	6.44	-78.10	55.47	77.55	13.50	-8.09	14
AT4	-1.82	-78.61	6.19	-77.47	53.46	76.80	13.42	-8.66	14
AT5	82.71	-37.32	-22.93	-52.38	-16.48	-48.62	27.89	25.40	15
AT5	82.17	-37.14	-23.05	-52.51	-16.61	-48.43	27.88	25.58	15
AT5	82.99	-35.85	-24.18	-51.59	-18.32	-47.69	28.53	25.19	15
AT5	82.96	-36.55	-24.73	-52.35	-17.26	-49.61	27.12	25.98	15
AT5	82.20	-36.32	-24.32	-51.04	-17.97	-49.08	27.40	24.31	15
AT5	83.08	-34.37	-23.65	-52.78	-19.21	-51.49	26.31	23.33	15
AT6	47.55	40.20	-122.72	-2.55	6.26	-7.59	-22.27	-1.02	16
AT6	48.25	40.80	-123.53	-2.91	6.00	-5.68	-21.37	-0.57	16
AT6	49.12	40.29	-122.82	-3.16	5.17	-6.30	-21.33	0.69	16
AT6	48.56	39.63	-123.32	-2.39	5.98	-6.13	-23.87	0.27	16
AT6	48.19	42.53	-121.63	-2.60	4.72	-7.01	-21.33	0.36	16
AT6	48.67	40.34	-124.90	-2.71	8.10	-6.75	-22.13	0.12	16
AT7	50.50	41.62	-126.67	1.16	14.31	-13.39	-2.56	-6.54	17
AT7	49.45	41.84	-128.43	-0.22	11.37	-10.32	-3.58	-4.42	17

AT7	51.38	39.64	-126.31	2.25	11.90	-11.02	-3.51	-6.29	17
AT7	50.81	41.45	-126.55	2.06	11.61	-10.84	-2.60	-5.65	17
AT7	49.91	40.54	-128.98	1.10	12.70	-12.62	-2.74	-6.18	17
AT7	49.73	41.68	-127.75	-1.27	11.60	-11.15	-4.91	-6.12	17
AT8	40.81	56.71	-113.77	2.22	9.09	7.33	-4.06	4.05	18
AT8	42.70	56.16	-114.99	2.15	9.66	8.46	-4.30	4.60	18
AT8	42.75	58.41	-114.40	1.73	7.64	7.64	-3.48	4.32	18
AT8	41.89	57.93	-114.36	1.21	8.53	7.38	-4.69	0.35	18
AT8	43.81	56.83	-114.67	0.82	10.27	7.14	-5.02	2.68	18
AT8	41.40	57.26	-115.71	0.07	9.17	7.16	-4.79	0.37	18
AT9	111.43	-230.15	3.91	17.73	-6.57	5.20	-13.86	-11.41	19
AT9	112.10	-228.42	5.60	19.05	-6.32	3.29	-15.96	-9.92	19
AT9	111.32	-227.81	5.53	18.15	-5.30	1.87	-15.35	-8.04	19
AT9	112.27	-228.41	4.40	17.32	-8.15	3.24	-15.31	-9.40	19
AT9	112.60	-229.61	4.74	18.34	-6.45	3.87	-14.48	-10.78	19
AT9	111.66	-229.66	5.06	18.12	-7.22	4.75	-15.62	-11.42	19
AT10	117.88	-195.94	12.75	24.03	4.84	-23.42	-23.94	12.05	2
AT10	118.35	-196.92	12.53	24.15	4.27	-22.95	-24.28	12.47	2
AT10	118.12	-196.55	12.72	24.45	3.27	-22.86	-24.75	12.02	2
AT10	118.26	-196.72	14.04	24.73	3.99	-22.87	-24.54	12.30	2
AT10	116.98	-196.79	13.72	24.66	4.49	-23.05	-24.82	12.43	2
AT10	117.53	-195.85	11.95	23.91	3.35	-22.74	-24.99	12.49	2
AT11	83.26	-181.26	5.41	-15.53	-47.73	-5.50	13.83	-10.51	3
AT11	82.61	-181.88	4.57	-15.63	-48.04	-4.58	14.37	-10.88	3
AT11	82.58	-181.82	4.76	-16.33	-47.69	-5.57	15.12	-10.41	3
AT11	82.94	-181.37	4.11	-14.57	-48.10	-5.73	12.55	-9.98	3
AT11	82.69	-181.74	5.33	-15.10	-49.22	-3.32	14.75	-11.73	3
AT11	82.08	-181.70	4.25	-15.13	-48.41	-4.63	14.08	-12.21	3
AT12	89.17	13.94	-17.52	106.37	-25.11	62.73	20.43	20.37	4
AT12	88.10	13.98	-19.32	108.35	-25.81	62.59	16.91	19.50	4
AT12	87.82	14.36	-19.44	107.67	-25.25	60.45	20.32	20.19	4
AT12	88.92	12.48	-19.06	107.67	-25.55	61.51	19.25	19.46	4
AT12	88.39	13.28	-17.40	105.26	-27.81	60.56	18.51	19.65	4
AT12	89.68	11.22	-17.13	106.95	-25.79	58.66	16.44	20.41	4
AT13	-1319.48	-14.05	5.63	7.78	-3.28	-3.72	-1.86	0.59	5
AT13	-1319.91	-14.83	5.60	8.96	-4.19	-6.78	1.01	0.73	5
AT13	-1314.87	-14.36	6.18	7.04	-2.06	-4.50	-0.11	-1.83	5
AT13	-1320.85	-14.37	5.49	7.97	-3.02	-3.50	-0.03	0.00	5
AT13	-1321.95	-14.49	6.54	9.48	-4.21	-6.75	-0.81	-0.49	5
AT13	-1318.72	-14.97	4.79	8.16	-3.92	-6.72	0.54	-1.04	5
AT14	93.85	45.56	12.37	42.21	11.36	-38.56	51.78	-21.35	6
AT14	93.34	47.20	9.28	41.76	9.25	-37.18	53.34	-22.05	6
AT14	93.58	48.42	12.37	45.06	7.92	-36.45	53.13	-23.26	6
AT14	95.33	45.62	11.51	41.82	8.55	-36.79	52.55	-19.63	6
AT14	94.84	47.39	9.28	42.78	9.14	-37.26	53.75	-20.99	6
AT14	95.25	47.27	10.21	41.85	8.05	-37.12	52.41	-20.94	6
AT15	82.37	-7.79	61.20	38.74	98.84	-24.21	1.97	-2.86	7
AT15	80.07	-5.31	61.51	38.31	100.51	-23.82	-0.75	-1.91	7
AT15	80.70	-6.99	59.68	39.96	100.48	-26.88	1.50	-3.43	7
AT15	80.58	-7.64	60.66	37.60	98.55	-24.18	-0.51	-1.43	7
AT15	81.14	-6.03	61.57	37.82	102.39	-25.90	2.43	-3.31	7
AT15	81.66	-9.53	60.13	38.87	100.40	-25.42	0.81	-2.36	7
AT16	70.44	65.59	50.62	-23.04	-32.60	8.74	-5.10	0.84	8
AT16	68.03	64.47	51.63	-25.08	-33.61	7.82	-3.73	-1.01	8
AT16	68.24	64.99	50.19	-26.38	-32.37	7.71	-3.55	1.47	8
AT16	67.79	63.90	51.82	-26.22	-32.30	8.34	-3.00	0.80	8
AT16	69.23	65.00	50.90	-26.68	-33.94	6.95	-5.17	1.81	8
AT16	69.27	64.06	48.82	-27.10	-34.89	7.31	-5.87	-0.11	8
AT17	49.24	65.44	44.73	-21.29	-10.58	13.09	-0.65	16.16	9
AT17	48.26	66.92	43.81	-20.04	-10.67	15.74	1.03	16.75	9
AT17	50.30	68.01	44.19	-21.77	-9.78	15.73	0.05	17.18	9
AT17	48.15	68.45	44.48	-20.59	-9.03	16.08	0.51	16.06	9
AT17	48.99	68.64	45.07	-21.18	-11.09	14.40	0.54	15.55	9
AT17	49.89	66.34	43.31	-21.05	-9.95	15.97	0.80	16.51	9
AT18	61.72	45.73	18.06	-41.35	-18.90	-7.29	14.27	-3.25	10
AT18	61.66	48.26	20.36	-43.09	-18.44	-8.02	12.56	-4.35	10
AT18	62.93	46.61	18.85	-40.10	-19.07	-8.03	14.97	-3.30	10
AT18	62.12	45.76	14.16	-44.00	-19.56	-7.20	15.45	-3.56	10
AT18	64.75	46.16	17.39	-39.46	-18.49	-7.42	13.91	-4.29	10
AT18	62.00	48.49	17.24	-42.35	-16.44	-7.18	12.59	-4.71	10
AT19	64.62	70.93	-6.81	-17.31	-2.19	-1.90	-10.69	-15.12	11
AT19	65.38	70.04	-5.58	-17.83	-5.29	-0.39	-11.48	-14.39	11

AT19	64.99	72.95	-8.03	-17.59	-2.40	-0.17	-12.32	-14.76	11
AT19	65.51	72.63	-5.10	-18.41	-3.74	-0.34	-12.38	-15.37	11
AT19	64.94	73.07	-5.68	-16.82	-3.95	-0.63	-10.45	-14.19	11
AT19	65.10	71.97	-7.39	-17.41	-1.27	-1.44	-12.47	-15.57	11
Control	74.93	76.65	43.22	16.55	-25.44	28.15	-8.12	-17.94	20
Control	74.27	75.24	45.32	14.80	-25.60	27.93	-8.70	-18.73	20
Control	74.25	76.67	43.66	15.45	-25.23	28.01	-10.53	-17.12	20
Control	77.22	75.70	44.56	15.40	-25.12	28.55	-8.80	-16.74	20
Control	74.47	73.60	44.95	13.52	-25.70	28.79	-8.53	-17.85	20
Control	74.91	75.13	45.54	14.21	-25.99	27.79	-7.71	-18.30	20

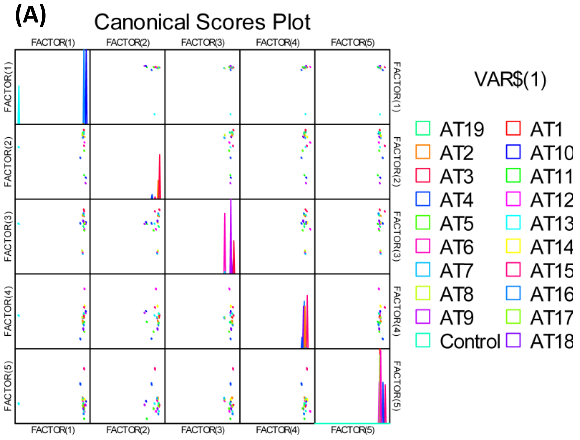

(B) **Jackknifed Classification Matrix**

	AT1	AT10	AT11	AT12	AT13	AT14	AT15	AT16	AT17	AT18	AT19	AT2	AT3	AT4	AT5	AT6	AT7	AT8	AT9	control	%correct
AT1	6	0	0	0	0	0	0	0	0	0	0	0	0	0	0	0	0	0	0	0	100
AT10	0	6	0	0	0	0	0	0	0	0	0	0	0	0	0	0	0	0	0	0	100
AT11	0	0	6	0	0	0	0	0	0	0	0	0	0	0	0	0	0	0	0	0	100
AT12	0	0	0	6	0	0	0	0	0	0	0	0	0	0	0	0	0	0	0	0	100
AT13	0	0	0	0	6	0	0	0	0	0	0	0	0	0	0	0	0	0	0	0	100
AT14	0	0	0	0	0	6	0	0	0	0	0	0	0	0	0	0	0	0	0	0	100
AT15	0	0	0	0	0	0	6	0	0	0	0	0	0	0	0	0	0	0	0	0	100
AT16	0	0	0	0	0	0	0	6	0	0	0	0	0	0	0	0	0	0	0	0	100
AT17	0	0	0	0	0	0	0	0	6	0	0	0	0	0	0	0	0	0	0	0	100
AT18	0	0	0	0	0	0	0	0	0	6	0	0	0	0	0	0	0	0	0	0	100
AT19	0	0	0	0	0	0	0	0	0	0	6	0	0	0	0	0	0	0	0	0	100
AT2	0	0	0	0	0	0	0	0	0	0	0	6	0	0	0	0	0	0	0	0	100
AT3	0	0	0	0	0	0	0	0	0	0	0	0	6	0	0	0	0	0	0	0	100
AT4	0	0	0	0	0	0	0	0	0	0	0	0	0	6	0	0	0	0	0	0	100
AT5	0	0	0	0	0	0	0	0	0	0	0	0	0	0	6	0	0	0	0	0	100
AT6	0	0	0	0	0	0	0	0	0	0	0	0	0	0	0	6	0	0	0	0	100
AT7	0	0	0	0	0	0	0	0	0	0	0	0	0	0	0	0	6	0	0	0	100
AT8	0	0	0	0	0	0	0	0	0	0	0	0	0	0	0	0	0	6	0	0	100
AT9	0	0	0	0	0	0	0	0	0	0	0	0	0	0	0	0	0	0	6	0	100
control	0	0	0	0	0	0	0	0	0	0	0	0	0	0	0	0	0	0	0	6	100
Total	6	6	6	6	6	6	6	6	6	6	6	6	6	6	6	6	6	6	6	6	100

Figure 107. (A) Correlations of canonical fluorescence response patterns from an array of sensor element S1-S30 against 19 antibiotics. The 95% confidence ellipses for the individual acids are also shown. **(B)** Jackknifed classification matrix showed the 100% correct classification.

Table 36. Training matrix of fluorescence response pattern from an optimized array of combined sensor element S2, S12, S18, S25, S28 and S29 against 19 antibiotics. LDA was carried out as described above resulting in the four factors of the canonical scores and group generation. Jackknifed classification matrix showed the 100% correct classification.

Analyte	Fluorescence response pattern						Results LDA						
Anti biotics	S2	S12	S18	S25	S28	S29	SCORE 1	SCORE 2	SCORE 3	SCORE 4	SCORE 5	SCORE 6	Gro up
AT1	-1138	383	1586	-499	-5638	3522	-56.52	-16.64	7.96	0.55	-7.66	3.66	1
AT1	-1032	715	1623	-391	-3984	5411	-55.72	-18.87	6.23	-0.33	-4.94	3.44	1
AT1	-1264	456	2160	-145	-5652	5935	-57.31	-17.94	6.88	-0.84	-4.96	5.37	1
AT1	-1163	834	1527	-879	-5112	4125	-56.53	-17.59	7.99	0.58	-6.21	3.04	1
AT1	-1098	568	1101	-161	-4550	3270	-56.12	-17.86	7.10	0.86	-8.29	2.96	1
AT1	-1045	467	1911	-1118	-2759	3861	-55.46	-17.81	6.38	-0.74	-5.47	0.94	1
AT2	7187	-1467	-1412	-530	-8613	2677	-12.44	-6.94	10.52	8.27	-9.51	7.61	12
AT2	7289	-1212	-2893	-950	-8268	2782	-11.90	-7.73	10.07	10.58	-9.01	6.68	12
AT2	7254	-1083	-1683	-1159	-8264	2528	-11.96	-7.17	11.04	8.90	-8.75	6.45	12
AT2	6263	-966	-1740	-1019	-7519	2333	-17.17	-8.55	10.20	8.44	-9.10	5.63	12
AT2	6848	-992	-1929	-1058	-8043	1252	-14.05	-7.36	11.27	9.26	-10.57	5.57	12
AT2	6550	-998	-1695	-1358	-8259	2941	-15.77	-7.84	10.73	8.73	-8.00	6.24	12
AT3	840	1016	-8978	-2496	-6382	1957	-46.51	-17.64	6.79	18.30	-9.30	0.01	13
AT3	929	2586	-8880	-881	-6248	2322	-45.88	-21.40	7.52	17.83	-11.11	1.65	13
AT3	857	1665	-8900	-1737	-8080	3354	-46.75	-18.83	7.69	18.43	-9.05	2.82	13
AT3	668	1734	-9077	-422	-5828	3117	-47.41	-21.39	5.35	17.43	-10.71	2.31	13
AT3	803	1175	-8977	-407	-8803	3558	-47.30	-18.97	6.71	18.18	-10.93	5.06	13
AT3	912	1015	-8098	-1146	-6709	2667	-46.21	-18.47	6.36	16.52	-10.22	2.31	13
AT4	7336	-15955	25615	-3110	-13579	970	-12.13	30.96	12.84	-32.25	-2.89	14.59	14
AT4	7603	-15792	25022	-3369	-13614	1912	-10.75	30.51	12.56	-31.30	-1.43	14.77	14
AT4	6900	-15890	25838	-3420	-13877	-678	-14.41	31.77	14.04	-32.21	-4.61	13.52	14
AT4	7592	-16202	25058	-3139	-14045	1459	-10.92	31.36	12.49	-31.30	-2.45	15.21	14
AT4	7580	-15560	24966	-2823	-13814	26	-10.80	30.60	13.56	-30.99	-4.71	14.49	14
AT4	7313	-15874	24492	-3386	-13827	-831	-12.26	31.52	13.59	-30.08	-5.13	13.34	14
AT5	-2458	-10820	-7780	-21026	-21688	8219	-68.15	18.93	10.49	24.08	21.44	-3.86	15
AT5	-2335	-10103	-7598	-20837	-21333	8226	-67.32	17.69	11.10	23.80	21.32	-4.01	15
AT5	-2472	-10265	-7787	-20861	-21321	7799	-68.07	17.94	10.98	24.08	20.76	-4.30	15
AT5	-2378	-10646	-7350	-20878	-21521	8315	-67.64	18.65	10.69	23.37	21.50	-3.73	15
AT5	-2411	-10539	-7322	-20534	-21410	8252	-67.79	18.16	10.57	23.19	20.96	-3.49	15
AT5	-2475	-9974	-7674	-20671	-22210	7715	-68.20	17.94	11.94	24.24	20.16	-3.47	15
AT6	677	1146	-33	-883	1868	15816	-46.06	-26.26	-2.42	-0.86	10.43	3.84	16
AT6	454	2233	725	-1475	3159	14498	-46.74	-27.37	-0.80	-1.86	10.10	1.32	16
AT6	443	3405	494	-713	2410	14916	-46.86	-29.58	0.35	-1.35	9.28	2.72	16

AT6	401	835	300	334	2990	14976	-47.37	-27.15	-3.82	-2.21	7.95	3.93	16
AT6	403	2810	1616	-350	3972	13721	-46.73	-28.94	-0.54	-3.65	7.90	1.54	16
AT6	345	2336	1278	480	4298	15563	-47.21	-30.09	-2.91	-3.98	9.07	3.21	16
AT7	1088	5202	696	-1284	2621	20688	-43.40	-33.79	0.16	-1.89	17.65	4.78	17
AT7	1137	6192	1643	-1527	2889	20186	-42.85	-34.55	2.00	-3.01	17.66	4.00	17
AT7	961	5422	2534	-1542	2569	21013	-43.94	-33.36	1.29	-4.57	18.85	4.90	17
AT7	1016	5553	1100	-663	3036	19872	-43.62	-34.58	0.49	-2.68	15.91	4.70	17
AT7	996	5265	1821	-1192	1531	21631	-44.06	-33.37	1.01	-3.38	18.69	6.36	17
AT7	1058	5118	3011	-590	1540	20677	-43.62	-32.72	1.57	-5.24	16.88	6.76	17
AT8	4642	5776	2407	1147	283	17978	-24.34	-30.84	4.87	-2.89	10.73	9.00	18
AT8	4478	6348	3079	700	983	18620	-24.99	-31.83	5.23	-4.02	12.53	8.23	18
AT8	4403	6173	2694	832	527	18488	-25.53	-31.58	5.12	-3.36	11.95	8.62	18
AT8	3907	6221	2120	885	1001	18793	-28.18	-32.69	4.15	-2.88	12.22	8.25	18
AT8	3927	5562	3138	1547	1303	16738	-27.94	-31.13	4.32	-4.54	8.95	7.96	18
AT8	4013	6272	2755	1298	705	17758	-27.57	-32.16	5.06	-3.66	10.37	8.51	18
AT9	-3120	-48775	12666	-21055	-21269	-11381	-73.79	90.49	-14.78	-11.75	1.32	-4.27	19
AT9	-3165	-48734	9614	-21017	-21906	-11381	-74.37	89.48	-15.82	-6.97	0.38	-4.20	19
AT9	-3091	-48596	8898	-21052	-22337	-11385	-74.08	89.32	-15.65	-5.69	0.14	-4.02	19
AT9	-3155	-48676	10245	-21033	-22482	-11398	-74.36	90.00	-15.01	-7.69	0.37	-3.69	19
AT9	-3217	-48601	12180	-21029	-21688	-11323	-74.41	90.15	-14.60	-10.88	1.13	-4.01	19
AT9	-3158	-48640	12597	-20949	-22658	-11309	-74.24	90.89	-13.77	-11.18	0.87	-3.07	19
AT10	-3028	-47861	-6991	-16704	-22235	-10843	-75.03	77.96	-25.44	16.58	-9.17	-1.42	2
AT10	-3083	-47801	-7129	-17020	-22536	-10749	-75.38	78.16	-25.11	16.99	-8.71	-1.54	2
AT10	-3025	-48011	-6975	-16732	-22820	-10722	-75.15	78.48	-25.23	16.73	-9.12	-0.90	2
AT10	-3069	-47838	-7044	-16670	-23063	-10669	-75.42	78.23	-24.97	16.91	-9.23	-0.66	2
AT10	-2949	-47882	-7112	-16927	-22620	-10769	-74.68	78.36	-25.12	16.99	-8.88	-1.32	2
AT10	-2970	-47891	-7339	-16642	-22971	-10788	-74.89	78.24	-25.16	17.34	-9.46	-0.77	2
AT11	-1927	-26788	17022	-22944	-26199	-7999	-65.24	63.84	16.63	-11.35	8.15	-4.04	3
AT11	-1860	-26407	16958	-22914	-26229	-7992	-64.84	63.30	17.07	-11.16	8.09	-4.04	3
AT11	-1893	-25950	18069	-22962	-26178	-8142	-64.85	63.13	18.21	-12.71	8.24	-4.15	3
AT11	-1928	-27071	16766	-22960	-26159	-8010	-65.29	64.15	16.15	-11.04	8.11	-4.07	3
AT11	-1893	-25314	18795	-22922	-26174	-7979	-64.73	62.39	19.21	-13.70	8.57	-4.03	3
AT11	-1822	-26039	18892	-22939	-26251	-8051	-64.44	63.63	18.54	-13.93	8.51	-3.86	3
AT12	5282	5412	3129	6425	39209	6041	-13.37	-50.51	-19.93	-17.65	-1.50	-21.59	4
AT12	5135	5005	3316	5821	40746	4820	-13.83	-49.78	-20.53	-18.19	-1.75	-24.05	4
AT12	5258	6041	3116	7341	38968	5138	-13.45	-51.69	-19.11	-17.60	-4.05	-20.98	4
AT12	4861	4798	3294	5983	40468	4036	-15.35	-49.33	-20.41	-18.11	-3.09	-24.09	4
AT12	4894	4181	2966	6319	39383	5013	-15.54	-48.63	-21.18	-17.64	-2.69	-22.27	4
AT12	4620	4755	2639	5370	40196	3798	-16.72	-48.95	-20.23	-16.86	-2.75	-24.84	4
AT13	159089	8454	2384	26105	94812	9814	827.92	9.50	-2.39	1.30	2.44	-1.88	5
AT13	159398	9846	1193	27342	94390	9293	829.58	6.65	-1.36	3.26	-0.39	-0.80	5
AT13	158571	9083	1846	26974	93271	10373	824.81	7.88	-1.82	2.24	1.31	0.26	5
AT13	159301	8878	1780	27266	93377	9513	828.78	8.76	-1.59	2.50	-0.14	0.28	5
AT13	159483	9294	2053	26417	94041	9284	830.01	8.83	-0.76	2.34	1.05	-1.31	5
AT13	158887	8948	2011	27142	93657	9571	826.62	8.37	-1.73	1.99	0.21	-0.14	5
AT14	-648	-76	-4317	9635	13897	12945	-51.79	-41.39	-19.75	-2.67	-6.35	3.94	6
AT14	-807	2912	-4032	9428	11930	14477	-52.68	-45.16	-15.40	-1.98	-4.57	5.48	6
AT14	-744	2393	-4336	10519	14684	14047	-51.95	-46.73	-18.52	-2.92	-6.02	4.38	6
AT14	-929	3029	-4009	9181	11756	12841	-53.25	-44.40	-14.23	-1.61	-6.36	4.43	6
AT14	-824	2680	-3888	9824	14252	12892	-52.30	-45.71	-16.71	-2.96	-6.51	3.33	6
AT14	-878	2294	-4045	10221	11162	13897	-53.28	-44.29	-15.78	-2.03	-6.67	6.77	6
AT15	-275	-24400	-12122	9528	18912	19306	-52.88	-14.17	-58.66	1.15	1.54	6.84	7
AT15	-215	-23505	-13718	9371	18331	20203	-52.72	-16.01	-58.32	3.86	2.39	7.19	7
AT15	-458	-22973	-13908	9164	19304	20507	-53.81	-17.55	-58.62	3.87	3.27	6.16	7
AT15	-289	-23743	-13152	8595	16677	19545	-53.33	-13.64	-56.39	3.91	2.35	7.39	7
AT15	-501	-23372	-13841	9297	18739	21540	-54.25	-17.21	-59.26	3.65	4.27	7.37	7
AT15	-437	-23648	-14075	9516	17720	22431	-54.20	-16.85	-59.51	4.10	4.77	8.92	7
AT16	-60	1760	-1156	-4248	-12857	-2055	-51.57	-9.42	18.77	10.08	-11.88	1.83	8
AT16	9	2130	-809	-5458	-12334	-2807	-50.93	-8.73	20.09	10.03	-10.87	-0.34	8
AT16	-45	3115	-429	-5632	-12690	-2470	-51.15	-9.86	21.60	9.79	-10.20	-0.23	8
AT16	50	2269	-1027	-5303	-11821	-2812	-50.63	-9.41	19.71	10.16	-11.01	-0.62	8
AT16	-100	2825	-821	-5912	-13311	-4049	-51.53	-8.38	22.43	10.87	-12.08	-0.89	8
AT16	-141	2859	-1273	-6746	-13968	-1898	-51.99	-8.51	22.10	11.73	-8.40	-0.27	8
AT17	4642	1710	3364	-1757	-8968	984	-25.37	-9.59	17.28	1.90	-9.09	5.06	9
AT17	4835	2504	4541	-1362	-6246	-257	-23.59	-11.44	17.32	-0.54	-10.23	2.78	9
AT17	4499	2673	3837	-2197	-8204	107	-25.78	-10.59	18.72	1.38	-9.27	3.35	9
AT17	4665	2098	4273	-686	-6721	245	-24.72	-11.59	16.34	-0.43	-10.77	4.17	9
AT17	4578	2694	3993	-2223	-8763	389	-25.45	-10.29	19.14	1.34	-8.98	3.95	9
AT17	4412	1525	3730	-2063	-5980	-678	-25.96	-10.04	16.00	0.56	-9.91	1.53	9
AT18	-449	2010	2133	-12694	-5929	-884	-51.88	-6.11	19.78	5.46	4.44	-12.15	10
AT18	-335	1744	3229	-12722	-7000	-1179	-51.39	-4.45	20.99	4.24	4.09	-11.25	10
AT18	-475	2010	2873	-13768	-6199	42	-52.02	-5.19	20.48	4.68	7.28	-12.56	10

AT18	-431	1843	2700	-13385	-6539	-1834	-51.79	-4.30	21.17	5.20	4.20	-12.82	10
AT18	-345	2006	2735	-12890	-5103	-1917	-51.05	-5.64	20.15	4.54	3.78	-13.44	10
AT18	-427	2151	3622	-12453	-6000	-935	-51.65	-5.84	20.63	3.22	4.36	-11.65	10
AT19	-553	-532	5236	-2399	4104	-3056	-50.99	-14.42	6.30	-6.65	-9.81	-8.70	11
AT19	-631	279	5442	-3728	4243	-3209	-51.21	-14.49	8.05	-6.35	-8.00	-10.53	11
AT19	-734	887	5614	-3083	5569	-3268	-51.46	-16.64	7.52	-7.20	-8.62	-10.99	11
AT19	-736	1312	5911	-3075	3335	-3105	-51.81	-15.97	9.68	-6.79	-8.96	-9.18	11
AT19	-669	999	5358	-2534	4917	-2673	-51.29	-17.20	7.41	-6.84	-8.89	-9.60	11
AT19	-762	490	6079	-2424	2782	-2678	-52.19	-15.13	8.60	-7.33	-9.46	-7.62	11

(A) Canonical Scores Plot

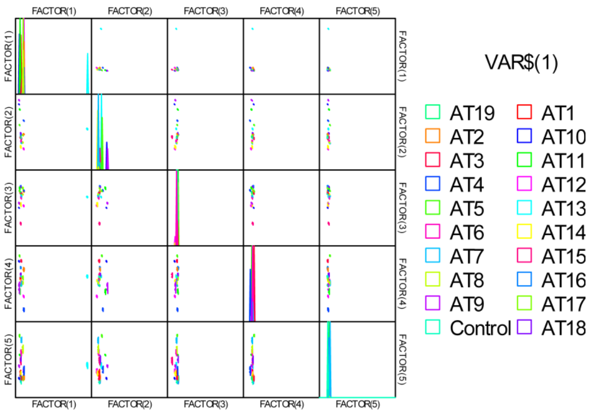

(B) **Jackknifed Classification Matrix**

	AT1	AT10	AT11	AT12	AT13	AT14	AT15	AT16	AT17	AT18	AT19	AT2	AT3	AT4	AT5	AT6	AT7	AT8	AT9	control	%correct
AT1	6	0	0	0	0	0	0	0	0	0	0	0	0	0	0	0	0	0	0	0	100
AT10	0	6	0	0	0	0	0	0	0	0	0	0	0	0	0	0	0	0	0	0	100
AT11	0	0	6	0	0	0	0	0	0	0	0	0	0	0	0	0	0	0	0	0	100
AT12	0	0	0	6	0	0	0	0	0	0	0	0	0	0	0	0	0	0	0	0	100
AT13	0	0	0	0	6	0	0	0	0	0	0	0	0	0	0	0	0	0	0	0	100
AT14	0	0	0	0	0	6	0	0	0	0	0	0	0	0	0	0	0	0	0	0	100
AT15	0	0	0	0	0	0	6	0	0	0	0	0	0	0	0	0	0	0	0	0	100
AT16	0	0	0	0	0	0	0	6	0	0	0	0	0	0	0	0	0	0	0	0	100
AT17	0	0	0	0	0	0	0	0	6	0	0	0	0	0	0	0	0	0	0	0	100
AT18	0	0	0	0	0	0	0	0	0	6	0	0	0	0	0	0	0	0	0	0	100
AT19	0	0	0	0	0	0	0	0	0	0	6	0	0	0	0	0	0	0	0	0	100
AT2	0	0	0	0	0	0	0	0	0	0	0	6	0	0	0	0	0	0	0	0	100
AT3	0	0	0	0	0	0	0	0	0	0	0	0	6	0	0	0	0	0	0	0	100
AT4	0	0	0	0	0	0	0	0	0	0	0	0	0	6	0	0	0	0	0	0	100
AT5	0	0	0	0	0	0	0	0	0	0	0	0	0	0	6	0	0	0	0	0	100
AT6	0	0	0	0	0	0	0	0	0	0	0	0	0	0	0	6	0	0	0	0	100
AT7	0	0	0	0	0	0	0	0	0	0	0	0	0	0	0	0	6	0	0	0	100
AT8	0	0	0	0	0	0	0	0	0	0	0	0	0	0	0	0	0	6	0	0	100
AT9	0	0	0	0	0	0	0	0	0	0	0	0	0	0	0	0	0	0	6	0	100
control	0	0	0	0	0	0	0	0	0	0	0	0	0	0	0	0	0	0	0	6	100
Total	6	6	6	6	6	6	6	6	6	6	6	6	6	6	6	6	6	6	6	6	100

Figure 108. (A) Correlations of canonical fluorescence response patterns from an optimized array of combined sensor element S2, S12, S18, S25, S28 and S29 against 19 antibiotics. The 95% confidence ellipses for the individual acids are also shown. **(B)** Jackknifed classification matrix showed the 100% correct classification.

Table 37. Detection and identification of unknown antibiotics samples using LDA with combined sensor element S2, S12, S18, S25, S28 and S29. All unknown samples could be assigned to the corresponding group defined by the training matrix according to the shortest Mahalanobis distance. According to the verification, all of 76 unknown samples were correct identified, representing an accuracy of 100%.

Analyte	Fluorescence response pattern						Results LDA								
Unknown samples	S2	S12	S18	S25	S28	S29	SCORE 1	SCORE 2	SCORE 3	SCORE 4	SCORE 5	SCORE 6	Group	Identi fication	Verifi cation
1	811	1483	-8573	-776	-6586	3113	-46.75	-19.99	6.11	17.06	-10.27	2.67	13	AT3	AT3
2	351	2753	1287	-77	3722	15008	-47.17	-29.67	-1.41	-3.41	9.01	2.67	16	AT6	AT6
3	5041	5177	3488	6412	39591	6296	-14.62	-50.52	-20.53	-18.48	-0.99	-21.74	4	AT12	AT12
4	-3081	-48542	11520	-20974	-21529	-11303	-73.69	89.76	-14.95	-9.92	0.97	-4.14	19	AT9	AT9
5	-457	-24148	-13579	9632	17876	21980	-54.29	-15.92	-59.81	3.22	4.18	8.86	7	AT15	AT15
6	-139	2038	3075	-13643	-6566	-949	-50.20	-4.37	21.44	4.73	5.81	-12.53	10	AT18	AT18
7	-567	2340	3125	-13281	-6499	-230	-52.51	-5.76	21.03	4.32	6.20	-11.97	10	AT18	AT18
8	-1113	-124	1086	136	-2585	4676	-56.03	-18.82	4.00	-0.30	-6.40	2.61	1	AT1	AT1
9	7173	-17073	24515	-3444	-14078	626	-13.29	32.73	11.63	-30.54	-3.25	14.43	14	AT4	AT4
10	4431	5582	2141	1281	1179	16494	-25.28	-30.79	4.43	-2.72	8.80	7.61	18	AT8	AT8
11	4240	6308	2415	1400	1555	16659	-26.15	-32.27	4.92	-3.24	8.98	7.39	18	AT8	AT8
12	-842	394	-4264	10238	15007	13454	-52.62	-43.54	-20.64	-3.40	-6.27	3.88	6	AT14	AT14
13	6935	-864	-1642	-1400	-9121	2146	-13.78	-6.87	12.12	9.24	-9.14	6.54	12	AT2	AT2
14	4604	2184	3993	-2013	-6465	781	-24.99	-11.15	16.59	0.28	-8.16	2.69	9	AT17	AT17
15	-2334	-10073	-7683	-20469	-21841	7870	-67.40	17.74	11.43	24.04	20.18	-3.40	15	AT5	AT5
16	159260	9359	2255	27069	91378	9730	828.29	9.41	0.63	2.63	-0.01	1.71	5	AT13	AT13
17	-206	2718	-1325	-4106	-12866	-1535	-52.28	-11.33	19.41	10.36	-11.48	2.02	8	AT16	AT16
18	-3048	-48127	-7432	-16338	-21587	-10852	-75.11	77.49	-26.65	16.82	-9.64	-1.54	2	AT10	AT10
19	6857	-1671	-1727	-2091	-8673	1692	-14.17	-5.26	11.40	9.34	-8.63	5.30	12	AT2	AT2
20	-2434	-10067	-8318	-20408	-22278	7751	-68.07	17.65	11.42	25.12	19.66	-3.17	15	AT5	AT5
21	-1932	-26447	18034	-22939	-26172	-7892	-65.14	63.68	17.45	-12.82	8.52	-3.91	3	AT11	AT11
22	-643	-24013	-13344	9926	17930	22001	-55.26	-16.45	-59.83	2.72	3.83	9.12	7	AT15	AT15
23	4783	5112	3336	6048	39515	3875	-15.90	-49.28	-19.33	-17.79	-3.64	-23.43	4	AT12	AT12
24	-3124	-48620	11261	-21025	-22633	-11258	-74.15	90.37	-14.39	-9.16	0.74	-3.34	19	AT9	AT9
25	913	5265	1990	-567	3446	21286	-44.15	-34.80	-0.50	-4.51	17.89	5.38	17	AT7	AT7
26	7102	-16213	24665	-3388	-13644	735	-13.48	31.15	12.28	-30.79	-3.05	14.05	14	AT4	AT4
27	-1153	-10	2009	-555	-2532	2937	-56.03	-17.35	5.79	-1.16	-7.39	0.99	1	AT1	AT1
28	743	5705	1086	-75	2901	21754	-45.23	-36.24	-0.63	-3.17	17.40	6.34	17	AT7	AT7
29	157688	9375	1871	26186	93195	9913	820.12	7.70	-1.12	2.39	1.77	-1.09	5	AT13	AT13
30	-163	3123	-1479	-5767	-12607	-3184	-51.81	-10.01	21.41	11.46	-11.15	-1.00	8	AT16	AT16
31	-3117	-47897	-7464	-16471	-21878	-10773	-75.50	77.33	-26.18	17.03	-9.44	-1.49	2	AT10	AT10

32	-665	741	5660	-2870	6509	-2821	-50.97	-17.25	6.38	-7.77	-8.09	-11.21	11	AT19	AT19
33	-1837	-25581	18700	-22915	-26231	-7781	-64.49	62.72	18.81	-13.61	8.78	-3.82	3	AT11	AT11
34	-2396	-10056	-7465	-20972	-22018	7781	-67.73	18.31	11.99	23.96	20.79	-3.86	15	AT5	AT5
35	4855	1407	4790	-1472	-7186	-122	-23.77	-9.16	16.84	-0.79	-10.09	3.73	9	AT17	AT17
36	-116	2108	3100	-13295	-4789	-2240	-49.68	-5.17	20.72	4.17	4.14	-14.22	10	AT18	AT18
37	-3062	-48013	-7524	-16450	-21378	-10794	-75.13	77.23	-26.68	16.93	-9.37	-1.84	2	AT10	AT10
38	185	2332	-197	-20	3305	15272	-48.33	-29.71	-2.57	-1.24	8.79	3.02	16	AT6	AT6
39	909	1643	-8529	-312	-6595	2434	-46.18	-20.22	6.45	17.00	-11.80	2.84	13	AT3	AT3
40	-1003	2921	-4105	10621	14747	13109	-53.21	-47.32	-17.53	-3.13	-7.32	3.82	6	AT14	AT14
41	4520	1978	3314	-1767	-6632	-169	-25.51	-10.89	16.42	1.36	-9.95	2.52	9	AT17	AT17
42	-703	641	5852	-2568	8373	-2797	-50.85	-18.35	4.82	-8.86	-7.95	-12.28	11	AT19	AT19
43	-553	-22484	-14001	9655	20344	22593	-54.22	-20.26	-60.20	3.20	5.48	6.85	7	AT15	AT15
44	438	1048	-8475	1	-6676	2397	-48.82	-19.88	5.47	16.58	-12.35	3.24	13	AT3	AT3
45	-2365	-10552	-7586	-20534	-21921	7763	-67.63	18.60	11.05	23.85	20.13	-3.37	15	AT5	AT5
46	-3136	-48675	11236	-20914	-21329	-11391	-73.98	89.67	-15.40	-9.62	0.75	-4.31	19	AT9	AT9
47	-1935	-26123	18652	-22943	-26219	-8153	-65.07	63.60	18.30	-13.62	8.33	-3.99	3	AT11	AT11
48	157654	9166	2241	25949	95842	9740	820.43	6.93	-2.87	0.95	2.69	-3.44	5	AT13	AT13
49	730	1464	-8499	-901	-6470	3114	-47.16	-19.95	6.08	16.92	-10.05	2.43	13	AT3	AT3
50	4249	6264	2369	844	1279	17171	-26.17	-31.82	5.11	-2.96	10.36	7.25	18	AT8	AT8
51	-725	3474	-4390	10310	12230	12992	-52.09	-46.32	-14.86	-1.48	-7.74	5.32	6	AT14	AT14
52	-515	1722	2918	-13351	-6333	-869	-52.26	-4.66	20.46	4.59	5.48	-12.41	10	AT18	AT18
53	-875	2327	-4345	8733	13878	12968	-52.68	-44.34	-16.52	-1.86	-5.05	2.43	6	AT14	AT14
54	6716	-1317	-2664	-2158	-8333	2319	-14.93	-6.67	10.77	10.58	-7.87	5.04	12	AT2	AT2
55	264	2242	74	-1017	2154	12907	-47.93	-26.92	0.06	-0.49	6.96	1.64	16	AT6	AT6
56	5042	4390	2409	5768	40051	3105	-14.51	-48.15	-20.36	-16.45	-4.27	-24.50	4	AT12	AT12
57	4254	6416	2120	651	1279	16833	-26.11	-31.83	5.44	-2.43	10.15	6.79	18	AT8	AT8
58	-266	2464	-1205	-6946	-13188	-1954	-52.55	-8.24	21.20	11.31	-7.97	-1.09	8	AT16	AT16
59	-1062	-79	1092	-802	-2900	3799	-55.72	-17.51	5.27	0.31	-6.24	1.35	1	AT1	AT1
60	-1976	-25916	17828	-22937	-26154	-7986	-65.32	62.82	17.98	-12.41	8.35	-4.12	3	AT11	AT11
61	-973	-76	1400	-635	-1149	4608	-54.95	-18.79	3.72	-0.94	-4.90	0.65	1	AT1	AT1
62	4998	4816	3396	6026	40865	5729	-14.63	-50.20	-21.43	-18.65	-0.84	-23.43	4	AT12	AT12
63	4664	2026	4365	-1434	-6747	592	-24.72	-10.97	16.58	-0.37	-9.23	3.56	9	AT17	AT17
64	6843	-760	-1515	-1819	-8135	1271	-14.01	-6.86	12.23	8.99	-9.37	4.81	12	AT2	AT2
65	-658	367	5422	-1844	5725	-2713	-51.18	-17.25	5.75	-7.59	-9.70	-9.34	11	AT19	AT19
66	318	2694	1526	128	2125	15193	-47.65	-28.87	-0.44	-3.32	8.57	4.29	16	AT6	AT6
67	-3081	-48650	11451	-20913	-23063	-11377	-73.98	90.73	-14.01	-9.31	0.36	-2.89	19	AT9	AT9
68	789	5932	773	-1416	2302	20494	-44.96	-34.67	1.32	-1.74	17.50	4.57	17	AT7	AT7
69	-90	3659	-1780	-5301	-12716	-3547	-51.38	-11.03	21.91	11.98	-12.38	-0.71	8	AT16	AT16
70	-665	220	5633	-2058	4910	-3077	-51.34	-16.17	6.57	-7.52	-10.03	-9.08	11	AT19	AT19
71	7577	-16474	25336	-3697	-13839	1398	-10.96	32.23	12.50	-31.64	-1.61	14.48	14	AT4	AT4
72	933	5849	629	-1018	2163	21279	-44.29	-35.10	0.70	-1.72	17.87	5.57	17	AT7	AT7
73	6950	-16335	25284	-3196	-13635	1583	-14.33	30.93	11.84	-32.00	-2.10	14.78	14	AT4	AT4
74	-3030	-48066	-7298	-16563	-22138	-10836	-75.08	77.96	-25.99	16.91	-9.41	-1.34	2	AT10	AT10
75	158122	9544	1608	25887	93915	10042	822.60	7.46	-1.27	2.78	2.54	-1.88	5	AT13	AT13
76	-604	-22616	-13719	8223	15865	21425	-55.18	-15.80	-55.63	5.03	4.92	8.21	7	AT15	AT15

Blind test: 76/76 (100% correct identified)

5.3.5 LDA Calculation (Chapter 3.1)

Table 38. Training matrix of fluorescence response pattern from an array of **PPE 1**, **PPE 2** (each at pH13, buffered) and their complex (at pH3 and 13, buffered) against 13 white wines. LDA was carried out as described above resulting in the four factors of the canonical scores and group generation.

Analyte	Fluorescence response pattern				Results LDA				
Wines	PPE 1 (pH13)	PPE 2 (pH13)	PPE 1+PPE 2 (pH13)	PPE 1+PPE 2 (pH3)	Factor 1	Factor 2	Factor 3	Factor 4	Group
Wine 1	-0.494	-0.939	-0.553	-0.935	-40.811	15.781	11.211	-2.996	6
Wine 1	-0.495	-0.939	-0.539	-0.935	-39.476	16.562	11.969	-4.039	6
Wine 1	-0.476	-0.940	-0.560	-0.939	-41.748	16.654	10.886	-1.122	6
Wine 1	-0.497	-0.938	-0.554	-0.936	-40.916	15.811	11.059	-3.216	6
Wine 1	-0.483	-0.934	-0.561	-0.936	-41.507	16.145	10.306	-1.499	6
Wine 1	-0.491	-0.932	-0.567	-0.938	-42.051	15.730	9.679	-1.741	6
Wine 2	-0.323	-0.678	-0.354	-0.506	13.822	4.561	7.311	2.876	7
Wine 2	-0.343	-0.660	-0.360	-0.533	12.206	6.289	4.331	1.665	7
Wine 2	-0.326	-0.677	-0.363	-0.523	11.940	5.482	6.319	3.048	7
Wine 2	-0.336	-0.679	-0.380	-0.514	10.803	3.214	5.790	3.487	7
Wine 2	-0.321	-0.685	-0.373	-0.513	11.273	4.073	6.858	4.242	7
Wine 2	-0.338	-0.664	-0.363	-0.499	13.787	3.129	5.582	2.487	7

Wine 3	-0.241	-0.634	-0.214	-0.656	19.856	30.767	6.648	-0.921	8
Wine 3	-0.224	-0.630	-0.225	-0.655	18.987	31.005	5.812	1.307	8
Wine 3	-0.251	-0.634	-0.222	-0.655	19.164	29.723	6.294	-1.193	8
Wine 3	-0.250	-0.623	-0.225	-0.653	19.364	29.807	5.016	-0.766	8
Wine 3	-0.233	-0.625	-0.216	-0.644	20.641	30.215	5.986	0.117	8
Wine 3	-0.250	-0.614	-0.231	-0.641	19.734	28.681	4.017	-0.097	8
Wine 4	-0.447	-0.727	-0.458	-0.325	12.911	-24.647	11.136	0.833	9
Wine 4	-0.450	-0.723	-0.459	-0.363	10.670	-21.369	9.722	0.442	9
Wine 4	-0.458	-0.729	-0.458	-0.343	11.843	-23.676	10.939	-0.260	9
Wine 4	-0.451	-0.722	-0.447	-0.366	11.689	-20.436	10.139	-0.481	9
Wine 4	-0.442	-0.732	-0.455	-0.346	11.792	-22.528	11.337	0.804	9
Wine 4	-0.455	-0.721	-0.449	-0.355	12.146	-21.711	10.259	-0.599	9
Wine 5	-0.234	-0.543	-0.260	-0.469	29.854	14.823	-0.140	5.246	10
Wine 5	-0.243	-0.563	-0.253	-0.474	29.562	14.589	2.081	3.791	10
Wine 5	-0.253	-0.559	-0.271	-0.477	27.816	13.514	0.622	4.194	10
Wine 5	-0.247	-0.531	-0.249	-0.497	29.648	17.632	-1.603	3.330	10
Wine 5	-0.229	-0.564	-0.239	-0.493	29.743	17.684	2.596	3.769	10
Wine 5	-0.249	-0.578	-0.254	-0.513	26.594	17.173	2.614	2.883	10
Wine 6	-0.482	-0.664	-0.495	-0.482	1.959	-12.317	-1.666	0.093	11
Wine 6	-0.487	-0.666	-0.494	-0.496	1.129	-11.289	-1.862	-0.547	11
Wine 6	-0.502	-0.658	-0.493	-0.500	1.233	-11.393	-2.730	-1.700	11
Wine 6	-0.488	-0.675	-0.500	-0.504	-0.181	-11.249	-1.477	-0.354	11
Wine 6	-0.474	-0.669	-0.489	-0.500	1.313	-10.132	-1.277	0.139	11
Wine 6	-0.493	-0.665	-0.489	-0.506	1.014	-10.373	-1.955	-1.418	11
Wine 7	-0.407	-0.664	-0.458	-0.598	-1.495	3.663	-2.616	2.731	12
Wine 7	-0.416	-0.684	-0.475	-0.594	-3.590	1.300	-1.339	3.029	12
Wine 7	-0.414	-0.656	-0.464	-0.592	-1.385	2.630	-3.521	2.665	12
Wine 7	-0.415	-0.658	-0.461	-0.603	-1.868	3.700	-3.466	2.331	12
Wine 7	-0.415	-0.671	-0.475	-0.597	-3.248	2.106	-2.771	3.158	12
Wine 7	-0.407	-0.672	-0.456	-0.612	-2.425	4.725	-1.960	2.433	12
Wine 8	-0.441	-0.702	-0.485	-0.407	6.202	-17.647	4.989	2.850	13
Wine 8	-0.445	-0.719	-0.491	-0.415	4.555	-18.046	6.095	2.780	13
Wine 8	-0.442	-0.702	-0.489	-0.413	5.489	-17.338	4.530	2.977	13
Wine 8	-0.457	-0.707	-0.482	-0.415	5.857	-17.698	5.339	1.197	13
Wine 8	-0.416	-0.718	-0.486	-0.403	5.856	-17.379	6.703	4.772	13
Wine 8	-0.444	-0.709	-0.483	-0.412	5.794	-17.499	5.628	2.394	13
Wine 9	-0.465	-0.612	-0.550	-0.811	-21.513	16.639	-18.936	3.370	5
Wine 9	-0.495	-0.608	-0.549	-0.817	-21.720	15.802	-19.493	0.886	5
Wine 9	-0.481	-0.628	-0.549	-0.819	-22.509	16.067	-17.498	1.833	5
Wine 9	-0.493	-0.622	-0.559	-0.821	-23.445	15.362	-18.720	1.567	5
Wine 9	-0.511	-0.613	-0.551	-0.820	-22.228	15.114	-19.193	-0.400	5
Wine 9	-0.482	-0.634	-0.540	-0.828	-22.384	17.109	-16.653	0.950	5
Wine 10	-0.516	-0.642	-0.549	-0.520	-4.858	-12.768	-8.039	1.058	1
Wine 10	-0.535	-0.640	-0.550	-0.517	-4.683	-13.872	-8.352	-0.468	1
Wine 10	-0.519	-0.658	-0.549	-0.519	-5.298	-13.380	-6.418	0.619	1
Wine 10	-0.544	-0.675	-0.548	-0.542	-7.233	-13.115	-5.359	-1.826	1
Wine 10	-0.524	-0.651	-0.564	-0.526	-6.915	-13.681	-8.102	1.248	1
Wine 10	-0.541	-0.667	-0.568	-0.550	-9.430	-13.064	-7.396	-0.196	1
Wine 11	-0.576	-0.696	-0.608	-0.521	-12.519	-20.324	-5.896	-0.351	2
Wine 11	-0.586	-0.692	-0.626	-0.556	-16.254	-18.561	-8.305	-0.153	2
Wine 11	-0.565	-0.700	-0.613	-0.528	-13.573	-19.571	-6.021	0.834	2
Wine 11	-0.551	-0.709	-0.617	-0.536	-14.753	-18.720	-5.376	2.024	2
Wine 11	-0.553	-0.703	-0.624	-0.527	-14.672	-19.731	-6.231	2.564	2
Wine 11	-0.557	-0.691	-0.623	-0.531	-14.462	-19.170	-7.471	2.258	2
Wine 12	-0.357	-0.368	-0.155	-0.219	61.426	-2.387	-6.062	-8.471	3
Wine 12	-0.322	-0.349	-0.150	-0.208	63.233	-0.800	-7.414	-5.655	3
Wine 12	-0.356	-0.362	-0.142	-0.214	63.162	-1.897	-5.907	-9.150	3
Wine 12	-0.327	-0.377	-0.141	-0.208	63.126	-1.498	-3.995	-7.028	3
Wine 12	-0.328	-0.372	-0.142	-0.202	63.558	-1.940	-4.431	-6.869	3
Wine 12	-0.316	-0.366	-0.133	-0.213	63.909	0.313	-4.869	-6.517	3
Wine 13	-0.649	-0.941	-0.711	-0.930	-55.990	-0.502	2.344	-4.564	4
Wine 13	-0.633	-0.937	-0.706	-0.932	-55.394	0.798	2.270	-3.604	4
Wine 13	-0.664	-0.940	-0.711	-0.930	-55.886	-1.285	2.287	-5.861	4
Wine 13	-0.638	-0.943	-0.714	-0.930	-56.251	-0.258	2.477	-3.587	4
Wine 13	-0.656	-0.942	-0.710	-0.931	-55.999	-0.834	2.476	-5.247	4
Wine 13	-0.644	-0.945	-0.709	-0.931	-55.995	-0.290	2.861	-4.379	4

Table 39. Detection and identification of unknown white wine samples using LDA. All unknown samples could be assigned to the corresponding group defined by the training matrix according to the shortest Mahalanobis distance. According to the verification, only 1 of 52 unknown wines was misclassified, representing an accuracy of 98%.

Sample	Fluorescence response pattern				Results LDA					Analyte	
#	PPE 1 (pH13)	PPE 2 (pH13)	PPE 1+PPE 2 (pH13)	PPE 1+PPE 2 (pH3)	Factor 1	Factor 2	Factor 3	Factor 4	Group	Identi fication	Verifi cation
1	-0.441	-0.839	-0.482	-0.439	-0.258	-18.963	18.351	1.006	13	Wine 8	Wine 8
2	-0.324	-0.386	-0.137	-0.340	55.114	10.414	-6.424	-8.091	3	Wine 12	Wine 12
3	-0.640	-0.940	-0.710	-0.937	-56.258	0.553	2.220	-3.949	4	Wine 13	Wine 13
4	-0.470	-0.623	-0.543	-0.874	-25.153	22.042	-19.135	1.928	5	Wine 9	Wine 9
5	-0.508	-0.653	-0.557	-0.554	-8.071	-10.117	-8.234	1.892	1	Wine 10	Wine 10
6	-0.496	-0.940	-0.570	-0.939	-42.719	15.209	10.242	-2.078	6	Wine 1	Wine 1
7	-0.427	-0.690	-0.457	-0.634	-4.481	5.157	-0.882	0.554	12	Wine 7	Wine 7
8	-0.244	-0.559	-0.248	-0.498	28.733	17.063	1.334	3.183	10	Wine 5	Wine 5
9	-0.489	-0.677	-0.494	-0.515	-0.339	-10.037	-1.217	-0.968	11	Wine 6	Wine 6
10	-0.440	-0.707	-0.485	-0.411	5.786	-17.470	5.347	2.850	13	Wine 8	Wine 8
11	-0.333	-0.655	-0.396	-0.554	7.617	6.889	1.397	4.821	7	Wine 2	Wine 2
12	-0.452	-0.736	-0.480	-0.415	5.014	-18.276	8.505	1.187	13	Wine 8	**Wine 4**
13	-0.248	-0.609	-0.218	-0.662	19.930	31.543	3.665	-0.897	8	Wine 3	Wine 3
14	-0.453	-0.722	-0.447	-0.348	12.774	-22.225	10.670	-0.525	9	Wine 4	Wine 4
15	-0.555	-0.696	-0.620	-0.543	-15.025	-18.047	-7.101	2.025	2	Wine 11	Wine 11
16	-0.485	-0.611	-0.547	-0.865	-24.512	20.688	-20.397	1.196	5	Wine 9	Wine 9
17	-0.222	-0.578	-0.243	-0.509	27.965	18.700	3.428	4.290	10	Wine 5	Wine 5
18	-0.427	-0.683	-0.461	-0.618	-3.634	3.698	-1.351	0.965	12	Wine 7	Wine 7
19	-0.344	-0.672	-0.390	-0.512	10.163	2.370	4.551	3.614	7	Wine 2	Wine 2
20	-0.501	-0.737	-0.502	-0.511	-3.024	-13.320	4.628	-1.990	11	Wine 6	Wine 6
21	-0.344	-0.381	-0.131	-0.336	56.156	9.522	-6.582	-9.987	3	Wine 12	Wine 12
22	-0.627	-0.943	-0.715	-0.938	-56.895	0.914	2.222	-2.594	4	Wine 13	Wine 13
23	-0.462	-0.723	-0.487	-0.370	7.496	-22.742	7.867	1.395	9	Wine 4	Wine 4
24	-0.490	-0.662	-0.487	-0.556	-1.684	-5.611	-3.443	-1.623	11	Wine 6	Wine 6
25	-0.244	-0.554	-0.246	-0.507	28.558	18.094	0.683	2.999	10	Wine 5	Wine 5
26	-0.504	-0.652	-0.549	-0.545	-6.708	-10.240	-7.732	1.684	1	Wine 10	Wine 10
27	-0.436	-0.723	-0.486	-0.414	4.936	-17.563	6.844	3.092	13	Wine 8	Wine 8
28	-0.249	-0.615	-0.233	-0.660	18.385	30.336	3.539	0.000	8	Wine 3	Wine 3
29	-0.510	-0.935	-0.572	-0.940	-42.775	14.612	9.588	-3.016	6	Wine 1	Wine 1
30	-0.601	-0.942	-0.710	-0.936	-56.279	2.348	2.568	-0.883	4	Wine 13	Wine 13
31	-0.276	-0.566	-0.238	-0.502	29.239	16.130	2.381	-0.159	10	Wine 5	Wine 5
32	-0.456	-0.627	-0.538	-0.871	-24.637	22.563	-18.326	2.698	5	Wine 9	Wine 9
33	-0.424	-0.668	-0.490	-0.604	-5.082	1.512	-4.140	3.510	12	Wine 7	Wine 7
34	-0.583	-0.701	-0.625	-0.535	-15.265	-20.503	-6.801	0.161	2	Wine 11	Wine 11
35	-0.439	-0.719	-0.486	-0.419	4.818	-17.110	6.305	2.832	13	Wine 8	Wine 8
36	-0.500	-0.650	-0.553	-0.559	-7.894	-8.965	-8.473	2.233	1	Wine 10	Wine 10
37	-0.428	-0.675	-0.475	-0.616	-4.569	3.014	-2.939	1.926	12	Wine 7	Wine 7
38	-0.348	-0.664	-0.386	-0.512	10.802	2.593	3.901	3.117	7	Wine 2	Wine 2
39	-0.562	-0.713	-0.623	-0.543	-15.896	-19.081	-5.526	1.479	2	Wine 11	Wine 11
40	-0.361	-0.380	-0.146	-0.335	54.734	7.856	-7.531	-10.290	3	Wine 12	Wine 12
41	-0.353	-0.662	-0.383	-0.522	10.530	3.543	3.516	2.526	7	Wine 2	Wine 2
42	-0.500	-0.933	-0.568	-0.938	-42.207	15.265	9.666	-2.415	6	Wine 1	Wine 1
43	-0.626	-0.937	-0.706	-0.935	-55.581	1.425	2.230	-3.075	4	Wine 13	Wine 13
44	-0.516	-0.660	-0.557	-0.557	-8.490	-10.372	-7.709	1.152	1	Wine 10	Wine 10
45	-0.458	-0.724	-0.461	-0.368	10.138	-21.417	9.531	-0.138	9	Wine 4	Wine 4
46	-0.476	-0.664	-0.499	-0.504	0.248	-10.315	-2.525	0.708	11	Wine 6	Wine 6
47	-0.546	-0.709	-0.627	-0.545	-16.252	-18.231	-6.221	3.102	2	Wine 11	Wine 11
48	-0.471	-0.609	-0.538	-0.878	-24.340	23.003	-20.337	1.590	5	Wine 9	Wine 9
49	-0.249	-0.627	-0.219	-0.651	19.878	29.896	5.787	-1.026	8	Wine 3	Wine 3
50	-0.331	-0.387	-0.143	-0.341	54.510	9.814	-6.637	-8.259	3	Wine 12	Wine 12
51	-0.500	-0.938	-0.583	-0.942	-44.127	14.599	9.281	-1.411	6	Wine 1	Wine 1
52	-0.227	-0.612	-0.245	-0.673	16.571	32.004	2.320	2.520	8	Wine 3	Wine 3

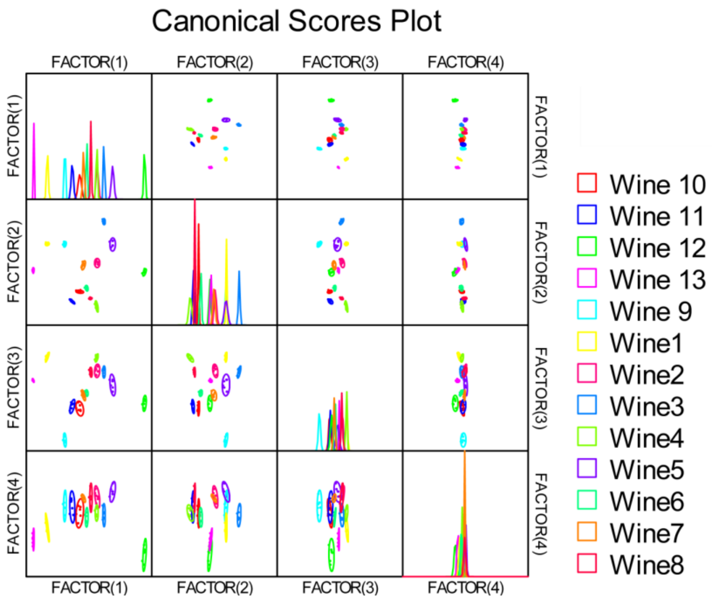

Figure 109. Correlations of canonical fluorescence response patterns obtained from an array of **PPE 1**, **PPE 2** (each at pH13, buffered) and their complex (at pH3 and 13, buffered) against 13 white wines. The 95% confidence ellipses for the individual acids are also shown.

5.3.6 LDA Calculation (Chapter 3.2)

Table 40. Training matrix of fluorescence response pattern from negatively charged water-soluble **P1** (2 µM, at pH3, pH7, and pH13, buffered) against commercial apple juice samples AJ1-AJ14 (50 µl). LDA was carried out as described above resulting in the three factors of the canonical scores and group generation.

Analytes	Fluorescence Response Pattern			Results LDA			
Apple juice	**P1** (pH3)	**P1** (pH7)	**P1** (pH13)	SCORE1	SCORE2	SCORE3	Group
AJ1	-0.95	-0.64	-0.67	-42.09	2.24	-7.20	1
AJ1	-0.95	-0.65	-0.68	-44.04	3.16	-8.13	1
AJ1	-0.95	-0.65	-0.68	-43.50	2.48	-7.39	1
AJ1	-0.95	-0.67	-0.68	-44.62	4.00	-5.82	1
AJ1	-0.95	-0.66	-0.67	-43.06	2.46	-4.88	1
AJ1	-0.95	-0.67	-0.68	-44.41	4.07	-4.97	1
AJ2	-0.90	-0.47	-0.59	-17.25	-8.10	-14.33	7
AJ2	-0.90	-0.47	-0.59	-16.95	-7.69	-13.77	7
AJ2	-0.89	-0.47	-0.60	-16.83	-6.81	-14.43	7
AJ2	-0.90	-0.48	-0.59	-17.49	-7.37	-12.34	7
AJ2	-0.89	-0.47	-0.59	-16.40	-7.93	-12.99	7
AJ2	-0.89	-0.46	-0.59	-15.62	-7.98	-14.45	7
AJ3	-0.91	-0.50	-0.54	-13.38	-13.74	-4.21	8
AJ3	-0.91	-0.51	-0.55	-15.11	-12.64	-4.98	8
AJ3	-0.91	-0.51	-0.54	-12.70	-12.72	-3.09	8
AJ3	-0.91	-0.52	-0.54	-13.78	-12.80	-2.89	8
AJ3	-0.91	-0.52	-0.54	-14.17	-12.73	-2.76	8
AJ3	-0.91	-0.52	-0.54	-13.41	-12.26	-2.81	8
AJ4	-0.75	-0.70	-0.67	-18.95	25.83	2.71	9
AJ4	-0.76	-0.71	-0.66	-18.59	24.91	3.82	9
AJ4	-0.75	-0.71	-0.67	-19.46	26.18	2.82	9
AJ4	-0.75	-0.71	-0.66	-16.89	25.59	5.05	9
AJ4	-0.75	-0.71	-0.66	-18.04	26.30	4.03	9
AJ4	-0.76	-0.71	-0.67	-19.84	25.60	2.90	9
AJ5	-0.80	-0.61	-0.63	-15.26	13.15	-2.76	10
AJ5	-0.80	-0.61	-0.62	-14.63	11.83	-1.19	10
AJ5	-0.80	-0.61	-0.63	-15.97	12.82	-2.34	10
AJ5	-0.80	-0.62	-0.62	-15.11	12.38	-0.89	10
AJ5	-0.80	-0.61	-0.62	-14.38	12.04	-2.05	10
AJ5	-0.80	-0.62	-0.63	-15.76	13.91	-1.85	10
AJ6	-0.88	-0.40	-0.51	0.71	-17.57	-10.12	11
AJ6	-0.88	-0.41	-0.51	-0.18	-16.85	-9.89	11
AJ6	-0.88	-0.40	-0.51	0.16	-17.73	-9.63	11

AJ6	-0.88	-0.40	-0.52	-0.55	-16.90	-10.55	11
AJ6	-0.88	-0.41	-0.51	0.42	-17.45	-9.29	11
AJ6	-0.88	-0.40	-0.51	-0.03	-17.46	-10.10	11
AJ7	-0.93	-0.88	-0.78	-65.02	24.85	3.18	12
AJ7	-0.93	-0.88	-0.77	-64.91	24.15	3.73	12
AJ7	-0.93	-0.88	-0.77	-65.10	24.23	3.88	12
AJ7	-0.93	-0.88	-0.77	-65.57	24.41	3.46	12
AJ7	-0.94	-0.88	-0.77	-65.31	23.95	3.63	12
AJ7	-0.93	-0.88	-0.77	-64.42	24.49	3.62	12
AJ8	-0.79	-0.35	-0.40	29.87	-22.59	0.28	5
AJ8	-0.79	-0.37	-0.40	29.40	-20.91	2.27	13
AJ8	-0.79	-0.40	-0.40	27.05	-19.07	4.31	13
AJ8	-0.79	-0.38	-0.40	27.62	-20.43	2.92	13
AJ8	-0.79	-0.39	-0.41	26.35	-18.77	2.66	13
AJ8	-0.79	-0.38	-0.41	26.12	-18.81	1.75	13
AJ9	-0.77	-0.67	-0.64	-15.02	19.64	2.44	14
AJ9	-0.76	-0.67	-0.65	-15.24	21.50	1.35	14
AJ9	-0.76	-0.67	-0.64	-14.35	21.35	1.80	14
AJ9	-0.76	-0.66	-0.64	-14.06	20.53	1.69	14
AJ9	-0.76	-0.65	-0.65	-15.66	20.99	-0.37	14
AJ9	-0.77	-0.66	-0.65	-15.74	20.10	1.23	14
AJ10	-0.82	-0.58	-0.46	5.71	-8.69	14.18	2
AJ10	-0.82	-0.61	-0.47	4.60	-6.25	16.25	2
AJ10	-0.82	-0.61	-0.47	4.39	-7.28	16.35	2
AJ10	-0.82	-0.58	-0.46	6.23	-8.01	14.61	2
AJ10	-0.82	-0.59	-0.47	5.44	-7.76	15.14	2
AJ10	-0.82	-0.60	-0.46	5.29	-7.78	16.23	2
AJ11	-0.92	-0.59	-0.50	-11.86	-16.23	9.10	3
AJ11	-0.92	-0.59	-0.50	-12.50	-15.29	9.10	3
AJ11	-0.92	-0.59	-0.49	-11.72	-16.06	9.50	3
AJ11	-0.92	-0.59	-0.50	-12.75	-15.47	8.40	3
AJ11	-0.92	-0.60	-0.49	-11.04	-16.25	11.05	3
AJ11	-0.92	-0.61	-0.49	-11.92	-15.19	11.56	3
AJ12	-0.81	-0.37	-0.42	23.66	-20.61	-0.50	4
AJ12	-0.81	-0.38	-0.42	22.86	-20.54	0.14	4
AJ12	-0.81	-0.38	-0.42	22.72	-19.92	0.45	4
AJ12	-0.81	-0.38	-0.41	24.12	-21.52	1.69	4
AJ12	-0.80	-0.39	-0.42	23.89	-18.81	1.98	4
AJ12	-0.82	-0.39	-0.41	23.23	-22.21	3.03	4
AJ13	-0.77	-0.35	-0.39	33.52	-20.49	1.69	5
AJ13	-0.78	-0.36	-0.40	30.93	-20.38	1.07	5
AJ13	-0.78	-0.35	-0.40	31.33	-19.83	-0.17	5
AJ13	-0.77	-0.36	-0.39	33.17	-19.57	2.10	5
AJ13	-0.77	-0.36	-0.41	30.43	-17.88	0.81	5
AJ13	-0.78	-0.37	-0.39	31.48	-20.29	2.83	5
AJ14	-0.21	-0.20	-0.40	112.16	36.17	-3.97	6
AJ14	-0.20	-0.21	-0.40	114.31	37.75	-2.86	6
AJ14	-0.23	-0.19	-0.40	111.66	33.61	-4.37	6
AJ14	-0.21	-0.21	-0.40	112.66	36.36	-3.25	6
AJ14	-0.22	-0.21	-0.40	111.23	35.52	-3.59	6
AJ14	-0.25	-0.22	-0.39	107.94	31.06	-1.57	6

Jackknifed classification matrix: 83/84 (99% corrected classification).

Table 41. Detection and Identification of 56 unknown commercial apple juice samples using LDA training matrix above (Table 40) from **P1** (2 µM, at pH3, pH7, and pH13, buffered). All unknown samples could be assigned to the corresponding acids group defined by the training matrix according to the shortest Mahalanobis distance. According to the verification, no unknown samples was misclassified, representing an accuracy of 100%.

Sample	Fluorescence Response Pattern			Results LDA				Analyte	
#	**P1** (pH3)	**P1** (pH7)	**P1** (pH13)	SCORE1	SCORE2	SCORE3	Group	Identification	Verification
1	-0.75	-0.71	-0.66	-17.23	25.88	4.92	9	AJ4	AJ4
2	-0.93	-0.88	-0.77	-65.13	24.29	3.62	12	AJ7	AJ7
3	-0.76	-0.66	-0.65	-14.53	21.13	1.06	14	AJ9	AJ9
4	-0.77	-0.66	-0.64	-15.39	20.21	1.15	14	AJ9	AJ9
5	-0.22	-0.20	-0.40	111.71	34.73	-4.06	6	AJ14	AJ14
6	-0.91	-0.52	-0.55	-14.25	-11.88	-3.77	8	AJ3	AJ3
7	-0.82	-0.60	-0.46	6.13	-7.95	16.91	2	AJ10	AJ10

8	-0.95	-0.67	-0.68	-45.03	3.69	-4.90	1	AJ1	AJ1
9	-0.80	-0.61	-0.63	-15.80	12.31	-2.52	10	AJ5	AJ5
10	-0.80	-0.38	-0.40	27.13	-21.46	3.39	13	AJ8	AJ8
11	-0.92	-0.60	-0.49	-11.56	-15.79	10.41	3	AJ11	AJ11
12	-0.78	-0.36	-0.39	31.78	-20.08	2.10	5	AJ13	AJ13
13	-0.77	-0.37	-0.40	31.35	-19.42	2.63	5	AJ13	AJ13
14	-0.91	-0.51	-0.55	-14.37	-12.52	-4.42	8	AJ3	AJ3
15	-0.89	-0.46	-0.59	-15.47	-8.55	-13.40	7	AJ2	AJ2
16	-0.80	-0.61	-0.62	-14.62	12.39	-1.66	10	AJ5	AJ5
17	-0.80	-0.61	-0.62	-14.40	11.34	-1.65	10	AJ5	AJ5
18	-0.90	-0.47	-0.59	-17.08	-8.00	-13.07	7	AJ2	AJ2
19	-0.92	-0.59	-0.50	-12.40	-15.53	9.33	3	AJ11	AJ11
20	-0.95	-0.66	-0.67	-43.73	2.86	-6.22	1	AJ1	AJ1
21	-0.75	-0.71	-0.66	-17.96	25.44	4.58	9	AJ4	AJ4
22	-0.89	-0.48	-0.59	-16.46	-7.33	-12.65	7	AJ2	AJ2
23	-0.88	-0.43	-0.51	-1.36	-15.72	-7.69	11	AJ6	AJ6
24	-0.82	-0.60	-0.47	4.69	-6.79	15.62	2	AJ10	AJ10
25	-0.95	-0.65	-0.67	-42.98	1.99	-6.37	1	AJ1	AJ1
26	-0.93	-0.88	-0.77	-65.15	24.26	3.42	12	AJ7	AJ7
27	-0.21	-0.21	-0.40	112.41	35.73	-2.09	6	AJ14	AJ14
28	-0.80	-0.37	-0.42	24.46	-20.11	0.00	4	AJ12	AJ12
29	-0.20	-0.20	-0.40	113.79	36.78	-3.53	6	AJ14	AJ14
30	-0.95	-0.68	-0.68	-44.51	4.23	-4.76	1	AJ1	AJ1
31	-0.76	-0.67	-0.64	-13.75	20.94	2.93	14	AJ9	AJ9
32	-0.91	-0.52	-0.55	-14.81	-12.79	-3.78	8	AJ3	AJ3
33	-0.90	-0.47	-0.61	-19.40	-6.24	-15.72	7	AJ2	AJ2
34	-0.80	-0.34	-0.41	27.57	-22.18	-1.56	13	AJ8	AJ8
35	-0.76	-0.66	-0.65	-16.12	21.08	0.77	14	AJ9	AJ9
36	-0.92	-0.59	-0.50	-11.58	-15.82	9.36	3	AJ11	AJ11
37	-0.75	-0.71	-0.65	-16.92	24.91	5.44	9	AJ4	AJ4
38	-0.82	-0.59	-0.46	6.04	-8.37	15.55	2	AJ10	AJ10
39	-0.81	-0.39	-0.42	22.39	-20.73	0.89	4	AJ12	AJ12
40	-0.91	-0.52	-0.54	-13.20	-13.63	-2.71	8	AJ3	AJ3
41	-0.92	-0.59	-0.49	-11.45	-16.25	9.66	3	AJ11	AJ11
42	-0.88	-0.40	-0.50	0.84	-18.10	-9.28	11	AJ6	AJ6
43	-0.79	-0.37	-0.40	28.79	-20.40	1.40	13	AJ8	AJ8
44	-0.76	-0.71	-0.66	-18.10	24.82	3.76	9	AJ4	AJ4
45	-0.81	-0.39	-0.42	22.41	-19.81	0.69	4	AJ12	AJ12
46	-0.88	-0.41	-0.50	0.87	-17.42	-8.07	11	AJ6	AJ6
47	-0.80	-0.61	-0.63	-15.72	12.95	-2.54	10	AJ5	AJ5
48	-0.81	-0.39	-0.42	22.19	-20.79	1.11	4	AJ12	AJ12
49	-0.93	-0.88	-0.77	-64.96	24.39	3.34	12	AJ7	AJ7
50	-0.82	-0.59	-0.47	5.83	-7.29	14.59	2	AJ10	AJ10
51	-0.78	-0.37	-0.40	30.74	-19.66	2.29	5	AJ13	AJ13
52	-0.88	-0.41	-0.51	0.32	-17.64	-9.25	11	AJ6	AJ6
53	-0.78	-0.37	-0.39	31.59	-20.18	2.95	5	AJ13	AJ13
54	-0.79	-0.36	-0.40	28.73	-21.34	1.01	13	AJ8	AJ8
55	-0.26	-0.21	-0.39	107.53	30.61	-2.57	6	AJ14	AJ14
56	-0.93	-0.88	-0.77	-64.89	24.06	3.73	12	AJ7	AJ7

Verification of unknown samples: 56/56 (100% accuracy).

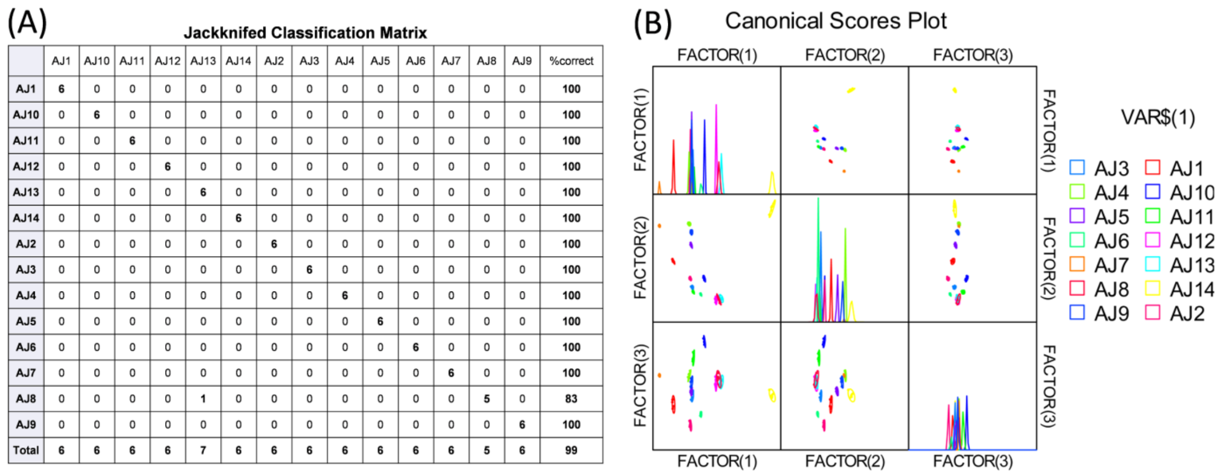

	AJ1	AJ10	AJ11	AJ12	AJ13	AJ14	AJ2	AJ3	AJ4	AJ5	AJ6	AJ7	AJ8	AJ9	%correct
AJ1	6	0	0	0	0	0	0	0	0	0	0	0	0	0	100
AJ10	0	6	0	0	0	0	0	0	0	0	0	0	0	0	100
AJ11	0	0	6	0	0	0	0	0	0	0	0	0	0	0	100
AJ12	0	0	0	6	0	0	0	0	0	0	0	0	0	0	100
AJ13	0	0	0	0	6	0	0	0	0	0	0	0	0	0	100
AJ14	0	0	0	0	0	6	0	0	0	0	0	0	0	0	100
AJ2	0	0	0	0	0	0	6	0	0	0	0	0	0	0	100
AJ3	0	0	0	0	0	0	0	6	0	0	0	0	0	0	100
AJ4	0	0	0	0	0	0	0	0	6	0	0	0	0	0	100
AJ5	0	0	0	0	0	0	0	0	0	6	0	0	0	0	100
AJ6	0	0	0	0	0	0	0	0	0	0	6	0	0	0	100
AJ7	0	0	0	0	0	0	0	0	0	0	0	6	0	0	100
AJ8	0	0	0	0	1	0	0	0	0	0	0	0	5	0	83
AJ9	0	0	0	0	0	0	0	0	0	0	0	0	0	6	100
Total	6	6	6	6	7	6	6	6	6	6	6	6	5	6	99

Figure 110. (A) Jackknifed classification matrix and **(B)** Canonical scores plots obtained from assay for negatively charged water-soluble **P1** (2 µM, at pH 3, pH7, and pH13, buffered) against commercial apple juice samples AJ1-AJ14 (50 µl).

Table 42. Training matrix of fluorescence response pattern from negatively charged water-soluble **P1** (2 µM, at pH3, pH7, and pH13, buffered) against commercial black currant juice samples BJ1-BJ5 (50 µl). LDA was carried out resulting in the three factors of the canonical scores and group generation.

Analytes	Fluorescence Response Pattern			Results LDA			
Juice	**P1** (pH3)	**P1** (pH7)	**P1** (pH13)	SCORE1	SCORE2	SCORE3	Group
BJ1	-0.85	-0.97	-0.75	16.74	7.09	-1.03	1
BJ1	-0.84	-0.97	-0.74	15.00	10.29	-1.77	1
BJ1	-0.85	-0.97	-0.76	15.20	7.55	0.97	1
BJ1	-0.85	-0.97	-0.74	13.74	7.57	-1.34	1
BJ1	-0.85	-0.97	-0.74	14.43	8.01	-1.88	1
BJ1	-0.85	-0.97	-0.75	14.00	8.72	-0.87	1
BJ2	-0.92	-0.98	-0.78	-14.01	5.42	1.89	2
BJ2	-0.92	-0.98	-0.79	-14.17	3.73	3.41	2
BJ2	-0.92	-0.98	-0.77	-13.82	4.53	1.24	2
BJ2	-0.92	-0.98	-0.78	-16.41	3.91	2.25	2
BJ2	-0.92	-0.98	-0.79	-13.88	3.09	3.67	2
BJ2	-0.92	-0.98	-0.78	-14.87	3.21	2.65	2
BJ3	-0.86	-0.96	-0.79	20.94	-8.03	3.57	3
BJ3	-0.86	-0.96	-0.77	21.91	-8.59	0.25	3
BJ3	-0.87	-0.96	-0.78	19.37	-10.30	1.20	3
BJ3	-0.87	-0.96	-0.77	20.84	-8.17	0.76	3
BJ3	-0.87	-0.96	-0.77	18.81	-8.92	-0.69	3
BJ3	-0.87	-0.96	-0.77	20.39	-8.69	0.14	3
BJ4	-0.96	-0.98	-0.78	-24.80	-3.61	-0.98	4
BJ4	-0.96	-0.98	-0.77	-24.86	-4.32	-2.13	4
BJ4	-0.96	-0.98	-0.77	-24.23	-5.34	-2.03	4
BJ4	-0.96	-0.98	-0.78	-24.27	-5.00	-1.67	4
BJ4	-0.96	-0.98	-0.78	-26.11	-3.73	-0.44	4
BJ4	-0.96	-0.98	-0.78	-24.69	-4.73	-1.75	4
BJ5	-0.89	-0.97	-0.76	4.76	0.33	-1.82	5
BJ5	-0.88	-0.97	-0.76	5.03	2.33	-0.88	5
BJ5	-0.89	-0.97	-0.76	2.12	0.96	-0.13	5
BJ5	-0.88	-0.97	-0.76	4.00	2.89	-0.21	5
BJ5	-0.89	-0.97	-0.76	4.54	-0.62	-0.76	5
BJ5	-0.89	-0.97	-0.76	4.33	0.43	-1.62	5

Jackknifed classification matrix: 30/30 (100% corrected classification)

Table 43. Detection and Identification of 20 unknown commercial black currant juice samples using LDA training matrix (Table 42) from **P1** (2 µM, at pH3, pH7, and pH13, buffered). All unknown samples could be assigned to the corresponding acids group defined by the training matrix according to the shortest Mahalanobis distance. According to the verification, no unknown samples was misclassified, representing an accuracy of 100%.

Sample	Fluorescence Response Pattern			Results LDA				Analyte	
#	**P1** (pH3)	**P1** (pH7)	**P1** (pH13)	SCORE1	SCORE2	SCORE3	Group	Identification	Verification
1	-0.87	-0.96	-0.78	17.90	-9.31	1.23	3	BJ3	BJ3
2	-0.87	-0.96	-0.79	19.87	-9.01	3.54	3	BJ3	BJ3
3	-0.88	-0.97	-0.76	3.36	2.49	0.01	5	BJ5	BJ5
4	-0.85	-0.97	-0.75	14.44	6.69	0.04	1	BJ1	BJ1
5	-0.89	-0.97	-0.76	2.87	2.96	-0.33	5	BJ5	BJ5

6	-0.92	-0.98	-0.79	-15.23	3.24	3.71	2	BJ2	BJ2
7	-0.85	-0.97	-0.75	15.88	5.84	-0.95	1	BJ1	BJ1
8	-0.96	-0.98	-0.78	-25.86	-3.35	-1.43	4	BJ4	BJ4
9	-0.87	-0.96	-0.78	18.65	-8.56	1.96	3	BJ3	BJ3
10	-0.96	-0.98	-0.78	-25.77	-2.82	-1.23	4	BJ4	BJ4
11	-0.89	-0.97	-0.76	1.82	1.87	-0.71	5	BJ5	BJ5
12	-0.92	-0.98	-0.79	-14.29	2.29	4.27	2	BJ2	BJ2
13	-0.96	-0.98	-0.78	-24.10	-4.10	-1.00	4	BJ4	BJ4
14	-0.92	-0.98	-0.79	-15.64	3.36	3.96	2	BJ2	BJ2
15	-0.85	-0.97	-0.74	13.17	8.02	-1.30	1	BJ1	BJ1
16	-0.89	-0.97	-0.76	2.85	2.48	-0.62	5	BJ5	BJ5
17	-0.88	-0.96	-0.77	16.76	-9.09	0.44	3	BJ3	BJ3
18	-0.96	-0.98	-0.78	-26.21	-3.69	-1.21	4	BJ4	BJ4
19	-0.93	-0.99	-0.80	-17.30	2.69	4.89	2	BJ2	BJ2
20	-0.85	-0.97	-0.77	15.91	4.38	2.73	1	BJ1	BJ1

Verification of unknown samples: 20/20 (100% accuracy).

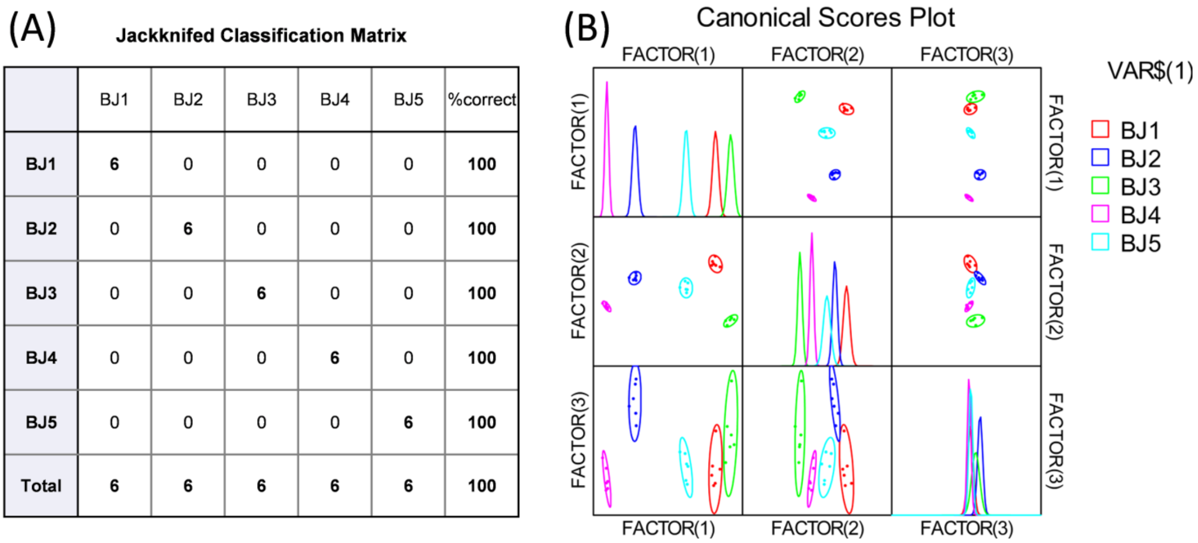

	BJ1	BJ2	BJ3	BJ4	BJ5	%correct
BJ1	6	0	0	0	0	100
BJ2	0	6	0	0	0	100
BJ3	0	0	6	0	0	100
BJ4	0	0	0	6	0	100
BJ5	0	0	0	0	6	100
Total	6	6	6	6	6	100

Figure 111. (A) Jackknifed classification matrix and **(B)** Canonical scores plots obtained from assay for negatively charged water-soluble **P1** (2 µM, at pH 3, pH7, and pH13, buffered) against commercial black currant juice samples BJ1-BJ5 (50 µl).

Table 44. Training matrix of fluorescence response pattern from negatively charged water-soluble **P1** (2 µM, at pH3, pH7, and pH13, buffered) against commercial grape juice samples GJ1-GJ6 (50 µl). LDA was carried out resulting in the three factors of the canonical scores and group generation.

Analytes	Fluorescence Response Pattern			Results LDA			
Grape juice	**P1** (pH3)	**P1** (pH7)	**P1** (pH13)	SCORE1	SCORE2	SCORE3	Group
GJ1	-0.94	-0.90	-0.62	-15.82	2.08	-4.91	1
GJ1	-0.94	-0.90	-0.62	-15.35	1.92	-3.85	1
GJ1	-0.94	-0.90	-0.62	-15.79	1.73	-4.90	1
GJ1	-0.94	-0.90	-0.62	-16.42	2.13	-4.23	1
GJ1	-0.94	-0.90	-0.62	-16.15	2.36	-5.18	1
GJ1	-0.94	-0.91	-0.62	-16.60	3.30	-5.32	1
GJ2	-0.95	-0.96	-0.69	-35.44	-7.23	1.64	2
GJ2	-0.94	-0.96	-0.69	-35.84	-6.48	2.46	2
GJ2	-0.95	-0.96	-0.69	-36.16	-5.70	1.42	2
GJ2	-0.95	-0.96	-0.69	-35.47	-7.37	0.81	2
GJ2	-0.95	-0.96	-0.69	-35.55	-6.64	1.74	2
GJ2	-0.95	-0.96	-0.69	-34.83	-7.65	1.39	2
GJ3	-0.91	-0.87	-0.62	-5.85	8.72	3.45	3
GJ3	-0.91	-0.88	-0.62	-8.31	10.14	3.28	3
GJ3	-0.91	-0.88	-0.63	-8.57	6.56	3.72	3
GJ3	-0.91	-0.89	-0.63	-9.52	9.24	4.93	3
GJ3	-0.91	-0.89	-0.63	-9.43	7.41	4.48	3
GJ3	-0.91	-0.88	-0.61	-8.45	10.31	1.48	3
GJ4	-0.91	-0.80	-0.60	16.70	0.09	-0.10	4
GJ4	-0.91	-0.80	-0.60	15.89	-0.73	0.08	4
GJ4	-0.91	-0.81	-0.61	15.02	0.19	1.48	4
GJ4	-0.91	-0.81	-0.60	14.98	1.00	-0.18	4
GJ4	-0.91	-0.81	-0.61	14.81	-0.27	0.53	4
GJ4	-0.91	-0.81	-0.60	14.25	1.27	0.82	4

GJ5	-0.91	-0.80	-0.59	18.27	3.26	0.36	5
GJ5	-0.92	-0.80	-0.59	16.07	0.53	-3.93	5
GJ5	-0.92	-0.81	-0.60	14.62	-0.19	-1.23	4
GJ5	-0.92	-0.80	-0.58	16.88	1.29	-3.89	5
GJ5	-0.92	-0.81	-0.59	14.99	1.08	-2.35	5
GJ5	-0.92	-0.80	-0.59	16.06	0.29	-2.19	5
GJ6	-0.91	-0.76	-0.61	29.85	-6.70	1.49	6
GJ6	-0.91	-0.76	-0.60	29.28	-4.61	1.19	6
GJ6	-0.91	-0.76	-0.61	27.99	-5.13	2.83	6
GJ6	-0.91	-0.76	-0.60	29.03	-6.35	0.57	6
GJ6	-0.91	-0.76	-0.61	28.24	-5.54	1.86	6
GJ6	-0.91	-0.77	-0.60	26.62	-4.32	0.25	6

Jackknifed classification matrix: 35/36 (97% corrected classification).

Table 45. Detection and Identification of 24 unknown commercial grape juice samples using LDA training matrix (Table 44) from **P1** (2 µM, at pH3, pH7, and pH13, buffered). All unknown samples could be assigned to the corresponding acids group defined by the training matrix according to the shortest Mahalanobis distance. According to the verification, 2 of the 24 samples were misclassified, representing an accuracy of 92%.

Sample	Fluorescence Response Pattern			Results LDA				Analyte	
#	**P1** (pH3)	**P1** (pH7)	**P1** (pH13)	SCORE1	SCORE2	SCORE3	Group	Identification	Verification
1	-0.94	-0.91	-0.63	-16.80	2.19	-3.71	1	GJ1	GJ1
2	-0.91	-0.88	-0.62	-8.37	9.04	4.10	3	GJ3	GJ3
3	-0.91	-0.81	-0.60	13.58	1.23	-0.11	4	GJ4	GJ4
4	-0.92	-0.81	-0.59	14.62	1.87	-2.02	5	GJ5	GJ5
5	-0.91	-0.76	-0.60	28.87	-4.94	1.11	6	GJ6	GJ6
6	-0.91	-0.80	-0.59	15.77	3.03	-1.48	5	GJ5	GJ4
7	-0.94	-0.91	-0.62	-16.81	2.81	-4.35	1	GJ1	GJ1
8	-0.94	-0.96	-0.68	-35.58	-4.88	1.49	2	GJ2	GJ2
9	-0.92	-0.79	-0.59	18.57	-1.16	-4.10	5	GJ5	GJ5
10	-0.91	-0.88	-0.62	-6.77	7.72	2.70	3	GJ3	GJ3
11	-0.91	-0.76	-0.60	29.11	-4.64	-0.01	6	GJ6	GJ6
12	-0.95	-0.96	-0.69	-35.97	-7.44	1.73	2	GJ2	GJ2
13	-0.94	-0.90	-0.63	-16.04	1.80	-4.00	1	GJ1	GJ1
14	-0.91	-0.88	-0.63	-8.07	7.10	4.71	3	GJ3	GJ3
15	-0.92	-0.81	-0.59	14.14	2.48	-2.39	5	GJ5	GJ4
16	-0.92	-0.81	-0.60	14.82	-1.10	-2.90	5	GJ5	GJ5
17	-0.95	-0.96	-0.69	-35.86	-5.67	1.46	2	GJ2	GJ2
18	-0.91	-0.76	-0.60	28.89	-4.80	1.19	6	GJ6	GJ6
19	-0.95	-0.96	-0.69	-35.33	-5.57	1.63	2	GJ2	GJ2
20	-0.91	-0.81	-0.60	14.86	0.00	0.08	4	GJ4	GJ4
21	-0.91	-0.88	-0.62	-8.49	8.65	3.36	3	GJ3	GJ3
22	-0.91	-0.76	-0.60	30.24	-5.53	0.49	6	GJ6	GJ6
23	-0.94	-0.91	-0.62	-16.33	3.69	-5.39	1	GJ1	GJ1
24	-0.92	-0.80	-0.59	17.98	-0.12	-1.68	5	GJ5	GJ5

Verification of unknown samples: 22/24 (92% accuracy).

(A) Jackknifed Classification Matrix

	GJ1	GJ2	GJ3	GJ4	GJ5	GJ6	%correct
GJ1	6	0	0	0	0	0	100
GJ2	0	6	0	0	0	0	100
GJ3	0	0	6	0	0	0	100
GJ4	0	0	0	6	0	0	100
GJ5	0	0	0	2	4	0	67
GJ6	0	0	0	0	0	6	100
Total	6	6	6	8	4	6	94

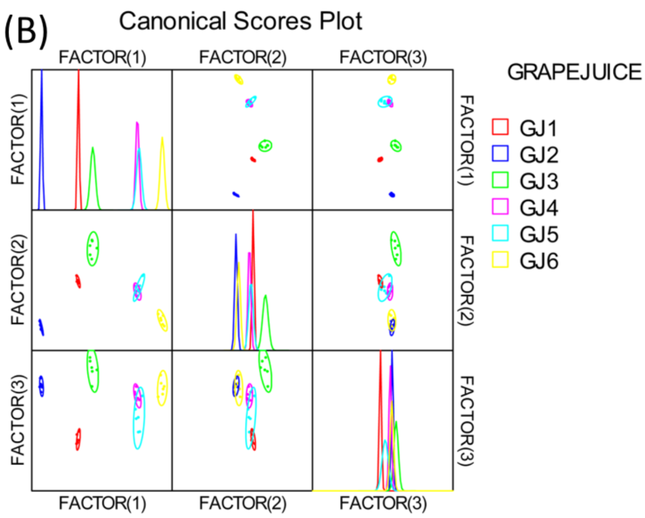

Figure 112. (A) Jackknifed classification matrix and **(B)** Canonical scores plots obtained from assay for negatively charged water-soluble **P1** (2 µM, at pH 3, pH7, and pH13, buffered) against commercial grape juice samples GJ1-GJ6 (50 µl).

Table 46. Training matrix of fluorescence response pattern from positively charged water-soluble **P2** (2 µM, at pH3, pH7, and pH13, buffered) against commercial apple juice samples AJ1-AJ14 (1 µl). LDA was carried out as described above resulting in the three factors of the canonical scores and group generation.

Analytes	Fluorescence Response Pattern			Results LDA			
Apple juice	**P2** (pH3)	**P2** (pH7)	**P2** (pH13)	SCORE1	SCORE2	SCORE3	Group
AJ1	-0.32	-0.58	-0.66	29.48	-10.81	7.53	1
AJ1	-0.31	-0.57	-0.66	29.10	-8.70	6.94	1
AJ1	-0.30	-0.56	-0.65	28.82	-8.02	6.96	1
AJ1	-0.31	-0.58	-0.65	28.45	-9.65	8.01	1
AJ1	-0.32	-0.58	-0.65	27.21	-10.45	7.47	1
AJ1	-0.33	-0.58	-0.66	30.06	-11.44	5.91	1
AJ2	-0.30	-0.50	-0.47	-9.37	-7.05	9.70	7
AJ2	-0.28	-0.49	-0.48	-6.33	-4.72	9.71	7
AJ2	-0.31	-0.50	-0.48	-7.21	-7.70	8.16	7
AJ2	-0.30	-0.49	-0.47	-8.15	-6.87	8.55	7
AJ2	-0.29	-0.51	-0.47	-9.12	-7.00	11.14	7
AJ2	-0.30	-0.50	-0.47	-9.14	-7.05	9.60	7
AJ3	-0.28	-0.46	-0.45	-12.30	-3.01	8.19	8
AJ3	-0.30	-0.47	-0.46	-11.02	-4.39	6.49	8
AJ3	-0.29	-0.46	-0.46	-11.15	-3.21	6.89	8
AJ3	-0.28	-0.46	-0.45	-11.97	-2.46	7.34	8
AJ3	-0.30	-0.48	-0.46	-11.26	-5.46	7.42	8
AJ3	-0.30	-0.48	-0.45	-13.22	-6.51	8.29	8
AJ4	-0.17	-0.46	-0.81	66.72	19.64	-0.35	9
AJ4	-0.16	-0.46	-0.81	66.05	20.42	0.14	9
AJ4	-0.16	-0.45	-0.81	67.02	21.01	-1.22	9
AJ4	-0.15	-0.46	-0.81	67.28	20.86	1.46	9
AJ4	-0.16	-0.46	-0.81	67.53	19.94	0.39	9
AJ4	-0.15	-0.47	-0.82	68.43	20.66	1.89	9
AJ5	-0.22	-0.44	-0.70	41.35	13.44	-1.63	10
AJ5	-0.22	-0.43	-0.70	41.30	14.17	-2.91	10
AJ5	-0.22	-0.44	-0.70	41.04	12.77	-1.97	10
AJ5	-0.22	-0.44	-0.70	42.78	12.98	-2.18	10
AJ5	-0.22	-0.44	-0.70	42.12	13.35	-1.96	10
AJ5	-0.23	-0.44	-0.70	40.97	12.04	-2.93	10
AJ6	-0.35	-0.42	-0.38	-29.43	-8.33	-0.72	11
AJ6	-0.33	-0.42	-0.38	-29.29	-6.40	1.92	11
AJ6	-0.35	-0.42	-0.38	-29.64	-7.67	0.59	11
AJ6	-0.35	-0.42	-0.37	-30.37	-8.03	1.04	11
AJ6	-0.33	-0.42	-0.38	-28.28	-6.45	1.38	11
AJ6	-0.34	-0.43	-0.38	-29.04	-8.42	1.98	11
AJ7	-0.48	-0.71	-0.88	68.42	-32.95	-4.59	12
AJ7	-0.48	-0.70	-0.88	68.04	-31.73	-6.99	12
AJ7	-0.50	-0.70	-0.88	66.74	-33.69	-8.38	12
AJ7	-0.50	-0.70	-0.88	67.82	-34.46	-8.10	12
AJ7	-0.48	-0.71	-0.88	67.45	-32.85	-4.95	12
AJ7	-0.48	-0.71	-0.88	68.32	-33.17	-5.52	12
AJ8	-0.31	-0.35	-0.30	-44.52	-0.59	0.30	13
AJ8	-0.31	-0.36	-0.29	-45.15	-0.59	0.91	13
AJ8	-0.31	-0.34	-0.30	-43.98	1.01	-1.68	13
AJ8	-0.31	-0.35	-0.30	-43.33	0.45	-0.23	13
AJ8	-0.32	-0.36	-0.31	-42.64	-1.22	-0.42	13
AJ8	-0.31	-0.35	-0.31	-42.39	0.06	-1.09	13
AJ9	-0.28	-0.40	-0.57	12.50	6.89	-5.56	14
AJ9	-0.26	-0.40	-0.56	10.99	8.07	-3.82	14
AJ9	-0.27	-0.39	-0.55	10.24	8.09	-4.54	14
AJ9	-0.27	-0.39	-0.55	9.94	7.52	-5.29	14
AJ9	-0.26	-0.39	-0.55	10.28	8.87	-3.48	14
AJ9	-0.28	-0.41	-0.56	10.05	5.50	-4.33	14
AJ10	-0.15	-0.38	-0.63	31.36	23.33	1.13	2
AJ10	-0.14	-0.38	-0.64	32.36	25.03	2.22	2
AJ10	-0.15	-0.36	-0.63	31.06	25.02	-1.19	2
AJ10	-0.14	-0.37	-0.64	32.51	25.40	0.39	2
AJ10	-0.15	-0.37	-0.64	32.89	24.72	0.56	2
AJ10	-0.16	-0.38	-0.65	33.48	23.17	0.34	2
AJ11	-0.40	-0.48	-0.47	-13.55	-16.55	-2.11	3
AJ11	-0.41	-0.47	-0.46	-15.81	-16.71	-3.91	3
AJ11	-0.42	-0.48	-0.47	-14.08	-17.42	-4.46	3
AJ11	-0.42	-0.47	-0.45	-16.86	-17.61	-4.01	3
AJ11	-0.41	-0.47	-0.46	-15.17	-16.98	-4.45	3
AJ11	-0.41	-0.49	-0.47	-14.04	-17.83	-2.92	3

AJ12	-0.34	-0.39	-0.35	-34.81	-4.81	-0.58	4
AJ12	-0.35	-0.40	-0.35	-35.73	-6.85	-1.28	4
AJ12	-0.34	-0.40	-0.34	-36.32	-6.50	-0.18	4
AJ12	-0.35	-0.41	-0.35	-34.20	-7.49	-0.31	4
AJ12	-0.35	-0.40	-0.36	-33.71	-6.74	-1.10	4
AJ12	-0.35	-0.41	-0.36	-32.40	-8.46	-0.33	4
AJ13	-0.31	-0.28	-0.26	-52.16	4.76	-5.63	5
AJ13	-0.31	-0.28	-0.26	-52.51	5.22	-6.10	5
AJ13	-0.30	-0.29	-0.26	-52.03	4.35	-4.03	5
AJ13	-0.31	-0.28	-0.27	-50.74	4.90	-5.98	5
AJ13	-0.32	-0.29	-0.26	-51.60	2.99	-6.47	5
AJ13	-0.31	-0.29	-0.27	-50.53	3.57	-5.42	5
AJ14	-0.23	-0.25	-0.23	-55.22	14.73	-0.59	6
AJ14	-0.24	-0.23	-0.23	-54.51	16.12	-4.01	6
AJ14	-0.23	-0.23	-0.24	-53.08	16.87	-3.90	6
AJ14	-0.23	-0.22	-0.23	-55.92	16.89	-3.51	6
AJ14	-0.24	-0.24	-0.23	-54.29	15.23	-2.24	6
AJ14	-0.23	-0.25	-0.24	-52.58	14.98	-1.43	6

Jackknifed classification matrix: 84/84 (100% corrected classification).

Table 47. Detection and Identification of 56 unknown commercial apple juice samples using LDA training matrix (Table 46) from **P2** (2 µM, at pH3, pH7, and pH13, buffered). All unknown samples could be assigned to the corresponding acids group defined by the training matrix according to the shortest Mahalanobis distance. According to the verification, 2 of the 56 samples were misclassified, representing an accuracy of 97%.

Sample	Fluorescence Response Pattern			Results LDA				Analyte	
#	**P2** (pH3)	**P2** (pH7)	**P2** (pH13)	SCORE1	SCORE2	SCORE3	Group	Identification	Verification
1	-0.23	-0.44	-0.69	40.40	11.55	-2.20	10	AJ5	AJ5
2	-0.31	-0.35	-0.30	-42.95	0.37	-0.47	13	AJ8	AJ8
3	-0.32	-0.34	-0.31	-42.55	0.05	-2.23	13	AJ8	AJ8
4	-0.26	-0.39	-0.55	8.55	8.34	-3.67	14	AJ9	AJ9
5	-0.14	-0.38	-0.65	35.69	25.55	1.34	2	AJ10	AJ10
6	-0.49	-0.71	-0.89	68.87	-33.89	-5.63	12	AJ7	AJ7
7	-0.30	-0.29	-0.26	-51.34	4.73	-4.63	5	AJ13	AJ13
8	-0.33	-0.57	-0.66	28.46	-11.04	5.48	1	AJ1	AJ1
9	-0.32	-0.48	-0.45	-14.10	-8.66	5.67	8	AJ3	AJ3
10	-0.15	-0.46	-0.81	66.85	21.01	1.28	9	AJ4	AJ4
11	-0.33	-0.51	-0.47	-10.64	-10.75	7.76	7	AJ2	AJ2
12	-0.36	-0.43	-0.38	-28.36	-9.67	0.68	11	AJ6	AJ6
13	-0.17	-0.46	-0.81	65.82	19.52	-0.02	9	AJ4	AJ4
14	-0.42	-0.47	-0.46	-16.25	-17.41	-4.24	3	AJ11	AJ11
15	-0.32	-0.57	-0.65	27.34	-10.23	6.98	1	AJ1	AJ1
16	-0.41	-0.47	-0.45	-16.59	-16.57	-4.21	3	AJ11	AJ11
17	-0.35	-0.41	-0.36	-34.23	-7.85	-0.82	4	AJ12	AJ12
18	-0.23	-0.23	-0.22	-57.45	15.88	-2.06	6	AJ14	AJ14
19	-0.30	-0.46	-0.45	-11.73	-4.47	6.03	8	AJ3	AJ3
20	-0.31	-0.48	-0.46	-10.80	-7.12	6.67	8	**AJ3**	**AJ2**
21	-0.49	-0.70	-0.88	68.25	-32.87	-6.50	12	AJ7	AJ7
22	-0.15	-0.38	-0.65	34.51	24.21	-0.08	2	AJ10	AJ10
23	-0.34	-0.43	-0.38	-29.40	-7.71	2.82	11	AJ6	AJ6
24	-0.31	-0.48	-0.45	-12.55	-6.74	7.51	8	AJ3	AJ3
25	-0.26	-0.41	-0.56	11.31	7.39	-1.41	14	AJ9	AJ9
26	-0.33	-0.29	-0.27	-50.75	2.23	-7.13	5	AJ13	AJ13
27	-0.32	-0.57	-0.66	29.91	-10.42	4.89	1	AJ1	AJ1
28	-0.32	-0.47	-0.46	-12.32	-7.31	4.43	8	AJ3	AJ3
29	-0.34	-0.43	-0.38	-27.55	-7.36	2.12	11	AJ6	AJ6
30	-0.15	-0.45	-0.82	68.93	22.51	-0.42	9	AJ4	AJ4
31	-0.23	-0.44	-0.69	39.45	11.69	-3.07	10	AJ5	AJ5
32	-0.14	-0.37	-0.65	34.67	26.31	0.59	2	AJ10	AJ10
33	-0.41	-0.47	-0.45	-17.01	-16.76	-3.53	3	AJ11	AJ11
34	-0.31	-0.48	-0.47	-8.57	-6.47	6.42	7	AJ2	AJ2
35	-0.31	-0.49	-0.46	-11.43	-7.98	7.07	8	**AJ3**	**AJ2**
36	-0.32	-0.58	-0.66	28.77	-10.58	7.18	1	AJ1	AJ1
37	-0.17	-0.45	-0.81	66.15	20.13	-1.07	9	AJ4	AJ4
38	-0.49	-0.71	-0.88	68.43	-33.09	-6.29	12	AJ7	AJ7
39	-0.26	-0.40	-0.55	9.36	8.34	-2.25	14	AJ9	AJ9
40	-0.36	-0.41	-0.36	-33.73	-8.28	-0.92	4	AJ12	AJ12
41	-0.33	-0.29	-0.28	-49.38	3.09	-7.75	5	AJ13	AJ13
42	-0.23	-0.43	-0.69	39.88	12.03	-3.97	10	AJ5	AJ5
43	-0.33	-0.35	-0.32	-41.53	-1.79	-3.51	13	AJ8	AJ8
44	-0.31	-0.35	-0.30	-43.40	-0.60	-0.18	13	AJ8	AJ8
45	-0.23	-0.24	-0.23	-54.34	16.19	-2.63	6	AJ14	AJ14

46	-0.26	-0.38	-0.54	8.33	9.53	-3.58	14	AJ9	AJ9
47	-0.23	-0.23	-0.24	-52.50	17.53	-3.56	6	AJ14	AJ14
48	-0.36	-0.41	-0.36	-32.84	-9.10	-1.81	4	AJ12	AJ12
49	-0.34	-0.41	-0.36	-32.75	-6.81	1.23	4	AJ12	AJ12
50	-0.33	-0.42	-0.39	-26.43	-6.19	1.03	11	AJ6	AJ6
51	-0.49	-0.70	-0.88	67.96	-33.02	-6.69	12	AJ7	AJ7
52	-0.15	-0.36	-0.66	35.67	25.82	-2.80	2	AJ10	AJ10
53	-0.22	-0.44	-0.69	40.67	13.04	-1.67	10	AJ5	AJ5
54	-0.41	-0.47	-0.45	-16.32	-16.90	-4.00	3	AJ11	AJ11
55	-0.32	-0.29	-0.27	-51.09	3.58	-6.04	5	AJ13	AJ13
56	-0.24	-0.24	-0.23	-55.80	14.62	-2.24	6	AJ14	AJ14

Verification of unknown samples: 54/56 (97% accuracy).

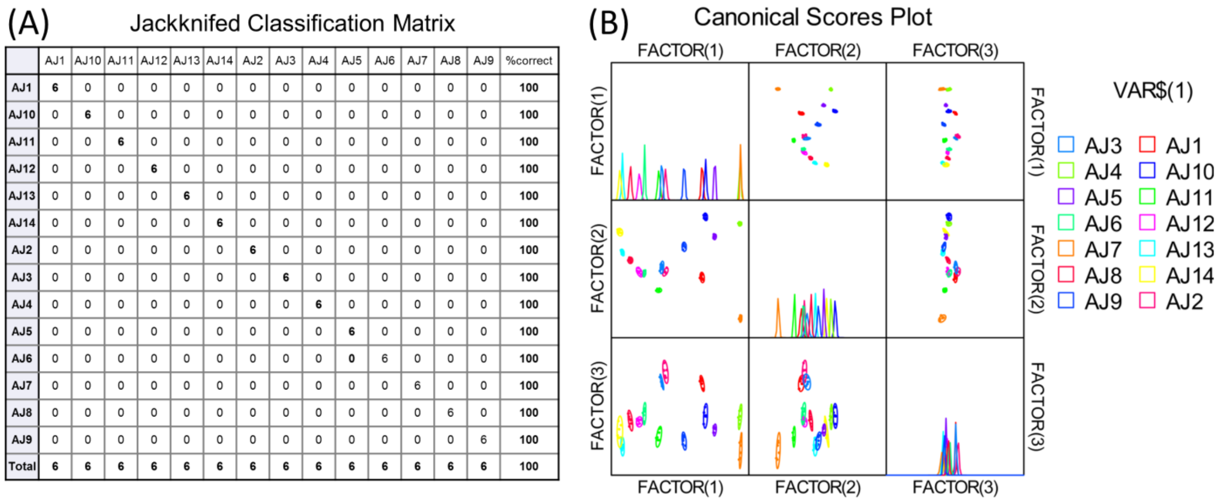

	AJ1	AJ10	AJ11	AJ12	AJ13	AJ14	AJ2	AJ3	AJ4	AJ5	AJ6	AJ7	AJ8	AJ9	%correct
AJ1	6	0	0	0	0	0	0	0	0	0	0	0	0	0	100
AJ10	0	6	0	0	0	0	0	0	0	0	0	0	0	0	100
AJ11	0	0	6	0	0	0	0	0	0	0	0	0	0	0	100
AJ12	0	0	0	6	0	0	0	0	0	0	0	0	0	0	100
AJ13	0	0	0	0	6	0	0	0	0	0	0	0	0	0	100
AJ14	0	0	0	0	0	6	0	0	0	0	0	0	0	0	100
AJ2	0	0	0	0	0	0	6	0	0	0	0	0	0	0	100
AJ3	0	0	0	0	0	0	0	6	0	0	0	0	0	0	100
AJ4	0	0	0	0	0	0	0	0	6	0	0	0	0	0	100
AJ5	0	0	0	0	0	0	0	0	0	6	0	0	0	0	100
AJ6	0	0	0	0	0	0	0	0	0	0	6	0	0	0	100
AJ7	0	0	0	0	0	0	0	0	0	0	0	6	0	0	100
AJ8	0	0	0	0	0	0	0	0	0	0	0	0	6	0	100
AJ9	0	0	0	0	0	0	0	0	0	0	0	0	0	6	100
Total	6	6	6	6	6	6	6	6	6	6	6	6	6	6	100

Figure 113. (A) Jackknifed classification matrix and **(B)** Canonical scores plots obtained from assay for water-soluble **P2** (2 µM, at pH 3, pH7, and pH13, buffered) against commercial apple juice samples AJ1-AJ14 (1 µl).

Table 48. Training matrix of fluorescence response pattern from water-soluble **P2** (2 µM, at pH3, pH7, and pH13, buffered) against commercial black currant juice samples **BJ1-BJ5** (1 µl). LDA was carried out resulting in the three factors of the canonical scores and group generation.

Analytes	Fluorescence Response Pattern			Results LDA			
Juice	**P2** (pH3)	**P2** (pH7)	**P2** (pH13)	SCORE1	SCORE2	SCORE3	Group
BJ1	-0.77	-0.99	-0.84	-2.28	6.42	-5.49	1
BJ1	-0.76	-0.98	-0.84	-1.72	6.32	-3.17	1
BJ1	-0.77	-0.99	-0.84	-2.34	6.34	-3.05	1
BJ1	-0.77	-0.98	-0.84	-2.38	5.85	-4.96	1
BJ1	-0.78	-0.99	-0.84	-3.50	4.60	-5.39	1
BJ1	-0.78	-0.98	-0.84	-2.98	5.02	-5.76	1
BJ2	-0.79	-0.98	-0.88	-8.47	-4.03	4.66	2
BJ2	-0.78	-0.98	-0.87	-6.87	-1.51	3.14	2
BJ2	-0.78	-0.98	-0.88	-8.94	-3.04	6.12	2
BJ2	-0.78	-0.98	-0.88	-7.54	-3.11	3.34	2
BJ2	-0.79	-0.98	-0.88	-8.91	-4.19	5.37	2
BJ2	-0.78	-0.98	-0.88	-7.17	-3.41	4.82	2
BJ3	-0.73	-0.98	-0.84	4.25	6.66	3.02	3
BJ3	-0.73	-0.98	-0.84	3.46	7.37	4.17	3
BJ3	-0.73	-0.98	-0.85	3.32	5.87	4.21	3
BJ3	-0.73	-0.97	-0.84	5.71	5.01	3.88	3
BJ3	-0.73	-0.98	-0.85	2.47	6.17	4.00	3
BJ3	-0.73	-0.98	-0.84	3.56	7.42	3.80	3
BJ4	-0.72	-0.95	-0.84	18.61	-3.93	-1.76	4
BJ4	-0.71	-0.95	-0.84	18.33	-3.32	-0.19	4
BJ4	-0.71	-0.94	-0.84	22.10	-4.82	-1.61	4
BJ4	-0.71	-0.94	-0.84	19.79	-4.38	0.38	4
BJ4	-0.72	-0.94	-0.84	18.77	-5.73	-1.87	4
BJ4	-0.72	-0.94	-0.84	17.98	-5.70	-1.98	4
BJ5	-0.82	-0.99	-0.87	-13.34	-3.91	-4.23	5
BJ5	-0.81	-0.99	-0.87	-12.85	-2.54	-1.98	5
BJ5	-0.82	-0.99	-0.87	-12.74	-3.62	-3.49	5
BJ5	-0.81	-0.99	-0.88	-12.26	-4.22	-2.20	5
BJ5	-0.82	-0.99	-0.88	-11.90	-5.45	-2.07	5
BJ5	-0.82	-0.98	-0.88	-12.15	-6.15	-1.71	5

Jackknifed classification matrix: 30/30 (100% corrected classification).

Table 49. Detection and Identification of 20 unknown commercial black currant juice samples using LDA training matrix (Table 48) from **P2** (2 µM, at pH3, pH7, and pH13, buffered). All unknown samples could be assigned to the corresponding acids group defined by the training matrix according to the shortest Mahalanobis distance. According to the verification, no unknown samples was misclassified, representing an accuracy of 100%.

Sample	Fluorescence Response Pattern			Results LDA				Analyte	
#	**P2** (pH3)	**P2** (pH3)	**P2** (pH3)	SCORE1	SCORE2	SCORE3	Group	Identification	Verification
1	-0.78	-0.98	-0.88	-7.19	-3.27	6.25	2	BCJ2	BCJ2
2	-0.71	-0.94	-0.84	20.57	-3.75	-0.17	4	BCJ4	BCJ4
3	-0.81	-0.99	-0.87	-11.70	-3.05	-3.89	5	BCJ5	BCJ5
4	-0.78	-0.98	-0.83	-1.87	6.13	-7.59	1	BCJ1	BCJ1
5	-0.72	-0.98	-0.84	3.03	8.17	5.85	3	BCJ3	BCJ3
6	-0.71	-0.95	-0.84	17.72	-3.28	1.04	4	BCJ4	BCJ4
7	-0.78	-0.98	-0.88	-6.08	-4.67	4.89	2	BCJ2	BCJ2
8	-0.78	-0.98	-0.87	-6.24	-3.34	1.85	2	BCJ2	BCJ2
9	-0.71	-0.95	-0.84	19.08	-3.66	-0.37	4	BCJ4	BCJ4
10	-0.82	-0.99	-0.88	-14.00	-6.15	-1.45	5	BCJ5	BCJ5
11	-0.77	-0.98	-0.83	-1.22	6.42	-6.78	1	BCJ1	BCJ1
12	-0.81	-0.98	-0.87	-10.98	-4.94	-3.19	5	BCJ5	BCJ5
13	-0.78	-0.99	-0.83	-2.26	6.22	-7.92	1	BCJ1	BCJ1
14	-0.72	-0.98	-0.84	4.33	7.29	4.37	3	BCJ3	BCJ3
15	-0.71	-0.95	-0.84	19.03	-3.02	-0.20	4	BCJ4	BCJ4
16	-0.78	-0.98	-0.88	-8.23	-2.95	4.31	2	BCJ2	BCJ2
17	-0.72	-0.98	-0.84	5.34	8.17	4.56	3	BCJ3	BCJ3
18	-0.82	-0.99	-0.87	-12.13	-4.68	-4.72	5	BCJ5	BCJ5
19	-0.78	-0.98	-0.83	-2.02	6.25	-7.52	1	BCJ1	BCJ1
20	-0.72	-0.98	-0.84	4.79	7.09	4.06	3	BCJ3	BCJ3

Verification of unknown samples: 20/20 (100% accuracy).

(A) Jackknifed Classification Matrix

	BCJ1	BCJ2	BCJ3	BCJ4	BCJ5	%correct
BCJ1	**6**	0	0	0	0	**100**
BCJ2	0	**6**	0	0	0	**100**
BCJ3	0	0	**6**	0	0	**100**
BCJ4	0	0	0	**6**	0	**100**
BCJ5	0	0	0	0	**6**	**100**
Total	**6**	**6**	**6**	**6**	**6**	**100**

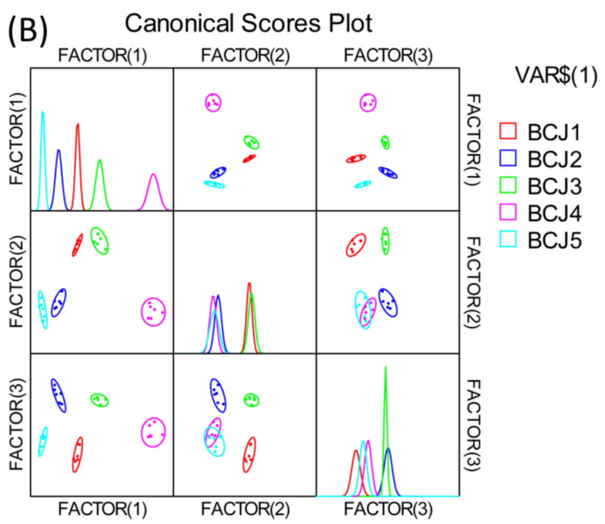

Figure 114. (A) Jackknifed classification matrix and **(B)** Canonical scores plots obtained from assay for water-soluble **P2** (2 µM, at pH 3, pH7, and pH13, buffered) against commercial black currant juice samples **BJ1-BJ5** (1 µl).

Table 50. Training matrix of fluorescence response pattern from water-soluble **P2** (2 µM, at pH3, pH7, and pH13, buffered) against commercial grape juice samples GJ1-GJ6 (1 µl). LDA was carried out resulting in the three factors of the canonical scores and group generation.

Analytes	Fluorescence Response Pattern			Results LDA			
Grape juice	**P2** (pH3)	**P2** (pH7)	**P2** (pH13)	SCORE1	SCORE2	SCORE3	Group
GJ1	-0.44	-0.65	-0.76	1.14	-9.25	-0.32	1
GJ1	-0.43	-0.65	-0.76	1.92	-10.22	0.05	1
GJ1	-0.43	-0.65	-0.75	3.26	-9.02	-0.53	1
GJ1	-0.42	-0.66	-0.75	2.11	-7.21	1.12	1
GJ1	-0.43	-0.65	-0.75	2.33	-8.65	-0.38	1
GJ1	-0.44	-0.65	-0.75	2.59	-8.35	-0.96	1
GJ2	-0.56	-0.80	-0.87	-22.74	-1.94	-2.21	2
GJ2	-0.56	-0.80	-0.86	-21.70	-0.89	-2.72	2
GJ2	-0.55	-0.79	-0.86	-21.21	-1.73	-1.40	2

GJ2	-0.54	-0.79	-0.87	-21.72	-1.90	0.12	2
GJ2	-0.55	-0.80	-0.86	-21.87	-0.80	-0.76	2
GJ2	-0.55	-0.80	-0.87	-22.67	-1.28	-1.18	2
GJ3	-0.48	-0.80	-0.80	-11.76	6.04	0.54	3
GJ3	-0.48	-0.79	-0.80	-11.54	4.82	0.58	3
GJ3	-0.46	-0.79	-0.79	-10.57	6.29	2.08	3
GJ3	-0.45	-0.80	-0.79	-10.91	6.98	2.83	3
GJ3	-0.46	-0.80	-0.80	-11.69	6.98	2.39	3
GJ3	-0.47	-0.81	-0.80	-12.45	8.09	1.82	3
GJ4	-0.40	-0.65	-0.71	8.49	-5.26	-0.31	4
GJ4	-0.39	-0.65	-0.72	7.97	-4.89	1.53	4
GJ4	-0.36	-0.64	-0.72	8.93	-5.20	3.47	4
GJ4	-0.37	-0.65	-0.72	7.95	-4.18	3.32	4
GJ4	-0.39	-0.67	-0.72	6.24	-2.44	1.80	4
GJ4	-0.40	-0.67	-0.72	5.85	-2.44	1.27	4
GJ5	-0.39	-0.67	-0.68	11.88	0.56	-1.61	5
GJ5	-0.38	-0.67	-0.68	11.94	1.32	-0.91	5
GJ5	-0.37	-0.66	-0.68	12.97	0.65	-0.06	5
GJ5	-0.39	-0.67	-0.67	12.11	1.09	-2.28	5
GJ5	-0.38	-0.67	-0.69	10.70	0.71	-0.48	5
GJ5	-0.40	-0.68	-0.69	8.95	-0.02	-1.46	5
GJ6	-0.37	-0.70	-0.65	13.11	7.61	-1.85	6
GJ6	-0.37	-0.70	-0.67	11.28	5.84	0.17	6
GJ6	-0.36	-0.70	-0.65	13.67	8.29	-1.13	6
GJ6	-0.37	-0.71	-0.66	11.99	7.52	-0.22	6
GJ6	-0.37	-0.70	-0.68	10.86	5.10	-0.18	6
GJ6	-0.38	-0.71	-0.66	12.57	7.75	-2.15	6

Jackknifed classification matrix: 36/36 (100% corrected classification).

Table 51. Detection and Identification of 24 unknown commercial grape juice samples using LDA training matrix (Table 50) from **P2** (2 µM, at pH3, pH7, and pH13, buffered). All unknown samples could be assigned to the corresponding acids group defined by the training matrix according to the shortest Mahalanobis distance. According to the verification, none of the samples were misclassified, representing an accuracy of 100%.

Sample	Fluorescence Response Pattern			Results LDA				Analyte	
#	**P2** (pH3)	**P2** (pH7)	**P2** (pH13)	SCORE1	SCORE2	SCORE3	Group	Identification	Verification
1	-0.42	-0.65	-0.75	2.83	-9.27	0.81	1	GJ1	GJ1
2	-0.45	-0.79	-0.80	-10.67	6.35	3.91	3	GJ3	GJ3
3	-0.40	-0.66	-0.71	7.46	-4.16	-0.62	4	GJ4	GJ4
4	-0.38	-0.70	-0.66	12.82	6.23	-2.73	6	GJ6	GJ6
5	-0.42	-0.65	-0.76	2.30	-8.76	0.85	1	GJ1	GJ1
6	-0.36	-0.65	-0.73	7.43	-4.34	4.54	4	GJ4	GJ4
7	-0.56	-0.80	-0.86	-22.22	-1.86	-2.05	2	GJ2	GJ2
8	-0.38	-0.67	-0.70	9.99	-0.75	0.32	5	GJ5	GJ5
9	-0.55	-0.80	-0.87	-22.11	-1.70	-0.60	2	GJ2	GJ2
10	-0.37	-0.67	-0.70	9.85	-0.97	1.53	5	GJ5	GJ5
11	-0.56	-0.79	-0.86	-21.53	-1.79	-2.13	2	GJ2	GJ2
12	-0.41	-0.67	-0.69	10.18	-0.42	-3.11	5	GJ5	GJ5
13	-0.38	-0.70	-0.65	13.35	7.89	-2.37	6	GJ6	GJ6
14	-0.42	-0.66	-0.76	0.97	-7.47	2.15	1	GJ1	GJ1
15	-0.39	-0.66	-0.72	6.97	-4.83	1.18	4	GJ4	GJ4
16	-0.57	-0.79	-0.87	-22.57	-2.89	-2.39	2	GJ2	GJ2
17	-0.37	-0.70	-0.68	10.85	5.31	0.41	6	GJ6	GJ6
18	-0.47	-0.80	-0.80	-11.98	5.65	1.64	3	GJ3	GJ3
19	-0.40	-0.66	-0.71	7.86	-4.10	-0.33	4	GJ4	GJ4
20	-0.37	-0.70	-0.67	11.52	6.59	0.00	6	GJ6	GJ6
21	-0.36	-0.67	-0.68	11.95	0.52	1.19	5	GJ5	GJ5
22	-0.45	-0.81	-0.80	-12.12	8.07	3.45	3	GJ3	GJ3
23	-0.44	-0.65	-0.76	1.34	-10.12	0.11	1	GJ1	GJ1
24	-0.46	-0.79	-0.80	-11.29	5.36	2.30	3	GJ3	GJ3

Verification of unknown samples: 24/24 (100% accuracy).

(A) Jackknifed Classification Matrix

	GJ1	GJ2	GJ3	GJ4	GJ5	GJ6	%correct
GJ1	6	0	0	0	0	0	100
GJ2	0	6	0	0	0	0	100
GJ3	0	0	6	0	0	0	100
GJ4	0	0	0	6	0	0	100
GJ5	0	0	0	0	6	0	100
GJ6	0	0	0	0	0	6	100
Total	6	6	6	6	6	6	100

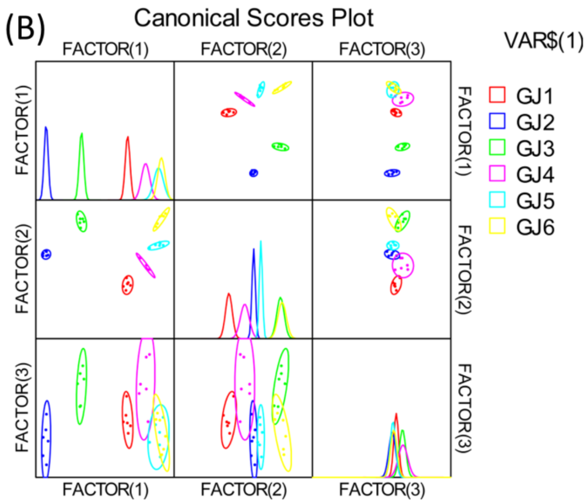

Figure 115. **(A)** Jackknifed classification matrix and **(B)** Canonical scores plots obtained from assay for water-soluble **P2** (2 µM, at pH 3, pH7, and pH13, buffered) against commercial grape juice samples GJ1-GJ6 (1 µl).

Table 52. Training matrix of fluorescence response pattern from water-soluble **P2** (2 µM, at pH3, pH7, and pH13, buffered) against juice mixtures (1 µl). LDA was carried out resulting in the three factors of the canonical scores and group generation.

Analytes	Fluorescence Response Pattern			Results LDA			
Mix juice	**P2** (pH3)	**P2** (pH7)	**P2**(pH13)	SCORE1	SCORE2	SCORE3	Group
BJ4-GJ1 (9:1)	-0.66	-0.92	-0.79	-19.73	8.75	-3.55	13
BJ4-GJ1 (9:1)	-0.65	-0.92	-0.79	-19.85	9.00	-3.32	13
BJ4-GJ1 (9:1)	-0.65	-0.92	-0.79	-19.56	9.10	-3.51	13
BJ4-GJ1 (8:2)	-0.63	-0.90	-0.76	-14.13	9.61	-6.50	12
BJ4-GJ1 (8:2)	-0.63	-0.90	-0.76	-13.75	9.25	-6.59	12
BJ4-GJ1 (8:2)	-0.63	-0.89	-0.76	-13.28	9.00	-5.46	12
BJ4-GJ1 (7:3)	-0.61	-0.86	-0.77	-6.83	4.87	-4.58	11
BJ4-GJ1 (7:3)	-0.61	-0.86	-0.77	-7.54	4.20	-3.65	11
BJ4-GJ1 (7:3)	-0.61	-0.86	-0.77	-7.22	5.33	-3.39	11
BJ4-GJ1 (6:4)	-0.61	-0.84	-0.76	-3.68	1.78	-4.87	10
BJ4-GJ1 (6:4)	-0.60	-0.83	-0.78	-3.31	1.16	-2.85	10
BJ4-GJ1 (6:4)	-0.61	-0.83	-0.73	-1.24	2.43	-9.40	10
BJ4-GJ1 (5:5)	-0.56	-0.79	-0.74	6.56	1.53	-6.54	9
BJ4-GJ1 (5:5)	-0.56	-0.79	-0.76	6.46	0.69	-3.09	9
BJ4-GJ1 (5:5)	-0.57	-0.79	-0.78	5.53	-2.47	-0.15	9
BJ4-GJ1 (4:6)	-0.53	-0.76	-0.75	12.66	-1.33	-2.45	8
BJ4-GJ1 (4:6)	-0.53	-0.76	-0.76	12.33	-1.75	-1.44	8
BJ4-GJ1 (4:6)	-0.53	-0.77	-0.75	11.93	-0.39	-2.05	8
BJ4-GJ1 (3:7)	-0.51	-0.76	-0.76	14.28	-0.01	0.14	7
BJ4-GJ1 (3:7)	-0.52	-0.76	-0.76	13.83	-0.58	-0.38	7
BJ4-GJ1 (3:7)	-0.52	-0.76	-0.76	13.79	-0.67	0.26	7
BJ4-GJ1 (2:8)	-0.49	-0.71	-0.76	22.55	-6.32	1.12	6
BJ4-GJ1 (2:8)	-0.49	-0.71	-0.76	22.40	-6.01	0.89	6
BJ4-GJ1 (2:8)	-0.50	-0.71	-0.76	21.94	-7.32	0.41	6
BJ4-GJ1 (1:9)	-0.47	-0.67	-0.75	30.46	-8.42	0.25	5
BJ4-GJ1 (1:9)	-0.47	-0.67	-0.75	30.05	-8.92	0.67	5
BJ4-GJ1 (1:9)	-0.47	-0.67	-0.75	29.77	-8.96	0.92	5
BJ5-GJ1 (9:1)	-0.81	-0.89	-0.86	-28.03	-15.89	-3.24	32
BJ5-GJ1 (9:1)	-0.81	-0.88	-0.85	-26.74	-17.00	-4.50	32
BJ5-GJ1 (9:1)	-0.81	-0.88	-0.86	-27.74	-17.62	-3.31	32
BJ5-GJ1 (8:2)	-0.77	-0.89	-0.85	-25.27	-11.64	-2.71	31
BJ5-GJ1 (8:2)	-0.77	-0.88	-0.85	-25.01	-12.50	-2.10	31
BJ5-GJ1 (8:2)	-0.78	-0.89	-0.85	-25.85	-12.38	-2.74	31
BJ5-GJ1 (7:3)	-0.75	-0.83	-0.84	-15.04	-19.09	-2.52	30
BJ5-GJ1 (7:3)	-0.74	-0.83	-0.83	-14.36	-17.50	-3.09	30
BJ5-GJ1 (7:3)	-0.76	-0.82	-0.84	-15.26	-20.51	-3.04	30
BJ5-GJ1 (6:4)	-0.72	-0.83	-0.84	-12.65	-15.77	-0.57	29
BJ5-GJ1 (6:4)	-0.73	-0.83	-0.84	-13.77	-16.52	-2.12	29
BJ5-GJ1 (6:4)	-0.72	-0.83	-0.84	-12.93	-15.21	-1.47	29
BJ5-GJ1 (5:5)	-0.67	-0.75	-0.82	1.42	-21.15	-1.18	28
BJ5-GJ1 (5:5)	-0.69	-0.76	-0.82	-0.51	-22.06	-2.46	28
BJ5-GJ1 (5:5)	-0.70	-0.76	-0.82	-1.47	-23.45	-2.90	28

BJ5-GJ1 (4:6)	-0.66	-0.76	-0.81	2.08	-17.23	-2.47	27
BJ5-GJ1 (4:6)	-0.64	-0.76	-0.81	2.92	-15.48	-1.34	27
BJ5-GJ1 (4:6)	-0.66	-0.76	-0.80	1.76	-17.08	-3.64	27
BJ5-GJ1 (3:7)	-0.57	-0.73	-0.79	13.77	-13.66	0.13	26
BJ5-GJ1 (3:7)	-0.59	-0.72	-0.79	12.97	-15.04	-0.43	26
BJ5-GJ1 (3:7)	-0.60	-0.72	-0.78	12.35	-16.69	-2.60	26
BJ5-GJ1 (2:8)	-0.51	-0.72	-0.77	18.98	-7.02	1.39	25
BJ5-GJ1 (2:8)	-0.53	-0.73	-0.77	16.33	-6.94	0.71	25
BJ5-GJ1 (2:8)	-0.54	-0.74	-0.78	14.59	-6.75	0.87	25
BJ5-GJ1 (1:9)	-0.50	-0.70	-0.77	22.68	-7.73	2.61	6
BJ5-GJ1 (1:9)	-0.52	-0.72	-0.77	18.49	-8.06	0.72	25
BJ5-GJ1 (1:9)	-0.52	-0.70	-0.77	21.41	-10.67	0.45	24
BJ4-GJ6 (9:1)	-0.62	-0.91	-0.81	-17.86	10.38	2.18	22
BJ4-GJ6 (9:1)	-0.62	-0.91	-0.81	-17.55	10.07	2.44	22
BJ4-GJ6 (9:1)	-0.62	-0.91	-0.82	-16.99	9.65	2.98	22
BJ4-GJ6 (8:2)	-0.62	-0.90	-0.81	-14.67	8.44	1.62	21
BJ4-GJ6 (8:2)	-0.62	-0.90	-0.80	-14.41	8.87	-0.16	21
BJ4-GJ6 (8:2)	-0.62	-0.89	-0.80	-13.89	8.43	0.67	21
BJ4-GJ6 (7:3)	-0.59	-0.86	-0.79	-7.19	7.41	0.60	20
BJ4-GJ6 (7:3)	-0.59	-0.88	-0.79	-9.03	9.13	-0.11	20
BJ4-GJ6 (7:3)	-0.59	-0.88	-0.79	-9.83	10.29	0.52	20
BJ4-GJ6 (6:4)	-0.57	-0.84	-0.78	-2.28	4.66	0.34	19
BJ4-GJ6 (6:4)	-0.57	-0.83	-0.78	-0.87	3.80	0.34	19
BJ4-GJ6 (6:4)	-0.58	-0.82	-0.78	-0.22	2.15	-0.32	19
BJ4-GJ6 (5:5)	-0.54	-0.82	-0.77	4.06	6.29	-0.33	18
BJ4-GJ6 (5:5)	-0.53	-0.82	-0.77	4.35	6.20	-0.10	18
BJ4-GJ6 (5:5)	-0.54	-0.82	-0.77	3.62	5.43	0.23	18
BJ4-GJ6 (4:6)	-0.50	-0.79	-0.76	10.84	5.46	0.63	17
BJ4-GJ6 (4:6)	-0.51	-0.79	-0.76	10.73	5.61	-0.11	17
BJ4-GJ6 (4:6)	-0.49	-0.79	-0.76	10.85	6.79	1.72	17
BJ4-GJ6 (3:7)	-0.45	-0.78	-0.74	15.81	11.57	1.97	16
BJ4-GJ6 (3:7)	-0.46	-0.78	-0.75	14.72	10.02	1.54	16
BJ4-GJ6 (3:7)	-0.45	-0.78	-0.75	15.23	10.43	2.14	16
BJ4-GJ6 (2:8)	-0.42	-0.74	-0.73	24.44	8.43	1.15	15
BJ4-GJ6 (2:8)	-0.42	-0.74	-0.72	24.88	8.88	-1.15	15
BJ4-GJ6 (2:8)	-0.42	-0.74	-0.72	24.28	8.70	0.15	15
BJ4-GJ6 (1:9)	-0.39	-0.72	-0.69	30.37	11.29	-2.81	14
BJ4-GJ6 (1:9)	-0.39	-0.73	-0.69	29.87	11.77	-3.19	14
BJ4-GJ6 (1:9)	-0.39	-0.72	-0.71	29.85	10.39	-0.57	14
BJ1	-0.77	-0.99	-0.84	-39.26	4.60	-2.94	1
BJ1	-0.76	-0.98	-0.84	-38.74	5.10	-2.05	1
BJ1	-0.77	-0.99	-0.84	-39.01	5.01	-2.01	1
BJ1	-0.77	-0.98	-0.84	-39.27	4.41	-2.64	1
BJ1	-0.78	-0.99	-0.84	-39.89	3.52	-2.59	1
BJ1	-0.78	-0.98	-0.84	-39.68	3.75	-2.80	1
BJ2	-0.79	-0.98	-0.88	-41.43	0.34	2.65	2
BJ2	-0.78	-0.98	-0.87	-40.75	1.56	1.65	2
BJ2	-0.78	-0.98	-0.88	-41.43	1.01	3.03	2
BJ2	-0.78	-0.98	-0.88	-41.11	0.70	2.00	2
BJ2	-0.79	-0.98	-0.88	-41.56	0.32	2.95	2
BJ2	-0.78	-0.98	-0.88	-40.79	0.90	2.60	2
BJ3	-0.73	-0.98	-0.84	-35.30	7.48	0.19	3
BJ3	-0.73	-0.98	-0.84	-35.50	7.90	0.50	3
BJ3	-0.73	-0.98	-0.85	-35.63	7.15	0.77	3
BJ3	-0.73	-0.97	-0.84	-34.62	7.09	0.79	3
BJ3	-0.73	-0.98	-0.85	-36.02	7.11	0.64	3
BJ3	-0.73	-0.98	-0.84	-35.49	7.87	0.35	3
BJ4	-0.72	-0.95	-0.84	-29.84	3.92	0.21	4
BJ4	-0.71	-0.95	-0.84	-29.76	4.46	0.69	4
BJ4	-0.71	-0.94	-0.84	-28.28	4.12	0.41	4
BJ4	-0.71	-0.94	-0.84	-29.08	4.31	1.08	4
BJ4	-0.72	-0.94	-0.84	-29.87	3.05	0.48	4
BJ4	-0.72	-0.94	-0.84	-30.24	2.90	0.43	4
BJ5	-0.82	-0.99	-0.87	-44.66	-2.14	-0.68	23
BJ5	-0.81	-0.99	-0.87	-44.11	-0.95	-0.08	23
BJ5	-0.82	-0.99	-0.87	-44.29	-1.75	-0.46	23
BJ5	-0.81	-0.99	-0.88	-43.95	-1.71	0.13	23
BJ5	-0.82	-0.99	-0.88	-43.83	-2.22	0.39	23
BJ5	-0.82	-0.98	-0.88	-43.94	-2.54	0.64	23
GJ1	-0.44	-0.65	-0.76	34.30	-8.98	3.77	33
GJ1	-0.43	-0.65	-0.76	36.06	-9.77	3.91	33
GJ1	-0.43	-0.65	-0.75	36.48	-8.57	2.41	33

GJ1	-0.42	-0.66	-0.75	34.83	-5.51	4.08	33
GJ1	-0.43	-0.65	-0.75	35.23	-8.16	2.95	33
GJ1	-0.44	-0.65	-0.75	35.03	-8.16	2.23	33
GJ2	-0.56	-0.80	-0.87	0.75	-4.75	13.06	34
GJ2	-0.56	-0.80	-0.86	0.97	-3.72	11.81	34
GJ2	-0.55	-0.79	-0.86	2.81	-3.77	12.93	34
GJ2	-0.54	-0.79	-0.87	3.17	-3.03	14.58	34
GJ2	-0.55	-0.80	-0.86	1.78	-2.34	13.62	34
GJ2	-0.55	-0.80	-0.87	0.95	-3.29	13.78	34
GJ3	-0.48	-0.80	-0.80	9.53	7.85	7.88	35
GJ3	-0.48	-0.79	-0.80	10.64	6.47	8.08	35
GJ3	-0.46	-0.79	-0.79	11.58	9.32	8.57	35
GJ3	-0.45	-0.80	-0.79	11.13	10.58	9.26	35
GJ3	-0.46	-0.80	-0.80	9.98	10.18	9.28	35
GJ3	-0.47	-0.81	-0.80	8.05	11.01	8.92	35
GJ4	-0.40	-0.65	-0.71	40.11	-3.34	-1.01	36
GJ4	-0.39	-0.65	-0.72	40.25	-1.76	0.81	36
GJ4	-0.36	-0.64	-0.72	42.61	-0.72	2.10	36
GJ4	-0.37	-0.65	-0.72	40.72	0.25	2.26	36
GJ4	-0.39	-0.67	-0.72	36.74	1.06	1.41	36
GJ4	-0.40	-0.67	-0.72	36.01	0.67	1.15	36
GJ5	-0.39	-0.67	-0.68	39.38	3.05	-5.28	37
GJ5	-0.38	-0.67	-0.68	39.31	4.42	-4.86	37
GJ5	-0.37	-0.66	-0.68	41.42	4.32	-4.51	37
GJ5	-0.39	-0.67	-0.67	38.92	3.25	-6.12	37
GJ5	-0.38	-0.67	-0.69	38.53	3.83	-3.69	37
GJ5	-0.40	-0.68	-0.69	36.47	2.09	-3.47	37
GJ6	-0.37	-0.70	-0.65	35.90	11.31	-7.75	38
GJ6	-0.37	-0.70	-0.67	36.09	10.34	-4.58	38
GJ6	-0.36	-0.70	-0.65	36.48	12.66	-7.56	38
GJ6	-0.37	-0.71	-0.66	35.56	12.14	-5.69	38
GJ6	-0.37	-0.70	-0.68	35.92	9.18	-4.51	38
GJ6	-0.38	-0.71	-0.66	35.03	11.20	-7.77	38

Jackknifed classification matrix: 97% corrected classification.

Table 53. Training matrix of fluorescence response pattern from water-soluble **P2** (2 µM, at pH3, pH7, and pH13, buffered) against self-made juice samples (1 µl). Commercial juice samples was calculated as blind. LDA was carried out resulting in the three factors of the canonical scores and group generation.

Analytes	Fluorescence Response Pattern			Results LDA		
self-made juice	**P2** (pH3)	**P2** (pH7)	**P2** (pH13)	SCORE1	SCORE2	SCORE3
GJ-green	-0.12	-0.14	-0.31	-100.50	-3.35	-1.82
GJ-green	-0.10	-0.15	-0.29	-102.33	-5.21	0.53
GJ-green	-0.09	-0.16	-0.29	-101.17	-4.80	2.12
GJ-green	-0.11	-0.14	-0.30	-102.11	-4.62	-0.73
GJ-green	-0.09	-0.14	-0.29	-103.72	-4.33	0.75
GJ-green	-0.11	-0.16	-0.29	-102.07	-6.56	-0.44
GJ green-red 7-3	-0.35	-0.46	-0.61	-24.68	0.55	-2.07
GJ green-red 7-3	-0.34	-0.48	-0.62	-22.26	1.07	-0.21
GJ green-red 7-3	-0.32	-0.45	-0.60	-26.33	2.13	-0.21
GJ green-red 7-3	-0.34	-0.44	-0.63	-22.49	5.02	-2.27
GJ green-red 7-3	-0.35	-0.48	-0.62	-21.41	0.41	-1.13
GJ green-red 7-3	-0.37	-0.46	-0.62	-23.17	0.58	-3.59
GJ green-red 5-5	-0.42	-0.60	-0.74	9.24	5.67	1.23
GJ green-red 5-5	-0.42	-0.62	-0.74	9.30	3.68	1.50
GJ green-red 5-5	-0.42	-0.59	-0.74	8.29	5.37	0.32
GJ green-red 5-5	-0.41	-0.59	-0.74	7.60	5.67	0.84
GJ green-red 5-5	-0.41	-0.61	-0.74	8.83	4.62	2.23
GJ green-red 5-5	-0.42	-0.62	-0.74	9.96	4.19	2.06
GJ green-red 3-7	-0.43	-0.64	-0.76	15.26	5.17	2.28
GJ green-red 3-7	-0.44	-0.65	-0.76	15.48	3.79	2.11
GJ green-red 3-7	-0.43	-0.64	-0.77	16.29	5.07	2.03
GJ green-red 3-7	-0.42	-0.65	-0.76	15.73	4.69	3.41
GJ green-red 3-7	-0.44	-0.64	-0.76	15.16	3.75	1.67
GJ green-red 3-7	-0.44	-0.65	-0.76	15.73	3.69	1.83
GJ-red	-0.53	-0.70	-0.86	36.30	6.71	-3.13
GJ-red	-0.52	-0.72	-0.86	38.01	6.52	-1.08
GJ-red	-0.52	-0.71	-0.86	36.28	7.16	-1.10
GJ-red	-0.53	-0.72	-0.86	37.63	6.47	-1.83
GJ-red	-0.54	-0.71	-0.86	36.83	6.10	-2.79
GJ-red	-0.53	-0.71	-0.86	36.82	6.59	-2.42
BJ	-0.68	-0.97	-0.89	63.21	-13.82	-1.03

BJ	-0.67	-0.97	-0.90	63.80	-12.43	0.16
BJ	-0.67	-0.97	-0.90	64.15	-12.26	0.56
BJ	-0.67	-0.97	-0.90	63.79	-12.31	0.54
BJ	-0.69	-0.97	-0.90	64.24	-12.92	-1.12
BJ	-0.67	-0.97	-0.90	64.34	-12.04	0.81
Set as blind (Commercial juice samples):						
BJ1	-0.77	-0.99	-0.84	53.32	-27.45	-9.19
BJ1	-0.76	-0.98	-0.84	53.84	-26.53	-8.51
BJ1	-0.77	-0.99	-0.84	54.04	-26.58	-8.61
BJ1	-0.77	-0.98	-0.84	53.62	-27.18	-9.21
BJ1	-0.78	-0.99	-0.84	54.08	-27.26	-9.84
BJ1	-0.78	-0.98	-0.84	53.74	-27.39	-9.73
BJ2	-0.79	-0.98	-0.88	60.17	-22.92	-10.33
BJ2	-0.78	-0.98	-0.87	58.75	-23.67	-9.80
BJ2	-0.78	-0.98	-0.88	60.50	-22.63	-9.83
BJ2	-0.78	-0.98	-0.88	59.34	-23.41	-10.26
BJ2	-0.79	-0.98	-0.88	60.53	-22.69	-10.28
BJ2	-0.78	-0.98	-0.88	59.72	-22.79	-9.88
BJ3	-0.73	-0.98	-0.84	53.84	-23.61	-5.65
BJ3	-0.73	-0.98	-0.84	54.23	-23.43	-5.36
BJ3	-0.73	-0.98	-0.85	54.61	-23.18	-5.73
BJ3	-0.73	-0.97	-0.84	54.03	-22.83	-5.52
BJ3	-0.73	-0.98	-0.85	54.72	-23.42	-5.88
BJ3	-0.73	-0.98	-0.84	54.09	-23.56	-5.42
BJ4	-0.72	-0.95	-0.84	50.77	-21.55	-6.39
BJ4	-0.71	-0.95	-0.84	51.16	-21.14	-5.91
BJ4	-0.71	-0.94	-0.84	50.02	-20.88	-5.84
BJ4	-0.71	-0.94	-0.84	51.14	-20.56	-5.71
BJ4	-0.72	-0.94	-0.84	51.08	-21.26	-6.80
BJ4	-0.72	-0.94	-0.84	51.26	-21.41	-6.99
BJ5	-0.82	-0.99	-0.87	59.01	-26.72	-13.54
BJ5	-0.81	-0.99	-0.87	59.20	-26.10	-12.55
BJ5	-0.82	-0.99	-0.87	58.98	-26.43	-13.16
BJ5	-0.81	-0.99	-0.88	59.34	-25.81	-12.88
BJ5	-0.82	-0.99	-0.88	59.54	-25.51	-13.06
BJ5	-0.82	-0.98	-0.88	59.87	-25.29	-13.19
GJ1	-0.44	-0.65	-0.76	16.59	3.41	2.36
GJ1	-0.43	-0.65	-0.76	15.71	4.16	2.36
GJ1	-0.43	-0.65	-0.75	13.96	2.89	2.66
GJ1	-0.42	-0.66	-0.75	16.41	3.60	4.54
GJ1	-0.43	-0.65	-0.75	15.21	2.93	2.78
GJ1	-0.44	-0.65	-0.75	14.64	2.23	2.50
GJ2	-0.56	-0.80	-0.87	45.29	0.36	-0.09
GJ2	-0.56	-0.80	-0.86	43.92	-0.74	0.15
GJ2	-0.55	-0.79	-0.86	43.90	0.85	0.91
GJ2	-0.54	-0.79	-0.87	45.24	2.36	1.93
GJ2	-0.55	-0.80	-0.86	45.12	1.02	1.69
GJ2	-0.55	-0.80	-0.87	45.81	0.96	1.02
GJ3	-0.48	-0.80	-0.80	34.53	-2.26	7.43
GJ3	-0.48	-0.79	-0.80	34.13	-1.62	6.98
GJ3	-0.46	-0.79	-0.79	33.90	-1.09	8.96
GJ3	-0.45	-0.80	-0.79	34.78	-0.72	9.79
GJ3	-0.46	-0.80	-0.80	35.51	-1.05	9.30
GJ3	-0.47	-0.81	-0.80	36.27	-2.05	9.21
GJ4	-0.40	-0.65	-0.71	8.28	0.67	5.37
GJ4	-0.39	-0.65	-0.72	9.88	2.21	6.88
GJ4	-0.36	-0.64	-0.72	9.67	4.04	8.43
GJ4	-0.37	-0.65	-0.72	10.90	3.49	8.59
GJ4	-0.39	-0.67	-0.72	12.42	1.39	7.86
GJ4	-0.40	-0.67	-0.72	12.62	0.95	7.38
GJ5	-0.39	-0.67	-0.68	4.33	-3.79	7.46
GJ5	-0.38	-0.67	-0.68	4.71	-3.54	8.35
GJ5	-0.37	-0.66	-0.68	3.80	-2.54	8.91
GJ5	-0.39	-0.67	-0.67	3.78	-4.70	7.20
GJ5	-0.38	-0.67	-0.69	6.33	-2.72	8.21
GJ5	-0.40	-0.68	-0.69	7.84	-3.07	6.82
GJ6	-0.37	-0.70	-0.65	3.66	-7.70	10.54
GJ6	-0.37	-0.70	-0.67	6.64	-4.78	11.05
GJ6	-0.36	-0.70	-0.65	3.44	-7.44	11.50
GJ6	-0.37	-0.71	-0.66	5.80	-6.06	11.59
GJ6	-0.37	-0.70	-0.68	6.86	-4.68	10.37
GJ6	-0.38	-0.71	-0.66	4.17	-7.99	10.27

5.3.7 LDA Calculation (Chapter 3.3)

Table 54. Whisky data obtained from normalized height of peaks and their resulted PCA scores.

Analyte	Height of Peaks*			Results PCA		
Whisky	Peak1	Peak2	Peak3	PC1	PC2	PC3
B-1	140.8	233.5	76.7	-0.609	0.234	-0.105
B-2	20.5	18.6	1.3	-1.599	-0.104	-0.112
Ib-1	19.2	124.0	23.4	-1.382	-0.204	0.058
Ib-2	24.3	47.0	9.5	-1.519	-0.116	-0.081
Is-1	12.3	19.3	3.7	-1.623	-0.153	-0.098
Is-2	132.5	277.7	65.7	-0.601	0.212	0.030
Is-3	179.3	339.7	69.9	-0.316	0.423	0.047
Is-4	48.3	184.6	42.8	-1.126	-0.128	0.075
Sb-1	49.4	212.1	105.8	-0.914	-0.316	-0.018
Sb-2	54.9	192.1	67.3	-1.025	-0.169	0.019
Sb-3	69.8	278.4	143.8	-0.633	-0.341	-0.014
Sb-4	7.2	101.9	31.3	-1.441	-0.283	0.020
Sb-5	39.8	197.2	64.4	-1.082	-0.238	0.069
Sb-6	53.5	209.7	92.2	-0.937	-0.254	0.000
Sb-Y8	282.4	709.2	250.3	1.126	0.320	0.167
Sb-Y12	342.6	1102.1	487.8	2.590	-0.178	0.295
Sb-Y21	453.9	1249.5	610.2	3.565	-0.008	0.071
Ss-1	66.7	152.4	53.3	-1.078	-0.056	-0.057
Ss-2	648.9	1343.6	585.3	4.388	1.041	-0.101
Ss-3	88.0	190.7	72.7	-0.887	-0.014	-0.069
Ss-4	165.5	195.2	27.3	-0.704	0.516	-0.123
Ss-5	245.1	409.1	100.7	0.124	0.651	-0.025
Ss-6	230.6	697.3	303.9	1.051	-0.101	0.130
Ss-7	349.3	1250.5	789.8	3.642	-1.076	-0.118
Ss-8	212.6	216.0	61.8	-0.401	0.650	-0.264
Ss-9	125.1	374.6	108.6	-0.366	0.021	0.148
Ss-10	122.3	385.7	86.8	-0.417	0.069	0.228
Ss-Y12	141.9	323.7	63.6	-0.499	0.254	0.110
Ss-Y15	199.7	601.0	202.3	0.516	0.067	0.235
Ss-Y18	386.0	724.7	307.2	1.694	0.679	-0.161

Table 55. Training matrix of fluorescence response pattern from an array of **P1**-**P3** against whiskies. LDA was carried out and resulting in 3 factors of the canonical scores and group generation. Jackknifed classification matrix showed the 99% correct classification.

Analyte	Fluorescence Response Pattern			Results LDA			
Whisky	**P2**	**P1**	**P3**	Factor 1	Factor 2	Factor 3	Group
B-1	0.670	-0.908	0.024	56.720	37.495	-10.011	1
B-1	0.677	-0.914	0.033	57.875	38.279	-10.708	1
B-1	0.666	-0.906	0.032	56.238	38.016	-10.981	1
B-1	0.691	-0.913	0.039	58.705	39.813	-10.402	1
B-1	0.687	-0.908	0.019	57.804	38.114	-8.581	1
B-1	0.645	-0.914	0.038	55.688	36.709	-12.886	1
B-2	0.224	-0.906	-0.140	26.443	-5.590	-19.661	2
B-2	0.230	-0.900	-0.143	26.194	-5.090	-18.794	2
B-2	0.212	-0.902	-0.148	25.181	-6.885	-19.466	2
B-2	0.246	-0.899	-0.155	27.147	-5.097	-16.789	2
B-2	0.243	-0.905	-0.142	27.596	-4.572	-18.414	2
B-2	0.236	-0.904	-0.145	27.100	-5.194	-18.432	2
Ib-1	0.104	-0.657	-0.142	-9.249	3.032	-16.752	3
Ib-1	0.115	-0.642	-0.150	-10.183	3.916	-14.775	3
Ib-1	0.121	-0.629	-0.150	-11.199	5.105	-14.002	3
Ib-1	0.108	-0.624	-0.158	-12.663	3.940	-13.842	3
Ib-1	0.113	-0.640	-0.148	-10.562	4.142	-15.029	3
Ib-1	0.111	-0.634	-0.129	-11.277	6.140	-16.707	3
Ib-2	0.206	-0.511	-0.227	-18.831	11.405	2.281	4
Ib-2	0.214	-0.508	-0.221	-18.559	12.695	2.258	4
Ib-2	0.194	-0.509	-0.227	-19.818	10.850	1.729	4
Ib-2	0.217	-0.512	-0.204	-17.861	14.108	0.761	4
Ib-2	0.217	-0.507	-0.219	-18.493	13.161	2.348	4
Ib-2	0.200	-0.521	-0.217	-18.109	11.255	0.641	4
Is-1	0.417	-0.525	-0.169	-3.100	29.167	8.194	5
Is-1	0.420	-0.527	-0.163	-2.631	29.823	7.733	5
Is-1	0.409	-0.516	-0.157	-4.602	30.415	6.921	5
Is-1	0.424	-0.541	-0.163	-0.813	29.060	7.381	5

Is-1	0.418	-0.522	-0.152	-3.325	30.908	6.767	5
Is-1	0.421	-0.546	-0.152	-0.468	29.619	6.101	5
Is-2	0.207	-0.542	-0.285	-15.409	4.226	6.622	6
Is-2	0.213	-0.523	-0.285	-17.084	5.786	7.592	6
Is-2	0.230	-0.520	-0.285	-16.331	7.072	8.677	6
Is-2	0.213	-0.525	-0.289	-16.913	5.374	7.940	6
Is-2	0.224	-0.527	-0.286	-15.903	6.160	8.112	6
Is-2	0.203	-0.542	-0.280	-15.637	4.392	5.873	6
Is-3	0.270	-0.455	-0.311	-20.897	11.600	15.709	7
Is-3	0.299	-0.452	-0.319	-19.283	12.989	18.189	7
Is-3	0.305	-0.451	-0.323	-19.053	13.068	18.962	7
Is-3	0.298	-0.453	-0.324	-19.283	12.380	18.592	7
Is-3	0.278	-0.443	-0.312	-21.697	12.859	16.734	7
Is-3	0.281	-0.454	-0.312	-20.269	12.265	16.436	7
Is-4	0.156	-0.576	-0.113	-14.705	14.200	-13.488	8
Is-4	0.171	-0.573	-0.117	-14.057	15.075	-12.135	8
Is-4	0.168	-0.571	-0.119	-14.439	14.760	-12.039	8
Is-4	0.180	-0.564	-0.123	-14.432	15.658	-10.719	8
Is-4	0.166	-0.572	-0.111	-14.451	15.349	-12.942	8
Is-4	0.158	-0.578	-0.116	-14.352	13.963	-13.138	8
Sb-1	-0.049	-0.634	-0.360	-22.363	-25.003	-4.281	9
Sb-1	-0.042	-0.650	-0.369	-20.078	-26.374	-3.668	**14**
Sb-1	-0.070	-0.635	-0.368	-23.637	-27.125	-4.717	9
Sb-1	-0.064	-0.661	-0.363	-20.355	-27.986	-5.767	9
Sb-1	-0.069	-0.651	-0.354	-21.781	-26.764	-6.546	9
Sb-1	-0.049	-0.639	-0.348	-21.786	-24.256	-5.588	9
Sb-2	0.023	-0.525	-0.242	-29.430	-2.503	-7.105	12
Sb-2	0.028	-0.538	-0.242	-27.671	-2.996	-7.272	12
Sb-2	0.031	-0.533	-0.240	-28.039	-2.308	-7.086	12
Sb-2	0.032	-0.523	-0.235	-29.037	-1.200	-7.095	12
Sb-2	0.030	-0.541	-0.230	-27.245	-2.027	-8.346	12
Sb-2	0.033	-0.532	-0.237	-28.027	-1.935	-7.178	12
Sb-3	-0.051	-0.698	-0.355	-15.325	-28.864	-7.258	10
Sb-3	-0.034	-0.675	-0.350	-16.738	-25.862	-5.862	10
Sb-3	-0.033	-0.695	-0.343	-14.434	-26.506	-7.267	10
Sb-3	-0.034	-0.679	-0.362	-16.348	-27.157	-4.869	10
Sb-3	-0.055	-0.709	-0.340	-14.339	-28.457	-9.293	10
Sb-3	-0.024	-0.679	-0.352	-15.703	-25.539	-5.325	10
Sb-4	0.072	-0.416	-0.046	-37.996	25.515	-18.343	11
Sb-4	0.067	-0.433	-0.019	-36.377	26.498	-21.674	11
Sb-4	0.075	-0.447	-0.040	-34.256	24.245	-19.890	11
Sb-4	0.072	-0.423	-0.021	-37.099	27.282	-20.852	11
Sb-4	0.080	-0.446	-0.028	-34.070	25.685	-20.593	11
Sb-4	0.062	-0.432	-0.025	-36.836	25.731	-21.368	11
Sb-5	0.051	-0.502	-0.304	-30.291	-4.870	1.108	13
Sb-5	0.054	-0.511	-0.294	-29.034	-4.334	0.072	13
Sb-5	0.051	-0.521	-0.298	-28.186	-5.524	-0.103	13
Sb-5	0.047	-0.506	-0.291	-30.038	-4.143	-0.422	13
Sb-5	0.066	-0.521	-0.284	-27.141	-3.269	-0.647	13
Sb-5	0.046	-0.510	-0.286	-29.717	-3.973	-1.147	13
Sb-6	-0.032	-0.636	-0.368	-20.950	-24.733	-2.678	14
Sb-6	-0.025	-0.646	-0.364	-19.383	-24.542	-3.015	14
Sb-6	-0.038	-0.644	-0.360	-20.474	-24.952	-4.098	14
Sb-6	-0.035	-0.639	-0.358	-20.794	-24.233	-3.851	14
Sb-6	-0.024	-0.648	-0.383	-19.226	-26.404	-1.239	14
Sb-6	-0.031	-0.647	-0.351	-19.656	-23.917	-4.558	14
Ss-1	0.533	-0.734	-0.111	28.032	27.940	1.367	15
Ss-1	0.538	-0.734	-0.106	28.394	28.718	1.210	15
Ss-1	0.532	-0.743	-0.121	28.926	26.485	1.936	15
Ss-1	0.528	-0.736	-0.099	27.942	28.617	-0.128	15
Ss-1	0.520	-0.740	-0.102	27.789	27.654	-0.444	15
Ss-1	0.525	-0.740	-0.086	28.215	29.337	-1.562	15
Ss-2	0.287	-0.829	-0.289	21.871	-10.097	0.512	17
Ss-2	0.278	-0.844	-0.294	22.830	-12.090	-0.037	17
Ss-2	0.266	-0.834	-0.293	20.998	-12.076	-0.401	17
Ss-2	0.276	-0.846	-0.297	23.013	-12.644	0.019	17
Ss-2	0.264	-0.838	-0.291	21.323	-12.311	-0.857	17
Ss-2	0.272	-0.836	-0.296	21.670	-12.127	0.066	17
Ss-3	0.310	-0.696	-0.429	8.351	-12.494	19.753	18
Ss-3	0.278	-0.699	-0.425	6.504	-14.294	17.445	18
Ss-3	0.290	-0.695	-0.434	6.893	-14.101	19.174	18
Ss-3	0.312	-0.704	-0.427	9.455	-12.665	19.400	18

Ss-3	0.282	-0.692	-0.421	6.066	-13.240	17.610	18
Ss-3	0.287	-0.709	-0.440	8.215	-15.811	19.034	18
Ss-4	0.226	-0.718	-0.365	5.276	-13.413	8.382	19
Ss-4	0.237	-0.728	-0.356	7.107	-12.592	7.770	19
Ss-4	0.234	-0.717	-0.344	5.823	-10.996	6.863	19
Ss-4	0.230	-0.725	-0.338	6.357	-11.226	5.808	19
Ss-4	0.224	-0.728	-0.356	6.300	-13.426	7.097	19
Ss-4	0.233	-0.729	-0.335	7.111	-11.042	5.600	19
Ss-5	0.207	-0.808	-0.401	13.996	-23.868	7.269	20
Ss-5	0.220	-0.806	-0.383	14.678	-21.312	6.326	20
Ss-5	0.225	-0.807	-0.387	15.081	-21.336	6.988	20
Ss-5	0.211	-0.814	-0.385	14.922	-22.532	5.796	20
Ss-5	0.212	-0.803	-0.386	13.759	-21.788	6.294	20
Ss-5	0.212	-0.816	-0.387	15.260	-22.826	5.869	20
Ss-6	0.405	-0.990	-0.271	47.621	-11.535	-0.613	21
Ss-6	0.405	-0.990	-0.268	47.605	-11.274	-0.854	21
Ss-6	0.396	-0.989	-0.282	46.963	-13.083	-0.043	21
Ss-6	0.406	-0.990	-0.283	47.677	-12.517	0.544	21
Ss-6	0.400	-0.989	-0.284	47.230	-13.024	0.324	21
Ss-6	0.396	-0.990	-0.286	47.001	-13.405	0.265	21
Ss-7	0.133	-0.989	-0.394	29.252	-39.918	-4.392	22
Ss-7	0.113	-0.990	-0.403	27.924	-42.072	-4.641	22
Ss-7	0.123	-0.990	-0.407	28.627	-41.815	-3.834	22
Ss-7	0.124	-0.990	-0.396	28.654	-40.733	-4.753	22
Ss-7	0.114	-0.989	-0.413	27.928	-42.915	-3.707	22
Ss-7	0.123	-0.990	-0.404	28.605	-41.525	-3.994	22
Ss-8	0.306	-0.646	-0.275	2.771	4.620	7.194	23
Ss-8	0.326	-0.664	-0.269	6.170	5.151	7.091	23
Ss-8	0.328	-0.646	-0.274	4.283	6.017	8.327	23
Ss-8	0.318	-0.670	-0.286	6.235	2.768	7.986	23
Ss-8	0.325	-0.651	-0.273	4.601	5.603	7.946	23
Ss-8	0.307	-0.647	-0.278	2.993	4.333	7.486	23
Ss-9	0.385	-0.513	-0.296	-6.779	16.456	18.581	24
Ss-9	0.385	-0.524	-0.284	-5.538	16.874	17.004	24
Ss-9	0.378	-0.504	-0.293	-8.197	16.887	18.174	24
Ss-9	0.374	-0.519	-0.284	-6.842	16.467	16.677	24
Ss-9	0.389	-0.511	-0.282	-6.684	18.033	17.583	24
Ss-9	0.387	-0.527	-0.283	-5.066	16.831	16.949	24
Ss-10	0.339	-0.577	-0.290	-2.680	9.893	13.018	16
Ss-10	0.352	-0.574	-0.271	-2.140	12.607	12.109	16
Ss-10	0.329	-0.570	-0.288	-4.134	9.904	12.560	16
Ss-10	0.351	-0.572	-0.296	-2.461	10.370	14.501	16
Ss-10	0.332	-0.567	-0.273	-4.239	11.601	11.412	16
Ss-10	0.351	-0.572	-0.280	-2.432	11.842	12.904	16

Table 56. Detection and identification of unknown whisky samples using LDA. All unknown samples could be assigned to the corresponding group defined by the training matrix according to the shortest Mahalanobis distance. According to the verification, only 4 of 120 unknown whiskies were misclassified, representing an accuracy of 96.7%.

Sample	Fluorescence Response Pattern			Results LDA				Analyte	
#	**P1**	**P2**	**P3**	Factor 1	Factor 2	Factor 3	Group	Identification	Verification
1	-0.452	0.303	-0.315	-19.029	13.501	18.032	7	Is-3	Is-3
2	-0.691	-0.032	-0.336	-14.891	-25.446	-7.701	10	Sb-3	Sb-3
3	-0.685	-0.048	-0.352	-16.636	-27.543	-6.851	10	Sb-3	Sb-3
4	-0.635	0.106	-0.126	-11.503	5.935	-17.292	3	Ib-1	Ib-1
5	-0.522	0.425	-0.163	-2.795	30.464	8.156	5	Is-1	Is-1
6	-0.553	0.390	-0.154	-1.718	26.921	4.158	5	Is-1	Is-1
7	-0.578	0.137	-0.135	-15.780	10.941	-12.585	8	Is-4	Is-4
8	-0.643	-0.047	-0.386	-21.244	-27.834	-2.143	**9**	**Sb-1**	**Sb-6**
9	-0.642	0.123	-0.135	-9.612	5.768	-15.759	3	Ib-1	Ib-1
10	-0.444	0.059	-0.065	-35.764	21.145	-18.336	11	Sb-4	Sb-4
11	-0.523	0.043	-0.306	-28.406	-6.960	0.095	13	Sb-5	Sb-5
12	-0.501	0.058	-0.296	-29.886	-3.580	0.841	13	Sb-5	Sb-5
13	-0.519	0.418	-0.144	-3.656	31.903	6.092	5	Is-1	Is-1
14	-0.640	0.104	-0.152	-11.108	3.218	-15.143	3	Ib-1	Ib-1
15	-0.458	0.298	-0.308	-18.753	13.449	16.936	7	Is-3	Is-3
16	-0.453	0.283	-0.306	-20.194	13.002	16.078	7	Is-3	Is-3
17	-0.579	0.167	-0.103	-13.602	15.646	-13.979	8	Is-4	Is-4
18	-0.730	0.251	-0.351	8.321	-11.311	7.999	19	Ss-4	Ss-4
19	-0.711	0.229	-0.349	4.792	-11.394	7.285	19	Ss-4	Ss-4
20	-0.802	0.199	-0.397	12.764	-23.613	6.578	20	Ss-5	Ss-5
21	-0.991	0.102	-0.398	27.301	-42.358	-5.780	22	Ss-7	Ss-7

22	-0.716	0.292	-0.419	9.412	-13.983	17.120	18	Ss-3	Ss-3
23	-0.738	0.503	-0.124	26.413	24.627	0.800	15	Ss-1	Ss-1
24	-0.807	0.192	-0.393	12.932	-24.040	5.694	20	Ss-5	Ss-5
25	-0.989	0.415	-0.279	48.232	-11.569	0.689	21	Ss-6	Ss-6
26	-0.578	0.318	-0.296	-4.031	7.874	12.407	16	Ss-10	Ss-10
27	-0.578	0.133	-0.108	-16.006	13.124	-15.263	8	Is-4	Is-4
28	-0.529	0.204	-0.280	-16.979	5.368	6.394	6	Is-2	Is-2
29	-0.668	-0.062	-0.354	-19.441	-27.444	-6.856	9	Sb-1	Sb-1
30	-0.899	0.240	-0.133	26.816	-3.594	-19.119	2	B-2	B-2
31	-0.903	0.226	-0.152	26.312	-6.382	-18.356	2	B-2	B-2
32	-0.677	-0.050	-0.350	-17.640	-26.998	-6.857	10	Sb-3	Sb-3
33	-0.461	0.069	-0.038	-33.145	22.998	-20.902	11	Sb-4	Sb-4
34	-0.570	0.141	-0.123	-16.406	12.858	-13.176	8	Is-4	Is-4
35	-0.735	0.517	-0.119	27.043	26.153	1.177	15	Ss-1	Ss-1
36	-0.748	0.532	-0.118	29.461	26.359	1.457	15	Ss-1	Ss-1
37	-0.911	0.651	0.020	55.772	35.730	-10.834	1	B-1	B-1
38	-0.898	0.249	-0.151	27.238	-4.485	-16.960	2	B-2	B-2
39	-0.521	0.053	-0.314	-28.042	-6.857	1.413	13	Sb-5	Sb-5
40	-0.652	-0.035	-0.377	-19.399	-26.819	-2.549	14	Sb-6	Sb-6
41	-0.813	0.194	-0.383	13.651	-23.392	4.665	20	Ss-5	Ss-5
42	-0.990	0.379	-0.275	45.943	-13.529	-1.691	21	Ss-6	Ss-6
43	-0.990	0.106	-0.399	27.539	-42.128	-5.519	22	Ss-7	Ss-7
44	-0.909	0.674	0.024	57.040	37.598	-9.807	1	B-1	B-1
45	-0.912	0.675	0.012	57.482	36.344	-8.771	1	B-1	B-1
46	-0.518	-0.004	-0.289	-32.065	-7.996	-3.985	**13**	**Sb-5**	**Sb-2**
47	-0.543	0.021	-0.253	-27.624	-4.807	-6.822	12	Sb-2	Sb-2
48	-0.529	0.216	-0.283	-16.217	5.749	7.308	6	Is-2	Is-2
49	-0.528	0.209	-0.285	-16.827	5.307	7.164	6	Is-2	Is-2
50	-0.444	0.287	-0.303	-21.023	14.171	16.393	7	Is-3	Is-3
51	-0.643	0.084	-0.154	-12.089	1.578	-16.217	3	Ib-1	Ib-1
52	-0.430	0.038	-0.040	-38.641	23.010	-21.290	11	Sb-4	Sb-4
53	-0.841	0.273	-0.311	22.182	-13.701	1.328	17	Ss-2	Ss-2
54	-0.903	0.219	-0.136	25.820	-5.472	-20.220	2	B-2	B-2
55	-0.907	0.678	0.016	57.067	37.266	-8.802	1	B-1	B-1
56	-0.913	0.699	0.028	59.244	39.370	-8.984	1	B-1	B-1
57	-0.658	0.300	-0.280	3.753	2.893	6.825	23	Ss-8	Ss-8
58	-0.656	0.306	-0.284	3.907	3.053	7.657	23	Ss-8	Ss-8
59	-0.518	0.037	-0.316	-29.417	-7.848	0.855	13	Sb-5	Sb-5
60	-0.547	0.056	-0.302	-24.913	-7.334	-0.476	13	Sb-5	Sb-5
61	-0.635	0.113	-0.148	-10.998	4.437	-14.875	3	Ib-1	Ib-1
62	-0.666	0.326	-0.273	6.356	4.682	7.427	23	Ss-8	Ss-8
63	-0.633	-0.032	-0.361	-21.304	-23.910	-3.157	14	Sb-6	Sb-6
64	-0.549	0.212	-0.213	-14.139	10.595	-0.136	4	Ib-2	Ib-2
65	-0.509	0.211	-0.266	-18.758	8.421	6.263	**6**	**Is-2**	**Ib-2**
66	-0.654	-0.031	-0.380	-18.974	-26.977	-2.188	14	Sb-6	Sb-6
67	-0.648	-0.029	-0.363	-19.490	-24.867	-3.346	14	Sb-6	Sb-6
68	-0.661	-0.049	-0.353	-19.325	-26.087	-5.886	9	Sb-1	Sb-1
69	-0.574	0.152	-0.116	-15.240	13.907	-13.339	8	Is-4	Is-4
70	-0.505	0.200	-0.207	-19.823	13.209	0.325	4	Ib-2	Ib-2
71	-0.534	0.422	-0.150	-1.705	30.609	6.407	5	Is-1	Is-1
72	-0.733	0.543	-0.123	28.532	27.646	3.090	15	Ss-1	Ss-1
73	-0.515	0.185	-0.206	-19.667	11.714	-0.920	4	Ib-2	Ib-2
74	-0.519	0.200	-0.223	-18.271	10.870	1.305	4	Ib-2	Ib-2
75	-0.675	0.313	-0.281	6.522	2.569	7.050	23	Ss-8	Ss-8
76	-0.705	0.309	-0.430	9.315	-13.190	19.486	18	Ss-3	Ss-3
77	-0.723	0.236	-0.368	6.504	-13.384	8.942	19	Ss-4	Ss-4
78	-0.990	0.372	-0.298	45.389	-16.032	0.006	21	Ss-6	Ss-6
79	-0.651	0.332	-0.287	5.019	4.826	9.531	23	Ss-8	Ss-8
80	-0.529	0.374	-0.283	-5.775	15.887	16.124	24	Ss-9	Ss-9
81	-0.540	0.373	-0.294	-4.536	14.086	16.705	24	Ss-9	Ss-9
82	-0.512	0.386	-0.310	-6.779	15.311	19.937	24	Ss-9	Ss-9
83	-0.990	0.135	-0.412	29.348	-41.476	-2.644	22	Ss-7	Ss-7
84	-0.539	0.353	-0.308	-5.976	11.613	16.858	**16**	**Ss-10**	**Ss-9**
85	-0.574	0.339	-0.284	-3.094	10.551	12.618	16	Ss-10	Ss-10
86	-0.574	0.317	-0.263	-4.461	11.001	9.434	16	Ss-10	Ss-10
87	-0.564	0.335	-0.275	-4.401	11.800	11.925	16	Ss-10	Ss-10
88	-0.584	0.334	-0.278	-2.253	10.157	11.427	16	Ss-10	Ss-10
89	-0.817	0.198	-0.388	14.438	-23.890	5.159	20	Ss-5	Ss-5
90	-0.808	0.205	-0.374	13.929	-21.622	4.579	20	Ss-5	Ss-5
91	-0.533	0.408	-0.160	-2.750	28.938	6.510	5	Is-1	Is-1
92	-0.531	0.374	-0.302	-5.532	14.115	17.830	24	Ss-9	Ss-9
93	-0.569	0.200	-0.282	-12.815	2.307	4.841	6	Is-2	Is-2

94	-0.527	0.241	-0.278	-14.842	8.021	8.330	6	Is-2	Is-2
95	-0.850	0.258	-0.292	22.180	-13.568	-1.579	17	Ss-2	Ss-2
96	-0.990	0.399	-0.289	47.195	-13.523	0.710	21	Ss-6	Ss-6
97	-0.990	0.415	-0.285	48.309	-12.144	1.249	21	Ss-6	Ss-6
98	-0.488	0.280	-0.312	-16.633	9.970	15.181	7	Is-3	Is-3
99	-0.685	-0.039	-0.334	-15.954	-25.311	-8.061	10	Sb-3	Sb-3
100	-0.990	0.116	-0.397	28.178	-41.312	-5.080	22	Ss-7	Ss-7
101	-0.641	-0.058	-0.360	-22.147	-25.986	-4.999	9	Sb-1	Sb-1
102	-0.425	0.050	-0.026	-38.391	25.356	-21.732	11	Sb-4	Sb-4
103	-0.450	0.062	-0.037	-34.817	23.488	-20.967	11	Sb-4	Sb-4
104	-0.990	0.120	-0.398	28.392	-41.120	-4.771	22	Ss-7	Ss-7
105	-0.719	0.236	-0.348	6.098	-11.370	7.252	19	Ss-4	Ss-4
106	-0.843	0.270	-0.286	22.306	-11.766	-1.166	17	Ss-2	Ss-2
107	-0.905	0.234	-0.144	26.996	-5.266	-18.670	2	B-2	B-2
108	-0.648	-0.048	-0.363	-20.659	-26.089	-4.474	9	Sb-1	Sb-1
109	-0.756	0.526	-0.122	29.968	25.128	1.165	15	Ss-1	Ss-1
110	-0.704	-0.053	-0.342	-14.741	-28.214	-8.765	10	Sb-3	Sb-3
111	-0.838	0.266	-0.309	21.407	-13.765	0.859	17	Ss-2	Ss-2
112	-0.550	0.033	-0.244	-26.024	-3.715	-7.263	12	Sb-2	Sb-2
113	-0.836	0.272	-0.312	21.584	-13.564	1.562	17	Ss-2	Ss-2
114	-0.541	0.031	-0.248	-27.156	-3.596	-6.632	12	Sb-2	Sb-2
115	-0.703	0.302	-0.436	8.518	-14.015	19.704	18	Ss-3	Ss-3
116	-0.647	-0.059	-0.354	-21.539	-25.893	-5.846	9	Sb-1	Sb-1
117	-0.531	0.035	-0.253	-28.033	-3.137	-5.631	12	Sb-2	Sb-2
118	-0.706	0.308	-0.418	9.379	-12.252	18.293	18	Ss-3	Ss-3
119	-0.729	0.225	-0.346	6.582	-12.506	6.096	19	Ss-4	Ss-4
120	-0.695	0.302	-0.443	7.745	-14.146	20.670	18	Ss-3	Ss-3

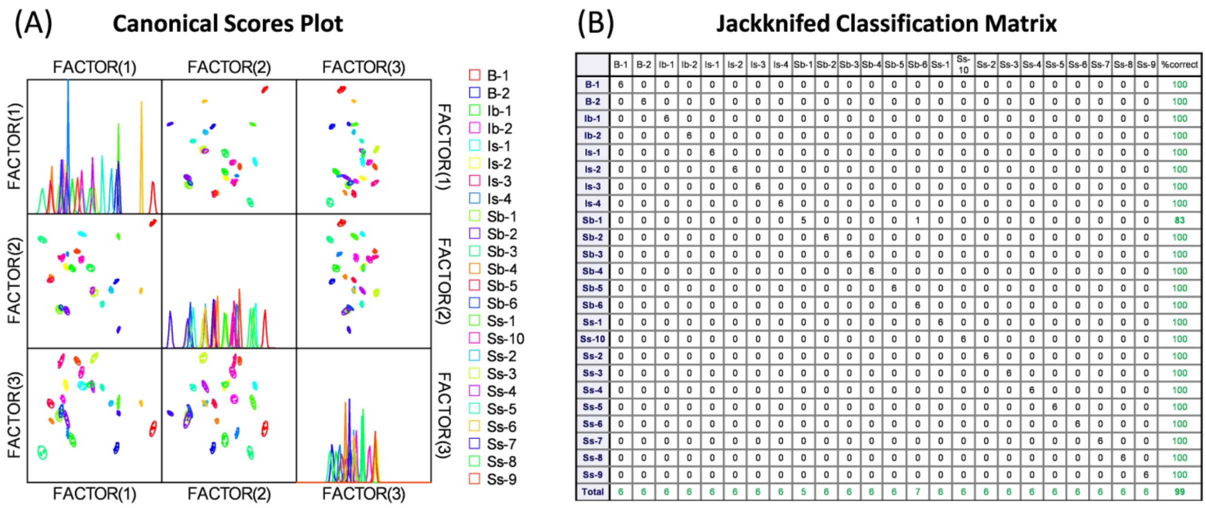

Figure 116. (A) Correlations of canonical fluorescence response patterns from an array of **P1-P3** against whiskies. The 95% confidence ellipses for the individual acids are also shown. **(B)**. Jackknifed classification matrix showed the 99% correct classification.

Table 57. Training matrix of fluorescence response pattern from PAE tongue (**P1-P3**) against various whisky origins. LDA was carried out and resulting in 3 factors of the canonical scores and group generation. Jackknifed classification matrix showed the 100% correct classification.

Analyte	Fluorescence Response Pattern			Results LDA			
Whisky	**P1**	**P2**	**P3**	Factor 1	Factor 2	Factor 3	Group
B-1	-0.9078	0.6705	0.0241	-66.751	22.376	5.048	1
B-1	-0.9142	0.6769	0.0329	-68.314	23.056	4.607	1
B-1	-0.9063	0.6655	0.0322	-66.622	23.369	4.148	1
B-1	-0.9129	0.6913	0.0388	-69.329	24.329	5.177	1
B-1	-0.9075	0.6873	0.0189	-67.535	22.256	6.584	1
B-1	-0.9135	0.6450	0.0375	-66.435	22.751	2.128	1
B-2	-0.9056	0.2241	-0.1396	-31.094	-10.775	-12.690	2
B-2	-0.8996	0.2304	-0.1428	-30.628	-10.427	-11.827	2
B-2	-0.9019	0.2116	-0.1478	-29.497	-11.811	-12.795	2
B-2	-0.8989	0.2463	-0.1546	-31.011	-11.352	-9.840	2
B-2	-0.9049	0.2425	-0.1418	-32.066	-10.441	-11.258	2
B-2	-0.9042	0.2365	-0.1449	-31.466	-10.935	-11.407	2
Ib-1	-0.6566	0.1041	-0.1417	6.316	8.618	-12.483	3
Ib-1	-0.6417	0.1151	-0.1505	7.804	9.241	-10.588	3

Ib-1	-0.6293	0.1207	-0.1504	8.931	10.573	-9.811	3
Ib-1	-0.6240	0.1076	-0.1579	10.725	9.754	-9.957	3
Ib-1	-0.6395	0.1130	-0.1481	8.091	9.681	-10.839	3
Ib-1	-0.6339	0.1111	-0.1288	8.011	12.531	-12.239	3
Ib-2	-0.5109	0.2056	-0.2270	21.214	14.630	5.576	4
Ib-2	-0.5082	0.2140	-0.2206	20.721	15.919	5.750	4
Ib-2	-0.5087	0.1945	-0.2269	22.169	14.521	4.891	4
Ib-2	-0.5124	0.2172	-0.2042	19.279	17.648	4.592	4
Ib-2	-0.5068	0.2174	-0.2190	20.603	16.347	5.904	4
Ib-2	-0.5209	0.1995	-0.2171	19.955	14.743	4.090	4
Is-3	-0.4552	0.2699	-0.3109	27.618	11.342	18.070	5
Is-3	-0.4521	0.2995	-0.3186	26.478	11.550	20.751	5
Is-3	-0.4507	0.3053	-0.3229	26.475	11.320	21.513	5
Is-3	-0.4528	0.2983	-0.3240	26.713	10.782	21.054	5
Is-3	-0.4429	0.2783	-0.3119	28.607	12.611	19.115	5
Is-3	-0.4543	0.2808	-0.3118	27.082	11.635	18.903	5
Is-4	-0.5762	0.1556	-0.1132	11.416	21.139	-8.520	6
Is-4	-0.5727	0.1712	-0.1170	11.027	21.454	-7.065	6
Is-4	-0.5712	0.1680	-0.1194	11.515	21.203	-7.051	6
Is-4	-0.5640	0.1803	-0.1233	11.780	21.754	-5.690	6
Is-4	-0.5721	0.1663	-0.1110	11.136	22.107	-7.829	6
Is-4	-0.5780	0.1580	-0.1162	11.185	20.671	-8.191	6
Sb-1	-0.6341	-0.0494	-0.3601	28.479	-20.785	-5.647	7
Sb-1	-0.6502	-0.0418	-0.3687	26.463	-23.123	-5.012	7
Sb-1	-0.6351	-0.0700	-0.3682	30.017	-22.485	-6.460	7
Sb-1	-0.6608	-0.0637	-0.3635	26.336	-24.112	-7.231	7
Sb-1	-0.6507	-0.0685	-0.3539	27.413	-22.127	-7.948	7
Sb-1	-0.6391	-0.0495	-0.3480	27.342	-19.759	-6.730	7
Sb-2	-0.5254	0.0229	-0.2415	31.601	6.114	-6.146	8
Sb-2	-0.5379	0.0283	-0.2416	29.771	5.097	-6.183	8
Sb-2	-0.5329	0.0312	-0.2398	30.106	5.870	-5.959	8
Sb-2	-0.5233	0.0321	-0.2352	30.991	7.359	-5.931	8
Sb-2	-0.5406	0.0299	-0.2301	28.830	6.313	-7.030	8
Sb-2	-0.5320	0.0328	-0.2374	30.005	6.297	-6.002	8
Ss-2	-0.8294	0.2866	-0.2892	-19.165	-20.325	5.307	9
Ss-2	-0.8435	0.2776	-0.2945	-20.048	-22.557	4.637	9
Ss-2	-0.8338	0.2662	-0.2934	-18.222	-21.853	4.102	9
Ss-2	-0.8463	0.2758	-0.2973	-20.144	-23.216	4.635	9
Ss-2	-0.8380	0.2641	-0.2915	-18.678	-22.071	3.679	9
Ss-2	-0.8365	0.2720	-0.2961	-18.787	-22.268	4.608	9
Ss-5	-0.8079	0.2073	-0.4013	-6.567	-34.505	9.107	10
Ss-5	-0.8063	0.2198	-0.3830	-7.984	-31.727	8.624	10
Ss-5	-0.8066	0.2253	-0.3869	-8.190	-32.075	9.280	10
Ss-5	-0.8135	0.2114	-0.3853	-8.215	-32.929	7.994	10
Ss-5	-0.8026	0.2122	-0.3856	-6.948	-31.928	8.428	10
Ss-5	-0.8163	0.2119	-0.3869	-8.509	-33.373	8.057	10

(A) **Canonical Scores Plot**

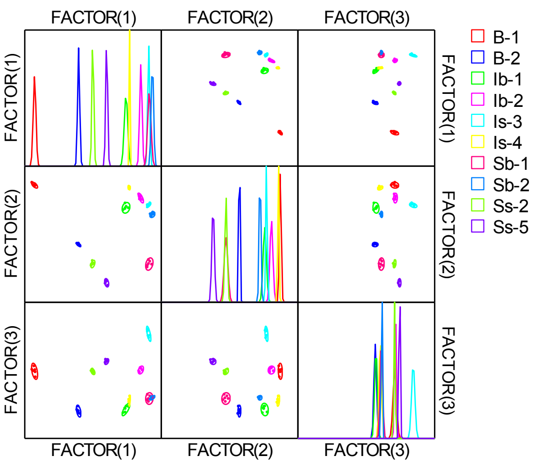

(B) **Jackknifed Classification Matrix**

	B-1	B-2	Ib-1	Ib-2	Is-3	Is-4	Sb-1	Sb-2	Ss-2	Ss-5	%correct
B-1	6	0	0	0	0	0	0	0	0	0	100
B-2	0	6	0	0	0	0	0	0	0	0	100
Ib-1	0	0	6	0	0	0	0	0	0	0	100
Ib-2	0	0	0	6	0	0	0	0	0	0	100
Is-3	0	0	0	0	6	0	0	0	0	0	100
Is-4	0	0	0	0	0	6	0	0	0	0	100
Sb-1	0	0	0	0	0	0	6	0	0	0	100
Sb-2	0	0	0	0	0	0	0	6	0	0	100
Ss-2	0	0	0	0	0	0	0	0	6	0	100
Ss-5	0	0	0	0	0	0	0	0	0	6	100
Total	6	6	6	6	6	6	6	6	6	6	100

Figure 117. (A). Correlations of canonical fluorescence response patterns from PAE tongue (**P1-P3**) against various whisky origins. The 95% confidence ellipses for the individual acids are also shown. **(B)**. Jackknifed classification matrix showed the 100% correct classification.

Table 58. Training matrix of fluorescence response pattern from GFP tongue (**GFP**, **GFP-K36**, and **GFP-E36**) against various whisky origins. LDA was carried out and resulting in 3 factors of the canonical scores and group generation. Jackknifed classification matrix showed the 100% correct classification.

Analyte	Fluorescence Response Pattern			Results LDA			
Whisky	**GFP**	**GFP-K36**	**GFP-E36**	Factor 1	Factor 2	Factor 3	Group
B-1	-0.963	-0.875	-0.967	-60.777	7.905	-0.162	1
B-1	-0.956	-0.873	-0.971	-60.235	8.306	0.939	1
B-1	-0.960	-0.870	-0.971	-60.420	7.557	0.802	1
B-1	-0.960	-0.873	-0.971	-60.683	7.892	0.737	1
B-1	-0.963	-0.875	-0.971	-61.187	7.830	0.501	1
B-1	-0.965	-0.877	-0.968	-61.400	7.986	-0.200	1
B-2	-0.956	-0.827	-0.968	-55.260	3.030	2.943	2
B-2	-0.960	-0.827	-0.967	-55.711	2.695	2.415	2
B-2	-0.954	-0.830	-0.968	-55.285	3.618	2.875	2
B-2	-0.960	-0.837	-0.963	-56.362	3.977	1.375	2
B-2	-0.951	-0.832	-0.966	-55.100	4.221	2.742	2
B-2	-0.957	-0.837	-0.966	-56.242	4.242	2.027	2
Ib-1	-0.827	-0.445	-0.790	14.267	-21.976	7.660	3
Ib-1	-0.839	-0.431	-0.807	12.717	-25.465	9.735	3
Ib-1	-0.825	-0.437	-0.792	15.017	-22.762	8.462	3
Ib-1	-0.827	-0.429	-0.809	14.037	-24.541	10.997	3
Ib-1	-0.833	-0.448	-0.814	10.951	-23.140	10.364	3
Ib-1	-0.826	-0.455	-0.802	12.216	-21.220	8.960	3
Ib-2	-0.800	-0.605	-0.676	11.800	3.255	-13.226	4
Ib-2	-0.795	-0.607	-0.693	10.730	3.443	-10.587	4
Ib-2	-0.798	-0.602	-0.686	11.453	2.729	-11.635	4
Ib-2	-0.798	-0.601	-0.689	11.263	2.560	-11.104	4
Ib-2	-0.795	-0.604	-0.676	12.459	3.688	-12.834	4
Ib-2	-0.799	-0.600	-0.676	12.590	2.874	-12.942	4
Is-3	-0.793	-0.517	-0.762	13.416	-9.141	3.236	5
Is-3	-0.789	-0.534	-0.786	10.029	-7.688	5.855	5
Is-3	-0.790	-0.529	-0.774	11.446	-7.887	4.445	5
Is-3	-0.785	-0.518	-0.772	13.344	-8.668	5.146	5
Is-3	-0.793	-0.540	-0.775	9.950	-7.011	3.844	5
Is-3	-0.791	-0.538	-0.770	10.835	-6.832	3.425	5
Is-4	-0.855	-0.373	-0.672	29.174	-29.208	-7.078	6
Is-4	-0.846	-0.378	-0.687	28.290	-28.229	-4.550	6
Is-4	-0.850	-0.375	-0.676	29.037	-28.660	-6.238	6
Is-4	-0.853	-0.366	-0.683	29.042	-30.188	-5.190	6
Is-4	-0.852	-0.376	-0.676	28.816	-28.676	-6.551	6
Is-4	-0.854	-0.380	-0.674	28.327	-28.417	-7.077	6
Sb-1	-0.468	-0.565	-0.601	60.887	35.496	5.566	7
Sb-1	-0.472	-0.568	-0.597	60.454	35.455	4.552	7
Sb-1	-0.487	-0.572	-0.605	57.514	34.149	4.236	7
Sb-1	-0.485	-0.579	-0.591	58.443	35.603	2.163	7
Sb-1	-0.474	-0.570	-0.608	59.075	35.058	5.703	7
Sb-1	-0.486	-0.579	-0.590	58.481	35.592	2.009	7
Sb-2	-0.544	-0.315	-0.504	86.175	1.746	-1.797	8
Sb-2	-0.552	-0.314	-0.501	85.672	0.888	-2.749	8
Sb-2	-0.528	-0.312	-0.505	88.271	3.100	-0.091	8
Sb-2	-0.522	-0.331	-0.508	86.667	5.798	-0.223	8
Sb-2	-0.528	-0.325	-0.518	85.804	4.157	1.047	8
Sb-2	-0.516	-0.328	-0.500	88.359	6.291	-0.603	8
Ss-2	-0.928	-0.715	-0.898	-34.465	-4.771	1.030	9
Ss-2	-0.932	-0.705	-0.895	-33.570	-6.198	0.908	9
Ss-2	-0.928	-0.710	-0.900	-34.153	-5.368	1.605	9
Ss-2	-0.933	-0.707	-0.898	-34.235	-6.210	1.029	9
Ss-2	-0.932	-0.719	-0.902	-35.679	-4.882	1.137	9
Ss-2	-0.935	-0.715	-0.904	-35.804	-5.669	1.248	9
Ss-5	-0.953	-0.898	-0.951	-60.524	12.137	-2.574	10
Ss-5	-0.953	-0.894	-0.949	-59.959	11.726	-2.647	10
Ss-5	-0.953	-0.892	-0.945	-59.283	11.789	-3.167	10
Ss-5	-0.953	-0.900	-0.949	-60.433	12.477	-2.931	10
Ss-5	-0.956	-0.895	-0.951	-60.425	11.568	-2.733	10
Ss-5	-0.952	-0.895	-0.948	-59.818	11.965	-2.828	10

(A) **Canonical Scores Plot**

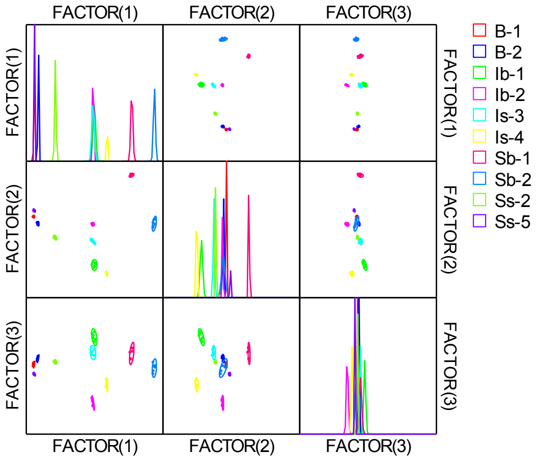

(B) **Jackknifed Classification Matrix**

	B-1	B-2	Ib-1	Ib-2	Is-3	Is-4	Sb-1	Sb-2	Ss-2	Ss-5	%correct
B-1	6	0	0	0	0	0	0	0	0	0	100
B-2	0	6	0	0	0	0	0	0	0	0	100
Ib-1	0	0	6	0	0	0	0	0	0	0	100
Ib-2	0	0	0	6	0	0	0	0	0	0	100
Is-3	0	0	0	0	6	0	0	0	0	0	100
Is-4	0	0	0	0	0	6	0	0	0	0	100
Sb-1	0	0	0	0	0	0	6	0	0	0	100
Sb-2	0	0	0	0	0	0	0	6	0	0	100
Ss-2	0	0	0	0	0	0	0	0	6	0	100
Ss-5	0	0	0	0	0	0	0	0	0	6	100
Total	6	6	6	6	6	6	6	6	6	6	100

Figure 118. (A). Correlations of canonical fluorescence response patterns from GFP tongue (**GFP**, **GFP-K36**, and **GFP-E36**) against various whisky origins. The 95% confidence ellipses for the individual acids are also shown. **(B)**. Jackknifed classification matrix showed the 100% correct classification.

Table 59. Training matrix of fluorescence response pattern from PAE/GFP tongue (six sensing elements) against various whisky origins. LDA was carried out and resulting in 6 factors of the canonical scores and group generation. Jackknifed classification matrix showed the 100% correct classification.

Analyte	Fluorescence Response Pattern						Results LDA				
Whisky	**P2**	**P1**	**P3**	**GFP**	**GFP-K36**	**GFP-E36**	Factor 1	Factor 2	Factor 3	Factor 4	Group
B-1	0.670	-0.908	0.024	-0.963	-0.875	-0.967	90.081	27.563	21.478	20.234	1
B-1	0.677	-0.914	0.033	-0.956	-0.873	-0.971	90.359	28.308	23.375	20.155	1
B-1	0.666	-0.906	0.032	-0.960	-0.870	-0.971	89.513	28.708	22.100	19.559	1
B-1	0.691	-0.913	0.039	-0.960	-0.873	-0.971	91.293	29.979	23.369	20.982	1
B-1	0.687	-0.908	0.019	-0.963	-0.875	-0.971	91.141	27.491	21.303	20.828	1
B-1	0.645	-0.914	0.038	-0.965	-0.877	-0.968	90.017	27.994	22.451	18.672	1
B-2	0.224	-0.906	-0.140	-0.956	-0.827	-0.968	66.421	-6.178	9.736	-11.695	2
B-2	0.230	-0.900	-0.143	-0.960	-0.827	-0.967	66.646	-5.836	8.543	-11.020	2
B-2	0.212	-0.902	-0.148	-0.954	-0.830	-0.968	65.606	-8.033	8.869	-11.962	2
B-2	0.246	-0.899	-0.155	-0.960	-0.837	-0.963	67.713	-7.737	7.652	-9.085	2
B-2	0.243	-0.905	-0.142	-0.951	-0.832	-0.966	66.918	-6.672	9.973	-9.858	2
B-2	0.236	-0.904	-0.145	-0.957	-0.837	-0.966	67.611	-7.326	9.024	-9.929	2
Ib-1	0.104	-0.657	-0.142	-0.827	-0.445	-0.790	-17.573	25.268	3.365	-19.237	3
Ib-1	0.115	-0.642	-0.150	-0.839	-0.431	-0.807	-16.567	27.615	0.528	-20.747	3
Ib-1	0.121	-0.629	-0.150	-0.825	-0.437	-0.792	-19.480	26.486	0.399	-17.610	3
Ib-1	0.108	-0.624	-0.158	-0.827	-0.429	-0.809	-19.363	26.337	-0.752	-20.243	3
Ib-1	0.113	-0.640	-0.148	-0.833	-0.448	-0.814	-15.319	25.830	0.525	-19.682	3
Ib-1	0.111	-0.634	-0.129	-0.826	-0.455	-0.802	-17.045	27.184	1.579	-17.509	3
Ib-2	0.206	-0.511	-0.227	-0.800	-0.605	-0.676	-23.881	5.237	-17.496	16.554	4
Ib-2	0.214	-0.508	-0.221	-0.795	-0.607	-0.693	-22.669	5.984	-16.885	16.288	4
Ib-2	0.194	-0.509	-0.227	-0.798	-0.602	-0.686	-24.107	5.161	-17.589	15.080	4
Ib-2	0.217	-0.512	-0.204	-0.798	-0.601	-0.689	-22.649	8.875	-15.614	16.185	4
Ib-2	0.217	-0.507	-0.219	-0.795	-0.604	-0.676	-24.270	6.555	-16.890	17.682	4
Ib-2	0.200	-0.521	-0.217	-0.799	-0.600	-0.676	-24.071	6.245	-15.601	15.457	4
Is-3	0.270	-0.455	-0.311	-0.793	-0.517	-0.762	-25.659	7.599	-25.340	8.500	5
Is-3	0.299	-0.452	-0.319	-0.789	-0.534	-0.786	-21.612	6.094	-25.999	9.965	5
Is-3	0.305	-0.451	-0.323	-0.790	-0.529	-0.774	-22.793	6.240	-26.306	10.813	5
Is-3	0.298	-0.453	-0.324	-0.785	-0.518	-0.772	-24.575	6.491	-25.471	9.583	5
Is-3	0.278	-0.443	-0.312	-0.793	-0.540	-0.775	-23.176	6.174	-27.231	10.559	5
Is-3	0.281	-0.454	-0.312	-0.791	-0.538	-0.770	-23.067	5.803	-25.740	10.351	5
Is-4	0.156	-0.576	-0.113	-0.855	-0.373	-0.672	-34.712	42.774	-3.825	-9.070	6
Is-4	0.171	-0.573	-0.117	-0.846	-0.378	-0.687	-33.494	41.890	-3.614	-8.517	6
Is-4	0.168	-0.571	-0.119	-0.850	-0.375	-0.676	-34.449	42.100	-4.285	-8.190	6
Is-4	0.180	-0.564	-0.123	-0.853	-0.366	-0.683	-34.355	43.480	-5.243	-8.423	6
Is-4	0.166	-0.572	-0.111	-0.852	-0.376	-0.676	-34.247	43.111	-3.887	-8.108	6
Is-4	0.158	-0.578	-0.116	-0.854	-0.380	-0.674	-33.769	41.684	-3.912	-8.643	6
Sb-1	-0.049	-0.634	-0.360	-0.468	-0.565	-0.601	-70.980	-49.835	17.856	4.664	7
Sb-1	-0.042	-0.650	-0.369	-0.472	-0.568	-0.597	-69.163	-51.219	18.644	4.454	7
Sb-1	-0.070	-0.635	-0.368	-0.487	-0.572	-0.605	-68.727	-50.797	15.311	3.007	7
Sb-1	-0.064	-0.661	-0.363	-0.485	-0.579	-0.591	-67.580	-51.869	18.461	3.676	7
Sb-1	-0.069	-0.651	-0.354	-0.474	-0.570	-0.608	-68.905	-50.242	19.097	2.361	7

Sb-1	-0.049	-0.639	-0.348	-0.486	-0.579	-0.590	-68.563	-48.431	17.142	6.003	7
Sb-2	0.023	-0.525	-0.242	-0.544	-0.315	-0.504	-96.805	2.967	12.732	1.010	8
Sb-2	0.028	-0.538	-0.242	-0.552	-0.314	-0.501	-95.214	3.395	13.412	0.503	8
Sb-2	0.031	-0.533	-0.240	-0.528	-0.312	-0.505	-97.808	2.135	15.345	1.207	8
Sb-2	0.032	-0.523	-0.235	-0.522	-0.331	-0.508	-97.156	0.831	14.627	3.423	8
Sb-2	0.030	-0.541	-0.230	-0.528	-0.325	-0.518	-95.083	1.841	16.417	0.915	8
Sb-2	0.033	-0.532	-0.237	-0.516	-0.328	-0.500	-98.063	0.020	16.072	3.412	8
Ss-2	0.287	-0.829	-0.289	-0.928	-0.715	-0.898	44.834	-11.736	-1.498	-9.070	9
Ss-2	0.278	-0.844	-0.294	-0.932	-0.705	-0.895	44.732	-12.076	-0.434	-11.209	9
Ss-2	0.266	-0.834	-0.293	-0.928	-0.710	-0.900	44.065	-12.767	-1.296	-11.127	9
Ss-2	0.276	-0.846	-0.297	-0.933	-0.707	-0.898	45.456	-12.683	-0.531	-11.581	9
Ss-2	0.264	-0.838	-0.291	-0.932	-0.719	-0.902	45.616	-13.257	-1.347	-11.026	9
Ss-2	0.272	-0.836	-0.296	-0.935	-0.715	-0.904	45.982	-12.883	-1.925	-11.043	9
Ss-5	0.207	-0.808	-0.401	-0.953	-0.898	-0.951	62.157	-44.140	-17.769	-3.469	10
Ss-5	0.220	-0.806	-0.383	-0.953	-0.894	-0.949	62.112	-40.842	-16.665	-2.590	10
Ss-5	0.225	-0.807	-0.387	-0.953	-0.892	-0.945	61.724	-41.091	-16.711	-2.081	10
Ss-5	0.211	-0.814	-0.385	-0.953	-0.900	-0.949	62.655	-42.368	-16.179	-2.983	10
Ss-5	0.212	-0.803	-0.386	-0.956	-0.895	-0.951	61.946	-41.224	-17.517	-2.921	10
Ss-5	0.212	-0.816	-0.387	-0.952	-0.895	-0.948	62.352	-42.208	-15.836	-3.456	10

(A) **Canonical Scores Plot**

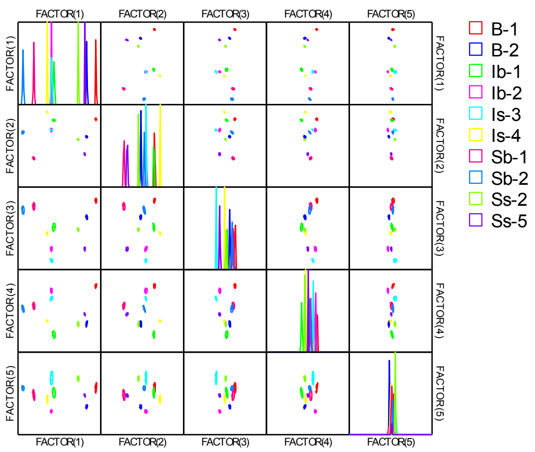

(B) **Jackknifed Classification Matrix**

	B-1	B-2	Ib-1	Ib-2	Is-3	Is-4	Sb-1	Sb-2	Ss-2	Ss-5	%correct
B-1	6	0	0	0	0	0	0	0	0	0	100
B-2	0	6	0	0	0	0	0	0	0	0	100
Ib-1	0	0	6	0	0	0	0	0	0	0	100
Ib-2	0	0	0	6	0	0	0	0	0	0	100
Is-3	0	0	0	0	6	0	0	0	0	0	100
Is-4	0	0	0	0	0	6	0	0	0	0	100
Sb-1	0	0	0	0	0	0	6	0	0	0	100
Sb-2	0	0	0	0	0	0	0	6	0	0	100
Ss-2	0	0	0	0	0	0	0	0	6	0	100
Ss-5	0	0	0	0	0	0	0	0	0	6	100
Total	6	6	6	6	6	6	6	6	6	6	100

Figure 119. (A). Correlations of canonical fluorescence response patterns from PAE/GFP tongue against various whisky origins. The 95% confidence ellipses for the individual acids are also shown. **(B)**. Jackknifed classification matrix showed the 100% correct classification.

Table 60. Training matrix of fluorescence response pattern from PAE tongue (**P1-P3**) against whisky (blending status). LDA was carried out and resulting in 3 factors of the canonical scores and group generation. Jackknifed classification matrix showed the 99% correct classification.

Analyte	Fluorescence Response Pattern			Results LDA			
Whisky	**P2**	**P1**	**P3**	Factor 1	Factor 2	Factor 3	Group
Sb-1	-0.049	-0.634	-0.360	-22.509	-21.340	1.299	1
Sb-1	-0.042	-0.650	-0.369	-20.061	-22.268	1.637	**6**
Sb-1	-0.070	-0.635	-0.368	-23.778	-23.652	1.416	1
Sb-1	-0.064	-0.661	-0.363	-20.779	-24.597	-0.155	1
Sb-1	-0.069	-0.651	-0.354	-22.423	-23.780	-0.806	1
Sb-1	-0.049	-0.639	-0.348	-22.308	-21.007	-0.215	1
Sb-2	0.023	-0.525	-0.242	-31.110	-0.941	-3.233	2
Sb-2	0.028	-0.538	-0.242	-29.413	-1.333	-3.671	2
Sb-2	0.031	-0.533	-0.240	-29.749	-0.638	-3.513	2
Sb-2	0.032	-0.523	-0.235	-30.780	0.356	-3.482	2
Sb-2	0.030	-0.541	-0.230	-29.303	-0.729	-4.952	2
Sb-2	0.033	-0.532	-0.237	-29.779	-0.302	-3.665	2
Sb-3	-0.051	-0.698	-0.355	-16.173	-25.550	-2.501	3
Sb-3	-0.034	-0.675	-0.350	-17.353	-22.258	-1.262	3
Sb-3	-0.033	-0.695	-0.343	-15.409	-23.181	-3.020	3
Sb-3	-0.034	-0.679	-0.362	-16.662	-23.141	-0.175	3
Sb-3	-0.055	-0.709	-0.340	-15.736	-25.774	-4.758	3
Sb-3	-0.024	-0.679	-0.352	-16.215	-21.670	-0.981	3
Sb-4	0.072	-0.416	-0.046	-43.523	21.813	-16.524	4
Sb-4	0.067	-0.433	-0.019	-42.805	21.751	-20.271	4
Sb-4	0.075	-0.447	-0.040	-40.186	20.345	-18.616	4
Sb-4	0.072	-0.423	-0.021	-43.342	22.735	-19.430	4

Sb-4	0.080	-0.446	-0.028	-40.242	21.519	-19.554	4
Sb-4	0.062	-0.432	-0.025	-43.147	21.074	-19.773	4
Sb-5	0.051	-0.502	-0.304	-29.813	-0.499	5.372	5
Sb-5	0.054	-0.511	-0.294	-28.864	-0.233	4.026	5
Sb-5	0.051	-0.521	-0.298	-28.029	-1.372	3.855	5
Sb-5	0.047	-0.506	-0.291	-29.979	-0.294	3.710	5
Sb-5	0.066	-0.521	-0.284	-27.236	0.722	2.795	5
Sb-5	0.046	-0.510	-0.286	-29.856	-0.351	2.911	5
Sb-6	-0.032	-0.636	-0.368	-20.734	-20.407	2.563	6
Sb-6	-0.025	-0.646	-0.364	-19.284	-20.206	1.890	6
Sb-6	-0.038	-0.644	-0.360	-20.614	-21.070	1.087	6
Sb-6	-0.035	-0.639	-0.358	-20.894	-20.310	1.297	6
Sb-6	-0.024	-0.648	-0.383	-18.612	-21.396	3.876	6
Sb-6	-0.031	-0.647	-0.351	-19.967	-20.156	0.335	6
Ss-1	0.533	-0.734	-0.111	26.042	36.321	-10.529	7
Ss-1	0.538	-0.734	-0.106	26.324	37.057	-10.865	7
Ss-1	0.532	-0.743	-0.121	27.114	35.180	-9.944	7
Ss-1	0.528	-0.736	-0.099	25.543	36.459	-12.079	7
Ss-1	0.520	-0.740	-0.102	25.361	35.403	-12.235	7
Ss-1	0.525	-0.740	-0.086	25.427	36.689	-13.654	7
Ss-2	0.287	-0.829	-0.289	21.424	-1.560	-4.840	9
Ss-2	0.278	-0.844	-0.294	22.315	-3.603	-5.290	9
Ss-2	0.266	-0.834	-0.293	20.421	-3.866	-5.292	9
Ss-2	0.276	-0.846	-0.297	22.535	-4.109	-5.197	9
Ss-2	0.264	-0.838	-0.291	20.644	-4.228	-5.770	9
Ss-2	0.272	-0.836	-0.296	21.209	-3.701	-4.956	9
Ss-3	0.310	-0.696	-0.429	13.043	1.626	17.172	10
Ss-3	0.278	-0.699	-0.425	10.740	-1.074	15.508	10
Ss-3	0.290	-0.695	-0.434	11.542	-0.252	17.107	10
Ss-3	0.312	-0.704	-0.427	14.053	1.426	16.619	10
Ss-3	0.282	-0.692	-0.421	10.306	-0.022	15.617	10
Ss-3	0.287	-0.709	-0.440	12.876	-1.860	16.950	10
Ss-4	0.226	-0.718	-0.365	7.247	-3.427	6.693	11
Ss-4	0.237	-0.728	-0.356	8.849	-2.692	5.599	11
Ss-4	0.234	-0.717	-0.344	7.300	-1.546	4.746	11
Ss-4	0.230	-0.725	-0.338	7.564	-2.093	3.621	11
Ss-4	0.224	-0.728	-0.356	7.929	-3.797	5.213	11
Ss-4	0.233	-0.729	-0.335	8.251	-1.924	3.250	11
Ss-5	0.207	-0.808	-0.401	15.975	-13.299	5.309	12
Ss-5	0.220	-0.806	-0.383	16.306	-11.072	3.894	12
Ss-5	0.225	-0.807	-0.387	16.856	-10.836	4.466	12
Ss-5	0.211	-0.814	-0.385	16.460	-12.422	3.497	12
Ss-5	0.212	-0.803	-0.386	15.411	-11.625	4.101	12
Ss-5	0.212	-0.816	-0.387	16.826	-12.661	3.540	12
Ss-6	0.405	-0.990	-0.271	46.464	-1.253	-10.868	13
Ss-6	0.405	-0.990	-0.268	46.384	-1.078	-11.136	13
Ss-6	0.396	-0.989	-0.282	46.032	-2.612	-9.951	13
Ss-6	0.406	-0.990	-0.283	46.850	-1.800	-9.591	13
Ss-6	0.400	-0.989	-0.284	46.381	-2.406	-9.652	13
Ss-6	0.396	-0.990	-0.286	46.156	-2.816	-9.609	13
Ss-7	0.133	-0.989	-0.394	28.739	-31.716	-6.979	14
Ss-7	0.113	-0.990	-0.403	27.461	-34.009	-6.660	14
Ss-7	0.123	-0.990	-0.407	28.342	-33.420	-6.039	14
Ss-7	0.124	-0.990	-0.396	28.086	-32.682	-7.101	14
Ss-7	0.114	-0.989	-0.413	27.733	-34.507	-5.628	14
Ss-7	0.123	-0.990	-0.404	28.266	-33.191	-6.239	14
Ss-8	0.306	-0.646	-0.275	3.715	13.536	3.497	15
Ss-8	0.326	-0.664	-0.269	6.998	14.292	2.642	15
Ss-8	0.328	-0.646	-0.274	5.420	15.410	4.117	15
Ss-8	0.318	-0.670	-0.286	7.396	12.289	3.845	15
Ss-8	0.325	-0.651	-0.273	5.658	14.908	3.730	15
Ss-8	0.307	-0.647	-0.278	4.026	13.375	3.779	15
Ss-9	0.385	-0.513	-0.296	-3.336	28.214	14.970	16
Ss-9	0.385	-0.524	-0.284	-2.527	28.189	13.115	16
Ss-9	0.378	-0.504	-0.293	-4.841	28.383	14.788	16
Ss-9	0.374	-0.519	-0.284	-3.866	27.563	13.104	16
Ss-9	0.389	-0.511	-0.282	-3.562	29.418	13.745	16
Ss-9	0.387	-0.527	-0.283	-2.084	28.162	12.967	16
Ss-10	0.339	-0.577	-0.290	-0.410	20.241	9.594	8
Ss-10	0.352	-0.574	-0.271	-0.229	22.616	8.209	8
Ss-10	0.329	-0.570	-0.288	-1.950	19.967	9.424	8
Ss-10	0.351	-0.572	-0.296	0.158	21.230	10.944	8

Ss-10	0.332	-0.567	-0.273	-2.415	21.222	8.069	8
Ss-10	0.351	-0.572	-0.280	-0.274	22.121	9.152	8

(A) **Canonical Scores Plot**

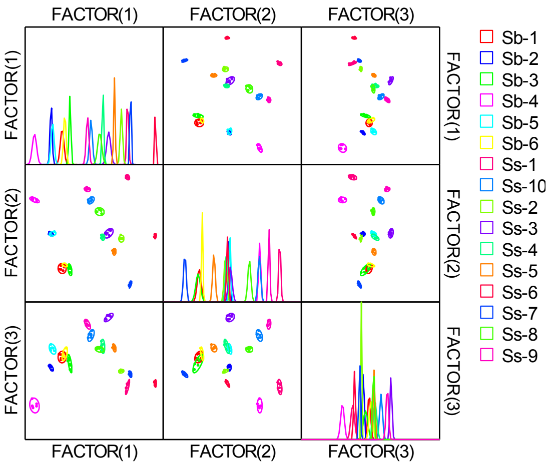

(B) **Jackknifed Classification Matrix**

	Sb-1	Sb-2	Sb-3	Sb-4	Sb-5	Sb-6	Ss-1	Ss-10	Ss-2	Ss-3	Ss-4	Ss-5	Ss-6	Ss-7	Ss-8	Ss-9	%correct
Sb-1	5	0	0	0	0	1	0	0	0	0	0	0	0	0	0	0	83
Sb-2	0	6	0	0	0	0	0	0	0	0	0	0	0	0	0	0	100
Sb-3	0	0	6	0	0	0	0	0	0	0	0	0	0	0	0	0	100
Sb-4	0	0	0	6	0	0	0	0	0	0	0	0	0	0	0	0	100
Sb-5	0	0	0	0	6	0	0	0	0	0	0	0	0	0	0	0	100
Sb-6	0	0	0	0	0	6	0	0	0	0	0	0	0	0	0	0	100
Ss-1	0	0	0	0	0	0	6	0	0	0	0	0	0	0	0	0	100
Ss-10	0	0	0	0	0	0	0	6	0	0	0	0	0	0	0	0	100
Ss-2	0	0	0	0	0	0	0	0	6	0	0	0	0	0	0	0	100
Ss-3	0	0	0	0	0	0	0	0	0	6	0	0	0	0	0	0	100
Ss-4	0	0	0	0	0	0	0	0	0	0	6	0	0	0	0	0	100
Ss-5	0	0	0	0	0	0	0	0	0	0	0	6	0	0	0	0	100
Ss-6	0	0	0	0	0	0	0	0	0	0	0	0	6	0	0	0	100
Ss-7	0	0	0	0	0	0	0	0	0	0	0	0	0	6	0	0	100
Ss-8	0	0	0	0	0	0	0	0	0	0	0	0	0	0	6	0	100
Ss-9	0	0	0	0	0	0	0	0	0	0	0	0	0	0	0	6	100
Total	5	6	6	6	6	7	6	6	6	6	6	6	6	6	6	6	99

Figure 120. (A). Correlations of canonical fluorescence response patterns from PAE tongue (**P1-P3**) against whisky (blending status). The 95% confidence ellipses for the individual acids are also shown. **(B)**. Jackknifed classification matrix showed the 99% correct classification.

Table 61. Training matrix of fluorescence response pattern from GFP tongue (**GFP**, **GFP-K36**, and **GFP-E36**) against whisky (blending status). LDA was carried out and resulting in 3 factors of the canonical scores and group generation. Jackknifed classification matrix showed the 93% correct classification.

Analyte	Fluorescence Response Pattern			Results LDA			
Whisky	**GFP**	**GFP-K36**	**GFP-E36**	Factor 1	Factor 2	Factor 3	Group
Sb-1	-0.468	-0.565	-0.601	49.967	20.279	21.931	1
Sb-1	-0.472	-0.568	-0.597	49.849	20.805	20.977	1
Sb-1	-0.487	-0.572	-0.605	47.488	20.169	20.012	1
Sb-1	-0.485	-0.579	-0.591	48.825	22.366	18.758	1
Sb-1	-0.474	-0.570	-0.608	48.476	20.039	21.773	1
Sb-1	-0.486	-0.579	-0.590	48.888	22.431	18.618	1
Sb-2	-0.544	-0.315	-0.504	67.862	-8.216	4.223	2
Sb-2	-0.552	-0.314	-0.501	67.592	-8.424	3.013	2
Sb-2	-0.528	-0.312	-0.505	69.261	-8.141	6.401	2
Sb-2	-0.522	-0.331	-0.508	68.316	-5.549	7.196	2
Sb-2	-0.528	-0.325	-0.518	67.190	-7.512	7.663	2
Sb-2	-0.516	-0.328	-0.500	69.774	-5.125	7.150	2
Sb-3	-0.841	-0.596	-0.716	5.370	1.226	-11.009	3
Sb-3	-0.832	-0.583	-0.705	8.081	0.853	-11.014	3
Sb-3	-0.842	-0.593	-0.711	5.961	1.230	-11.593	3
Sb-3	-0.842	-0.585	-0.703	7.286	0.961	-12.488	3
Sb-3	-0.836	-0.591	-0.717	6.017	0.772	-10.241	3
Sb-3	-0.833	-0.587	-0.714	6.809	0.470	-10.245	3
Sb-4	-0.395	-0.222	-0.148	123.124	15.441	-13.879	4
Sb-4	-0.378	-0.221	-0.158	123.430	14.880	-10.768	4
Sb-4	-0.376	-0.239	-0.157	122.688	17.505	-10.727	4
Sb-4	-0.391	-0.234	-0.184	118.831	13.919	-9.743	4
Sb-4	-0.362	-0.224	-0.152	125.144	16.386	-9.520	4
Sb-4	-0.376	-0.250	-0.152	122.612	19.571	-11.327	4
Sb-5	-0.577	-0.309	-0.464	69.719	-6.690	-3.743	5
Sb-5	-0.578	-0.290	-0.455	71.649	-8.630	-4.630	5
Sb-5	-0.565	-0.301	-0.460	71.599	-6.986	-2.627	5
Sb-5	-0.576	-0.324	-0.494	65.716	-7.295	-0.559	5
Sb-5	-0.558	-0.308	-0.475	70.192	-7.115	-0.360	5
Sb-5	-0.575	-0.319	-0.468	68.907	-5.523	-3.197	5
Sb-6	-0.837	-0.452	-0.785	6.411	-24.249	-2.640	6
Sb-6	-0.825	-0.447	-0.789	7.169	-24.927	-0.786	6
Sb-6	-0.838	-0.451	-0.791	5.656	-24.965	-2.068	6
Sb-6	-0.839	-0.450	-0.791	5.744	-25.070	-2.227	6
Sb-6	-0.834	-0.449	-0.781	7.194	-24.213	-2.635	6
Sb-6	-0.833	-0.452	-0.788	6.388	-24.385	-1.903	6
Ss-1	-0.946	-0.696	-0.949	-33.457	-8.996	-0.206	7
Ss-1	-0.941	-0.699	-0.948	-33.154	-8.332	0.345	7

Ss-1	-0.938	-0.710	-0.949	-33.661	-6.833	0.739	7
Ss-1	-0.943	-0.697	-0.950	-33.359	-8.875	0.195	7
Ss-1	-0.937	-0.710	-0.948	-33.349	-6.653	0.688	7
Ss-1	-0.942	-0.709	-0.943	-33.229	-6.602	-0.410	7
Ss-2	-0.928	-0.715	-0.898	-27.682	-1.384	-3.463	9
Ss-2	-0.932	-0.705	-0.895	-27.104	-2.665	-4.053	9
Ss-2	-0.928	-0.710	-0.900	-27.628	-2.227	-3.152	9
Ss-2	-0.933	-0.707	-0.898	-27.652	-2.659	-3.991	9
Ss-2	-0.932	-0.719	-0.902	-28.666	-1.395	-3.487	9
Ss-2	-0.935	-0.715	-0.904	-28.870	-2.119	-3.692	9
Ss-3	-0.907	-0.695	-0.887	-23.727	-2.373	-1.917	10
Ss-3	-0.907	-0.699	-0.884	-23.607	-1.703	-2.257	10
Ss-3	-0.914	-0.683	-0.881	-22.946	-3.754	-3.294	10
Ss-3	-0.907	-0.707	-0.884	-23.977	-0.529	-2.286	10
Ss-3	-0.913	-0.693	-0.877	-22.952	-2.032	-3.718	10
Ss-3	-0.907	-0.702	-0.883	-23.597	-1.107	-2.382	10
Ss-4	-0.899	-0.508	-0.888	-12.751	-27.712	0.234	11
Ss-4	-0.906	-0.543	-0.885	-14.948	-23.027	-1.034	11
Ss-4	-0.901	-0.535	-0.887	-14.285	-24.013	-0.330	11
Ss-4	-0.902	-0.527	-0.888	-14.078	-25.312	-0.203	11
Ss-4	-0.897	-0.519	-0.891	-13.524	-26.540	0.694	11
Ss-4	-0.898	-0.536	-0.884	-13.800	-23.520	-0.321	11
Ss-5	-0.953	-0.898	-0.951	-45.488	18.105	-2.004	12
Ss-5	-0.953	-0.894	-0.949	-45.073	17.720	-2.188	12
Ss-5	-0.953	-0.892	-0.945	-44.423	17.959	-2.589	12
Ss-5	-0.953	-0.900	-0.949	-45.302	18.570	-2.191	12
Ss-5	-0.956	-0.895	-0.951	-45.434	17.680	-2.356	12
Ss-5	-0.952	-0.895	-0.948	-44.898	18.002	-2.252	12
Ss-6	-0.961	-0.954	-0.959	-50.000	24.836	-2.489	13
Ss-6	-0.964	-0.950	-0.959	-50.046	24.154	-2.837	13
Ss-6	-0.958	-0.950	-0.956	-49.247	24.738	-2.419	**14**
Ss-6	-0.956	-0.951	-0.954	-48.909	25.031	-2.412	**14**
Ss-6	-0.957	-0.951	-0.956	-49.289	24.812	-2.300	**14**
Ss-6	-0.963	-0.951	-0.955	-49.592	24.717	-3.168	13
Ss-7	-0.960	-0.950	-0.951	-48.896	25.013	-3.206	14
Ss-7	-0.957	-0.953	-0.955	-49.263	25.259	-2.502	14
Ss-7	-0.957	-0.950	-0.957	-49.278	24.659	-2.164	14
Ss-7	-0.961	-0.953	-0.953	-49.413	25.225	-3.120	14
Ss-7	-0.959	-0.949	-0.956	-49.268	24.601	-2.510	**13**
Ss-7	-0.955	-0.950	-0.957	-49.206	24.709	-1.967	14
Ss-8	-0.917	-0.571	-0.919	-20.990	-22.520	0.992	15
Ss-8	-0.920	-0.573	-0.925	-21.956	-22.866	1.084	15
Ss-8	-0.923	-0.571	-0.928	-22.481	-23.437	1.072	15
Ss-8	-0.919	-0.577	-0.927	-22.331	-22.421	1.484	15
Ss-8	-0.918	-0.570	-0.922	-21.323	-22.880	1.098	15
Ss-8	-0.924	-0.571	-0.922	-21.930	-22.984	0.427	15
Ss-9	-0.841	-0.676	-0.935	-22.258	-6.890	10.962	16
Ss-9	-0.817	-0.669	-0.934	-19.837	-6.802	13.738	16
Ss-9	-0.816	-0.670	-0.934	-19.745	-6.626	13.880	16
Ss-9	-0.833	-0.671	-0.933	-21.212	-7.058	11.810	16
Ss-9	-0.828	-0.663	-0.930	-19.967	-7.719	12.152	16
Ss-9	-0.844	-0.674	-0.933	-22.212	-7.097	10.508	16
Ss-10	-0.942	-0.754	-0.956	-37.157	-1.653	0.669	8
Ss-10	-0.937	-0.759	-0.955	-36.863	-0.686	1.128	8
Ss-10	-0.944	-0.767	-0.957	-38.048	0.028	0.388	8
Ss-10	-0.939	-0.767	-0.955	-37.466	0.397	0.821	8
Ss-10	-0.939	-0.764	-0.957	-37.543	-0.113	0.984	8
Ss-10	-0.937	-0.760	-0.954	-36.838	-0.388	0.994	8

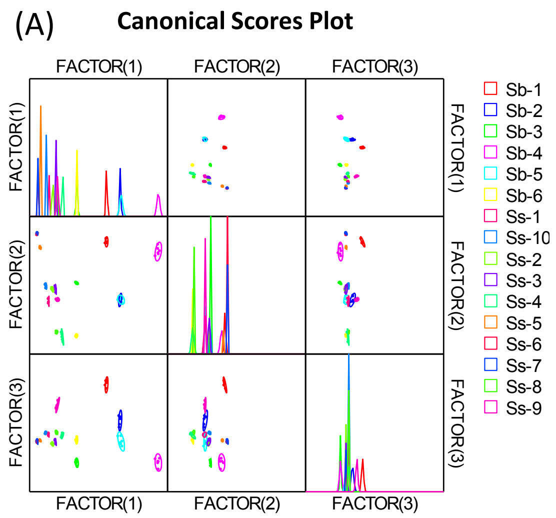

(B) **Jackknifed Classification Matrix**

	Sb-1	Sb-2	Sb-3	Sb-4	Sb-5	Sb-6	Ss-1	Ss-10	Ss-2	Ss-3	Ss-4	Ss-5	Ss-6	Ss-7	Ss-8	Ss-9	%correct
Sb-1	6	0	0	0	0	1	0	0	0	0	0	0	0	0	0	0	100
Sb-2	0	6	0	0	0	0	0	0	0	0	0	0	0	0	0	0	100
Sb-3	0	0	6	0	0	0	0	0	0	0	0	0	0	0	0	0	100
Sb-4	0	0	0	6	0	0	0	0	0	0	0	0	0	0	0	0	100
Sb-5	0	0	0	0	6	0	0	0	0	0	0	0	0	0	0	0	100
Sb-6	0	0	0	0	0	6	0	0	0	0	0	0	0	0	0	0	100
Ss-1	0	0	0	0	0	0	6	0	0	0	0	0	0	0	0	0	100
Ss-10	0	0	0	0	0	0	0	6	0	0	0	0	0	0	0	0	100
Ss-2	0	0	0	0	0	0	0	0	6	0	0	0	0	0	0	0	100
Ss-3	0	0	0	0	0	0	0	0	0	6	0	0	0	0	0	0	100
Ss-4	0	0	0	0	0	0	0	0	0	0	6	0	0	0	0	0	100
Ss-5	0	0	0	0	0	0	0	0	0	0	0	6	0	0	0	0	100
Ss-6	0	0	0	0	0	0	0	0	0	0	0	0	3	3	0	0	50
Ss-7	0	0	0	0	0	0	0	0	0	0	0	0	4	2	0	0	33
Ss-8	0	0	0	0	0	0	0	0	0	0	0	0	0	0	6	0	100
Ss-9	0	0	0	0	0	0	0	0	0	0	0	0	0	0	0	6	100
Total	6	6	6	6	6	6	6	6	6	6	6	6	7	5	6	6	93

Figure 121. (A). Correlations of canonical fluorescence response patterns from GFP tongue (**GFP**, **GFP-K36**, and **GFP-E36**) against whisky (blending status). The 95% confidence ellipses for the individual acids are also shown. **(B)**. Jackknifed classification matrix showed the 93% correct classification.

Table 62. Training matrix of fluorescence response pattern from PAE/GFP tongue against whisky (blending status). LDA was carried out and resulting in 6 factors of the canonical scores and group generation. Jackknifed classification matrix showed the 100% correct classification.

Analyte	Fluorescence Response Pattern						Results LDA				
Whisky	**P2**	**P1**	**P3**	**GFP**	**GFP-K36**	**GFP-E36**	Factor 1	Factor 2	Factor 3	Factor 4	Group
Sb-1	-0.049	-0.634	-0.360	-0.468	-0.565	-0.601	-64.511	-29.941	-1.168	21.700	1
Sb-1	-0.042	-0.650	-0.369	-0.472	-0.568	-0.597	-63.028	-30.957	-0.243	20.335	1
Sb-1	-0.070	-0.635	-0.368	-0.487	-0.572	-0.605	-62.943	-31.774	-2.590	21.074	1
Sb-1	-0.064	-0.661	-0.363	-0.485	-0.579	-0.591	-62.961	-33.519	0.553	18.742	1
Sb-1	-0.069	-0.651	-0.354	-0.474	-0.570	-0.608	-63.644	-31.893	-1.782	19.716	1
Sb-1	-0.049	-0.639	-0.348	-0.486	-0.579	-0.590	-63.527	-30.374	1.584	20.237	1
Sb-2	0.023	-0.525	-0.242	-0.544	-0.315	-0.504	-83.219	2.534	-6.863	-2.048	2
Sb-2	0.028	-0.538	-0.242	-0.552	-0.314	-0.501	-82.057	2.375	-6.183	-3.987	2
Sb-2	0.031	-0.533	-0.240	-0.528	-0.312	-0.505	-83.938	2.610	-6.414	-1.746	2
Sb-2	0.032	-0.523	-0.235	-0.522	-0.331	-0.508	-83.654	2.233	-4.960	1.120	2
Sb-2	0.030	-0.541	-0.230	-0.528	-0.325	-0.518	-82.066	2.204	-5.989	-1.471	2
Sb-2	0.033	-0.532	-0.237	-0.516	-0.328	-0.500	-84.610	1.451	-4.308	0.338	2
Sb-3	-0.051	-0.698	-0.355	-0.841	-0.596	-0.716	-16.708	-22.170	-11.148	-6.874	3
Sb-3	-0.034	-0.675	-0.350	-0.832	-0.583	-0.705	-19.402	-19.149	-10.483	-5.401	3
Sb-3	-0.033	-0.695	-0.343	-0.842	-0.593	-0.711	-16.679	-20.042	-9.521	-7.426	3
Sb-3	-0.034	-0.679	-0.362	-0.842	-0.585	-0.703	-18.065	-19.906	-10.663	-5.868	3
Sb-3	-0.055	-0.709	-0.340	-0.836	-0.591	-0.717	-17.547	-22.148	-10.730	-8.548	3
Sb-3	-0.024	-0.679	-0.352	-0.833	-0.587	-0.714	-17.455	-18.512	-10.555	-5.164	3
Sb-4	0.072	-0.416	-0.046	-0.395	-0.222	-0.148	-143.547	12.867	30.507	-5.688	4
Sb-4	0.067	-0.433	-0.019	-0.378	-0.221	-0.158	-144.278	12.967	30.921	-7.091	4
Sb-4	0.075	-0.447	-0.040	-0.376	-0.239	-0.157	-142.044	10.449	32.370	-5.896	4
Sb-4	0.072	-0.423	-0.021	-0.391	-0.234	-0.184	-139.917	14.216	29.307	-5.219	4
Sb-4	0.080	-0.446	-0.028	-0.362	-0.224	-0.152	-144.507	11.933	32.467	-6.584	4
Sb-4	0.062	-0.432	-0.025	-0.376	-0.250	-0.152	-143.827	10.217	33.522	-4.228	4
Sb-5	0.051	-0.502	-0.304	-0.577	-0.309	-0.464	-82.288	2.484	-5.935	-0.903	5
Sb-5	0.054	-0.511	-0.294	-0.578	-0.290	-0.455	-83.706	3.705	-5.870	-4.130	5
Sb-5	0.051	-0.521	-0.298	-0.565	-0.301	-0.460	-83.509	1.803	-5.346	-2.802	5
Sb-5	0.047	-0.506	-0.291	-0.576	-0.324	-0.494	-78.961	2.803	-7.082	0.304	5
Sb-5	0.066	-0.521	-0.284	-0.558	-0.308	-0.475	-81.813	3.585	-4.676	-1.887	5
Sb-5	0.046	-0.510	-0.286	-0.575	-0.319	-0.468	-82.050	2.112	-4.540	-1.328	5
Sb-6	-0.032	-0.636	-0.368	-0.837	-0.452	-0.785	-18.172	-6.491	-31.200	-10.343	6
Sb-6	-0.025	-0.646	-0.364	-0.825	-0.447	-0.789	-18.261	-6.116	-31.157	-10.875	6
Sb-6	-0.038	-0.644	-0.360	-0.838	-0.451	-0.791	-17.719	-6.732	-31.664	-11.484	6
Sb-6	-0.035	-0.639	-0.358	-0.839	-0.450	-0.791	-17.833	-6.009	-31.543	-11.197	6
Sb-6	-0.024	-0.648	-0.383	-0.834	-0.449	-0.781	-17.593	-7.431	-31.152	-10.825	6
Sb-6	-0.031	-0.647	-0.351	-0.833	-0.452	-0.788	-18.141	-6.195	-30.359	-11.750	6
Ss-1	0.533	-0.734	-0.111	-0.946	-0.696	-0.949	48.798	36.532	16.556	-9.642	7
Ss-1	0.538	-0.734	-0.106	-0.941	-0.699	-0.948	48.619	36.839	17.429	-9.167	7
Ss-1	0.532	-0.743	-0.121	-0.938	-0.710	-0.949	49.449	34.436	17.481	-8.208	7
Ss-1	0.528	-0.736	-0.099	-0.943	-0.697	-0.950	48.124	36.617	16.950	-10.110	7
Ss-1	0.520	-0.740	-0.102	-0.937	-0.710	-0.948	47.759	34.626	17.888	-8.816	7

Ss-1	0.525	-0.740	-0.086	-0.942	-0.709	-0.943	47.601	35.847	19.205	-10.082	7
Ss-2	0.287	-0.829	-0.289	-0.928	-0.715	-0.898	37.793	-0.280	4.320	-11.481	9
Ss-2	0.278	-0.844	-0.294	-0.932	-0.705	-0.895	37.535	-1.435	3.307	-13.870	9
Ss-2	0.266	-0.834	-0.293	-0.928	-0.710	-0.900	36.885	-1.919	2.547	-12.194	9
Ss-2	0.276	-0.846	-0.297	-0.933	-0.707	-0.898	38.148	-1.887	3.058	-13.902	9
Ss-2	0.264	-0.838	-0.291	-0.932	-0.719	-0.902	37.866	-2.582	3.119	-12.227	9
Ss-2	0.272	-0.836	-0.296	-0.935	-0.715	-0.904	38.623	-1.793	2.796	-12.330	9
Ss-3	0.310	-0.696	-0.429	-0.907	-0.695	-0.887	33.658	2.247	-5.009	7.238	10
Ss-3	0.278	-0.699	-0.425	-0.907	-0.699	-0.884	31.664	-0.357	-5.827	6.734	10
Ss-3	0.290	-0.695	-0.434	-0.914	-0.683	-0.881	31.997	1.336	-6.779	5.711	10
Ss-3	0.312	-0.704	-0.427	-0.907	-0.707	-0.884	34.283	1.250	-3.267	7.259	10
Ss-3	0.282	-0.692	-0.421	-0.913	-0.693	-0.877	31.007	0.815	-5.377	6.124	10
Ss-3	0.287	-0.709	-0.440	-0.907	-0.702	-0.883	33.022	-1.370	-5.440	6.764	10
Ss-4	0.226	-0.718	-0.365	-0.899	-0.508	-0.888	18.373	9.722	-21.577	-13.538	11
Ss-4	0.237	-0.728	-0.356	-0.906	-0.543	-0.885	21.120	8.311	-17.236	-12.446	11
Ss-4	0.234	-0.717	-0.344	-0.901	-0.535	-0.887	19.576	9.758	-17.760	-12.288	11
Ss-4	0.230	-0.725	-0.338	-0.902	-0.527	-0.888	19.310	9.903	-18.391	-13.998	11
Ss-4	0.224	-0.728	-0.356	-0.897	-0.519	-0.891	19.114	8.864	-20.432	-13.837	11
Ss-4	0.233	-0.729	-0.335	-0.898	-0.536	-0.884	19.306	9.232	-16.688	-13.597	11
Ss-5	0.207	-0.808	-0.401	-0.953	-0.898	-0.951	51.671	-19.938	4.447	10.075	12
Ss-5	0.220	-0.806	-0.383	-0.953	-0.894	-0.949	51.442	-17.751	5.781	9.137	12
Ss-5	0.225	-0.807	-0.387	-0.953	-0.892	-0.945	51.265	-17.650	6.228	9.109	12
Ss-5	0.211	-0.814	-0.385	-0.953	-0.900	-0.949	51.505	-19.321	5.953	9.006	12
Ss-5	0.212	-0.803	-0.386	-0.956	-0.895	-0.951	51.282	-18.206	5.132	9.498	12
Ss-5	0.212	-0.816	-0.387	-0.952	-0.895	-0.948	51.333	-19.268	5.662	8.371	12
Ss-6	0.405	-0.990	-0.271	-0.961	-0.954	-0.959	71.027	-12.089	29.370	-7.360	13
Ss-6	0.405	-0.990	-0.268	-0.964	-0.950	-0.959	71.040	-11.585	29.116	-8.041	13
Ss-6	0.396	-0.989	-0.282	-0.958	-0.950	-0.956	70.096	-13.272	28.391	-7.039	13
Ss-6	0.406	-0.990	-0.283	-0.956	-0.951	-0.954	70.364	-12.712	29.134	-6.870	13
Ss-6	0.400	-0.989	-0.284	-0.957	-0.951	-0.956	70.399	-13.144	28.514	-6.837	13
Ss-6	0.396	-0.990	-0.286	-0.963	-0.951	-0.955	70.581	-13.399	28.345	-7.302	13
Ss-7	0.133	-0.989	-0.394	-0.960	-0.950	-0.951	57.755	-38.946	9.887	-4.505	14
Ss-7	0.113	-0.990	-0.403	-0.957	-0.953	-0.955	57.177	-41.125	8.349	-3.652	14
Ss-7	0.123	-0.990	-0.407	-0.957	-0.950	-0.957	57.867	-40.373	8.211	-3.664	14
Ss-7	0.124	-0.990	-0.396	-0.961	-0.953	-0.953	57.754	-39.889	9.352	-4.254	14
Ss-7	0.114	-0.989	-0.413	-0.959	-0.949	-0.956	57.504	-41.288	7.461	-3.610	14
Ss-7	0.123	-0.990	-0.404	-0.955	-0.950	-0.957	57.728	-40.203	8.343	-3.575	14
Ss-8	0.306	-0.646	-0.275	-0.917	-0.571	-0.919	25.150	22.330	-12.737	-4.960	15
Ss-8	0.326	-0.664	-0.269	-0.920	-0.573	-0.925	27.844	23.165	-11.389	-6.843	15
Ss-8	0.328	-0.646	-0.274	-0.923	-0.571	-0.928	27.874	24.382	-12.430	-5.116	15
Ss-8	0.318	-0.670	-0.286	-0.919	-0.577	-0.927	28.412	21.134	-12.308	-6.178	15
Ss-8	0.325	-0.651	-0.273	-0.918	-0.570	-0.922	26.748	23.682	-11.886	-5.466	15
Ss-8	0.307	-0.647	-0.278	-0.924	-0.571	-0.922	26.312	22.439	-13.105	-5.388	15
Ss-9	0.385	-0.513	-0.296	-0.841	-0.676	-0.935	24.831	26.984	-4.977	24.410	16
Ss-9	0.385	-0.524	-0.284	-0.817	-0.669	-0.934	22.463	26.768	-4.317	24.029	16
Ss-9	0.378	-0.504	-0.293	-0.816	-0.670	-0.934	21.393	26.808	-5.503	26.416	16
Ss-9	0.374	-0.519	-0.284	-0.833	-0.671	-0.933	23.081	26.483	-4.969	23.481	16
Ss-9	0.389	-0.511	-0.282	-0.828	-0.663	-0.930	22.369	28.371	-4.658	23.807	16
Ss-9	0.387	-0.527	-0.283	-0.844	-0.674	-0.933	25.144	27.118	-3.927	22.115	16
Ss-10	0.339	-0.577	-0.290	-0.942	-0.754	-0.956	39.312	18.472	-1.721	17.327	8
Ss-10	0.352	-0.574	-0.271	-0.937	-0.759	-0.955	39.046	20.117	0.353	17.687	8
Ss-10	0.329	-0.570	-0.288	-0.944	-0.767	-0.957	39.191	17.486	-1.255	18.834	8
Ss-10	0.351	-0.572	-0.296	-0.939	-0.767	-0.955	40.182	18.337	-0.265	19.516	8
Ss-10	0.332	-0.567	-0.273	-0.939	-0.764	-0.957	38.293	18.653	-0.619	18.641	8
Ss-10	0.351	-0.572	-0.280	-0.937	-0.760	-0.954	39.117	19.525	0.059	18.297	8

(A) **Canonical Scores Plot**

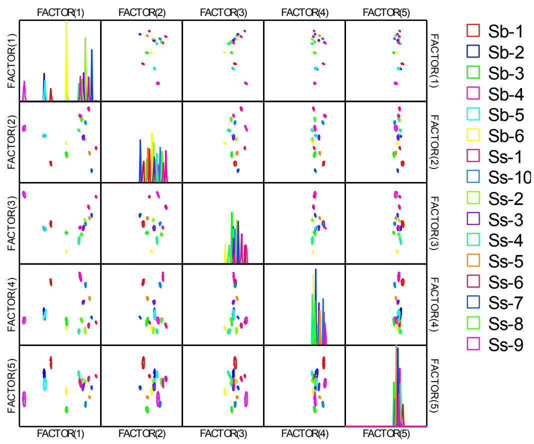

(B) **Jackknifed Classification Matrix**

	Sb-1	Sb-2	Sb-3	Sb-4	Sb-5	Sb-6	Ss-1	Ss-10	Ss-2	Ss-3	Ss-4	Ss-5	Ss-6	Ss-7	Ss-8	Ss-9	%correct
Sb-1	6	0	0	0	0	0	0	0	0	0	0	0	0	0	0	0	100
Sb-2	0	6	0	0	0	0	0	0	0	0	0	0	0	0	0	0	100
Sb-3	0	0	6	0	0	0	0	0	0	0	0	0	0	0	0	0	100
Sb-4	0	0	0	6	0	0	0	0	0	0	0	0	0	0	0	0	100
Sb-5	0	0	0	0	6	0	0	0	0	0	0	0	0	0	0	0	100
Sb-6	0	0	0	0	0	6	0	0	0	0	0	0	0	0	0	0	100
Ss-1	0	0	0	0	0	0	6	0	0	0	0	0	0	0	0	0	100
Ss-10	0	0	0	0	0	0	0	6	0	0	0	0	0	0	0	0	100
Ss-2	0	0	0	0	0	0	0	0	6	0	0	0	0	0	0	0	100
Ss-3	0	0	0	0	0	0	0	0	0	6	0	0	0	0	0	0	100
Ss-4	0	0	0	0	0	0	0	0	0	0	6	0	0	0	0	0	100
Ss-5	0	0	0	0	0	0	0	0	0	0	0	6	0	0	0	0	100
Ss-6	0	0	0	0	0	0	0	0	0	0	0	0	6	0	0	0	100
Ss-7	0	0	0	0	0	0	0	0	0	0	0	0	0	6	0	0	100
Ss-8	0	0	0	0	0	0	0	0	0	0	0	0	0	0	6	0	100
Ss-9	0	0	0	0	0	0	0	0	0	0	0	0	0	0	0	6	100
Total	6	6	6	6	6	6	6	6	6	6	6	6	6	6	6	6	100

Figure 122. (A). Correlations of canonical fluorescence response patterns from PAE-GFP tongue against whisky (blending status). The 95% confidence ellipses for the individual acids are also shown. **(B)**. Jackknifed classification matrix showed the 100% correct classification.

Table 63. Training matrix of fluorescence response pattern from PAE tongue (**P1-P3**) against whisky (age). LDA was carried out and resulting in 3 factors of the canonical scores and group generation. Jackknifed classification matrix showed the 100% correct classification.

Analyte	Fluorescence Response Pattern			Results LDA			
Whisky	**P2**	**P1**	**P3**	**Factor 1**	**Factor 2**	**Factor 3**	**Group**
Sb-Y8	-0.0677	-0.9279	-0.4409	-22.3857	-21.4991	-5.1043	3
Sb-Y8	-0.0690	-0.9301	-0.4353	-20.1415	-21.7504	-5.97812	3
Sb-Y8	-0.0654	-0.9297	-0.4332	-20.0399	-22.1685	-5.59489	3
Sb-Y8	-0.0613	-0.9279	-0.4439	-22.6203	-20.9414	-4.32462	3
Sb-Y8	-0.0673	-0.9331	-0.4472	-19.6229	-18.9029	-6.03933	3
Sb-Y8	-0.0672	-0.9334	-0.4471	-19.399	-18.8269	-6.10363	3
Sb-Y12	-0.0744	-0.9209	-0.5956	-48.2678	1.245174	1.962598	1
Sb-Y12	-0.0490	-0.9242	-0.6002	-45.9284	3.280951	3.990877	1
Sb-Y12	-0.0462	-0.9211	-0.5982	-47.7315	2.051424	4.931551	1
Sb-Y12	-0.0557	-0.9228	-0.5945	-46.3074	1.860075	3.403423	1
Sb-Y12	-0.0615	-0.9217	-0.5962	-47.4523	1.73368	3.130527	1
Sb-Y12	-0.0633	-0.9262	-0.6036	-45.3811	4.269733	2.176583	1
Sb-Y21	0.0160	-0.9903	-0.5765	4.771828	20.24388	-5.80369	2
Sb-Y21	-0.0269	-0.9901	-0.5714	4.182455	18.86438	-10.3901	2
Sb-Y21	-0.0290	-0.9896	-0.5826	2.270477	20.49439	-10.0469	2
Sb-Y21	-0.0094	-0.9906	-0.5815	3.631486	20.84696	-8.30102	2
Sb-Y21	-0.0189	-0.9905	-0.5829	3.121384	20.93242	-9.20363	2
Sb-Y21	-0.0217	-0.9904	-0.5753	4.002435	19.64431	-9.7695	2
Ss-Y12	0.1249	-0.9700	-0.5320	-0.39852	8.177443	8.472316	4
Ss-Y12	0.1240	-0.9704	-0.5444	-1.81711	10.28758	8.774825	4
Ss-Y12	0.1257	-0.9692	-0.5451	-2.69748	10.05646	9.260832	4
Ss-Y12	0.1183	-0.9704	-0.5409	-1.49651	9.65727	8.047717	4
Ss-Y12	0.1210	-0.9698	-0.5373	-1.35507	8.926241	8.325844	4
Ss-Y12	0.1169	-0.9703	-0.5450	-2.15567	10.27183	8.08857	4
Ss-Y15	0.1798	-0.9883	-0.3944	32.28363	-7.8273	4.398006	5
Ss-Y15	0.1748	-0.9889	-0.3927	32.79569	-7.97745	3.672941	5
Ss-Y15	0.1703	-0.9889	-0.4070	30.74838	-5.72386	3.772811	5
Ss-Y15	0.1631	-0.9887	-0.3921	32.42758	-8.27023	2.487619	5
Ss-Y15	0.1758	-0.9894	-0.3926	33.182	-7.83047	3.654498	5
Ss-Y15	0.1711	-0.9884	-0.3969	31.78497	-7.49461	3.57437	5
Ss-Y18	0.1289	-0.9946	-0.4113	33.01781	-3.78236	-1.67744	6
Ss-Y18	0.1329	-0.9945	-0.4145	32.62328	-3.25041	-1.11425	6
Ss-Y18	0.1315	-0.9945	-0.4131	32.77488	-3.49234	-1.31418	6
Ss-Y18	0.1345	-0.9944	-0.4115	33.00093	-3.7459	-1.04387	6
Ss-Y18	0.1368	-0.9947	-0.4037	34.32132	-4.886	-1.185	6
Ss-Y18	0.1550	-0.9943	-0.4057	34.25762	-4.47408	0.868507	6

(A) **Canonical Scores Plot**

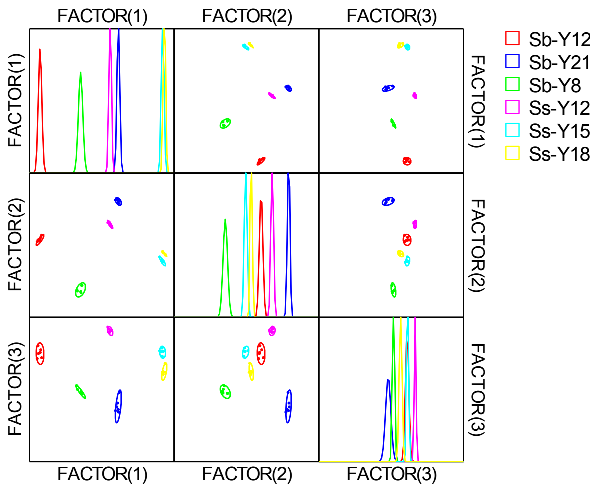

(B) **Jackknifed Classification Matrix**

	Sb-Y12	Sb-Y21	Sb-Y8	Ss-Y12	Ss-Y15	Ss-Y18	%correct
Sb-Y12	6	0	0	0	0	0	100
Sb-Y21	0	6	0	0	0	0	100
Sb-Y8	0	0	6	0	0	0	100
Ss-Y12	0	0	0	6	0	0	100
Ss-Y15	0	0	0	0	6	0	100
Ss-Y18	0	0	0	0	0	6	100
Total	6	6	6	6	6	6	100

Figure 123. (A). Correlations of canonical fluorescence response patterns from PAE tongue (P1-P3) against whisky (age). The 95% confidence ellipses for the individual acids are also shown. **(B)**. Jackknifed classification matrix showed the 100% correct classification.

Table 64. Training matrix of fluorescence response pattern from GFP tongue (**GFP**, **GFP-K36**, and **GFP-E36**) against whisky (age). LDA was carried out and resulting in 3 factors of the canonical scores and group generation. Jackknifed classification matrix showed the 97% correct classification.

Analyte	Fluorescence Response Pattern			Results LDA			
Whisky	**GFP**	**GFP-K36**	**GFP-E36**	**Factor 1**	**Factor 2**	**Factor 3**	**Group**
Sb-Y8	-0.9417	-0.8905	-0.9359	9.518044	0.44832	-0.29909	3
Sb-Y8	-0.9419	-0.8919	-0.9385	8.587454	-0.06842	0.285109	3
Sb-Y8	-0.9443	-0.8912	-0.9333	9.577601	0.393594	-1.33115	3
Sb-Y8	-0.9437	-0.8924	-0.9363	8.690633	-0.00848	-0.52833	3
Sb-Y8	-0.9478	-0.8885	-0.9312	10.6789	-0.44766	-2.30266	3
Sb-Y8	-0.9430	-0.8913	-0.9334	9.594344	0.762292	-1.11999	3
Sb-Y12	-0.9316	-0.8381	-0.9248	29.9899	-0.13737	-0.52726	1
Sb-Y12	-0.9284	-0.8273	-0.9302	32.97524	-1.77563	1.483515	1
Sb-Y12	-0.9263	-0.8318	-0.9306	31.46553	-0.72322	1.796965	1
Sb-Y12	-0.9262	-0.8288	-0.9269	33.12779	-0.16134	0.958914	1
Sb-Y12	-0.9316	-0.8374	-0.9251	30.18094	-0.29231	-0.43934	1
Sb-Y12	-0.9357	-0.8393	-0.9255	29.2436	-1.36433	-0.97308	1
Sb-Y21	-0.9424	-0.9311	-0.9430	-5.71845	3.349745	0.540953	2
Sb-Y21	-0.9412	-0.9311	-0.9359	-4.46187	5.405391	-1.03575	2
Sb-Y21	-0.9377	-0.9351	-0.9386	-6.11252	6.256671	0.057795	2
Sb-Y21	-0.9385	-0.9347	-0.9449	-7.07566	4.462825	1.503211	2
Sb-Y21	-0.9413	-0.9286	-0.9451	-5.1515	2.871757	1.268095	2
Sb-Y21	-0.9404	-0.9294	-0.9449	-5.34674	3.278215	1.333337	2
Ss-Y12	-0.9557	-0.9381	-0.9505	-10.0906	-1.51733	0.322258	4
Ss-Y12	-0.9486	-0.9366	-0.9545	-9.87395	-0.57508	2.36798	4
Ss-Y12	-0.9529	-0.9376	-0.9462	-9.04851	0.275777	-0.32206	4
Ss-Y12	-0.9475	-0.9389	-0.9525	-10.2735	0.499721	1.988486	4
Ss-Y12	-0.9552	-0.9381	-0.9535	-10.5688	-2.09089	1.134495	4
Ss-Y12	-0.9597	-0.9349	-0.9497	-9.06152	-2.87632	-0.39124	4
Ss-Y15	-0.9611	-0.9457	-0.9544	-13.6508	-3.13487	0.349436	5
Ss-Y15	-0.9584	-0.9475	-0.9543	-14.1136	-2.10659	0.680409	5
Ss-Y15	-0.9525	-0.9454	-0.9570	-13.5342	-1.27498	2.243535	5
Ss-Y15	-0.9531	-0.9459	-0.9567	-13.6877	-1.31951	2.072595	5
Ss-Y15	-0.9545	-0.9469	-0.9555	-13.9042	-1.32315	1.553768	5
Ss-Y15	-0.9621	-0.9454	-0.9543	-13.5828	-3.43937	0.185755	5
Ss-Y18	-0.9578	-0.9421	-0.9463	-10.8742	-0.65054	-1.0976	6
Ss-Y18	-0.9627	-0.9437	-0.9449	-11.4473	-1.56046	-2.1852	6
Ss-Y18	-0.9591	-0.9409	-0.9420	-9.80533	-0.14152	-2.32247	6
Ss-Y18	-0.9621	-0.9479	-0.9478	-13.3524	-1.58307	-1.46683	6
Ss-Y18	-0.9594	-0.9434	-0.9424	-10.7507	-0.0292	-2.31717	6
Ss-Y18	-0.9617	-0.9485	-0.9395	-12.1429	0.597315	-3.46739	6

(A) **Canonical Scores Plot**

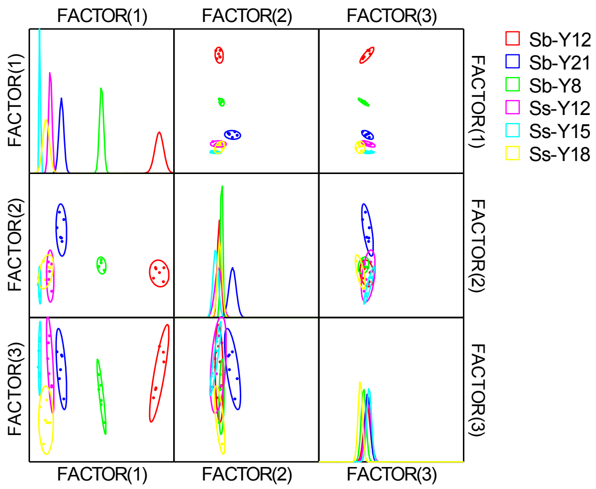

(B) **Jackknifed Classification Matrix**

	Sb-Y12	Sb-Y21	Sb-Y8	Ss-Y12	Ss-Y15	Ss-Y18	%correct
Sb-Y12	6	0	0	0	0	0	100
Sb-Y21	0	6	0	0	0	0	100
Sb-Y8	0	0	6	0	0	0	100
Ss-Y12	0	0	0	6	0	0	100
Ss-Y15	0	0	0	0	6	0	100
Ss-Y18	0	0	0	0	1	5	**83**
Total	6	6	6	6	**7**	**5**	**97**

Figure 124. (A) Correlations of canonical fluorescence response patterns from GFP tongue (**GFP**, **GFP-K36**, and **GFP-E36**) against whisky (age). The 95% confidence ellipses for the individual acids are also shown. **(B)**. Jackknifed classification matrix showed the 97% correct classification.**).**

Table 65. Training matrix of fluorescence response pattern from PAE/GFP tongue against whisky (age). LDA was carried out and resulting in 3 factors of the canonical scores and group generation. Jackknifed classification matrix showed the 100% correct classification.

Analyte	Fluorescence Response Pattern						Results LDA					
Whisky	**P2**	**P1**	**P3**	**GFP**	**GFP-K36**	**GFP-E36**	Factor 1	Factor 2	Factor 3	Factor 4	Factor 5	Group
Sb-Y8	-0.068	-0.928	-0.441	-0.942	-0.891	-0.936	-27.571	-20.284	-3.707	-6.872	-0.412	3
Sb-Y8	-0.069	-0.930	-0.435	-0.942	-0.892	-0.938	-25.062	-20.823	-4.566	-6.913	-1.140	3
Sb-Y8	-0.065	-0.930	-0.433	-0.944	-0.891	-0.933	-25.714	-21.288	-4.320	-6.083	0.484	3
Sb-Y8	-0.061	-0.928	-0.444	-0.944	-0.892	-0.936	-27.398	-19.641	-2.677	-7.380	-0.109	3
Sb-Y8	-0.067	-0.933	-0.447	-0.948	-0.888	-0.931	-25.913	-18.463	-4.914	-4.545	1.413	3
Sb-Y8	-0.067	-0.933	-0.447	-0.943	-0.891	-0.933	-24.739	-17.974	-5.058	-5.332	0.318	3
Sb-Y12	-0.074	-0.921	-0.596	-0.932	-0.838	-0.925	-60.253	2.363	1.137	4.043	0.816	1
Sb-Y12	-0.049	-0.924	-0.600	-0.928	-0.827	-0.930	-59.410	3.255	2.128	8.278	-1.307	1
Sb-Y12	-0.046	-0.921	-0.598	-0.926	-0.832	-0.931	-60.200	2.774	3.430	6.293	-1.380	1
Sb-Y12	-0.056	-0.923	-0.595	-0.926	-0.829	-0.927	-59.852	2.229	1.439	7.859	-0.741	1
Sb-Y12	-0.062	-0.922	-0.596	-0.932	-0.837	-0.925	-59.573	2.695	2.106	4.903	0.796	1
Sb-Y12	-0.063	-0.926	-0.604	-0.936	-0.839	-0.925	-57.151	4.857	1.293	5.230	1.221	1
Sb-Y21	0.016	-0.990	-0.576	-0.942	-0.931	-0.943	9.820	21.142	-5.928	-0.411	-0.165	2
Sb-Y21	-0.027	-0.990	-0.571	-0.941	-0.931	-0.936	8.507	19.985	-10.605	-0.987	1.134	2
Sb-Y21	-0.029	-0.990	-0.583	-0.938	-0.935	-0.939	8.040	22.314	-9.935	-2.799	0.280	2
Sb-Y21	-0.009	-0.991	-0.582	-0.938	-0.935	-0.945	9.804	22.278	-8.115	-2.497	-1.157	2
Sb-Y21	-0.019	-0.990	-0.583	-0.941	-0.929	-0.945	8.039	21.704	-9.071	-1.376	-1.167	2
Sb-Y21	-0.022	-0.990	-0.575	-0.940	-0.929	-0.945	8.970	20.438	-9.726	-1.518	-1.319	2
Ss-Y12	0.125	-0.970	-0.532	-0.956	-0.938	-0.950	5.677	9.841	10.245	-4.879	0.907	4
Ss-Y12	0.124	-0.970	-0.544	-0.949	-0.937	-0.954	4.885	12.281	10.282	-4.885	-0.997	4
Ss-Y12	0.126	-0.969	-0.545	-0.953	-0.938	-0.946	3.354	12.286	10.786	-4.509	1.819	4
Ss-Y12	0.118	-0.970	-0.541	-0.947	-0.939	-0.952	5.445	11.926	9.518	-5.311	-0.596	4
Ss-Y12	0.121	-0.970	-0.537	-0.955	-0.938	-0.954	5.192	10.631	10.308	-5.571	0.069	4
Ss-Y12	0.117	-0.970	-0.545	-0.960	-0.935	-0.950	3.441	11.661	10.060	-4.534	1.527	4
Ss-Y15	0.180	-0.988	-0.394	-0.961	-0.946	-0.954	35.771	-10.191	3.939	2.599	-0.737	5
Ss-Y15	0.175	-0.989	-0.393	-0.958	-0.947	-0.954	36.716	-10.124	3.092	2.266	-1.067	5
Ss-Y15	0.170	-0.989	-0.407	-0.953	-0.945	-0.957	35.038	-7.545	3.004	2.254	-2.471	5
Ss-Y15	0.163	-0.989	-0.392	-0.953	-0.946	-0.957	36.439	-10.294	1.687	2.128	-2.522	5
Ss-Y15	0.176	-0.989	-0.393	-0.954	-0.947	-0.955	37.172	-9.879	2.809	2.588	-1.899	5
Ss-Y15	0.171	-0.988	-0.397	-0.962	-0.945	-0.954	35.284	-9.890	3.246	2.287	-0.656	5
Ss-Y18	0.129	-0.995	-0.411	-0.958	-0.942	-0.946	35.461	-6.330	-2.872	4.403	0.370	6
Ss-Y18	0.133	-0.995	-0.414	-0.963	-0.944	-0.945	35.189	-5.832	-1.949	3.986	1.493	6
Ss-Y18	0.131	-0.995	-0.413	-0.959	-0.941	-0.942	34.588	-6.039	-2.703	5.302	1.654	6
Ss-Y18	0.135	-0.994	-0.412	-0.962	-0.948	-0.948	36.575	-6.052	-1.553	2.556	0.835	6
Ss-Y18	0.137	-0.995	-0.404	-0.959	-0.943	-0.942	36.416	-7.439	-2.545	5.016	1.614	6
Ss-Y18	0.155	-0.994	-0.406	-0.962	-0.948	-0.939	37.012	-6.571	-0.266	4.411	3.091	6

(A) **Canonical Scores Plot**

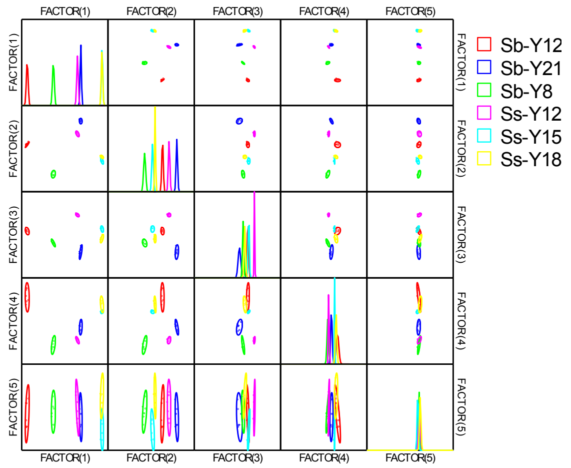

(B) **Jackknifed Classification Matrix**

	Sb-Y12	Sb-Y21	Sb-Y8	Ss-Y12	Ss-Y15	Ss-Y18	%correct
Sb-Y12	6	0	0	0	0	0	100
Sb-Y21	0	6	0	0	0	0	100
Sb-Y8	0	0	6	0	0	0	100
Ss-Y12	0	0	0	6	0	0	100
Ss-Y15	0	0	0	0	6	0	100
Ss-Y18	0	0	0	0	0	6	100
Total	6	6	6	6	6	6	100

Figure 125. (A). Correlations of canonical fluorescence response patterns from PAE/GFP tongue against whisky (age). The 95% confidence ellipses for the individual acids are also shown. **(B).** Jackknifed classification matrix showed the 100% correct classification.

Table 66. Training matrix of fluorescence response pattern from PAE tongue (**P1-P3**) against whisky (taste). LDA was carried out and resulting in 3 factors of the canonical scores and group generation. Jackknifed classification matrix showed the 98% correct classification.

Analyte	Fluorescence Response Pattern			Results LDA			
Whisky	**P2**	**P1**	**P3**	Factor 1	Factor 2	Factor 3	Group
Ss-1	0.533	-0.734	-0.111	49.192	26.690	-2.776	1
Ss-1	0.538	-0.734	-0.106	49.575	27.505	-2.813	1
Ss-1	0.532	-0.743	-0.121	47.578	26.518	-1.334	1
Ss-1	0.528	-0.736	-0.099	48.574	28.196	-4.555	1
Ss-1	0.520	-0.740	-0.102	47.406	27.962	-4.858	1
Ss-1	0.525	-0.740	-0.086	47.772	30.051	-6.017	1
Ss-2	0.287	-0.829	-0.289	14.096	6.284	-2.191	5
Ss-2	0.278	-0.844	-0.294	10.847	6.971	-1.809	5
Ss-2	0.266	-0.834	-0.293	11.889	5.439	-3.483	5
Ss-2	0.276	-0.846	-0.297	10.191	6.897	-1.539	5
Ss-2	0.264	-0.838	-0.291	10.980	6.087	-3.702	5
Ss-2	0.272	-0.836	-0.296	11.761	5.691	-2.496	5
Ss-3	0.310	-0.696	-0.429	39.568	-25.696	9.472	6
Ss-3	0.278	-0.699	-0.425	36.961	-26.202	5.986	6
Ss-3	0.290	-0.695	-0.434	38.476	-27.277	8.080	6
Ss-3	0.312	-0.704	-0.427	38.228	-24.306	9.882	6
Ss-3	0.282	-0.692	-0.421	38.526	-26.389	5.705	6
Ss-3	0.287	-0.709	-0.440	35.615	-26.482	9.109	6
Ss-5	0.207	-0.808	-0.401	12.145	-13.183	1.698	7
Ss-5	0.220	-0.806	-0.383	13.382	-10.644	0.782	7
Ss-5	0.225	-0.807	-0.387	13.673	-10.841	1.762	7
Ss-5	0.211	-0.814	-0.385	11.470	-10.407	0.565	7
Ss-5	0.212	-0.803	-0.386	13.545	-11.730	0.168	7
Ss-5	0.212	-0.816	-0.387	10.975	-10.238	0.923	7
Ss-6	0.405	-0.990	-0.271	-7.639	32.954	14.668	8
Ss-6	0.405	-0.990	-0.268	-7.580	33.258	14.366	8
Ss-6	0.396	-0.989	-0.282	-8.192	31.163	15.069	8
Ss-6	0.406	-0.990	-0.283	-7.599	31.580	16.107	8
Ss-6	0.400	-0.989	-0.284	-7.991	31.130	15.636	8
Ss-6	0.396	-0.990	-0.286	-8.260	30.795	15.473	8
Ss-8	0.306	-0.646	-0.275	49.598	-13.393	-10.492	9
Ss-8	0.326	-0.664	-0.269	47.509	-9.632	-8.326	9
Ss-8	0.328	-0.646	-0.274	50.948	-12.323	-8.438	9
Ss-8	0.318	-0.670	-0.286	45.852	-11.302	-6.957	9
Ss-8	0.325	-0.651	-0.273	49.934	-11.820	-8.564	9
Ss-8	0.307	-0.647	-0.278	49.409	-13.541	-9.980	9
Ss-11	-0.064	-0.977	-0.506	-37.932	-16.909	-4.909	2
Ss-11	-0.055	-0.976	-0.504	-37.277	-16.313	-4.249	2
Ss-11	-0.052	-0.976	-0.501	-36.945	-15.892	-4.395	2
Ss-11	-0.059	-0.975	-0.509	-37.286	-17.290	-4.113	2
Ss-11	-0.060	-0.976	-0.507	-37.490	-17.042	-4.426	2

Ss-11	-0.048	-0.976	-0.508	-36.816	-16.528	-3.197	2
Ss-12	0.032	-0.975	-0.345	-30.211	6.355	-13.724	3
Ss-12	0.023	-0.975	-0.355	-30.889	4.714	-13.466	3
Ss-12	0.023	-0.975	-0.357	-30.946	4.517	-13.283	3
Ss-12	0.016	-0.974	-0.361	-31.293	3.669	-13.549	3
Ss-12	0.018	-0.975	-0.355	-31.242	4.534	-13.987	3
Ss-12	0.011	-0.974	-0.358	-31.606	3.771	-14.259	3
Ss-13	0.030	-0.976	-0.353	-30.675	5.373	-12.913	3
Ss-13	0.038	-0.977	-0.357	-30.261	5.295	-11.677	4
Ss-13	0.025	-0.978	-0.366	-31.394	3.824	-11.907	4
Ss-13	0.018	-0.977	-0.367	-31.800	3.440	-12.514	4
Ss-13	0.015	-0.978	-0.365	-32.033	3.605	-13.008	4
Ss-13	0.013	-0.977	-0.372	-32.097	2.590	-12.435	4
Ss-Y12	0.125	-0.970	-0.532	-24.184	-12.765	15.918	10
Ss-Y12	0.124	-0.970	-0.544	-24.383	-14.241	17.229	10
Ss-Y12	0.126	-0.969	-0.545	-24.053	-14.398	17.424	10
Ss-Y12	0.118	-0.970	-0.541	-24.748	-14.065	16.298	10
Ss-Y12	0.121	-0.970	-0.537	-24.436	-13.590	16.127	10
Ss-Y12	0.117	-0.970	-0.545	-24.846	-14.630	16.616	10
Ss-Y18	0.129	-0.995	-0.411	-27.804	4.891	3.958	11
Ss-Y18	0.133	-0.995	-0.414	-27.535	4.666	4.696	11
Ss-Y18	0.131	-0.995	-0.413	-27.621	4.774	4.405	11
Ss-Y18	0.135	-0.994	-0.412	-27.393	5.082	4.510	11
Ss-Y18	0.137	-0.995	-0.404	-27.251	6.154	3.874	11
Ss-Y18	0.155	-0.994	-0.406	-25.968	6.645	5.833	11

(A) Canonical Scores Plot

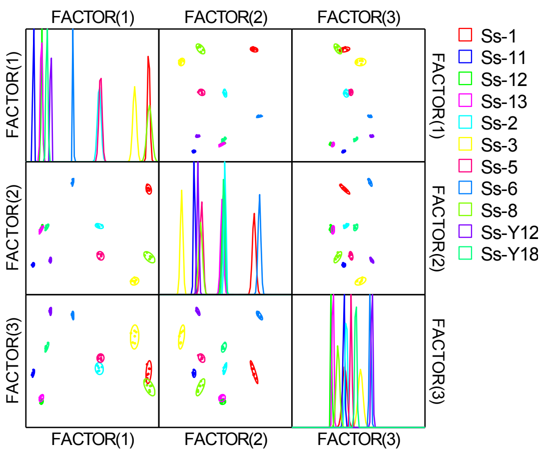

(B) Jackknifed Classification Matrix

	Ss-1	Ss-11	Ss-12	Ss-13	Ss-2	Ss-3	Ss-5	Ss-6	Ss-8	Ss-Y12	Ss-Y18	%correct
Ss-1	6	0	0	0	0	0	0	0	0	0	0	100
Ss-11	0	6	0	0	0	0	0	0	0	0	0	100
Ss-12	0	0	6	0	0	0	0	0	0	0	0	100
Ss-13	0	0	1	5	0	0	0	0	0	0	0	83
Ss-2	0	0	0	0	6	0	0	0	0	0	0	100
Ss-3	0	0	0	0	0	6	0	0	0	0	0	100
Ss-5	0	0	0	0	0	0	6	0	0	0	0	100
Ss-6	0	0	0	0	0	0	0	6	0	0	0	100
Ss-8	0	0	0	0	0	0	0	0	6	0	0	100
Ss-Y12	0	0	0	0	0	0	0	0	0	6	0	100
Ss-Y18	0	0	0	0	0	0	0	0	0	0	6	100
Total	6	6	7	5	6	6	6	6	6	6	6	98

Figure 126. (A). Correlations of canonical fluorescence response patterns from PAE tongue (**P1-P3**) against whisky (taste). The 95% confidence ellipses for the individual acids are also shown. **(B).** Jackknifed classification matrix showed the 98% correct classification.

Table 67. Training matrix of fluorescence response pattern from GFP tongue (**GFP**, **GFP-K36**, and **GFP-E36**) against whisky (taste). LDA was carried out and resulting in 3 factors of the canonical scores and group generation. Jackknifed classification matrix showed the 100% correct classification.

Analyte	Fluorescence Response Pattern			Results LDA			
Whisky	**GFP**	**GFP-K36**	**GFP-E36**	Factor 1	Factor 2	Factor 3	Group
Ss-1	-0.9458	-0.6961	-0.9488	25.32987	-15.9564	-1.1686	1
Ss-1	-0.9406	-0.6993	-0.9483	25.25798	-14.9792	0.394703	1
Ss-1	-0.9378	-0.7103	-0.9495	23.06766	-14.4527	1.599395	1
Ss-1	-0.9431	-0.6968	-0.9496	25.4986	-15.7972	-0.23166	1
Ss-1	-0.9366	-0.7101	-0.9476	23.29162	-13.7571	1.703616	1
Ss-1	-0.9419	-0.7089	-0.9430	22.96282	-13.1912	-0.53956	1
Ss-2	-0.9285	-0.7149	-0.8980	23.90525	1.784807	-2.42465	5
Ss-2	-0.9317	-0.7047	-0.8954	25.88091	1.644144	-3.92422	5
Ss-2	-0.9281	-0.7101	-0.9003	25.02618	0.95831	-2.0802	5
Ss-2	-0.9334	-0.7069	-0.8981	25.12323	0.743607	-4.03656	5
Ss-2	-0.9323	-0.7186	-0.9024	22.51419	0.186281	-2.91721	5
Ss-2	-0.9354	-0.7150	-0.9038	22.93037	-0.79	-3.7313	5
Ss-3	-0.9073	-0.6954	-0.8873	31.20976	6.776055	2.204365	6
Ss-3	-0.9075	-0.6985	-0.8844	30.51298	7.724012	1.809477	6
Ss-3	-0.9141	-0.6831	-0.8811	33.26391	7.097938	-0.90568	6
Ss-3	-0.9070	-0.7067	-0.8840	28.69801	8.278434	2.053299	6

Ss-3	-0.9134	-0.6927	-0.8767	31.20854	8.891902	-1.11385	6
Ss-3	-0.9071	-0.7018	-0.8829	29.82639	8.358179	1.787822	6
Ss-5	-0.9532	-0.8977	-0.9513	-21.9497	-8.47498	0.524625	7
Ss-5	-0.9533	-0.8937	-0.9494	-21.0169	-8.12439	0.167707	7
Ss-5	-0.9526	-0.8922	-0.9446	-20.5168	-6.72087	-0.29223	7
Ss-5	-0.9527	-0.8995	-0.9490	-22.2679	-7.66601	0.398972	7
Ss-5	-0.9556	-0.8947	-0.9505	-21.5522	-8.6992	-0.36257	7
Ss-5	-0.9525	-0.8946	-0.9479	-21.1017	-7.54658	0.224269	7
Ss-6	-0.9609	-0.9536	-0.9587	-35.8661	-9.07481	0.186328	8
Ss-6	-0.9641	-0.9495	-0.9588	-35.3295	-9.71355	-0.84162	8
Ss-6	-0.9579	-0.9502	-0.9557	-34.6645	-7.97073	0.630296	8
Ss-6	-0.9561	-0.9506	-0.9537	-34.5012	-7.13972	0.91333	8
Ss-6	-0.9573	-0.9509	-0.9562	-34.7566	-8.00315	0.891515	8
Ss-6	-0.9632	-0.9507	-0.9546	-35.4328	-8.33304	-1.11225	8
Ss-8	-0.9165	-0.5709	-0.9193	58.20062	-9.30419	1.499531	9
Ss-8	-0.9202	-0.5727	-0.9246	57.24604	-11.2346	1.124268	9
Ss-8	-0.9232	-0.5714	-0.9279	57.11991	-12.6389	0.636767	9
Ss-8	-0.9187	-0.5771	-0.9270	56.391	-11.5254	1.979116	9
Ss-8	-0.9178	-0.5702	-0.9218	58.16238	-10.2264	1.429619	9
Ss-8	-0.9238	-0.5713	-0.9223	57.14553	-11.1137	-0.29904	9
Ss-11	-0.9225	-0.8773	-0.8869	-12.4881	13.16198	0.796381	2
Ss-11	-0.9226	-0.8780	-0.8880	-12.6769	12.86455	0.926418	2
Ss-11	-0.9225	-0.8784	-0.8851	-12.7156	13.72927	0.574137	2
Ss-11	-0.9204	-0.8739	-0.8867	-11.4393	13.34246	1.344267	2
Ss-11	-0.9234	-0.8787	-0.8862	-12.9135	13.30779	0.454977	2
Ss-11	-0.9211	-0.8707	-0.8910	-10.8527	11.86862	1.65317	2
Ss-12	-0.9249	-0.8913	-0.8914	-16.07	12.18888	0.92461	3
Ss-12	-0.9215	-0.8902	-0.8891	-15.3561	13.24947	1.624699	3
Ss-12	-0.9247	-0.8903	-0.8964	-15.885	10.73314	1.639138	3
Ss-12	-0.9256	-0.8900	-0.8984	-15.9577	10.02574	1.630208	3
Ss-12	-0.9223	-0.8891	-0.8845	-15.14	14.41529	0.74491	3
Ss-12	-0.9240	-0.8902	-0.8845	-15.6072	14.24048	0.250151	3
Ss-13	-0.9099	-0.7806	-0.8549	11.76325	19.62088	-1.41604	4
Ss-13	-0.9112	-0.7738	-0.8551	13.15847	19.08184	-1.90382	4
Ss-13	-0.9036	-0.7740	-0.8565	14.05201	19.69409	0.587451	4
Ss-13	-0.9049	-0.7789	-0.8572	12.75255	19.54407	0.375571	4
Ss-13	-0.9074	-0.7796	-0.8575	12.27207	19.15901	-0.32807	4
Ss-13	-0.9116	-0.7890	-0.8523	9.655489	20.52551	-2.12994	4
Ss-Y12	-0.9557	-0.9381	-0.9505	-31.5345	-6.73645	0.381387	10
Ss-Y12	-0.9486	-0.9366	-0.9545	-30.3499	-7.01481	3.04041	10
Ss-Y12	-0.9529	-0.9376	-0.9462	-31.0061	-5.15325	0.641891	10
Ss-Y12	-0.9475	-0.9389	-0.9525	-30.7115	-6.1899	3.145534	10
Ss-Y12	-0.9552	-0.9381	-0.9535	-31.5134	-7.53231	0.935787	10
Ss-Y12	-0.9597	-0.9349	-0.9497	-31.293	-7.18144	-0.9935	10
Ss-Y18	-0.9578	-0.9421	-0.9463	-32.6596	-5.62533	-0.74703	11
Ss-Y18	-0.9627	-0.9437	-0.9449	-33.6259	-5.79844	-2.38923	11
Ss-Y18	-0.9591	-0.9409	-0.9420	-32.4878	-4.6164	-1.73958	11
Ss-Y18	-0.9621	-0.9479	-0.9478	-34.5556	-6.36112	-1.74309	11
Ss-Y18	-0.9594	-0.9434	-0.9424	-33.1056	-4.6572	-1.732	11
Ss-Y18	-0.9617	-0.9485	-0.9395	-34.5268	-3.896	-2.72663	11

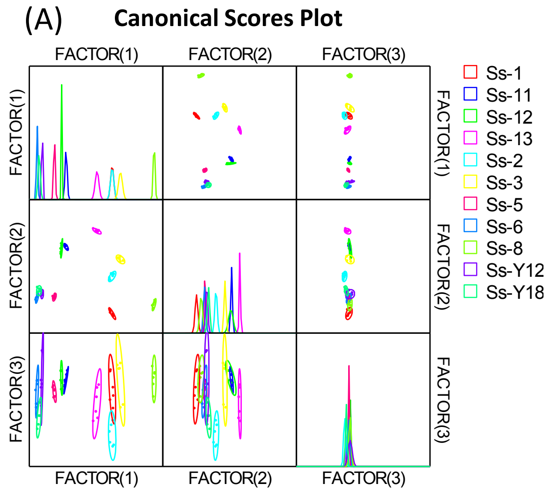

(B) Jackknifed Classification Matrix

	Ss-1	Ss-11	Ss-12	Ss-13	Ss-2	Ss-3	Ss-5	Ss-6	Ss-8	Ss-Y12	Ss-Y18	%correct
Ss-1	6	0	0	0	0	0	0	0	0	0	0	100
Ss-11	0	6	0	0	0	0	0	0	0	0	0	100
Ss-12	0	0	6	0	0	0	0	0	0	0	0	100
Ss-13	0	0	1	5	0	0	0	0	0	0	0	100
Ss-2	0	0	0	0	6	0	0	0	0	0	0	100
Ss-3	0	0	0	0	0	6	0	0	0	0	0	100
Ss-5	0	0	0	0	0	0	6	0	0	0	0	100
Ss-6	0	0	0	0	0	0	0	6	0	0	0	100
Ss-8	0	0	0	0	0	0	0	0	6	0	0	100
Ss-Y12	0	0	0	0	0	0	0	0	0	6	0	100
Ss-Y18	0	0	0	0	0	0	0	0	0	0	6	100
Total	6	6	6	6	6	6	6	6	6	6	6	**100**

Figure 127. (A). Correlations of canonical fluorescence response patterns from GFP tongue (**GFP**, **GFP-K36**, and **GFP-E36**) against whisky (taste). The 95% confidence ellipses for the individual acids are also shown. **(B)**. Jackknifed classification matrix showed the 100% correct classification.

Table 68. Training matrix of fluorescence response pattern from PAE/GFP tongue against whisky (taste). LDA was carried out and resulting in 6 factors of the canonical scores and group generation. Jackknifed classification matrix showed the 100% correct classification.

Analyte	Fluorescence Response Pattern						Results LDA				
Whisky	**P2**	**P1**	**P3**	**GFP**	**GFP-K36**	**GFP-E36**	Factor 1	Factor 2	Factor 3	Factor 4	Group
Ss-1	0.5328	-0.7345	-0.1113	-0.9458	-0.6961	-0.9488	52.08289	26.01185	-19.7023	-2.13512	1
Ss-1	0.5381	-0.7345	-0.1064	-0.9406	-0.6993	-0.9483	52.5345	26.26705	-20.2284	-2.27116	1
Ss-1	0.5325	-0.7428	-0.1210	-0.9378	-0.7103	-0.9495	49.77051	26.45613	-18.7091	-1.57421	1
Ss-1	0.5278	-0.7364	-0.0989	-0.9431	-0.6968	-0.9496	52.21295	25.6096	-21.8386	-3.64955	1
Ss-1	0.5200	-0.7398	-0.1015	-0.9366	-0.7101	-0.9476	50.29423	25.56622	-21.1149	-4.42507	1
Ss-1	0.5253	-0.7402	-0.0864	-0.9419	-0.7089	-0.9430	50.27001	26.12881	-23.1128	-4.52952	1
Ss-2	0.2866	-0.8294	-0.2892	-0.9285	-0.7149	-0.8980	23.77149	-6.75584	-10.4209	5.217806	5
Ss-2	0.2776	-0.8435	-0.2945	-0.9317	-0.7047	-0.8954	22.42482	-9.57526	-12.7743	7.163706	5
Ss-2	0.2662	-0.8338	-0.2934	-0.9281	-0.7101	-0.9003	23.09863	-9.06309	-11.1955	4.17492	5
Ss-2	0.2758	-0.8463	-0.2973	-0.9334	-0.7069	-0.8981	21.54392	-9.08158	-12.6372	7.054078	5
Ss-2	0.2641	-0.8380	-0.2915	-0.9323	-0.7186	-0.9024	21.02619	-7.51018	-11.3021	3.477068	5
Ss-2	0.2720	-0.8365	-0.2961	-0.9354	-0.7150	-0.9038	21.57795	-6.84504	-10.5728	4.516037	5
Ss-3	0.3096	-0.6962	-0.4292	-0.9073	-0.6954	-0.8873	42.30557	-7.06081	28.62264	9.33156	6
Ss-3	0.2775	-0.6988	-0.4246	-0.9075	-0.6985	-0.8844	40.36649	-9.53363	27.58013	6.486635	6
Ss-3	0.2901	-0.6949	-0.4341	-0.9141	-0.6831	-0.8811	42.29277	-10.2095	28.5799	9.482932	6
Ss-3	0.3124	-0.7045	-0.4270	-0.9070	-0.7067	-0.8840	39.83765	-6.13383	28.03431	9.8846	6
Ss-3	0.2820	-0.6921	-0.4210	-0.9134	-0.6927	-0.8767	41.34519	-9.79669	27.99529	7.319655	6
Ss-3	0.2867	-0.7089	-0.4404	-0.9071	-0.7018	-0.8829	38.56467	-9.37928	28.56185	9.602489	6
Ss-5	0.2073	-0.8079	-0.4013	-0.9532	-0.8977	-0.9513	-4.57196	20.21738	24.12727	-11.6179	7
Ss-5	0.2198	-0.8063	-0.3830	-0.9533	-0.8937	-0.9494	-2.95993	20.83338	21.60845	-11.7615	7
Ss-5	0.2253	-0.8066	-0.3869	-0.9526	-0.8922	-0.9446	-2.78498	20.31616	22.07531	-10.2226	7
Ss-5	0.2114	-0.8135	-0.3853	-0.9527	-0.8995	-0.9490	-4.96547	20.43569	21.19056	-11.9485	7
Ss-5	0.2122	-0.8026	-0.3856	-0.9556	-0.8947	-0.9505	-3.18942	20.92082	22.64658	-12.7332	7
Ss-5	0.2119	-0.8163	-0.3869	-0.9525	-0.8946	-0.9479	-4.70971	19.48835	20.55007	-11.0714	7
Ss-6	0.4049	-0.9898	-0.2712	-0.9609	-0.9536	-0.9587	-24.7694	38.06557	-16.5111	7.401573	8
Ss-6	0.4050	-0.9896	-0.2685	-0.9641	-0.9495	-0.9588	-24.4686	37.96738	-17.1112	7.425247	8
Ss-6	0.3962	-0.9893	-0.2825	-0.9579	-0.9502	-0.9557	-24.6575	36.04001	-15.2776	8.11152	8
Ss-6	0.4062	-0.9897	-0.2830	-0.9561	-0.9506	-0.9537	-24.2735	36.39296	-15.1744	9.290933	8
Ss-6	0.3999	-0.9895	-0.2843	-0.9573	-0.9509	-0.9562	-24.603	36.37239	-14.9883	8.505774	8
Ss-6	0.3963	-0.9896	-0.2859	-0.9632	-0.9507	-0.9546	-25.4618	36.53532	-14.6091	8.602062	8
Ss-8	0.3063	-0.6456	-0.2746	-0.9165	-0.5709	-0.9193	69.32152	-13.9396	3.912924	-5.4346	9
Ss-8	0.3261	-0.6642	-0.2691	-0.9202	-0.5727	-0.9246	67.39188	-11.9148	0.538563	-3.14733	9
Ss-8	0.3280	-0.6462	-0.2740	-0.9232	-0.5714	-0.9279	69.57231	-10.3624	4.076451	-4.53146	9
Ss-8	0.3183	-0.6698	-0.2858	-0.9187	-0.5771	-0.9270	65.60742	-12.3889	2.214047	-2.45133	9
Ss-8	0.3253	-0.6507	-0.2733	-0.9178	-0.5702	-0.9218	69.45732	-12.3268	3.032894	-3.63434	9
Ss-8	0.3075	-0.6470	-0.2776	-0.9238	-0.5713	-0.9223	68.36566	-12.6883	4.35675	-5.26304	9
Ss-11	-0.0641	-0.9766	-0.5059	-0.9225	-0.8773	-0.8869	-35.0318	-25.5072	7.320541	-2.06103	2
Ss-11	-0.0550	-0.9765	-0.5040	-0.9226	-0.8780	-0.8880	-34.6945	-24.5182	7.202767	-1.60247	2
Ss-11	-0.0523	-0.9757	-0.5007	-0.9225	-0.8784	-0.8851	-34.5457	-24.5183	6.966802	-1.38716	2
Ss-11	-0.0589	-0.9749	-0.5092	-0.9204	-0.8739	-0.8867	-34.0374	-25.8021	7.740637	-1.25814	2
Ss-11	-0.0603	-0.9756	-0.5073	-0.9234	-0.8787	-0.8862	-35.1077	-24.9728	7.87668	-1.68286	2
Ss-11	-0.0485	-0.9762	-0.5079	-0.9211	-0.8707	-0.8910	-33.2833	-24.8607	7.125579	-0.6567	2

Ss-12	0.0324	-0.9747	-0.3446	-0.9249	-0.8913	-0.8914	-28.8559	-12.3731	-12.9128	-9.03182	3
Ss-12	0.0230	-0.9747	-0.3550	-0.9215	-0.8902	-0.8891	-29.0473	-14.1157	-11.7148	-8.64667	3
Ss-12	0.0228	-0.9749	-0.3567	-0.9247	-0.8903	-0.8964	-29.2369	-12.8962	-11.5009	-9.38176	3
Ss-12	0.0159	-0.9741	-0.3606	-0.9256	-0.8900	-0.8984	-29.4869	-13.155	-10.9137	-9.9547	3
Ss-12	0.0179	-0.9748	-0.3547	-0.9223	-0.8891	-0.8845	-29.3407	-15.1245	-11.8226	-8.47087	3
Ss-12	0.0113	-0.9742	-0.3582	-0.9240	-0.8902	-0.8845	-29.9351	-15.3214	-11.142	-8.86144	3
Ss-13	0.0300	-0.9761	-0.3534	-0.9099	-0.7806	-0.8549	-14.2848	-33.8987	-21.5937	2.771632	4
Ss-13	0.0379	-0.9766	-0.3574	-0.9112	-0.7738	-0.8551	-13.3913	-34.1138	-21.5935	4.270985	4
Ss-13	0.0249	-0.9777	-0.3661	-0.9036	-0.7740	-0.8565	-13.4014	-36.0384	-20.9261	3.709314	4
Ss-13	0.0181	-0.9775	-0.3666	-0.9049	-0.7789	-0.8572	-14.4111	-35.6698	-20.4241	2.755668	4
Ss-13	0.0152	-0.9778	-0.3645	-0.9074	-0.7796	-0.8575	-14.8558	-35.4495	-20.6538	2.287182	4
Ss-13	0.0132	-0.9772	-0.3716	-0.9116	-0.7890	-0.8523	-16.9246	-34.562	-18.5365	2.786969	4
Ss-Y12	0.1249	-0.9700	-0.5320	-0.9557	-0.9381	-0.9505	-37.3269	8.980094	19.32006	5.156584	10
Ss-Y12	0.1240	-0.9704	-0.5444	-0.9486	-0.9366	-0.9545	-36.6344	8.118247	20.56246	5.714489	10
Ss-Y12	0.1257	-0.9692	-0.5451	-0.9529	-0.9376	-0.9462	-37.3206	7.939659	21.22336	6.829597	10
Ss-Y12	0.1183	-0.9704	-0.5409	-0.9475	-0.9389	-0.9525	-37.0084	7.670741	20.21137	5.000725	10
Ss-Y12	0.1210	-0.9698	-0.5373	-0.9552	-0.9381	-0.9535	-37.4316	8.897566	20.00025	4.872238	10
Ss-Y12	0.1169	-0.9703	-0.5450	-0.9597	-0.9349	-0.9497	-38.0471	8.06024	20.89057	5.933513	10
Ss-Y18	0.1289	-0.9946	-0.4113	-0.9578	-0.9421	-0.9463	-37.9842	10.40395	-1.0843	-2.37924	11
Ss-Y18	0.1329	-0.9945	-0.4145	-0.9627	-0.9437	-0.9449	-38.6995	11.29285	-0.25589	-1.62898	11
Ss-Y18	0.1315	-0.9945	-0.4131	-0.9591	-0.9409	-0.9420	-38.051	10.0535	-0.78937	-1.37948	11
Ss-Y18	0.1345	-0.9944	-0.4115	-0.9621	-0.9479	-0.9478	-38.9403	12.32074	-0.34127	-2.37826	11
Ss-Y18	0.1368	-0.9947	-0.4037	-0.9594	-0.9434	-0.9424	-37.9788	11.0406	-1.87048	-1.90353	11
Ss-Y18	0.1550	-0.9943	-0.4057	-0.9617	-0.9485	-0.9395	-38.3266	13.05959	-0.78873	-0.07063	11

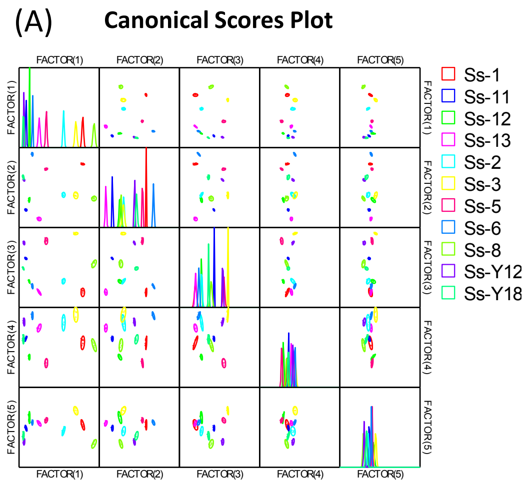

(B) **Jackknifed Classification Matrix**

	Ss-1	Ss-11	Ss-12	Ss-13	Ss-2	Ss-3	Ss-5	Ss-6	Ss-8	Ss-Y12	Ss-Y18	%correct
Ss-1	6	0	0	0	0	0	0	0	0	0	0	100
Ss-11	0	6	0	0	0	0	0	0	0	0	0	100
Ss-12	0	0	6	0	0	0	0	0	0	0	0	100
Ss-13	0	0	1	5	0	0	0	0	0	0	0	100
Ss-2	0	0	0	0	6	0	0	0	0	0	0	100
Ss-3	0	0	0	0	0	6	0	0	0	0	0	100
Ss-5	0	0	0	0	0	0	6	0	0	0	0	100
Ss-6	0	0	0	0	0	0	0	6	0	0	0	100
Ss-8	0	0	0	0	0	0	0	0	6	0	0	100
Ss-Y12	0	0	0	0	0	0	0	0	0	6	0	100
Ss-Y18	0	0	0	0	0	0	0	0	0	0	6	100
Total	6	6	6	6	6	6	6	6	6	6	6	100

Figure 128. (A). Correlations of canonical fluorescence response patterns from PAE/GFP tongue against whisky (taste). The 95% confidence ellipses for the individual acids are also shown. **(B).** Jackknifed classification matrix showed the 100% correct classification.

5.4 Titration Experiments for Binding Constants (log K_{sv})

5.4.1 Titration Experiments (Chapter 2.1)

(A)

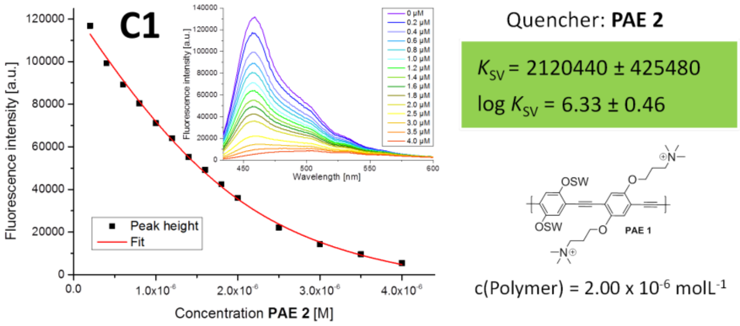

(B)

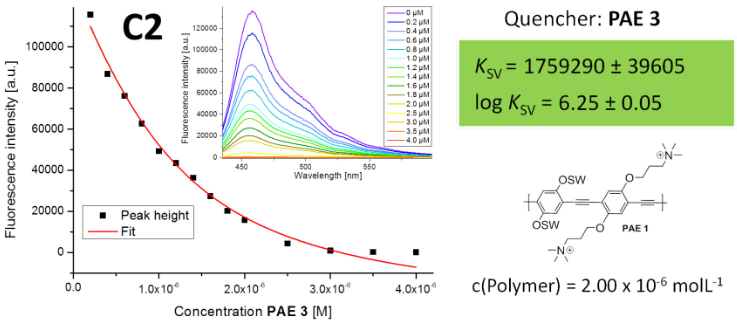

(C)

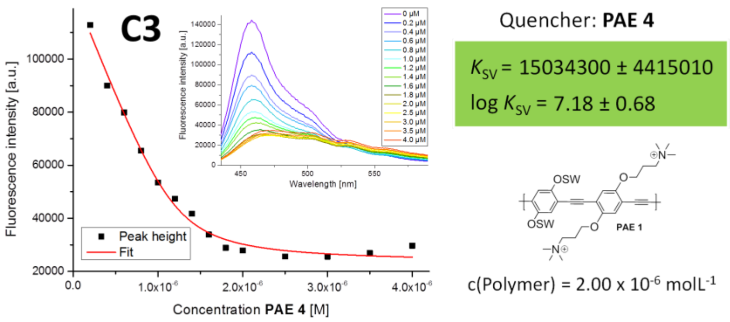

(D)

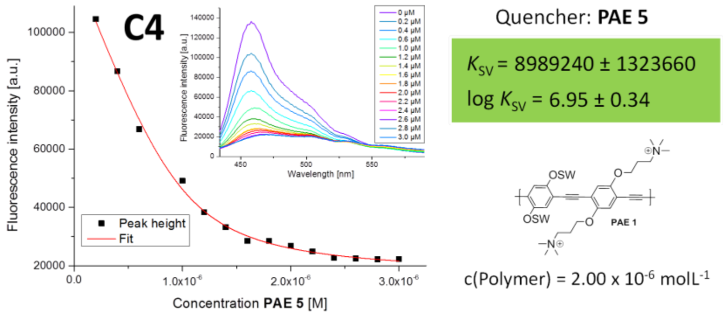

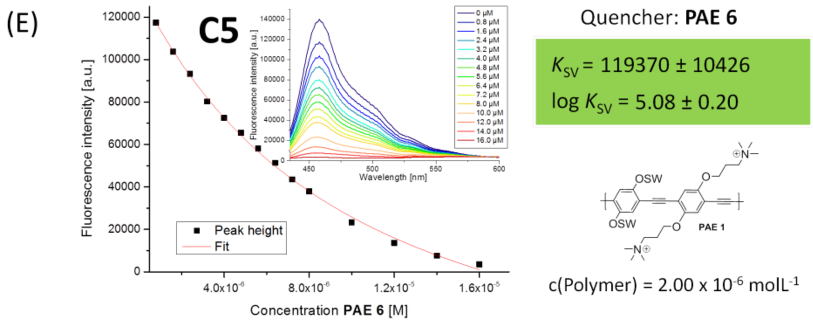

Figure 129. Stern-Volmer plot using a modified Stern-Volmer equation for fluorescence quenching of **PAE 1** (2.0 x 10^{-6} M) with PAE **2-6** (A-E). The inset shows the emission quenching data.

5.4.2 Titration Experiments (Chapter 2.2)

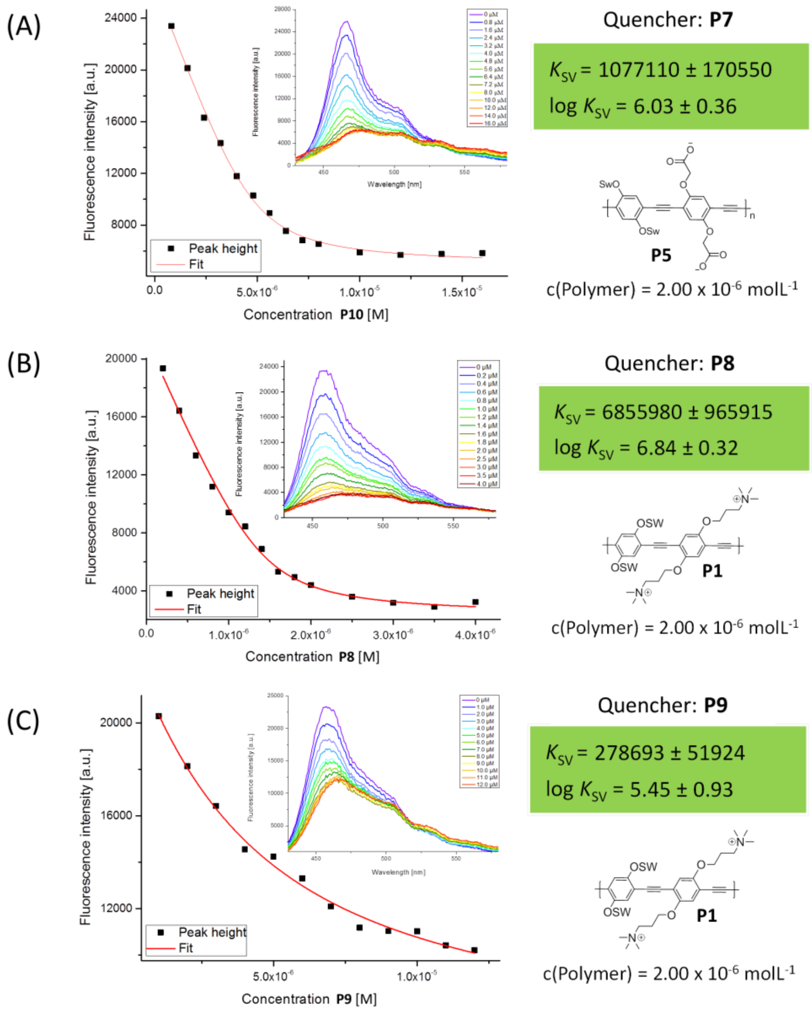

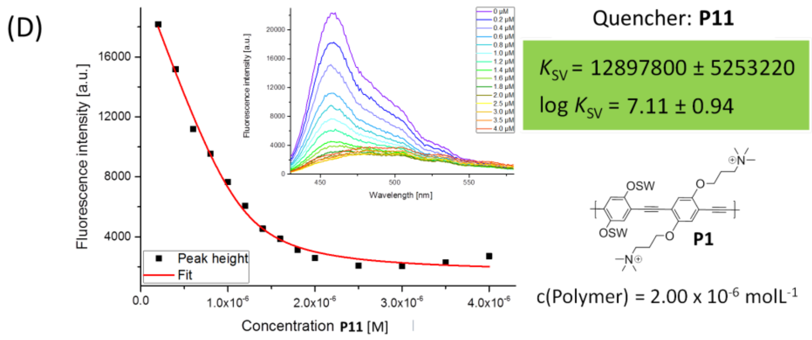

Figure 130. Volmer plot using a modified Stern–Volmer equation for fluorescence quenching of **(A) P5** (2.0×10^{-6} M) with **P7**, **(B) P1** (2.0×10^{-6} M) with **P8**, **(C) P1** (2.0×10^{-6} M) with **P9**, **(D) P1** (2.0×10^{-6} M) with **P11.** The inset shows the emission quenching data.

5.4.3 Titration Experiments (Chapter 2.3)

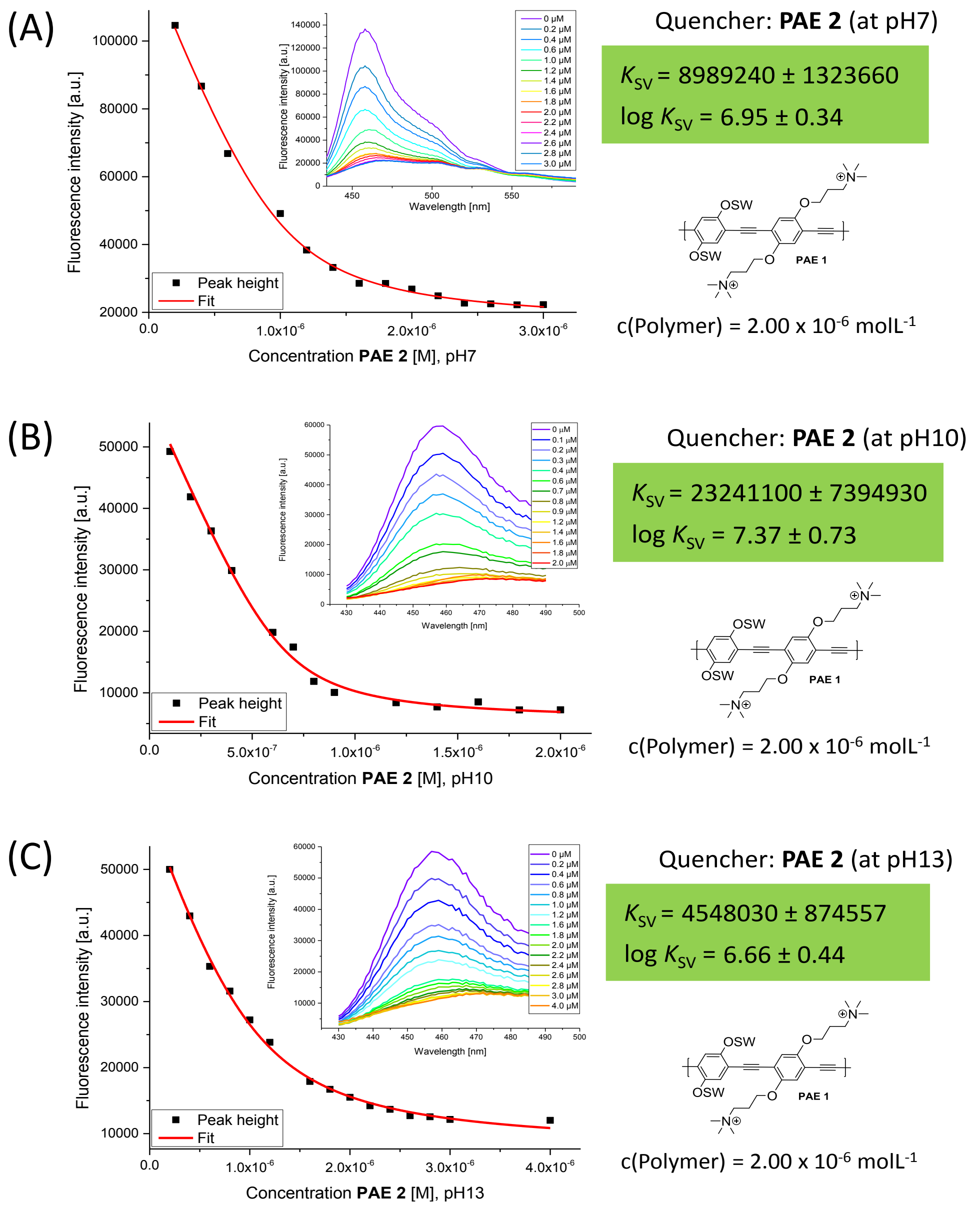

Figure 131. Volmer plot using a modified Stern–Volmer equation for fluorescence quenching of **P1** (2.0×10^{-6} M) with **P2** (1.0×10^{-6} M) at (**A**) pH 7, (**B**) pH 10 and (**C**) pH 13. The inset shows the emission quenching data.

5.4.4 Titration Experiments (Chapter 2.4)

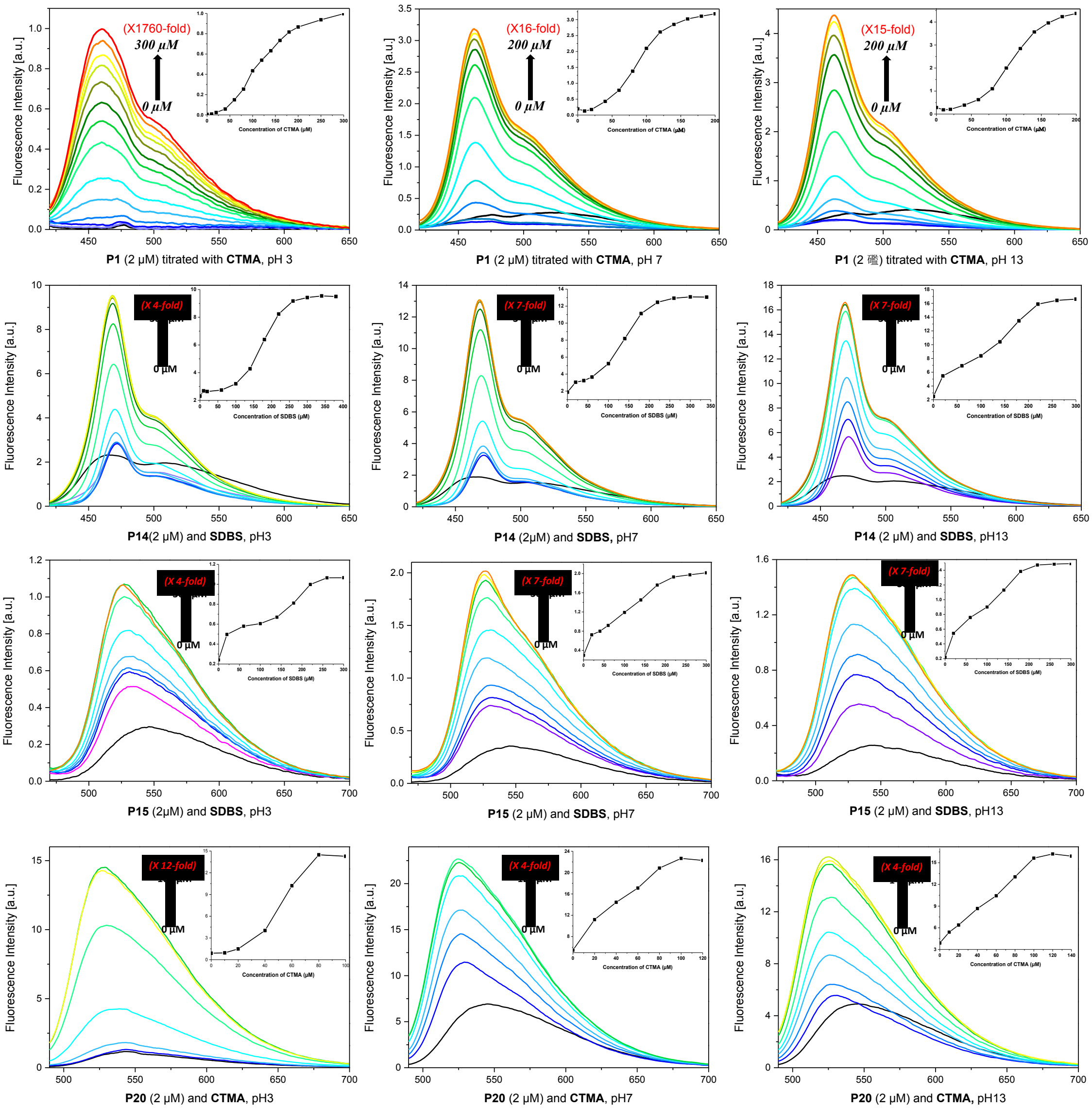

Figure 132. P1-P4 (2 µM, black line) with **SDBS** or **CTMA** at pH 3, pH 7, and pH 13. The inset graph shows the change of I_{Fl} with increasing surfactant concentration.

5.4.5 Titration Experiments (Chapter 4.1)

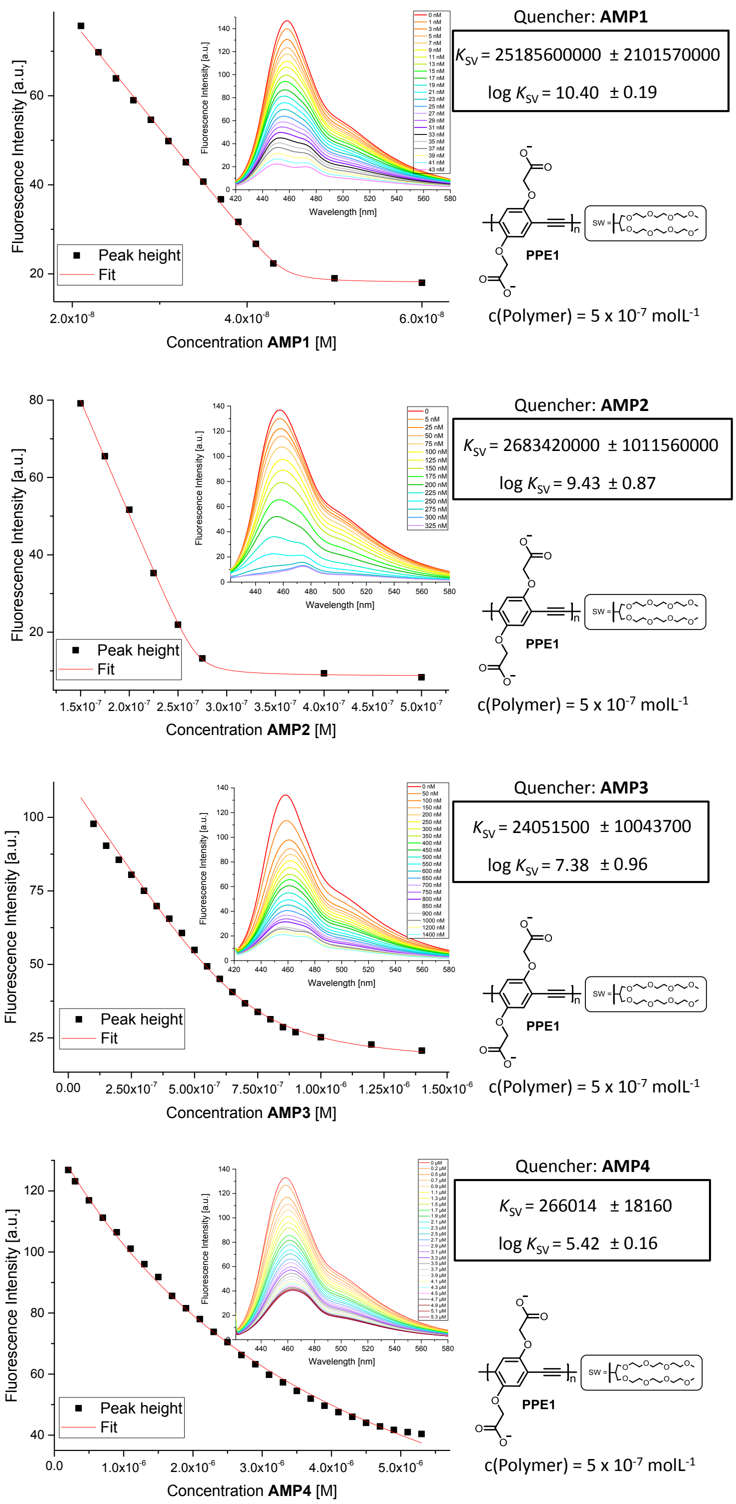

Figure 133. Titration of **PPE 1** with various concentration of AMPs **1-4** in water solution.

5.5 Other Experiment Details

5.5.1 Preparation of Juice Sample (Chapter 3.2)

Sample Preparation

14 apple juices (AJ1-AJ14), 5 black currant juices (BJ1-BJ5) and 6 red grape juices (GJ1-GJ6) were purchased from local supermarkets (detailed information see Table 12) and used directly in discrimination experiments with **P1** and **P2**; pH values of the juices were measured immediately after opening with a pH-meter. Chemicals, solvents and buffers (pH 3, citric acid/NaOH/NaCl; pH 7, KH_2PO_4/Na_2HPO_4; pH 13, glycine/NaOH/NaCl) were purchased from commercial laboratory suppliers. Reagents were used without further purification unless otherwise noted.

Preparations of Red and Green Grape Juices.

Seedless green grapes, Sugarone, Spain, 500 g, and red grapes Summer Royal, Italy, 500 g, were purchased from local supermarkets. Grapes were removed from their stems and washed with cold water, drained off and mashed with a potato masher. The resulting grape sludge was centrifuged with an ultracentrifuge Beckman L7-55 (20000 rpm, 0.5 h, 20 ^{o}C) to isolate clear grape juice as supernatant.

Preparation of Black Currant Juice.

Black currants, Germany, 500 g, were purchased from local supermarkets. The black currants were washed and de-stemmed. 250 mL of water were added, the mixture was mashed with a potato masher and heated for 10 min to gentle boil to furnish 550 mL of a thick solution. Ultracentrifugation (20000 rpm, 0.5 h, 20 ^{o}C) furnished a clear dark black currant juice, which was diluted to 40% of its original concentration by distilled water.

5.5.2 Experimental Details for Bacterial Sensing (Chapter 4.1)

Preparation of Antimicrobial Peptides.

PAF26 and Jelleine-I were synthesized by solid-phase synthesis via fluorenylmethoxycarbonyl/t-butyl (Fmoc/tBu) strategy on an Applied Biosystems 433A peptide synthesizer. The purification was done with a preparativ HPLC system on a Waters Xbridge BEH130 PREP C18 (5 µm, 19 × 150 mm). Analyses were performed on an Agilent 1100 HPLC system using a Chromolith Performance RP-C18 column (100 × 3 mm). The identity of the peptides was verified by HPLC-MS analysis (Exactive, Thermo Fisher Scientific). Ib-AMP4 was firstly synthesized by solid-phase synthesis via fluorenylmethoxycarbonyl/t-butyl (Fmoc/tBu) strategy on an Applied Biosystems 433A peptide synthesizer. The first disulfide bridge was made with the Allyl/Tetrakis/Palladium strategy. The second disulfide bridge was linked via oxidation with a solution of iodine in acetic acid. Excessive iodine was inactivated with ascorbic acid. The purification was done done with a preparativ HPLC system on a Waters Xbridge BEH130 PREP C18 (5 µm, 19 × 150 mm). Analyses were performed on an Agilent 1100 HPLC system using a Chromolith Performance RP-C18 column (100 × 3 mm). The identity of the peptides was verified by HPLC-MS analysis (Exactive, Thermo Fisher Scientific).

Bacteria culturing.

Bacteria were cultured in liquid LB medium overnight at 37°C. The bacterial cells were collected by centrifuged (3500 g for 10 min), the supernatant was removed, and then the bacterial pellets were suspended in water. The number of bacteria are estimated by OD_{600} and confirmed by viable count in an inverted microscope.

Table 69. Numbers of bacteria (/mL) at OD_{600}=0.01, counted under microscope.

Nr.	*Abbreviation of Bacteria*	**OD_{600}**	**Corresponding Numbers of Bacteria** (numbers/mL)
1	*B. megaterium*	0.01	4.7×10^{6}
2	*S. auricularis*	0.01	5.2×10^{6}
3	*M. leteus*	0.01	7.3×10^{6}
4	*K. kristinae*	0.01	2.2×10^{6}
5	*K. marina*	0.01	1.6×10^{6}
6	*K. rhizophilia*	0.01	2.4×10^{6}
7	*K. salsicia*	0.01	2.8×10^{6}
8	*K. varians*	0.01	2.0×10^{6}
9	*P. fluorescens*	0.01	3.1×10^{6}
10	*Y. mollaretii*	0.01	6.2×10^{6}
11	*E. coli K12*	0.01	3.3×10^{6}
12	*E. coli HT115*	0.01	5.4×10^{6}
13	*E. coli OP50*	0.01	7.7×10^{6}
14	*E. coli DH5α*	0.01	3.7×10^{6}

Experimental Details for Bacterial Detection.

The number average molecular weight (M_n=11 kDa) of **PPE 1** was determined by gel permeation chromatography, with polydispersity (PDI=2.7) and degree of polymerization (P_n=13). Generally, the solutions of complex **C1-C4 (**1.5 μM**)** and 14 bacteria (OD_{600} = 0.3) were first prepared in DI water. Complex solution (1.5 μM, 180 μL) was respectively loaded into a well on a 96-well plate. Subsequently, 90 μL of different bacterial solutions were added. After incubation for 30 min, the fluorescence intensity at the peak was recorded on a CLARIOstar (firmware version 1.13) microplate reader with the excitation at 410 nm. Similar procedures were employed to the same (or lower) concentration of bacteria in human urine and in serum.

References

[1] M. C. Gather, A. Kohnen and K. Meerholz, *Adv. Mater.* **2011**, *23*, 233-248.

[2] M. T. Bernius, M. Inbasekaran, J. O'Brien and W. S. Wu, *Adv. Mater.* **2000**, *12*, 1737-1750.

[3] C. J. Brabec, N. S. Sariciftci and J. C. Hummelen, *Adv. Funct. Mater.* **2001**, *11*, 15-26.

[4] G. Dennler, M. C. Scharber and C. J. Brabec, *Adv. Mater.* **2009**, *21*, 1323-1338.

[5] C. D. Dimitrakopoulos and P. R. L. Malenfant, *Adv. Mater.* **2002**, *14*, 99-117.

[6] Y. F. Li and Y. P. Zou, *Adv. Mater.* **2008**, *20*, 2952-2958.

[7] S. W. Thomas, G. D. Joly and T. M. Swager, *Chem. Rev.* **2007**, *107*, 1339-1386.

[8] D. T. McQuade, A. E. Pullen and T. M. Swager, *Chem. Rev.* **2000**, *100*, 2537-2574.

[9] U. H. F. Bunz, *Chem. Rev.* **2000**, *100*, 1605-1644.

[10] U. H. F. Bunz, K. Seehafer, M. Bender and M. Porz, *Chem. Soc. Rev.* **2015**, *44*, 4322-4336.

[11] L. H. Feng, C. L. Zhu, H. X. Yuan, L. B. Liu, F. T. Lv and S. Wang, *Chem. Soc. Rev.* **2013**, *42*, 6620-6633.

[12] C. Zhu, L. Liu, Q. Yang, F. Lv and S. Wang, *Chem. Rev.* **2012**, *112*, 4687-4735.

[13] U. H. F. Bunz, *Acc. Chem. Res.* **2001**, *34*, 998-1010.

[14] U. H. F. Bunz, *Adv. Polym. Sci.* **2005**, *177*, 1-52.

[15] L. B. Buck, *Angew. Chem. Int. Ed.* **2005**, *44*, 6128-6140.

[16] P. Mombaerts, F. Wang, C. Dulac, S. K. Chao, A. Nemes, M. Mendelsohn, J. Edmondson and R. Axel, *Cell* **1996**, *87*, 675-686.

[17] B. Malnic, J. Hirono, T. Sato and L. B. Buck, *Cell* **1999**, *96*, 713-723.

[18] L. Buck and R. Axel, *Cell* **1991**, *65*, 175-187.

[19] K. Persaud and G. Dodd, *Nature* **1982**, *299*, 352-355.

[20] J. Janata, *Principles of chemical sensors*, Springer Science & Business Media, **2010**.

[21] S. Katada, T. Hirokawa, Y. Oka, M. Suwa and K. Touhara, *J. Neurosci.* **2005**, *25*, 1806-1815.

[22] J. R. Stetter and J. Li, *Chem. Rev.* **2008**, *108*, 352-366.

[23] M. U. Ahmed, M. M. Hossain and E. Tamiya, *Electroanal* **2008**, *20*, 616-626.

[24] C. Mandenius, L. Bülow, B. Danielsson and K. Mosbach, *Appl. Microbiol. Biotechnol.* **1985**, *21*, 135-142.

[25] B. Xie, K. Ramanathan and B. Danielsson, *Trac-Trend Anal Chem* **2000**, *19*, 340-349.

[26] B. Xie, M. Mecklenburg, B. Danielsson, O. Ohman and F. Winquist, *Anal. Chim. Acta* **1994**, *299*, 165-170.

[27] P. Bataillard, E. Steffgen, S. Haemmerli, A. Manz and H. M. Widmer, *Biosensors & Bioelectronics* **1993**, *8*, 89-98.

[28] Y. Y. Zhang and S. Tadigadapa, *Biosensors & Bioelectronics* **2004**, *19*, 1733-1743.

[29] M. Shimohigoshi and I. Karube, *Sens. Actuators, B* **1996**, *30*, 17-21.

[30] M. Mecklenburg, C. Lindbladh, H. S. Li, K. Mosbach and B. Danielsson, *Anal. Biochem.* **1993**, *212*, 388-393.

[31] F. Scheller, N. Siegbahn, B. Danielsson and K. Mosbach, *Anal. Chem.* **1985**, *57*, 1740-1743.

[32] K. Nassau, *The Physics and Chemistry of Color: The Fifteen Causes of Color, 2nd Edition, by Kurt Nassau, pp. 496. ISBN 0-471-39106-9. Wiley-VCH, July 2001.* **2001**, *1*.

[33] C. Albrecht, *Anal. Bioanal. Chem.* **2008**, *390*, 1223-1224.

[34] C. McDonagh, C. S. Burke and B. D. MacCraith, *Chem. Rev.* **2008**, *108*, 400-422.

[35] F. Baldini, A. N. Chester, J. Homola and S. Martellucci, *Optical chemical sensors*, Springer Science & Business Media, **2006**.

[36] J. R. Askim, M. Mahmoudi and K. S. Suslick, *Chem. Soc. Rev.* **2013**, *42*, 8649-8682.

[37] L. You, D. J. Zha and E. V. Anslyn, *Chem. Rev.* **2015**, *115*, 7840-7892.

[38] W. Huang, E. Smarsly, J. Han, M. Bender, K. Seehafer, I. Wacker, R. R. Schroder and U. H. Bunz, *ACS Appl. Mater. Interfaces* **2017**, *9*, 3068-3074.

[39] J. Han, B. Wang, M. Bender, S. Kushida, K. Seehafer and U. H. Bunz, *ACS Appl. Mater. Interfaces* **2017**, *9*, 790-797.

[40] J. Han, B. Wang, M. Bender, K. Seehafer and U. H. F. Bunz, *ACS Appl. Mater. Interfaces* **2016**, *8*, 20415-20421.

[41] J. Han, M. Bender, S. Hahn, K. Seehafer and U. H. Bunz, *Chem-Eur J* **2016**, *22*, 3230-3233.

[42] S. G. Elci, D. F. Moyano, S. Rana, G. Y. Tong, R. L. Phillips, U. H. F. Bunz and V. M. Rotello, *Chem. Sci.* **2013**, *4*, 2076-2080.

[43] I. B. Kim, M. H. Han, R. L. Phillips, B. Samanta, V. M. Rotello, Z. J. Zhang and U. H. F. Bunz, *Chem-Eur J* **2009**, *15*, 449-456.

[44] I. B. Kim and U. H. F. Bunz, *J. Am. Chem. Soc.* **2006**, *128*, 2818-2819.

[45] I. B. Kim, A. Dunkhorst, J. Gilbert and U. H. F. Bunz, *Macromolecules* **2005**, *38*, 4560-4562.

[46] J. Han, B. Wang, M. Bender, K. Seehafer and U. H. Bunz, *Analyst* **2017**, *142*, 537-543.

[47] J. Han, M. Bender, K. Seehafer and U. H. Bunz, *Angew. Chem. Int. Ed.* **2016**, *55*, 7689-7692.

[48] S. Rana, S. G. Elci, R. Mout, A. K. Singla, M. Yazdani, M. Bender, A. Bajaj, K. Saha, U. H. F. Bunz, F. R. Jirik and V. M. Rotello, *J. Am. Chem. Soc.* **2016**, *138*, 4522-4529.

[49] D. F. Moyano, S. Rana, U. H. F. Bunz and V. M. Rotello, *Faraday Discuss.* **2011**, *152*, 33-42.

[50] O. R. Miranda, H. T. Chen, C. C. You, D. E. Mortenson, X. C. Yang, U. H. F. Bunz and V. M. Rotello, *J. Am. Chem. Soc.* **2010**, *132*, 5285-5289.

[51] U. H. F. Bunz and V. M. Rotello, *Angew. Chem. Int. Ed.* **2010**, *49*, 3268-3279.

[52] A. Bajaj, S. Rana, O. R. Miranda, J. C. Yawe, D. J. Jerry, U. H. F. Bunz and V. M. Rotello, *Chem. Sci.* **2010**, *1*, 134-138.

[53] A. Bajaj, O. R. Miranda, R. Phillips, I. B. Kim, D. J. Jerry, U. H. F. Bunz and V. M. Rotello, *J. Am. Chem. Soc.* **2010**, *132*, 1018-1022.

[54] M. De, S. Rana, H. Akpinar, O. R. Miranda, R. R. Arvizo, U. H. F. Bunz and V. M. Rotello, *Nat. Chem.* **2009**, *1*, 461-465.

[55] A. Bajaj, O. R. Miranda, I. B. Kim, R. L. Phillips, D. J. Jerry, U. H. F. Bunz and V. M. Rotello, *Proc. Natl. Acad. Sci. U. S. A.* **2009**, *106*, 10912-10916.

[56] R. L. Phillips, O. R. Miranda, C. C. You, V. M. Rotello and U. H. F. Bunz, *Angew. Chem. Int. Ed.* **2008**, *47*, 2590-2594.

[57] C. C. You, O. R. Miranda, B. Gider, P. S. Ghosh, I. B. Kim, B. Erdogan, S. A. Krovi, U. H. F. Bunz and V. M. Rotello, *Nature Nanotechnology* **2007**, *2*, 318-323.

[58] O. R. Miranda, C. C. You, R. Phillips, I. B. Kim, P. S. Ghosh, U. H. F. Bunz and V. M. Rotello, *J. Am. Chem. Soc.* **2007**, *129*, 9856-9857.

[59] R. A. Johnson and D. W. Wichern, *Applied multivariate statistical analysis*, Prentice hall Upper Saddle River, NJ, **2002**.

[60] R. E. Anderson, R. L. Tatham and W. C. Black, *Upper Saddle River, NJ: Prentice Hall. Hancock D (2004). Cooperative learning and peer orientation effects on motivation achievement. J. Educ. Res* **1998**, *97*, 159-166.

[61] S. Stewart, M. A. Ivy and E. V. Anslyn, *Chem. Soc. Rev.* **2014**, *43*, 70-84.

[62] Y. L. Liu and M. Bonizzoni, *J. Am. Chem. Soc.* **2014**, *136*, 14223-14229.

[63] P. C. Jurs, G. A. Bakken and H. E. McClelland, *Chem. Rev.* **2000**, *100*, 2649-2678.

[64] D. L. Massart and L. Kaufman, *The interpretation of analytical chemical data by th e use of cluster analysis*, Wiley, **1983**.

[65] Z. Li, H. Li, M. K. LaGasse and K. S. Suslick, *Anal. Chem.* **2016**, *88*, 5615-5620.

[66] J. R. Askim, Z. Li, M. K. LaGasse, J. M. Rankin and K. S. Suslick, *Chem. Sci.* **2016**, *7*, 199-206.

[67] C. J. Musto and K. S. Suslick, *Curr. Opin. Chem. Biol.* **2010**, *14*, 758-766.

[68] L. A. Feng, C. J. Musto, J. W. Kemling, S. H. Lim, W. X. Zhong and K. S. Suslick, *Anal. Chem.* **2010**, *82*, 9433-9440.

[69] S. H. Lim, L. Feng, J. W. Kemling, C. J. Musto and K. S. Suslick, *Nat. Chem.* **2009**, *1*, 562-567.

[70] M. C. Janzen, J. B. Ponder, D. P. Bailey, C. K. Ingison and K. S. Suslick, *Anal. Chem.* **2006**, *78*, 3591-3600.

[71] K. S. Suslick, N. A. Rakow and A. Sen, *Tetrahedron* **2004**, *60*, 11133-11138.

[72] K. L. Diehl and E. V. Anslyn, *Chem. Soc. Rev.* **2013**, *42*, 8596-8611.

[73] S. H. Shabbir, L. A. Joyce, G. M. da Cruz, V. M. Lynch, S. Sorey and E. V. Anslyn, *J. Am. Chem. Soc.* **2009**, *131*, 13125-13131.

[74] A. Akdeniz, M. G. Caglayan and P. Anzenbacher, *Chem. Commun.* **2016**, *52*, 1827-1830.

[75] L. Mosca, R. S. Khnayzer, M. S. Lazorski, E. O. Danilov, F. N. Castellano and P. Anzenbacher, *Chem-Eur J* **2015**, *21*, 4056-4064.

[76] A. Akdeniz, L. Mosca, T. Minami and P. Anzenbacher, *Chem. Commun.* **2015**, *51*, 5770-5773.

[77] T. Minami, Y. L. Liu, A. Akdeniz, P. Koutnik, N. A. Esipenko, R. Nishiyabu, Y. Kubo and P. Anzenbacher, *J. Am. Chem. Soc.* **2014**, *136*, 11396-11401.

[78] T. Minami, N. A. Esipenko, B. Zhang, L. Isaacs and P. Anzenbacher, *Chem. Commun.* **2014**, *50*, 61-63.

[79] T. Minami, N. A. Esipenko, A. Akdeniz, B. Zhang, L. Isaacs and P. Anzenbacher, *J. Am. Chem. Soc.* **2013**, *135*, 15238-15243.

[80] Y. L. Liu, T. Minami, R. Nishiyabu, Z. Wang and P. Anzenbacher, *J. Am. Chem. Soc.* **2013**, *135*, 7705-7712.

[81] N. A. Esipenko, P. Koutnik, T. Minami, L. Mosca, V. M. Lynch, G. V. Zyryanov and P. Anzenbacher, *Chem. Sci.* **2013**, *4*, 3617-3623.

[82] P. Anzenbacher, L. Mosca, M. A. Palacios, G. V. Zyryanov and P. Koutnik, *Chem-Eur J* **2012**, *18*, 12712-12718.

[83] M. A. Palacios, Z. Wang, V. A. Montes, G. V. Zyryanov and P. Anzenbacher, *J. Am. Chem. Soc.* **2008**, *130*, 10307-10314.

[84] M. A. Palacios, Z. Wang, V. A. Montes, G. V. Zyryanov, B. J. Hausch, K. Jursikova and P. Anzenbacher, *Chem. Commun.* **2007**, 3708-3710.

[85] T. Minami, N. A. Esipenko, B. Zhang, L. Isaacs, R. Nishiyabu, Y. Kubo and P. Anzenbacher, *J. Am. Chem. Soc.* **2012**, *134*, 20021-20024.

[86] M. Qin, F. Y. Li, Y. Huang, W. Ran, D. Han and Y. L. Song, *Anal. Chem.* **2015**, *87*, 837-842.

[87] G. He, N. Yan, H. Cui, T. H. Liu, L. P. Ding and Y. Fang, *Macromolecules* **2011**, *44*, 7096-7099.

[88] M. A. Palacios, R. Nishiyabu, M. Marquez and P. Anzenbacher, *J. Am. Chem. Soc.* **2007**, *129*, 7538-7544.

[89] G. V. Zyryanov, M. A. Palacios and P. Anzenbacher, *Angew. Chem. Int. Ed.* **2007**, *46*, 7849-7852.

[90] Z. Li and K. S. Suslick, *Acs Sensors* **2016**, *1*, 1330-1335.

[91] J. M. Rankin, Q. F. Zhang, M. K. LaGasse, Y. N. Zhang, J. R. Askim and K. S. Suslick, *Analyst* **2015**, *140*, 2613-2617.

[92] P. J. Mazzone, X. F. Wang, Y. M. Xu, T. Mekhail, M. C. Beukemann, J. Na, J. W. Kemling, K. S. Suslick and M. Sasidhar, *J Thorac Oncol* **2012**, *7*, 137-142.

[93] H. W. Lin, M. Jang and K. S. Suslick, *J. Am. Chem. Soc.* **2011**, *133*, 16786-16789.

[94] H. W. Lin and K. S. Suslick, *J. Am. Chem. Soc.* **2010**, *132*, 15519-15521.

[95] H. Haick, Y. Y. Broza, P. Mochalski, V. Ruzsanyi and A. Amann, *Chem. Soc. Rev.* **2014**, *43*, 1423-1449.

[96] Y. Y. Broza and H. Haick, *Nanomedicine-Uk* **2013**, *8*, 785-806.

[97] F. Rock, N. Barsan and U. Weimar, *Chem. Rev.* **2008**, *108*, 705-725.

[98] A. P. F. Turner and N. Magan, *Nat Rev Microbiol* **2004**, *2*, 161-166.

[99] R. F. Machado, D. Laskowski, O. Deffenderfer, T. Burch, S. Zheng, P. J. Mazzone, T. Mekhail, C. Jennings, J. K. Stoller, J. Pyle, J. Duncan, R. A. Dweik and S. C. Erzurum, *Am J Resp Crit Care* **2005**, *171*, 1286-1291.

[100] Y. Y. Broza, R. Kremer, U. Tisch, A. Gevorkyan, A. Shiban, L. A. Best and H. Haick, *Nanomed-Nanotechnol* **2013**, *9*, 15-21.

[101] K. S. Suslick, *MRS Bull.* **2004**, *29*, 720-725.

[102] Z. Li, W. P. Bassett, J. R. Askim and K. S. Suslick, *Chem. Commun.* **2015**, *51*, 15312-15315.

[103] S. J. Toal and W. C. Trogler, *J. Mater. Chem.* **2006**, *16*, 2871-2883.

[104] J. Cho, R. Anandakathir, A. Kumar, J. Kumar and P. U. Kurup, *Sens. Actuators, B* **2011**, *160*, 1237-1243.

[105] N. Fahimi-Kashani and M. R. Hormozi-Nezhad, *Anal. Chem.* **2016**, *88*, 8099-8106.

[106] S. E. Ebeler, *Food Rev Int* **2001**, *17*, 45-64.

[107] T. J. Evans, C. E. Butzke and S. E. Ebeler, *J. Chromatogr. A* **1997**, *786*, 293-298.

[108] L. Nyadong, M. D. Green, V. R. De Jesus, P. N. Newton and F. M. Fernandez, *Anal. Chem.* **2007**, *79*, 2150-2157.

[109] R. M. Alberici, G. D. Fernandes, A. M. Porcari, M. N. Eberlin, D. Barrera-Arellano and F. M. Fernandez, *Food Chem.* **2016**, *211*, 661-668.

[110] C. Nerin, P. Alfaro, M. Aznar and C. Domeno, *Anal. Chim. Acta* **2013**, *775*, 14-24.

[111] E. A. Baldwin, J. H. Bai, A. Plotto and S. Dea, *Sensors* **2011**, *11*, 4744-4766.

[112] A. Legin, A. Rudnitskaya, Y. Vlasov, C. Di Natale, F. Davide and A. D'Amico, *Sensors and Actuators B-Chemical* **1997**, *44*, 291-296.

[113] M. Sliwinska, P. Wisniewska, T. Dymerski, J. Namiesnik and W. Wardencki, *J. Agric. Food Chem.* **2014**, *62*, 1423-1448.

[114] I. Mafra, I. M. P. L. V. O. Ferreira and M. B. P. P. Oliveira, *Eur. Food Res. Technol.* **2008**, *227*, 649-665.

[115] A. K. Lockley and R. G. Bardsley, *Trends Food Sci. Technol.* **2000**, *11*, 67-77.

[116] P. Anzenbacher, P. Lubal, P. Bucek, M. A. Palacios and M. E. Kozelkova, *Chem. Soc. Rev.* **2010**, *39*, 3954-3979.

[117] T. L. Nelson, C. O'Sullivan, N. T. Greene, M. S. Maynor and J. J. Lavigne, *J. Am. Chem. Soc.* **2006**, *128*, 5640-5641.

[118] M. S. Maynor, T. L. Nelson, C. O'Sullivan and J. J. Lavigne, *Org. Lett.* **2007**, *9*, 3217-3220.

[119] B. A. Suslick, L. Feng and K. S. Suslick, *Anal. Chem.* **2010**, *82*, 2067-2073.

[120] S. L. Wiskur and E. V. Anslyn, *J. Am. Chem. Soc.* **2001**, *123*, 10109-10110.

[121] C. Zhang, D. P. Bailey and K. S. Suslick, *J. Agric. Food. Chem.* **2006**, *54*, 4925-4931.

[122] C. Zhang and K. S. Suslick, *J. Agric. Food. Chem.* **2007**, *55*, 237-242.

[123] A. P. Umali, S. E. LeBoeuf, R. W. Newberry, S. Kim, L. Tran, W. A. Rome, T. A. Tian, D. Taing, J. Hong, M. Kwan, H. Heymann and E. V. Anslyn, *Chem. Sci.* **2011**, *2*, 439-445.

[124] A. M. Piatek, Y. J. Bomble, S. L. Wiskur and E. V. Anslyn, *J. Am. Chem. Soc.* **2004**, *126*, 6072-6077.

[125] L. T. Gallagher, J. S. Heo, M. A. Lopez, B. M. Ray, J. Xiao, A. P. Umali, A. Zhang, S. Dharmarajan, H. Heymann and E. V. Anslyn, *Supramol. Chem.* **2012**, *24*, 143-148.

[126] M. Mahmoudi, S. E. Lohse, C. J. Murphy and K. S. Suslick, *Acs Sensors* **2016**, *1*, 17-21.

[127] Z. Li, M. Jang, J. R. Askim and K. S. Suslick, *Analyst* **2015**, *140*, 5929-5935.

[128] N. A. Rakow and K. S. Suslick, *Nature* **2000**, *406*, 710-713.

[129] A. P. Umali and E. V. Anslyn, *Curr. Opin. Chem. Biol.* **2010**, *14*, 685-692.

[130] B. T. Nguyen and E. V. Anslyn, *Coordination Chemistry Reviews* **2006**, *250*, 3118-3127.

[131] B. S. Reisner and G. L. Woods, *J. Clin. Microbiol.* **1999**, *37*, 2024-2026.

[132] J. Wang, X. Wang, Y. Li, S. Yan, Q. Zhou, B. Gao, J. Peng, J. Du, Q. Fu, S. Jia, J. Zhang and L. Zhan, *Anal. Sci.* **2012**, *28*, 237-241.

[133] P. L. Zarain, G. Lopez-Tellez, R. D. Rocha-Gracia, C. Romero-Lopez, Y. Martinez-Laguna, A. Rivera and E. Brambila, *Afr. J. Microbiol. Res.* **2012**, *6*, 4601-4607.

[134] Y. Hu, J. Liu, D. Xia and S. Chen, *J. Basic Microbiol.* **2012**, *52*, 27-34.

[135] U. Ruffing, R. Akulenko, M. Bischoff, V. Helms, M. Herrmann and L. von Muller, *PLoS One* **2012**, *7*, e52487.

[136] P. Krader and D. Emerson, *Extremophiles* **2004**, *8*, 259-268.

[137] C. Mello, D. Ribeiro, F. Novaes and R. J. Poppi, *Anal. Bioanal. Chem.* **2005**, *383*, 701-706.

[138] C. Wang and J. Irudayaraj, *Small* **2008**, *4*, 2204-2208.

[139] A. K. Singh, D. Senapati, S. G. Wang, J. Griffin, A. Neely, P. Candice, K. M. Naylor, B. Varisli, J. R. Kalluri and P. C. Ray, *Acs Nano* **2009**, *3*, 1906-1912.

[140] Y. S. Kim, J. Chung, M. Y. Song, J. Jurng and B. C. Kim, *Biosensors & Bioelectronics* **2014**, *54*, 195-198.

[141] R. G. van der Merwe, P. D. van Helden, R. M. Warren, S. L. Sampson and N. C. Gey van Pittius, *Analyst* **2014**, *139*, 2617-2626.

[142] R. Edgar, M. McKinstry, J. Hwang, A. B. Oppenheim, R. A. Fekete, G. Giulian, C. Merril, K. Nagashima and S. Adhya, *Proc. Natl. Acad. Sci. U. S. A.* **2006**, *103*, 4841-4845.

[143] M. D. Disney, J. Zheng, T. M. Swager and P. H. Seeberger, *J. Am. Chem. Soc.* **2004**, *126*, 13343-13346.

[144] J. Chen, S. M. Andler, J. M. Goddard, S. R. Nugen and V. M. Rotello, *Chem. Soc. Rev.* **2016**.

[145] S. C. Hayden, G. X. Zhao, K. Saha, R. L. Phillips, X. N. Li, O. R. Miranda, V. M. Rotello, M. A. El-Sayed, I. Schmidt-Krey and U. H. F. Bunz, *J. Am. Chem. Soc.* **2012**, *134*, 6920-6923.

[146] A. Duarte, A. Chworos, S. F. Flagan, G. Hanrahan and G. C. Bazan, *J. Am. Chem. Soc.* **2010**, *132*, 12562-12564.

[147] W. Chen, Q. Li, W. Zheng, F. Hu, G. Zhang, Z. Wang, D. Zhang and X. Jiang, *Angew. Chem. Int. Ed.* **2014**, *53*, 13734-13739.

[148] U. H. F. Bunz, *Macromol. Rapid Commun.* **2009**, *30*, 772-805.

[149] H. A. Ho, A. Najari and M. Leclerc, *Acc. Chem. Res.* **2008**, *41*, 168-178.

[150] R. L. Phillips, O. R. Miranda, D. E. Mortenson, C. Subramani, V. M. Rotello and U. H. F. Bunz, *Soft Matter* **2009**, *5*, 607-612.

[151] J. S. Wu, B. Kwon, W. M. Liu, E. V. Anslyn, P. F. Wang and J. S. Kim, *Chem. Rev.* **2015**, *115*, 7893-7943.

[152] W. J. Peveler, M. Yazdani and V. M. Rotello, *Acs Sensors* **2016**, *1*, 1282-1285.

[153] X. L. Feng, L. B. Liu, S. Wang and D. B. Zhu, *Chem. Soc. Rev.* **2010**, *39*, 2411-2419.

[154] K. Seehafer, M. Bender, S. T. Schwaebel and U. H. F. Bunz, *Macromolecules* **2014**, *47*, 7014-7020.

[155] K. Seehafer, M. Bender and U. H. F. Bunz, *Macromolecules* **2014**, *47*, 922-927.

[156] I. B. Kim, R. Phillips and U. H. F. Bunz, *Macromolecules* **2007**, *40*, 5290-5293.

[157] D. Zamora-Olivares, T. S. Kaoud, J. Jose, A. Ellington, K. N. Dalby and E. V. Anslyn, *Angew. Chem. Int. Ed.* **2014**, *53*, 14064-14068.

[158] T. Z. Zhang, N. Y. Edwards, M. Bonizzoni and E. V. Anslyn, *J. Am. Chem. Soc.* **2009**, *131*, 11976-11984.

[159] J. J. Lavigne and E. V. Anslyn, *Angew. Chem. Int. Ed.* **2001**, *40*, 3118-3130.

[160] J. J. Lavigne, *Nat Mater* **2007**, *6*, 548-549.

[161] K. L. Bicker, J. Sun, J. J. Lavigne and P. R. Thompson, *ACS Comb. Sci.* **2011**, *13*, 232-243.

[162] K. J. Albert, N. S. Lewis, C. L. Schauer, G. A. Sotzing, S. E. Stitzel, T. P. Vaid and D. R. Walt, *Chem. Rev.* **2000**, *100*, 2595-2626.

[163] B. Creran, U. H. F. Bunz and V. M. Rotello, *Curr. Org. Chem.* **2015**, *19*, 1054-1062.

[164] E. A. Davey, A. Zucchero, O. Trapp and U. H. F. Bunz, *J. Am. Chem. Soc.* **2011**, *133*, 7716-7718.

[165] A. T. Wright, M. J. Griffin, Z. L. Zhong, S. C. McCleskey, E. V. Anslyn and J. T. McDevitt, *Angew. Chem. Int. Ed.* **2005**, *44*, 6375-6378.

[166] A. T. Wright and E. V. Anslyn, *Chem. Soc. Rev.* **2006**, *35*, 14-28.

[167] N. T. Greene and K. D. Shimizu, *J. Am. Chem. Soc.* **2005**, *127*, 5695-5700.

[168] C. H. Fan, K. W. Plaxco and A. J. Heeger, *J. Am. Chem. Soc.* **2002**, *124*, 5642-5643.

[169] A. Buryak and K. Severin, *J. Am. Chem. Soc.* **2005**, *127*, 3700-3701.

[170] M. Bender, K. Seehafer, M. Findt and U. H. F. Bunz, *Rsc Adv* **2015**, *5*, 96189-96193.

[171] G. M. L. Nayyar, J. G. Breman, P. N. Newton and J. Herrington, *Lancet Infect Dis* **2012**, *12*, 488-496.

[172] P. N. Newton, M. D. Green, F. M. Fernandez, N. P. J. Day and N. J. White, *Lancet Infect. Dis.* **2006**, *6*, 602-613.

[173]*http://www.fda.gov/Drugs/ResourcesForYou/Consumers/BuyingUsingMedicineSafely/CounterfeitMedicine/default.htm* **2016**.

[174] P. Aldhous, *Nature* **2005**, *434*, 132-136.

[175] A. K. Deisingh, *The Analyst* **2005**, *130*, 271-279.

[176] P. M. Rudolf and I. B. Bernstein, *The New England journal of medicine* **2004**, *350*, 1384-1386.

[177] C. Sheridan, *Nature biotechnology* **2007**, *25*, 707-709.

[178] A. A. Weaver, H. Reiser, T. Barstis, M. Benvenuti, D. Ghosh, M. Hunckler, B. Joy, L. Koenig, K. Raddell and M. Lieberman, *Anal. Chem.* **2013**, *85*, 6453-6460.

[179] A. A. Weaver and M. Lieberman, *Am J Trop Med Hyg* **2015**, *92*, 17-23.

[180] L. A. Baumes, M. B. Sogo, P. Montes-Navajas, A. Corma and H. Garcia, *Chem-Eur J* **2010**, *16*, 4489-4495.

[181] C. Huang, B. Lucas, C. Vervaet, K. Braeckmans, S. Van Calenbergh, I. Karalic, M. Vandewoestyne, D. Deforce, J. Demeester and S. C. De Smedt, *Advanced materials* **2010**, *22*, 2657-2662.

[182] R. Martino, M. Malet-Martino, V. Gilard and S. Balayssac, *Anal Bioanal Chem* **2010**, *398*, 77-92.

[183] O. Y. Rodionova, L. P. Houmoller, A. L. Pomerantsev, P. Geladi, J. Burger, V. L. Dorofeyev and A. P. Arzamastsev, *Anal Chim Acta* **2005**, *549*, 151-158.

[184] S. H. F. Scafi and C. Pasquini, *The Analyst* **2001**, *126*, 2218-2224.

[185] A. Parthasarathy, H. C. Pappas, E. H. Hill, Y. Huang, D. G. Whitten and K. S. Schanze, *ACS Appl Mater Interfaces* **2015**, *7*, 28027-28034.

[186] D. Wu and K. S. Schanze, *ACS Appl Mater Interfaces* **2014**, *6*, 7643-7651.

[187] Y. Wu, Y. Tan, J. T. Wu, S. Y. Chen, Y. Z. Chen, X. W. Zhou, Y. Y. Jiang and C. Y. Tan, *Acs Applied Materials & Interfaces* **2015**, *7*, 6882-6888.

[188] J. S. Yang and T. M. Swager, *J. Am. Chem. Soc.* **1998**, *120*, 11864-11873.

[189] C. Zhang and K. S. Suslick, *J. Agric. Food. Chem.* **2007**, *55*, 237-242.

[190] A. A. Weaver, H. Reiser, T. Barstis, M. Benvenuti, D. Ghosh, M. Hunckler, B. Joy, L. Koenig, K. Raddell and M. Lieberman, *Anal. Chem.* **2013**, *85*, 6453-6460.

[191] S. Kovacs, S. E. Hawes, S. N. Maley, E. Mosites, L. Wong and A. Stergachis, *PLoS One* **2014**, *9*.

[192] P. N. Newton, F. M. Fernandez, A. Plancon, D. C. Mildenhall, M. D. Green, L. Ziyong, E. M. Christophel, S. Phanouvong, S. Howells, E. McIntosh, P. Laurin, N. Blum, C. Y. Hampton, K. Faure, L. Nyadong, C. W. R. Soong, B. Santoso, W. Zhiguang, J. Newton and K. Palmer, *PLoS Med.* **2008**, *5*, 209-219.

[193] C. Patze, K. Broedner, F. Rominger, O. Trapp and U. H. Bunz, *Chemistry* **2011**, *17*, 13720-13725.

[194] M. Kitamura, S. H. Shabbir and E. V. Anslyn, *J. Org. Chem.* **2009**, *74*, 4479-4489.

[195] J. J. Lavigne, D. L. Broughton, J. N. Wilson, B. Erdogan and U. H. F. Bunz, *Macromolecules* **2003**, *36*, 7409-7412.

[196] P. Jonathan, W. V. McCarthy and A. M. I. Roberts, *J. Chemom.* **1996**, *10*, 189-213.

[197] A. R. Henderson, *Clin. Chim. Acta* **2005**, *359*, 1-26.

[198] L. Holmberg, *International Journal of Wine Research* **2010**, *2010*, 105-113.

[199] A. CAVICChI and C. SAntInI, *Tourism Review International* **2011**, *15*, 253-267.

[200] E. Ghanem, H. Hopfer, A. Navarro, M. S. Ritzer, L. Mahmood, M. Fredell, A. Cubley, J. Bolen, R. Fattah, K. Teasdale, L. Lieu, T. Chua, F. Marini, H. Heymann and E. V. Anslyn, *Molecules* **2015**, *20*, 9170-9182.

[201] I. B. Kim, H. Shin, A. J. Garcia and U. H. F. Bunz, *Bioconjugate Chem.* **2007**, *18*, 815-820.

[202] R. L. Phillips, I. B. Kim, L. M. Tolbert and U. H. F. Bunz, *J. Am. Chem. Soc.* **2008**, *130*, 6952-+.

[203] J. N. Wilson, Y. Q. Wang, J. J. Lavigne and U. H. F. Bunz, *Chem. Commun.* **2003**, 1626-1627.

[204] P. Wisniewska, T. Dymerski, W. Wardencki and J. Namiesnik, *J. Sci. Food Agric.* **2015**, *95*, 2159-2166.

[205] D. Gonzalez-Arjona, G. Lopez-Perez, V. Gonzalez-Gallero and A. G. Gonzalez, *J. Agric. Food. Chem.* **2006**, *54*, 1982-1989.

[206] M. L. Xu, Y. Yu, H. S. Ramaswamy and S. M. Zhu, *Sci. Rep.* **2017**, *7*, 39671.

[207] A. G. Mignani, L. Ciaccheri, B. Gordillo, A. A. Mencaglia, M. L. Gonzalez-Miret, F. J. Heredia and B. Culshaw, *Sens. Actuators, B* **2012**, *171*, 458-462.

[208] D. Picque, P. Lieben, G. Corrieu, R. Cantagrel, O. Lablanquie and G. Snakkers, *J. Agric. Food. Chem.* **2006**, *54*, 5220-5226.

[209] D. Wishart, *Significance* **2009**, *6*, 20-26.

[210] D. Broom, *The World Atlas of Whisky: More Than 200 Distilleries Explored and 750 Expressions Tasted*, **2014**.

[211] D. Wishart, *Whisky Classified: Choosing Single Malts by Flavour*, Pavilion, **2006**.

[212] K. Liu, D. Pesce, C. Ma, M. Tuchband, M. Shuai, D. Chen, J. J. Su, Q. Liu, J. Y. Gerasimov, A. Kolbe, W. Zajaczkowski, W. Pisula, K. Mullen, N. A. Clark and A. Herrmann, *Adv. Mater.* **2015**, *27*, 2459-2465.

[213] D. Pesce, Y. Z. Wu, A. Kolbe, T. Weil and A. Herrmann, *Biomaterials* **2013**, *34*, 4360-4367.

[214] H. G. Yang, C. Ma, K. Y. Li, K. Liu, M. Loznik, R. Teeuwen, J. C. M. van Hest, X. Zhou, A. Herrmann and J. J. Wang, *Adv. Mater.* **2016**, *28*, 5008-5012.

[215] P. Wisniewska, M. Sliwinska, J. Namiesnik, W. Wardencki and T. Dymerski, *J. Anal. Methods Chem.* **2016**.

[216] J. K. S. Moller, R. R. Catharino and M. N. Eberlin, *Analyst* **2005**, *130*, 890-897.

[217] C. Nathan and O. Cars, *N. Engl. J. Med.* **2014**, *371*, 1761-1763.

[218] S. B. Levy and B. Marshall, *Nat. Med.* **2004**, *10*, S122-129.

[219] M. Zasloff, *Nature* **2002**, *415*, 389-395.

[220] P. Nicolas and A. Mor, *Annu. Rev. Microbiol.* **1995**, *49*, 277-304.

[221] J. D. Hale and R. E. Hancock, *Expert Rev. Anti-Infect. Ther.* **2007**, *5*, 951-959.

[222] J. R. Uzarski and C. M. Mello, *Anal. Chem.* **2012**, *84*, 7359-7366.

[223] H. Yuan, Z. Liu, L. Liu, F. Lv, Y. Wang and S. Wang, *Adv. Mater.* **2014**, *26*, 4333-4338.

[224] M. R. Yeaman and N. Y. Yount, *Pharmacol. Rev.* **2003**, *55*, 27-55.

[225] J. Han, B. Wang, M. Bender, J. Pfisterer, W. Huang, K. Seehafer, M. Yazdani, V. M. Rotello, C. M. Rotello and U. H. F. Bunz, *Polym. Chem.* **2017**, *8*, 2723-2732.

[226] S. O. Kelley, *Acs Sensors* **2017**, *2*, 193-197.

[227] G. Helmchen, G. Nill, D. Flockerzi, W. Schuhle and M. S. K. Youssef, *Angew. Chem. Int. Ed.* **1979**, *18*, 62-63.

[228] G. R. Fulmer, A. J. M. Miller, N. H. Sherden, H. E. Gottlieb, A. Nudelman, B. M. Stoltz, J. E. Bercaw and K. I. Goldberg, *Organometallics* **2010**, *29*, 2176-2179.

[229] W. H. Melhuish, *J Phys Chem-Us* **1961**, *65*, 229-235.

[230] D. J. Haydon, J. M. Bennett, D. Brown, I. Collins, G. Galbraith, P. Lancett, R. Macdonald, N. R. Stokes, P. K. Chauhan, J. K. Sutariya, N. Nayal, A. Srivastava, J. Beanland, R. Hall, V. Henstock, C. Noula, C. Rockley and L. Czaplewski, *J. Med. Chem.* **2010**, *53*, 3927-3936.

[231] A. H. Berrie, G. T. Newbold and F. S. Spring, *J. Chem. Soc.* **1952**, 2042-2046.

[232] P. Herguch, X. Z. Jiang, M. S. Liu and A. K. Y. Jen, *Macromolecules* **2002**, *35*, 6094-6100.

[233] A. Kolbe, L. L. del Mercato, A. Z. Abbasi, P. Rivera-Gil, S. J. Gorzini, W. H. C. Huibers, B. Poolman, W. J. Parak and A. Herrmann, *Macromol. Rapid Commun.* **2011**, *32*, 186-190.

Eidesstattliche Versicherung gemäß § 8 der Promotionsordnung der Naturwissenschaftlich-Mathematischen Gesamtfakultät der Universität Heidelberg

Bei der eingereichten Dissertation zu dem Thema

„Conjugated Polymer-Based Chemical Tongues: Hypothesis-Free Sensor Arrays for the Discrimination of Chemical and Biological Analytes“

handelt es sich um meine eigenständig erbrachte Leistung.

Ich habe nur die angegebenen Quellen und Hilfsmittel benutzt und mich keiner unzulässigen Hilfe Dritter bedient. Insbesondere habe ich wörtlich oder sinngemäß aus anderen Werken übernommene Inhalte als solche kenntlich gemacht.

Die Arbeit oder Teile davon habe ich bislang nicht an einer Hochschule des In- oder Auslands als Bestandteil einer Prüfungs- oder Qualifikationsleistung vorgelegt.

Die Richtigkeit der vorstehenden Erklärung bestätige ich.

Die Bedeutung der eidesstaatlichen Versicherung und die strafrechtlichen Folgen einer unrichtigen oder unvollständigen eidesstattlichen Versicherung sind mir bekannt.

Ich versichere an Eides statt, dass ich nach bestem Wissen die reine Wahrheit erklärt und nichts verschwiegen habe.

____________________ ____________________

Ort und Datum Unterschrift